SAN DIEGO REGIONAL LAGOON PLANNING STUDIES PHASE 2

SUMMARY OF FINDINGS FOR WETLAND ENHANCEMENT OPPORTUNITIES USING THE HYDRODYNAMIC APPROACH FOR OPTIMIZATION OF BRIDGE DESIGN AT BATIQUITOS AND AGUA HEDIONDA LAGOONS

Interstate 5 North Coast Corridor Project
SAN DIEGO COUNTY, CALIFORNIA
DISTRICT 11-SD-5 (PM R28.4/R55.4)
EA 235800 (P ID 11-000-0159)

OCTOBER 2010

SAN DIEGO REGIONAL LAGOON PLANNING STUDIES
PHASE 2

SUMMARY OF FINDINGS
FOR WETLAND ENHANCEMENT OPPORTUNITIES
USING THE HYDRODYNAMIC APPROACH
FOR OPTIMIZATION OF BRIDGE DESIGN
AT BATIQUITOS AND AGUA HEDIONDA LAGOONS

Based on studies prepared for Caltrans/SANDAG

Prepared by

University of California, San Diego
Marine Physical Laboratory, Scripps Institute of Oceanography
291 Rosecrans Street
San Diego, CA 92110

Chang Consultants
PO Box 9492
Rancho Santa Fe, CA 92067

WRA, Inc.
2169 E Francisco Boulevard, Suite G
San Rafael, CA 94901

AECOM
1420 Kettner Boulevard
Suite 500
San Diego, CA 92101

October 2010

TABLE OF CONTENTS

1.0 INTRODUCTION 1
1.1 Background 1
1.2 Phase II Study 1
2.0 METHODS 3
2.1 Overview 3
2.2 Bathymetry 4
2.3 Models 4
2.3.1 Tidal dynamics 4
2.3.2 Sea level analysis 6
2.3.3 Flood model 7
2.4 Field investigation 7
2.5 Alternatives investigated 8
3.0 SUMMARY OF FINDINGS 15
3.1 Batiquitos Lagoon 15
3.1.1 Tidal dynamics 15
3.1.2 Flood flow passage 17
3.1.3 Habitat benefits 17
3.1.4 Sea level rise effects 20
3.1.5 Summary 20
3.2 Agua Hedionda 21
3.2.1 Tidal dynamics 21
3.2.2 Flood flow passage 23
3.2.3 Habitat benefits 23
3.2.4 Sea level rise effects 25
3.2.5 Summary 25
3.3 San Dieguito Lagoon 26
3.3.1 Tidal dynamics 26
3.3.2 Flood flows 27
3.3.3 Habitat Considerations 27
3.3.4 Summary 27
4.0 CONCLUSIONS 28

Appendices

Appendix A: Hydrodynamic Approach to Wetland Restoration by Optimization of Bridge Waterways. Prepared by Marine Physical Laboratory, Scripps Institution of Oceanography, University of California.

Appendix B: Hydraulic and Scour Studies for Proposed Interstate 5 Bridge Widening across Three Lagoons. Prepared by Chang Consultants.

Appendix C: Topographic and Vegetation Analysis of Batiquitos Lagoon and Agua Hedionda Lagoon. Prepared by WRA, Inc.

1.0 INTRODUCTION

1.1 Background

The California Department of Transportation (Caltrans), District 11, is developing plans and supporting environmental studies for the proposed Interstate 5 (I-5) North Coast Corridor Project. The project would improve an approximately 27-mile-long portion of I-5 within the County of San Diego, extending from the City of San Diego north to the City of Oceanside. Improvements would include widening of existing bridge structures at coastal lagoons to provide for additional travel lanes and would therefore have impacts to tidal and nontidal wetlands that would require mitigation.

A Phase I Study conducted by WRA, Inc. and AECOM in 2009 evaluated the potential restoration opportunities within six coastal lagoons traversed by I-5: Buena Vista, Agua Hedionda, Batiquitos, San Elijo, San Dieguito, and Los Peñasquitos (listed north to south). The Phase I analysis sought to specifically identify (a) conventional earth-moving restoration opportunities, and (b) potential changes in bridge structures where constraints to tidal flow could be reduced to improve tidal amplitude and circulation east of the I-5 bridges (hydrodynamic approach).

The hydrodynamic approach refers to improvements in the tidal range that result from removing flow restrictions imposed by causeways and bridge structures. Tidal muting or damping is caused by narrow channel configurations that reduce the volume of tidal water transferred between basins, which results in a smaller tidal range and modified tidal inundation and exposure frequencies within the intertidal zone. The frequency of tidal inundation and exposure directly affects the distribution of various habitat types (i.e., vegetated marsh and mudflat) within tidal ecosystems. In addition, reducing tidal damping increases tidal flushing or exchange between the ocean and lagoon areas and results in improved water quality for aquatic organisms. The potential to increase tidal heights through reduction in bridge constrictions may also increase the amount of wetland habitat by inundating current upland areas.

1.2 Phase II Study

The Phase I Study identified Batiquitos and Agua Hedionda lagoons as having the greatest potential for tidal flow enhancement using the hydrodynamic approach. Batiquitos and

Agua Hedionda lagoons have large basins east of the existing I-5 bridges that are subject to daily tidal action and have relatively narrow channels at the point of the bridge crossing. Based on these criteria, the potential for improvements in tidal exchange and increased tidal range was substantial at these two lagoons. On the other hand, the I-5 bridge structure near Penasquitos Lagoon is not being changed and is upstream of any tidal habitat. Buena Vista Lagoon was not studied as it does not currently have tidal action and the final restoration alternative has not been selected. San Elijo Lagoon is undergoing a study to evaluate restoration alternatives and therefore was not included in this study.

At San Dieguito Lagoon, the current bridge structure will be retained and additional lanes added. However, given the recently completed Southern California Edison/Joint Powers Authority tidal basin restoration and the proposed Caltrans tidal wetland creation project at San Dieguito Lagoon, the effect of any changes in the bridge structure on tidal exchange east of I-5 was investigated in this Phase II study to ensure the proposed modifications would not result in unanticipated impacts to those areas.

Caltrans engaged the Scripps Institute of Oceanography, WRA, Inc., and AECOM to evaluate existing tidal conditions and, if warranted, alternative bridge designs from the proposed design that might increase tidal flushing east of the bridges at the two identified lagoons—Batiquitos and Agua Hedionda. Along with the studies on tidal exchange, Chang Consultants conducted studies to evaluate whether the alternative bridge designs would have any adverse impacts on flood flows by increasing flood levels or causing additional scour that might affect bridge stability. WRA conducted field studies on the distribution of wetland vegetation along the margin of the lagoons to determine if additional tidal action would result in any increase in wetland habitat.

Three reports were prepared for the Phase II Study to assess the potential benefits of the hydrodynamic approach for salt marsh habitat and their effectiveness:

1. A tidal modeling study that evaluated the existing tidal flow dynamics and the resulting changes in the tidal inundation frequencies under various bridge alternatives (Jenkins and Wasyl 2010; see Appendix A).
2. A flood flow analysis to determine whether the bridge alternatives passed 100-year flood flows without materially affecting sediment flow dynamics downstream of the bridge (Chang Consultants 2010; see Appendix B).

3. A habitat distribution analysis to determine whether higher tidal ranges would result in an overall increase in tidal habitat within the lagoons (WRA, Inc. 2010; see Appendix C).

This report summarizes the content of these analyses and the findings reached on the potential for hydrodynamic enhancement of wetland habitats in Batiquitos and Agua Hedionda lagoons. In addition, the effects of the bridge design for San Dieguito Lagoon on existing tidal and flood flows are provided. The full reports for each of the separate studies are attached as appendices to this summary report.

2.0 METHODS

2.1 Overview

Background information was collected on each of the lagoon systems during the Phase I study, and these data were used in the tidal and flood models. The overall approach to the study consisted of a number of steps. The first step was to collect information on the existing and the proposed bridge designs[1] for the new I-5 crossings at each of the study lagoons and cross reference elevation data. In addition, bathymetric and cross-sectional data were needed for the models and this required gathering existing information as well as generating data for the upper portions of the lagoon where detailed topographic information was lacking. The hydraulic models could then be calibrated for the specific configurations within each lagoon against measured tidal data and flood conditions. Once the models were calibrated, existing and proposed bridge designs could be evaluated in terms of their effect on tidal damping and flood conditions. With that information, a series of iterative steps were undertaken to identify and evaluate additional bridge alternatives that might result in improved tidal circulation without affecting flood levels or scour. A set of alternatives that resulted in improved hydraulic conditions based on preliminary modeling was then subject to more rigorous evaluation. The tidal models were used to generate tidal range, tidal circulation, and tidal inundation frequency determinations to estimate the changes in habitat that may result from the bridge design. The bridge designs that had the greatest potential benefit to tidal flows were then evaluated in terms of whether they would have any adverse impacts on flood flow and scour.

[1] The alternative that was modeled was referred to as 10+4 w/buffer.

2.2 Bathymetry

Accurate bathymetric data were a critical input for the model parameters but were not readily available from a single source so various data sources were used.

For Batiquitos Lagoon, the most recent bathymetry was from Merkel and Associates (2009); however, the survey data did not provide topographic information above +5 feet Mean Lower Low Water (MLLW), so additional data were needed. WRA conducted field surveys of elevation transects in 2010 around the tidal basin east of I-5. WRA merged these data with the existing bathymetric data to produce a final bathymetric map for Batiquitos Lagoon using 1-foot contours. These merged data provided the base bathymetric and topographic data for the full tidal range experienced in the lagoon.

For Agua Hedionda Lagoon, the most recent bathymetry was from lagoon soundings taken by Cabrillo Power in 2007. However, the survey data did not provide topographic information above +2 feet MLLW. In this case, upper intertidal and low marsh data were obtained from an April 1997 field survey and supplemented with high marsh and upland data collected by WRA in 2010. These data were merged, corrected using averaging, and then summarized into a 1-foot contour map for the lagoon that allowed for a full tidal range to be modeled.

For San Dieguito Lagoon, the most recent bathymetry was from Coastal Environments (2009), which was supplemented with the topographic information using the as-built San Dieguito Wetlands Restoration Plan provided by Southern California Edison. No additional field surveys were required for this analysis as the topographic data covered the full tidal range.

2.3 Models

The computer models used for the analysis, assumptions used in their operation, and outputs are detailed in the technical reports in the appendices. A brief summary is provided below.

2.3.1 Tidal dynamics

For the tidal dynamics modeling, the TIDE_FEM model was used for tidal hydraulics and the littoral transport model was TIDE_FEM/SEDEXPORT. Jenkins and Wasyl (2010) provide background on this model and its use in Southern California, as well as the extensive peer review that has been undertaken on its performance. The model was calibrated against

recently collected field data from each of the lagoons and was then run using a 30-year simulation time period, 1980–2010. This time period includes a number of significant climate cycles including both El Niño and La Niña events. The output from these models provided information on flow patterns (direction and velocity) within the lagoon systems, as well as calculations of tidal heights and inundation frequency under the various alternatives.

An inundation-duration model developed by Josselyn and Whelchel (1999) was used to determine the change in wetland habitats associated with the duration of tidal inundation as calculated by the hydrodynamic models. The key parameter of this model is the amount of exposure to air (or its opposite, the degree of inundation by tidal waters) as it affects the distribution of various habitat types. The distribution breaks for habitat types within the lagoon were based on the following exposure times during the tidal cycle:

Subtidal Exposure = 0%;
0% < Frequently Flooded Mud Flat Exposure < 50%;
50% < Frequently Exposed Mud Flat Exposure < 61.8%
61.8% < Low Salt Marsh Exposure < 81.7%
81.7% < Mid Salt Marsh Exposure < 96.2%
96.2% < High Salt Marsh Exposure < 99.8%
99.8% < Transitional Exposure < 100%

The TIDE_FEM model calculated the hydroperiod data to predict exposure/inundation for various elevations, and the distribution of habitat types were then predicted based on the inundation/duration model for habitat distributions (see Figure S-1 for an example).

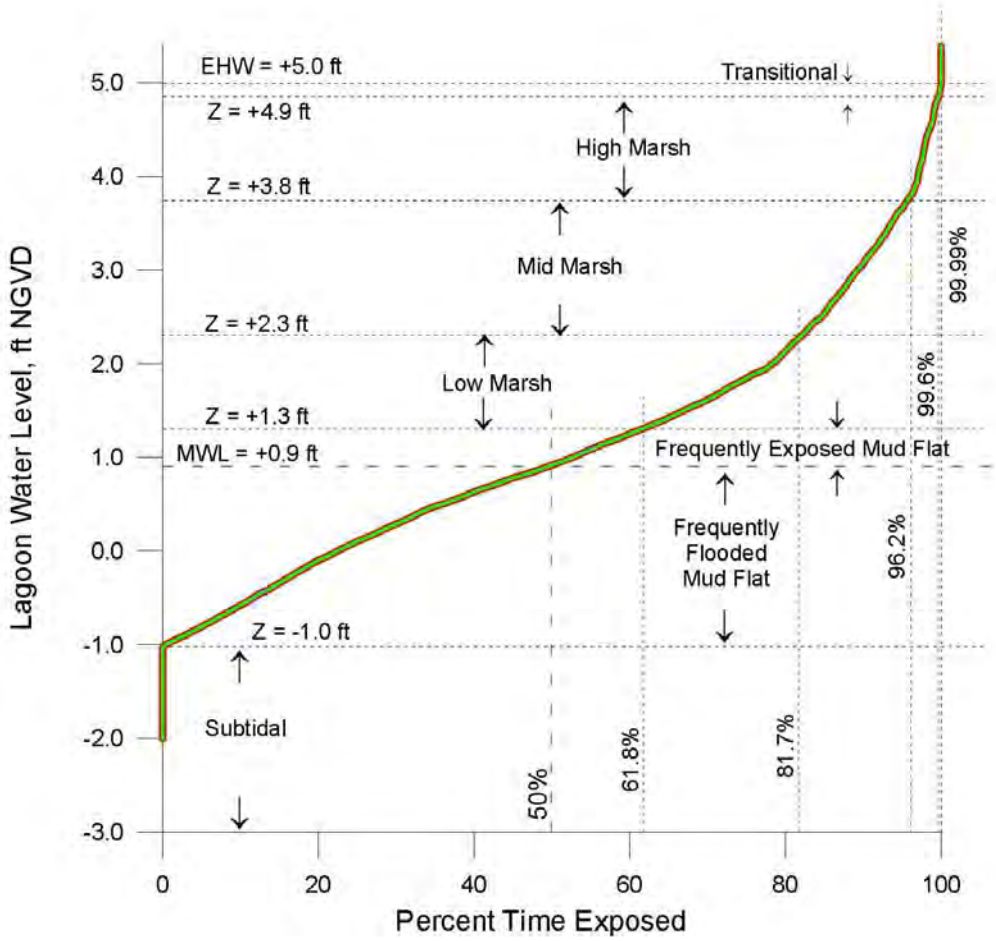

Figure S-1: Habitat distribution related to exposure as predicted by tidal model. Figure for San Dieguito Lagoon from Jenkins and Wasyl (2010). Lines for existing and proposed condition overlap in this figure.

2.3.2 Sea level analysis

The mean of six global climate model predictions used by the Intergovernmental Panel on Climate Change calls for 0.41 m (1.33 ft) of sea level rise by 2100, while the most aggressive prediction calls for that amount of sea level rise by 2050. This predicted sea level rise was linearly combined with the historic ocean water level record and used to drive the tidal hydraulics model. Although sea level rise will undoubtedly erode neighboring beaches, we did not attempt to quantify beach impacts on the lagoon bathymetry and tidal hydraulics due to the numerous assumptions that must be made on future beach sand supplies in such an analysis. The proposed replacement bridges and Alternative 4 were both evaluated for sea level rise effects on tidal exchange. Alternative 4 was used because it provided tidal regime conditions

equivalent or better than the other alternatives and therefore would represent the highest degree of tidal inundation under sea level rise scenarios.

2.3.3 Flood model

For the flood conditions, the HEC-2 or HEC-RAS model was used to determine the hydraulic performance for the 100-year flood event. This work was completed after the tidal dynamics model demonstrated the effectiveness of bridge alternatives in improving tidal flows. The purpose of the model was to determine whether the alternative designs would have any adverse effect on flood levels or scour[2]. The flooding model provided output on water surface elevation, flow velocity, and overtopping flow. In addition, the two-dimensional FESWNS model was used to distribute flood flow velocity distributions within the lagoon during the 100-year flood event. It provided information on the effective flow area (the region of the lagoon that has significant flow velocities and contributes to the conveyance of most of the flood flows) and the ineffective flow area (the region that primarily experiences elevated water levels and not strong velocities). Flood levels will change based on static sea-level rise; however, sea-level rise was not modeled in the flood flow analysis because the channel cross-section enlarges with sea-level rise and therefore bridge design itself will not result in increased flooding over that caused by sea-levels.

2.4 Field investigation

WRA conducted a detailed analysis of elevation and vegetation changes above the existing Mean High Water (MHW) within the portion of the lagoons east of I-5 for Batiquitos and Agua Hedionda lagoons. The fieldwork and data collection were conducted between February 22 and February 25, 2010. Using an Auto Level and a hand-held Trimble Global Positioning System (GPS) unit with sub-foot accuracy, elevation transects were shot and vegetation composition transects were collected throughout the two lagoons.

For the elevation transects, representative areas of topography were selected using existing topographic data mapped on lagoon aerials. For each representative area, a metered transect tape was run from MHW, moving upslope and perpendicular to the edge of water.

[2] The proposed bridge and the lengthened span alternatives result in an enlargement of the cross-sectional area that would result in lowered flood levels and flow velocity through the bridge opening. These alternatives were not analyzed in detail; only those that involved deepening of the channel cross-section or addition of flow fences were analyzed to determine if they exacerbated flood levels or flow over the existing bridge configuration.

During data collection, MHW was determined through the use of physical and biological field indicators such as wrack lines, vegetation changes, and algae growth on the ground and on vegetation. Using an Auto Level, an MHW elevation was recorded and a geo-referenced point was taken using the Trimble GPS.

By combining topographic and bathymetric data, along with collected elevation and vegetation data, WRA was able to model the area of wetland habitat located within 6-inch bands from MHW to 2 feet above MHW. This analysis was conducted to facilitate the assessment of the net increase of salt marsh habitat that could be expected from incremental increases in tidal levels within the lagoon. In addition, these data could be used to verify existing elevation conditions for marsh communities.

2.5 Alternatives investigated

The analysis investigated the existing and proposed bridge configurations for the new I-5 improvement as defined in the environmental impact report/environmental impact statement for the project. In addition, several alternatives were explored for effect on tidal dynamics or flood flows. The alternatives investigated for each of the lagoons are described below and summarized in Table S-1.

The alternatives were developed after initial investigation of the proposed bridge designs and with the objectives of enhancing the lagoon systems through improved tidal circulation, water quality, and increased tidal inundation and intertidal habitat. Alternative 1 considered whether the additional of flow fences to the proposed bridge design would improve circulation and reduce tidal damping. Flow fences are essentially steel or concrete sheet walls placed on the channel edge and at the ends of vertical walls to create a sheer wall along the entire depth of the channel and to reduce frictional eddy flow at the ends of the channel. The flow fence is narrowed toward the center with the flared expansion sections extending into the east and central basins, where they are free-standing without backfill and use the deeply driven sheet pile footings for support. The flow fences result in a vertically walled channel and result in optimal flow under the bridges to relieve tidal damping forces.

Table S-1. Alternatives Investigated for Agua Hedionda and Batiquitos Lagoons

ALTERNATIVE	AGUA HEDIONDA	BATIQUITOS
Existing Bridge	230-foot span with 4 rows of pilings with hard bottom at -19 feet and sediment surface[3] at -5 ft MLLW Bed width[4]: 76 ft	246-foot span with 2 rows of 3 vertical piers with armored bottom at -3 feet MLLW Bed width: 106 ft
Proposed Bridge [Alt 10+4 w/buffer]	230-foot replacement span with 2 rows of pilings with hard bottom at -19 feet and sediment surface at -5 feet MLLW Bed width: 76 ft	246-foot replacement span with 2 rows of 6 vertical piers with armored bottom at -3 feet MLLW Bed width: 106 ft
Alternative 1 [Add flow fence to proposed bridge span]	230-foot replacement span with flow fences Bed width: 113 ft	246-foot span with flow fences with armored bottom at -3 feet MLLW with flow fences Bed width: 140 ft
Alternative 2 [Doubling the length[5] of proposed bridge span]	460-foot replacement span with hard bottom at -19 feet MLLW and sediment surface at -5 ft MLLW Bed width: 152 ft	492-foot span with hard bottom at -3 feet MLLW Bed width: 212
Alternative 3 [Chang channel]	230-foot span with steeper side slopes to create 100-foot channel bed width with hard bottom at -19 feet MLLW and sediment surface at -5 ft MLLW Bed width: 128 feet	Modify 246-foot span with steeper side slopes to create 180-foot bed width with hard bottom at -4.7 feet MLLW Bed Width: 180 feet
Alternative 4 [Chang channel with flow fence]	Alternative 3 with flow fences	Alternative 3 with flow fences

Alternative 2 considered how increasing the bridge span by removing causeway fill (referred to in the reports as "double wide"[6]) would affect tidal dynamics. A third alternative modified the proposed design to create a larger cross-sectional area by removing some

[3] At Agua Hedionda, sediment backfills into the channel during the equilibrium non-flooding condition; during extreme flood events, the channel can scour to the hard bottom. The equilibrium condition was modeled in the tidal modeling; but the flood model allows for scour to the hard bottom of the channel.

[4] Bed width at sediment surface.

[5] This is also referred to as the "double-wide" alternative in the technical reports.

[6] The use of the term "double-wide" and bridge widening as used in the technical reports refers to lengthening the bridge span over the channel. It should not be confused with the fact that the bridge decks are also being widened for additional traffic lanes.

causeway fill beneath the span, creating steeper sidewalls, and deepening the channel bottom. This alternative (referred to as the “Chang Channel” in the attached technical reports) would increase the cross-sectional area of the channel similar to what could be achieved under the double-wide alternative by replacing sloped surfaces with steeper side walls and by deepening the channel. This third alternative was further modified with the use of flow fences to create a fourth alternative for evaluation.

Conceptual drawings for each alternative are shown in Figures S-2a and b and S-3a and b.

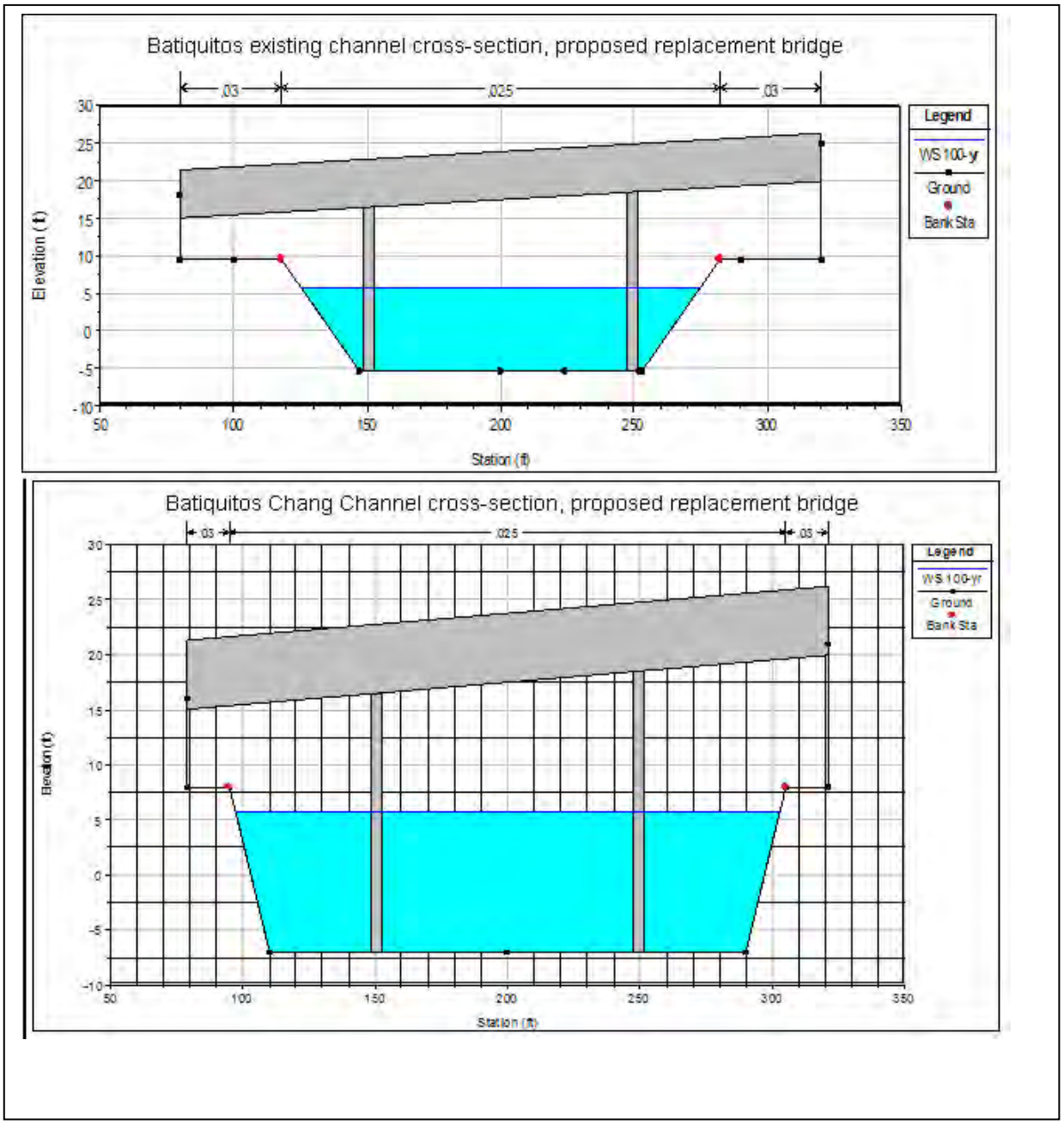

Figure S-2a. Conceptual drawings of the channel cross-sections considered for Batiquitos Lagoon. Upper is the channel cross-section used for both the existing and proposed replacement bridge. The lower is the channel cross-section used for Alternative 3 (Chang channel)

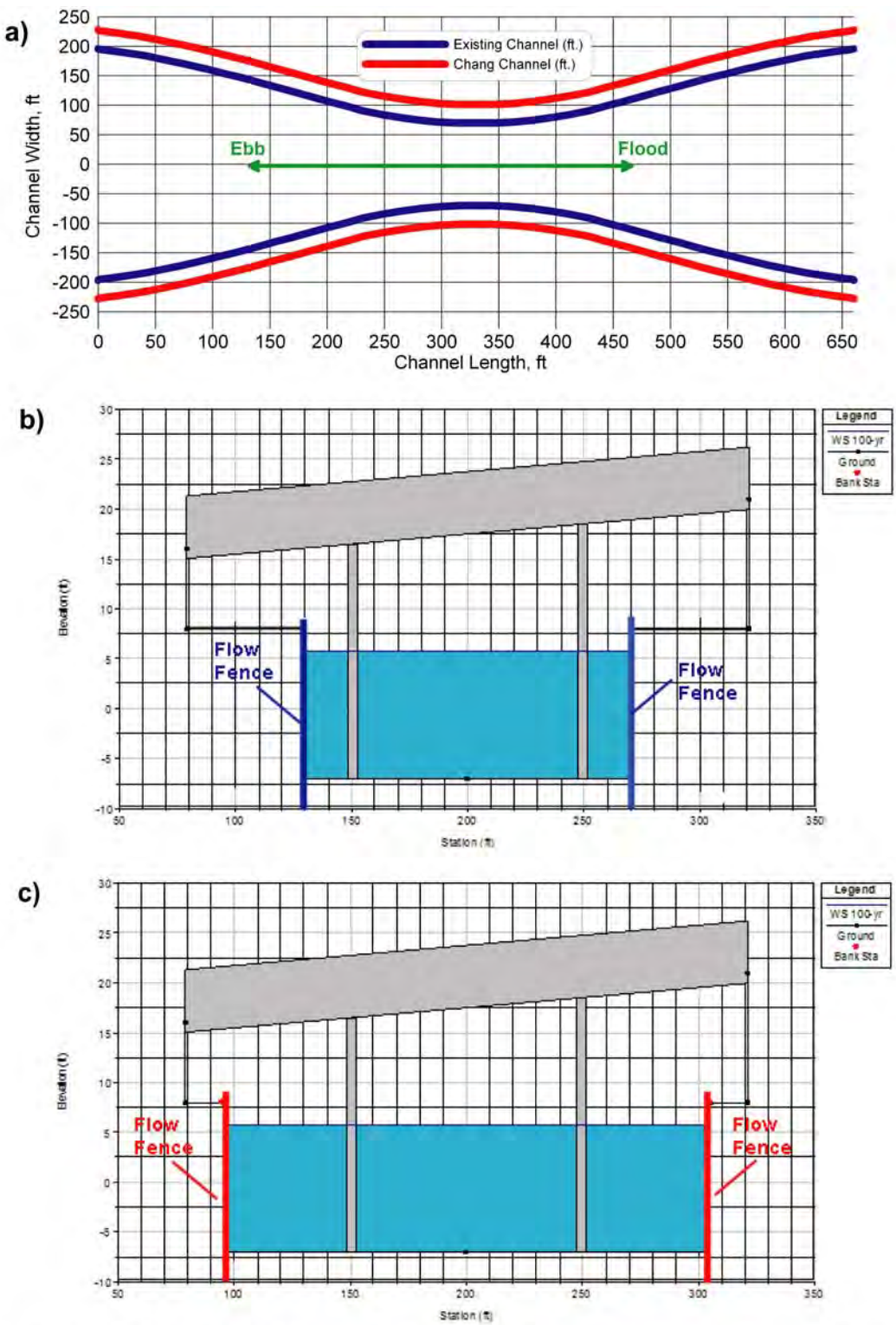

Figure S-2b. Conceptual drawings of the channel cross-sections for Batiquitos Lagoon with flow fences. (a) Flow fence plan views for Alternative 1 (blue) and 4 (red). (b) Cross-sections for Alternative 1. (c) Cross-sections for Alternative 4.

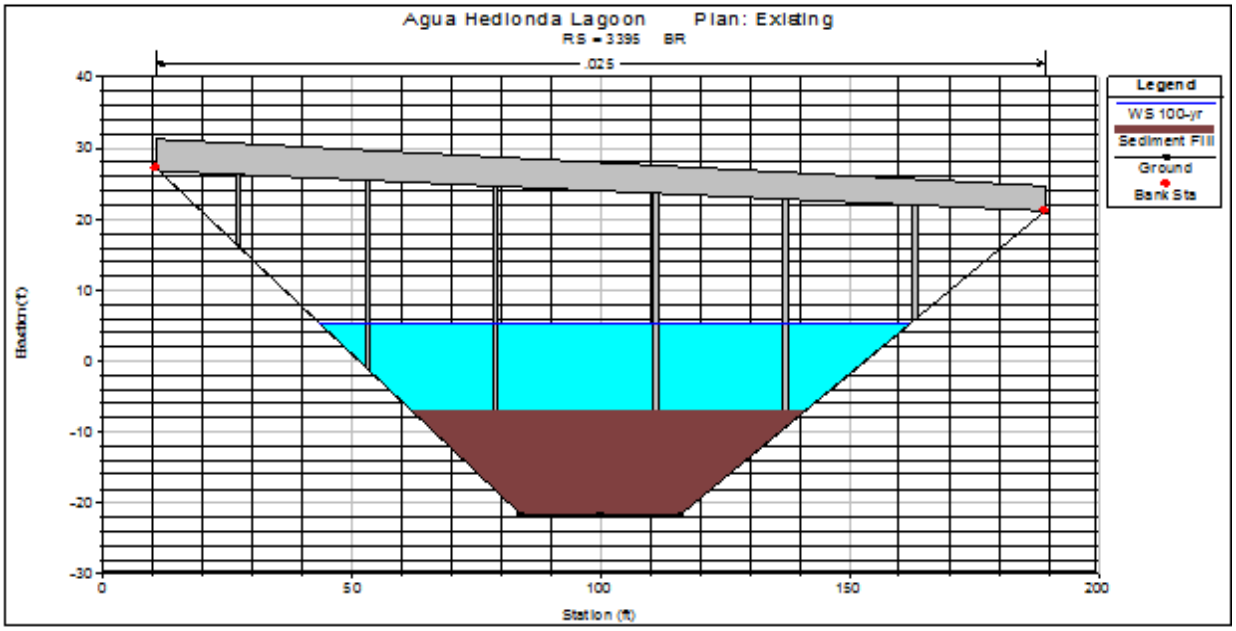

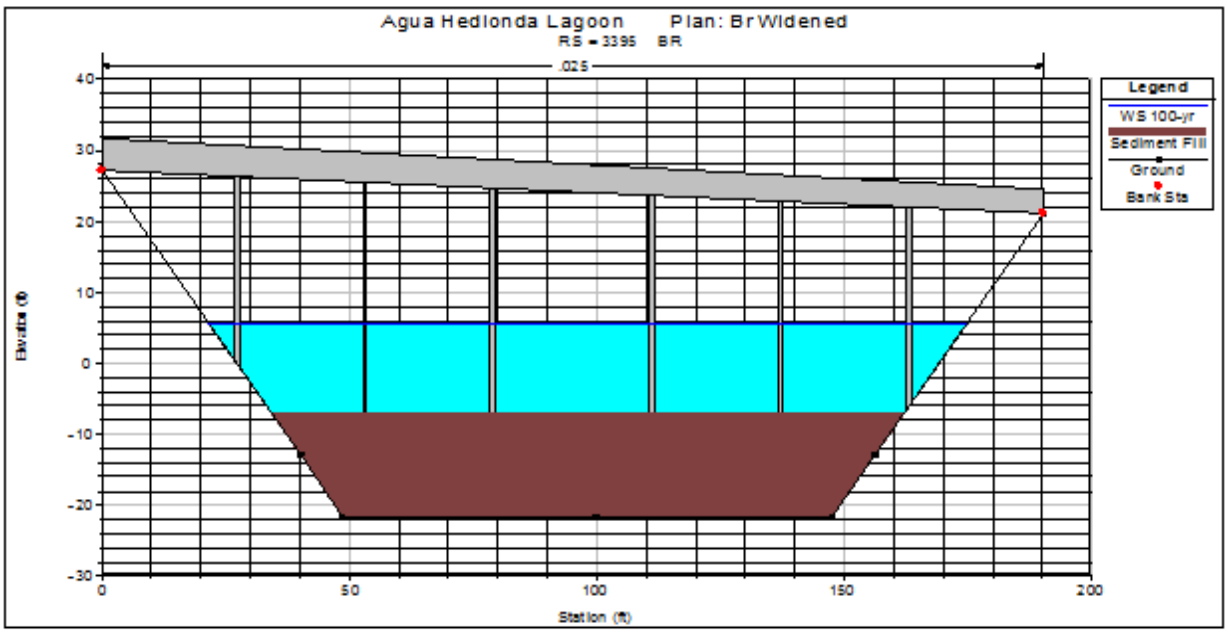

Figure S-3a. Conceptual channel cross-sections used for Agua Hedionda. Upper is the cross-section used for both the existing and the proposed bridge design. The lower cross-section is Alternative 3 (Chang channel).

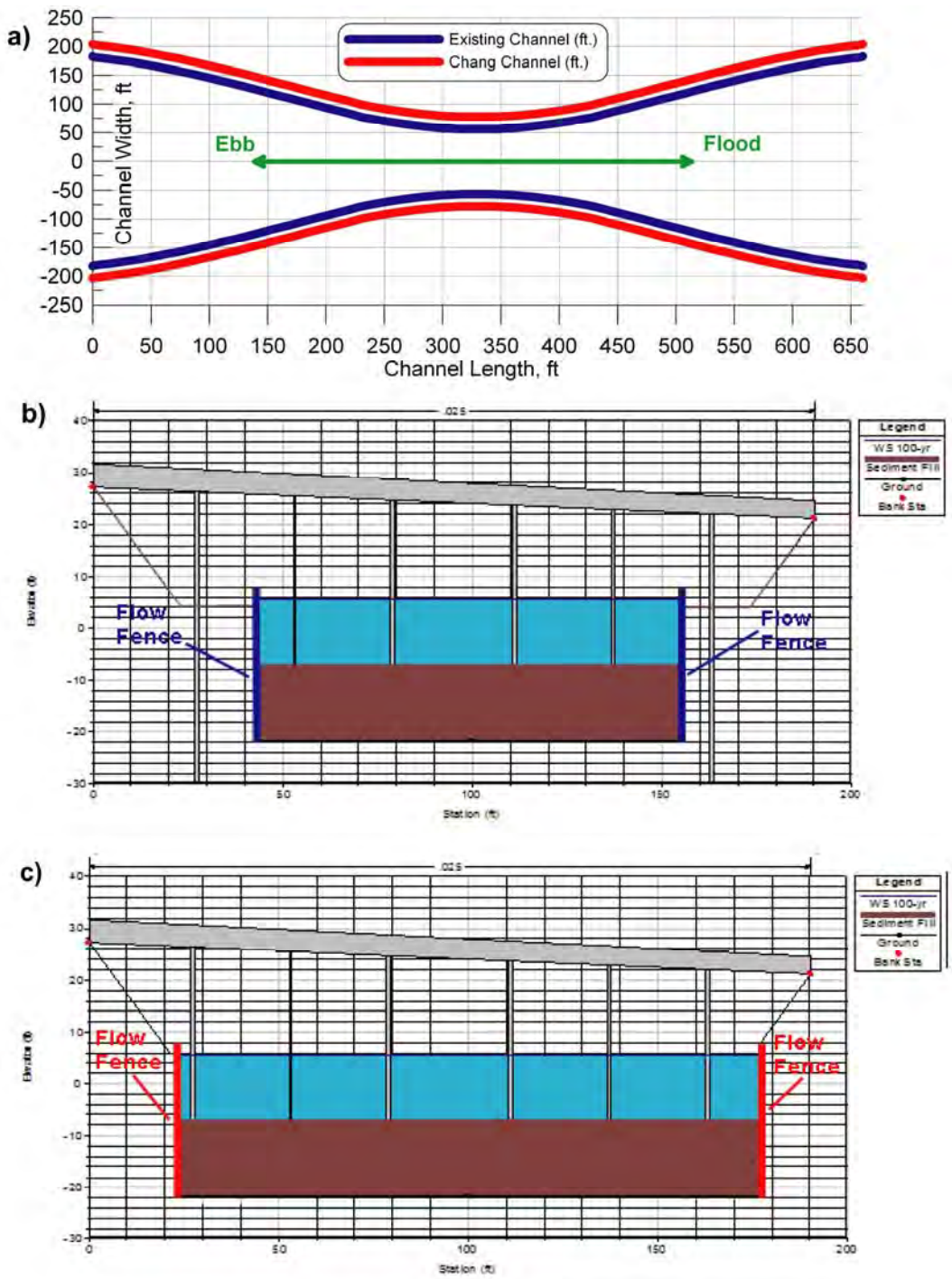

Figure S-3b. Conceptual channel cross-sections for Agua Hedionda. (a) Flow fence plan view for both Alternative 1 (blue) and 4 (red). (b) Cross-section for Alternative 1 (c) Cross-section for Alternative 4.

3.0 SUMMARY OF FINDINGS

3.1 Batiquitos Lagoon

3.1.1 Tidal dynamics

The current tidal range of the east basin (east of I-5) at Batiquitos Lagoon is affected by the existing bridge configuration. There is an approximately 50-minute lag between the tidal wave in the ocean and that in the east basin, while the high tide levels in the basin are slightly higher (approximately 0.3 foot) than those in the ocean. This is likely due to the "trapped tidal mode," or standing wave, that can occur in lagoon systems with multiple constrictions. At low tide levels, water in the east basin does not drain as low as the water levels in the ocean; the basin level is about +2.5 feet higher. Similar damping of the low tide water levels occurs within the central and west basins of Batiquitos Lagoon, though the tidal muting is less pronounced than within the east basin. This suggests that existing I-5 bridge conditions have an effect on tidal exchange in the east basin and that modification of the channel, and potentially the bridge structure, may be able to reduce the damping to at least the ranges in the central and western basins. The presence of scour holes (up to -24 feet) on either side of the existing bridge hard bottom also suggests that flow constriction and high current velocities reduce tidal exchange and amplitudes.

Figure S-4. Existing I-5 Bridge over Batiquitos Lagoon.

3.1.1.1 Proposed bridge condition

With the proposed bridge replacement, the flow velocities and potential for scour at either side of the bridge would still occur, and the model predicts minimal to no change in the lowest daily lagoon water level or in the phase lag with the ocean tides.

3.1.1.2 Alternatives

Under Alternative 1, a flow fence would be installed beneath the bridge by driving vertical interlocking sheet pile members into the channel at the point where the sloping rock revetment meets the water level. This would improve water flow through the channel in comparison with more turbulent flows over the rock revetment. This alternative would provide

some improvement in the drainage of the lagoon—approximately 0.15-foot lower water level at low tides.

Under Alternative 2, a substantial change would occur in water levels due to the removal of the flow restrictions by increasing the length of the span to the south. While this alternative would increase the number of pilings within the channel, the cross-sectional area of the channel would increase substantially. The most substantial change would be to the drainage of the east basin at low tide (MLLW), which will be lowered to +1.1 feet above MLLW[7], 0.5 foot lower than existing conditions. There is a much smaller change in the high tide level (MHHW) which is projected to be approximately 6.2 feet above MLLW, or about 0.1 foot above existing conditions.

Under Alternative 3, the bottom width of the channel would be increased using vertical side walls with the proposed bridge design rather than sloping rock revetments. In addition, the hard bottom would be increased in depth by 1.7 feet. With 80 percent more channel cross-sectional area than the existing bridge waterway; this alternative would improve tidal exchange compared to the existing or proposed conditions. While the flow velocities would be slightly higher than with Alternative 2, they would be sufficiently reduced such that scour holes on either side of the channel would likely fill over time. Compared to Alternative 2, the MHHW elevation would be similar and the MLLW elevation is only 0.1 ft higher. Therefore, Alternative 3 would result in almost similar tidal range conditions to Alternative 2 without the additional costs associated with increasing the span of the proposed bridge design.

Alternative 4 would add flow fences to Alternative 3. The flow fences would be placed on either side of the vertical walls to reduce eddies and consequential drag at the end of the walls. The tidal model showed very little difference in performance. There would be a small improvement in low tide drainage compared to Alternative 3, resulting in Alternative 4 being very similar to Alternative 2 in tidal performance in terms of tidal range and inundation frequency (Figure S-5); however, this small difference may not result in significant changes in habitat types.

[7]When providing elevation relative to MLLW, the ocean tidal datum of MLLW is being referenced. Therefore, an elevation of +1.1 feet above MLLW means that the low water elevation within the lagoon is still dampened (i.e., does not drain as readily) in comparison to the ocean tide. For reference, MLLW in the ocean is approximately 2.3 feet below NGVD29 (National Geodetic Vertical Datum) and 0.19 foot below NAVD1988 (North American Vertical Datum).

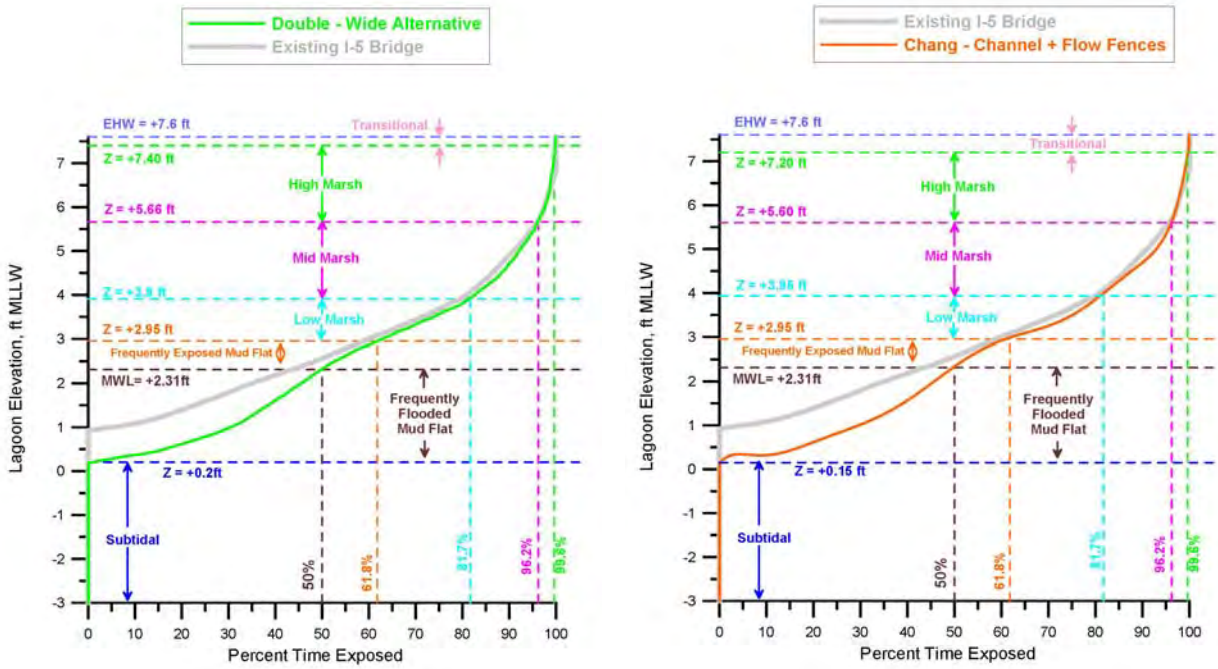

Figure S-5. Tidal exposure frequency related to lagoon elevation comparing existing conditions (grey line) with bridge design Alternatives 2 (on left) and 4 (on right). Low tide elevations lowered by similar amount under either alternative.

3.1.2 Flood flow passage

The flood flow analysis focused on a comparison of Alternative 3 with the proposed conditions. This is because under Alternative 2, 100-year flood levels and velocities would be reduced due to the increase in width and cross-sectional area. Alternative 3 is a narrower channel so it was investigated to determine if flood height or scour would increase. The HEC-RAS modeling demonstrated that the bridge under Alternative 3 would perform as well or better than Alternative 1 under the 100-year flood conditions. Because Alternative 4 has the same cross-sectional area as Alternative 3, it would be expected to perform similarly. None of the alternatives will exacerbate flooding or flow velocities over the existing condition.

3.1.3 Habitat benefits

The tidal dynamics study shows that, under existing conditions, the high tide elevations in the east basin are elevated compared to the ocean. In addition, at low tide, drainage is restricted and the low tide is 0.9 foot higher than experienced in the ocean. The result is that under existing conditions, subtidal habitat is greater and intertidal habitat is less than would exist with no restrictions to tidal flows.

3.1.3.1 Proposed bridge design

Under the proposed bridge design, some improvement would occur in reducing low tide levels with a resulting increase in intertidal habitat (Figure S-6). However, there would be little change in other habitat types.

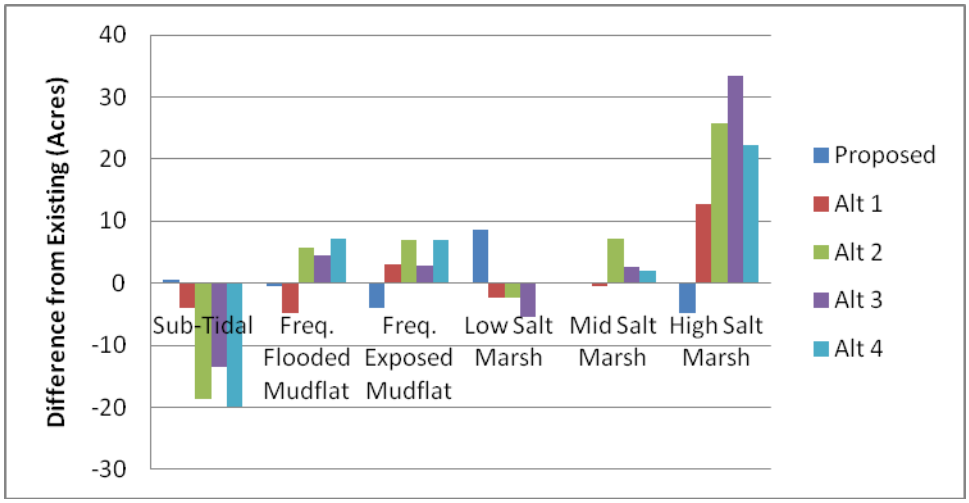

Figure S-6. Difference in habitat types from existing conditions for each alternative at Batiquitos Lagoon

3.1.3.2 Alternatives

The addition of flow fences to the proposed bridge design (Alternative 1) would result in a small increase in intertidal mudflat and the distribution of vegetated habitats within the east basin (Figure S-6). This is primarily due to an increase in exposure as opposed to increasing wetland through expansion of habitat at high tide. This would occur because the 12.5-acre area that lies between 5.9 feet and 6.3 feet MLLW is already 95 percent wetland (11.9 acres) (Appendix C). The upland acreage in this band consists of 0.6 acre of herbaceous habitat and 0.01 acre of rock. Alternative 1 had an increase of 0.1 foot in elevation of MHHW and this small increase would result in only a small conversion of upland habitat to wetland habitat (less than 0.5 acre).

Alternative 2 would substantially improve tidal range performance and would result in a substantial increase in both intertidal mudflat and vegetated marsh, primarily through changes in the distribution of high marsh habitat. Again, while some additional inundation would occur at the highest tide levels, most of the change in habitat distribution would occur due to changes in

tidal inundation frequency within the intertidal zones and reduction in continuously submerged (subtidal areas).

Similarly, Alternative 3 reduces tidal damping compared to the proposed bridge design and Alternative 1 through an increase in the intertidal habitat and would have the highest increase in total vegetated habitat by 31 acres. Most of this increase would result from the greater exposure of the upper mudflat such that tidal marsh vegetation would colonize to a lower elevation under the model's prediction of exposure frequency.

Alternative 4 (the addition of flow fences to Alternative 3) would result in net increase of 14 acres of mudflats and would result in an increase of 22 acres vegetated habitat through conversion of existing mudflat to salt marsh.

A summary of the change in maximum intertidal area, mean intertidal area, and total area of saltwater inundation is shown for the proposed project and each alternative in Figure S-7. It is apparent from this analysis that Alternative 2 and 4 are very similar in overall performance in terms of establishing additional intertidal habitat. The increase in tidal exchange would result in greater intertidal mudflats and an increase in vegetated habitat as marsh vegetation would be able to extend lower into the intertidal zone.

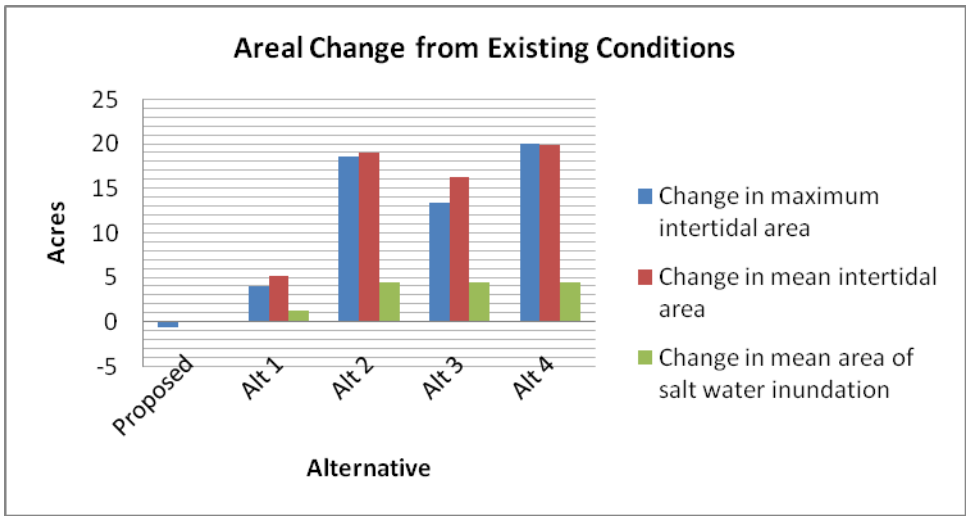

Figure S-7: Habitat change associated with bridge alternatives for Batiquitos Lagoon.

These changes in habitat distribution would have benefits to specific species such as shorebirds, which would have greater foraging opportunities on mudflats that are exposed more

frequently, and to passerine bird species, such as the Belding's savannah sparrow, that inhabit high marsh habitat. They would also benefit water quality by increased tidal flushing and reduced residence time in the east basin. While there are no current water quality problems in the lagoon, the improved flushing could reduce nutrient concentrations that may be contributed to the lagoon from the surrounding watershed; especially from urban runoff and excess summer irrigation flows.

3.1.4 Sea level rise effects

The general impact from sea level rise of 1.33 ft was found to be an increase in both the maximum and average areas of salt water inundation in the East Basin of Batiquitos Lagoon. However, these increases involved significant expansion in subtidal habitat and mudflats due to greater inundation while producing moderate reductions in low and mid salt marsh and significant reductions in high salt marsh habitat due to greater frequency of inundation. The incremental increases in tidally inundated habitat in response to sea level rise were moderately greater for Alternative 4 (Chang channel + flow fences) than for the proposed replacement bridge. The unbalanced habitat shift away from salt marsh induced by sea level rise was less for Alternative 4 than for the proposed replacement bridge.

3.1.5 Summary

A number of bridge alternatives were investigated for the replacement bridge structure at Batiquitos Lagoon. Each alternative was observed to provide benefits to tidal exchange, especially in reducing tidal damping and improving of ebb flow drainage. This led to reduction of the low tide levels, improved tidal exchange and flushing, and substantial increases in the distribution of intertidal mudflat and vegetated habitats. Deepening the channel bottom and adding vertical walls and flow fences (Alternative 4) were found to result in tidal exchange improvements over the proposed bridge design and were comparable in hydraulic performance to an increased span length alternative (Alternative 2). In addition, neither Alternative 2 nor Alternative 4 would compromise the conveyance of flood flows. Alternative 4 is likely to also represent a lower construction cost to lengthening the bridge span.

While there would be only a small conversion of upland to wetland in any of the alternatives, there is a projected increase in intertidal habitat (both tidally influenced vegetated wetland and intertidal mudflat) that would benefit a number of species that utilize these two habitat types. Improvements in tidal circulation would also benefit water quality through greater flushing of the east basin. In addition, implementation of Alternatives 2, 3, or 4 at the I-5

corridor would increase the channel cross-sectional area and thereby reduce restrictions to tidal and flood flows at this point. By removing the tidal restriction at the I-5 corridor under these alternatives, any further modification of the lagoon inlet at Pacific Coast Highway and/or the railroad bridge for the purpose of improving tidal ebb flows would translate to the east basin as well.

In Alternative 2, there would be some increase in aquatic habitat due to the removal of fill and conversion to open water habitat. Approximately 1.5 acres of additional open water habitat would be created under the lengthened bridge span. Because of the need to armor the bridge abutments, there would be no increase in vegetated wetland habitat.

3.2 Agua Hedionda

3.2.1 Tidal dynamics

The tidal dynamics of Agua Hedionda Lagoon have been altered by the Encina Power Station, which utilizes ocean water for cooling. The maximum once-through flow rate in the power plant is 800 million gallons/day (mgd) but averages about 500 mgd[8]. The result is that the ocean inlet to the lagoon experiences a higher net inflow of water each day rather than the higher net outflow (tidal + stream input) that occurs in most natural systems. While this effect is most substantial at the inlet and in the west basin of the lagoon, it has some benefits to the east basin (east of I-5) in that it reduces tidal damping that might occur due to restrictions in flow at the I-5 bridge and downstream at the ocean inlet (e.g., railroad bridge and PCH).

Figure S-8. Existing I-5 Bridge over Agua Hedionda Lagoon

Under existing conditions, there is a slightly higher MHHW level in the east basin (6.1 feet MLLW) compared to the ocean (5.7 feet MLLW); however, low tide is close to that of the ocean (a difference of only 0.4 foot for MLW and 0.2 foot for MLLW). Although the tidal prism exchange with the ocean is similar to Batiquitos Lagoon, tidal damping and phase lag in the

[8] The recently approved Carlsbad Desalination Project will reduce flows to approximately 40 percent of present-day averages and 62 percent of peak flow.

east basin of Agua Hedionda were found to be four to six times less than modeled at Batiquitos. This difference is attributable to the “suction induced horsepower” contributed by the power plant to more effectively drain the lagoon on the ebbing tide.

3.2.1.1 Proposed design

The proposed replacement bridge design would have fewer pilings and therefore would result in some benefits by reducing flow resistance and slightly increasing the tidal range.

3.2.1.2 Alternatives

Alternative 1 would achieve some reduction in flow resistance within the channel due to the placement of flow fences. However, the flow fences would not result in substantial increases in the tidal range within the intertidal zone.

Alternative 2 would result in a reduced time phase lag (compared to the ocean tidal wave) and achieve more complete drainage of the east basin during low tide. MLLW would be reduced to +0.55 foot MLLW (compared to +0.64 foot MLLW under existing conditions) and the diurnal range would be 5.58 feet, an increase of 0.16 foot over existing conditions.

Alternative 3 would increase channel cross-sectional area without increasing structural span. While it would have some benefits over the proposed bridge design, the benefits would not be as substantial as benefits from Alternative 2. MHHW would remain similar to Alternative 2; however, MLLW would be reduced to +0.60 foot MLLW for a diurnal range of 5.5 feet, slightly less than that under Alternative 2.

Alternative 4 would increase both the cross-sectional area of Alternative 3 and the flow capacity through the channel with the installation of flow fences. This alternative would achieve the best result in MLLW elevation at +0.54 foot MLLW (Figure S-9). In addition, the modeling shows that flow eddies during flooding tide are more organized than in Alternative 2 and would result in a better stirring action within the east basin. This could be beneficial to improving dissolved oxygen and reducing areas of potential nutrient concentrations in the east basin.

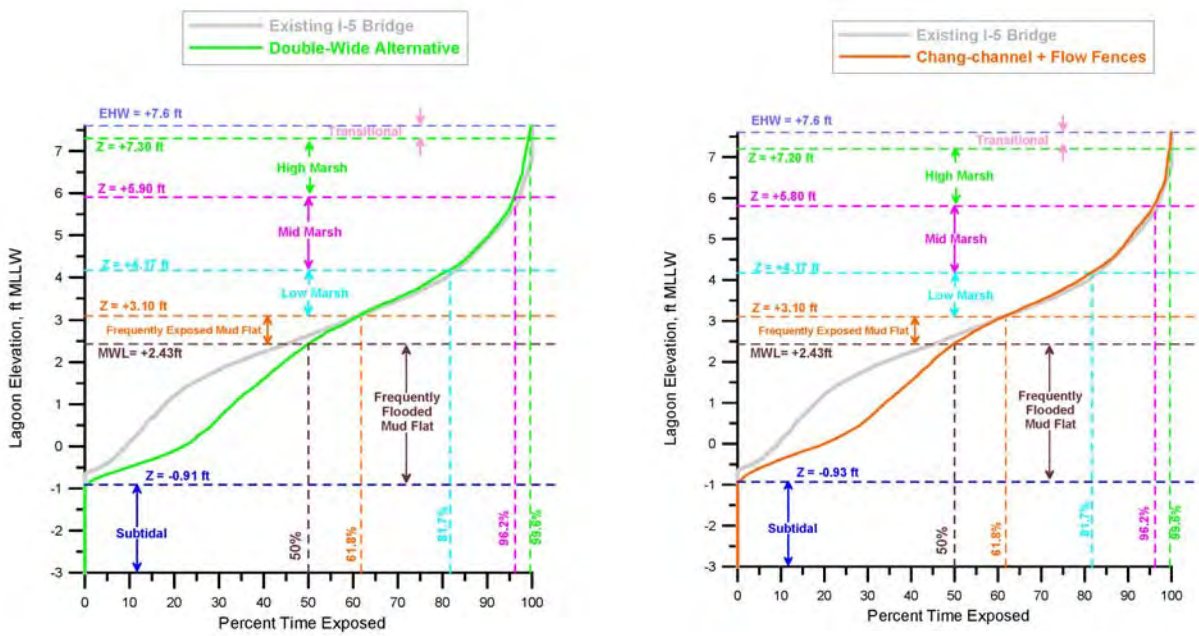

Figure S-9. Tidal exposure related to lagoon elevation in comparison to existing conditions (grey line) for Alternative 2 (on left) and Alternative 4 (on right) for Agua Hedionda Lagoon. Most of the change in tidal exposure occurs below Mean Water Line (MWL).

3.2.2 Flood flow passage

The doubling of the span under Alternative 2 is expected to have greater capacity to pass flood flows and therefore was not analyzed in the flood modeling. However, Alternatives 3 and 4 would change the cross-sectional area under the bridge without increasing the span. Therefore they were modeled to determine if they would have an effect on flood levels or scour. The HEC-RAS modeling demonstrated that the bridge under Alternative 3 would perform as well as or better than either the existing or proposed bridge design in the 100-year flood conditions. Alternative 4, being similar to Alternative 3, would be expected to perform as well.

3.2.3 Habitat benefits

Compared to Batiquitos Lagoon, Agua Hedionda contains much more open water and subtidal habitat. In addition, the northern and southern sides of the lagoon are much steeper and lack shallow grades that could be available for the formation of wetland habitat with rising water levels. Only the far eastern end of the lagoon has shallow wetland habitat that may be affected by changing tidal exposure patterns.

The area of land that extends from MHW up to an elevation 2 feet above MHW totals 32.5 acres. The total distribution of land cover types in this elevation range is 30.2 acres of wetlands, 0.9 acre of uplands, and 1.4 acres of sand/rock. None of the project alternatives would substantially change the high tide inundation area, and no additional wetland area would be created as a result of bridge design.

3.2.3.1 Proposed bridge design

Under the proposed bridge design, there would be relatively small changes in habitat types, usually within 1 acre of existing conditions (Figure S-10). Intertidal mudflat would increase slightly and high marsh habitat would decrease.

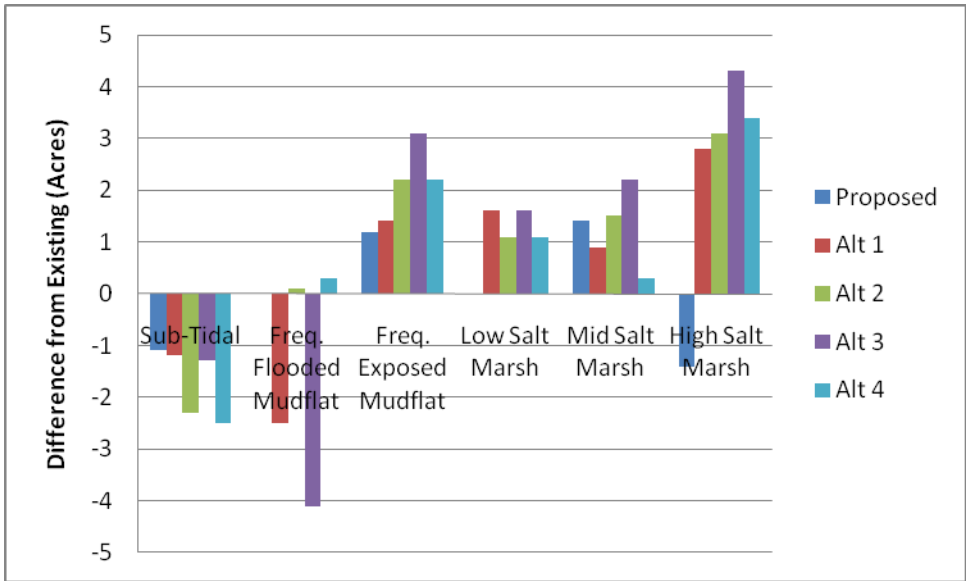

Figure S-10. Differences in habitat types from the existing conditions under various bridge designs for Agua Hedionda Lagoon.

3.2.3.2 Alternatives

Most of the alternatives would result in a slight decrease of subtidal and frequently flooded mudflat habitat (1 to 2 acres) and an increase in frequently exposed mudflat and vegetated marsh habitat. It is difficult to distinguish between the effectiveness of any alternatives since the differences in performance would be small and likely within the error margin of the response of the vegetative communities to changing water levels; however, Alternative 3 and 4 appear to result in the greatest increase in frequently exposed mudflat and vegetated marsh habitat.

In terms of maximum and mean intertidal range and the mean area of salt water inundated, both Alternatives 2 and 4 appear to be as effective (Figure S-11). However, these differences overall would be very small compared to the size of the east basin itself and may not be substantial given potential errors in the model and its predictive tools.

3.2.4 Sea level rise effects

In general, sea level rise effects in the East Basin of Agua Hedionda are less pronounced than what was found for the East Basin of Batiquitos Lagoon. Net gains in areas of tidal inundation are significantly less at Agua Hedionda, and losses of salt marsh habitat are also less. This is due to the differences in grading designs between the two lagoons. The east basin of Batiquitos Lagoon was designed to be a wetland restoration with broad shallow sloping marsh plains in the upper intertidal zone, whereas Agua Hedionda Lagoon was designed to be a cooling water reservoir with predominant sub-tidal area and steep slopes in the upper intertidal zone. Consequently sea level rise impacts on salt marsh are substantially less at Agua Hedionda Lagoon because that lagoon was designed with substantially less of that habitat type.

3.2.5 Summary

The Encina Power Plant effectively acts as an “iron lung” in helping the east basin of Agua Hedionda Lagoon to more effectively drain on the ebbing tide. This reduces the opportunity to achieve habitat gains and expansion of the intertidal zone with more efficient I-5 bridge waterway alternatives. While there are slight differences between the proposed and the various alternatives, they are relatively small in magnitude.

Of the alternatives investigated, Alternative 4 would create more efficient flow through the bridge channel and thereby increasing the tidal range in the east basin. This alternative would result in 2.5 acres of new mudflat creation and would increase the exposure time of existing mudflats; a benefit to shorebird foraging. It would also allow expansion of the present intertidal habitat by 5 acres through lowering the elevation that could be colonized by vegetated tidal marsh, but that habitat type makes up only a minor fraction of the existing east basin habitat, 77 percent of which is subtidal. It is important to note that while the model predicts these changes; the response of the vegetative communities is likely to be more variable. As a result, for Agua Hedionda Lagoon, the benefits of any of these alternatives are likely to be for water quality improvement primarily, not habitat change.

As noted for Batiquitos Lagoon, additional open water habitat would be created in Alternative 2 as the bridge span would be widened. Approximately 1-2 acres of additional habitat would be created; all of which would be either intertidal rocky or subtidal habitat.

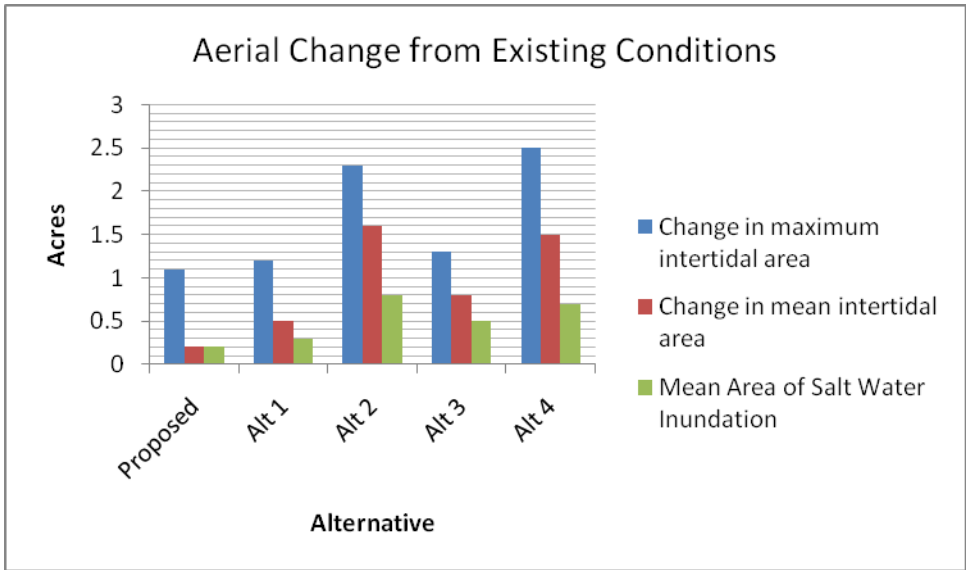

Figure S-11. Habitat change predicted for Agua Hedionda.

3.3 San Dieguito Lagoon

3.3.1 Tidal dynamics

The I-5 Bridge over the tidal/river channel of San Dieguito Lagoon would not be replaced under the proposed plan; but lanes would be added to increase its width using the existing span length as proposed in the environmental documents for the project. Therefore, this bridge was only studied in terms of any constraints it places on current tidal flows and flood conveyance.

Figure S-12. Existing I-5 Bridge over San Dieguito River

The hydrodynamics model considered the effect of the bridge on the current restoration as completed by Southern California Edison (SCE) and the effect of an additional 40 acres of created wetlands habitat should a plan be approved for the Caltrans tidal

wetland restoration project at San Dieguito Lagoon. This latter plan is being developed by the Joint Powers Authority for the San Dieguito River and by Caltrans. The modeling results found that neither the current wetland restoration as completed by SCE nor that proposed by Caltrans would be affected by any changes associated with the additional lanes being added to the current bridge.

3.3.2 Flood flows

The computed water-surface elevations at the bridge crossing and adjacent channels under 100-year flood flow conditions and with the additional W-19 basin as preliminarily designed by the JPA and Caltrans show that the proposed bridge design would not result in a rise of the flood level. The 100-year water surface would stay well below the bridge under existing sea-levels. Modeling was not conducted for this bridge under sea-level rise conditions.

3.3.3 Habitat Considerations

The tidal dynamics modeling indicates that habitat distribution within the lands east of I-5 would not be materially altered by the wider I-5 bridge. In considering patterns of tidal flow, water level, areas of tidal inundation and hydroperiod in total, the proposed additional lanes on the I-5 bridge would not result in substantial changes in habitat distribution or extent.

3.3.4 Summary

The proposed widening of the I-5 bridge would not result in substantial changes to tidal exchange and habitat types relative to existing conditions in San Dieguito Lagoon. This finding was expected, since neither the existing nor the proposed I-5 bridges have any structural footprint (e.g., support piles) located in the active tidal channel under the I-5 bridge. Due to the long bridge span at San Dieguito Lagoon (209 meters or 686 feet), both the existing and proposed bridge bridges would be transparent to tidal circulation and would have no differing effects on flood flows. In addition, Caltrans and SANDAG are planning on creating a tidal wetland of approximately 40 acres east of I-5. The modeling showed that there was no effect of the proposed bridge on tidal exchange in the new wetland area.

4.0 CONCLUSIONS

The hydrodynamic approach to wetland enhancement was investigated to determine the potential to improve tidal range and flushing within areas east of the I-5 corridor in Batiquitos and Agua Hedionda lagoons. The hydrodynamic approach focuses on optimization of the channel configuration beneath the bridge structure to reduce tidal damping, thereby altering ebb flows allowing for greater drainage and flushing of the lagoon. Changes in the tidal inundation and exposure frequency have a direct influence on the distribution of habitat types within the lagoon.

For Batiquitos Lagoon, substantial changes in habitat distribution in the east basin were predicted under various bridge alternatives. In particular, increasing the channel cross-section and flow efficiency through the channel (Alternatives 2 and 4) would result in more frequent ebb tide exposure of current subtidal habitats, converting them to mudflats and vegetated marsh habitats. This could result in improved habitat for shorebirds and species associated with vegetated marshes such as light-footed clapper rail and Belding's savannah sparrow. While the amount of new wetland habitat created by reducing tidal damping would be small, bridge alternatives were shown to result in substantial increases (e.g.15–25 acres) in intertidal mudflat and vegetated marsh with a concomitant reduction in subtidal habitat. Reducing tidal damping would also improve circulation within the east basin of the lagoon. This may have an effect on water quality (e.g. reduced temperatures, higher dissolved oxygen) and may also promote greater movement of fine sediments out of the lagoon towards the ocean. These benefits were not quantified in the modeling effort to date; however, they are expected to be a result of improved tidal exchange.

It is important to note that Alternatives 2, 3, and 4 at Batiquitos Lagoon would maximize the ebb flow drainage from the east basin. Further reduction in tidal damping would require alteration of the railroad bridge crossing and more frequent dredging of the inlet shoal that has developed just west of the railroad bridge. If these restrictions were removed to ebb flow passage, the proposed alternatives at the I-5 corridor would also allow for improved tidal drainage in the east basin.

For Agua Hedionda, potential changes in habitat distribution were smaller (e.g. 1–3 acres). This is due primarily to the effect of the Encina Power Plant, which discharges cooling water that is extracted from the lagoon, thereby improving ebb flows from the entire lagoon system. While all the alternatives examined would result in improved tidal circulation, the differences between them are relatively small and probably within the margin of error on the prediction of intertidal

communities by tidal exposure models. Although some small conversion of subtidal to intertidal habitat would be expected under various alternatives investigated, no conversion of upland to wetland habitats was predicted due to small change in high tide levels. On the other hand, the tidal circulation models show some improvement in tidal circulation and this could have benefits on water quality. These benefits have not been quantified in this analysis; however, the coupling the modeling results to a water quality model could provide such information.

For San Dieguito Lagoon, the bridge structure under existing and proposed conditions showed no effect on the tidal exchange east of the I-5 corridor for either the existing conditions or with the addition of a new tidal wetland basin proposed by Caltrans. The bridge does not appear to be constraining tidal flows. SCE is required to implement inlet maintenance and therefore tidal damping is not expected to be an issue once SCE completes its restoration project.

REFERENCES

Chang Consultants. 2010. Hydraulic and Scour Studies for Proposed Interstate 5 Bridge Widening across Three Lagoons. 148 pp.

Coastal Environments. 2009. 2009 Monitoring Program for San Dieguito Lagoon: Topography, Hydrology, and Water Quality Surveys. Submitted to Southern California Edison Company. 134 pp and app.

Jenkins, S. and J. Wasyl. 2010. Hydrodynamic Approach to Wetland Restoration by Optimization of Bridge Waterways. Prepared by Marine Physical Laboratory, Scripps Institution of Oceanography, University of California. 256 pp.

Josselyn, M. and A. Whelchel. 1999. Determining the upper extent of tidal marsh habitat for San Dieguito Lagoon. Prepared by WRA, Inc. for Southern California Edison.

Merkel and Associates. 2009. Batiquitos Lagoon: Long-term Biological Monitoring Report Program. Final Report. Prepared for the Port of Los Angeles and City of Carlsbad.

WRA, Inc. 2010. Topographic and Vegetation Analysis of Batiquitos Lagoon and Agua Hedionda Lagoon. Prepared by WRA, Inc. 8 pp + Figures.

Appendix A

Jenkins, S. and J. Wasyl. 2010. Hydrodynamic Approach to Wetland Restoration by Optimization of Bridge Waterways. Prepared by Marine Physical Laboratory, Scripps Institution of Oceanography, University of California 291 Rosecrans Street San Diego, CA 92016 256 pp

HYDRODYNAMIC APPROACH TO WETLAND RESTORATION BY OPTIMIZATION OF BRIDGE WATERWAYS

Interstate 5 North Coast Corridor Project

SAN DIEGO COUNTY, CALIFORNIA
DISTRICT 11-SD-5 (PM R28.4/R55.4)
EA 235800 (P ID 11-000-0159)

OCTOBER 2010

Hydrodynamic Approach to Wetland Restoration by Optimization of Bridge Waterways

Technical Agreement # 11A1766

Submitted by: Scott A. Jenkins, Ph.D., Principal Development Engineer
Joseph Wasyl, Associate Development Engineer
Marine Physical Laboratory
Scripps Institution of Oceanography
University of California, San Diego
291 Rosecrans Street
San Diego, CA 92016

Submitted to: Sue Scatolini
Department of Transportation, District 11
Environmental Division, MS-242
4050 Taylor St.
San Diego, CA 92110

Revised 21 October 2010

Table of Contents

Executive Summary……...4

1.0) Phase 2 Chronology……..23

2.0) Hydrodynamic Model and Input Variables……...24
2.1) Ocean Water Level Data and Sea Level Rise Predictions…….26

3.0) Tidal Hydraulics Impacts of Widening Existing I-5 Bridge Span at San Dieguito Lagoon……32
3.1) Model Input……32
3.2) Model Calibration and Assessment of Existing Conditions……..35
3.3) Simulated Tidal Hydraulics Impacts from I-5 Bridge Widening……46

4.0) Tidal Hydraulics Impacts of Replacing and Widening the I-5 Bridge at Batiquitos Lagoon……56
4.1) Model Input……56
4.2) Model Calibration and Assessment of Existing Conditions……..68
4.3) Simulated Tidal Hydraulics Impacts from I-5 Bridge Replacement and Widening……78
4.3.1) Tidal Hydraulics Impacts of Proposed I-5 Bridge Replacement……78
4.3.2) Tidal Hydraulics Impacts of I-5 Bridge Replacement with Fill Removal (*Double-Wide Alternative*)……87
4.3.3) Tidal Hydraulics Impacts of I-5 Bridge Replacement with Reduced Fill Removal (*Chang-channel Alternative*)……98
4.3.4) Tidal Hydraulics Impacts of the Proposed I-5 Bridge Replacement + Flow Fences……...111
4.3.5) Tidal Hydraulics Impacts of the Chang-channel Alternative + Flow Fences……..121

5.0) Tidal Hydraulics Impacts of Replacing and Widening the I-5 Bridge at Agua Hedionda Lagoon……..133
5.1) Model Input……..134
5.1.1 Power Plant Flow Rates……..142
5.2) Model Calibration and Assessment of Existing Conditions……147
5.3) Simulated Tidal Hydraulics Impacts from I-5 Bridge Replacement and Widening……...159
5.3.1) Tidal Hydraulics Impacts of Proposed I-5 Bridge Replacement….159
5.3.2) Tidal Hydraulics Impacts of I-5 Bridge Replacement with Fill Removal (*Double-Wide Alternative*)……..173
5.3.3) Tidal Hydraulics Impacts of I-5 Bridge Replacement with Reduced Fill Removal (*Chang-channel Alternative*)……...183
5.3.4) Tidal Hydraulics Impacts of the Proposed I-5 Bridge Replacement + Flow Fences……192

Table of Contents (continued)….

5.3.5) Tidal Hydraulics Impacts of the Chang-channel Alternative + Flow Fences……..201

6.0) Sea level Rise Effects…….210
6.1) Sea level Rise Effects at Batiquitos Lagoon for Replacement Bridges……210
6.2) Sea level Rise Effects at Batiquitos Lagoon for Chang-channel + Flow Fences…….216
6.3) Sea level Rise Effects at Agua Hedionda Lagoon for Replacement Bridges……223
6.4) Sea level Rise Effects at Agua Hedionda Lagoon for Chang-channel + Flow Fences……...228

7.0) Conclusions…….235
7.1) San Dieguito Lagoon……..235
7.2) Batiquitos Lagoon……...236
7.3) Agua Hedionda Lagoon…….242
7.4) Sea level Rise Effects…….248

REFERENCES……..253

Executive Summary:

This study constitutes Phase 2 of a multi-phase project already underway. The purpose of the study is to evaluate the potential for wetlands habitat enhancement associated with bridge configurations designed to minimize the muting of tidal exchange in the wetlands east of I-5 in Batiquitos Lagoon and Agua Hedionda Lagoon. In addition, the combination of the proposed W-19 tidal basin and a wider I-5 bridge at San Dieguito Lagoon will be evaluated by hydrodynamic modeling to determine potential effects on tidal inundation in the newly constructed Edison restoration project. This work focuses on the Batiquitos, Agua Hedionda and San Dieguito lagoons, because these are the most opportune lagoon systems along the I-5 corridor that have the largest areas of potential tidal inundation east of I-5. The primary objective of this study is to formulate and evaluate hydraulically more efficient bridge design concepts that minimize impacts and maximize wetland habitat in the context of the overall system dynamics of each lagoon, and under the influence of climate variability. The specific study goals were 1) determine what effects wider I-5 bridges will have on tidal inundation at Batiquitos, Agua Hedionda and San Dieguito Lagoons; and then, 2) determine whether or not tidal inundation of wetlands habitat east of I-5 in Batiquitos and Agua Hedionda can be increased through innovative changes in bridge waterways design, and whether or not this action will increase functional capacity, provide additional mid- and high-salt marsh habitat, improve water quality by reducing residence time and improve tidal flushing of littoral sediments by increasing the tidal prism of the overall wetland systems.

It is an observational fact that extreme high water (EHW) and mean higher high water (MHHW) levels in all three lagoons exceed ocean water level elevations under existing conditions (cf. Elwany, et. al, 2005; Merkel, 2008; and Coastal Environments, 2009). This is due to a well known phenomenon involving the formation of trapped tidal modes (standing oscillations or seiches) in enclosed water bodies isolated from open ocean tides by constricted inlets and choke points. These trapped modes are comprised of a number of higher harmonics and resonant triads at the K1 and M2 tidal frequencies, which pump up the lagoon high water elevations to elevations that equal or slightly exceed ocean high water elevations. Because of this high water effect, it is difficult to increase the absolute numbers of acres inundated at high tide with better bridge waterway designs. The net effect of the existing bridge designs on tidal exchange is to limit the ability of the east basins of the lagoons to fully drain during ebb tide, resulting in mean lower low water levels (MLLW) in the lagoons well above the ocean MLLW. This in turn limits and compresses the intertidal habitat by raising the zonation of low, mid and high marsh vegetation. Although we attempt in this study to increase tidal inundation east of I-5 with new bridge waterway alternatives, most of the benefits from these alternatives come from

improving the drainage of the eastern tidal basins during ebbing tide, thereby expanding the intertidal habitat, and increasing the amount of mud flats and expanding the vertical zonation of low, mid and high marsh habitat.

The computer models used in this study are finite element types. The tidal hydraulics model is the research model, *TIDE_FEM*, [Inman & Jenkins, 1996] and the littoral transport model is TIDE_FEM/SEDXPORT**.** TIDE_FEM was built from some well-studied and proven computational methods and numerical architecture that have done well in predicting shallow water tidal propagation in numerous bays, estuaries and lagoons. Five independent peer review episodes of TIDE_FEM/SEDXPORT have been conducted by 9 independent experts and can be found in the public records of the State Water Resources Control Board, the California Coastal Commission and the City of Huntington Beach.

San Dieguito Lagoon: The study begins in Section 3 with a hydrodynamic evaluation of potential tidal exchange effects from widening the I-5 Bridge at San Dieguito Lagoon; and the potential mitigation credits that may be derived for the North Coast Corridor Project by constructing a new tidal basin east of the I-5 Bridge referred to as Basin W-19. The I-5 Bridge over the tidal/river channel of San Dieguito Lagoon will not be replaced under the current plans for the North Coast Corridor Project; but rather will be widened in place using the existing span. We conclude that the effect of the W-19 tidal basin on tidal inundation overwhelms potential changes in the San Dieguito Lagoon system; and that no significant impact from bridge width changes can be found in the model results. Hydroperiod computations indicate that the habitat breaks of the lagoon system are not materially altered by the wider I-5 bridge. Regardless of whether the hydroperiod is calculated for the existing bridge or the widened bridge, we find that W-19 will create the following mix of wetland habitat: a) 4.84 acres of sub-tidal (fish) habitat; b) 5.09 acres of frequently flooded mud flat; c) 4.98 acres of frequently exposed mud flat; d) 12.24 acres of low salt marsh; e) 9.92 acres of mid salt marsh; f) 1.94 acres of high salt marsh; and, g) 0.24 acres of transitional habitat. This mix of habitat adds up to 39.25 acres of new wetlands habitat created by the W-19 basin at San Dieguito Lagoon. In considering patterns of tidal flow, water level, areas of tidal inundation and hydroperiod in total, it is concluded that the proposed widening of the I-5 bridge results in no significant changes to tidal exchange and habitat divisions relative to existing conditions in San Dieguito Lagoon. This finding was expected since neither the existing nor the widened I-5 bridges have any structural footprint (eg. support piles) located in the active tidal channel under the I-5 bridge. Due to the long bridge span at San Dieguito lagoon (209 m or 686 ft), both the existing and widened bridges are transparent to the tidal circulation.

The study proceeds to evaluate potential impacts to tidal circulation from replacement I-5 bridges at Batiquitos Lagoon in Section 4 and at Agua Hedionda Lagoon in Section 5. In both sections, tidal hydraulics of these lagoons are first evaluated in detail for existing conditions to establish a comparative baseline, and then re-evaluated for the proposed replacement bridges. The replacement bridges are wider and have a different structural footprint in the tidal channel under the bridge (bridge waterway) as compared to the existing bridges; with the replacement bridge at Batiquios Lagoon having double the number of piles as the existing bridge, while at Agua Hedionda Lagoon the replacement bridge has one-half the number of piles as the existing bridge. Evaluation of the existing and replacement bridge tidal hydraulics provides a comparative baseline for assessing potential wetland habitat gains and improvements from replacement bridges and bridge waterway alternatives.

The first generic class of alternatives that was considered is referred to as *soft-alternatives*, and involves reductions of fill and earth works along transportation crossings in order to increase the cross sectional area of the tidal channel under the bridges. This alternative is referred to herein as the "double-wide" alternative and involves the excavation of a wider tidal channel along the existing grade. It also requires doubling of the replacement bridge spans.

The second generic class of bridge waterways that were studied is based on fixed, hardened channels beneath the bridges whose geometries and dimensions are optimized for rigid boundary flow conditions. There are three basic types of these *hardened-alternatives* that were studied: 1) increasing the choke point channel cross section of the bridge waterway, referred to herein as the *Chang-channel* concept; 2) adding structural amendments to the present bridge waterway configurations that provide high hydrodynamic efficiency; referred to as *flow-fences*, and 3) a combination of Chang-channel geometry and flow fences.

Batiquitos Lagoon: Table ES-1 summarizes the habitat distributions in the east basin of Batiquitos Lagoon resolved from the hydrodynamic simulations for the existing and replacement bridge baselines, and compares them against the soft and hard replacement bridge waterway alternatives. Table ES-2 summarizes the net changes in habitat distributions arising from these replacement bridge waterway alternatives.

We find the proposed replacement bridge at Batiquitos Lagoon does have a minor effect on the tidal elevations, phase lags and hydroperiod function of the East Basin. Minimum (perpetual) sub-tidal area of the East Basin increases by 0.6 acres with the replacement bridge, to 91.9 acres vs 91.3 acres for the existing bridge; frequently flooded mud flat is

Table ES-1: East Basin Habitat Area Distribution for I-5 Bridge Alternatives at Batiquitos Lagoon.

East Basin Habitat Areas	Existing I-5 Bridge	Replacement I-5 Bridge	Replacement I-5 Bridge + Flow Fences	Double-Wide Alternative	Chang-Channel Alternative	Chang-Channel +Flow Fences
Perpetual Sub-Tidal (acres)	91.3	91.9	87.3	73.4	78.2	71.8
Mean Sub-Tidal (acres)	111.3	111.3	107.4	97.7	99.9	96.5
Frequently Flooded Mud Flat (acres)	58.6	58.1	53.8	64.5	63.2	65.7
Frequently Exposed Mud Flat (acres)	13.6	9.6	16.6	20.6	16.6	20.6
Low Salt Marsh (acres)	42.3	50.9	40.0	40.1	36.9	42.3
Mid Salt Marsh (acres)	77.0	77.2	76.5	84.4	79.7	79.1
High Salt Marsh (acres)	45.8	41.0	58.5	71.7	79.2	68.1
Transitional Habitat (acres)	30.2	30.2	26.2	5.5	5.5	11.7
Maximum Intertidal Area (acres)	267.6	267.0	271.6	286.8	281.1	287.6
Maximum Area of Salt Water Inundation (acres)	358.9	358.9	358.9	360.2	359.3	359.4
Mean Intertidal Area (acres)	191.4	191.4	196.6	210.6	207.6	211.2
Mean Area of Salt Water Inundation (acres)	302.7	302.7	304.0	308.3	307.5	307.7

Table ES-2: Net Change of East Basin Habitat Areas Resulting from I-5 Bridge Alternatives at Batiquitos Lagoon.

Changes in East Basin Habitat Areas	Replacement I-5 Bridge	Replacement I-5 Bridge + Flow Fences	Double-Wide Alternative	Chang-Channel Alternative	Chang-Channel +Flow Fences
Perpetual Sub-Tidal (acres)	0.6	-4.0	-17.9	-13.1	-19.5
Mean Sub-Tidal (acres)	0.0	-3.9	-13.6	-11.4	-14.8
Frequently Flooded Mud Flat (acres)	-0.5	-4.8	5.9	4.6	7.1
Frequently Exposed Mud Flat (acres)	-4.0	3.0	7.0	3.0	7.0
Low Salt Marsh (acres)	8.6	-2.3	-2.2	-5.4	0.0
Mid Salt Marsh (acres)	0.2	-0.5	7.4	2.7	2.1
High Salt Marsh (acres)	-4.8	12.7	25.9	33.4	22.3
Transitional Habitat (acres)	0.0	-4.0	-24.7	-24.7	-18.5
Maximum Intertidal Area (acres)	-0.6	4.0	19.2	13.5	20.0
Maximum Area of Salt Water Inundation (acres)	0.0	0.0	1.3	0.4	0.5
Mean Intertidal Area (acres)	0.0	5.2	19.2	16.2	19.8
Mean Area of Salt Water Inundation (acres)	0.0	1.3	5.6	4.8	5.0

reduced by 0.5 acres, from 58.6 acres for the existing bridge to 58.1 acres for the replacement bridge; frequently exposed mud flat is reduced by 4.0 acres, from 13.6 acres for the existing bridge to 9.6 acres for the replacement bridge; low salt marsh is increased by 8.6 acres, from 42.3 acres for the existing bridge to 50.9 acres for the replacement bridge; mid salt marsh is relatively unchanged, increasing by only 0.2 acres, from 77.0 acres for the existing bridge to 77.2 acres for the replacement bridge; high salt marsh is reduced by 4.8 acres, from 45.8 acres for the existing bridge to 41.0 acres for the replacement bridge; transitional habitat is unchanged at 30.2 acres. Because the maximum area inundated by salt water at extreme high water is unchanged at 358.9, the maximum intertidal habitat is reduced by only 0.6 with the replacement bridge; and the mean area experiencing tidal inundation up to MHHW is unchanged at 302.7 acres with an average of 191.4 acres of intertidal habit, and a mean sub-tidal habitat of 111.3 acres for both existing and replacement bridges. Therefore, the small deviations in the distributions of areas among intertidal habitat types are not considered as being a significant impact of the replacement bridge since the aggregate totals of habitat and their split between intertidal and sub-tidal remain essentially unchanged. The small deviations in intertidal habitat splits are likely due to the turbulence and drag effects associated with the increase in numbers of piles on the replacement bridge. Maximum intertidal habitat is increased by 18.6 acres with the double-wide alternative.

The addition of the *flow fence retrofit* to the replacement bridge would have negligible footprint over existing lagoon habitat, as it is envisioned as being constructed from vertical inter-locking sheet pile members driven into the lagoon and existing bridge waterway along a hydrodynamic efficient arc computed from Stratford turbulent pressure recovery relations. It would be constructed in phases, with the sheet piles driven immediately after the removal of sections of the existing bridge and prior to the construction of the replacement sections. It has been sized to adapt to the + 4 ft MLLW contours of the existing channel under the I-5 bridge, maintaining the existing channel bed at -3 ft MLLW. Generally, we find that the flow fence retrofit to the replacement bridge will create small amounts of new East Basin habitat with small reduction of the compression of present intertidal habitat. The flow fence retrofit to the proposed replacement bridge produces an average of 196.6 intertidal acres in the East Basin, or a net gain of 5.2 intertidal acres over existing conditions. Most of this gain has resulted from conversion of sub-tidal to intertidal habitat, as the mean area of tidal inundation in the East Basin has increased by only 1.3 acres over existing conditions. Maximum intertidal habitat is increased by 4.0 acres to 271.6 acres with the flow fence retrofit, as compared to 267.6 acres for existing conditions. These benefits are modest by comparison to what was achieved by expanding the bridge waterway channel cross section with the double-wide or Chang-channel alternatives.

To remediate tidal muting effects of the narrow bridge waterway at the Batiquitos Lagoon I-5 bridge, we first pose the *double-wide* alternative that would require removal of a portion of the road bed fill to accommodate doubling the width of the tidal channel along the existing grade of the south bank and increasing the span of the replacement bridge from 246 ft (78 m) to 492 ft (156 m). Doubling of the span also places two additional rows of 12 piles each in the active transport region of the channel, but increases channel cross section two-fold. Channel width increases effect only the south bank because the I-5 grades upward to higher ground toward the north (requiring more fill and longer bridge spans if the channel were widened in that direction), and grades downward toward the south. Also, most of the vegetation around the bridge footings and road bed on the south side of the channel appears to be ruderal. The double-wide concept retains the hard channel bottom feature at -3 ft MLLW.

The reductions in flow speeds and phase lags due to the double-wide waterway alternative results in more complete conversion of velocity into potential energy of water elevation, thereby increasing the tidal range in the east basin of Batiquitos Lagoon. MHHW in the East Basin has been raised to +6.2 ft MLLW with the double-wide alternative, while MLLW in the East Basin has been lowered to +1.1 ft MLLW, producing a mean diurnal tidal range of 5.1 ft, an increase of 0.6 ft over existing conditions. The double-wide channel eliminates nearly all tidal muting due to the I-5 choke point, but some tidal muting still remains in the system from the seaward choke points at the railroad and PCH bridges. Regardless, substantial habitat gains and improvements are achieved in the East Basin. Maximum intertidal habitat is increased by 19.2 acres to 286.8 acres with the double-wide alternative as compared to 267.6 acres for existing conditions; and the mean area experiencing tidal inundation up to MHHW is increased by 5.6 acres from 302.7 acres for the existing bridge to 308.3 acres for the double-wide alternative, resulting in an average 210.6 acres of intertidal habit, an increase of 19.2 acres over existing conditions. The double-wide channel will create 12.9 acres of new mud flats and increase the exposure time of existing mud flats; a benefit to shorebird foraging and a feature of the East Basin that has been lacking to some degree. It will also reduce the compression of present intertidal habitat by lowering the zonation of low, mid, and high marsh vegetation allowing for some expansion of the cordgrass currently in the lagoon and providing some improved habitat for clapper rail. The new hydroperiod function promoted by the double-wide alternative brings the functionality of the east basin of Batiquitos Lagoon in closer alignment with its original restoration goals.

Under existing conditions, depth constrictions under the railroad bridge are the leading order cause of limited ebb tide drainage out of the central basin of Batiquitos Lagoon,

which in turn limits further drainage from the East Basin, even with the double-wide channel improvements in place. About 76% of the tidal muting of the east basin of Batiquitos Lagoon is attributable to the combination of choke points at the PCH and railroad bridges. Attempts to relieve these choke points through application of a double-wide type of concept would be problematic, and attempts to eliminate them altogether are probably infeasible. The depth of the channel under the railroad bridge is hardened at only -3 ft to -4 ft MLLW. Removal of fill at the rail road bridge to widen the channel would have constraints with respect to fill disposal and removal of large stone, as the bed fill is armored by rip rap and could have contaminant issues. Attempts to convert the footprint of this fill into functioning wetland would suffer degradation from shading. The remaining constriction at the ocean inlet is due to the West Basin inlet bar, which in turn, is a consequence of failure to perform timely and adequate maintenance dredging. Attempts to recover the footprint of the PCH road bed fill for restorative improvement would make the entire West Basin vulnerable to sand infilling by wave overtopping of the beach berm, as the PCH road bed fill functions as a sea wall to protect the West Basin of the lagoon. In spite of these concerns, if the constrictions at the railroad bridge, the West Basin inlet bar, and the PCH bridge were remediated, the double-wide alternative for the I-5 bridge would function optimally as it was sized to convey the entire potential tidal prism of the East Basin.

The *Chang-channel* alternative would require removal of a smaller portion of the road bed fill than the double-wide alternative, and would not require doubling the span of the replacement, thereby providing a significant cost advantage. Channel width increases associated with the *Chang-channel* alternative are symmetric with respect to existing conditions, but the channel is deepened from -3 ft MLLW to -4.7 ft MLLW. While the double-wide alternative provided a 100% increase in channel cross section over existing conditions, the *Chang-channel* alternative provides an 80% increase. Maximum intertidal habitat is increased by 13.5 acres to 281.1 acres with the Chang-channel alternative as compared to 267.6 acres for existing conditions; and the mean area experiencing tidal inundation up to MHHW is increased by 4.8 acres from 302.7 acres for the existing bridge to 307.5 acres for the Chang-channel alternative, resulting in an average 207.6 acres of intertidal habit, an increase of 16.2 acres over existing conditions. The Chang-channel will create 7.6 acres of new mud flats and increase the exposure time of existing mud flats. Although this gain is slightly less than achieved by the double-wide alternative, it is, none the less, still a benefit to shorebird foraging.

Combining the Stratford flow fences with the Chang-channel produces tidal inundation in the east basin of Batiquitos Lagoon that is roughly comparable in hydraulic performance to the double-wide alternative without the added cost of doubling the span of the

replacement bridge. The Chang-channel + flow fences alternative will create 14.1 acres of new mud flats (1.3 acres more than the double-wide alternative). Maximum intertidal habitat is increased by 20.0 acres to 287.6 acres with the Chang-channel + flow fences alternative as compared to 267.6 acres for existing conditions and 286.8 acres for the double-wide alternative; and the mean area experiencing tidal inundation up to MHHW is increased by 5.0 acres from 302.7 acres for the existing bridge to 307.7 acres for the Chang-channel + flow fences alternative, resulting in an average 211.2 acres of intertidal habit, an increase of 19.8 acres over existing conditions.

Agua Hedionda Lagoon: The utilization of lagoon water for once-through cooling by the Encina Power Station renders Agua Hedionda's hydraulics distinctly different from any other natural tidal lagoon. Power plant cooling water uptake acts as a kind of "negative river." Whereas natural lagoons have a river or stream adding water to the lagoon, causing a net outflow at the ocean inlet, the power plant infall removes water from Agua Hedionda Lagoon, resulting in a net inflow of water through the ocean inlet. This net inflow has several consequences for sediment transport into and out of the lagoon: 1) it draws nutritive particulate and suspended sediment from the surf zone into the lagoon, the latter forming bars and shoals that subsequently restrict the tidal circulation, and 2) the net inflow of water diminishes or at times cancels the ebb flow velocities out of the inlet, and provides an artificial suction head on the Central and East Basins that helps to drain those water bodies on ebbing tide. Therefore, the plant demand for lagoon water strongly controls the tidal circulation of the lagoon.

Remarkably little tidal muting occurs under existing conditions at Agua Hedionda Lagoon, despite the fact that on average nearly the same mean tidal prism is exchanged with the ocean as at Batiquitos Lagoon, where East Basin tidal muting and phase lags are four to six times greater. This difference is attributable to the controlling effects of the power plant whose suction induced horsepower from its seawater circulation pumps acts as an "iron lung" in helping the east basin of Agua Hedionda to more effectively drain on ebbing tide. This reduces the opportunity to achieve habitat gains and expansion of the intertidal zone with more efficient I-5 bridge waterway alternatives at Agua Hedionda Lagoon. The other limiting aspect for achieving significant habitat gains at Agua Hedionda Lagoon is that these bridge waterway alternatives essentially work only on the intertidal zone by improving tidal exchange. However, that habitat type makes up only a minor fraction of the existing East Basin habitat, 77% of which is sub-tidal based on mean ranges of tidal inundation.

Table ES-3 summarizes the habitat distributions in the east basin of Agua Hedionda Lagoon resolved from the hydrodynamic simulations for the existing and replacement

bridge baselines, and compares them against the soft and hard replacement bridge waterway alternatives. In the simulations of these alternatives, power plant flow rates were set at 304 mgd, the expected future consumption rate for the Carlsbad Desalination Project that is expected to take over operations of the Encina sea water circulation system once Cabrillo Power LLC repowers the generating facility using air cooling systems. Table ES-4 summarizes the net changes in habitat distributions arising from these replacement bridge waterway alternatives. Comparing Table ES-4 with Table ES-2, it is apparent how limited the habitat gains and improvements at Agua Hedionda Lagoon are in comparison to those achieved at Batiquitos Lagoon using the same soft and hard bridge waterway alternatives.

Table ES-3 indicates that the slight reductions of East Basin tidal muting achieved by the Agua Hedionda replacement bride (as a consequence of a significant number of piles in the bridge waterway channel), will slightly expand the intertidal habitat zonation and increase the exposure of mud flats to a small degree, while making a small reduction in the sub-tidal habitat. Table ES-3 shows that the minimum (perpetual) sub-tidal area of the East Basin decreases by 1.1 acres with the replacement bridge, to 179.0 acres vs 180.1 acres for the existing bridge; the areas of frequently flooded mud flats remain unchanged at 30.3 acres; while frequently exposed mud flats are increased by 1.2 acres, from 4.3 acres for the existing bridge to 5.5 acres for the replacement bridge; low salt marsh remain unchanged at 11.5 acres; mid salt marsh increases by 1.4 acres, from 20.0 acres for the existing bridge to 21.4 acres for the replacement bridge; high salt marsh is reduced by 1.4 acres, from 11.7 acres for the existing bridge to 10.3 acres for the replacement bridge; and transitional habitat is unchanged at 8.1 acres. The maximum area inundated by salt water at extreme high water is unchanged at 266.0, but the maximum the intertidal habitat is increased by 1.1 acres with the replacement bridge; and the mean area experiencing tidal inundation up to MHHW is increased slightly from 250.8 acres for the existing bridge to 251.0 acres with an average 60.0 acres of intertidal habit (an increase of 0.2 acres over existing conditions), while the mean sub-tidal habitat remains unchanged at 191 acres for both the existing bridge and the replacement bridge. These deviations in the distributions of areas among sub-tidal and intertidal habitat types are less than what replacement bridges caused at Batiquitos, because the preponderance of habitat at Agua Hedionda is one type, namely, sub-tidal. These small changes of a couple of acres or less are not considered as being a significant impact of the replacement bridge since the aggregate totals of habitat and their split between intertidal and sub-tidal remain essentially unchanged. The small deviations in intertidal habitat splits in Table ES-3 are likely due to reductions in turbulence and drag effects associated with fewer numbers of piles in the waterway channel of the replacement bridge.

Table ES-3: East Basin Habitat Area Distribution for I-5 Bridge Alternatives at Agua Hedionda Lagoon.

East Basin Habitat Areas	Existing I-5 Bridge	Replacement I-5 Bridge	Replacement I-5 Bridge + Flow Fences	Double-Wide Alternative	Chang-Channel Alternative	Chang-Channel +Flow Fences
Perpetual Sub-Tidal (acres)	180.1	179.0	178.9	178.6	179.0	178.1
Mean Sub-Tidal (acres)	191.0	191.0	190.8	191.0	190.9	190.7
Frequently Flooded Mud Flat (acres)	30.3	30.3	27.8	30.6	26.2	30.6
Frequently Exposed Mud Flat (acres)	4.3	5.5	5.7	6.5	7.4	6.5
Low Salt Marsh (acres)	11.5	11.5	13.1	12.7	13.1	12.6
Mid Salt Marsh (acres)	20.0	21.4	20.9	21.6	22.2	20.3
High Salt Marsh (acres)	11.7	10.3	14.5	14.9	16.0	15.1
Transitional Habitat (acres)	8.1	8.1	5.1	2.4	2.4	3.2
Maximum Intertidal Area (acres)	85.9	87.0	87.1	88.7	87.3	88.4
Maximum Area of Salt Water Inundation (acres)	266.0	266.0	266.0	267.3	266.3	266.5
Mean Intertidal Area (acres)	59.8	60.0	60.3	61.8	60.6	61.3
Mean Area of Salt Water Inundation (acres)	250.8	251.0	251.1	252.8	251.5	252.0

Table ES-4: Net Change of East Basin Habitat Areas Resulting from I-5 Bridge Alternatives at Agua Hedionda Lagoon.

Changes in East Basin Habitat Areas	Replacement I-5 Bridge	Replacement I-5 Bridge + Flow Fences	Double-Wide Alternative	Chang-Channel Alternative	Chang-Channel +Flow Fences
Perpetual Sub-Tidal (acres)	-1.1	-1.2	-1.5	-1.1	-2.0
Mean Sub-Tidal (acres)	0	-0.2	0.0	-0.1	-0.3
Frequently Flooded Mud Flat (acres)	0	-2.5	0.3	-4.1	0.3
Frequently Exposed Mud Flat (acres)	1.2	1.4	2.2	3.1	2.2
Low Salt Marsh (acres)	0	1.6	1.2	1.6	1.1
Mid Salt Marsh (acres)	1.4	0.9	1.6	2.2	0.3
High Salt Marsh (acres)	-1.4	2.8	3.2	4.3	3.4
Transitional Habitat (acres)	0	-3	-5.7	-5.7	-4.9
Maximum Intertidal Area (acres)	1.1	1.2	2.8	1.4	2.5
Maximum Area of Salt Water Inundation (acres)	0	0	1.3	0.3	0.5
Mean Intertidal Area (acres)	0.2	0.5	2.0	0.8	1.5
Mean Area of Salt Water Inundation (acres)	0.2	0.3	2.0	0.7	1.2

The addition of *flow fence retrofit* to the replacement bridge at Agua Hedionda Lagoon would also have a negligible footprint on existing lagoon habitat, as it is envisioned as being constructed from vertical inter-locking sheet pile members driven into the lagoon and existing bridge waterway along a hydrodynamic efficient arc computed from Stratford turbulent pressure recovery relations. It has been sized to adapt to the + 4 ft MLLW contours of the existing channel under the I-5 bridge with a bed width of 113 ft (Figure 68b) comprised of rip rap at a depth of -19.22 ft MLLW (-21.52 ft NGVD) with sediment fill to a depth of -5 ft MLLW (-7.3 ft NGVD). Despite noticeable changes in the hydroperiod function with the flow fence waterway, those changes do not map into appreciable changes in habitat areas when factored against the stage area function in of the East Basin. This is due to the fact that the preponderance of the East Basin habitat is sub-tidal, while the more significant changes in the hydroperiod function involve the intertidal habitat that comprises a relatively minor constituent. Altogether, net habitat gains and conversions to higher quality intertidal habitats are meager with the flow fence waterway retrofit. Maximum intertidal habitat is increased by 1.2 acres to 87.1 acres with the flow fence waterway retrofit as compared to 85.9 acres for existing conditions; while the mean area experiencing tidal inundation up to MHHW is increased by only 0.3 acres from 250.8 acres for the existing bridge to 251.1 acres for the flow fence waterway retrofit resulting in an average 60.3 acres of intertidal habit, an increase of 0.5 acres over existing conditions.

The *double-wide* bridge waterway alternative that gave significant gains in habitat amount and quality at Batiquitos Lagoon was also tested at Agua Hedionda Lagoon. Here the double-wide alternative would require removal of a portion of the road bed fill to accommodate doubling the width of the tidal channel along the existing grade of the north bank and increasing the span of the replacement bridge from 230 ft (70.1 m) to 460 ft (140.2 m). Doubling of the span also places two additional rows of 16 piles each in the active transport region of the channel, but increases channel cross sectional two-fold. Channel width increases effect only the north bank because the present tidal channel runs along the south bank of the Central Basin, and there is no free basin space to expand the channel to the south. Due to buried infrastructure concerns, the double-wide concept retains the hard channel bottom feature at -19.22 ft MLLW (-21.52 ft NGVD) with sediment fill at -5 ft MLLW (-7.3 ft NGVD).

The reductions in flow speeds and phase lags due to the double-wide waterway alternative results in more complete conversion of velocity head into potential energy of water elevation, thereby increasing the tidal range in the east basin of Agua Hedionda Lagoon. We find that both the mean and maximum diurnal tidal ranges in the East Basin

are slightly increased with the double-wide alternative. MHHW in the East Basin has been raised to +6.13 ft MLLW with the double-wide alternative, while MLLW in the East Basin has been lowered to +0.55 ft MLLW, producing a mean diurnal tidal range of 5.58 ft, an increase of 0.16 ft over existing conditions. While extreme high water levels in the East Basin remain unchanged with the double-wide alternative, extreme low water levels are lowered to -0.91 ft MLLW, resulting in a maximum tidal range of 8.51 ft, an increase of 0.25 ft over existing conditions. With these increases in maximum and mean tidal ranges came small increases in intertidal habitat. Maximum intertidal habitat is increased by 2.8 acres to 88.7 acres with the double-wide alternative as compared to 85.9 acres for existing conditions; while the mean area experiencing tidal inundation up to MHHW is increased by 2.0 acres from 250.8 acres for the existing bridge to 252.8 acres for the double-wide alternative resulting in an average 61.8 acres of intertidal habit, an increase of 2.0 acres over existing conditions. The double-wide channel will create 2.5 acres of new mud flats in the east basin of Agua Hedionda Lagoon and increase the exposure time of existing mud flats. These gains are about eight to nine times smaller than the gains achieved with the double-wide alternative at Batiquitos Lagoon. Because of the "iron-lung" effect that the power plant exerts on tidal ventilation of the east basin of Agua Hedionda, it is difficult to achieve substantial habitat gains or conversions through improved bridge designs, even one involving rather significant removal of I-5 road bed fill such as the double-wide alternative.

Implementing the *Chang-channel* alternative at Agua Hedionda Lagoon would also require removal of a smaller portion of the road bed fill than the double-wide alternative, and would not require doubling the span of the replacement, again providing a significant cost advantage. Channel width increases associated with the *Chang-channel* alternative increase the bed width of the hard bottom channel to 99.1 ft while maintaining the existing depth of the hard bottom channel at -19.22 ft MLLW (-21.52 ft NGVD) along 1 on 1 side slopes**.** While the double-wide alternative increases the channel cross section by a factor of 2 over existing conditions, the *Chang-channel* alternative provides an increase by a factor of 1.4. Maximum intertidal habitat is increased by 1.4 acres to 87.3 acres with the Chang-channel alternative as compared to 85.9 acres for existing conditions; while the mean area experiencing tidal inundation up to MHHW is increased by only 0.7 acres from 250.8 acres for the existing bridge to 251.5 acres for the Chang-channel alternative resulting in an average 60.6 acres of intertidal habit, an increase of 0.8 acres over existing conditions. The Chang-channel will result in the loss of 1.0 acres of new mud flats but increase the exposure time of existing mud flats; a bit of a wash in terms of net benefit to foraging birds. Of the 0.8 acres of intertidal area created on average by the Chang-channel alternative, 0.7 acres represents net wetland habitat gain. Again, the "iron-lung" effect that the power plant exerts on tidal ventilation of the East Basin makes it difficult

to achieve substantial habitat gains or conversions through by removal of I-5 road bed fill as attempted with the Chang-channel alternative.

Combining the Stratford flow fences with the Chang-channel produces tidal inundation in the east basin of Agua Hedionda Lagoon that is slightly better in hydraulic performance than the double-wide alternative without the added cost of doubling the span of the replacement bridge. It has been sized to adapt to the Chang-channel +4 ft MLLW contours under the I-5 bridge using a bed width of 156 ft comprised of rip rap at a depth of -19.22 ft MLLW (-21.52 ft NGVD) with sediment fill to a depth of -5 ft MLLW (-7.3 ft NGVD), and provides 80% more channel cross section than the existing bridge. The Chang-channel + flow fences alternative will increase the maximum intertidal habitat by 2.5 acres to 88.4 acres with the Chang-channel + flow fences alternative as compared to 85.9 acres for existing conditions; while the mean area experiencing tidal inundation up to MHHW is increased by only 1.2 acres from 250.8 acres for the existing bridge to 252.0 acres for the Chang-channel + flow fences alternative resulting in an average 61.3 acres of intertidal habit, an increase of 1.5 acres over existing conditions. The Chang-channel + flow fences will create 2.5 acres of new mud flats and increase the exposure time of existing mud flats. Of the 1.5 acres of intertidal area created on average by the Chang-channel + flow fences alternative, 1.2 acres represents net wetland habitat gain. The “iron-lung” effect that the power plant exerts on lagoon tidal exchange and the preponderance of East Basin area that is comprised of sub-tidal habitat make substantial habitat gains or conversions through improved bridge designs difficult to attain, even one involving rather significant structural amendments to bridge under-works as the Chang-channel + flow fences alternative.

Sea level Rise Effects: The mean of six climate model predictions calls for 0.41 m (1.33 ft) of sea level rise by 2100, while the most aggressive prediction calls for that amount of sea level rise by 2050. This predicted sea level rise was linearly combined with the historic ocean water level record and used to drive the tidal hydraulics model and thereby resolve the potential effects on tidal exchange and habitat mix for replacement bridges and the Chang Channel + flow fences I-5 bridge alternative, both using existing bathymetric conditions. Although sea level rise will undoubtedly erode neighboring beaches, we did not attempt to quantify beach impacts on the lagoon bathymetry and tidal hydraulics due to the numerous assumptions that must be made on future beach sand supplies in such an analysis. We chose the Chang Channel + flow fences alternative to make comparisons against the proposed replacement bridges because it was generally found to be the most cost effective of the alternatives considered.

Batiquitos Lagoon: Sea level rise effects on the east basin of Batiquitos Lagoon are summarized in Table ES-5. Despite the 0.41 m (1.33 ft.) increase in elevations of salt water inundation at future sea levels, the maximum area inundated by salt water at extreme high water is increased by only 9.2 acres, from 358.9 acres for the replacement bridge at present sea level to 368.1 acres at future sea level. While the sub-tidal and mud flat habitats increase significantly at future sea levels, maximum the intertidal habitat is reduced by 30.3 acres, from 267.0 acres for the replacement bridge at present sea level to 236.7 acres at future sea level with the replacement bridge. The mean area experiencing tidal inundation up to MHHW at future sea level is substantially increased by 51.6 acres to 354.3 acres from 302.7 acres at present sea level with the replacement bridge; but this increase is primarily sub-tidal in nature as the mean intertidal habit increases by only 5.6 acres to 197.0 with replacement bridge at future sea level versus 191.4 acres at present sea levels. The increase in mean sub-tidal area at future sea level is 46 acres, from 111.3 acres at present sea level to 157.3 acres at future sea level.

Inspection of Table ES-5 reveals that even at higher sea levels, the Chang-channel + flow fences alternative delivers benefits over the replacement bridges in terms of East Basin habitat gains and diversity. Maximum intertidal habitat is increased by 27.1 acres to 263.8 acres with the Chang-channel + flow fences alternative as compared to 236.7 acres for the replacement bridge at future sea level and 267.0 acres for the present sea level conditions. The mean area experiencing tidal inundation up to MHHW is increased by 2.7 acres from 354.3 acres for the replacement bridge at future sea level to 357.0 acres for the Chang-channel + flow fences alternative, 54.3 acres more than for present sea level and resulting in an average 219.8 acres of intertidal habit, an increase of 22.8 acres over the replacement bridge at future sea level and 28.4 acres more than at present sea level.

As expected, the general impact from sea level rise was found to be an increase in both the maximum and average areas of salt water inundation in the east basin of Batiquitos Lagoon, and this result held for both the proposed replacement bridge and the Chang-channel + flow fences alternative. However, these increases involved significant expansion in areas of sub-tidal habitat and mud flats while producing moderate reductions in low and mid salt marsh and significant reductions in high salt marsh habitat. The incremental increases in tidally inundated habitat in response to sea level rise were moderately greater for the Chang-channel + flow fences alternative than for the proposed replacement bridge. The unbalanced habitat shift away from salt marsh induced by sea level rise was less for the Chang-channel + flow fences alternative than for the proposed replacement bridge. The transitional habitat was nearly eliminated in the East Basin by sea level rise, with less than an acre remaining for both the proposed replacement bridge and the Chang-channel + flow fences alternative.

Table ES-5: Batiquitos East Basin Habitat Area Distribution from Hydroperiod & Stage Area Functions with Proposed Replacement Bridge vs Chang-channel + flow fences alternative with +0.41 m (1.33 ft) of Sea Level Rise

East Basin Habitat Areas	Replacement I-5 Bridge Present Sea Level	Replacement I-5 Bridge Future Sea Level	Chang-channel+flow fences Future Sea Level
Perpetual Sub-Tidal (acres)	91.9	131.4	108.2
Mean Sub-Tidal (acres)	111.3	157.3	137.2
Frequently Flooded Mud Flat (acres)	58.1	68.9	78.4
Frequently Exposed Mud Flat (acres)	9.6	21.9	29.0
Low Salt Marsh (acres)	50.9	47.6	48.3
Mid Salt Marsh (acres)	77.2	70.8	74.2
High Salt Marsh (acres)	41.0	26.9	30.2
Transitional Habitat (acres)	30.2	0.5	0.3
Maximum Intertidal Area (acres)	267.0	236.7	263.8
Maximum Area of Salt Water Inundation (acres)	358.9	368.1	368.6
Mean Intertidal Area (acres)	191.4	197.0	219.8
Mean Area of Salt Water Inundation (acres)	302.7	354.3	357.0

Other adverse consequences of sea level rise at Batiquitos Lagoon can be inferred from the tidal velocities predicted by the model. While the model assumes rigid boundaries and stationary, existing bathymetry, the flood tide currents at higher sea levels form jets and boundary streams that are significantly stronger than during spring tides at present sea level, and remain above the threshold of sediment motion the entire distance from the ocean inlet to the East Basin. Thus rapidly shoaling sand bars and localized scour and

erosion are likely to occur under future high sea levels in all three basins of Batiquitos Lagoon with either the proposed replacement bridges or with the Chang-channel + flow fences alternative.

Agua Hedionda Lagoon: Sea level rise effects on the east basin of Agua Hedionda Lagoon are summarized in Table ES-6. Despite 0.41 m (1.33 ft.) increases in elevations of salt water inundation at future sea levels, the maximum area inundated by salt water at extreme high water is increased by only 4.6 acres, from 266.0 acres for the replacement bridge at present sea level to 270.6 acres at future sea level. While the sub-tidal and mud flat habitats increase significantly at future sea levels, maximum the intertidal habitat is reduced by 6.7 acres, from 87.0 acres for the replacement bridge at present sea level to 80.3 acres at future sea level with the replacement bridge. The mean area experiencing tidal inundation up to MHHW at future sea level is increased by 13.6 acres to 264.6 acres from 251.0 acres at present sea level with the replacement bridge; but this increase is primarily sub-tidal in nature as the mean intertidal habit increases by only 1.7 acres to 61.7 acres with replacement bridge at future sea level versus 60.0 acres at present sea levels. The increase in mean sub-tidal area at future sea level is 11.9 acres, from 191.0 acres at present sea level to 202.9 acres at future sea level.

Inspection of Table ES-6 reveals that at higher sea levels, the Chang-channel + flow fences alternative delivers only minor benefits over the replacement bridges in terms of East Basin habitat gains and diversity. Little transitional habitat at higher sea levels because the upper limits of salt water inundation have nearly reached the day light contour of the upper limit of grading during the lagoon excavation in 1955. Maximum intertidal habitat is increased by 1.4 acres to 81.7 acres with the Chang-channel + flow fences alternative as compared to 80.3 acres for the replacement bridge at future sea level but 5.3 acres less than for the present sea level conditions. The mean area experiencing tidal inundation up to MHHW is increased by only 0.3 acres from 264.6 acres for the replacement bridge at future sea level to 264.9 acres for the Chang-channel + flow fences alternative, 13.9 acres more than for present sea level and resulting in an average 62.9 acres of intertidal habit, an increase of 1.2 acres over the replacement bridge at future sea level and 2.9 acres more than at present sea level. Therefore, the modest gains in intertidal habitat by the Chang-channel + flow fences alternative at present sea level are reduced to only meager gains at future sea levels.

In general, sea level rise effects in the east basin of Agua Hedionda are less pronounced than what was found for the east basin of Batiquitos Lagoon. Net gains in areas of tidal inundation are significantly less at Agua Hedionda, and losses of salt marsh habitat are also less. This is due to the differences in grading designs between the two lagoons. The

Table ES-6: Agua Hedionda East Basin Habitat Area Distribution from Hydroperiod & Stage Area Functions with Proposed Replacement Bridge vs Chang- channel + flow fences alternative with +0.41 m (1.33 ft) of Sea Level Rise

East Basin Habitat Areas	Replacement I-5 Bridge Present Sea Level	Replacement I-5 Bridge Future Sea Level	Chang-channel+flow fences Future Sea Level
Perpetual Sub-Tidal (acres)	179.0	190.3	189.4
Mean Sub-Tidal (acres)	191.0	202.9	202.0
Frequently Flooded Mud Flat (acres)	30.3	33.2	33.6
Frequently Exposed Mud Flat (acres)	5.5	7.1	4.9
Low Salt Marsh (acres)	11.5	12.3	13.4
Mid Salt Marsh (acres)	21.4	19.3	18.2
High Salt Marsh (acres)	10.3	6.5	8.2
Transitional Habitat (acres)	8.1	1.9	0.1
Maximum Intertidal Area (acres)	87.0	80.3	81.7
Maximum Area of Salt Water Inundation (acres)	266.0	270.6	271.1
Mean Intertidal Area (acres)	60.0	61.7	62.9
Mean Area of Salt Water Inundation (acres)	251.0	264.6	264.9

east basin of Batiquitos Lagoon was designed to be a wetland restoration with broad shallow sloping marsh plains in the upper intertidal zone, whereas Agua Hedionda Lagoon was designed to be a cooling water reservoir with predominant sub-tidal area and steep slopes in the upper intertidal zone. Consequently sea level rise impacts on salt marsh are substantially less at Agua Hedionda Lagoon because that lagoon was designed with substantially less of that habitat type. Sediment transport inferred from modeled tidal velocities indicate rapidly shoaling sand bars and localized scour and erosion are likely to occur under future high sea levels in all three basins of Agua Hedionda Lagoon with either the proposed replacement bridges or with the Chang-channel + flow fences alternative.

Hydrodynamic Approach to Wetland Restoration by Optimization of Bridge Waterways, by: Scott A. Jenkins, Ph. D., and Joseph Wasyl

1.0) Phase 2 Chronology:

The Technical Agreement # 11A1766 between CalTrans and UCSD was executed on 17 December, 2009, in accordance with scope of work under UCSD proposal # 20092713R6. This agreement will involve preparation of a supporting environmental study for the proposed Interstate 5 (I-5) North Coast Corridor Project that consists of tidal hydraulics model analysis of bridge widening and waterways concepts for Batiquitos, Agua Hedionda and San Dieguito Lagoons. This is the second quarterly progress report to be submitted to CalTrans, as required within three months of the date of execution of the agreement (see Section V, page 14 of Technical Agreement # 11A1766). Planning Meeting #1 (as required by Section V) was held 28 January 2010 at CalTrans District 11 headquarters. Materials to be supplied by CalTrans listed under Section 10 were not received in total until 1 February 2010, when the last CADD files of the I-5 corridor and widening alternatives were delivered via e-mail attachment. Additional updates to bathymetry at Agua Hedionda Lagoon were received 17 February 2010 when Sue Scatolini and Scott Jenkins met with NRG representatives at Encina Power Station.

At the 28 January 2010 planning meeting it was agreed that tidal hydraulics model analysis would begin with San Dieguito Lagoon. Here the I-5 bridge will not be re-built, but merely widened to accommodate the planned new lanes of the Interstate 5 North Coast Corridor Project. The objective of the tidal hydraulics model analysis at San Dieguito is to determine whether widening of the existing bridge would result in any adverse effects on tidal exchange in the newly completed San Dieguito Lagoon Restoration (the Edison Project) or future new tidal basins planned for the W-19 parcel east of I-5.

Upon completion of the San Dieguito analysis, it was contemplated at the 28 January 2010 planning meeting that analysis of a new bridge alternative at Agua Hedionda would be next in the work schedule. However, delays in securing an up-to-date set of bathymetry for Agua Hedionda Lagoon caused the analysis effort to proceed with evaluation of a new bridge alternative at Batiquitos Lagoon.

During the month of February, work was divided between the Batiquitos bridge analysis and building the necessary data bases for Agua Hedionda. Encina flow rate data sets were processed and delivered to Howard Chang, Mike Josselyn and Sue Scatolini on 24 February 2010, and bridge alternative analysis on a *double-wide* waterway concept at

Batiquitos Lagoon that involved removal of a portion of the exisiting road bed fill and doubling the span of the replacement bridge to provide a wider tidal channel with increased cross section and improved pressure recovery of velocity head. The tidal simulations and modified bathymetry of the double-wide alternative were delivered to Howard Chang and Sue Scatolini on 3 March 2010. Additional channel cross sections of the double-wide bridge waterway alternative were delivered to Howard Chang and Sue Scatolini on 11 March 2010. Howard Chang performed 100 yr flood plane analysis on the double-wide waterway at Batiquitos and concluded the alternative created no adverse flood impacts, and actually lowered the flood plane elevation east of I-5 and reduced scour immediately west of I-5. Chang's analysis was forwarded to Mike Josselyn and Scott Jenkins on 12 March 2010.

In April 2010 tidal hydraulics analysis of the existing and double-wide alternatives were performed on the replacement bridge for Agua Hedionda Lagoon. Then on 10 May 2010, Dr. Chang determined that the double-wide channel cross section could be accommodated under the existing bridge span at Batiquitos by using steeper channel slopes than the version_1 double-wide waterway alternative. We refer to this alternative as the "*Chang-channel*". It was subsequently studied in hydraulic simulations of replacement bridges at both Batiquitos and Agua Hedionda Lagoons. In addition to the double–wide and Chang-channel alternatives, flow fence alternatives were studied from late May to early July 2010 as retrofits to both the existing bridge waterways and the Chang-channel alternatives. These flow fences were configured from "incipient separation" pressure recovery algorithms designed to optimally convert velocity head into pressure recovery. Although not as effective on the existing channel cross sections at Batiquitos and Agua Hedionda Lagoons, the flow fences were found to provide a significant reduction in tidal muting when combined with the Chang-channel alternatives.

2.0) Hydrodynamic Model and Input Variables

The computer models used in this study are finite element types. The tidal hydraulics model is the research model, *TIDE_FEM*, [Inman & Jenkins, 1996] and the littoral transport model is TIDE_FEM/SEDXPORT**.** TIDE_FEM was built from some well-studied and proven computational methods and numerical architecture that have been successful in predicting shallow water tidal propagation in Massachusetts Bay [Connor & Wang, 1974] and estuaries in Rhode Island, [Wang, 1975], and have been reviewed in basic text books [Weiyan, 1992] and symposia on the subject, e.g., Gallagher (1981). A discussion of the physics of TIDE_FEM is given in Jenkins and Wasyl (2003 & 2005).

In its most recent version, the TIDE_FEM/TIDE_FEM/SEDXPORT modeling system has been integrated into the Navy's Coastal Water Clarity Model and the Littoral Remote Sensing Simulator (LRSS) (see Hammond, et al., 1995). The TIDE_FEM/SEDXPORT code has been validated in mid-to-inner shelf waters (see Hammond, et al., 1995; Schoonmaker, et al., 1994). Detailed description of the architecture and codes of the TIDE_FEM/SEDXPORT are given in Jenkins and Wasyl (1998a), Jenkins and Inman (1999), and Jenkins and Wasyl (2005) that is available on-line at the University of California digital library at:
http://repositories.cdlib.org/sio/techreport/58/.

Validation of the TIDE_FEM/SEDXPORT code was shown by three independent methods: 1) direct measurement of suspended particle transport and particle size distributions by means of a laser particle sizer; 2) measurements of water column optical properties; and, 3) comparison of computed stratified plume dispersion patterns with LANDSAT imagery. Besides being validated in coastal waters of Southern California, the TIDE_FEM/SEDXPORT modeling system has been extensively peer reviewed. Although some of the early peer review was confidential and occurred inside the Office of Naval Research and the Naval Research Laboratory, the following is a listing of 5 independent peer review episodes of TIDE_FEM/SEDXPORT that were conducted by 9 independent experts and can be found in the public records of the State Water Resources Control Board, the California Coastal Commission and the City of Huntington Beach.

1997- Reviewing Agency: State Water Resources Control Board
Project: NPDES 316 a/b Permit renewal, Scripps Beach, Carlsbad, CA
Reviewer: Dr. Andrew Lissner, SAIC, La Jolla, CA

1998- Reviewing Agency: California Coastal Commission
Project: Coastal Development Permit, San Dieguito Lagoon Restoration
Reviewers: Prof. Ashish Mehta, University of Florida, Gainesville;
Prof. Paul Komar, Oregon State University, Corvallis;
Prof. Peter Goodwin, University of Idaho, Moscow

2000- Reviewing Agency: California Coastal Commission
Project: Coastal Development Permit, Crystal Cove Development
Reviewers: Prof. Robert Wiegel, University of California, Berkeley;
Dr.Ron Noble, Noble Engineers, Irvine, CA

2002- Reviewing Agency: California Coastal Commission
Project: Coastal Development Permit, Dana Point Headland Reserve
Reviewers: Prof. Robert Wiegel, University of California, Berkeley;
Dr. Richard Seymour, University of California, San Diego

2003- Reviewing Agency: City of Huntington Beach
Project: EIR Certification, Poseidon Desalination Project
Reviewer: Prof. Stanley Grant, University of California, Irvine

Lagoon water levels and tidal currents are studied using numerical transport models that are run over a historic surrogate time period for which environmental forcing is well-known. A 30-year simulation time period, 1980-2010, was used to drive the model in the present analysis. This period was chosen because it represents the longest unbroken record for which there existed the simultaneous availability of a number of critical input data sets, in particular an unbroken verified ocean water level record. This time period is sufficiently long to characterize and capture the effects of climate variability, and contained a number of significant climate cycles, including the warm/wet El Niño events of 1980, 1983, 1993, 1995 and 1997, as well as the cool/dry La Niña events of 1986-88 and 2000-01. These climate events embedded in the 1980-2010 period of record assure that the hydrodynamic simulations were able to account for the effects of climate cycle extremes on ocean water levels and ultimately on tidal inundation of the lagoons.

In all such *boundary value problems* input variables are divided between two general classes, forcing functions and boundary conditions. The primary forcing function is ocean water level variation (Section 2.1.1), although Encina Power Station flow rates are a significant augmentation to forcing at Agua Hedionda Lagoon. The important boundary conditions are lagoon bathymetry, sediment grain size, dredge disposal volumes, watershed washload volumes, and bridge configurations. Input for ocean water level variations are discussed below in Section 2.1.1. The remaining variables are site specific and will be dealt with separately for San Dieguito Lagoon in Section 3.1.1, Batiquitos Lagoon in Section 4.1.1 and Agua Hedionda Lagoon in Sections 5.1.1.

2.1 Ocean Water Level Data and Sea Level Rise Predictions: The flow of sea water into and out of the lagoons is driven by the time variation in ocean water level. Ocean water level variations for the 1980-2010 simulation period were obtained from the nearest ocean tide gage station to the three lagoons, located at Scripps Pier, La Jolla, CA. This tide gage (NOAA #941-0230) was last leveled using the 1983-2001 tidal epoch. Elevations of tidal datums referenced to Mean Lower Low Water (MLLW), in METERS are as follows:

Table 1: Tidal Datums for Scripps Pier Tide Gage during 1983-2001 Epoch:

HIGHEST OBSERVED WATER LEVEL (11/13/1997) = 2.332 m
MEAN HIGHER HIGH WATER (MHHW) = 1.624 m
MEAN HIGH WATER (MHW) = 1.402 m
MEAN TIDE LEVEL (MTL) = 0.839 m
MEAN SEA LEVEL (MSL) = 0.833 m
MEAN LOW WATER (MLW) = 0.276 m
NORTH AMERICAN VERTICAL DATUM-1988 (NAVD) = 0.058 m
NGVD29 = 0.700 m
MEAN LOWER LOW WATER (MLLW) = 0.000 m
LOWEST OBSERVED WATER LEVEL (12/17/1933) = -0.874 m

The use of observations of historic ocean water levels in hydraulic modeling exercises requires reconstruction of the water level time series at time steps much shorter than the observation intervals (6 minutes to 1 hour). Due to the shallow water marsh plains of the lagoons, reconstruction of water level variations at 2 second time step intervals is necessary for achieving stable modeling simulations of the hydraulic response of the lagoon. The ocean water levels were reconstructed at 2 second time step intervals from astronomic tidal constituents for Scripps Pier using daily offsets to the astronomic tidal elevations to compensate for sea level anomalies (see Flick & Cayan, 1984) and achieve agreement with the daily high and low water elevations measured by the Scripps Pier tide gage. These daily offsets were obtained by a minimization of the mean squared error between the predicted and measured water level. The short time step reconstruction from tidal constituents with daily offsets was accomplished with the TID_DAYS program, detailed in Jenkins and Wasyl (2005).

It is interesting to note from Table 1 that mean sea level as determined by the 1983-2001 tidal epoch statistics has risen $\Delta\eta = 0.436$ ft above the level at which mean sea level was in 1929 when the National Geodetic Vertical Datum (NGVD) was established (where from Table 1: $\Delta\eta =$ MSL - NGVD29 = 0.833m – 0.700 m = 0.133m = 0.436 ft). This is due to the long-term upward creep in eustatic sea level during the last part of the modern sea level high stand. Global warming is believed to be a factor in this gradual rise of mean sea which has been estimated at 0.7 ft./100 yr. during the preceding 20th century. However, sea level rise rates are expected to accelerate in the 21st century. Figure 1 gives the envelope of variability in predicted sea level rise over the next century from six independent global climate models. The mean of these six predictions calls for 0.41 m

(16 in) of sea level rise by 2100, while the most aggressive prediction calls for that amount of sea level rise by 2050. We will apply the maximum and mean predicted rise functions to the tidal hydraulics model and resolve the potential effects on tidal exchange and habitat mix for both existing conditions and with the I-5 bridge modifications in place. While it is clear that sea level rise will have a favorable effect on tidal exchange, tidal prism, and area of salt water inundation within the wetland domains, it will definitely increase the percentage of sub-tidal habitat and have an adverse effect on beach widths in the neighborhood of the ocean inlets. The latter will likely increase the influx of littoral sediment into the wetland systems because transport into these systems will remain flood tide dominant at higher sea levels owing to the fact that the majority portion of the tidal prism will remain above the higher mean sea levels. We will quantify these impacts with the outputs from the TIDE_FEM numerical model over the range of predicted sea level rise as anticipated from Figure 1.

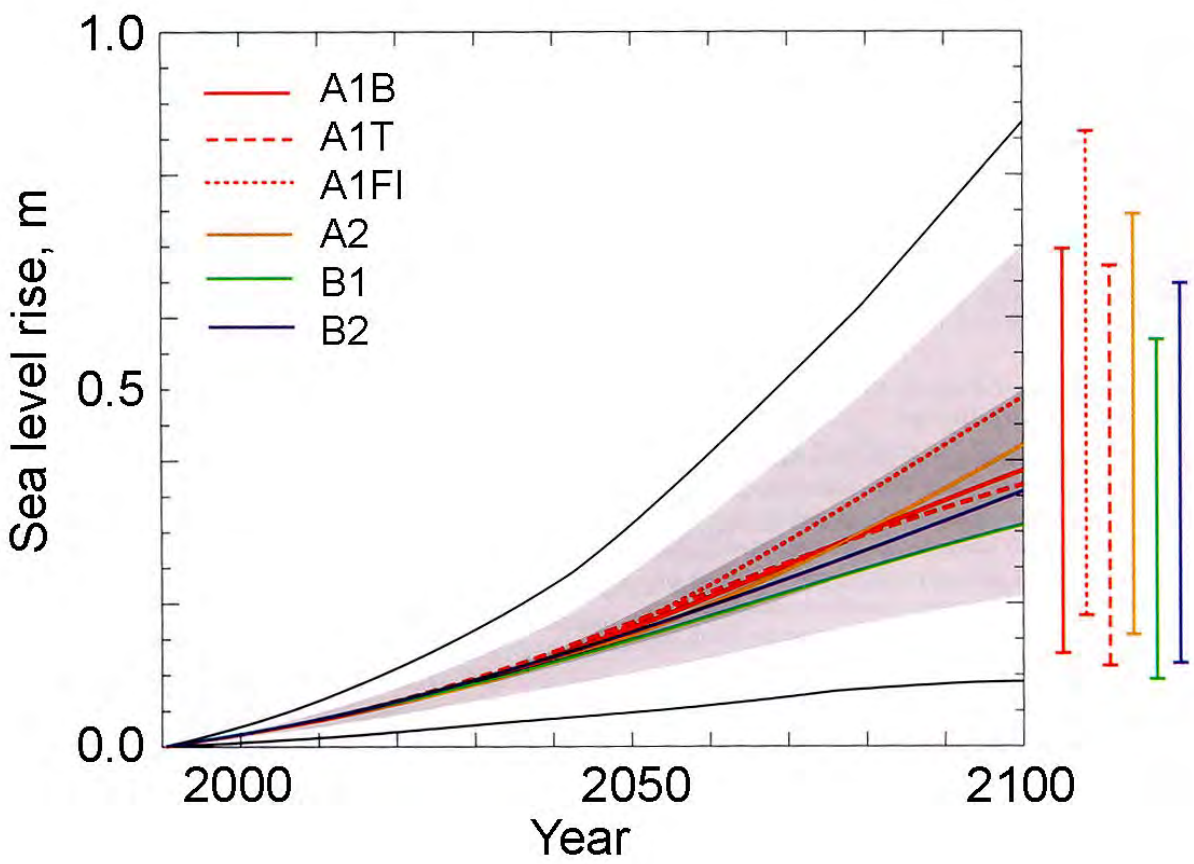

Figure 1: Range of sea level rise scenarios predicted out to year 2100 by six separate global climate models (from Houghton, 2004)

There are other factors which influence the mean sea level about which the astronomic tides oscillate. These factors are illustrated schematically in Figure 2. We begin on the right hand side where the astronomic tides are shown to generate tidal oscillations modulated in a spring-neap cycle about mean sea level. But mean sea level is not an invariant quantity, and as we have already mentioned, is creeping upward in an apparently accelerating rate from its historic rise of 0.7 ft per century as shown by the notation immediately to the left of the spring/neap astronomic oscillations in Figure 2. Further to the left in Figure 2 is the seasonal oscillation in mean sea level. Flick and Cayan (1984) have shown that seasonal warming and cooling accounts for an inter-annual variation in mean sea level of about 0.5 ft., as shown by the 1960-83 average of the monthly mean sea levels.

In addition to these seasonal anomalies, sea level anomalies are also produce by climate cycles such as ENSO. These climate cycles typically have 3-7 year periodicity, with El Niño events raising mean sea level by as much as 1-1.5 ft, and sustaining those higher sea levels for as long as 9 – 12 months at a time. Cool/dry La Niña events typically depress mean sea levels by about 0.5 ft and sustain such anomalies for comparable periods of time. When the astronomic tides oscillate around mean sea levels displaced by the aggregate effects of a number of differing sea level anomalies (Figure 2), the extreme higher high water levels (EHHW) of a Perigean Spring Tide (Wood, 1977) can be significantly greater than what would have been calculated from tidal constituents derived from the 1983-2001 tidal epoch. The most dramatic effects of these aggregate sea level anomalies produced the highest ever observed sea level in November 1997. Figure 3 shows that the 1997 El Niño produced more than a 1.47 ft. rise in mean sea level above the 1983-2001 datum in Table 1, due to the thermal expansion effects of the coastal warm water anomalies associated with this powerful El Niño and by the inverse barometer effects associated with the companion ENSO-induced North Pacific low pressure anomaly.

The **TID_DAYS** code in Jenkins and Wasyl (2005) was configured for 6 minute time step intervals to reconstruct the Scripps Pier tidal elevations for the 30-year period of 1980-2010. The record was searched for a two-day block having the maximum and minimum diurnal range and for another two-day block whose diurnal range most closely matches the 5.33 ft. range between the MHHW and MLLW of the 1983-2001 tidal epoch. Once these two-day blocks were identified at six minute time step intervals, they were subsequently reassembled in $\Delta t = 2$ sec. time step intervals to produce the tidal forcing functions, η_o used in the high resolution tidal circulation analysis of each lagoon. The spring tide range resulted from a higher-high water (HHW) of +4.26 ft. NGVD;

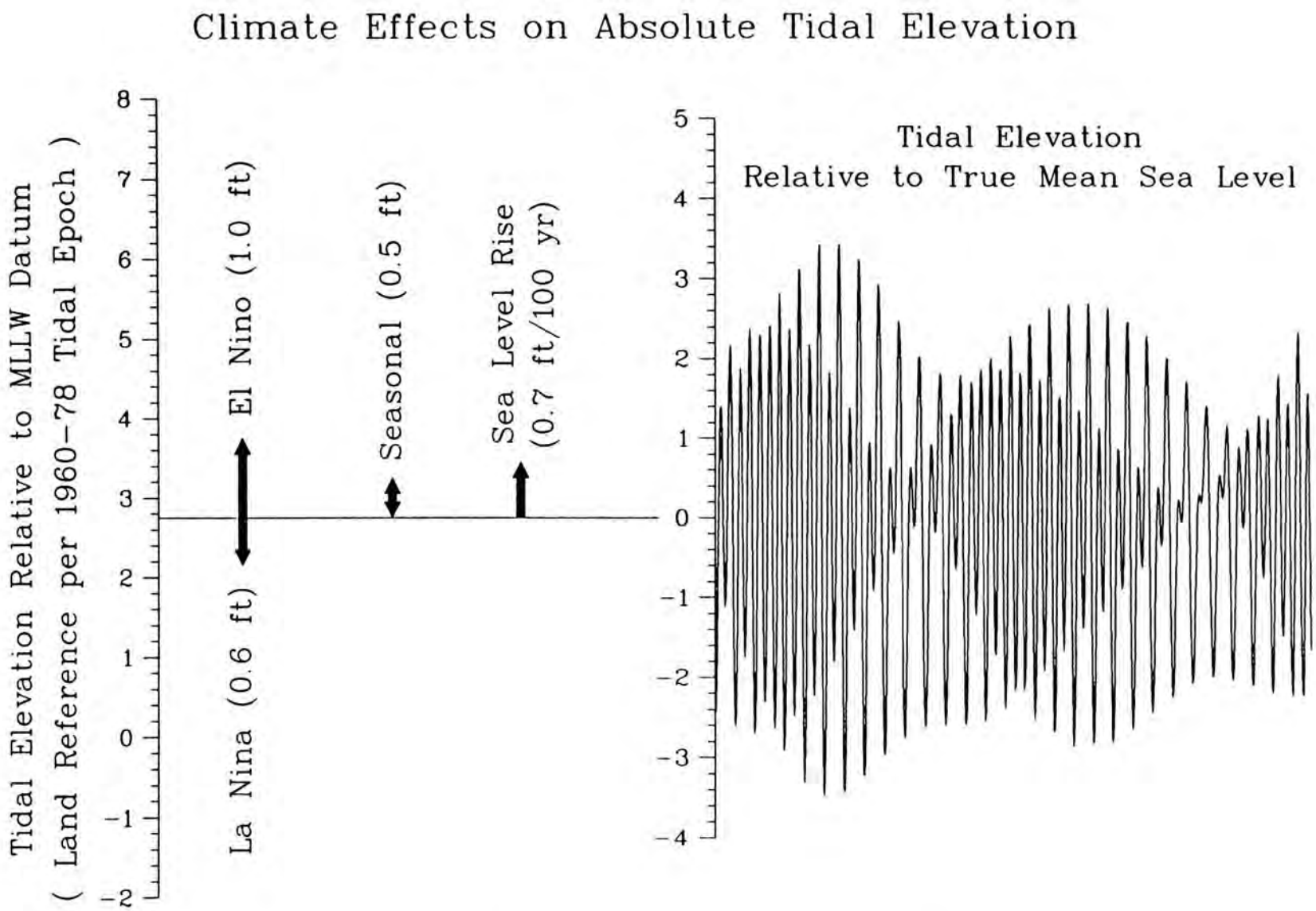

Figure 2. Seasonal and long-term climate effects on sea level and tidal elevations.

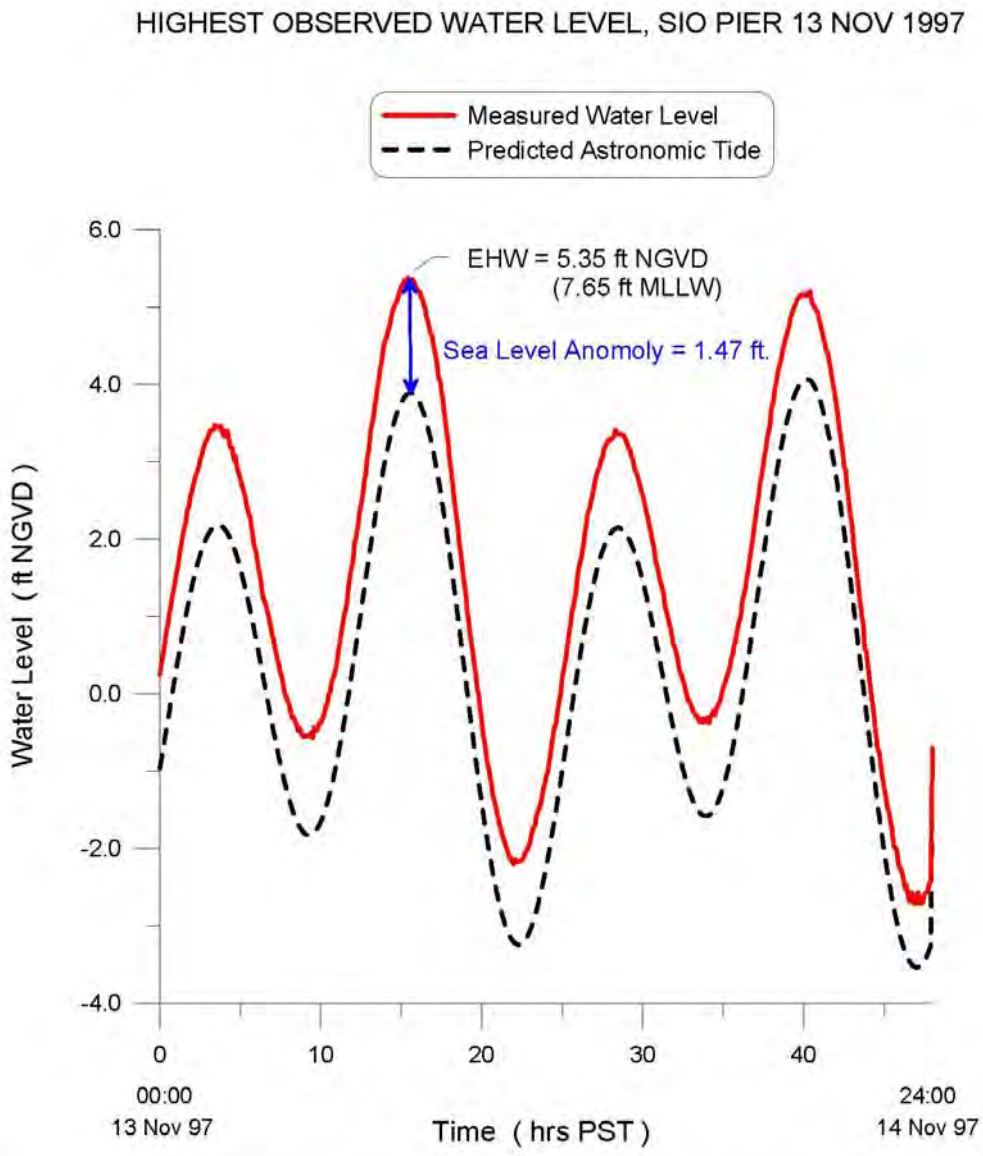

Figure 3: Comparison of measured ocean water level (red) at the Scripps Pier Tide gage vs predicted water level based on tidal constituents (black dashed) for the EHW event of 13 November 1997.

and an astronomic extreme lower-low water (LLW) of -4.58 ft. NGVD; yielding a maximum diurnal range of 8.84 ft. These extreme tidal ranges, or so-called Perigean Spring Tides, occur every 4-1/2 years when the declination angle reaches a minimum at the perigee of the lunar orbit, Wood (1977).

The minimum diurnal tidal range provides the weakest tidal forcing which the lagoon system will experience and will thus represent the condition of greatest susceptibility to inlet closure if coinciding with large oblique waves. For this minimum tidal range the

highest water level of this extreme neap tide reaches only +1.22 ft. NGVD, while the LLW level reaches -1.89 ft. NGVD. This extreme neap tide produces a diurnal tidal range of only 3.11 ft. While this condition is a time of enhanced vulnerability to inlet closure, such extreme neap tides occur only once every 18.6 years, (Wood, 1977).

The numerical search of the 30-year block of predicted astronomic tides 1980-2010 revealed some difficulty in finding an actual tidal day whose diurnal range, MHHW, and MLLW elevations all matched the values in Table 1 from long-term averages of the 1983-2001 tidal epoch. The tidal hydraulics model cannot be made to run on tidal forcing by average statistics; rather it requires an actual tidal time history. Therefore, it was necessary to adopt a two-day tidal block that came closest to the values in Table 3, even though it did not exactly match these values. The two-day record that was adapted as an astronomic mean range tide proxy has a MHHW = +3.02 ft. NGVD and a MLLW = -2.29 ft. NGVD. Although there is a small offset in the MHHW of this two-day time series relative to the NOAA datum, the diurnal range of the time series is 5.31 ft., and matches the mean diurnal range of Table 1 within 0.01 ft.

3.0) Tidal Hydraulics Impacts of Widening Existing I-5 Bridge Span at San Dieguito Lagoon:

The I-5 bridge over the tidal/river channel of San Dieguito Lagoon will not be replaced under the current plans for the North Coast Corridor Project; but rather will be widened in place using the existing span. Specifications for the widened I-5 bridge proposed for the San Dieguito Lagoon (referred to as 10+4 buffer) are:

Total Length (span): 649.5 ft
Width of existing bridge deck (7-7-2003): 179 ft (54.5 m)
Width of proposed/new bridge deck: 253 ft (77.1 m)
Side slope of channel: 2 to 1
Channel depth: +1.0 ft NGVD

3.1) Model Input: The TIDE_FEM model was gridded for the San Dieguito Lagoon bathymetry, including both the newly constructed lagoon restoration (the Edison Plan), as well as the W-19 tidal basin east of I-5 being proposed to partially mitigate for wetlands impacts associated with the North Coast Corridor Project. Figure 4 details the bathymetry contours of the W-19 tidal basin merged with the Edison Plan and San Dieguito River bathymetry. We consider two basic sets of tidal hydraulics simulations: 1) the Edison Plan with the W-19 basin using the existing bridge design and its associated hard-bottom channel dimensions; and 2) the Edison Plan with the W-19 tidal basin using

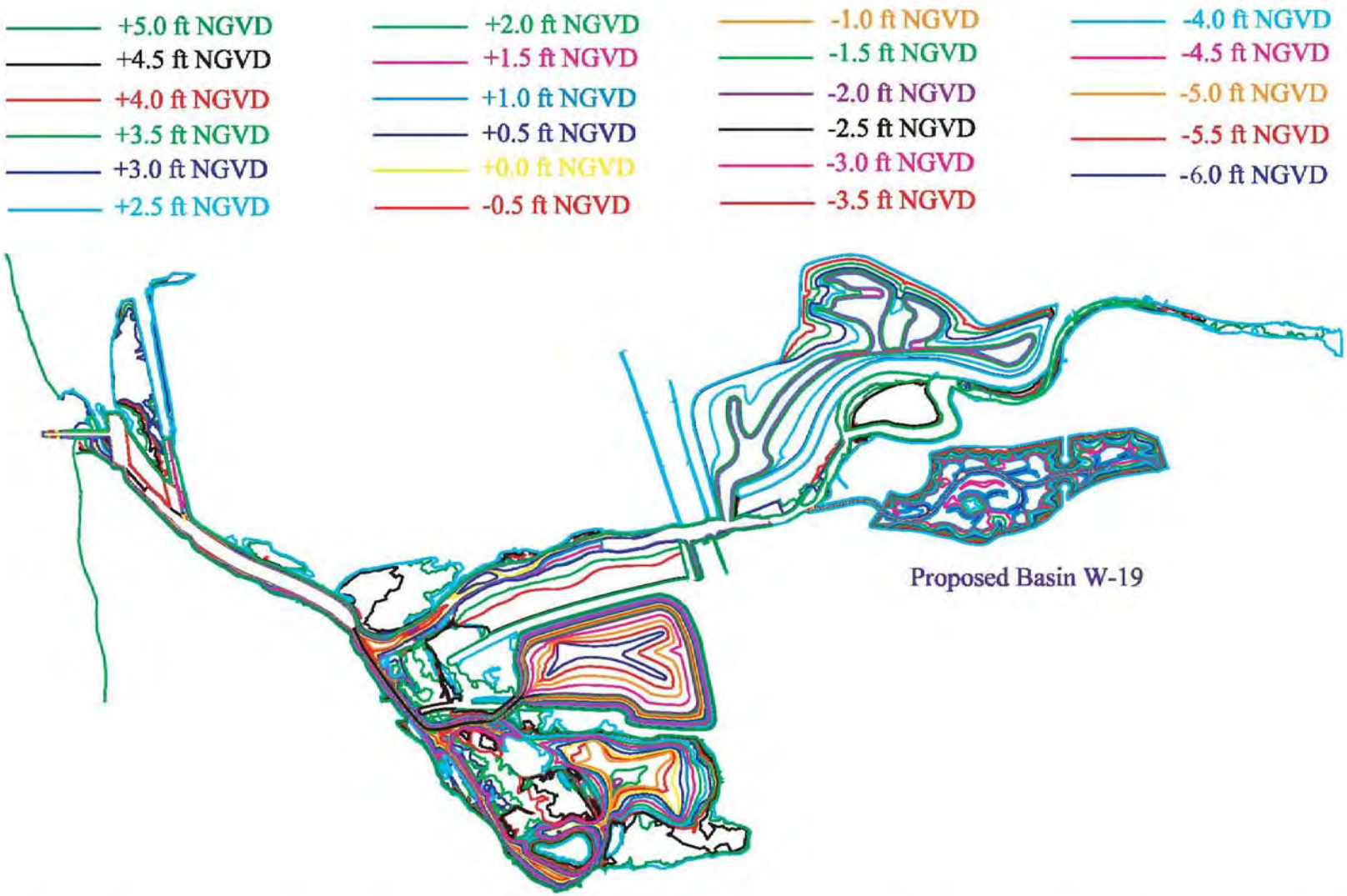

Figure 4: Bathymetry of San Dieguito Lagoon system with the Edison Plan and newly proposed W-19 tidal basin. Contours shown in feet NGVD.

an elongated channel hard-bottom channel to accommodate the wider span associated with the North Coast Corridor Project. We examine specifically incremental changes in total area of salt water inundation and incremental changes in area of intertidal habit as a consequence of the wider bridge span and elongated channel under that wider span.

Of particular interest to the finite element mesh derived from the bathymetry in Figure 4 is the *hydraulic friction slope coefficient*, S_{fj}, providing tidal muting effects. Two separate formulations are used. One is given for the 3-node triangular elements situated in the interior of the mesh in Figure 16 which do not experience successive wetting and drying during each tide cycle. The other formulation is for the elements situated along the wet and dry boundaries of the lagoon. These have been formulated as 3-node triangular elements with one curved side based upon the cubic-spline matrices developed by Weiyan (1992). These two sets of elements were assembled into a computational mesh of the lagoon conforming to the lagoon extreme high waterline in Figure 4. The wet-dry boundary coordinates of the curved waterline, (x', y'), are linearly interpolated for any given water elevation from the contours stored in the lagoon bathymetry file.

Stage area and storage rating functions were calculated from the bathymetric contours shown in Figure 4. These contours are based on a merging of the bathymetric surveys by Coastal Environments, 2009 of the as-built Edison plan with the KTU+A restoration design for the W-19 parcel originally commissioned by Poseidon Resources. The stage area and storage rating functions convert the physical details of the lagoon bathymetry into a mathematical form that is used by the tidal hydraulics model to make its calculations of tidal exchange and salt water inundation. Stage area functions give the wetted area of the lagoon at variable water levels, while storage rating functions give the variation in water volume stored in the lagoon in response to water level changes. The stage area and storage rating functions used in the initialization of the TIDE_FEM tidal hydraulics model have been modified relative to the original EIR/EIS analysis of the Edison Plan (see Jenkins & Wasyl 1998; 1999a) to reflect the modifications to W-19 grading shown in Figure 4. A series of high-order polynomials were computed from the areas within grading contours of the original grading design of the Edison plan, and from newly created contours for the W-19 tidal basin. Due to slope variations over the full elevation range in the grading plan, separate polynomials were developed for the portions of the stage area function above and below 0.0 ft NGVD. The resulting stage area functions in Figures 5 and 6 show the grading contour areas (cross points) vs the polynomial fits (solid line) for the portion of the stage area functions below 0.0 ft NGVD (the black line segments); while the red line segments give the wetted areas of the portion of the grading plan that extends from 0 ft. NGVD up to the "daylight" contour or contour above which salt water inundation never occurs. To accommodate possible future sea

level rise, the daylight contour was chosen at +5.5 ft NGVD, even though the inundation in the lagoon has never been observed above +5.0 ft NGVD.

Figure 5 gives the stage area function of the W-19 basin in isolation, while Figure 6 gives the composite stage area function of the San Dieguito lagoon system with the Edison Plan and W-19 added. These functions were integrated vertically to compute polynomial coefficients for the storage rating function also required in the initialization of the TIDE_FEM tidal hydraulics model. Figure 7 shows the storage rating function for W-19 and its feeder channel, while Figure 8 gives the storage rating function of the San Dieguito lagoon system with the Edison Plan and W-19 added. The previous EIR/EIS analyses in Jenkins & Wasyl (1998, 1999) and Jenkins, Josselyn and Wasyl (1999) indicate that the historic extreme high water (EHW) event will cause lagoon water levels to reach the neighborhood of +5.0 ft. NGVD. However, the California Coastal Commission only awarded restoration credit for tidal inundation up to +4.5 ft NGVD, (see SCE, 2005). The work of Zedler & Cox, 1985 and Josselyn & Whelchel, 1999, indicates that this elevation of tidal inundation must be achieved at least one day per year to sustain tidally influenced salt marsh habitats. Therefore the relevant metric for evaluating maximum tidal prism is based on diurnal tides reaching a higher high water (HHW) of +4.5 ft. NGVD rather than the historic extreme high water (EHW) of + 5.0 ft NGVD. The extreme low water (ELW) definitions are based on the design values of the San Dieguito Lagoon Final Restoration Plan (SCE, 2009). The combined potential tidal prism of the San Dieguito Lagoon with Edison Plan was found to be 886 acre ft (see Jenkins and Wasyl, 2001). However, Figure 8 and the present tidal hydraulics modeling effort indicates that this tidal prism can be increased to 1,012 acre ft when the W-19 tidal basin is added to the system, an increase of 13 % or 114 acre ft.

3.2) Model Calibration and Assessment of Existing Conditions: Spring, neap and mean tidal range simulations of the hydraulics of San Dieguito Lagoon were performed using astronomic tidal forcing functions at = 2 sec time step intervals for the period 1980-2007, as discussed in Section 2.1. Computed water surface elevations and depth-averaged velocities from the global solution matrix were converted to lagoon waterline contours and flow trajectories. Calibrations for determining the appropriate Manning factors and eddy viscosities were performed by running the TIDE_FEM model on the Figure 4 bathymetry file and comparing calculated water surface elevations in the W-1 and W-16 tidal basins against water level measurements by Coastal Environments (2009) during September 2009. Iterative selection of Manning factor n_0 = 0.03511 and an eddy viscosity of ε = 7.129 ft^2/sec gave calculations of water surface elevation and inlet that reproduced the measured values to within 2% over the 2009 monitoring period.

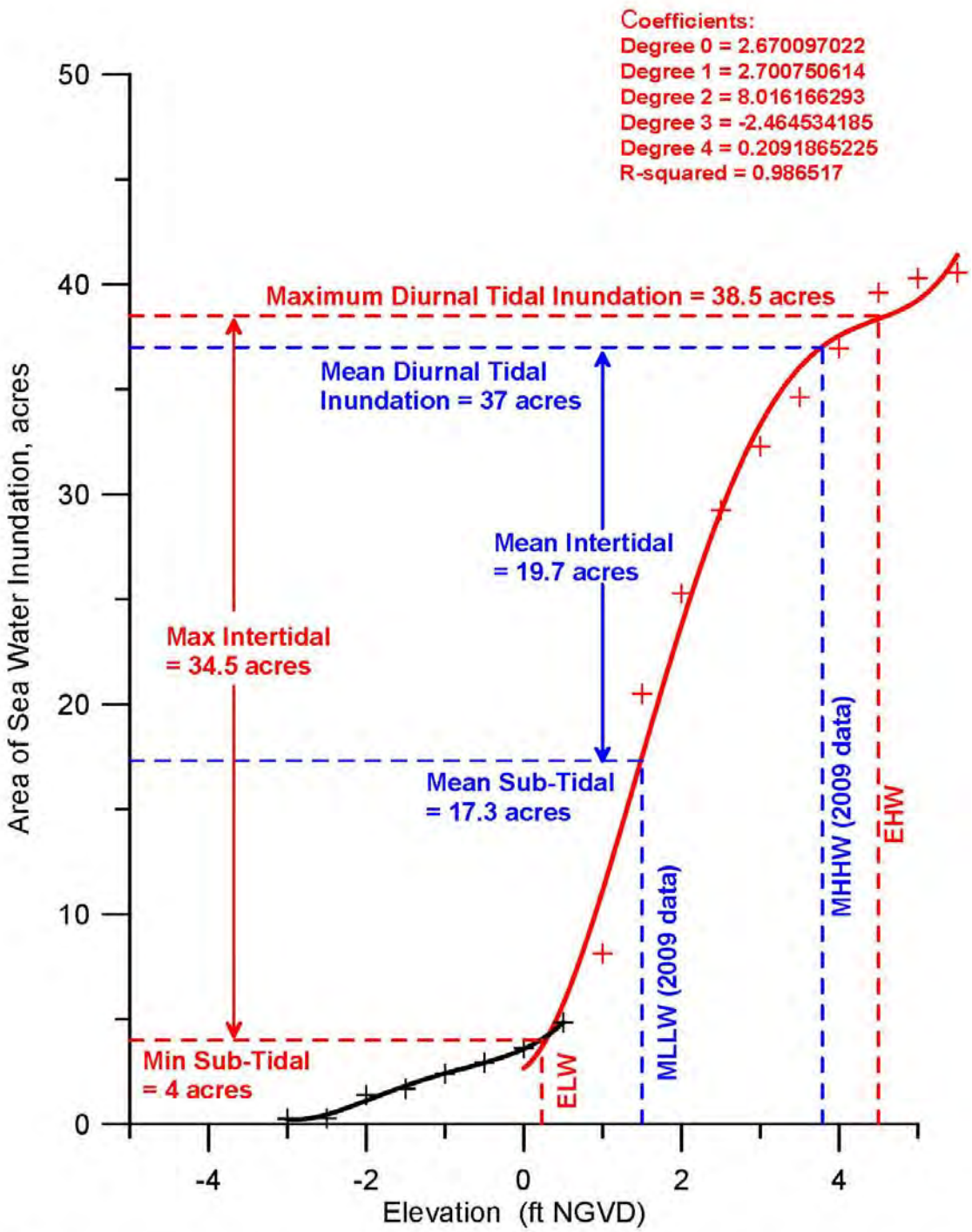

Figure 5. Stage area function of the W-19 tidal basin and feeder channel, San Dieguito Lagoon. Water level data from Coastal Environments, (2009). Extreme water levels based on San Dieguito Final Restoration Plan, SCE (2005).

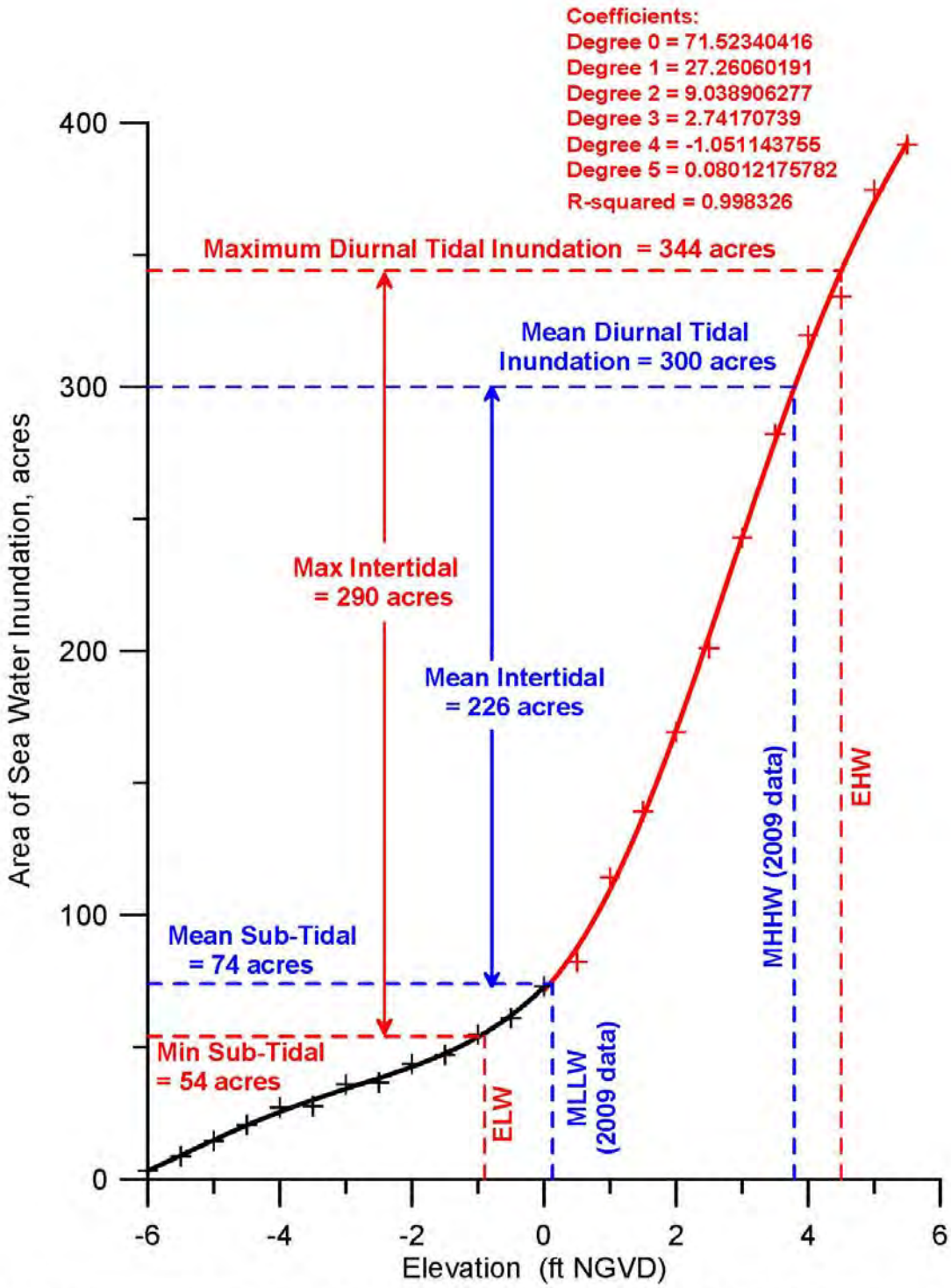

Figure 6. Stage area function of the Edison Plan with the W-19 tidal basin added, San Dieguito Lagoon. Water level data from Coastal Environments, (2009). Extreme water levels based on San Dieguito Final Restoration Plan, SCE, (2005).

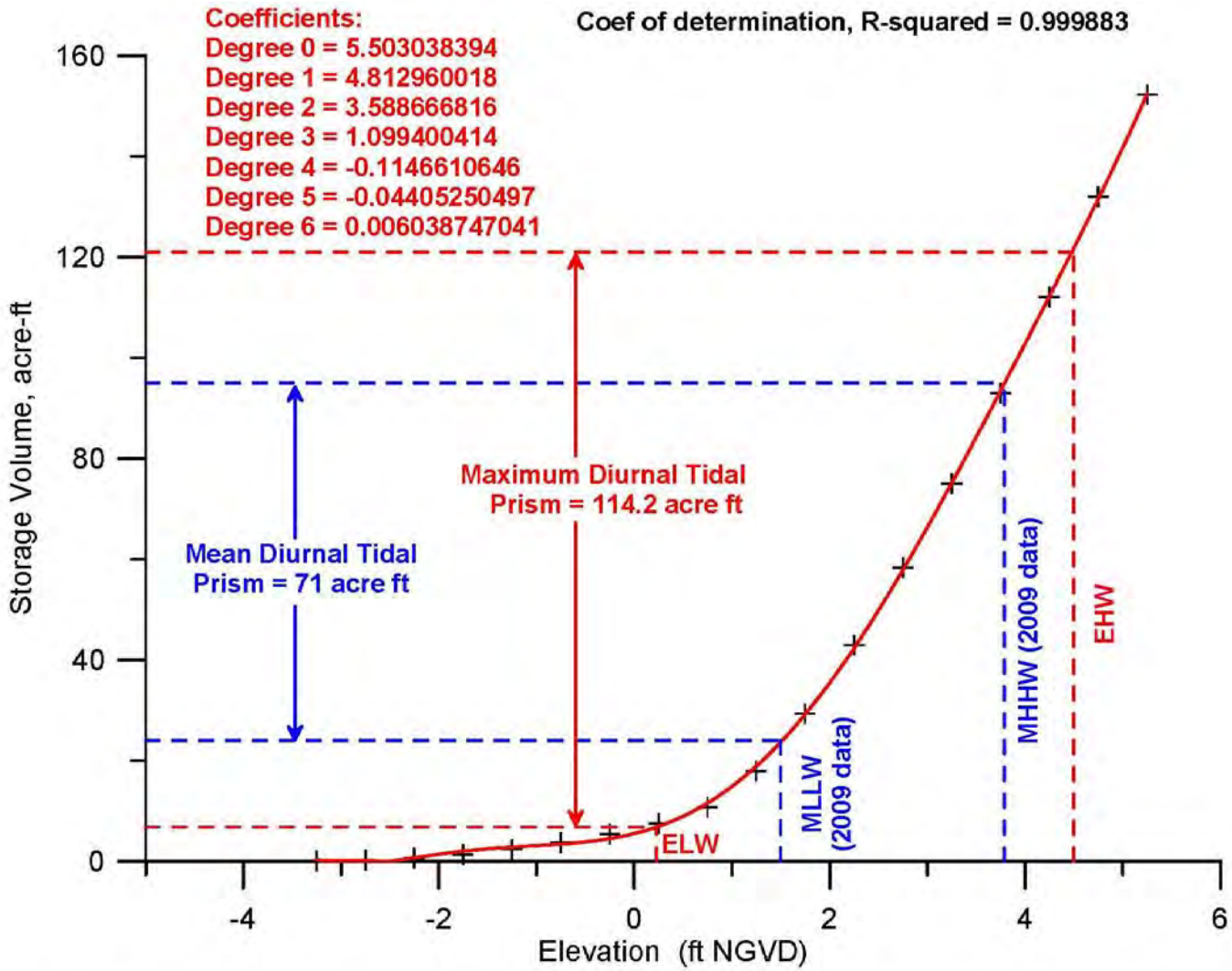

Figure 7. Storage rating function of the W-19 tidal basin and feeder channel, San Dieguito Lagoon. Water level data from Coastal Environments, (2009). Extreme water levels based on San Dieguito Final Restoration Plan, SCE, (2005).

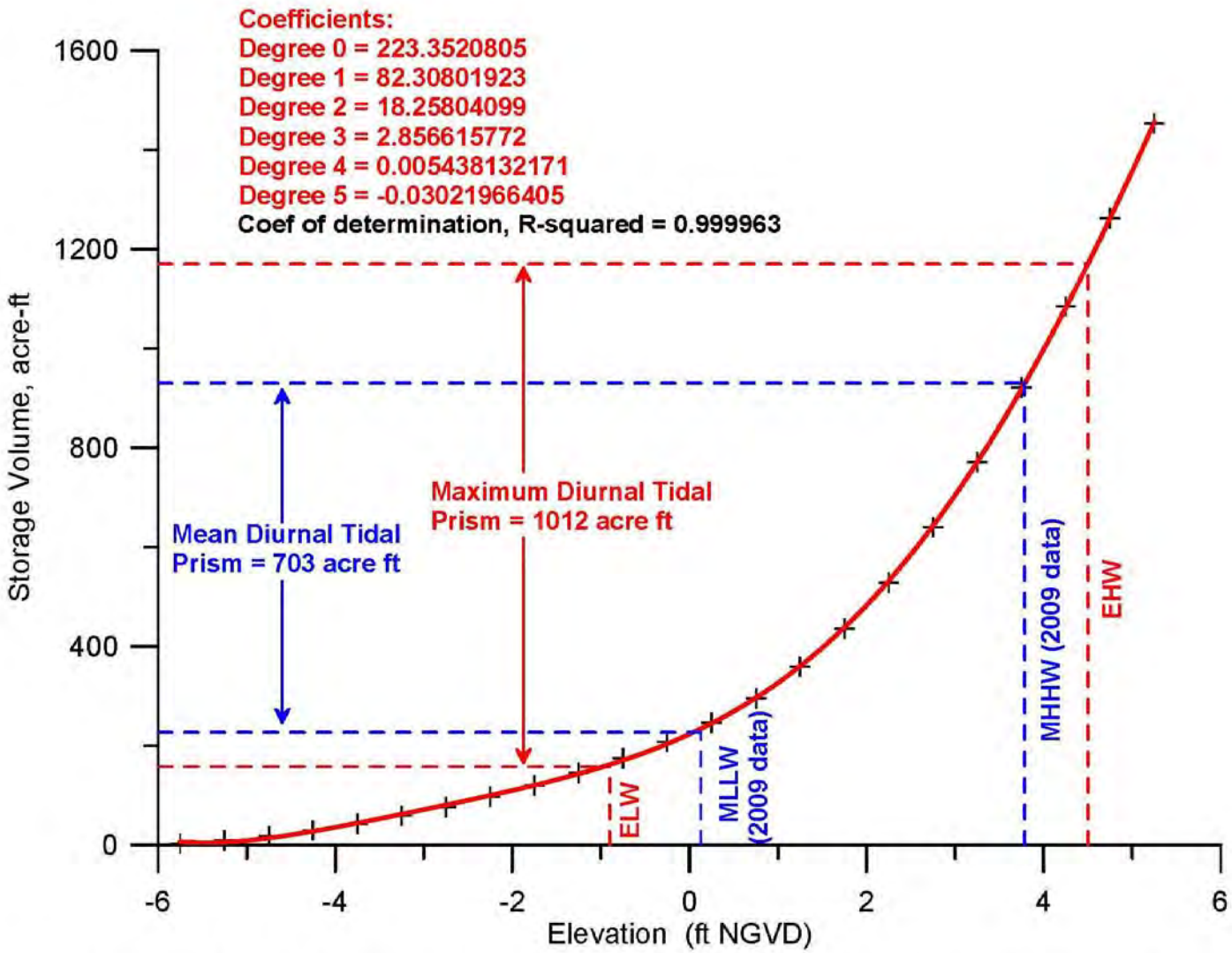

Figure 8. Storage rating function, Edison Plan with W-19 tidal basin added, San Dieguito Lagoon. Water level data from Coastal Environments, (2009). Extreme water levels based on San Dieguito Final Restoration Plan, SCE, (2005).

Figure 9 provides a quantitative assessment of the accuracy of the calibrated TIDE_FEM model over the calibration period of 14-18 September 2009 using water level measurements in the newly created W-1 tidal basin located west of I-5 and east of Jimmy Durante Blvd. Here we compare W-1 Tidal Basin water level variations predicted by the model (red trace) with the actual water level measurements (black crosses) during the post-construction monitoring of the Edison Plan by Coastal Environments, (2009). The W-1 Basin water level variations are found to lag the ocean water levels by as much as 2.43 hr during the mid-range tides of the monitoring period. Low tide water levels in the W-1 basin never drop below + 0.13 ft NGVD and are well above ocean low tide water levels due to the inlet channel sill formed across the beach berm. The amplitudes and degree of non-linearity in the W-1 Basin water level time series simulated by the model closely duplicate that observed in the measured lagoon tides. The maximum error in simulating the low tide elevations was found to be ε_L = +0.1 ft. The maximum high tide error in the model simulation relative to observations was found to be ε_H = -0.05 ft.

Figure 10 provides similar calibration and predictive skill assessment using water level measurements in the newly created W-16 Tidal Basin located east of I-5 off the north bank of the San Dieguito River. Here we compare W-16 Tidal Basin water level variations predicted by the model (purple trace) with the water level measurements (black crosses) during the post-construction monitoring of the Edison Plan by Coastal Environments, (2005). The W-16 Basin water level variations are found to lag the ocean water levels by as much as 3.79 hr during the mid-range tides of the monitoring period. Low tide water levels in the W-16 basin never drop below + 1.49 ft NGVD and are well above ocean low tide water levels due to the erosion of the upper slopes of a mud flat due to storm drain discharge, and the subsequent deposition of those sediments in the W-16 feeder channel, forming a plug that prevents total drainage of W-16 during ebb tide. Even without this depositional plug, low tide levels in W-16 could fall no lower than +0.23 ft NGVD due to the present elevation of the hard channel bottom under the I-5 bridge. Again, the amplitudes and degree of non-linearity in the W-16 Basin water level time series are accurately simulated by the model and closely duplicate those features observed in the measured lagoon tides.

In both Figures 9 and 10, the calibration error appears to exhibit a systematic tendency. When amplitude errors occur, they tend to over estimate the water elevation of the LLW tidal stage and under estimate the water elevation of the HHW tidal stage. Although

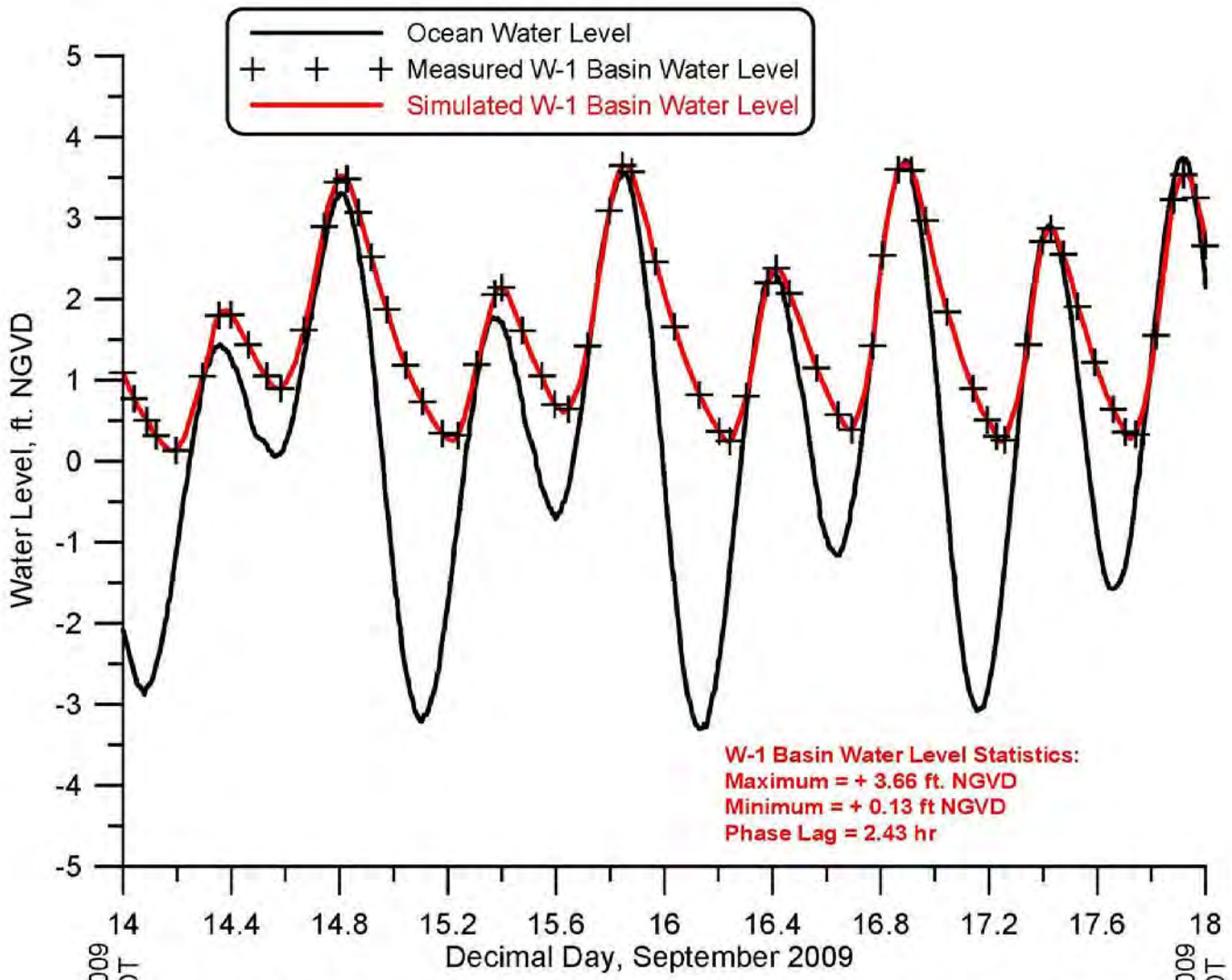

Figure 9. Water level calibration based on the W-1 tidal basin measurements, San Dieguito Lagoon, 14 - 18 September 2009. Ocean water level (black) compared to measured W-1 basin water levels (black crosses) vs calibrated model simulation (red). Measurements by Coastal Environments (2009).

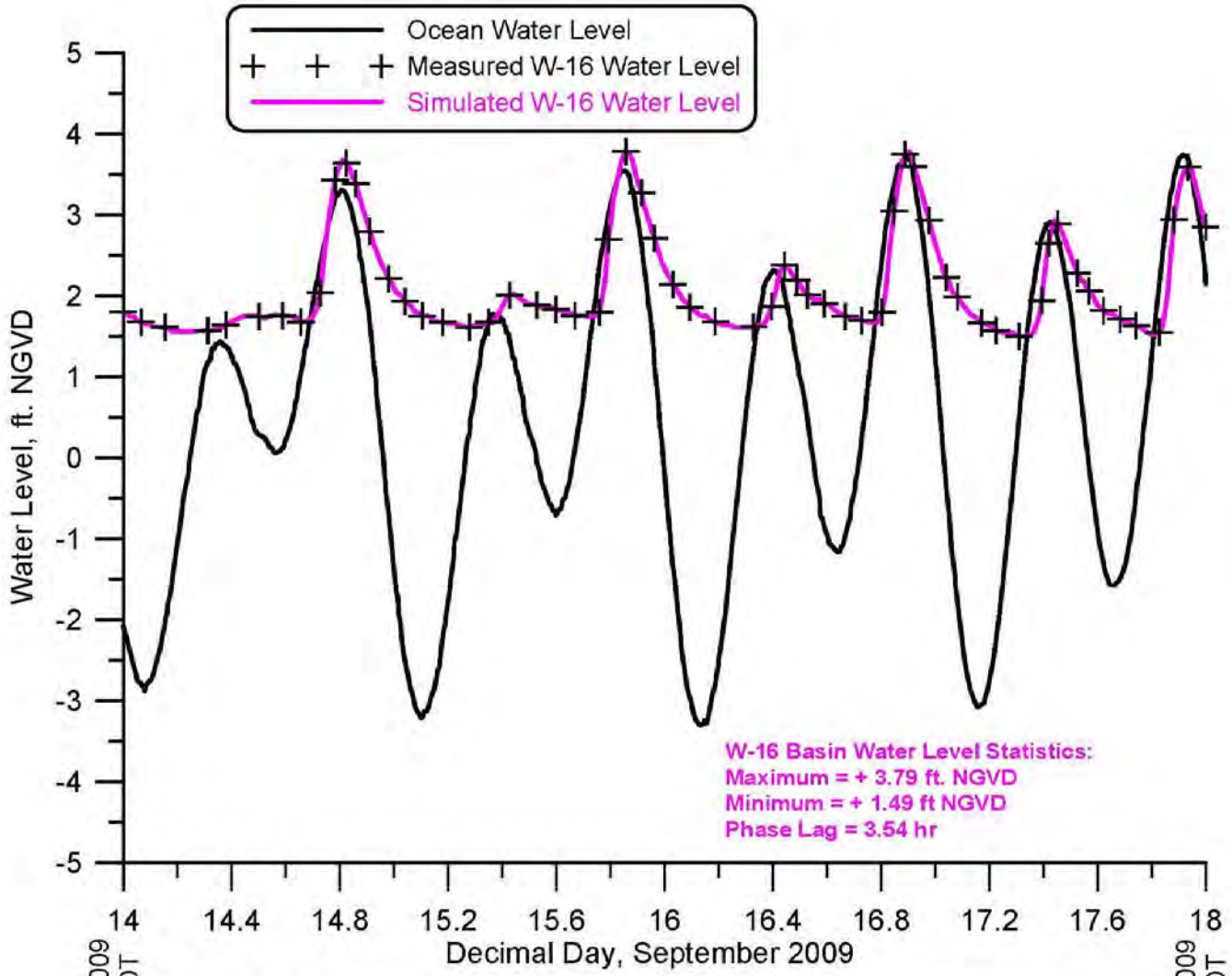

Figure 10. Water level calibration based on the W-16 tidal basin measurements, San Dieguito Lagoon, 14 - 18 September 2009. Ocean water level (black) compared to measured W-16 basin water levels (black crosses) vs calibrated model simulation (red). Measurements by Coastal Environments (2009).

these errors are quite small and may be considered high predictive skill, this error mode is consistent with *bathymetry errors* in which depth has been under estimated, Weiyan (1992). Bathymetry errors are the most common cause of modeling errors. Other sources of errors include:

ELEMENT INTERPOLATION ERROR: Due to the degree of the polynomial used to specify shape function, N_i.

DISCRETIZATION ERRORS: Due to mesh coarseness and approximating the curved wet/dry boundary side of an element with a quadratic spline.

QUADRATURE ERRORS: Due to reducing the weighted residual integrals with the influence coefficient matrices.

ITERATION ERRORS: Due to solving the system of algebraic equations reduced from the Galerkin Equations.

ROUNDOFF ERRORS: Due to time integration by the trapezoidal rule.

SEA LEVEL ANOMALIES: Due to discrepancies between the astronomic tides and the actual observed water levels in the ocean.

INSUFFICIENT CALIBRATION DATA: Due to limitations in the period of record.

Power "auto-" spectra are useful tools for determining how the energy in complex time series like Figures 9 & 10 is distributed among various frequencies of oscillation. The predominant frequencies, where most of the tidal energy appears (spectral peaks), can give clues that identify the mechanisms that predominate in the local tidal system. In Figures 11a and 12a, auto spectra of the ocean tides (black, upper panel) show the predominant energy is centered on a diurnal frequency of the K1 lunar-solar diurnal tidal constituent at $f_{K1} = 1.16079 \text{ x } 10^{-5}$ Hz. The energy in this peak is disproportionately high relative to the next largest spectral peak occurring at the M2 principal lunar semi-diurnal tidal constituent, $f_{M2} = 2.2365 \text{ x } 10^{-5}$ Hz. The excess energy at diurnal frequencies is believed to be non-tidal and attributable to a wind-driven current component that has a diurnal fluctuation in response to daily heating of the land. With the onset of Santa Anna winds in September 2009, this diurnal land breeze component would be strengthened in the time frame of the lagoon monitoring.

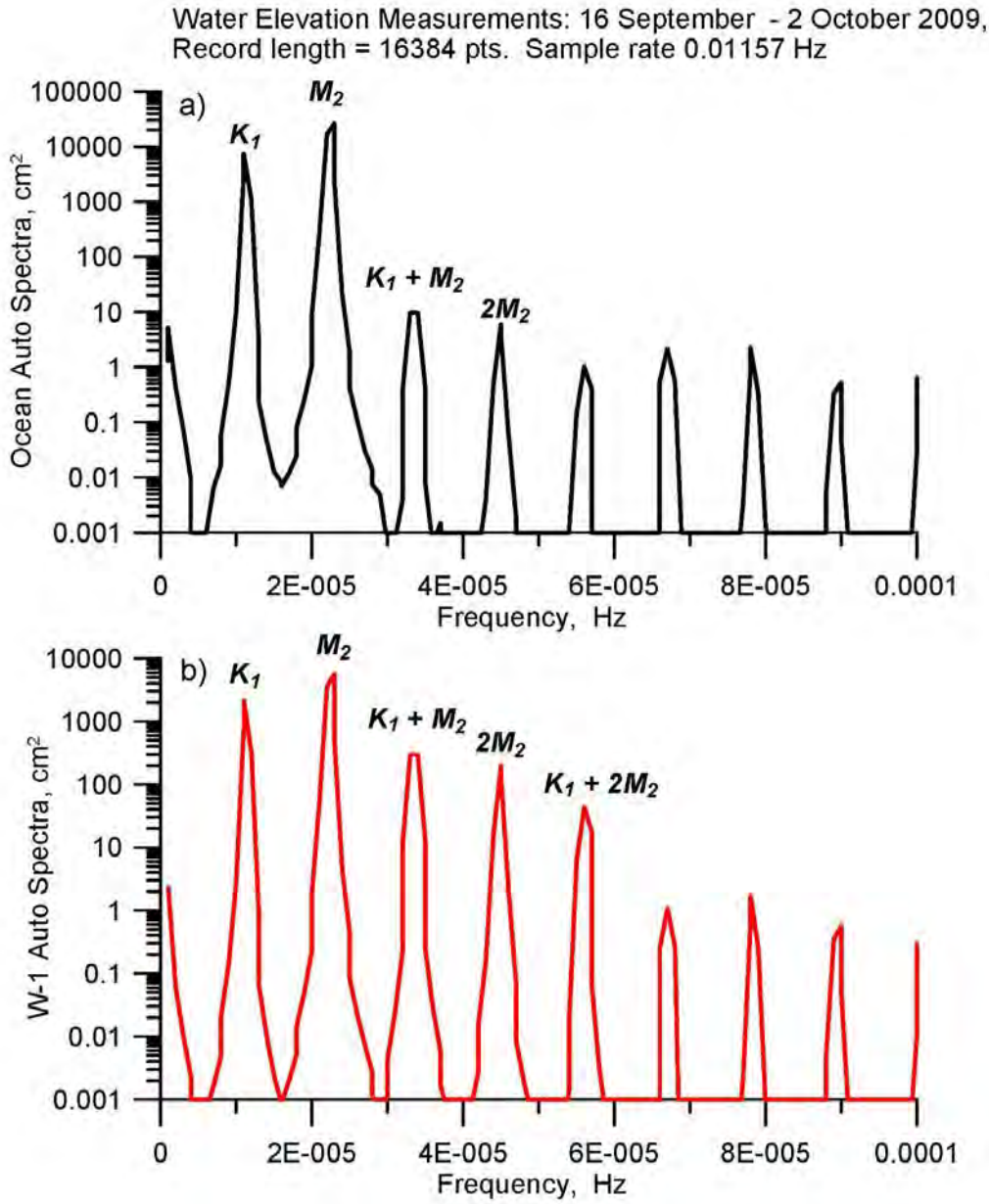

Figure 11. Auto spectra of water level measurements: a) Ocean water level at mouth of San Dieguito River, b) water level in the W-1 tidal basin of San Dieguito Lagoon.

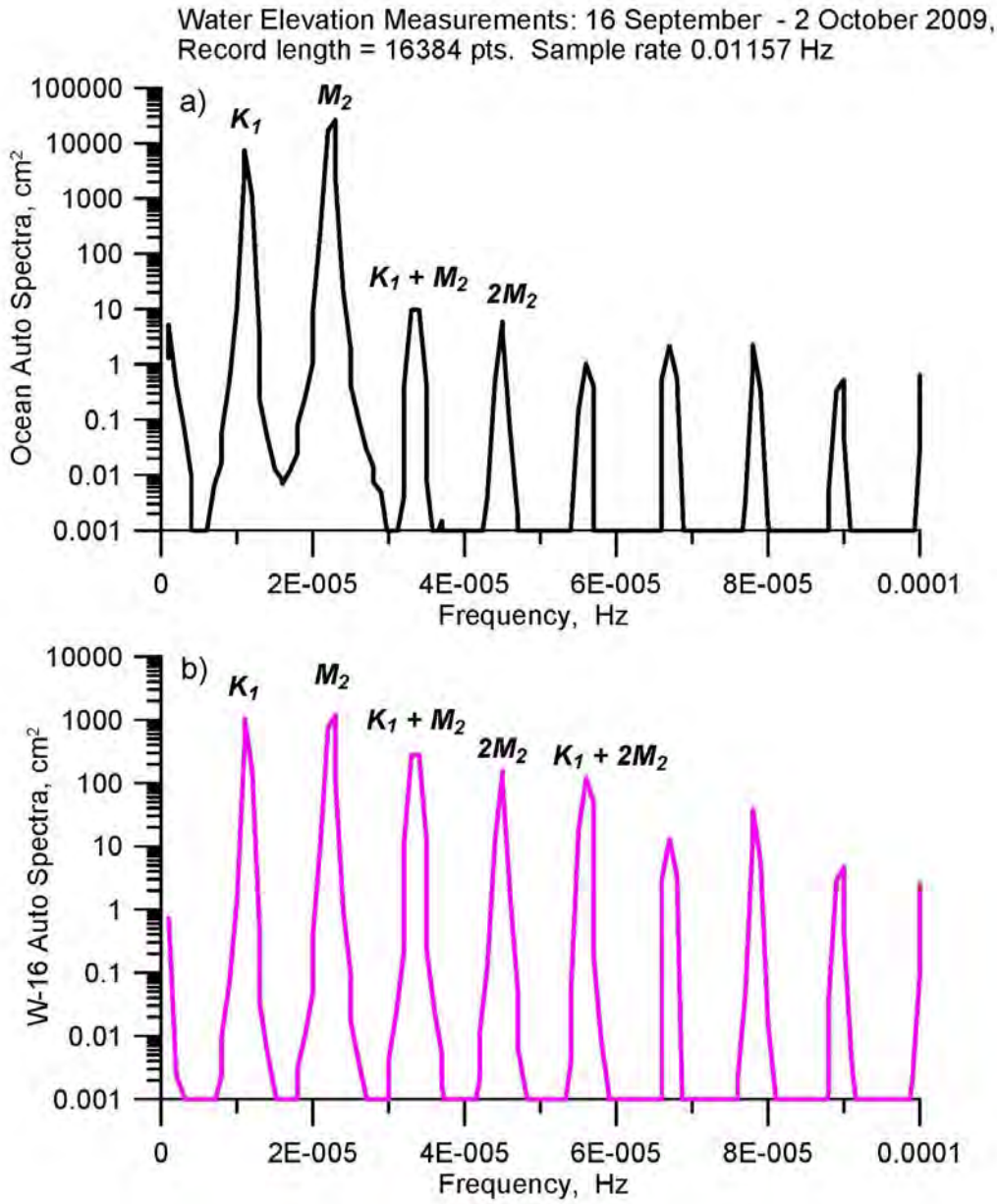

Figure 12. Auto spectra of water level measurements: a) Ocean water level at mouth of San Dieguito River, b) water level in the W-16 tidal basin of San Dieguito Lagoon.

Other less energetic tidal peaks are also found in the spectra of Figures 11a & 12a, including one believed to be a baroclinic *shelf resonance* formed by a resonant *triad* at the sum of the frequencies of the K1 and M2 barotropic tides, ie., a diurnal third harmonic at a frequency $f_3 = f_{K1} + f_{M2} = 3.3973 \text{ x } 10^{-5}$ Hz. This diurnal third harmonic is a baroclinic tide excited by the barotropic K1 and M2 tides interacting with the bottom topography, in particular the local shelf and Scripps Submarine Canyon to the south. Another baroclinic shelf resonance apparent in the spectra of the ocean tides in Figures 11a & 12a is a second harmonic of the barotropic M2 tide appearing at a frequency of $2 f_{M2} = 4.4730 \text{ x } 10^{-5}$ Hz. The auto spectra of the East Basin tides shown in red in the lower panel of Figure 11b exhibits the same primary barotropic and baroclinic tidal peaks as the ocean tides in the upper panel, with one exception, an additional non-linear resonance appears as a triad formed by the sum of the K1 barotropic mode and the baroclinic second harmonic of the M2 tide, $f_{K1} + 2 f_{M2} = 5.6338 \text{ x } 10^{-5}$ Hz. Apparently this mode is excited by non-linear tidal interaction with the lagoon bathymetry.

Figure 12b compares the auto spectra of the W-16 tidal basin in purple in the lower panel against the ocean tidal spectra from Figures 11a & 12a in black in the upper panel. Spectral peaks in the ocean tides are all found in the W-16 spectra but, similar to the W-1 tidal basin spectra in Figure 11b, some of the higher harmonics of the W-16 spectra are disproportionately large. The diurnal third harmonic is present in the W-16 tidal basin water levels at the sum of the frequencies of the K1 and M2 barotropic tides, as well as the second harmonic of the M2 tides, and a triad formed by the sum of the K1 barotropic mode and the baroclinic second harmonic of the M2 tide.

3.3) Simulated Tidal Hydraulics Impacts from I-5 Bridge Widening: The 13% boost in tidal prism which will result from addition of the W-19 tidal basin will increase the flushing of sediments from the ocean inlet, forestall tendencies for inlet closure and reduce the required frequency of dredging the sediment trap in the inlet channel. We will not attempt to quantify in detail or monetize the benefits of the W-19 basin to long term maintenance. Instead our focus here will be on the effects which the increased tidal prism will have on increasing the current speeds in the channel under the bridge, (referred to as a *bridge waterway*), and on assessing whether higher speeds in combination with a longer bridge waterway under widened span increases frictional losses enough to reduce either area of salt water inundation of intertidal area.

Fine scale flow details in the tidal channel near the I-5 bridge over San Dieguito Lagoon are shown in Figure 13 for maximum flooding spring tides and in Figure 14 for

maximum ebbing spring tides. The examples shown in Figures 13 and 14 are for the widened I-5 bridge but flow trajectories are identical with those found for the existing bridge. In either case, the W-19 tidal basin has increased tidal speeds in the bridge waterway by 14% over those reported in the EIR/EIS of the Edison Plan (see Jenkins & Wasyl 1998; 1999a). Despite this increase, flow speeds exiting the hard bottom channel are at most 0.18 m/s during flood tide and 0.08 during ebb tide, well below the threshold transport velocity of the river bed sediments found on either side of the bridge. Therefore, the addition of the W-19 tidal basin will not result in tidal channel scour with either the existing or widened I-5 bridge.

The ocean water levels 1980-2010 were used to drive the TIDE_FEM model at the ocean boundary in order to solve for the time series of the water level variation throughout the lagoon system based on the stage area and storage rating functions of the Edison Plan (Figures 5-8). Daily highest high and lowest low water levels for each day during this 30-year simulation period were mapped onto the stage area functions to calculated acreages of salt water inundation and assembled into the histograms in Figures 51 & 16. Figure 15 gives the computed acreage of salt water inundated habitat in the proposed W-19 tidal basin and its feeder channel, based on ocean water level forcing for surrogate year 1997. Figure 15a gives total area of salt water inundation with the existing I-5 bridge, while Figure 15b gives an identical result for the wider bridge. The lagoon system with the fully implemented Edison Plan is shown in Figure 15 to increase the annual maximum area receiving salt water inundation to 374 acres, greater than the maximum 344 acre diurnal estimate of tidal inundation in Figure 6 because the historic inundation levels in 1997 exceeded by 0.61 ft the EHW levels for which the Coastal Commission was willing to grant restoration credits under the San Dieguito Final Restoration Plan (SCE, 2005). The inundation simulations in Figure 15b also find that the Edison Plan with the W-19 tidal basin and wider I-5 bridge will give 240 acres of salt water inundation at least half the time.

Figure 16 shows that San Dieguito Lagoon remains a predominantly intertidal system with the W-19 basin added, and that widening the bridge makes no change in the intertidal acreage. Maximum intertidal acreage exceeds the 290 acre estimate from Figure 6 because tidal inundation exceeds the +4.5 ft NGVD for the EHW datum that the Coastal Commission was willing to admit. The tides of 13 November 1997 would cause salt water inundation in W-19 up to an actual extreme high water elevation of EHW = 5.11 ft NGVD for both the existing and widened I-5 bridge. Consequently, the maximum intertidal acreage of the system is expanded to 315 acres with the addition of W-19 while the annual median intertidal acreage of this combined system would be 184 acres.

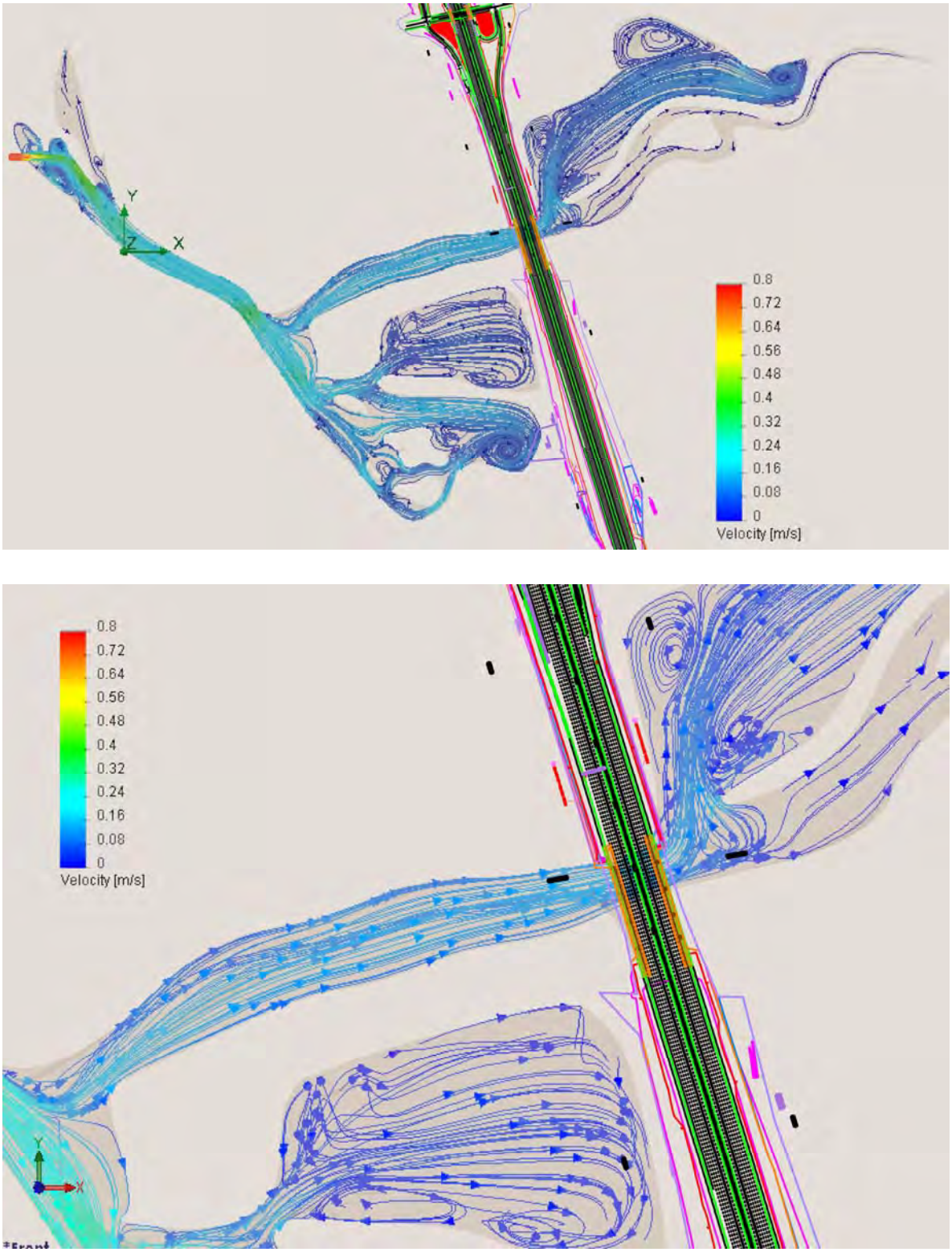

Figure 13: Hydrodynamic simulation of maximum flood flow during mean range tides at San Dieguito Lagoon (upper panel); with tidal channel flow detail under the proposed I-5 bridge widening alternative of the North Coast Corridor Project (lower panel).

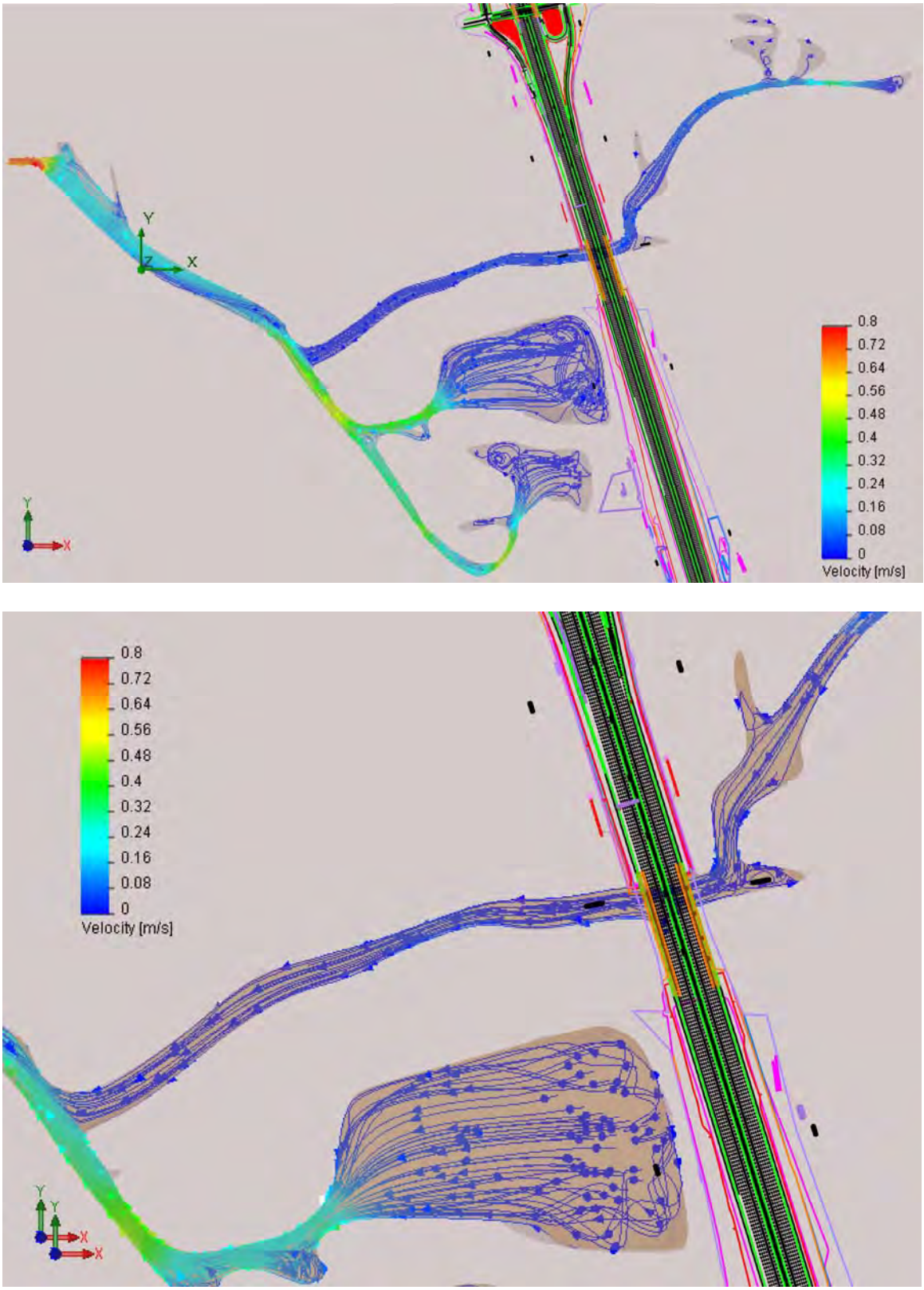

Figure 14: Hydrodynamic simulation of maximum ebb flow during mean range tides at San Dieguito Lagoon (upper panel); with tidal channel flow detail under the proposed I-5 bridge widening alternative of the North Coast Corridor Project (lower panel).

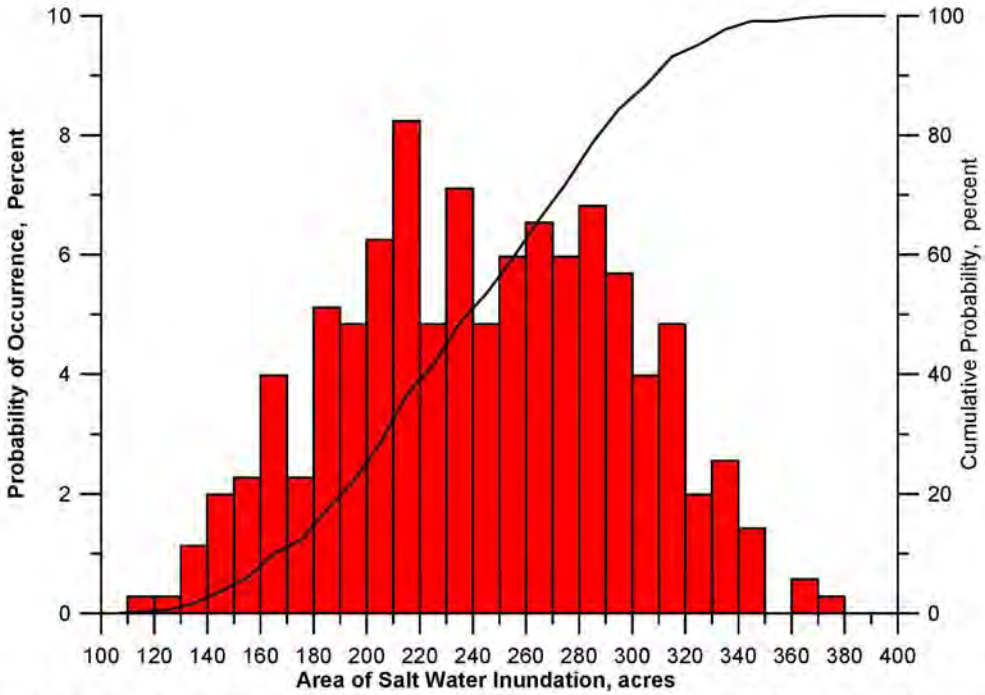

Figure 15a. Probability density function of area inundated by sea water at San Dieguito Lagoon with the existing I-5 bridge. Based on long term tidal hydraulics simulation of the Edison Plan + W - 19 tidal basin.

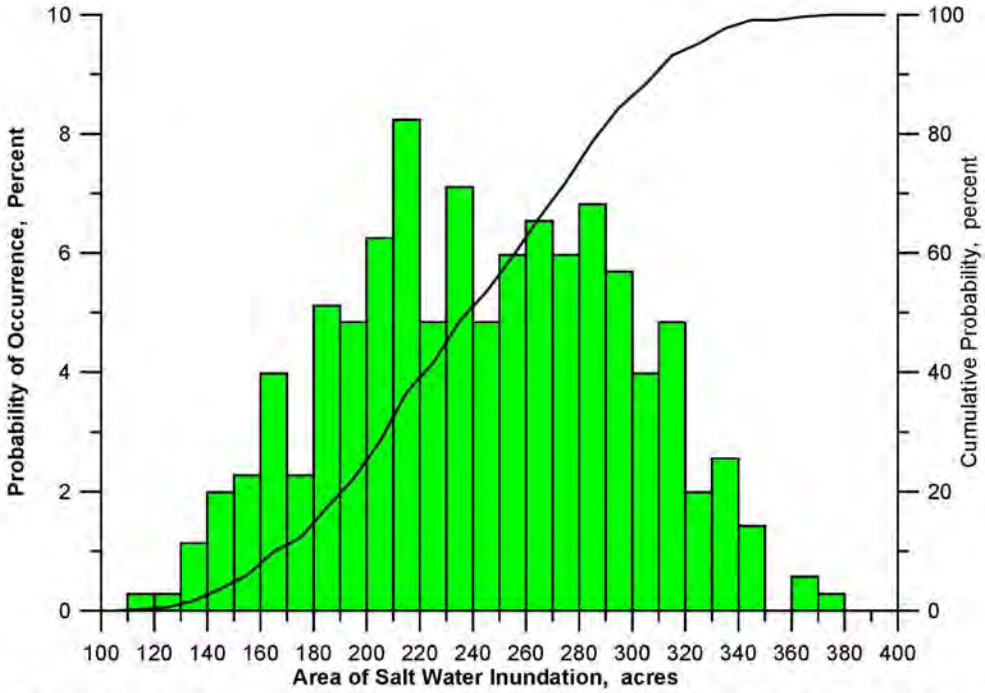

Figure 15b. Probability density function of area inundated by sea water at San Dieguito Lagoon with the widened I-5 bridge. Based on long term tidal hydraulics simulation of the Edison Plan + W - 19 tidal basin.

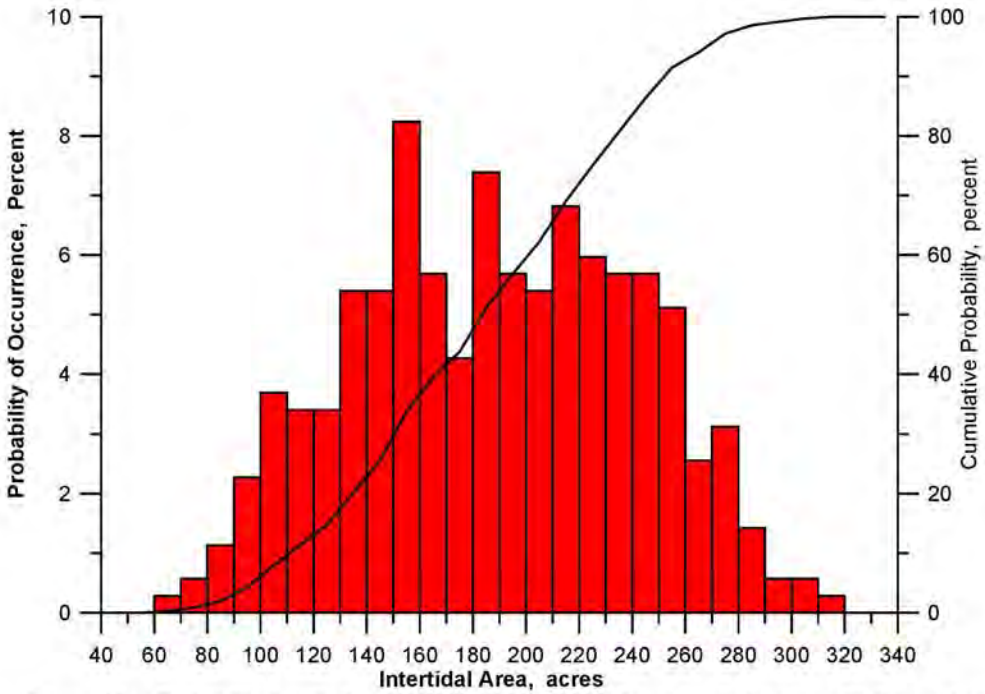

Figure 16a. Probability density function of intertidal area at San Dieguito Lagoon with the existing I-5 bridge. Based on long term tidal hydraulics simulation of the Edison Plan + W - 19 tidal basin.

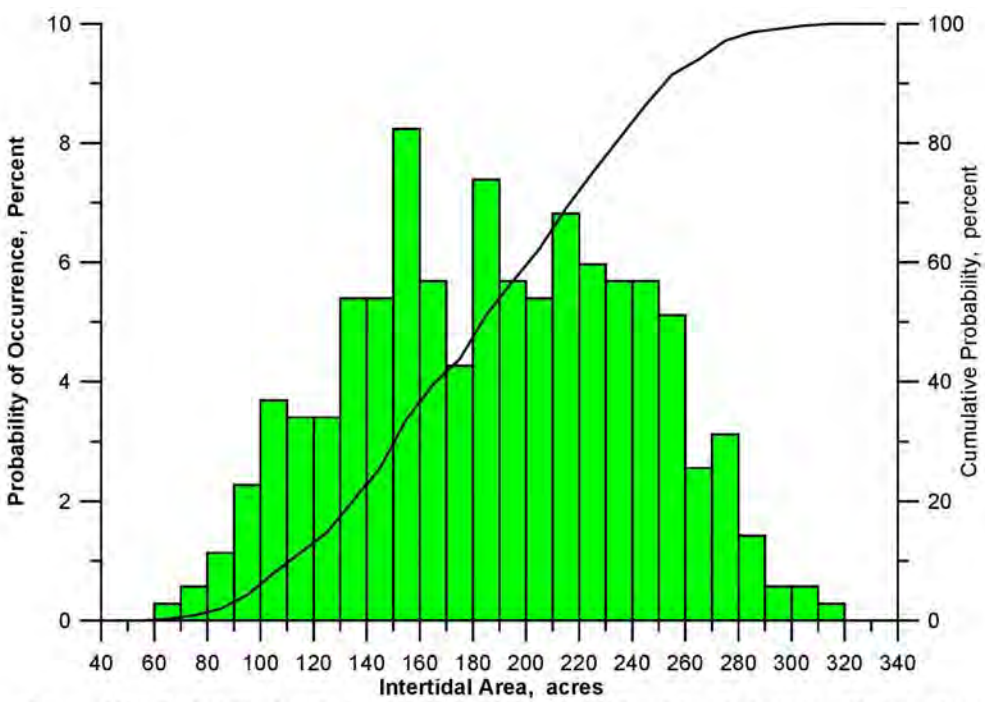

Figure 16b. Probability density function of intertidal area at San Dieguito Lagoon with the widened I-5 bridge. Based on long term tidal hydraulics simulation of the Edison Plan + W - 19 tidal basin.

Thus, on average, 76.7% of the combined wetland system (including W-19) is intertidal. From these findings of long-term tidal inundation simulation, we conclude that the effect of the W-19 tidal basin on tidal inundation overwhelms potential changes in the San Dieguito Lagoon system; and that no significant impact from bridge width changes can be found in the model results.

The hydroperiod function gives the percentage of exposure for each elevation throughout the full range of lagoon water level variation. This is the primary physical factor limiting the type of habitat that will thrive at a particular elevation in the lagoon. The astronomic tides alone give rise to ocean water levels that only reach a maximum elevation of +4.26 ft. NGVD during Perigean spring tides, (based on tidal constituents derived from the 1983-01 tidal epoch, see NOAA, 1998, and Jenkins & Wasyl, 1998). The fact that ocean water level elevations have been measured as high as +5.38 ft. NGVD and that tidal inundation in the pre-restoration lagoon reaches +5.0 ft. NGVD is due to positive sea level anomalies occurring seasonally and/or concurrent with ENSO cycles (Flick & Cayan, 1984). Therefore, in order to model the hydroperiod function over the full range of observed water level variation, it is necessary to select an historic water level record that involved a positive sea level anomaly. To be consistent with the Edison Plan EIR/EIS, and to permit direct comparisons with previously computed hydroperiod functions in that document, the year selected for this purpose was 1997, (Jenkins, Josselyn and Wasyl, 1999; SCE, 2005). Several considerations led to this selection including: 1) Temporal proximity to the 1992 biological survey of the existing habitat; 2) Complete annual spring tidal range. (These months occur late summer and early winter when the moon is either near its perigee or the declination angle is low or both); 3) High water level inundation reaching elevations of observed tidal habitat recruitment. The 1997 ENSO cycle event had a maximum daily higher high water level of HHW = +5.38 ft. NGVD. This occurred on 13 November 1997 and is the extreme high water event of the period of record. Daily high ocean water levels exceeded +5.0 ft. NGVD in 1992, 1993 and 1997, and exceeded +4.75 ft. NGVD in 1990, 1991, 1992, 1993, 1994, 1995 and 1997 (NOAA, 1998).

The ocean water levels of 1997 were used to drive the TIDE_FEM model at the ocean boundary in order to solve for the time series of the water level variation throughout the lagoon system based on the stage area and storage rating functions in Figures 5-8. The computations involved N_o = 7,760,520 time steps. At each time step the average lagoon water elevation, η_0 was calculated from the ensemble average of the solutions at the nodes in the computational mesh, see Jenkins & Wasyl (1998a). Conditional if statements and counting loops inserted into the TIDE_FEM code would count the number time steps, N, for which the average lagoon water elevation was less than a particular

elevation, Z_i. The percent time that elevation Z_i was exposed over a tidal month was calculated as:

$$\varepsilon_i = \frac{100\%}{N_o} \sum N(\hat{\eta} < Z_i) \qquad (1)$$

The red line in Figures 17 shows the hydroperiod function calculated for the Edison Plan with the W-19 tidal basins and the existing I-5 bridge. The elevations dividing the various sub-tidal and intertidal habitat types are based on the 1992 biological survey and supporting literature data as detailed in Josselyn & Whelchel (1999). These elevations were mapped into the corresponding exposure percentages for each habitat type using the hydroperiod function computed for the existing lagoon at the time of the biological survey. From this procedure, the following exposure times were assigned to each habitat break:

Subtitidal Exposure < 0%;
0% < Frequently Flooded Mud Flat Exposure < 50%;
50% < Frequently Exposed Mud Flat Exposure < 61.8%
61.8% < Low Salt Marsh Exposure < 81.7%
81.7% < Mid Salt Marsh Exposure < 96.2%
96.2% < High Salt Marsh Exposure < 99.8%
99.8% < Transitional Exposure < 100%

Inspection of Figure 17 shows that the intertidal range of the Edison Plan has been significantly increased over pre-restoration conditions due to the hydraulic efficiencies achieved by the combined restoration (SCE, 2005). The intertidal mud flats have expanded to lower elevations due to depression of the pre-restoration inlet sill depths, and the upper limits of mid and high marsh have been raised due to reduced tidal muting above mean higher-high water (MHHW = +2.81ft. NGVD). However, the addition of W-19 with it's 13.7% additional tidal prism will depress the inlet sill by 0.13 ft from its original calculated depth at z = -0.89 ft with the Edison Plan to z = 1.03 ft with the addition of W-19. This change will slightly reduce the amount of sub-tidal habitat supported by the restoration relative to that quoted in the EIR/EIS, but will increase the area of frequently flooded mud flat.

The green line in Figures 17 shows the hydroperiod function calculated for the Edison Plan with the W -19 tidal basins and the widened I-5 bridge. The fact that the green and red lines in Figure 17 have exactly the same footprint indicates that the habitat breaks of the lagoon system are not materially altered by the wider I-5 bridge. Regardless of bridge

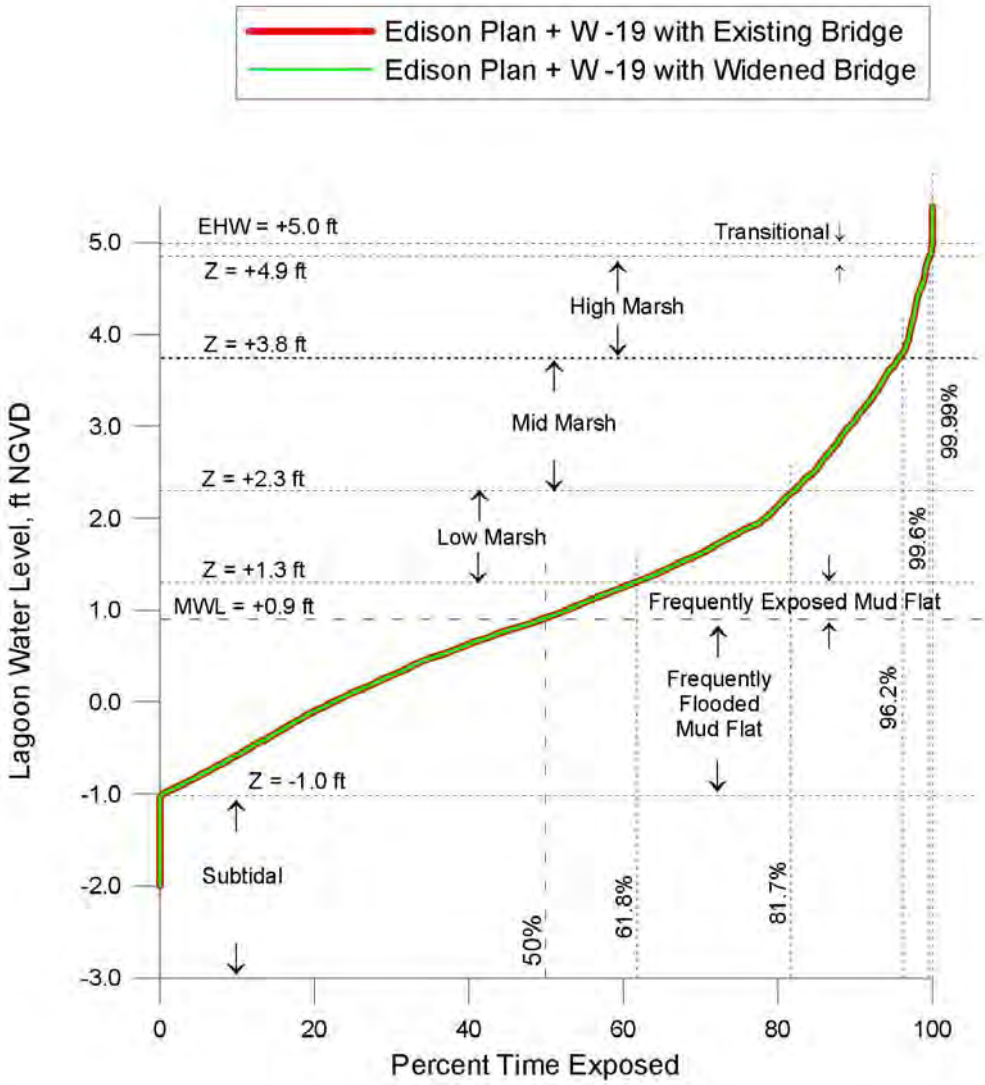

Figure 17: Hydroperiod function for the Edison Plan with Basin W-19 added for: existing I-5 bridge (red) propsed widened I-5 bridge (green). Inlet Sediment Trap at -2 ft NGVD. Habitat divisions from Josselyn and Whelchel (1999).

type, we find that W-19 will create the following mix salt marsh habitat: a) 4.84 acres of sub-tidal (fish) habitat; b) 5.09 acres of frequently flooded mud flat; c) 4.98 acres of frequently exposed mud flat; d) 12.24 acres of low salt marsh; e) 9.92 acres of mid salt marsh; f) 1.94 acres of high salt marsh; and, g) 0.24 acres of transitional habitat. This mix of habitat adds up to 39.25 acres. The 0.75 acre discrepancy between the hydroperiod derived habitat count and the inundation histogram in Figure 6 is due to the fact that the hydroperiod protocol in Figure 17 (as adopted from the certified EIR/EIS) does not acknowledge any salt water influenced or transitional habitat above +5.0 ft NGVD,

whereas the 1980-2007 tides used to derive Figure 6 caused salt water inundation in W-19 up to +5.11 ft NGVD. Moreover, the Coastal Commission did not give Edison any restoration credit for habitat above +4.5 ft NGVD. Using this +4.5 ft NGVD standard, the salt water influenced habitat accounting for W-19 would yield 38.35 acres of coastal wetland creation.

In considering patterns of tidal flow, water level, areas of tidal inundation and hydroperiod in total, it is concluded that the proposed widening of the I-5 bridge results in no significant changes to tidal exchange and habitat divisions relative to existing conditions in San Dieguito Lagoon. This finding was expected since neither the existing nor the widened I-5 bridges have any structural footprint (eg. support piles) located in the active tidal channel under the I-5 bridge. Due to the long bridge span at San Dieguito lagoon (209 m or 686 ft), both the existing and widened bridge bridges are transparent to the tidal circulation.

4) Tidal Hydraulics Impacts of Replacing and Widening the I-5 Bridge at Batiquitos Lagoon:

The I-5 bridge over the tidal channel of Batiquitos Lagoon will be replaced and widened under the current plans for the North Coast Corridor Project; and increases in span length may be a viable option if proven to be cost effective by comparison to conventional wetlands construction or restoration. The present specifications for the replacement I-5 bridge span at Batiquitos Lagoon (referred to as 10+4 buffer) are as follows:

Length of bridge span: 246 feet (75 meters)
Width for existing bridge deck: 154 feet
Width for proposed bridge deck: 229.3 feet (69.88 meters)
Three bridge spans with two rows of cylindrical piers.
Number of piles in each row increased from 6 (existing) to 12 (replacement)
Bridge low chard elevation: 15 feet at south end, 20 feet at north end
Elevation of armored bed: -5.3 feet NGVD (-3 ft MLLW)
Bed width of trapezoidal channel: 106 feet
Side slope of trapezoidal channel: 2 to 1
Width of bench: 38 feet
Elevation of bench: 9.5 feet

4.1) Model Input: The TIDE_FEM model was gridded for the Batiquitos Lagoon bathymetry, based on the most resent lagoon soundings by Merkel and Associates, (2008). The 2008 survey did not provide bathymetric information above +5 ft MLLW; so consequently those data had to be merged with other survey data to obtain a complete picture of the lagoon over the entire tidal range. We began this merging exercise by building a bathymetric contour map from the 2008 survey data, obtaining bathymetric detail between -20 ft MLLW and + 5 ft MLLW. To fill in the upper mid- and high-marsh intertidal regions, bathymetric contours from the 2009 topographic survey were stitched into the 2008 bathymetric survey contours. The mid-marsh and high marsh contours were obtained from field surveys conducted by WRA for the City of Carlsbad that were overlaid on a 3D terrain map to determine the elevation of each point. There was some variation in the elevations of these points from different transects (due primarily to the limitations in accuracy of both the GPS data and the original 1' contours). To compensate for this and to determine the appropriate MHW elevation for the lagoon, WRA took the mean elevation of all of the MHW points. WRA repeated this averaging procedure to create the 0.5 ft, 1 ft, 1.5 ft and 2 ft above MHW contour lines. While this procedure worked quite well throughout much of the lagoon, when creating a 3D model

of the terrain in very flat (or topographically complex) portions of the lagoon the software encountered data gaps that resulted in fairly erroneous topographic data in these areas. This could not be avoided when using 1 ft contours. There were relatively few regions of error, and based on fairly straightforward vegetative signatures on the aerials; and using this vegetation data, WRA was able to manually correct the topography.

Upon completion of vetting the topographic data using vegetation types for co-registration, the six mid and high marsh contours between + 2 ft MLLW and extreme high water at + 7.7 ft MLLW were stitched into the master bathymetric file for Batiquitos Lagoon, producing the bathymetric map shown in Figure 17. The TIDE_FEM tidal hydraulics model presented in Jenkins and Inman (1999) was gridded for a computational mesh of Batiquitos Lagoon built off the Figure 18 bathymetry. Of particular interest to the finite element mesh is the *hydraulic friction slope coefficient*, S_{fj}, providing tidal muting effects. Two separate formulations are used. One is given for the 3-node triangular elements situated in the interior of the mesh which do not experience successive wetting and drying during each tide cycle. The other formulation is for the elements situated along the wet and dry boundaries of the lagoon. These have been formulated as 3-node triangular elements with one curved side based upon the cubic-spline matrices developed by Weiyan (1992). These two sets of elements were assembled into a computational mesh of the lagoon conforming to the lagoon extreme high waterline in Figure 18. The wet-dry boundary coordinates of the curved waterline, (x', y'), are linearly interpolated for any given water elevation from the contours stored in the lagoon bathymetry file based on the updated lagoon bathymetry.

We consider five sub-sets of lagoon bathymetry for alternative tidal hydraulics simulations: 1) The existing lagoon bathymetry using the proposed 246 ft replacement bridge span (Figure 19a) with its associated hard-bottom channel at -3 ft MLLW (-5.3 ft NGVD); 2) The existing lagoon bathymetry using the proposed 246 ft replacement bridge span with flow fences (Figure 20a, blue) retrofitted to the existing hard-bottom channel; 3) Slight modification to existing lagoon bathymetry by removal of a portion of the road bed fill to accommodate doubling the width of the existing channel along existing grade with hard bottom at -3 ft MLLW. This alternative requires doubling the replacement bridge span to 492 ft (*double-wide* alternative); 4) Slight modification to existing lagoon bathymetry by removal of a portion of the road bed fill to increase the bed width of the hard bottom channel to 180 ft while lowering the channel bottom to -4.7 ft MLLW (-7 ft NGVD) along 2 on 1 side slopes (*Chang-channel*, Figure 19b). This alternative allows the replacement bridge span to remain at 246 ft; and 5) The slightly modified lagoon

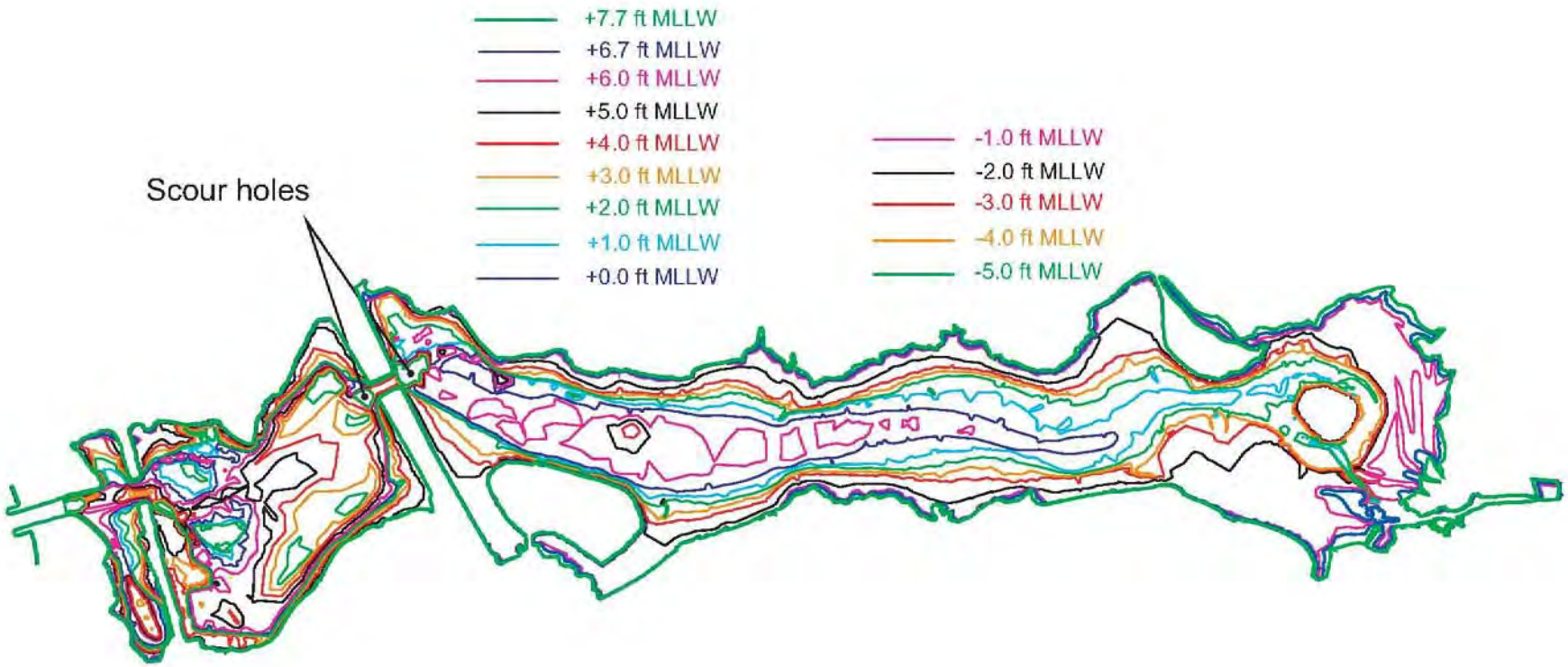

Figure 18. Bathymetry of Batiquitos Lagoon based on 2008 survey merged with land topographic survey 2009, contours in ft MLLW.

bathymetry with the Chang-channel and flow fences (Figure 20b) using the proposed 246 ft replacement bridge span.

The theory behind the double-wide channel alternative (alternative 3) is to remediate tidal muting effects of the narrow bridge waterway at the Batiquitos I-5 bridge choke point. The double-wide channel alternative would double the width of the tidal channel along the existing grade of the south bank and require increasing the span of the North Coast Corridor Project from 246 ft (78) m to 492 ft (156 m). Channel width increases effect only the south bank because the I-5 grades upward to higher ground toward the north (requiring more fill and longer bridge spans if the channel were widened in that direction); while the I-5 road bed and fill grades downward toward the south. Also, most of the vegetation around the bridge footing and road bed on the south side of the channel appears to be ruderal. Due to buried infrastructure concerns, the double-wide concept retains the hard channel bottom feature at -3 ft MLLW (-4.7 ft NGVD).

The theory behind the Chang-channel was to increase the cross section of the bridge waterway channel without requiring an increase in the span of the replacement bridge. The specifications for the Chang-channel alternative in Figure 18 b are:

1) Bridge span: Use the existing bridge span of 75 m (246 feet) with no change.
2) Bridge deck width: The planned new deck width of 229.3 feet is wider than the existing deck width of 154 feet.
3) Channel bottom elevation: The existing bed elevation of 0 foot will be lowered to the new bottom elevation of -7 feet NGVD (-4.7 ft MLLW), to be consistent with the adjacent channel bed.
4) Armoring of the channel: The channel cross section at the bridge crossing will be armored to avoid excessive abutment scour.
5) Channel bench: A 16-foot wide bench will be installed on each side of the channel. The bench has the top elevation of 8 feet in order to cover the pile caps supporting the bridge piers.
6) Side slope of channel: The channel has the one-on-one side slope, steeper than the 2 on 1 existing side slope.
7) Bed width of channel: The channel has the bed width of 180 feet.

The concept behind the flow fence is to achieve more complete pressure recovery of the velocity head through the narrowest portion of the bridge waterway channel (choke point). These flow fences are typically constructed of vertically driven sheet pile and are referred to as the “Stratford Fence” because they are based on the optimal turbulent

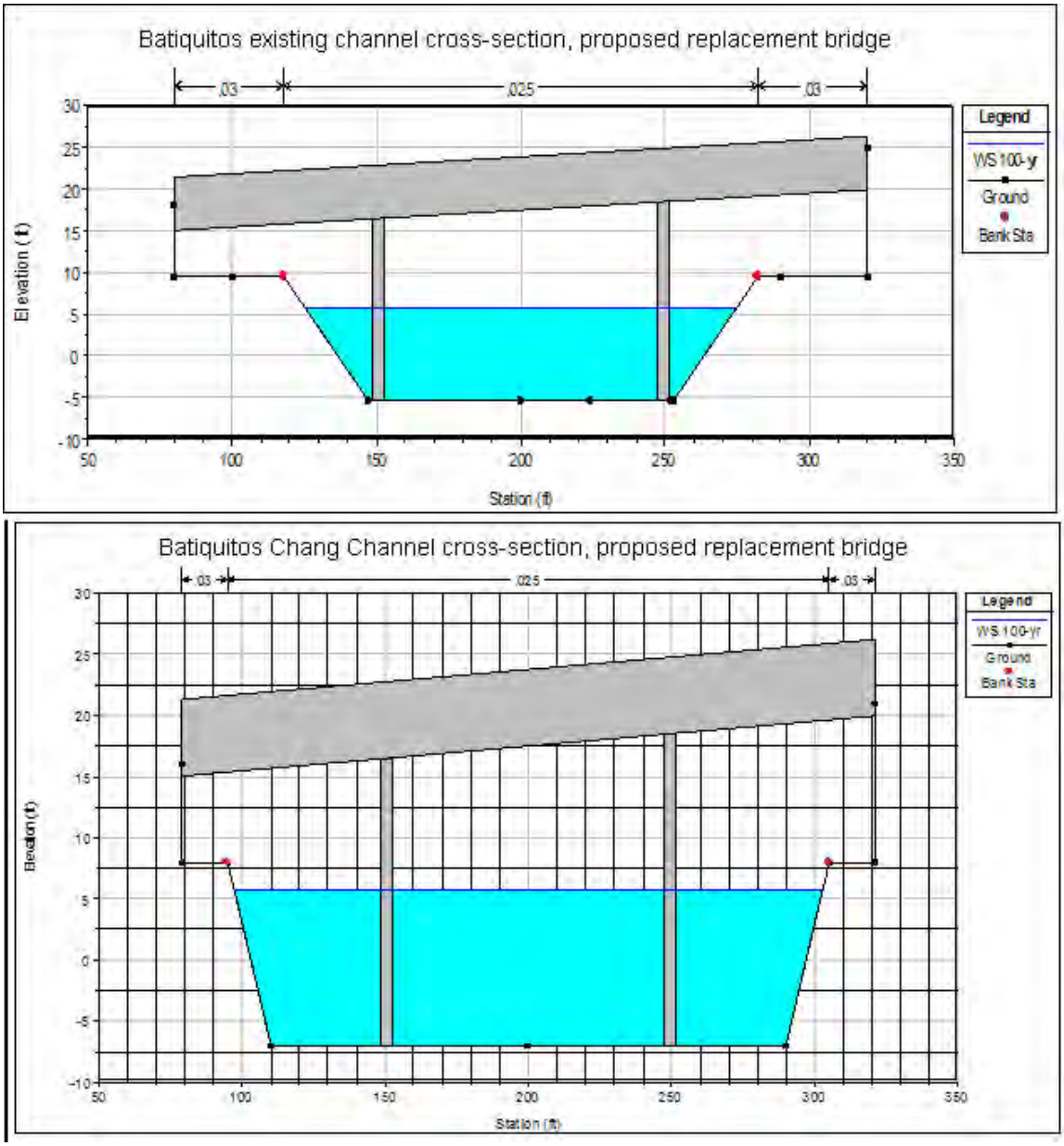

Figure 19: Bridge and Channel Cross Sections: a) proposed I-5 replacement span and existing bridge waterway channel cross section (upper panel); b) proposed I-5 replacement span with increased bridge waterway channel cross section (lower panel), referred to as the *Chang-channel* (lower panel). All elevations are in feet NGVD.

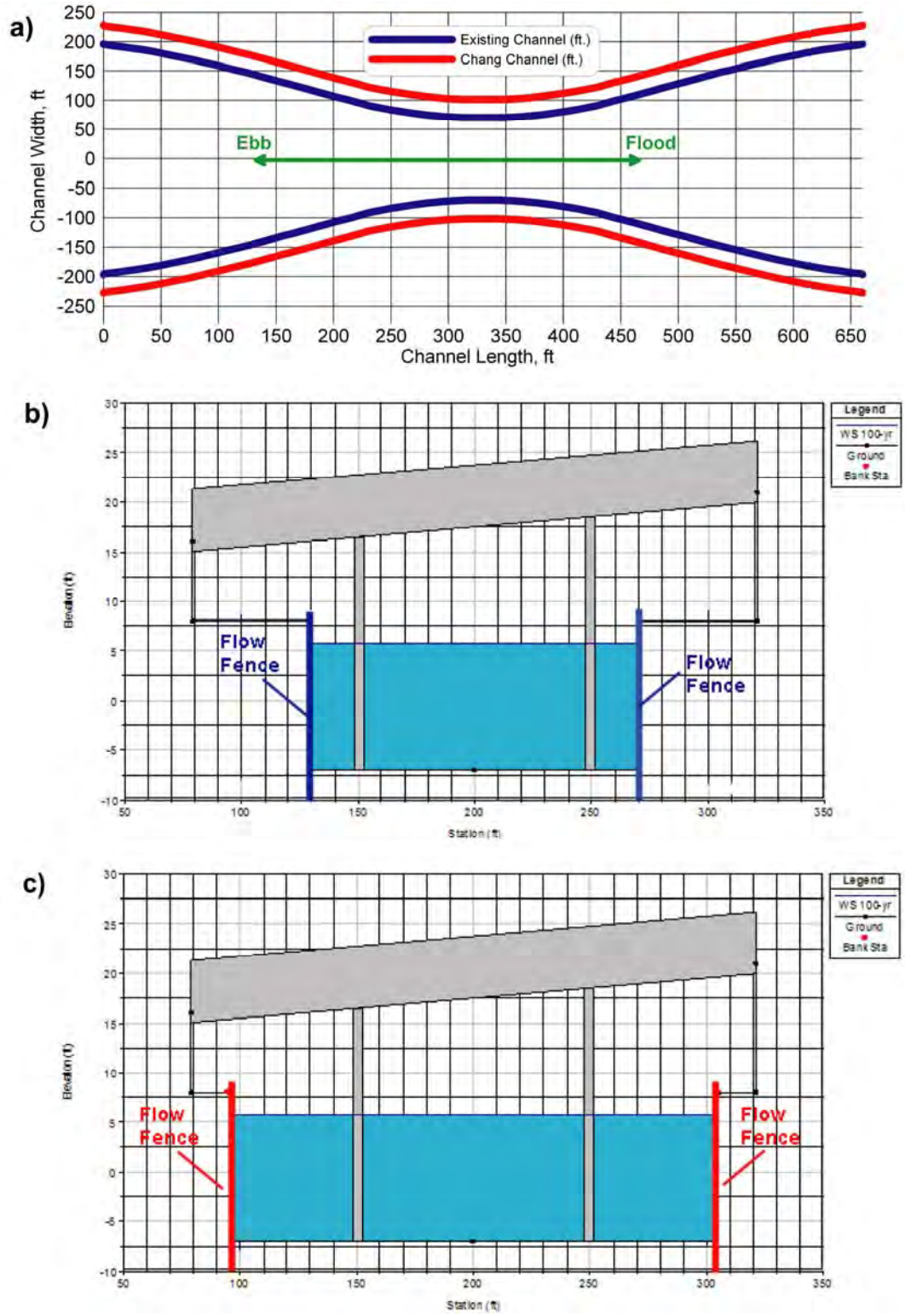

Figure 20. a) Flow Fence design for pressure recover of velocity head through I-5 bridge waterway; b) existing channel cross section with flow fence; c) Chang channel cross section with flow fence.

pressure recovery relations due to Stratford (1959 a and b). B.S. Stratford developed an analytic solution for a pressure recovery distribution in a turbulent flow which both avoids flow separation while maintaining zero wall friction over the entire pressure recovery length. This solution is now widely regarded as a universal law for the minimum energy dissipation in a turbulent flow. It has been used to optimize turbine blades, lifting bodies, aircraft wings, ground effects tunnels and wings for race cars, flow nozzles and diffusers (see Liebeck, 1976). The present application of the Stratford pressure recovery to tidal channel choke points is very similar to the prior applications to flow nozzles. The primary distinction is that tidal flow through a choke point is bi-directional, whereas prior nozzle applications have been made for unidirectional flows.

Stratford recovery is sometimes referred to as "imminent separation recovery" because it works by keeping the flow on the verge of separation throughout the entire deceleration without actually separating. This principle works by keeping the flows downstream of the choke point on the verge of separation without actually separating. In this condition, vortex formation is prevented while velocity shear at the wall is close to zero; and, consequently, the friction nearly vanishes. While this occurs, kinetic energy of the velocity head is reconverted into pressure as the local flow decelerates into the receiving basin, hence the notion of pressure recovery. To avoid dependence on the exact pressure and velocity of a particular flow, the pressure recovery is expressed in terms of pressure coefficient, $\overline{C}_P$, and local Reynolds number $R_{e\sigma_0}$ defined as

$$\overline{C}_p = \frac{p - p_0}{1/2\rho v_0^2}\ , \qquad R_{e\sigma_0} = \frac{v_0\sigma_0}{\nu} \tag{2}$$

Here $v = v_0$ is the maximum local velocity of the flow at a point $\sigma = \sigma_0$ where the pressure recovery is initiated; p_0 is the static pressure at $\sigma = \sigma_0$; and p is the local static pressure at any point along the pressure recovery length $\sigma > \sigma_0$. The canonical coordinate, σ, is a non-dimensional form of the curvilinear coordinate s that is measured along the surface of the flow fence from the upstream stagnation point at $s = s_p$; and σ_0 corresponds to the location of the choke point at $s = s_0$. To maximize the expanse of low drag laminar boundary layers along the flow fence , Liebeck (1976) has shown that the optimal placement of the choke point channel half-width, *t*, is given by:

$$\sigma_0 = 38.2\left(R_{e\sigma_0}\right)^{-3/8}\left[\int_{s_p}^{s_o}\left(\frac{v}{v_0}\right)^5 d\left(\frac{s}{s_0 - s_p}\right)\right]^{-5/8} \qquad (3)$$

When $\overline{C}_P = 0$ the flow is at its maximum velocity, v_0, and is about to convert the velocity head, $1/2\rho v_0^{\ 2}$, back into pressure, whence $\overline{C}_P > 0$. If the flow reconverts all of its velocity head into pressure (total pressure recovery), then the flow would be brought to rest or $v = 0$ at $\sigma = 1.0$. This is a condition known as stagnation for which the pressure coefficient has a maximum value of $\overline{C}_P = 1.0$.

In the design of our flow fences we use an analytic formulation to specify the pressure recovery distribution in terms of $\overline{C}_P$ versus σ, and then solve the inverse problem for the physical shape of a given thickness that produces that pressure distribution. The analytic relation for the pressure recovery distribution is in the public domain and was published by Stratford, (1959 a & b). It is given by:

$$\overline{C}_P = 0.49\left\{\left(R_{e\sigma_0}\right)^{1/5}\left[\left(\frac{\sigma}{\sigma_0}\right)^{1/5} - 1.0\right]\right\}^{1/3} \qquad \text{for} \quad \overline{C}_P \le \frac{4}{7}$$

(4a)

Or:

$$\overline{C}_P = 1.0 - \frac{t}{\left[\dfrac{\sigma}{\sigma_0} + c\right]^{1/2}} \qquad \text{for} \quad \overline{C}_P > \frac{4}{7}$$

(4b)

The pressure recovery relations in (4a & 4b) produce an initial sharp increase in $\overline{C}_P$ (deceleration) immediately after the pressure recovery begins at $\sigma = \sigma_0$. This places the flow on the verge of separation; but the initial flow deceleration is not made so large as to

actually induce separation. Further flow deceleration and increases in $\overline{C}_p$ are made progressively more and more gradual in the downstream direction. This produces a concave pressure recovery distribution known as a "pressure recovery bucket." Stratford proved that the concave pressure recovery distribution had a stabilizing influence on a decelerating flow that was close to separation. The use of these pressure recovery relations gives our flow fence plan view contours in Figure 20a their distinctive concave expansion section.With this expansion section, eddy formation is prevented while velocity shear at the wall is close to zero; consequently, the turbulent wall friction nearly vanishes. This is how most of the energy dissipation is avoided and how most of the kinetic energy of the velocity head is reconverted into pressure. These relations specify a change in flow velocity with distance along the waterway channel axis that allows for maximum conversion of velocity head in the channel to pressure head once the channel empties into the tidal basin. Examples of the optimal velocity curves in the plan-view channel space of the I-5 bridge at Batiquitos Lagoon are shown in Figure 20 when retrofitted to the existing bridge waterway channel (red) and the Chang-channel (blue). This optimal velocity curve is constrained by existing depths of the tidal basins and by the width of the bridge waterway, and is used to solve the inverse problem for the physical shape of either a flow fence or a contoured hard bottom.

Aside from gridding the TIDE_FEM tidal model, stage area and storage rating functions were calculated from the bathymetric contours of Figure 18. Figure 21 gives the stage area function of the intertidal East Basin in isolation, while Figure 22 gives the stage area function of the sub-tidal portion of the East Basin. From calculations of the historic MHHW and MLLW water levels in the East Basin (see Table 2.1, Merkel, 2008), Batiquitos Lagoon presently supports 191.4 acres of intertidal habitat east of the I-5 bridge. The intertidal polynomial in Figure 20 is almost linear, suggesting a man-made basin at constant grade. It suggests that more efficient bridge waterways could create 3.2 acres of new high marsh from for every tenth of a foot increase in tidal inundation achieved above the historic MHHW, (red dashed line). The sub-tidal stage area function in Figure 22 is also interesting because it is exponential, suggesting a scour feature; and indeed, nearly all of the sub-tidal area is contained within the scour holes immediately east of the I-5 bridge. Figure 23 gives the composite storage rating function of the entire Batiquitos Lagoon system. The stage area functions of each basin were integrated vertically to compute polynomial coefficients for the storage rating function of the entire system, as plotted in Figure 23. The polynomial derived from Figure 23 is also required in the initialization of the TIDE_FEM tidal hydraulics model. From historic MHHW and MLLW levels in the lagoon, as reported in Merkel (2008), it is concluded that the mean diurnal tidal prism of Batiquitos Lagoon is presently 1,515 acre-ft.

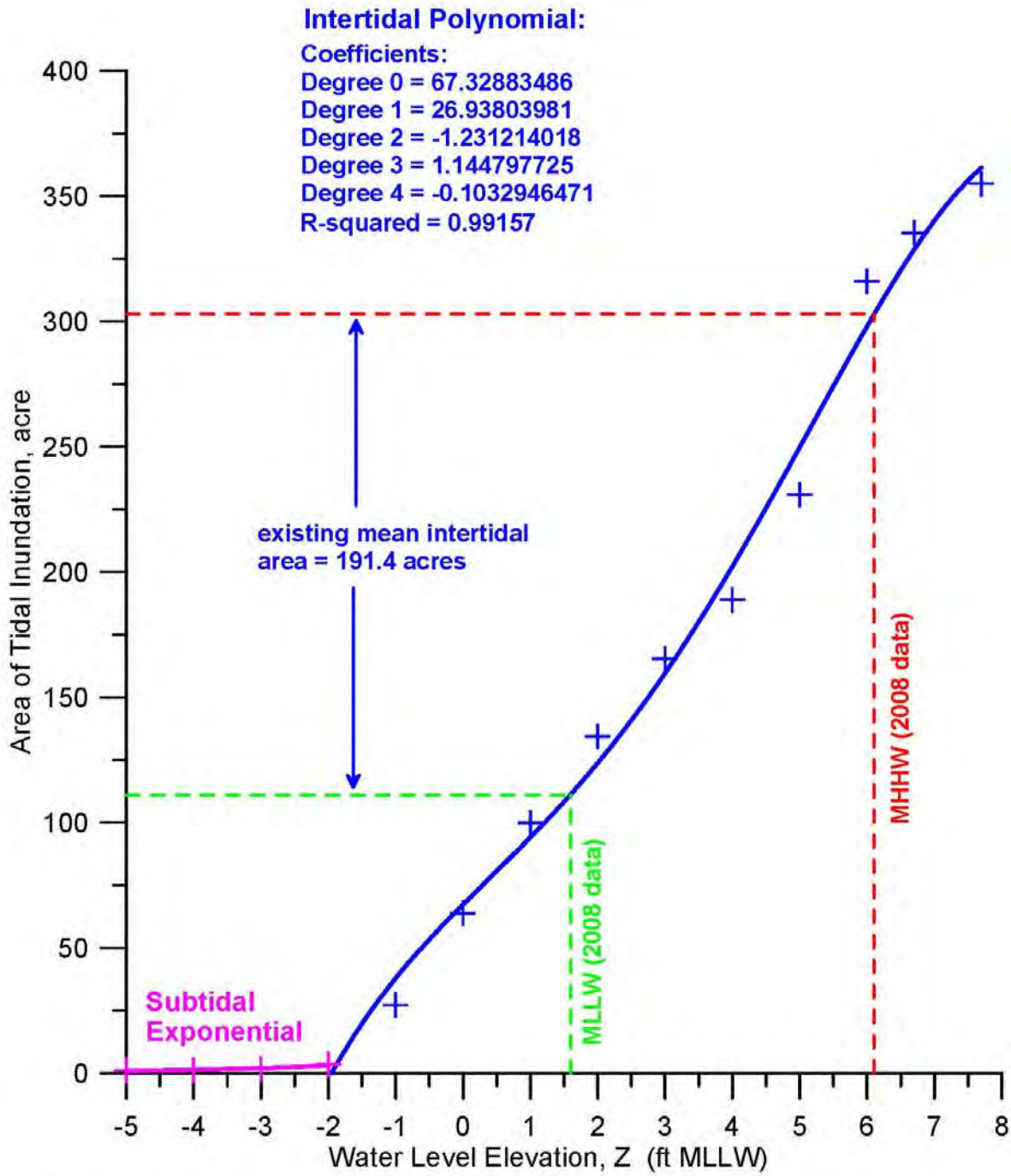

Figure 21. Area of tidal inundation in the east basin of Batiquitos Lagoon as a function of water level elevation (stage area function from 2008 soundings). Mean water levels for existing conditions from Merkel (2008, Table 2.1)

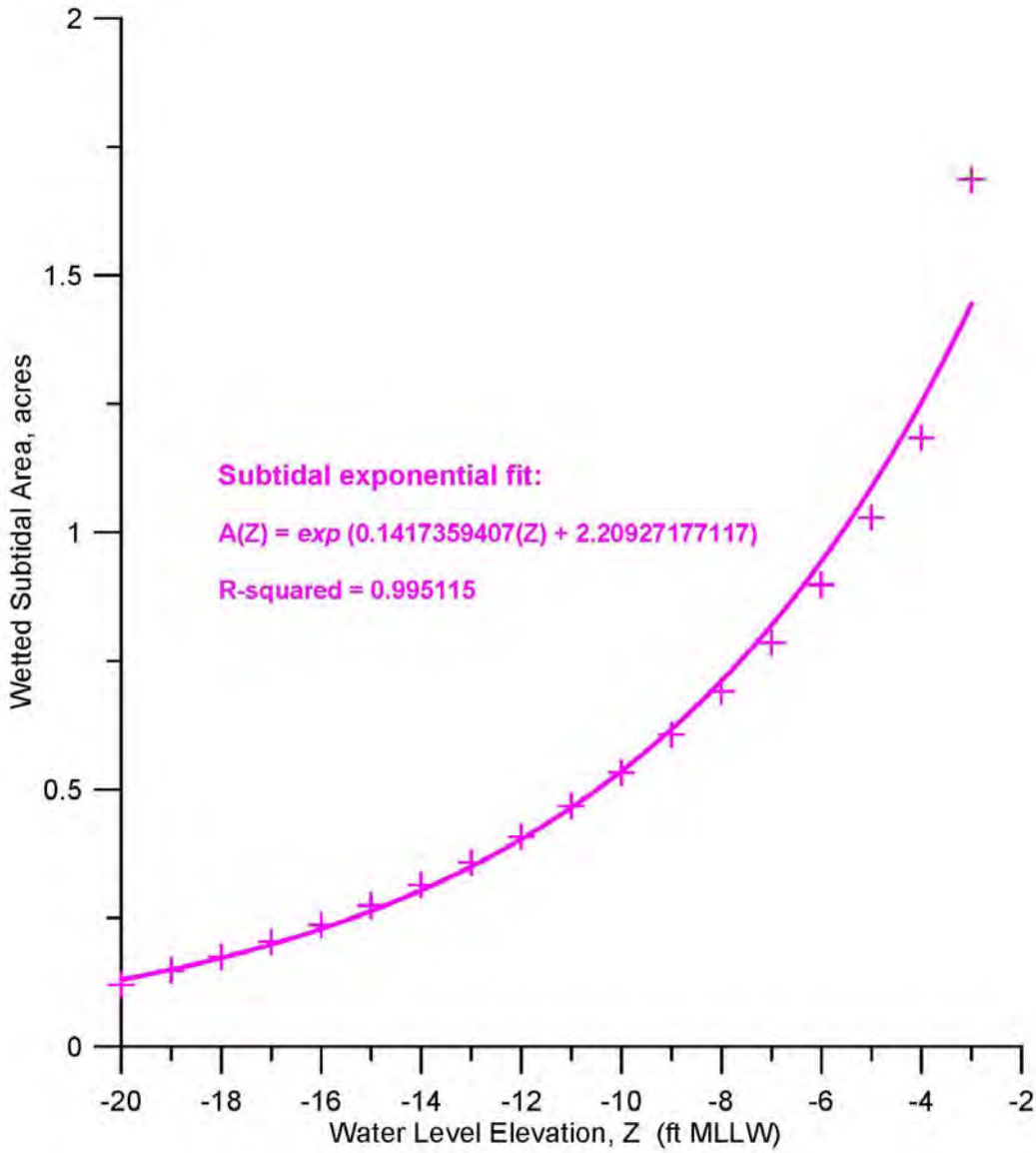

Figure 22. Subtidal area in the east basin of Batiquitos Lagoon as a function of depth (from 2008 soundings)

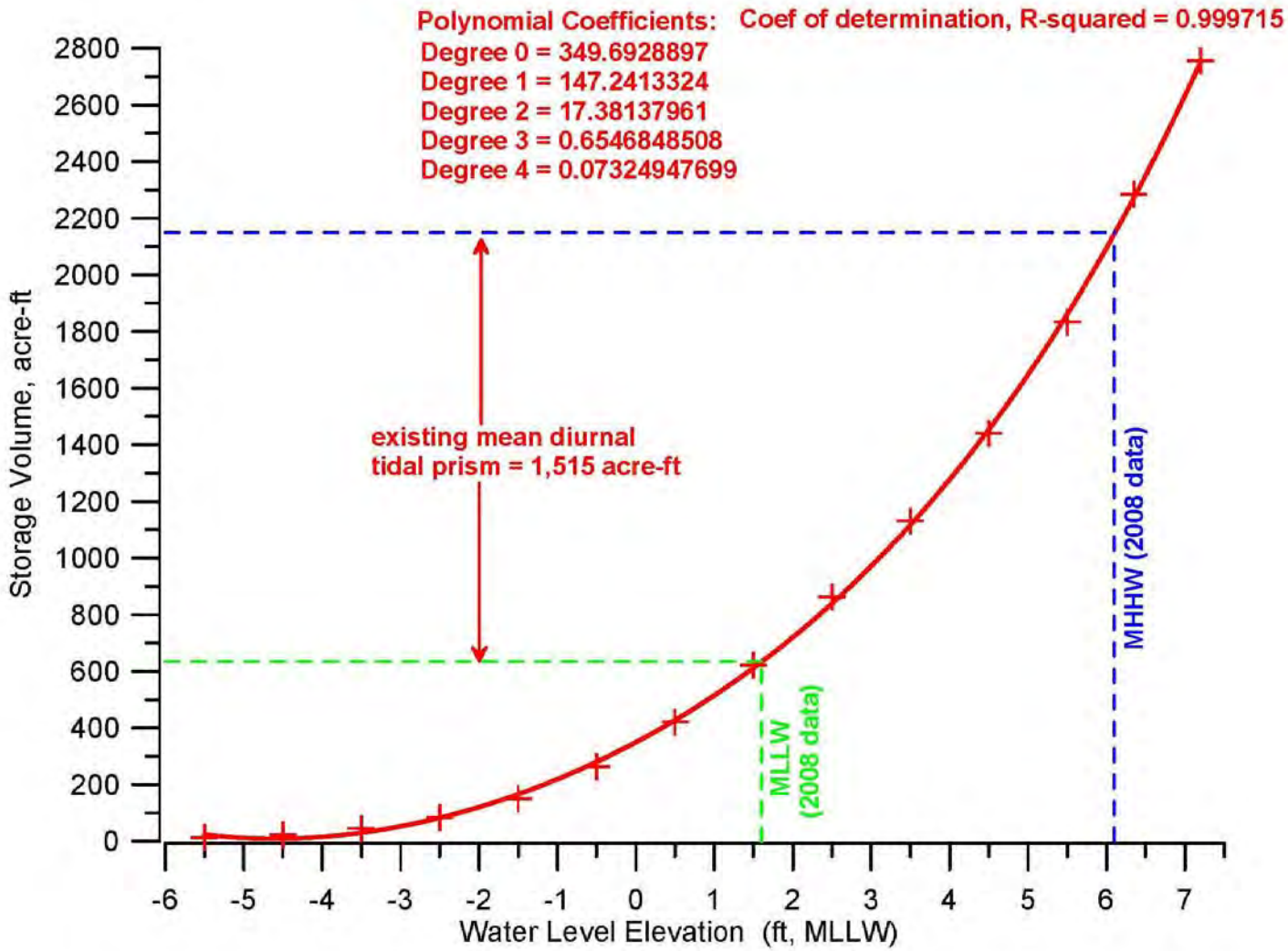

Figure 23. Storage rating function for Batiquitos Lagoon, based on 2008 sounding. Mean water levels for existing conditions from Merkel (2008, Table 2.1)

4.2) Model Calibration and Assessment of Existing Conditions: Spring, neap and mean tidal range simulations of the hydraulics of Batiquitos Lagoon were performed using astronomic tidal forcing functions at 2 sec time step intervals for the period 1980-2007, as discussed in Section 2.1. Computed water surface elevations and depth-averaged velocities from the global solution matrix were converted to lagoon waterline contours and flow trajectories. Calibrations for determining the appropriate Manning factors and eddy viscosities were performed by running the TIDE_FEM model on the Figure 17 bathymetry file and comparing calculated water surface elevations in the West, Central and East Tidal Basins against water level measurements reported in Merkel (2008) during September 2009. Iterative selection of Manning factor n_0 = 0.03406 and an eddy viscosity of ε = 7.355 ft^2/sec gave calculations of water surface elevation in the West, Central and East Basins that reproduced the measured values to within 2% over the 2008 monitoring period.

The most recent water level measurements in Batiquitos Lagoon were taken over a monitoring period of 2 July thru 6 October 2008, (Merkel, 2008). Figure 24 provides a quantitative assessment of the accuracy of the calibrated TIDE_FEM model using water level measurements during spring tides in the east basin of Batiquitos Lagoon during the period of 2-14 July 2008. Figure 24 provides a comparison between East Basin water level variations predicted by the model (red trace) versus the actual water level measurements (black crosses) reported in Merkel (2008). The East Basin water level variations in red are found to lag the ocean water levels (blue trace) by as much as 53.7 minutes at higher high water (HHW) levels on flooding tides while this phase lag averages 180.4 minutes at lower low water (LLW) level during ebb tides. Higher high water levels in the East Basin exceed those in the ocean by +0.22 ft, due to a trapped tidal mode (standing wave) typical of lagoons with large tidal basins and multiple choke point linkages to the ocean tides (Lamb, 1932; LeBlond & Mysak, 1978). Lower low water levels in the East Basin are +2.47 ft above ocean water levels. Thus the East Basin does not fully drain on ebbing tides due to the 180 minute phase lag, and consequently the East Basin tidal range suffers from 2.25 ft of tidal muting relative to ocean tidal ranges, where diurnal spring tide ranges in the ocean are $\Delta\eta$ = 8.89 ft. The amplitudes and degree of non-linearity in the East Basin water level time series simulated by the model closely duplicate that observed in the measured lagoon tides. The maximum error in simulating the low tide elevations was found to be ε_L = +0.08 ft. The maximum high tide error in the model simulation relative to observations was found to be ε_H = -0.04 ft.

Figure 25 compares East Basin water level variations predicted by the model (purple trace) with the actual water level measurements (black crosses) reported in Merkel (2008). The West Basin water level variations in purple are found to lag the ocean water levels (blue trace) by as much as 40.3 minutes at higher high water (HHW) levels on flooding tides; while this phase lag averages 109.4 minutes at lower low water (LLW) level during ebb tides. Higher high water levels in the West Basin are 0.10 ft lower than those in the ocean, while lower low water levels in the west basin are +1.31 ft above ocean water levels. Therefore, the West Basin does not fully drain either on ebbing tides due its 109 minute phase lag, and consequently the West Basin tidal range suffers from

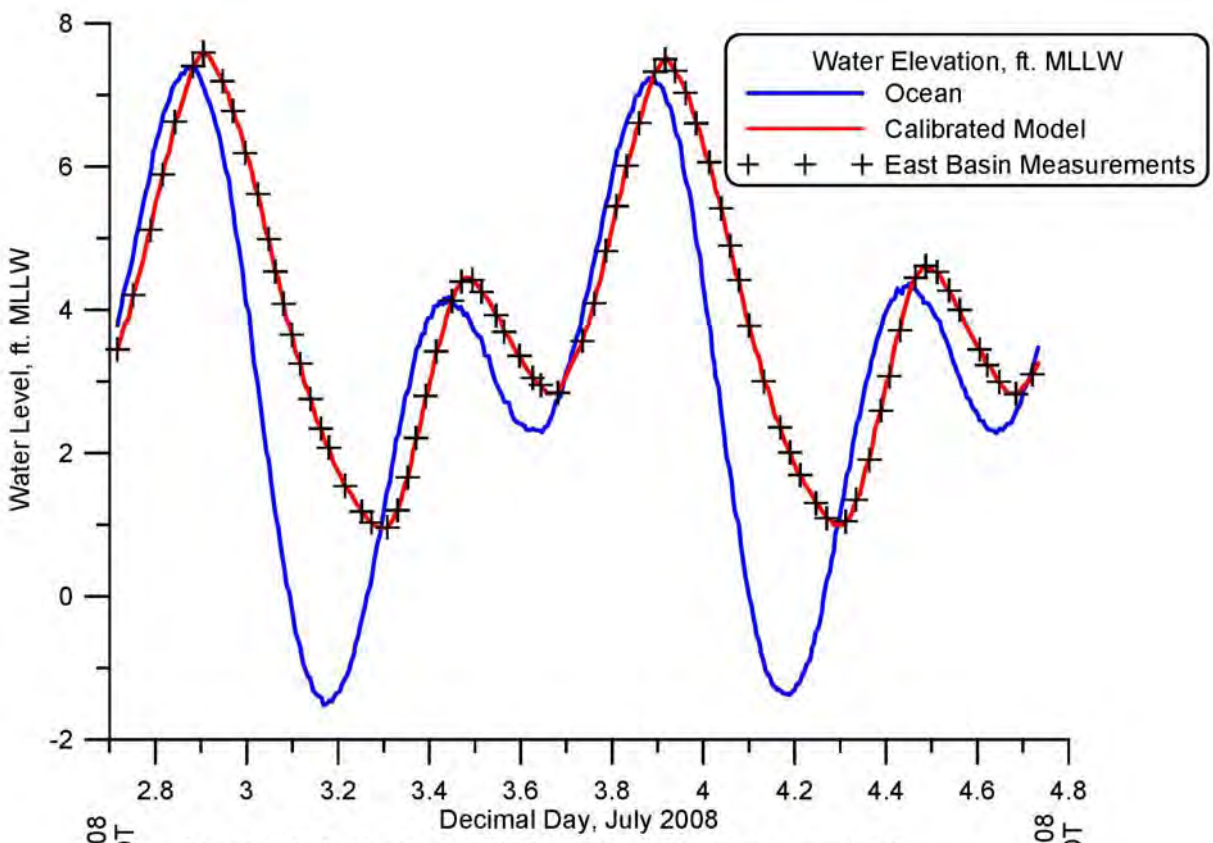

Figure 24. Calibration of TIDE_FEM model using water level measurements at Batiquitos Lagoon, Carlsbad, CA, during spring tides 2 July - 4 July 2008. East Basin water level simulation (red) versus water level measurements (black crosses).

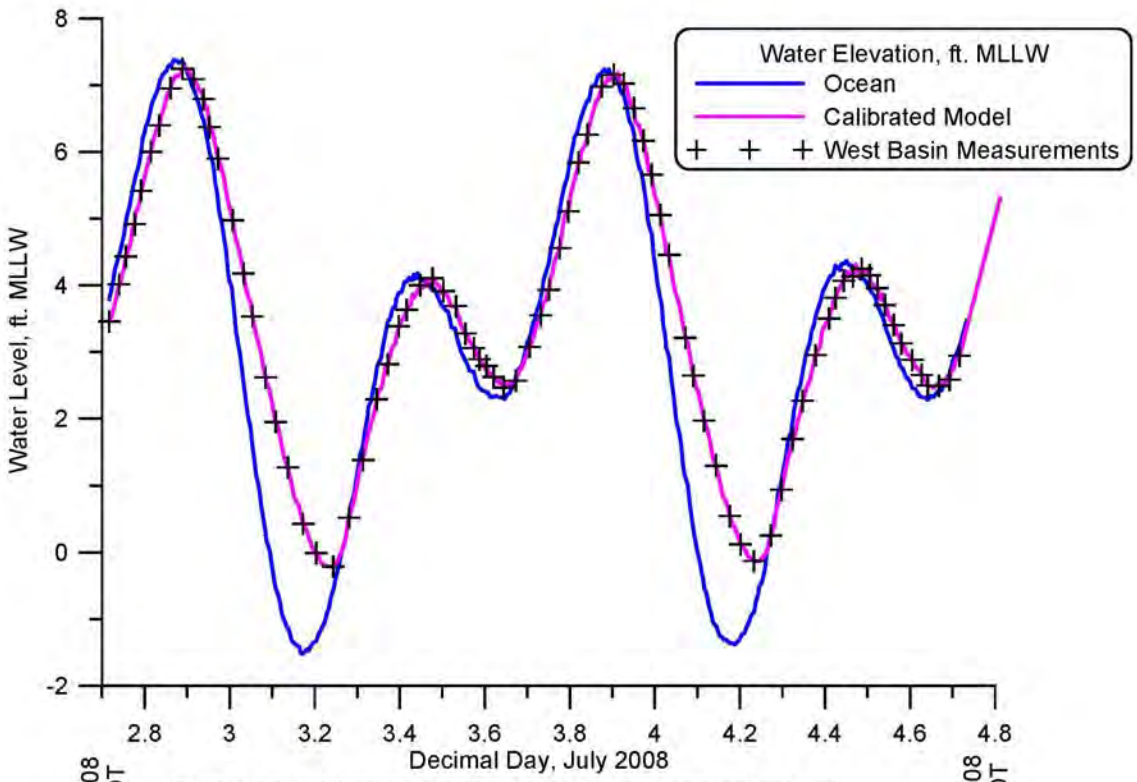

Figure 25. Calibration of TIDE_FEM model using water level measurements at Batiquitos Lagoon, Carlsbad, CA, during spring tides 2 July - 4 July 2008. West Basin water level simulation (purple) versus water level measurements (black crosses).

1.41 ft of tidal muting relative to ocean tidal ranges. From these numbers it is apparent that about 63% of the tidal muting of the East Basin is attributable to the choke point at the PCH where the hardened ocean inlet channel crosses the barrier sand spit that segregates the lagoon from the beach. The amplitudes and degree of non-linearity in the West Basin water level time series simulated by the model closely duplicate that observed in the measured lagoon tides. The maximum error in simulating the low tide elevations was found to be ε_L = +0.075 ft. The maximum high tide error in the model simulation relative to observations was found to be ε_H = -0.035 ft.

Figure 26 compares Central Basin water level variations predicted by the model (green trace) with the actual water level measurements (black crosses) reported in Merkel (2008). The Central Basin water level variations in green are found to lag the ocean water levels (blue trace) by as much as 43.8 minutes at higher high water (HHW) levels on flooding tides; while this phase lag averages 124 minutes at lower low water (LLW) level during ebb tides. Higher high water levels in the Central Basin are 0.04 ft higher than those in the ocean, while lower low water levels in the West Basin are +1.77 ft above

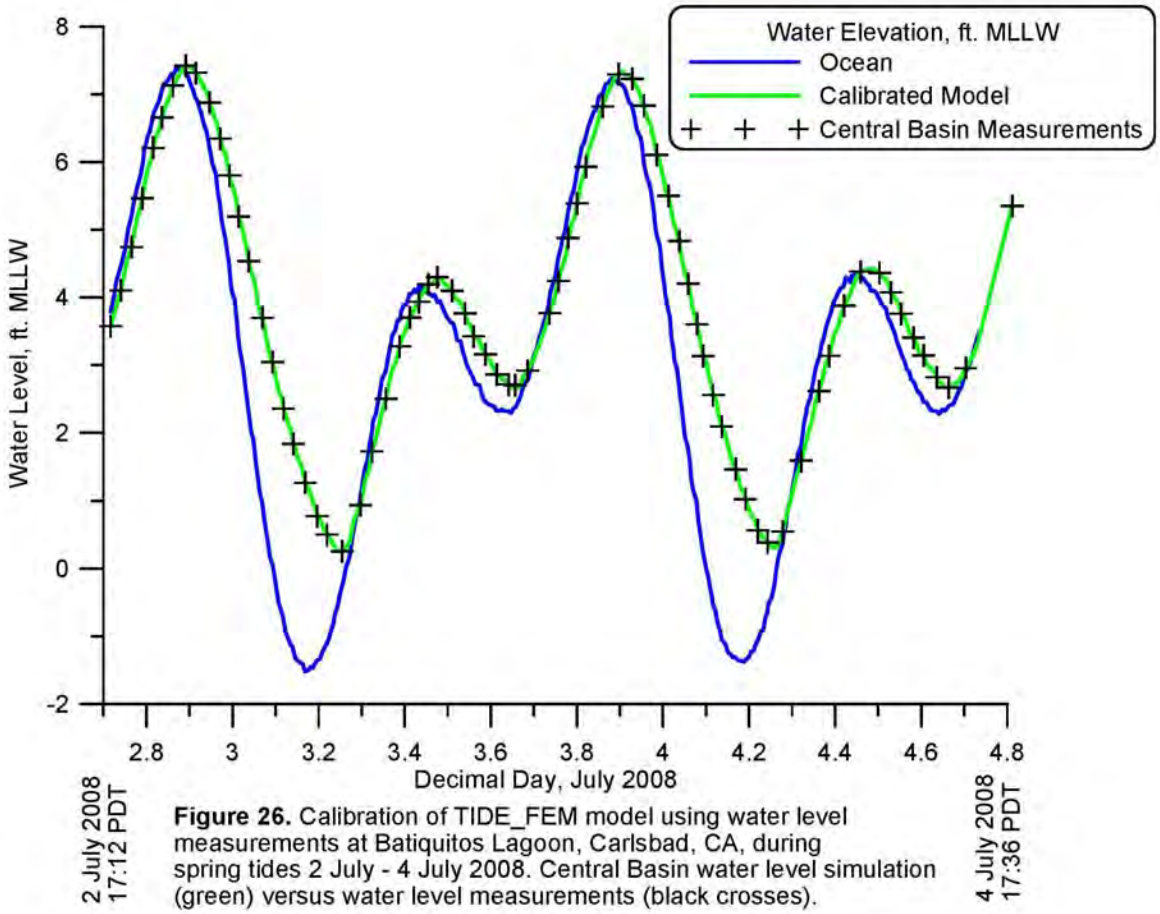

Figure 26. Calibration of TIDE_FEM model using water level measurements at Batiquitos Lagoon, Carlsbad, CA, during spring tides 2 July - 4 July 2008. Central Basin water level simulation (green) versus water level measurements (black crosses).

ocean water levels. Therefore the Central Basin also does not fully drain on ebbing tides due its 124 minute phase lag, and consequently the Central Basin tidal range suffers from 1.72 ft of tidal muting relative to ocean tidal ranges. From these numbers it is apparent that about 76% of the tidal muting of the East Basin is attributable to the combination of choke points at the PCH and railroad bridges. The amplitudes and degree of non-linearity in the West Basin water level time series simulated by the model closely duplicate that observed in the measured lagoon tides. The maximum error in simulating the low tide elevations was found to be ε_L = +0.075 ft. The maximum high tide error in the model simulation relative to observations was found to be ε_H = -0.035 ft.

In all three cases of the West, Central and East Basin water levels, the calibration error appears to exhibit a systematic tendency. When amplitude errors occur they tend to over estimate the water elevation of the LLW tidal stage, and under estimate the water elevation of the HHW tidal stage. Although these errors are quite small and may be considered high predictive skill, this error mode would be consistent with *bathymetry errors* in which depth has been under estimated, Weiyan (1992). Bathymetry errors are the most common cause of modeling errors. Other sources of errors include:

ELEMENT INTERPOLATION ERROR: Due to the degree of the polynomial used to specify shape function, N_i.

DISCRETIZATION ERRORS: Due to mesh coarseness and approximating the curved wet/dry boundary side of an element with a quadratic spline.

QUADRATURE ERRORS: Due to reducing the weighted residual integrals with the influence coefficient matrices.

ITERATION ERRORS: Due to solving the system of algebraic equations reduced from the Galerkin Equations.

ROUNDOFF ERRORS: Due to time integration by the trapezoidal rule.

SEA LEVEL ANOMALIES: Due to discrepancies between the astronomic tides and the actual observed water levels in the ocean.

INSUFFICIENT CALIBRATION DATA: Due to limitations in the period of record.

In Figure 27a, auto spectra of the ocean tides (black, upper panel) shows the predominant energy is centered on a diurnal frequency of the K1 lunar-solar diurnal tidal constituent at $f_{K1} = 1.16079 \text{ x } 10^{-5}$ Hz. The energy in this peak is disproportionately high relative to the next largest spectral peak occurring at the M2 principal lunar semi-diurnal tidal constituent, $f_{M2} = 2.2365 \text{ x } 10^{-5}$ Hz. The excess energy at diurnal frequencies is believed to be non-tidal and attributable to a wind-driven current component that has a diurnal fluctuation in response to daily heating of the land. With the onset of a strong thermal low over the inland deserts during July 2008, this diurnal sea breeze component would be expected to be very strong in the time frame of the lagoon monitoring.

Other less energetic tidal peaks are also found in the spectra of Figure 27a, including one believed to be a baroclinic *shelf resonance* formed by a resonant *triad* at the sum of the frequencies of the K1 and M2 barotropic tides, ie a diurnal third harmonic at a frequency $f_3 = f_{K1} + f_{M2} = 3.3973 \text{ x } 10^{-5}$ Hz. This diurnal third harmonic is a baroclinic tide excited by the barotropic K1 and M2 tides interacting with the bottom topography, in particular the local shelf and Scripps Submarine Canyon to the south. Another baroclinic shelf resonance apparent in the spectra of the ocean tides in Figure 27a is a second harmonic of the barotropic M2 tide appearing at a frequency of $2f_{M2} = 4.4730 \text{ x } 10^{-5}$ Hz. The auto spectra of the East Basin tides shown in red in the lower panel of Figure 27b exhibits the same primary barotropic and baroclinic tidal peaks as the ocean tides in the upper panel; with one exception; an additional non-linear resonance appears as a triad formed by the sum of the K1 barotropic mode and the baroclinic second harmonic of the M2 tide, $f_{K1} + 2f_{M2} = 5.6338 \text{ x } 10^{-5}$ Hz. Apparently this mode is excited by non-linear tidal interaction with the lagoon bathymetry.

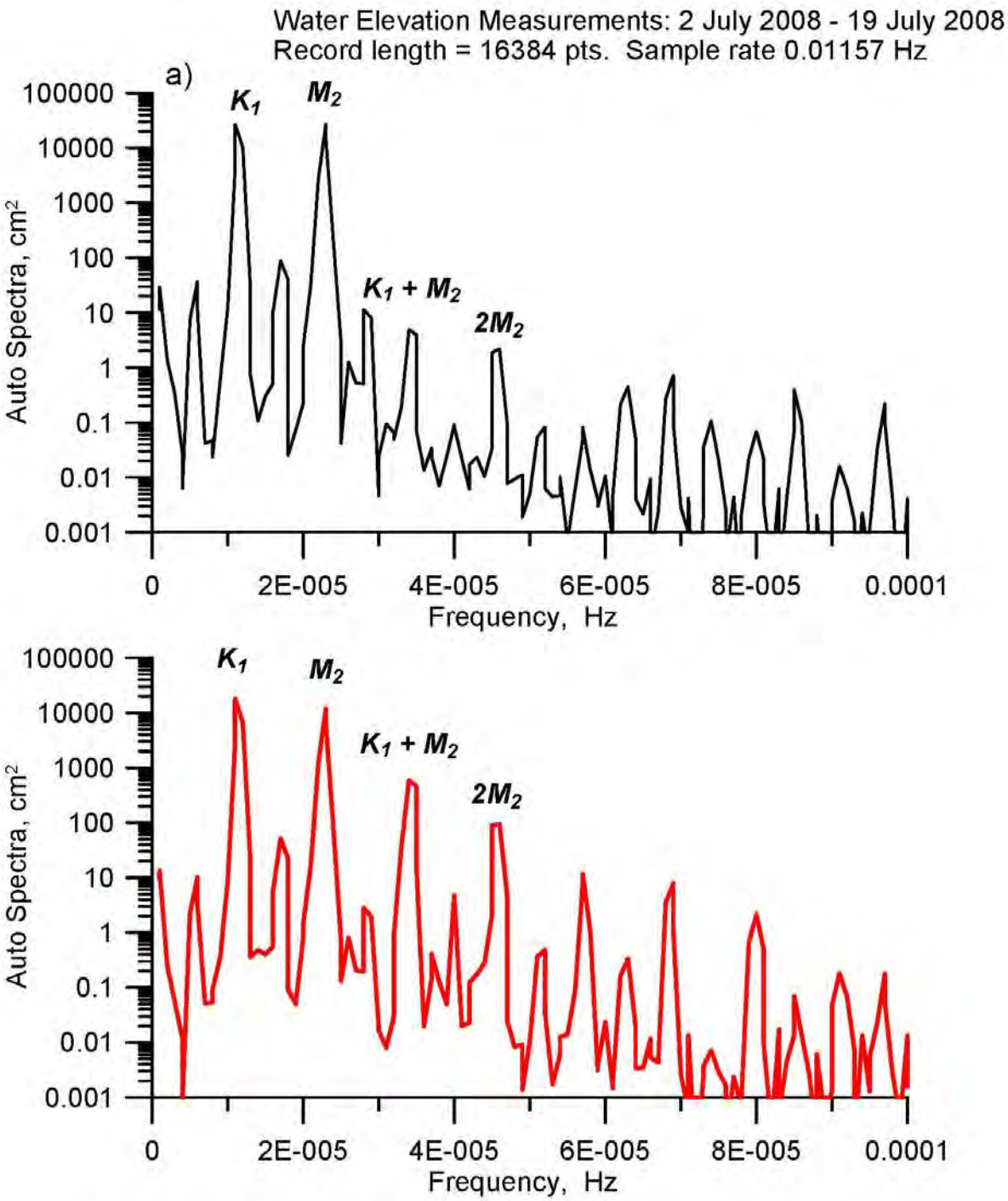

Figure 27. Auto spectra of water level measurements: a) Ocean water level at inlet to Batiquitos Lagoon, b) water level in the East Basin of Batiquitos Lagoon.

Table 4.1 gives a summary of the water level elevations calculated by the calibrated model for Batiquitos Lagoon with the existing I-5 bridge based on long-term tidal simulations using historic ocean water level forcing for the 2008 period of record.

Table 4.1: Water Levels for Batiquitos Lagoon With Existing I-5 Bridge, 2008 Forcing

Elevations Feet MLLW	Ocean	West Basin	Central Basin	East Basin
MEAN HIGHER HIGH WATER (MHHW)	5.7	5.8	6.0	6.1
MEAN HIGH WATER (MHW)	5.0	5.0	5.2	5.3
MEAN LOW WATER (MLW)	1.3	1.6	1.9	2.2
MEAN LOWER LOW WATER (MLLW)	0.4	0.9	1.2	1.6
LOWEST OBSERVED WATER LEVEL	-1.5	-0.2	0.3	0.9
HIGHEST OBSERVED WATER LEVEL	7.4	7.3	7.4	7.6
MAXIMUM TIDAL RANGE	8.9	7.5	7.1	6.7

A quantitative assessment of the predictive skill of the calibrated model over the entire period of monitoring 2 July – 6 October 2008 is provided by Figure 28 for lowest daily water levels in the West, Central, and East Basins, and for phase lags in the three basins in Figure 29. The coefficient of determination of model predictions of daily lowest water level in Figure 28 for the East Basin is found to be R-squares = 0.906, while R-squares = 0.950 for the Central Basin, and R-squares = 0.977 was found for the West Basin. Predictive skill of phase lags in Figure 29 was found to be R-squares = 0.884 in the East Basin; R-squares = 0.697 in the Central Basin and R-squares = 0.551 for the West Basin. Figures 28 and 29 serve to emphasize the controlling effects that the choke points of the I-5, railroad and PCH bridges have on constraining tidal range under existing conditions in the three basins at Batiquitos Lagoon. In Section 4.3.1 we will examine the effects which the I-5 replacement bridge may have on existing conditions and explore possible alternative bridge waterway channels and road bed fill removal options for partially relaxing these choke point constraints on tidal exchange.

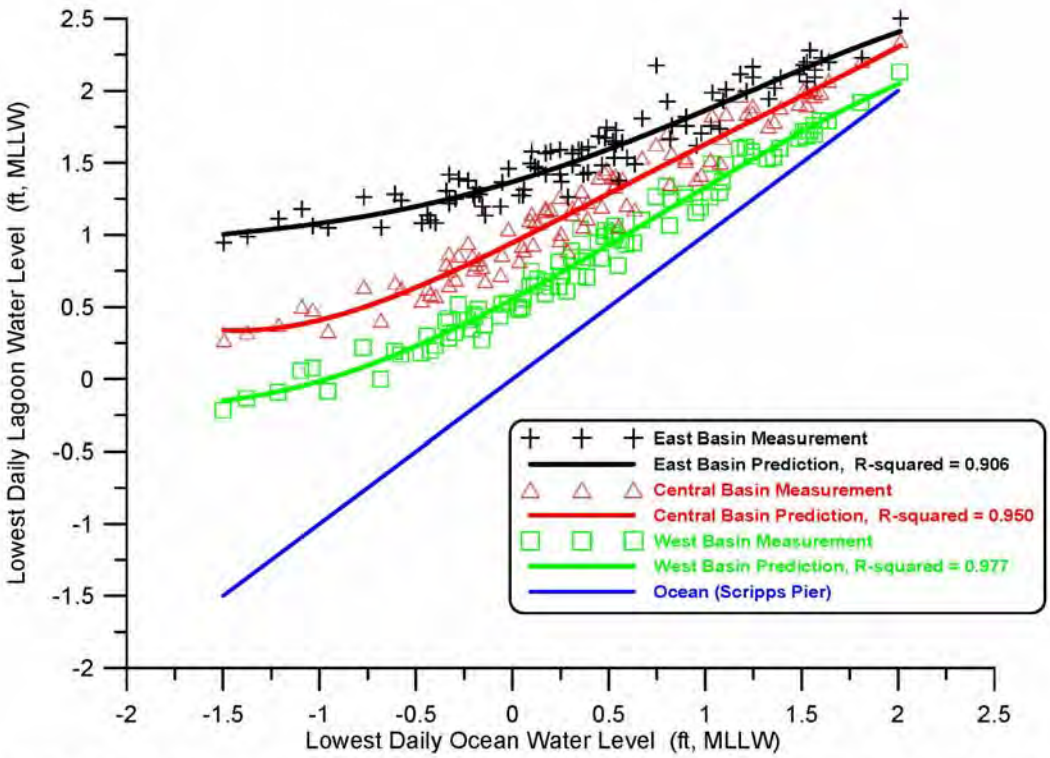

Figure 28. Daily lowest water level in Batiquitos Lagoon versus daily lowest water level in the local ocean as measured at the Scripps Pier tide gage (NOAA #941- 0230). Measured values indicated by symbols, model predictions according to solid lines of matching colors. Water level data after Merkel, (2008)

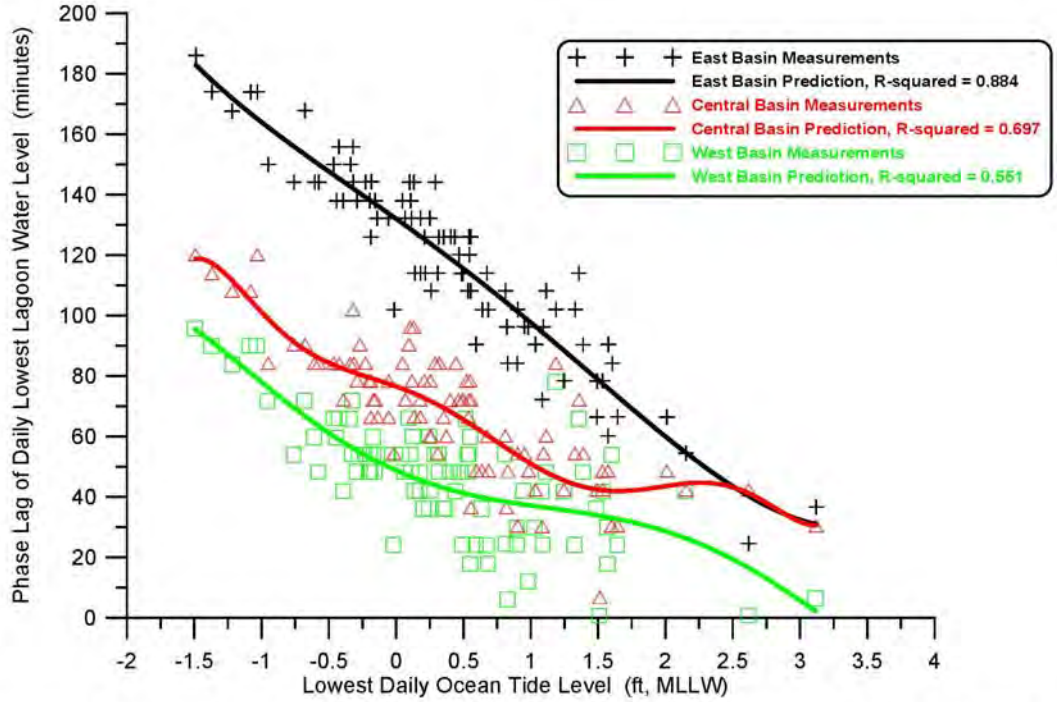

Figure 29. Phase lag of daily lowest water level in Batiquitos Lagoon relative to daily lowest water level in the local ocean as measured at the Scripps Pier tide gage (NOAA #941- 0230). Measured values indicated by symbols, model predictions according to solid lines of matching colors. Water level data after Merkel, (2008)

Figure 30 gives the hydroperiod function for the east basin of Batiquitos lagoon with the existing I-5 bridge, based on the relationships between habitat breaks and exposure used for San Dieguito Lagoon, as discussed in Section 3.3, Figure 17. The hydroperiod function in Figure 30 is based on tidal forcing using the Scripps Pier ocean water level measurements 1980-2010 to drive the tidal hydraulics model at its ocean inlet and compute the percent time the East Basin is exposed at a particular elevation from Equation 1. Comparing Figure 30 with the hydroperiod function for San Dieguito Lagoon in Figure 17, it is apparent how the phase lag in the east basin of Batiquitos lagoon and its inability to fully drain on lower low water stages has compressed the present intertidal habitat and raised the zonation of low mid and high marsh vegetation. This also greatly

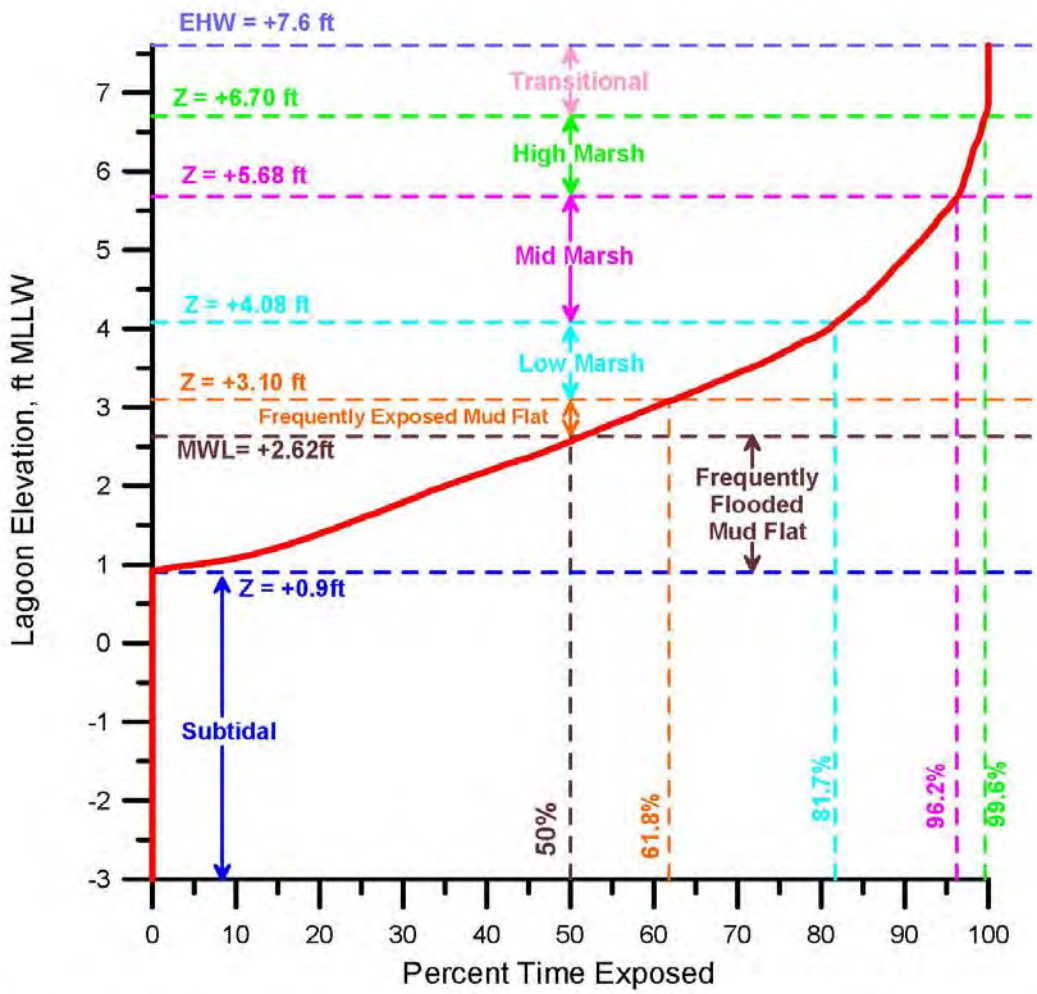

Figure 30. Hydroperiod function for the East Basin of Batiquitos Lagoon with existing I-5 bridge and bathymetry. Based on hydrodynamic simulation of East Basin water levels in response to tidal forcing from the Scripps Pier tide gage (NOAA # 941-0230). Habitat breaks based on habitat delineation from Josselyn and Whelchel (1999).

diminishes the amount of frequently exposed mud flats that support bird habitat. Remediating this compression of intertidal and mud flat habitat is one of the primary objectives of the replacement bridge alternatives considered in Section 4.3. To establish a quantitative baseline for determining the degree to which these objectives can be met by these replacement bridge alternatives, we can map the elevations of the habitat breaks of the hydroperiod function in Figure 30 against the stage area function Figure 21 to estimate the proportions of habitat types of the existing East Basin. This procedure gives the minimum sub-tidal and maximum intertidal habitat types since the hydroperiod function is based on the full range of water level variation over long periods of time (2008 period of record). By that procedure, the minimum (perpetual) sub-tidal area of the East Basin is 91.3 acres; there are maximum of 58.6 acres of frequently flooded mud flat; 13.6 acres of frequently exposed mud flat; 42.3 acres of low salt marsh; 77.0 acres of mid salt marsh; 45.8 acres of high salt marsh; and 30.2 acres of transitional habitat. The maximum area inundated by salt water at extreme high water is 358.9 acres of which 91.3 acres are sub tidal with at most 267.7 acres of intertidal habitat that experiences tidal inundation at least once in the period of record. An average of 302.7 acres experiences tidal inundation up to MHHW resulting in an average of 191.4 acres of intertidal habitat and 111.3 acres of sub-tidal habitat.

4.3) Simulated Tidal Hydraulics Impacts from I-5 Bridge Replacement and Widening:

In this section we consider five possible alternatives for the replacement I-5 bridge at Batiquitos Lagoon: In Section 4.3.1, the proposed 246 ft replacement bridge span (Figure 19a) with its associated hard-bottom channel at -3 ft MLLW (-5.3 ft NGVD); In Section 4.3.2, removal of a portion of the road bed fill to accommodate doubling the width of the existing channel along existing grade with hard bottom at -3 ft MLLW. This alternative requires doubling the replacement bridge span to 492 ft (*double-wide* alternative); In Section 4.3.3, removal of a portion of the road bed fill to increase the bed width of the hard bottom channel to 180 ft while lowering the channel bottom to -4.7 ft MLLW (-7 ft NGVD) along 2 on 1 side slopes (*Chang-channel*, Figure 19b). This alternative allows the replacement bridge span to remain at 246 ft; In Section 4.3.4, the proposed 246 ft replacement bridge span with flow fences (Figure 20a, blue) retrofitted to the existing hard-bottom channel; and in Section 4.3.5, the Chang-channel and flow fences (Figure 20b), using the proposed 246 ft replacement bridge span.

4.3.1) Tidal Hydraulics Impacts of the Proposed I-5 Bridge Replacement: Here we evaluate possible hydrodynamic impacts of the proposed replacement I-5 bridge design on the tidal exchange of the east basin of Batiquitos Lagoon. The potential source of any such impacts is the doubling of the numbers of bridge piles associated with the replacement span relative to existing conditions. These additional piles create additional drag and turbulence in the high-speed channel flow under the bridge.

Figure 31 (upper panel) gives the flow trajectories and depth-averaged tidal currents computed by the calibrated TIDE_FEM model for the proposed replacement bridge during the mean range flooding tides selected at the end of Section 2.0. Figure 31 (lower panel) shows fine scale flow details in the tidal channel near the proposed replacement I-5 bridge, while Figure 32 provides the same for mean ebbing tides. The examples shown in Figures 31 and 32 use the existing hard bottom bridge waterway channel at -3 ft MLLW. Streamline patterns, flow trajectories and velocities are indistinguishable from those found for the narrower, present day I-5 bridge using the same hard bottom channel cross section. With both existing an replacement bridges, maximum flood currents in the inlet channel reach 0.97 m/sec or 3.18 ft/sec. Flood tide currents entering the lagoon form

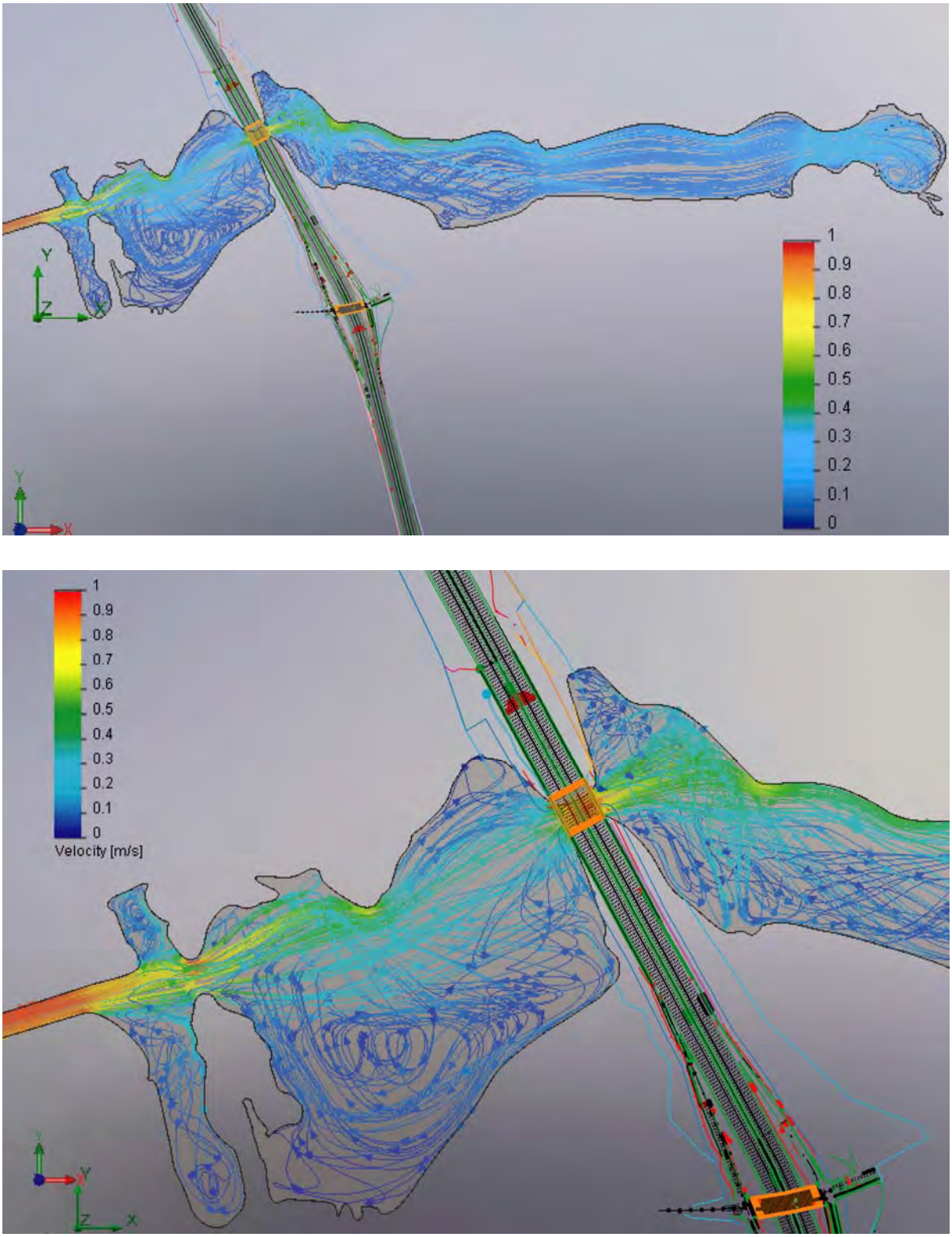

Figure 31: Hydrodynamic simulation of maximum flood flow during mean range tides at Batiquitos Lagoon with the proposed I-5 replacement bridge for the North Coast Corridor Project

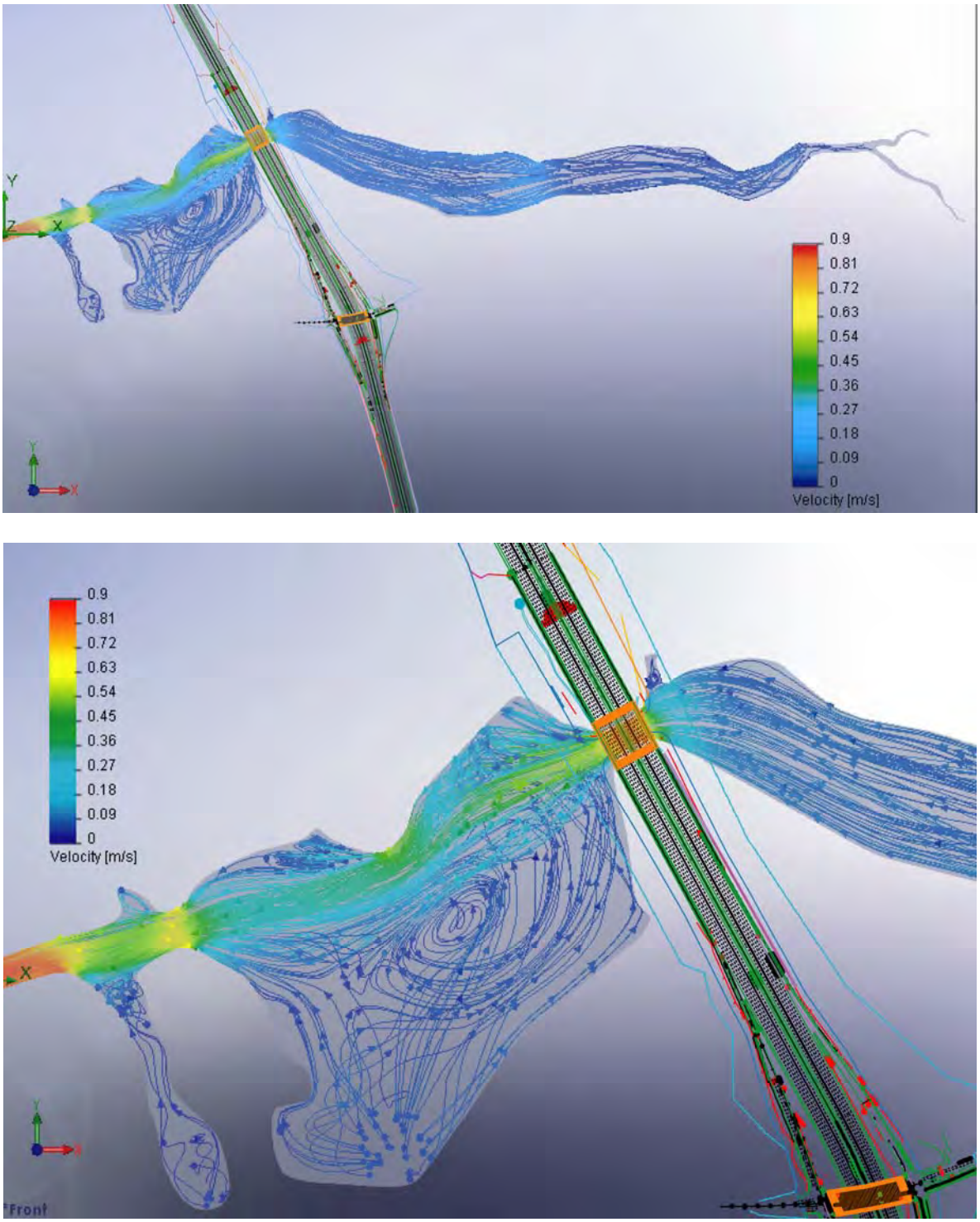

Figure 32: Hydrodynamic simulation of maximum ebb flow during mean range tides at Batiquitos Lagoon with the proposed I-5 replacement bridge for the North Coast Corridor Project.

a well defined jet through the West Basin and into the Central Basin at speeds of roughly 0.6 m/s (1.96 ft/sec), sufficient to transport fine grained beach sand in the 120-210 micron size regime into the West Basin and beyond. A sluggish disorganized eddy persists in the south arm of the West Basin while the middle portion is near stagnation, ideal conditions for fine sand to settle and form sand bars of beach grade sand. The flood tide jet exiting the West Basin speeds back up to as high as to 0.9 m/sec (2.95 ft/sec) as it passes through the hardened channel under the rail road bridge and then loses energy as it diverges into the Central Basin, spinning up a somewhat disorganized Central Basin eddy. The core of the Central Basin eddy is at stagnation, again providing ideal conditions for suspended beach grade sand to settle and deposit as a Central Basin sand bar. Flood tide currents speed back up to 0.7 m/sec (2.3 ft/sec) through the hardened channel under the both the existing and replacement I-5 bridge before diverging into a complex set of swirls and counter rotating eddies that populate the East Basin. East Basin swirl and eddy speeds are on the order of 0.1 m/sec (0.3 ft/sec), insufficient to transport fine sand but an important stirring mechanism for mixing the East Basin water mass to maintain high oxygen levels and to maintain silt and clay sized sediment particles in suspension.

Figure 32 plots the TIDE_FEM simulation of ebbing mean range tidal flows. The wetted area of the lagoon is significantly reduced relative to the flood tide area in Figure 31, due to the lower water levels acting on the storage rating curve in Figure 21. A creeping flow with complex structure on the order of -0.1 m/sec (-0.3 ft/sec) evacuates the East Basin and accelerates to -0.6 m/s (-1.9 ft/sec) as it passes through the hardened channel under either the existing or replacement I-5 bridge. A vigorous well-ordered Central Basin eddy is spun up by an ebb-tide jet flowing along the northern bank of the Central Basin. This jet accelerates to -0.63 m/sec (-2.1 ft/sec) as it passes through the hardened channel under the rail road bridge; and then splits into a south branch current as it diverges into the West Basin. The south branch current flows along the west bank of the West Basin at a rate of about -0.1 m/sec (-0.3 ft/sec) and exits the lagoon through the ocean inlet. Maximum ebb flow currents in the inlet channel are -0.9 m/sec (-2.95 ft/sec) slightly less than on flooding tide due to the flood tide dominance of the lagoon system. It is this flood tide dominance of the inlet channel flows that leads to the continuous net influx of beach sand into the lagoon that has required 206,838 cubic yards of maintenance dredging of the West and Central Basins between 1998 and 2008.

The fine-scale flow similarities between the existing and proposed replacement I-5 bridge simulations is born out in duplicate scour features found for these two sets of simulations. In either case tidal flows under the I-5 bridge reach 0.7 m/sec (2.3 ft/sec) during flood tide and 0.6 m/s (1.9 ft/sec) during ebb. These velocities through the existing and

proposed I-5 bridge waterway are about double the threshold of motion of the relict sediments of the lower San Marcos Creek. The preponderance of sediments near the I-5 bridge at channel station 3750 are in the medium to coarse sand size with a mean grain size of about 0.6 mm to 1 mm (Merkel, 2008). Figure 33 gives several of the most commonly used threshold of motion criteria, after (Everest 2007), indicating that these sands would reach the threshold of motion in tidal stream flows greater than 0.8 ft/sec to 1 ft/sec (0.24 m/sec to 0.31 m/sec), or about one half the maximum currents under the existing and proposed replacement I-5 bridges during mean range tides. Consequently, when the tidal current exits from the hard channel bottom under the bridge to the soft sedimentary bottom of the lagoon tidal basin, these super-critical tidal currents scour deep holes on either side of the I-5 bridge, both for the existing bridge and the proposed replacement bridge being proposed for the North Coast Corridor Project. In either case, the channel is so narrow and constrained in cross section by the 246 ft bridge span that two 20 ft deep scour holes have formed on either side of the I-5 bridge (see Figure 18) due to the excess velocity head of the tidal flow passing under the bridge.

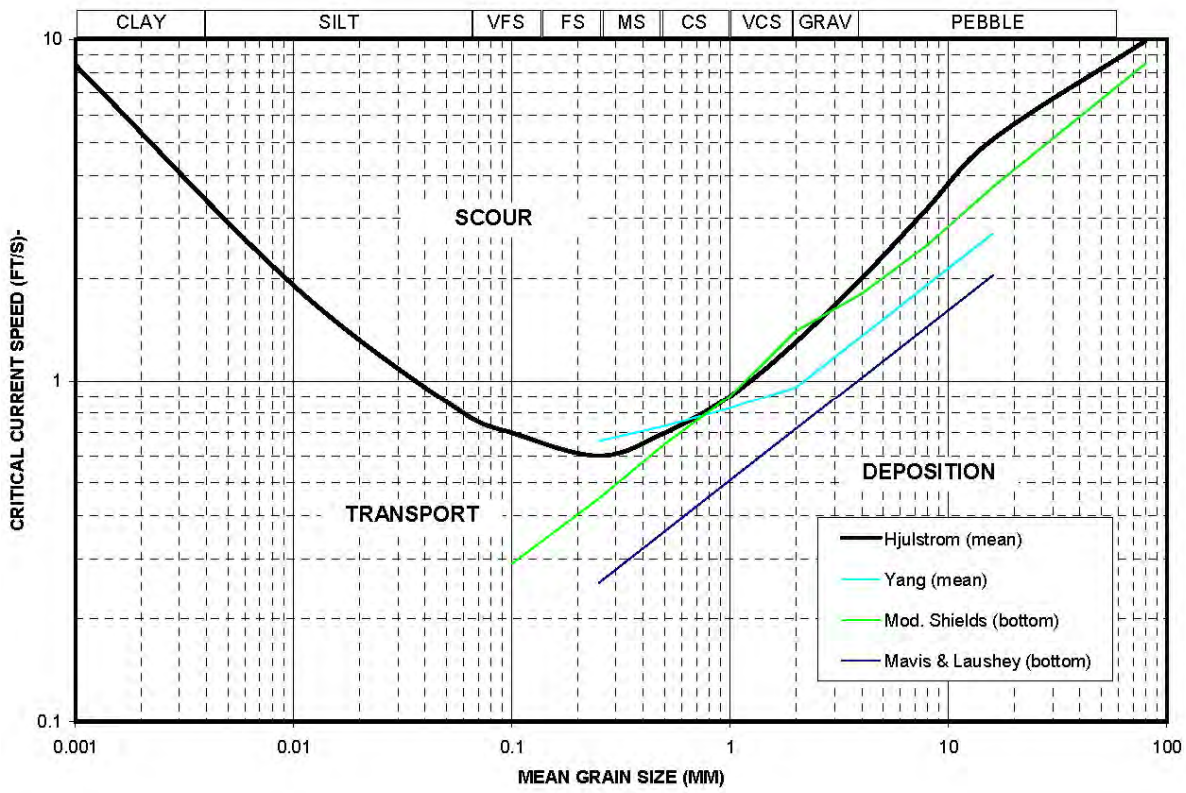

Figure 33: Critical current speeds for quartz sediment as a function of mean grain size, (from Everest, 2007).

The bridge waterway is presently too narrow, and that condition is not corrected by the replacement bridge proposed for the North Coast Corridor Project. As a result the kinetic energy of the high speed tidal flows (velocity head) in this narrow, hardened channel is being wasted in turbulence and sediment transport to scour the 20 ft deep holes in the lagoon bathymetry, rather than being reconverted into potential energy as pressure (water level elevation) after passing under the bridge into the eastern tidal basin. This results in as much as 2.2 ft of tidal muting in the East Basin relative to the ocean tides, and a phase lag at MLLW of as much as 186 minutes between the East Basin and the ocean that is not improved by the present proposed replacement bridge design. With either bridge design, the East Basin phase lag averages 117 minutes.

Flow similitude between the existing and replacement bridge designs is born out in Figures 34 and 35 giving comparisons of the lowest low water level and phase lag in the East Basin. In both figures, the replacement bridge in red gives nearly the same East Basin response as the existing bridge in black, with relatively minor variance between the two at the upper and lower end of ocean low water levels. Although these small differences do not appear significant, they are due to the increase in numbers of piles used in the replacement bridge design (where piles are increased from 6 in each of two rows for existing, to 12 piles per row for the replacement design). Greater numbers of piles increase velocity head loss to turbulence and form drag which further inhibits the ability of the East Basin to drain. In particular, the rather significant phase lags in Figure 35 causes the East Basin to not fully drain at low tide, as ocean tides begin to rise before East Basin water levels reach potential minimums. As a result, the hydrodynamic model results in Figure 31 and 32 show flood tide dominance to the tidal transport, with ebb flow speeds under the bridge being slightly less than flood flow and daily low water levels in the East Basin remains well above those in the ocean (Figure 34). The highest daily low water level in the East Basin is η_{LLW} = +2.50 ft MLLW, while the average is $\overline{\eta}_{LLW}$ = + 1.58 ft MLLW. This compresses present intertidal habitat by lowering the zonation of low mid and high marsh vegetation and reducing the exposure time of mud flats.

Compression of the intertidal habitat zonation due to restricted drainage through the narrow channel under the existing I-5 bridge is not remediated to any degree by the proposed replacement bridge span, as found in the hydroperiod function in Figure 36 that compares the existing bridge (green) versus the replacement bridge (red). The elevations of the habitat breaks in Figure 36 can be mapped against the East Basin stage area function (Figure 21) and used to estimate the sub-tidal and intertidal habitat types for both the existing and replacement bridges. By that procedure Table 4.2 shows that the

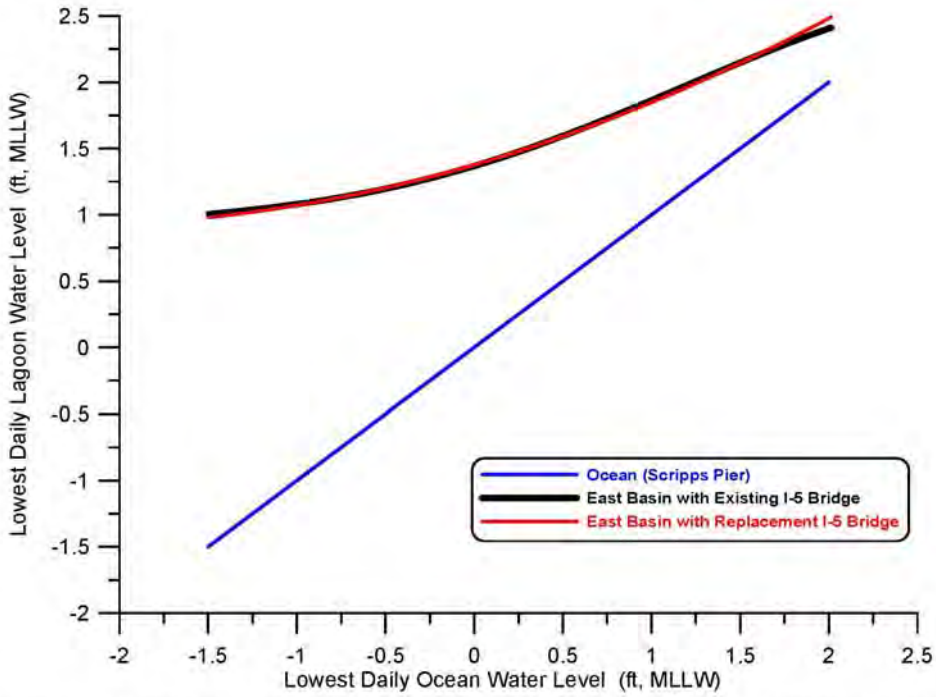

Figure 34. Comparison of daily lowest water level in east basin of Batiquitos Lagoon for existing I-5 bridge (black) versus the proposed replacement I-5 bridge (red). Both shown as functions of daily lowest water level in the local ocean as measured at the Scripps Pier tide gage (NOAA #941- 0230).

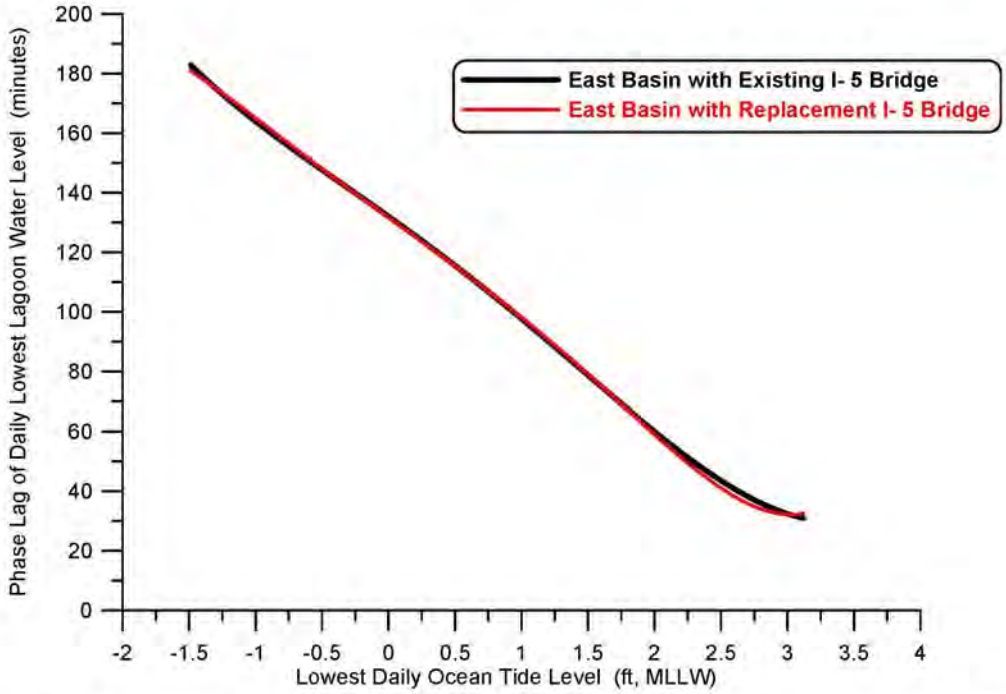

Figure 35. Comparison of the phase lag of lowest low water level in east basin of Batiquitos Lagoon for existing I-5 bridge (black) versus the proposed replacement I-5 bridge (red). Both shown as functions of daily lowest water level in the local ocean as measured at the Scripps Pier tide gage (NOAA #941- 0230).

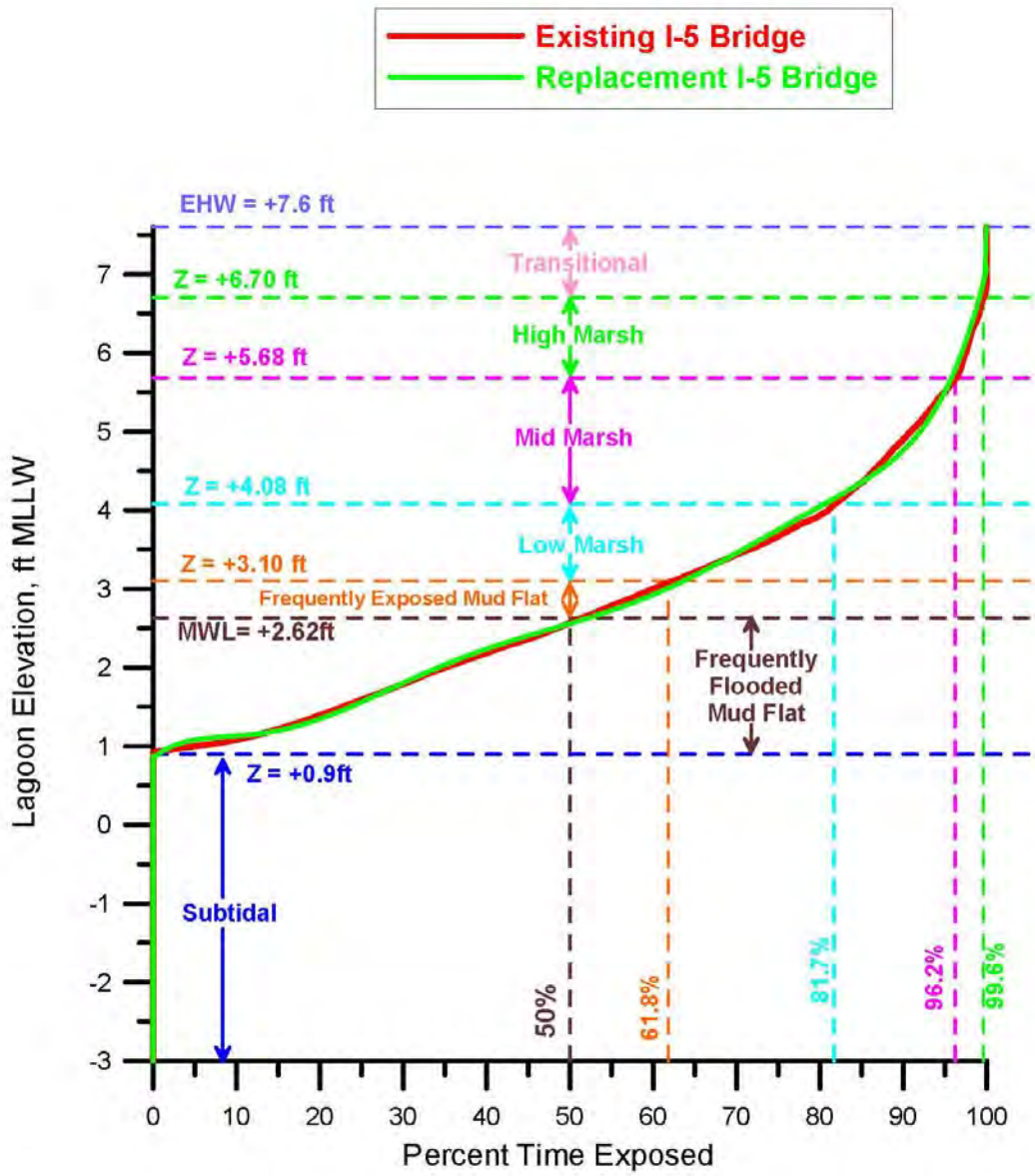

Figure 36. Hydroperiod function for the East Basin of Batiquitos Lagoon comparing existing I-5 bridge (red) against the proposed replacement I-5 bridge (green). Based on hydrodynamic simulation of East Basin water levels in response to tidal forcing from the Scripps Pier tide gage (NOAA # 941-0230). Habitat breaks based on habitat delineation from Josselyn and Whelchel (1999).

minimum (perpetual) sub-tidal area of the East Basin increases by 0.6 acres with the replacement bridge, to 91.9 acres vs 91.3 acres for the existing bridge; frequently flooded mud flat is reduced by 0.5 acres, from 58.6 acres for the existing bridge to 58.1 acres for the replacement bridge; frequently exposed mud flat is reduced by 4.0 acres, from 13.6 acres for the existing bridge to 9.6 acres for the replacement bridge; low salt marsh is increased by 8.6 acres, from 42.3 acres for the existing bridge to 50.9 acres for the

replacement bridge; mid salt marsh is relatively unchanged, increasing by only 0.2 acres, from 77.0 acres for the existing bridge to 77.2 acres for the replacement bridge; high salt marsh is reduced by 4.8 acres, from 45.8 acres for the existing bridge to 41.0 acres for the replacement bridge; transitional habitat is unchanged at 30.2 acres. Because the maximum area inundated by salt water at extreme high water is unchanged at 358.9 acres, maximum the intertidal habitat is reduced by only 0.6 acres with the replacement bridge; and the mean area experiencing tidal inundation up to MHHW is unchanged at 302.7 acres with an average 191.4 acres of intertidal habit and a mean sub-tidal habitat of 111.3 acres for both existing and replacement bridges. Therefore, the small deviations in the distributions of areas among intertidal habitat types are not considered as being a significant impact of the replacement bridge since the aggregate totals of habitat and their split between intertidal and sub-tidal remain essentially unchanged. The small deviations in intertidal habitat splits in Table 4.2 and Figure 36 are likely due to the turbulence and drag effects associated with the increase in numbers of piles on the replacement bridge.

Table 4.2: East Basin Habitat Area Distribution from Hydroperiod & Stage Area Functions with Existing Bridge vs. Proposed Replacement Bridge

East Basin Habitat Areas	Existing I-5 Bridge	Replacement I-5 Bridge
Perpetual Sub-Tidal (acres)	91.3	91.9
Mean Sub-Tidal (acres)	111.3	111.3
Frequently Flooded Mud Flat (acres)	58.6	58.1
Frequently Exposed Mud Flat (acres)	13.6	9.6
Low Salt Marsh (acres)	42.3	50.9
Mid Salt Marsh (acres)	77.0	77.2
High Salt Marsh (acres)	45.8	41.0
Transitional Habitat (acres)	30.2	30.2
Maximum Intertidal Area (acres)	267.6	267.0
Maximum Area of Salt Water Inundation (acres)	358.9	358.9
Mean Intertidal Area (acres)	191.4	191.4
Mean Area of Salt Water Inundation (acres)	302.7	302.7

4.3.2) Tidal Hydraulics Impacts of I-5 Bridge Replacement with Fill Removal (*Double-Wide Alternative*): To remediate these tidal muting effects of the narrow bridge waterway at Batiquitos I-5 bridge, we evaluate the *double-wide* alternative that would require removal of a portion of the road bed fill to accommodate doubling the width of the tidal channel along the existing grade of the south bank and increasing the span of the replacement bridge from 246 ft (78 m) to 492 ft (156 m). Doubling of the span also places two additional rows of 12 piles each in the active transport region of the channel, but increases channel cross sectional two-fold. Channel width increases effect only the south bank because the I-5 grades upward to higher ground toward the north (requiring more fill and longer bridge spans if the channel were widened in that direction); and grades downward toward the south. Also, most of the vegetation around the bridge footings and road bed on the south side of the channel appears to be ruderal. The double-wide concept retains the hard channel bottom feature at -3 ft MLLW. Figure 37 compares the existing and double-wide channel bottom profiles on both the west side (Section 9) and the east side (Section 10) of the I-5 bridge.

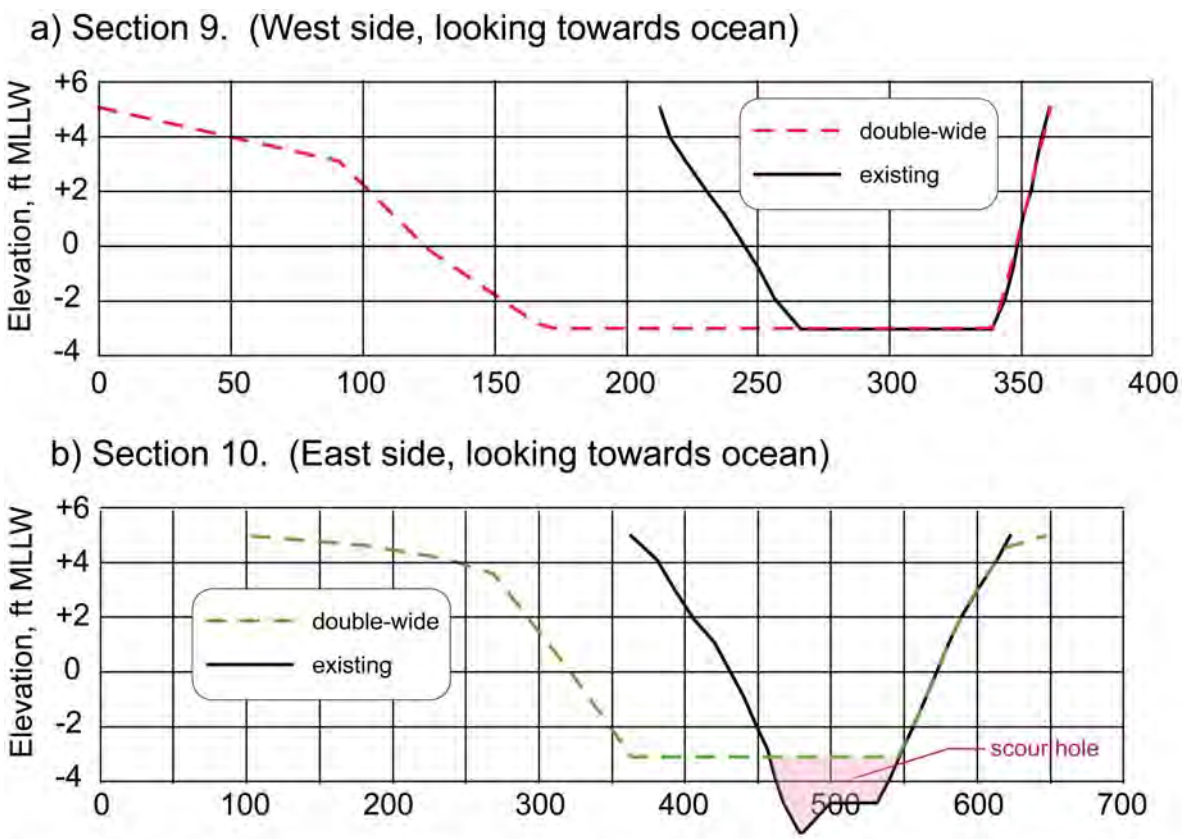

Figure 37. Comparison of existing vs. double-wide I-5 bridge channel at Batiquitos Lagoon, a) cross section #9, west side of bridge; b) cross section #10, east side of bridge.

Figure 38 gives flow trajectories and depth-averaged tidal currents in Batiquitos Lagoon with the double-wide alternative for maximum flood flow during mean range tides. Note the replacement bridge span has been doubled to accommodate the wider bridge waterway channel. This wider bridge waterway reduces the velocities of the flow exiting the hard bottom section of the channel to 0.3 m/sec (1 ft/sec) during maximum flood flow. In Figure 39, velocities of the flow exiting the hard bottom section of the channel are reduced to 0.24 m/sec (0.8 ft/sec) during maximum ebbing flow. Both of these examples are less than the threshold of incipient motion of the local relict San Marcos Creek sediments, and insufficient to cause significant scour. These sub-scour threshold channel velocities are insufficient to maintain the scour holes that presently exist on either side of the I-5 bridge (Figure 18); and consequently these holes will in-fill over time, further reducing losses of tidal energy to form drag. Hence the double-wide channel cross section in Figure 37b does not exhibit the hashed area due to scour in the existing channel.

Eddy structures and jets elsewhere in the East, Central and West Basins are similar in the case of the double-wide channel but not identical to those found for the existing and replacement spans on mean range flooding and ebbing tides in Figure 31 & 32. Maximum flood currents in the inlet channel reach 1 m/sec or (3.28 ft/sec) with the double-wide alternative; while maximum ebb flow currents in the inlet channel are -0.93 m/sec (-3.05 ft/sec) slightly more than existing conditions but the inlet is still flood tide dominated. Eddy structures in the Central Basin are a bit more well organized with the double-wide channel, possible because more volume is flowing in and out of the East Basin.

The reduced drag and more complete pressure recovery of the velocity head in the double-wide channel will reduce flood dominance of the tidal exchange as evidenced when velocity scales in Figures 38 and 39 are compared with those in Figures 31 & 32. Drag reduction achieved by the double-wide channel cross section in Figure 37 ultimately reduce the East Basin phase lag and thereby achieve more complete drainage of the East Basin during low tide. To that point, Figure 40 compares long term simulations of the daily low water levels in the East Basin with the existing I-5 bridge (black), the proposed I-5 bridge (red) and the double-wide alternative (purple) with its double-wide channel cross section from Figure 37. The double-wide channel reduces the maximum daily lower low water levels to η_{LLW} = 2.24 ft MLLW from η_{LLW} = 2.5 ft MLLW for the existing I-5 bridge; and, reduces average daily lowest water levels to $\overline{\eta}_{LLW}$ = 1.11 ft MLLW from the existing average of $\overline{\eta}_{LLW}$ = 1.58 ft MLLW. The minimum daily low water level achieved by the double-wide channel is lowered most significantly to +0.17 ft MLLW,

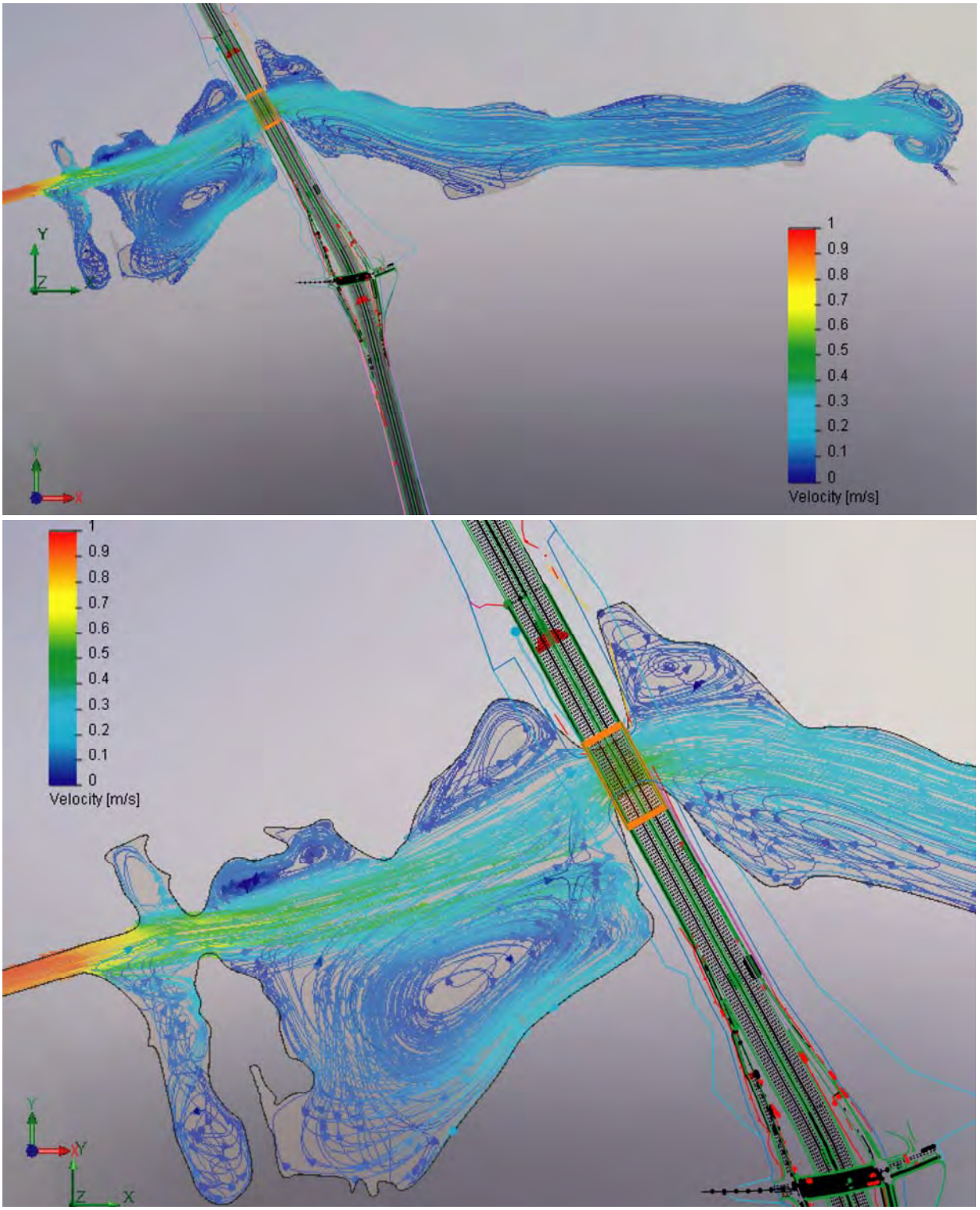

Figure 38: Hydrodynamic simulation of maximum flood flow during mean range tides at Batiquitos Lagoon with the *double-wide* alternative for the replacement bridge of North Coast Corridor Project.

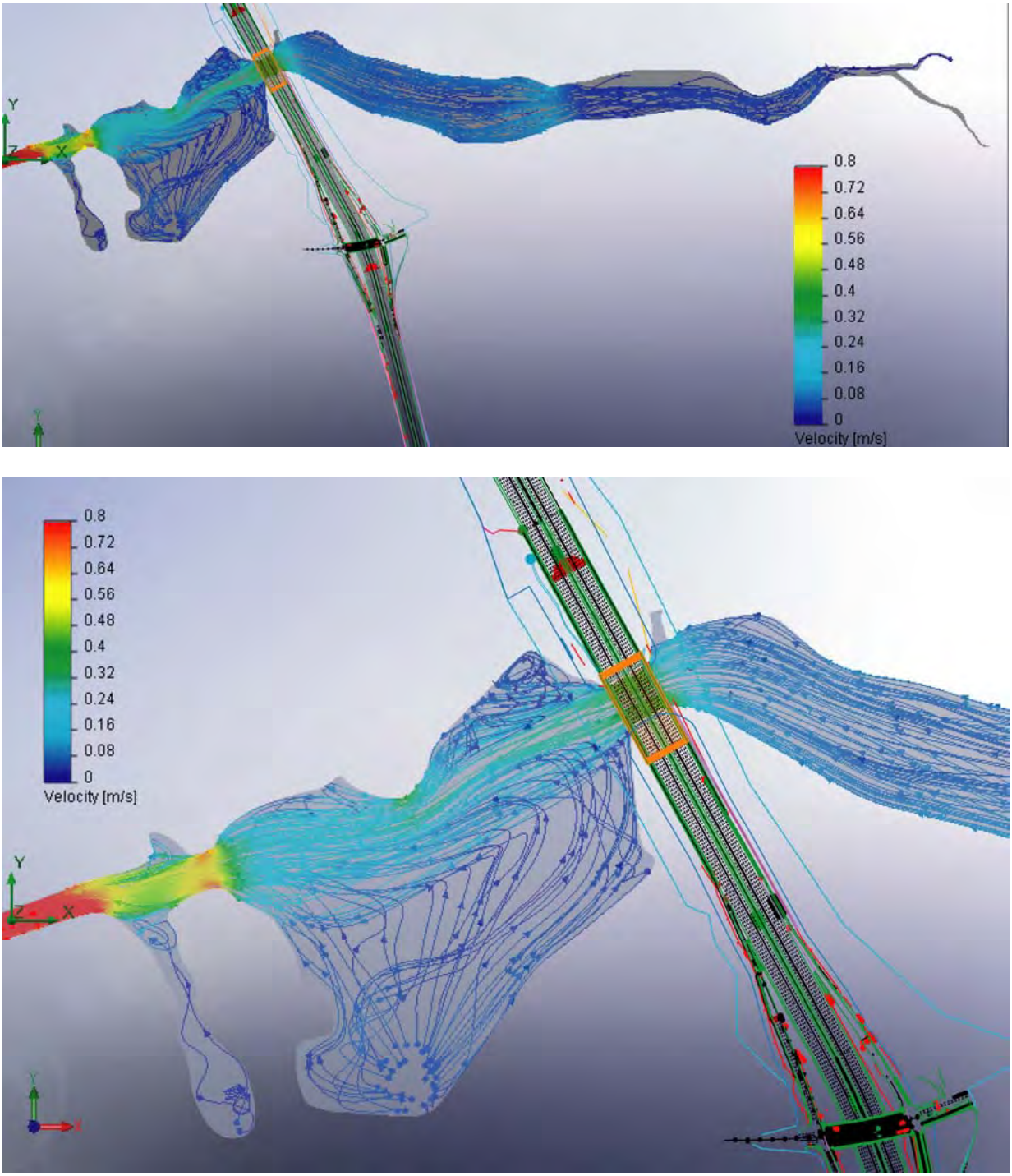

Figure 39: Hydrodynamic simulation of maximum ebb flow during mean range tides at Batiquitos Lagoon with the *double-wide* alternative for the replacement bridge of North Coast Corridor Project.

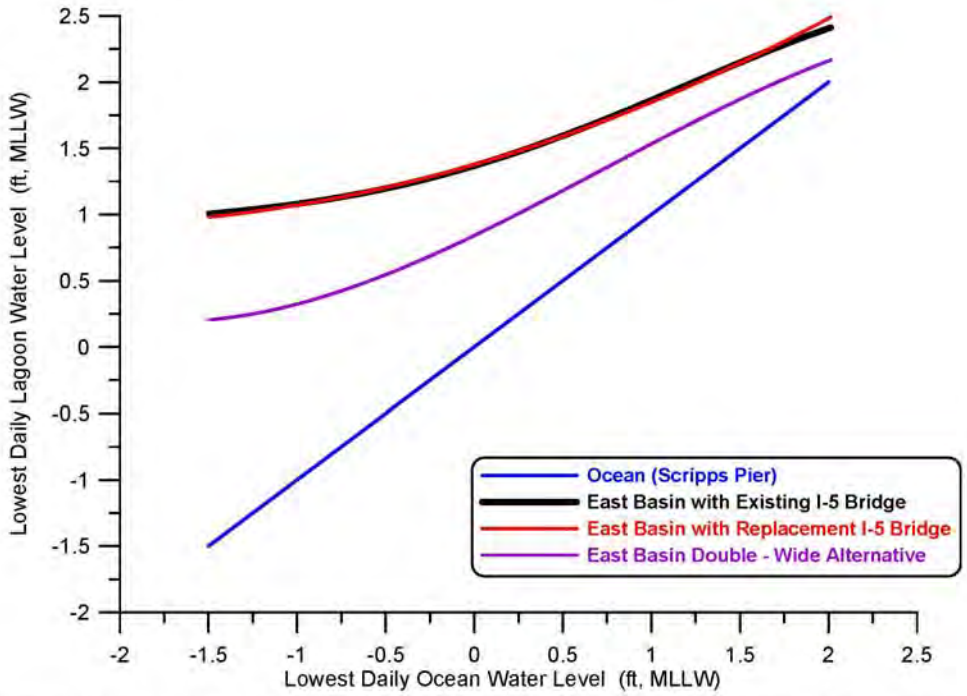

Figure 40. Comparison of daily lowest water level in east basin of Batiquitos Lagoon for existing I-5 bridge (black) and the proposed replacement I-5 bridge (red), versus the double-wide alternative (purple). All shown as functions of daily lowest water level in the local ocean as measured at the Scripps Pier tide gage.

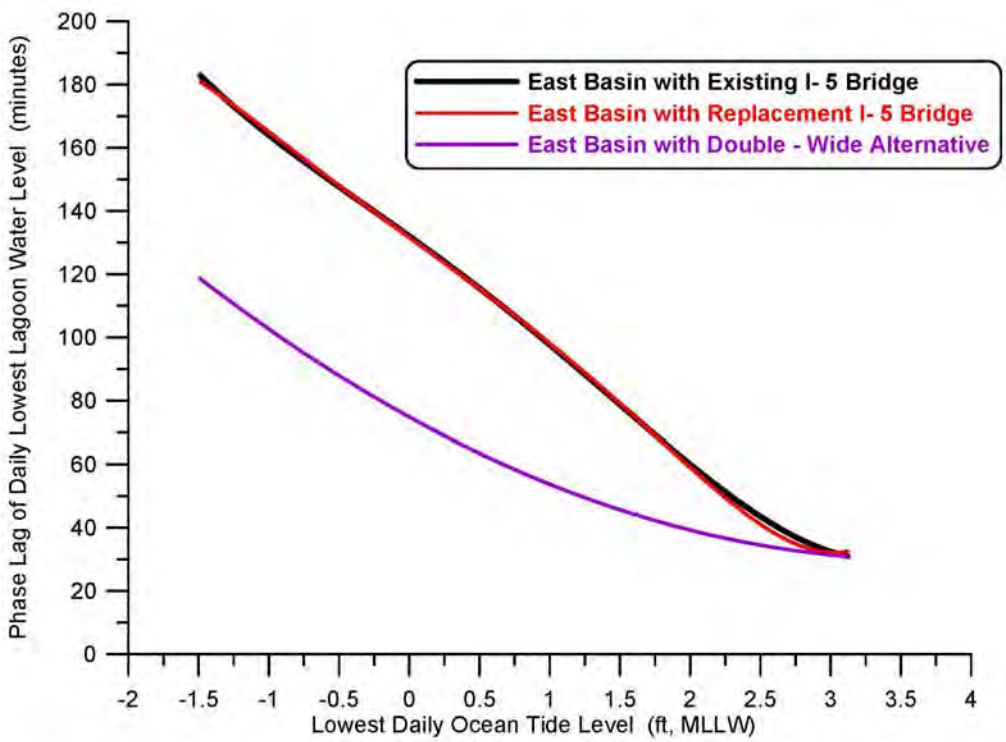

Figure 41. Comparison of the phase lag of lowest low water level in east basin of Batiquitos Lagoon for existing I-5 bridge (black) and the proposed replacement I-5 bridge (red) versus the double-wide alternative (purple). All shown as functions of daily lowest water level in the local ocean as measured at the Scripps Pier.

down from 0.9 ft MLLW for existing conditions (cf. Table 4.1). East Basin phase lags are substantially diminished with the double-wide alternative. Figure 41 shows that in long term simulation the maximum East Basin phase lag is reduced from θ_{max} = 186 minutes with the existing I-5 bridge to θ_{max} = 120 minutes with the double-wide alternative. Average East Basin phase lags are reduced from $\bar{\theta}$ = 117 minutes with the existing I-5 bridge to $\bar{\theta}$ = 68 minutes with the double-wide alternative. The minimum phase lag for East Basin tides remains unchanged with the double-wide alternative at 31 minutes, as this minimum occurs during neap tides, where the choke points at the inlet channel and railroad bridge retain ultimate hydraulic control for these small range tidal events.

The reductions in flow speeds and phase lags due to the double-wide waterway alternative results in more complete conversion of velocity into potential energy of water elevation, thereby increasing the tidal range in the east basin of Batiquitos Lagoon. Table 4.3 gives a summary of the water level elevations calculated for Batiquitos Lagoon with the double-wide I-5 bridge alternative based on long-term tidal simulations using historic ocean water level forcing for the 2008 period of record. Comparing Table 4.3 against existing conditions in Table 4.1, we find that both the mean and maximum diurnal tidal ranges in the East Basin are substantially increased with the double-wide alternative. MHHW in the East Basin has been raised to +6.2 ft MLLW with the double-wide alternative, while MLLW in the East Basin has been lowered to +1.1 ft MLLW, producing a mean diurnal tidal range of 5.1 ft, an increase of 0.6 ft over existing conditions. While extreme high water levels in the East Basin remain unchanged with

Table 4.3: Water Levels for Batiquitos Lagoon with Double-Wide Alternative I-5 Bridge

Elevations Feet MLLW	Ocean	West Basin	Central Basin	East Basin
MEAN HIGHER HIGH WATER (MHHW)	5.7	5.8	6.0	6.2
MEAN HIGH WATER (MHW)	5.0	5.0	5.2	5.3
MEAN LOW WATER (MLW)	1.3	1.6	1.8	1.8
MEAN LOWER LOW WATER (MLLW)	0.4	0.9	1.1	1.1
EXTREME LOW WATER LEVEL (ELW)	-1.5	-0.2	0.2	0.2
EXTREME HIGH WATER LEVEL (EHW)	7.4	7.3	7.4	7.6
MAXIMUM TIDAL RANGE	8.9	7.5	7.2	7.4

the double-wide alternative, extreme low water levels are lowered to +0.2 ft MLLW, resulting in a maximum tidal range of 7.4 ft, an increase of 0.7 ft over existing conditions. More complete drainage of the East Basin with the double-wide alternative also makes a small hydraulic improvement in the Central Basin, where MLW is lowered by 0.1 ft to +1.8 ft MLLW, MLLW is lowered by 0.1 ft to +1.1 ft MLLW; ELW is lowered by 0.1 ft to +0.2 ft MLLW; and the maximum tidal range is increased by 0.1 ft to 7.2 ft.

Figure 42 overlays the new MHHW and MLLW levels with the double-wide bridge waterway alternative on the East Basin stage area function, producing an average of 210.4 intertidal acres in the East Basin, or a net gain of 19 intertidal acres over existing conditions (cf. Figure 21). However, most of this gain has resulted from conversion of sub-tidal to intertidal habitat, as the mean area of tidal inundation in the East Basin has increased by only 4.5 acres over existing conditions. A complete accounting of this conversion of sub-tidal to intertidal area and the realignment of the expanded intertidal area is revealed by the hydroperiod function computed in Figure 43 from 1980-2010 ocean water level forcing. Comparing the new habitat breaks for the hydroperiod function of the double-wide alternative in Figure 43 against those for existing conditions in Figure 36, we find that the improved drainage of the East Basin promoted by the double-wide channel lowers the zonation of mud flats, and thereby allows vertical expansion of the low, mid and high marsh habitat. This is shown in Table 4.4 where the elevations of the habitat breaks of the hydroperiod function in Figure 43 have been mapped against the stage area function (Figure 21) and used to estimate the sub-tidal and intertidal areas.

Table 4.4 shows that the perpetual sub-tidal area of the East Basin decreases by 17.9 acres with the double-wide alternative, from 91.3 acres for the existing bridge to 73.4 acres, while the mean sub-tidal area with the double-wide alternative decreases by 13.6 acres to 97.7 acres, from 111.3 acres for the existing bridge; frequently flooded mud flat is increased by 5.9 acres, from 58.6 acres for the existing bridge to 64.5 acres for the double-wide alternative; frequently exposed mud flat is increased by 7.0 acres, from 13.6 acres for the existing bridge to 20.6 acres for the double-wide alternative; low salt marsh is reduced slightly by 2.2 acres, from 42.3 acres for the existing bridge to 40.1 acres for the double-wide alternative; mid salt marsh is increased by 7.4 acres, from 77.0 acres for the existing bridge to 84.4 acres for the double-wide alternative; high salt marsh is increased considerably by 25.9 acres, from 45.8 acres for the existing bridge to 71.7 acres for the double-wide alternative replacement bridge; and much of the transitional habitat is converted into high salt marsh, reducing transitional habitat by 24.7 acres from 30.2 acres for the existing bridge to 5.5 acres for the double-wide alternative. Maximum intertidal habitat is increased by 19.2 with the double-wide alternative to 286.8 acres, as compared

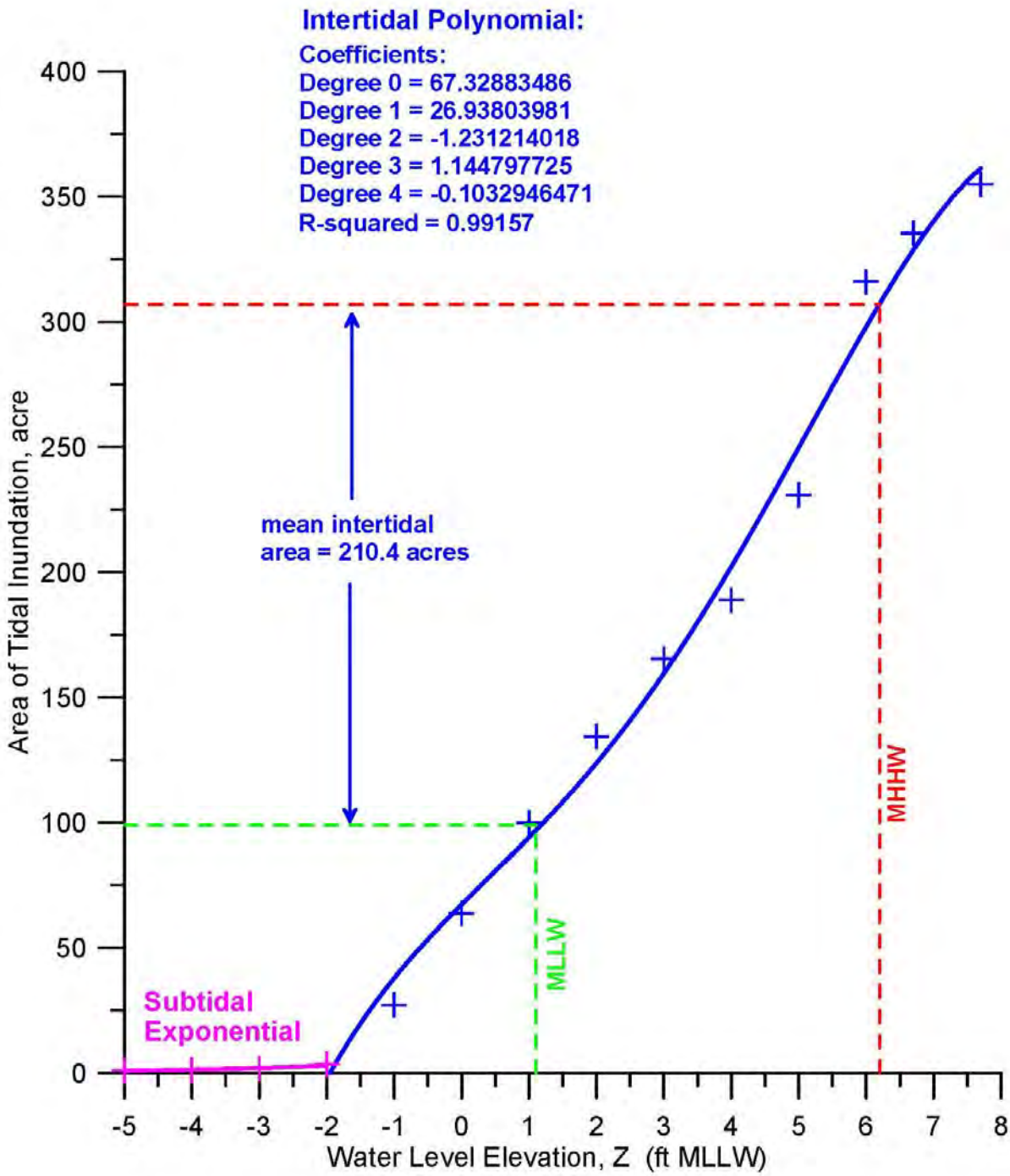

Figure 42. Area of tidal inundation in the east basin of Batiquitos Lagoon as a function of water level elevation for the double - wide alternative. Mean water levels from long-term hydrodynamic simulation using 2008 tidal forcing.

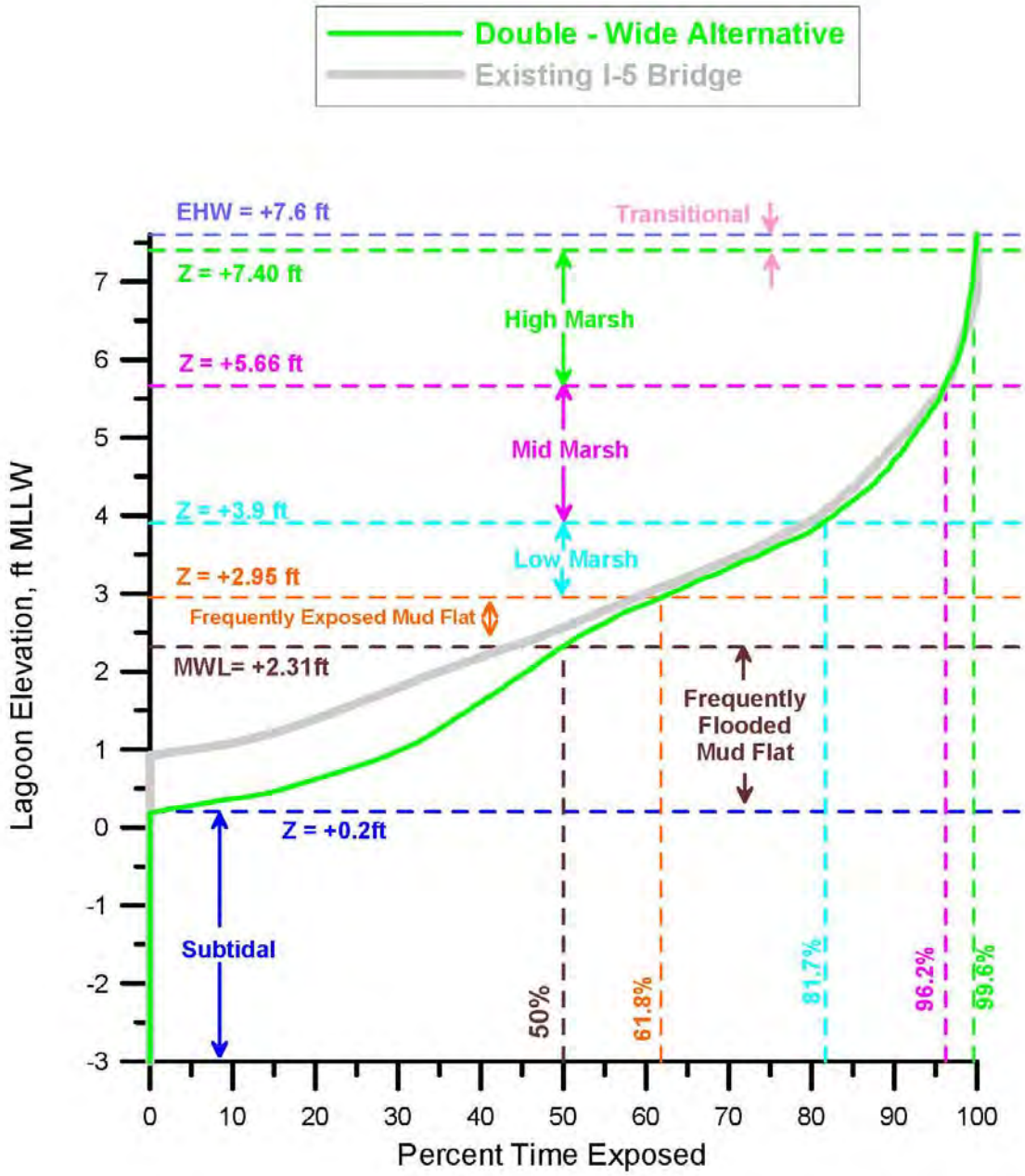

Figure 43. Hydroperiod function for the East Basin of Batiquitos Lagoon due to the double - wide alternative. Based on hydrodynamic simulation of East Basin water levels in response to tidal forcing from the Scripps Pier tide gage (NOAA # 941-0230). Habitat breaks based on habitat delineation from Josselyn and Whelchel (1999).

Table 4.4: East Basin Habitat Area Distribution from Hydroperiod and Stage Area Functions with Existing Bridge vs. Double-Wide Alternative

East Basin Habitat Areas	Existing I-5 Bridge	Double-Wide Alternative
Perpetual Sub-Tidal (acres)	91.3	73.4
Mean Sub-Tidal (acres)	111.3	97.7
Frequently Flooded Mud Flat (acres)	58.6	64.5
Frequently Exposed Mud Flat (acres)	13.6	20.6
Low Salt Marsh (acres)	42.3	40.1
Mid Salt Marsh (acres)	77.0	84.4
High Salt Marsh (acres)	45.8	71.7
Transitional Habitat (acres)	30.2	5.5
Maximum Intertidal Area (acres)	267.6	286.8
Maximum Area of Salt Water Inundation (acres)	358.9	360.2
Mean Intertidal Area (acres)	191.4	210.6
Mean Area of Salt Water Inundation (acres)	302.7	308.3

to 267.6 acres for existing conditions; and the mean area experiencing tidal inundation up to MHHW is increased by 5.6 acres from 302.7 acres for the existing bridge to 308.3 acres for the double-wide alternative resulting in an average 210.6 acres of intertidal habit, an increase of 19.2 acres over existing conditions.

Generally, Figure 43 and Table 4.4 indicate that the double-wide channel will create 12.8 acres of new mud flats and increase the exposure time of existing mud flats; a benefit to shorebird foraging and a feature of the East Basin that has been lacking to some degree. It will also reduce the compression of present intertidal habitat by lowering the zonation of low mid and high marsh vegetation allowing for some expansion of the cordgrass currently in the lagoon and providing some improved habitat for clapper rail. The new hydroperiod function promoted by the double-wide alternative in Figure 44 brings the functionality of the east basin of Batiquitos in closer alignment with its original restoration goals (see Merkel, 2008).

Under existing conditions, depth constrictions under the railroad bridge are the leading order cause of limited ebb tide drainage out of the Central Basin of Batiquitos Lagoon, which in turn limits further drainage from the East Basin, even with the double-wide channel improvements in place. About 76% of the tidal muting of the East Basin of Batiquitos Lagoon is attributable to the combination of choke points at the PCH and railroad bridges and 63% of that muting is attributable to the choke point at the PCH where the hardened ocean inlet channel crosses the barrier sand spit that segregates the lagoon from the beach. Attempts to relieve these choke points through application of a double-wide type of concept would be problematic, and attempts to eliminate them altogether are probably infeasible. The depth of the channel under the railroad bridge is hardened at only -3 ft to -4 ft MLLW. Removal of fill at the rail road bridge to widen the channel would have constraints with respect to disposal, as the bed fill is armored by rip rap and could have contaminant issues. Attempts to convert the footprint of this fill into functioning wetland would suffer degradation from shading. The remaining constriction at the ocean inlet is due to the West Basin inlet bar, which in turn, is a consequence of failure to perform timely and adequate maintenance dredging. Attempts to recover the footprint of the PCH road bed fill for restorative improvement would make the entire West Basin vulnerable to sand infilling by wave overtopping of the beach berm, as the PCH road bed fill functions as a sea wall to protect the West Basin of the lagoon. In spite of these concerns, if the constrictions at the railroad bridge, the West Basin inlet bar, and the PCH bridge were remediated, the double-wide alternative for the I-5 bridge would function optimally as it was sized to convey the entire potential tidal prism of the East Basin.

4.3.3) Tidal Hydraulics Impacts of I-5 Bridge Replacement with Reduced Fill Removal (*Chang-channel Alternative*): Here we evaluate the *Chang-channel* alternative as a means to remediate tidal muting effects of the existing narrow bridge waterway at Batiquitos I-5 bridge. The *Chang-channel* alternative (Figure 19) would require removal of a smaller portion of the road bed fill than the double-wide alternative in Section 4.3.2, and would not require doubling the span of the replacement, thereby providing a significant cost advantage. Channel width increases associated with the *Chang-channel* alternative are symmetric with respect to the existing, but the channel is deepened from -3 ft MLLW to -4.7 ft MLLW. While the double-wide alternative provided a 100% increase in channel cross section over existing conditions, the *Chang-channel* alternative provides an 80% increase.

Figure 44 gives flow trajectories and depth-averaged tidal currents in Batiquitos Lagoon with the *Chang-channel* alternative for maximum flood flow during mean range tides. With 80% more channel cross section than the existing bridge waterway, this alternative reduces the velocities of the flow exiting the hard bottom section of the channel to 0.38 m/sec (1.24 ft/sec) during maximum flood flow. In Figure 45, velocities of the flow exiting the hard bottom section of the channel are reduced to 0.3 m/sec (0.98 ft/sec) during maximum ebbing flow. While these flood and ebb velocities under the I-5 bridge with the Chang-channel are greater than with the double-wide alternative, they remain are less than the threshold of incipient motion of the local relict San Marcos Creek sediments, and insufficient to cause significant scour. These sub-scour threshold channel velocities are insufficient to maintain the scour holes that presently exist on either side of the I-5 bridge (Figure 18); and consequently these holes will in-fill over time, further reducing losses of tidal energy to form drag. Hence the Chang-channel cross section in Figure 19 does not exhibit scour holes indicated by the hashed area in Figure 37b (red) for the existing channel.

Eddy structures and jets in the East, Central and West Basins with the Chang-channel are similar to those for the double-wide channel but not identical to those found for the existing and replacement spans on mean range flooding and ebbing tides in Figure 31 & 32. Maximum flood currents in the inlet channel reach 0.99 m/sec or (3.25 ft/sec) with the double-wide alternative; while maximum ebb flow currents in the inlet channel are -0.92 m/sec (-3.01 ft/sec) slightly more than existing conditions but the inlet is still flood tide dominated. Eddy structures in the East Basin during flooding tide are more well organized than with either the double-wide channel or existing channel. This is possible due to the symmetric expansion of the Chang-channel about the existing channel,

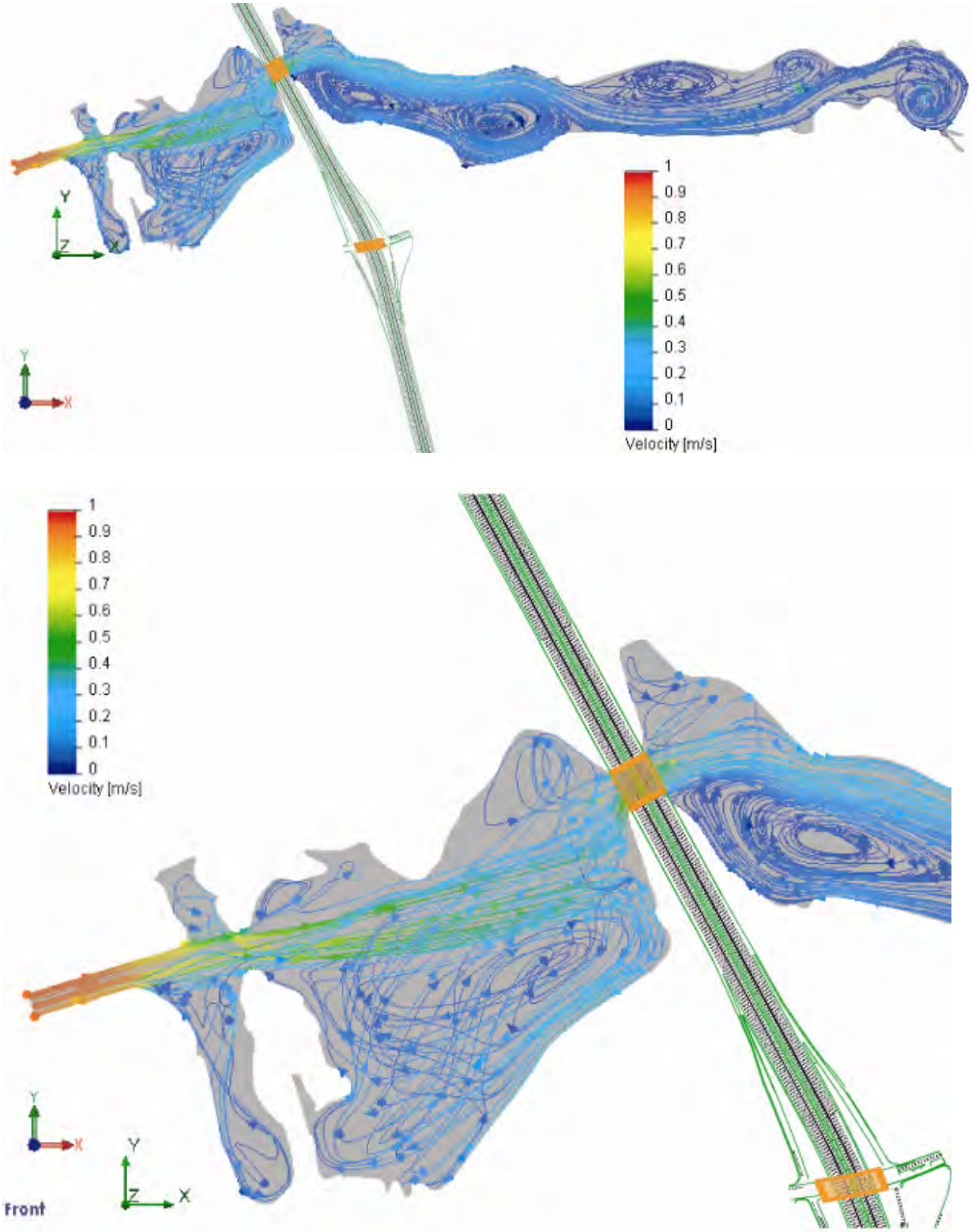

Figure 44: Hydrodynamic simulation of maximum flood flow during mean range tides at Batiquitos Lagoon with the *Chang-channel* alternative for the replacement bridge of North Coast Corridor Project.

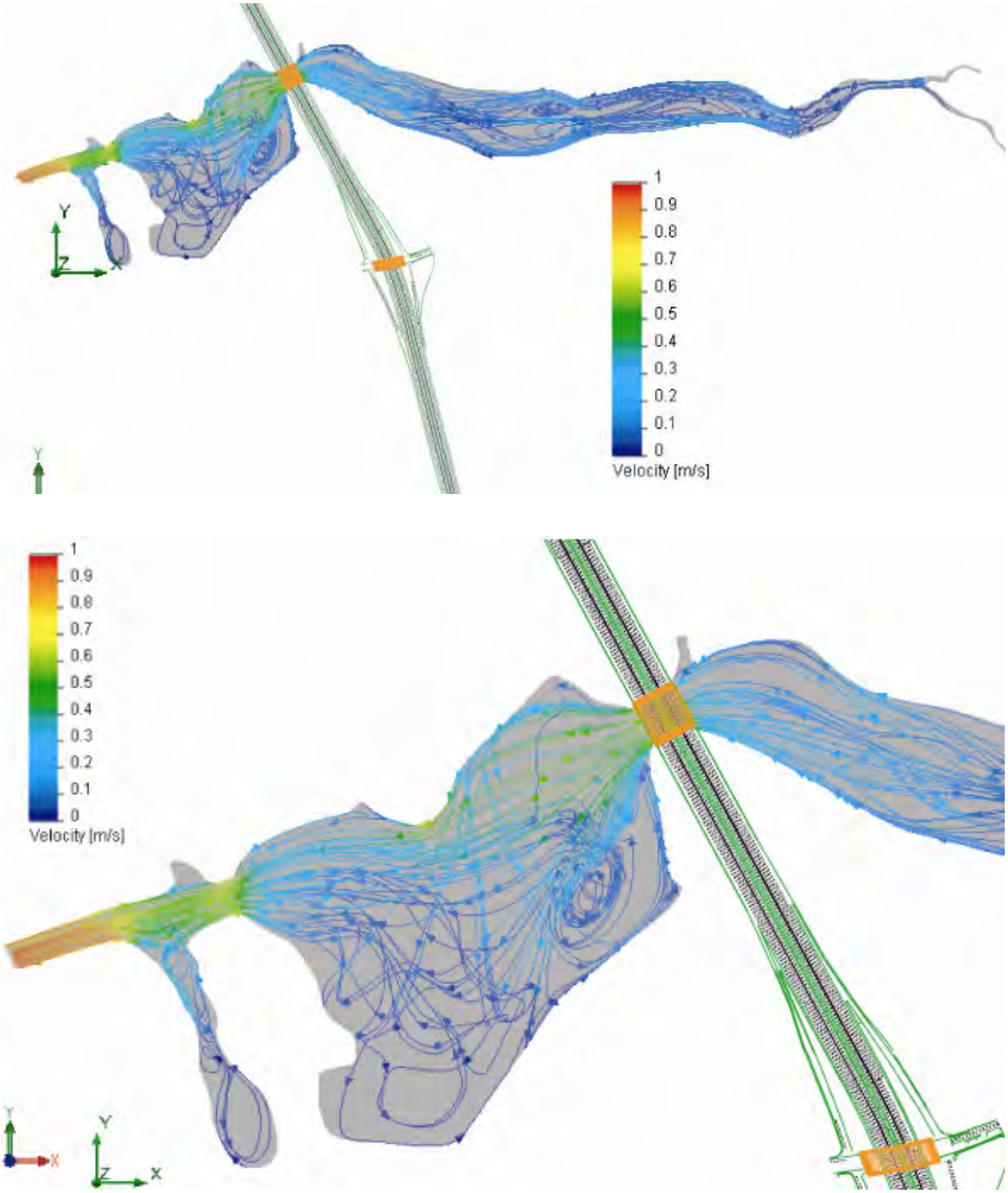

Figure 45: Hydrodynamic simulation of maximum ebb flow during mean range tides at Batiquitos Lagoon with the *Chang-channel* alternative for the replacement bridge of North Coast Corridor Project.

creating a boundary jet along the north bank of the East Basin during flooding tide that drives a system of counter rotating eddies throughout the East Basin. This stirring action should be beneficial to dissolved oxygen and nutrient distribution in the East Basin.

For flow similarity comparisons, Figures 46 and 47 give flow trajectories and depth-averaged tidal currents in Batiquitos Lagoon with the *Chang-channel* alternative for maximum flood and ebb flow during spring tides. Figures 46 & 47 display many similar flow structures to the mean range tide simulations in Figures 44 & 45. Figure 46 reveals maximum currents in the inlet channel reach 1.2 m/sec or 3.94 ft/sec. The flood tide jet through the West Basin sustains speeds of between 0.8 m/s (2.62 ft/sec) to 0.9 m/sec (2.95 ft/sec), well above the threshold of motion of the fine-grained beach sand on the bar in the West and Central Basins and more than sufficient to induce scour and erosion of those sands. The eddy in the central basin spins at as much as 0.3 m/sec (0.98 ft/sec) but the middle portion over the bar remains near stagnation, again providing ideal conditions for entrained beach sediment to settle and deposit. Flooding spring tide currents speed back up to 0.53 m/sec (1.7 ft/sec) through the Chang-channel under the I-5 bridge before diverging into a complex set of rather vigorous swirls that populate the East Basin. The more organized eddy system during flooding mean range tides in Figure 44 is still apparent in the East Basin during spring flooding tides. East Basin eddy speeds are on the order of at 0.1 m/sec (0.3 ft/sec). The high marsh area at the east end of the East Basin exhibits a disorganized meandering flow system during flooding spring tides. During ebbing spring tides (Figure 47), the East Basin creeping flows at -0.05 m/sec to -0.1 m/sec are more rectilinear, while the flow through the Chang-channel at the I-5 bridge, spreads into the Central Basin as a fairly uniform jet with velocities of about -0.5 m/sec (-1.6 ft/sec), indicating that the flood tide dominance of tidal flow under the I-5 bridge has been greatly diminished by the Chang-channel. The linear structures in I-5 ebb flow jet and the absence of significant swirl and turbulence indicate reduced drag and higher volume fluxes from the East Basin with more complete drainage.

The reduced drag and more complete pressure recovery of the velocity head in the Chang-channel relative to existing conditions has also reduced flood dominance during mean range tides as evidenced when velocity scales in Figures 44 and 45 are compared with those in Figures 31 & 32. Drag reduction achieved by the Chang-channel cross section in Figure 19 ultimately reduce the East Basin phase lag and thereby achieving

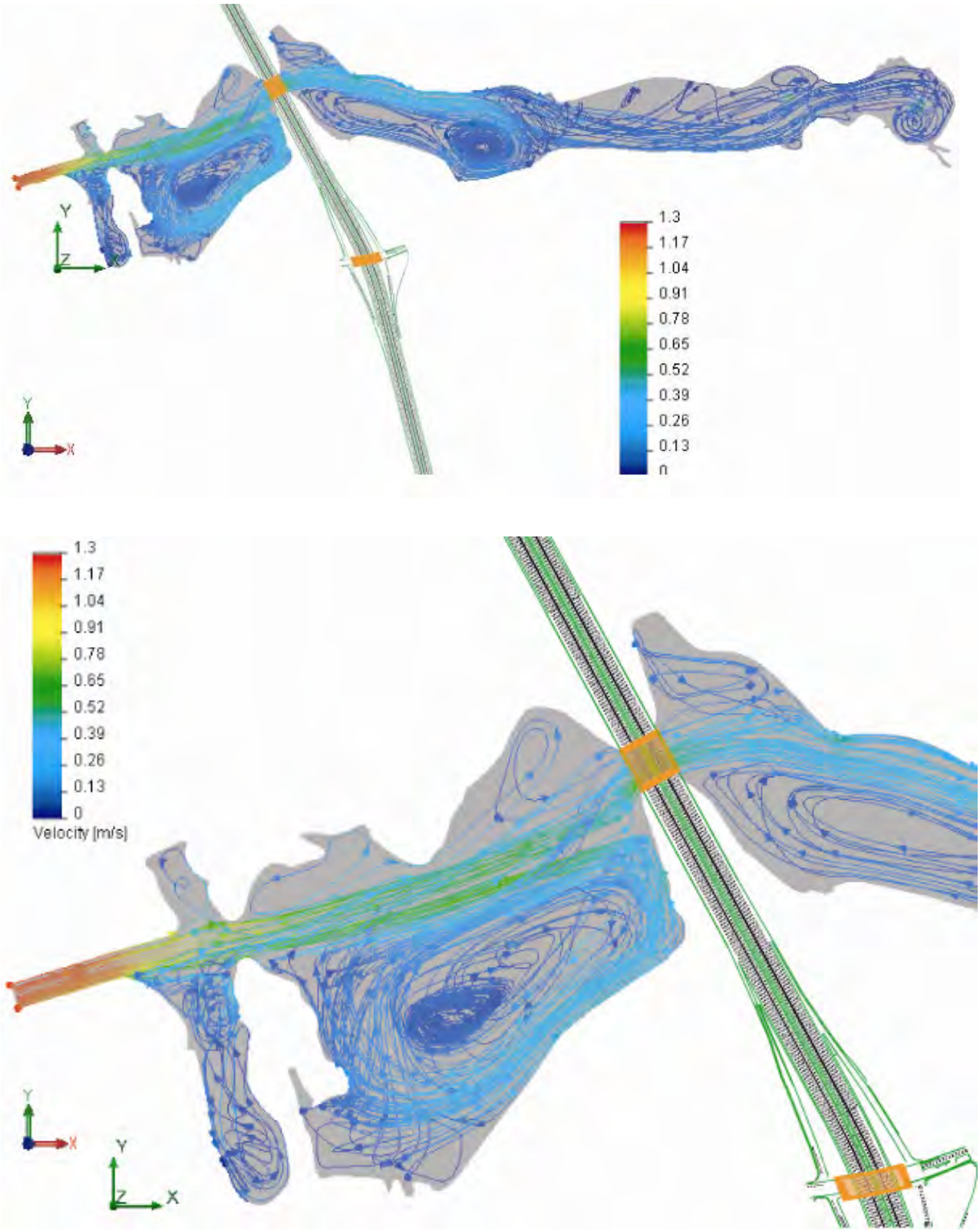

Figure 46: Hydrodynamic simulation of maximum flood flow during spring tides at Batiquitos Lagoon with the *Chang-channel* alternative for the replacement bridge of North Coast Corridor Project.

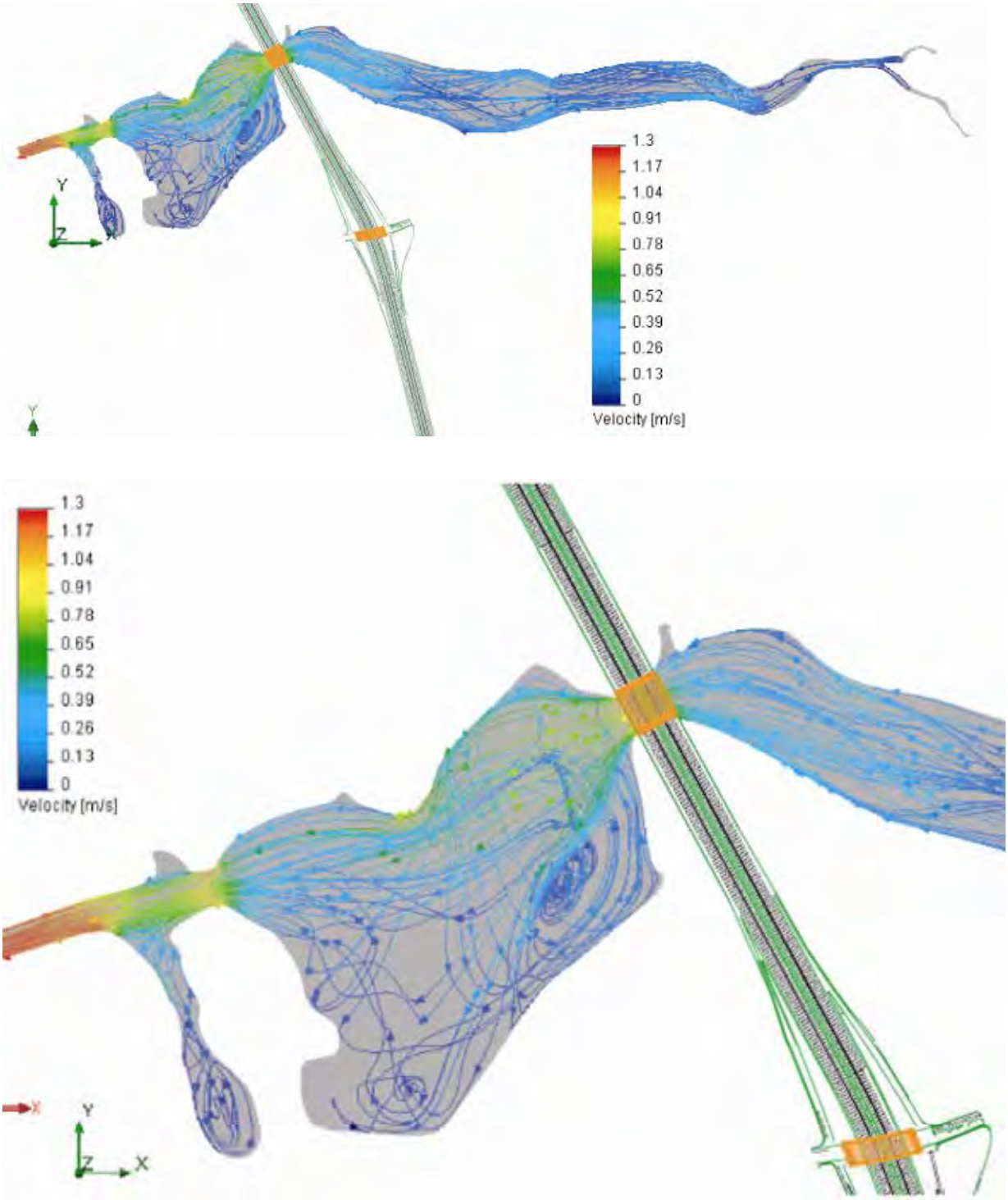

Figure 47: Hydrodynamic simulation of maximum ebb flow during spring tides at Batiquitos Lagoon with the *Chang-channel* alternative for the replacement bridge of North Coast Corridor Project.

more complete drainage of the East Basin during low tide. Figure 48 compares long term simulations of the daily low water levels in the East Basin with the existing I-5 bridge (black), the proposed I-5 bridge (red) and the double-wide channel alternative (purple) and the Chang-channel (green). The Chang-channel reduces the maximum daily lower low water levels to η_{LLW} = 2.35 ft MLLW from η_{LLW} = 2.5 ft MLLW for the existing I-5 bridge; and, reduces average daily lowest water levels to $\overline{\eta}_{LLW}$ = 1.24 ft MLLW from the existing average of $\overline{\eta}_{LLW}$ = 1.58 ft MLLW. The minimum daily low water level achieved by the Chang-channel is lowered most significantly to +0.36 ft MLLW, down from 0.9 ft MLLW for existing conditions (cf. Table 4.1). East Basin phase lags are substantially

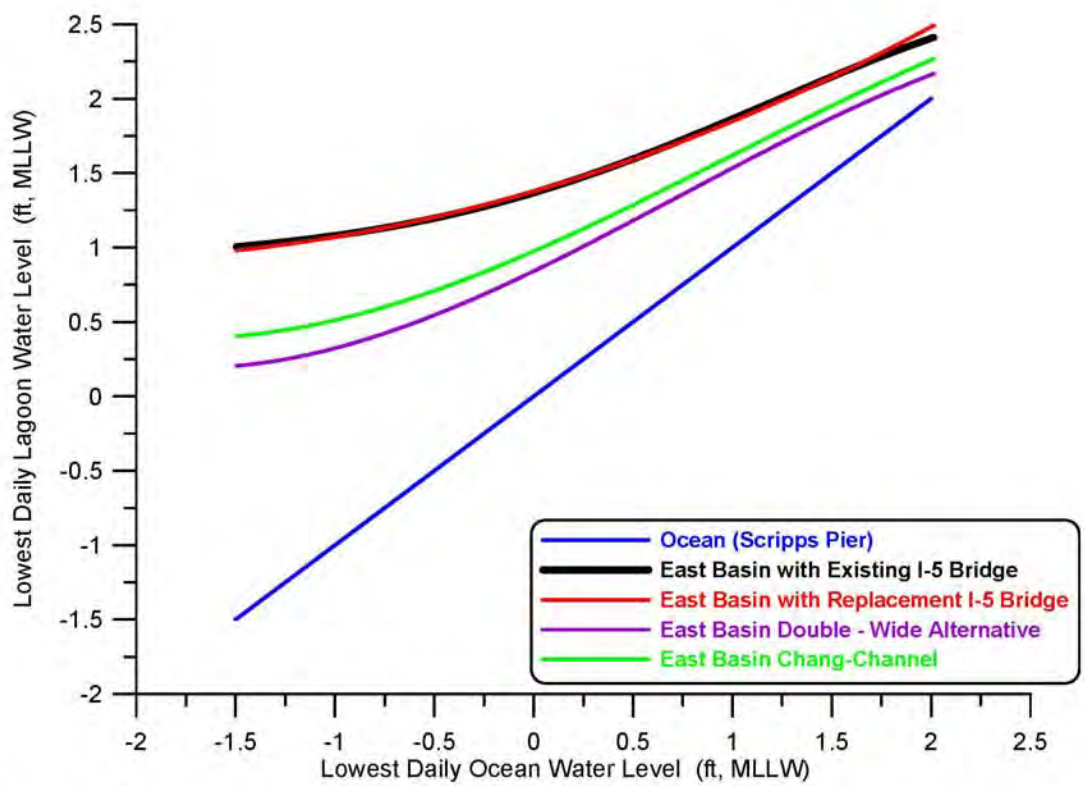

Figure 48. Comparison of daily lowest water level in east basin of Batiquitos Lagoon for existing I-5 bridge (black) and the proposed replacement I-5 bridge (red), the double-wide (purple), versus the Chang Channel (green). All shown as functions of daily lowest water level in the local ocean per Scripps Pier tide gage.

diminished with the Chang-channel alternative. Figure 49 shows that in long term simulation the maximum East Basin phase lag is reduced from $\theta_{\max}$ = 186 minutes with the existing I-5 bridge to $\theta_{\max}$ = 136 minutes with the double-wide alternative. Average East Basin phase lags are reduced from $\overline{\theta}$ = 117 minutes with the existing I-5 bridge to $\overline{\theta}$ = 79 minutes with the double-wide alternative. The minimum phase lag for East Basin

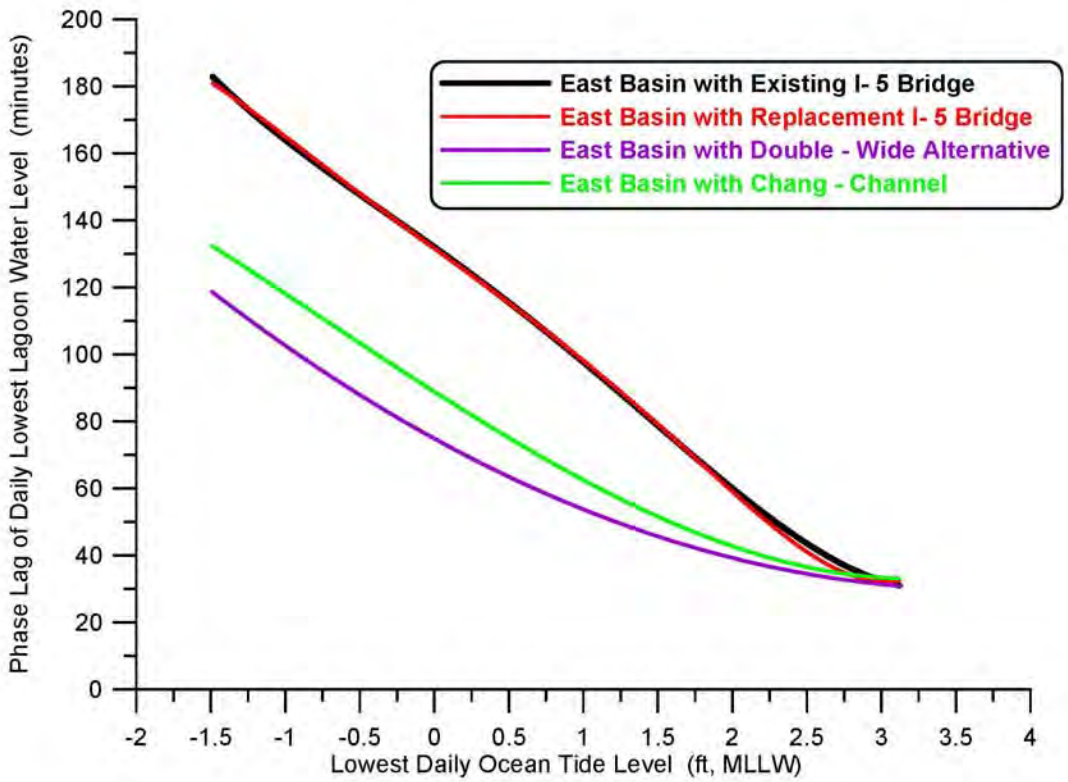

Figure 49. Comparison of the phase lag of lowest low water level in east basin of Batiquitos Lagoon for existing I-5 bridge (black), the proposed replacement I-5 bridge (red), the double-wide alternative (purple), versus the Chang-Channel (green). All shown as functions of daily lowest water level in the local ocean.

tides remains unchanged with the Chang-channel alternative at 31 minutes, as this minimum occurs during neap tides the choke points at the inlet channel and railroad bridge retain ultimate hydraulic control for these small range tidal events.

Reductions in flow speeds and phase lags due to the Chang-channel waterway alternative result in a more complete conversion of velocity head into potential energy of water elevation, and thereby increase the tidal range in the east basin of Batiquitos Lagoon. Table 4.5 gives a summary of the water level elevations calculated for Batiquitos Lagoon with the Chang-channel I-5 bridge alternative based on long-term tidal simulations using historic ocean water level forcing for the 2008 period of record. Comparing Table 4.5 against existing conditions in Table 4.1, we find that both the mean and maximum diurnal tidal ranges in the East Basin are substantially increased with the Chang-channel alternative. MHHW in the East Basin has been raised to +6.18 ft MLLW with the Chang-channel alternative, while MLLW in the East Basin has been lowered to +1.88 ft MLLW,

Table 4.5: Water Levels for Batiquitos Lagoon with Chang-channel Bridge Alternative

Elevations Feet MLLW	Ocean	West Basin	Central Basin	East Basin
MEAN HIGHER HIGH WATER (MHHW)	5.7	5.8	6.0	6.2
MEAN HIGH WATER (MHW)	5.0	5.0	5.2	5.3
MEAN LOW WATER (MLW)	1.3	1.6	1.9	1.88
MEAN LOWER LOW WATER (MLLW)	0.4	0.9	1.2	1.2
EXTREME LOW WATER LEVEL (ELW)	-1.5	-0.2	0.3	0.34
HIGHEST OBSERVED WATER LEVEL	7.4	7.3	7.4	7.6
MAXIMUM TIDAL RANGE	8.9	7.5	7.1	7.26

producing a mean diurnal tidal range of 5.0 ft, an increase of 0.5 ft over existing conditions. While extreme high water levels in the East Basin remain unchanged with the Chang-channel alternative, extreme low water levels are lowered to +0.34 ft MLLW, resulting in a maximum tidal range of 7.26 ft, an increase of 0.56 ft over existing conditions. Water elevations in the Central Basin remain unchanged with the Chang-channel alternative.

Figure 50 overlays the new MHHW and MLLW levels with the Chang-channel bridge waterway alternative on the East Basin stage area function, producing an average of 207.6 intertidal acres in the East Basin, or a net gain of 16.2 intertidal acres over existing conditions (cf. Figure 21) although 2.8 acres smaller than the net gain for the double-wide alternative. Again, most of this gain has resulted from conversion of sub-tidal to intertidal habitat, as the mean area of tidal inundation in the East Basin has increased by only 4.5 acres over existing conditions. A complete accounting of this conversion of sub-tidal to intertidal area and the realignment of the expanded intertidal area is revealed by the hydroperiod function in Figure 51, based on 1980-2010 ocean water level forcing. Comparing the new habitat breaks for the hydroperiod function of the Chang-channel alternative in Figure 51 against those for existing conditions in Figure 36, we find that the improved drainage of the East Basin promoted by the Chang-channel channel lowers the zonation of mud flats and marsh and thereby allows vertical expansion of the low, mid and high marsh habitat. This is shown in Table 4.6 where the elevations of the habitat

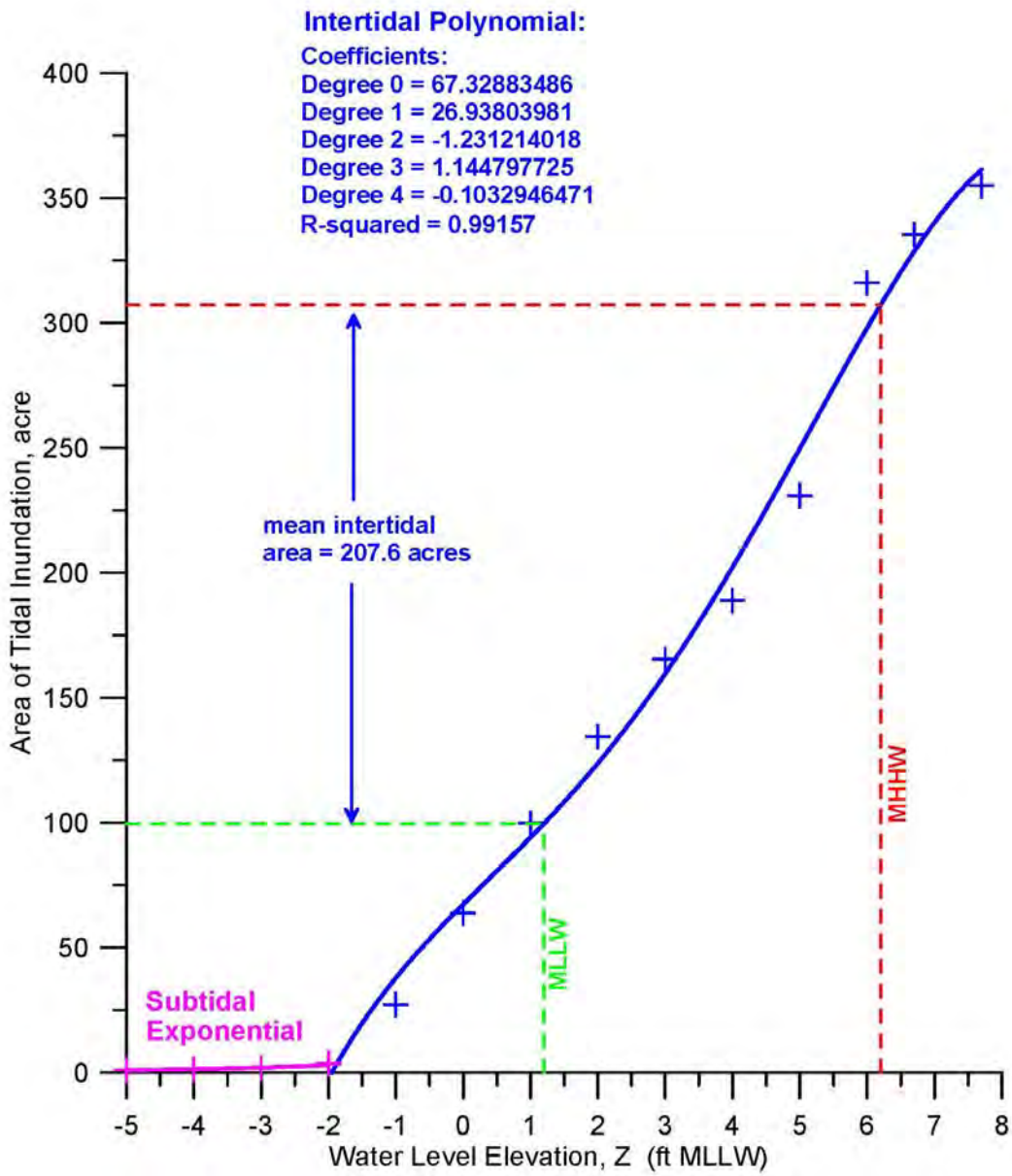

Figure 50. Area of tidal inundation in the east basin of Batiquitos Lagoon as a function of water level elevation for the Chang - Channel alternative. Mean water levels from long-term hydrodynamic simulation using 2008 tidal forcing.

breaks of the hydroperiod function in Figure 51 have been mapped against the stage area function (Figure 21) and used to estimate the sub-tidal and intertidal areas.

Table 4.6 shows that the perpetual sub-tidal area of the East Basin decreases with the Chang-channel alternative by 13.1 acres, to 78.2 acres from 91.3 acres for the existing bridge, while the mean sub-tidal area with the Chang-channel alternative decreases by 11.4 acres to 99.9 acres, from 111.3 acres for the existing bridge; frequently flooded mud flat is increased by 4.6 acres, from 58.6 acres for the existing bridge to 63.2 acres for the Chang-channel alternative; frequently exposed mud flat is increased by 3.0 acres, from 13.6 acres for the existing bridge to 16.6 acres for the Chang-channel alternative; low salt marsh is reduced slightly by 5.4 acres, from 42.3 acres for the existing bridge to 36.9 acres for the Chang-channel alternative; mid salt marsh is increased by 2.7 acres, from 77.0 acres for the existing bridge to 79.7 acres for the Chang-channel alternative; high salt marsh is increased considerably by 33.4 acres, from 45.8 acres for the existing bridge to 79.2 acres for the Chang-channel alternative; much of the transitional habitat is converted into high salt marsh, reducing transitional habitat by 24.7 acres from 30.2 acres for the existing bridge to 5.5 acres for the Chang-channel alternative. Maximum intertidal habitat is increased by 13.5 acres to 281.1 acres with the Chang-channel alternative as compared to 267.6 acres for existing conditions; and the mean area experiencing tidal inundation up to MHHW is increased by 4.8 acres from 302.7 acres for the existing bridge to 307.5 acres for the Chang-channel alternative resulting in an average 207.6 acres of intertidal habit, an increase of 16.2 acres over existing conditions.

Generally, Figure 51 and Table 4.6 indicate that the Chang-channel will create 7.6 acres of new mud flats and increase the exposure time of existing mud flats. Although this gain is slightly less than achieved by the double-wide alternative, it is, none the less, still a benefit to shorebird foraging and a feature of the East Basin that has been lacking to some degree. It will also reduce the compression of present intertidal habitat by lowering the zonation of low mid and high marsh vegetation allowing for some expansion of the cordgrass currently in the lagoon and providing some improved habitat for clapper rail. The new hydroperiod function promoted by the Chang-channel alternative in Figure 51 brings the functionality of the east basin of Batiquitos in closer alignment with its original restoration goals (see Merkel, 2008).

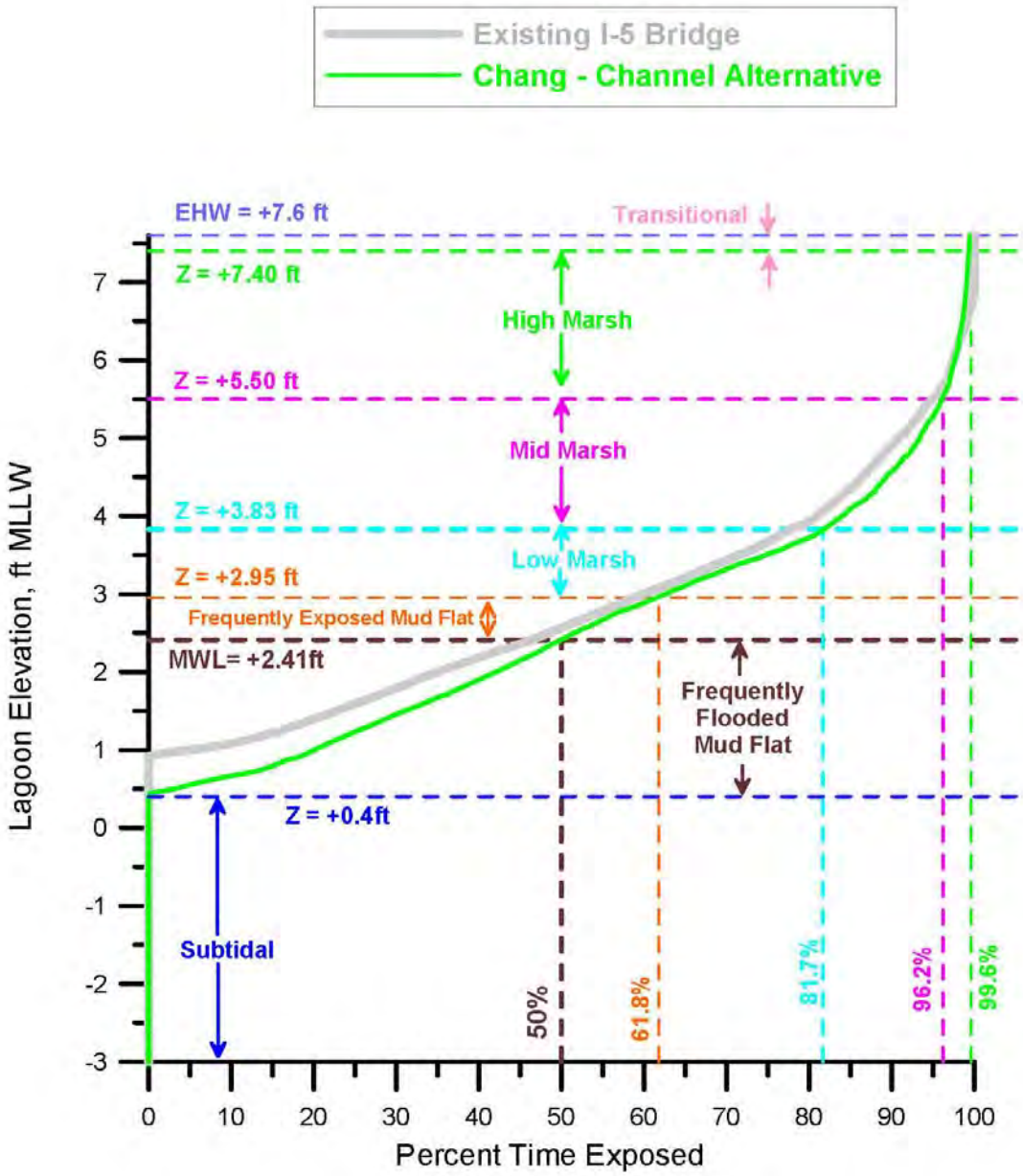

Figure 51. Hydroperiod function for the East Basin of Batiquitos Lagoon due to the Chang - Channel alternative. Based on hydrodynamic simulation of East Basin water levels in response to tidal forcing from the Scripps Pier tide gage (NOAA # 941-0230). Habitat breaks based on habitat delineation from Josselyn and Whelchel (1999).

Table 4.6: East Basin Habitat Area Distribution from Hydroperiod and Stage Area Functions with Existing Bridge vs. Chang-channel Alternative

East Basin Habitat Areas	Existing I-5 Bridge	Chang-channel
Perpetual Sub-Tidal (acres)	91.3	78.2
Mean Sub-Tidal (acres)	111.3	99.9
Frequently Flooded Mud Flat (acres)	58.6	63.2
Frequently Exposed Mud Flat (acres)	13.6	16.6
Low Salt Marsh (acres)	42.3	36.9
Mid Salt Marsh (acres)	77.0	79.7
High Salt Marsh (acres)	45.8	79.2
Transitional Habitat (acres)	30.2	5.5
Maximum Intertidal Area (acres)	267.6	281.1
Maximum Area of Salt Water Inundation (acres)	358.9	359.3
Mean Intertidal Area (acres)	191.4	207.6
Mean Area of Salt Water Inundation (acres)	302.7	307.5

4.3.4) Tidal Hydraulics Impacts of the Proposed I-5 Bridge Replacement + Flow Fences: Here we evaluate potential remediation of tidal range muting in the east basin of Batiquitos Lagoon by retrofitting Stratford flow fencing as shown in blue in Figure 20a to the proposed replacement I-5 bridge design with its 75 m (246 feet) bridge span. The *flow fence* alternative (Figure 20a) would have negligible footprint over existing lagoon habitat as it is envisioned as being constructed from vertical inter-locking sheet pile members driven into the lagoon and existing bridge waterway along the blue contours shown in Figure 20a. It would be constructed in phases, with the sheet piles driven immediately after the removal of sections of the existing bridge and prior to the construction of the replacement sections. It has been sized to adapt to the + 4 ft MLLW contours of the existing channel under the I-5 bridge along the using a channel bed at -3 ft MLLW with a bed width of 140 ft (Figure 20b)

Figure 52 and 53 give flow trajectories and depth-averaged tidal currents in Batiquitos Lagoon with the *replacement bridge + flow fence* alternative for maximum flood and ebb flow during mean range tides. With its hydrodynamic efficient channel expansion sections, this alternative reduces velocities in the bridge waterway channel by about 0.1 ft/sec for both flood and ebb flow and also reduces the swirl in the flanking sections of the receiving basins. Both actions result in more complete recovery of velocity head in the channel into pressure and tidal elevation of the receiving basin. The flood flow entering the East Basin the hard bottom expansion section of the channel and flow fence reaches to a maximum of 0.5 m/sec (1.9 ft/sec) during maximum flood flow (Figure 52), down from 0.7 m/sec (2.3 ft sec) for the replacement bridge without the flow fence (Figure 31). In Figure 53, velocities of the ebb flow exiting the hard bottom expansion section form a very uniform jet into the Central Basin with very little swirl, thereby reducing drag that would otherwise retard the ability of the East Basin to drain. Although the flow fence has cleaned up the structure of the tidal jets under the I-5 bridge, the velocities in those jets remain significantly higher than what was achieved with the larger channel cross sections of the double–wide and Chang-channel alternatives. With more velocity head to convert into pressure, the flow fence does not produce as much pressure and tidal elevation recovery in the receiving basins as the double–wide and Chang-channel alternatives.

Drag reduction and improved ebb flow structures achieved by the Stratford flow fence cross section in Figure 53 ultimately reduce the East Basin phase lag and thereby achieve more complete drainage of the East Basin during low tide. Figure 54 compares long term simulations of the daily low water levels in the East Basin with the existing I-5 bridge (black), the proposed I-5 bridge (red) and the flow fence retrofit the proposed I-5 bridge (cyan). The flow fence reduces the maximum daily lower low water levels to η_{LLW} = 2.4

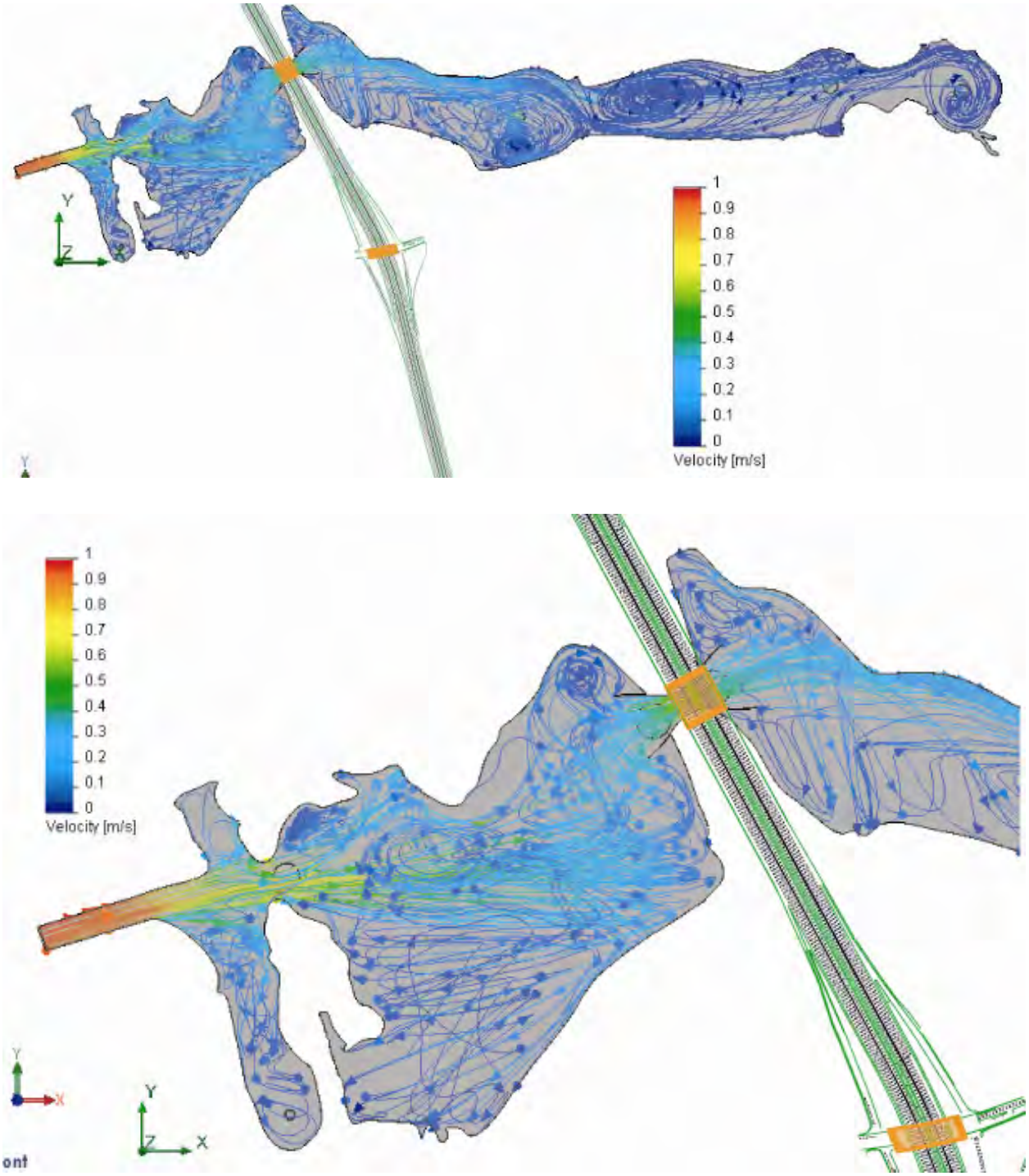

Figure 52: Hydrodynamic simulation of maximum flood flow during mean range tides at Batiquitos Lagoon with the proposed I-5 replacement bridge plus flow fences for the North Coast Corridor Project

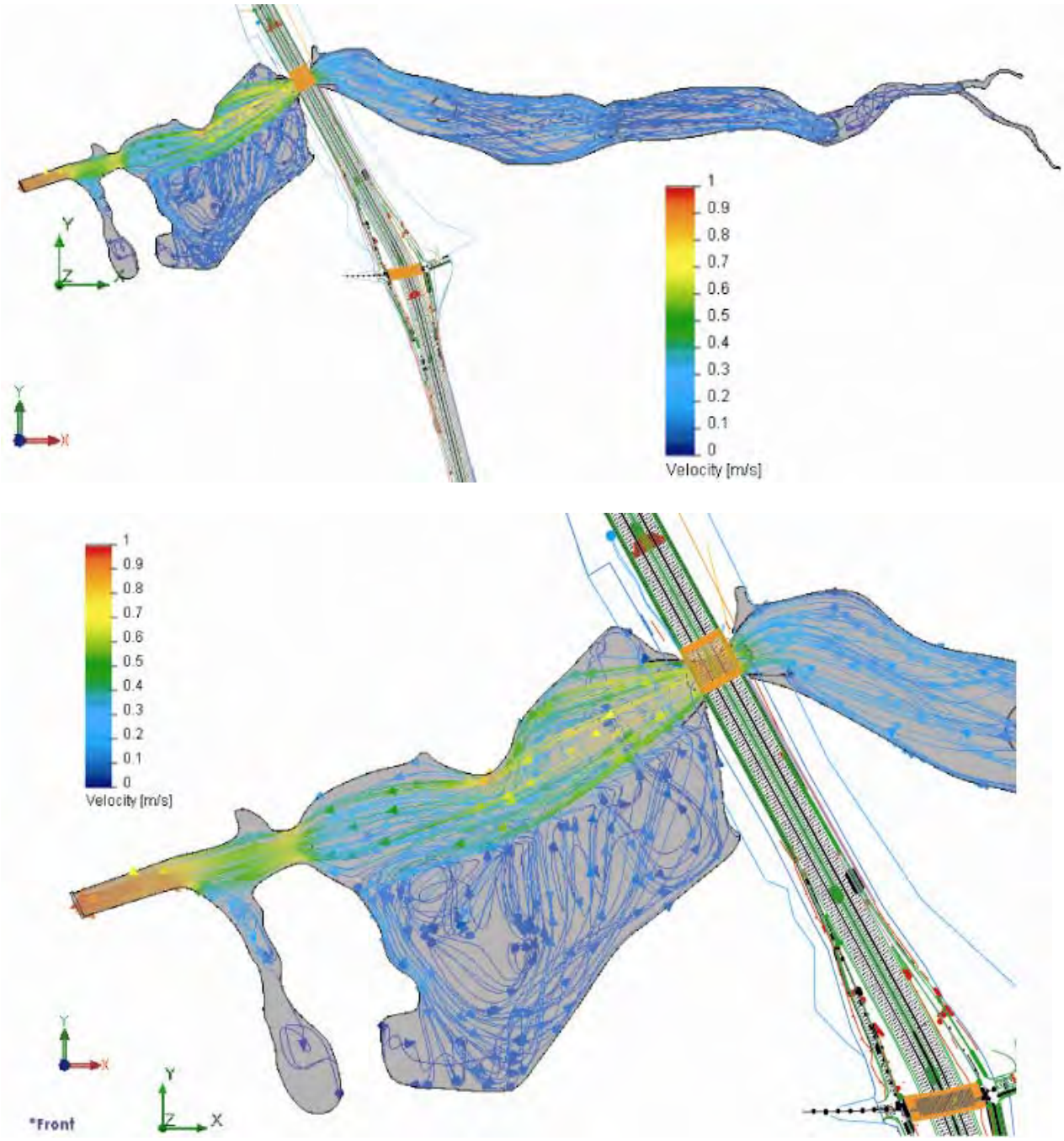

Figure 53: Hydrodynamic simulation of maximum ebb flow during mean range tides at Batiquitos Lagoon with the proposed I-5 replacement bridge plus flow fences for the North Coast Corridor Project.

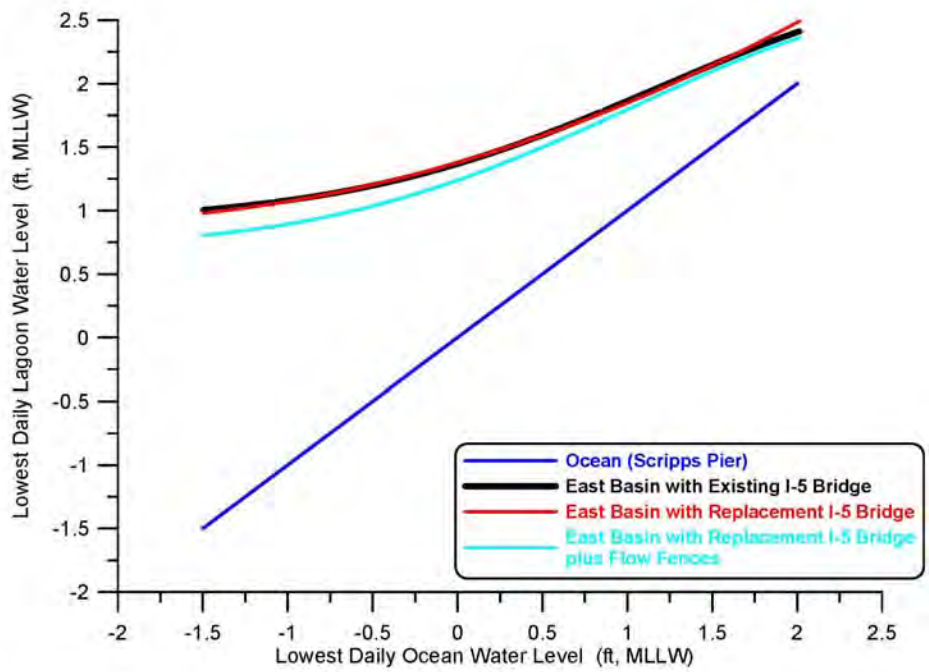

Figure 54. Comparison of daily lowest water level in east basin of Batiquitos Lagoon for existing I-5 bridge (black) and the proposed replacement I-5 bridge (red), versus the proposed replacement bridge with flow fences (cyan). All shown as functions of daily lowest water level in the local ocean per Scripps Pier tide gage.

ft MLLW from η_{LLW} = 2.5 ft MLLW for the existing I-5 bridge; and reduces average daily lowest water levels to $\overline{\eta}_{LLW}$ = 1.47 ft MLLW from the existing average of $\overline{\eta}_{LLW}$ = 1.58 ft MLLW. The minimum daily low water level achieved by the flow fence is lowered to +0.75 ft MLLW, down from 0.9 ft MLLW for existing conditions (cf. Table 4.1). Thus the flow fence in combination with the proposed replacement bridge is only able to achieve about one quarter the improvements of East Basin drainage as achieved by the double-wide alternative, and only about one third the improvements of the Chang-channel.

East Basin phase lags are diminished by the addition of the Stratford flow fence to the proposed replacement bridge. Figure 45 shows that in long term simulation the maximum East Basin phase lag is reduced from $\theta_{\max}$ = 186 minutes with the existing I-5 bridge to $\theta_{\max}$ = 169 minutes with the flow fence added to the proposed replacement bridge. Average East Basin phase lags are reduced from $\overline{\theta}$ = 117 minutes with the existing I-5 bridge to $\overline{\theta}$ = 103 minutes with the flow fences. The minimum phase lag for East Basin

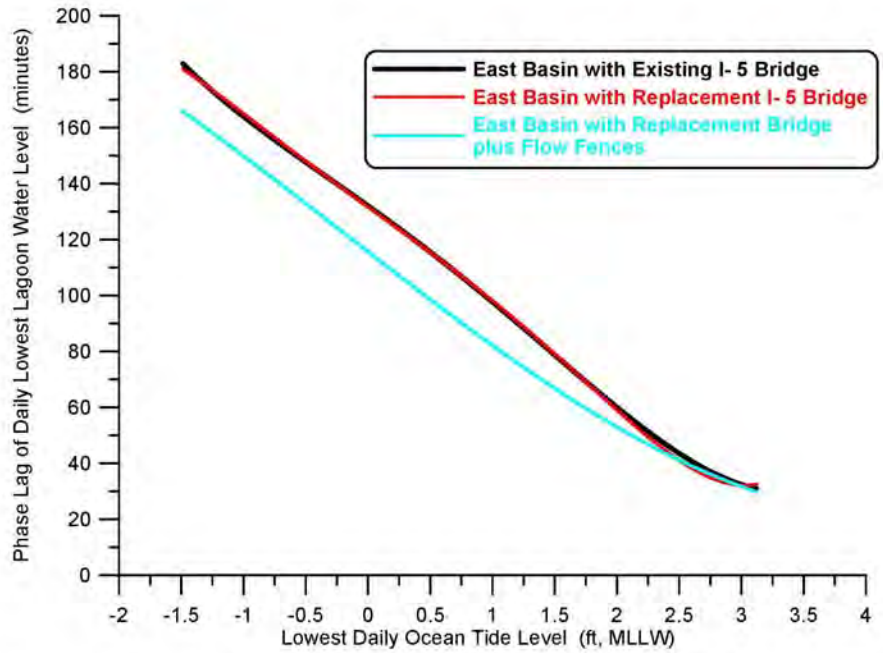

Figure 55. Comparison of the phase lag of lowest low water level in east basin of Batiquitos Lagoon for existing I-5 bridge (black), the proposed replacement I-5 bridge (red), versus the proposed replacement bridge + flow fences (cyan). All shown as functions of daily lowest water level in the local ocean.

tides remains unchanged at 31 minutes, as was found with the other alternatives because this minimum occurs during neap tides, where the choke points at the inlet channel and railroad bridge retain ultimate hydraulic control for these small range tidal events.

The reductions in flow speeds and phase lags due to the flow fence waterway are not as significant as found with the double-wide and Chang-channel alternatives because the smaller channel cross section of the proposed replacement bridge still produces more velocity head that must ultimately be recovered into potential energy of water elevation. Consequently, the flow fence by itself, although an improvement on the proposed replacement bridge, can not achieve as much of the benefits of the double-wide or Chang-channel alternatives. This is apparent in Table 4.7, which gives a summary of the water level elevations calculated for Batiquitos Lagoon with the I-5 replacement bridge and flow fencing based on long-term tidal simulations using historic ocean water level forcing for the 2008 period of record. Comparing Table 4.7 against existing conditions in Table 4.1, we find that both the mean and maximum diurnal tidal ranges in the East Basin are slightly increased by the addition of the flow fencing. MHHW in the East Basin has been raised to +6.13 ft MLLW with the Chang-channel alternative, while MLLW in the East Basin has been lowered to +1.47 ft MLLW, producing a mean diurnal tidal range of 4.66 ft., an increase of 0.16 ft over existing conditions. While extreme high water levels

Table 4.7: Water Levels for Batiquitos Lagoon with the Proposed Replacement Bridge Plus Flow Fence

Elevations Feet MLLW	Ocean	West Basin	Central Basin	East Basin
MEAN HIGHER HIGH WATER (MHHW)	5.7	5.8	6.0	6.13
MEAN HIGH WATER (MHW)	5.0	5.0	5.2	5.3
MEAN LOW WATER (MLW)	1.3	1.6	1.9	2.1
MEAN LOWER LOW WATER (MLLW)	0.4	0.9	1.2	1.47
EXTREME LOW WATER LEVEL (ELW)	-1.5	-0.2	0.3	0.75
HIGHEST OBSERVED WATER LEVEL	7.4	7.3	7.4	7.6
MAXIMUM TIDAL RANGE	8.9	7.5	7.1	6.85

in the East Basin remain unchanged with the flow fence retrofit, extreme low water levels are lowered by 0.15 ft to +0.75 ft MLLW, resulting in a maximum tidal range of 6.85 ft, an increase of 0.15 ft over existing conditions. Water elevations in the Central Basin remain unchanged with the flow fence retrofit.

Figure 56 overlays the new MHHW and MLLW levels with the flow fence retrofit to the proposed replacement on the East Basin stage area function, producing an average of 196.6 intertidal acres in the East Basin, or a net gain of 5.2 intertidal acres over existing conditions (cf. Figure 21), substantially less than the net gain for the double-wide or Chang-channel alternatives. Again, most of this gain has resulted from conversion of sub-tidal to intertidal habitat, as the mean area of tidal inundation in the East Basin has increased by only 1.3 acres over existing conditions. A complete accounting of this conversion of sub-tidal to intertidal area and the realignment of the expanded intertidal area is revealed by the hydroperiod function in Figure 57 based on 1980-2010 ocean water level forcing. Comparing the new habitat breaks for the hydroperiod function of the flow fence retrofit in Figure 57 against those for existing conditions in Figure 36, we find that the small improvements to drainage of the East Basin promoted by the flow fence retrofit slightly lowers the zonation of mud flats and marsh thereby allows a small vertical expansion of the low, mid and high marsh habitat. This is shown in Table 4.8

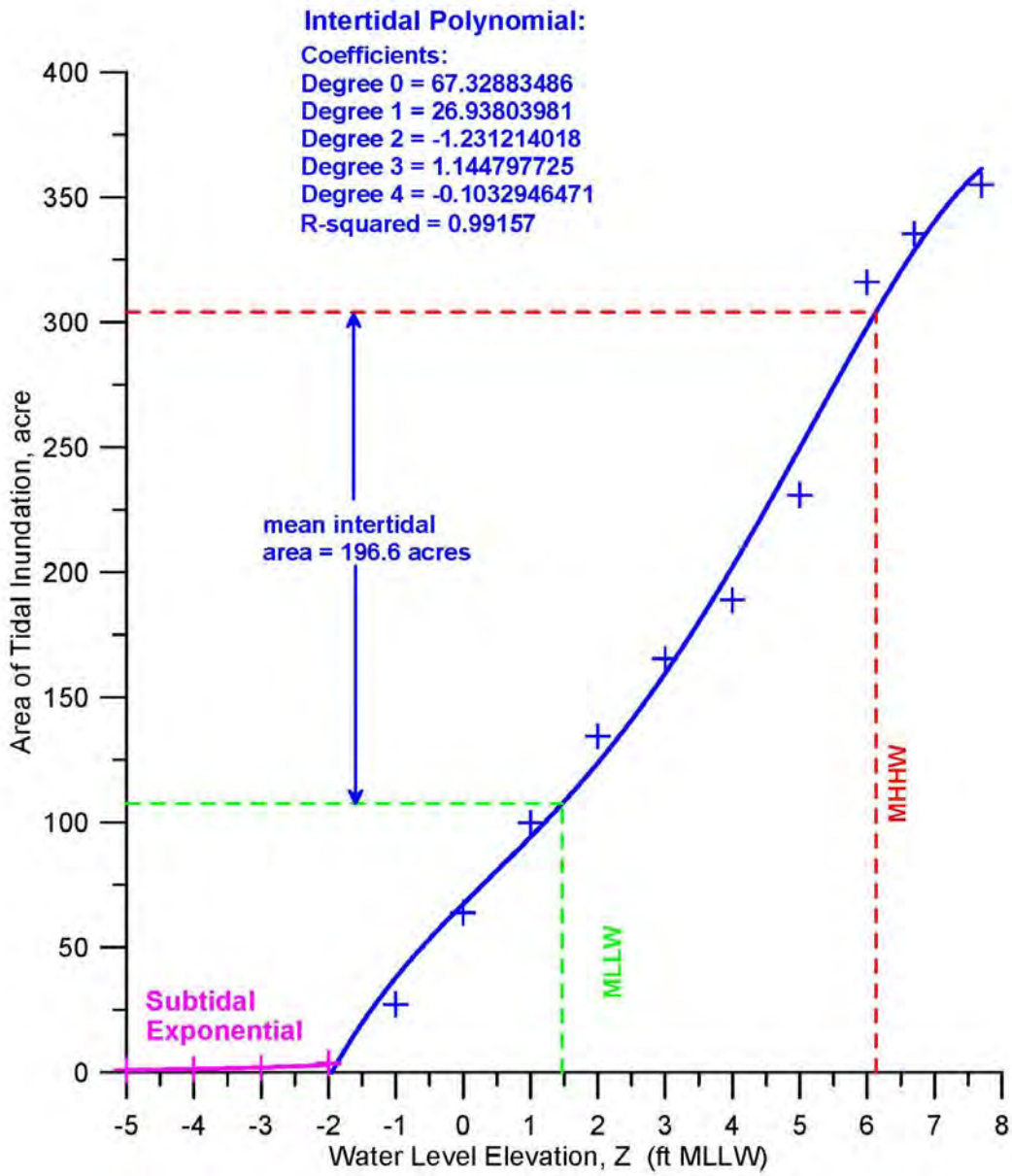

Figure 56. Area of tidal inundation in the east basin of Batiquitos Lagoon as a function of water level elevation for the proposed replacement bridge with flow fences. Mean water levels from hydrodynamic simulation using 2008 tidal forcing.

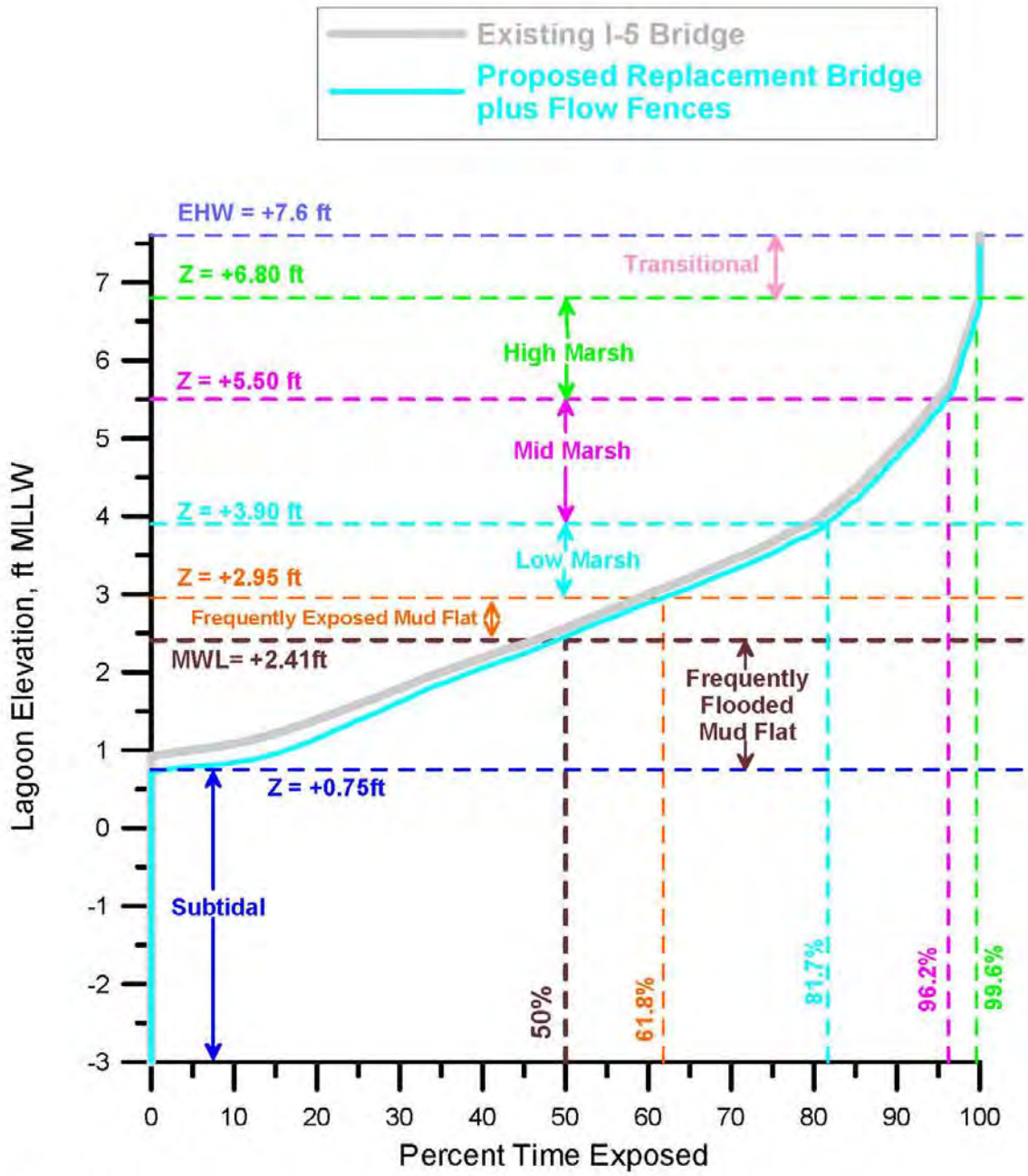

Figure 57. Hydroperiod function for the East Basin of Batiquitos Lagoon due to the proposed replacement bridge + flow fence. Based on hydrodynamic simulation of East Basin water levels in response to tidal forcing from the Scripps Pier tide gage (NOAA # 941-0230). Habitat breaks based on habitat delineation from Josselyn and Whelchel (1999).

Table 4.8: East Basin Habitat Area Distribution from Hydroperiod & Stage Area Functions for Existing Bridge vs. Proposed Replacement Bridge and Proposed Replacement Bridge plus Flow Fences

East Basin Habitat Areas	Existing I-5 Bridge	Replacement I-5 Bridge	Replacement I-5 Bridge + Flow Fences
Perpetual Sub-Tidal (acres)	91.3	91.9	87.3
Mean Sub-tidal (acres)	111.3	111.3	107.4
Frequently Flooded Mud Flat (acres)	58.6	58.1	53.8
Frequently Exposed Mud Flat (acres)	13.6	9.6	16.6
Low Salt Marsh (acres)	42.3	50.9	40.0
Mid Salt Marsh (acres)	77.0	77.2	76.5
High Salt Marsh (acres)	45.8	41.0	58.5
Transitional Habitat (acres)	30.2	30.2	26.2
Maximum Intertidal Area (acres)	267.6	267.0	271.6
Maximum Area of Salt Water Inundation (acres)	358.9	358.9	358.9
Mean Intertidal Area (acres)	191.4	191.4	196.6
Mean Area of Salt Water Inundation (acres)	302.7	302.7	304.0

where the elevations of the habitat breaks of the hydroperiod function in Figure 57 have been have been mapped against the stage area function (Figure 21) and used to estimate the sub-tidal and intertidal areas.

Table 4.8 shows that the perpetual sub-tidal area of the East Basin decreases with the flow-fence retrofit by 4.0 acres, to 87.3 acres from 91.3 acres for the existing bridge, while the mean sub-tidal area with the flow-fence retrofit decreases by 3.9 acres to 107.4 acres, from 111.3 acres for the existing bridge; frequently flooded mud flat is decreased by 4.3 acres, from 58.6 acres for the existing bridge to 53.8 acres for the flow fence retrofit alternative; frequently exposed mud flat is increased by 3.0 acres, from 13.6 acres

for the existing bridge to 16.6 acres for the flow fence retrofit; low salt marsh is reduced slightly by 2.3 acres, from 42.3 acres for the existing bridge to 40.0 acres for the flow fence retrofit alternative; mid salt marsh is decreased slightly by 0.5 acres, from 77.0 acres for the existing bridge to 76.5 acres for the flow fence retrofit; high salt marsh is increased considerably by 12.7 acres, from 45.8 acres for the existing bridge to 58.5 acres for the flow fence retrofit; some transitional habitat is converted into high salt marsh, reducing transitional habitat by 4.0 acres from 30.2 acres for the existing bridge to 26.2 acres for the flow fence retrofit. Maximum intertidal habitat is increased by only 4.0 acres to 271.6 acres with the flow fence retrofit as compared to 267.6 acres for existing conditions; and the mean area experiencing tidal inundation up to MHHW is increased by 1.3 acres from 302.7 acres for the existing bridge to 304.0 acres for the flow fence retrofit alternative resulting in an average 196.6 acres of intertidal habit, an increase of 5.2 acres over existing conditions.

Generally, Figure 57 and Table 4.8 indicate that the flow fence retrofit will create small amounts of new East Basin habitat with small reduction of the compression of present intertidal habitat by lowering the zonation of low mid and high marsh vegetation. These benefits are modest by comparison to what was achieved by expanding the bridge waterway channel cross section with the double-wide or Chang-channel alternatives.

4.3.5) Tidal Hydraulics Impacts of the Chang-channel Alternative + Flow Fences: Here we evaluate potential remediation of tidal range muting in the east basin of Batiquitos Lagoon by retrofitting Stratford flow fencing as shown in red in Figure 20a to the Chang-channel I-5 bridge waterway with its 75 m (246 feet) bridge span. The Chang-channel + flow fences alternative (Figure 20a) would have negligible footprint over existing lagoon habitat as it is envisioned as being constructed from vertical inter-locking sheet pile members driven into the lagoon and existing bridge waterway along the red contours shown in Figure 20a. It would be constructed in phases, with the sheet piles driven immediately after the removal of sections of the existing bridge and prior to the construction of the replacement sections. It has been sized to adapt to the Chang-channel contours under the I-5 bridge along the using a channel bed at -4.7 ft MLLW with a bed width of 203 ft (Figure 20c).

Figure 58 gives flow trajectories and depth-averaged tidal currents in Batiquitos Lagoon with the *Chang-channel + flow fences* alternative for maximum flood flow during mean range tides. With 80% more channel cross section than the existing bridge waterway in combination with an efficient flow fence expansion section for optimal pressure recovery, this alternative reduces the velocities of the flow exiting the hard bottom section of the channel to 0.3 m/sec (0.98 ft/sec) during maximum flood flow. In Figure 59, velocities of the ebb flow exiting the hard bottom expansion section form a very uniform jet into the Central Basin with very little swirl, thereby reducing drag that would otherwise retard the ability of the East Basin to drain. Ebbing flow velocities exiting the hard bottom section of the channel are reduced to 0.3 m/sec (0.98 ft/sec). While these flood and ebb velocities under the I-5 bridge are nearly comparable to the double-wide alternative, and remain less than the threshold of incipient motion of the local relict San Marcos Creek sediments, and thereby insufficient to cause significant scour. These sub-scour threshold channel velocities are insufficient to maintain the scour holes that presently exist on either side of the I-5 bridge (Figure 18); and consequently these holes will in-fill over time, further reducing losses of tidal energy to form drag. Hence the Chang-channel + flow fences cross section in Figure 20c does not exhibit scour holes.

Eddy structures and jets in the East, Central and West Basins with the Chang-channel + flow fences alternative are similar to those for the double-wide channel but display less swirl in the tidal streams exiting the expansion section of the flow fence, resulting in nearly uniform streams across large expanses of the receiving basins. Maximum flood currents in the inlet channel reach 0.99 m/sec or (3.25 ft/sec) with the Chang-channel + flow fences alternative; while maximum ebb flow currents in the inlet channel are -0.92 m/sec (-3.01 ft/sec) slightly more than existing conditions but the inlet is still flood tide dominated.

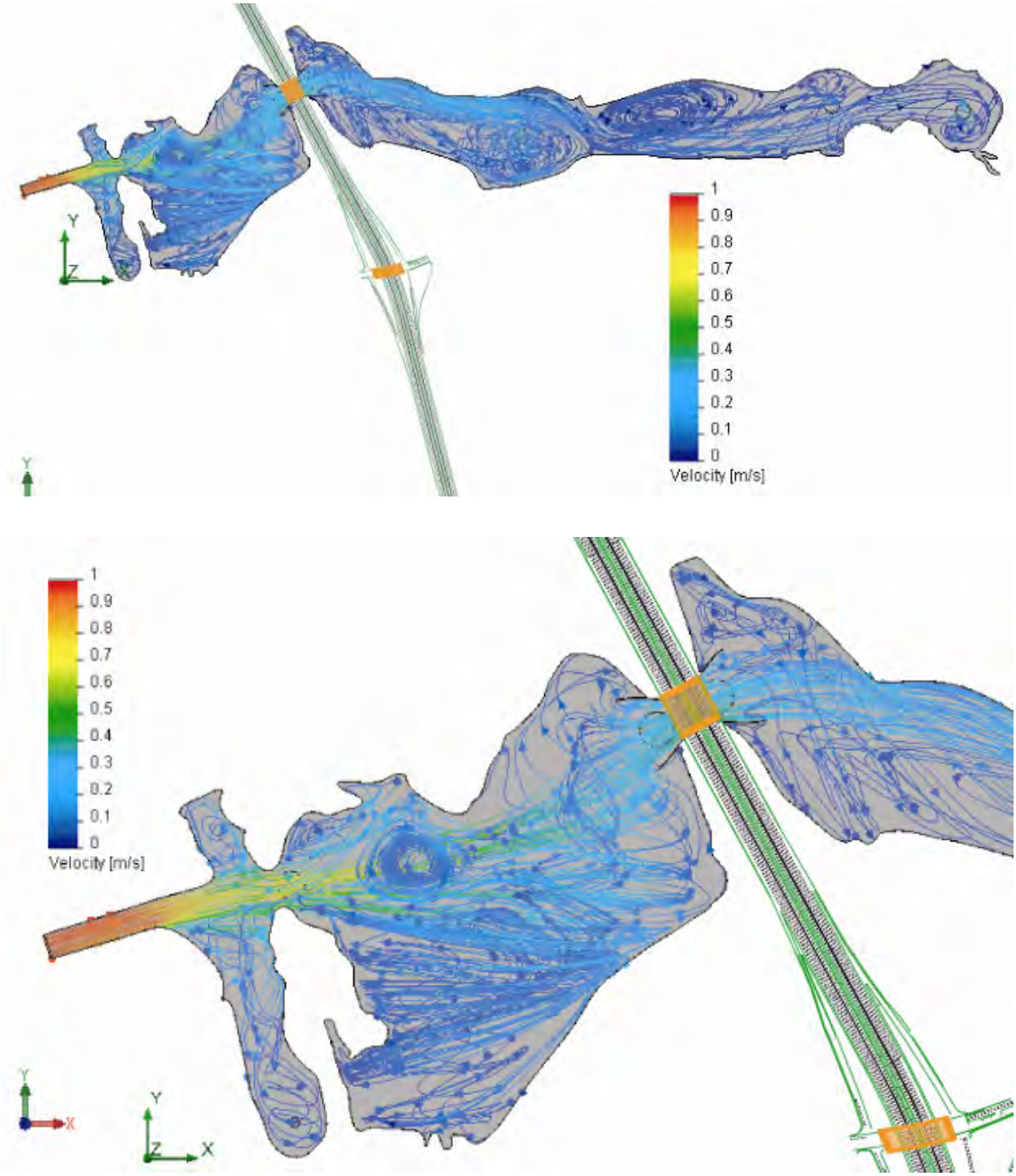

Figure 58: Hydrodynamic simulation of maximum flood flow during mean range tides at Batiquitos Lagoon with the *Chang-channel +flow fences* alternative for the replacement bridge of North Coast Corridor Project.

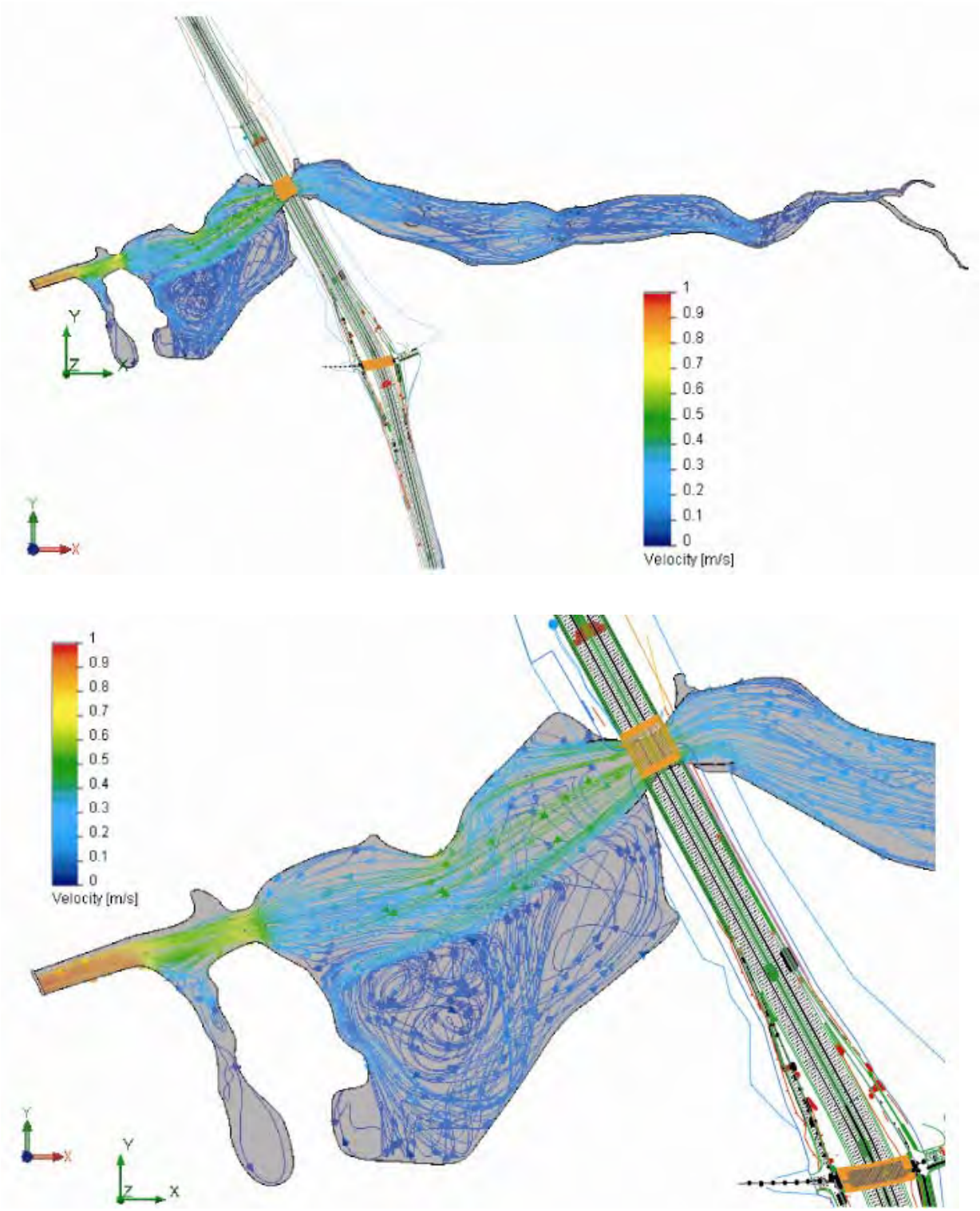

Figure 59: Hydrodynamic simulation of maximum ebb flow during mean range tides at Batiquitos Lagoon with the *Chang-channel + flow fences* alternative for the replacement bridge of North Coast Corridor Project.

Eddy structures in the East Basin during flooding tide are more well organized than with either the double-wide channel or existing channel. This is attributable to the swirl-free tidal stream exiting the expansion section of the flow fence, creating a boundary jet along the north bank of the East Basin during flooding tide that drives a system of counter rotating eddies throughout the East Basin. This stirring action should be beneficial to dissolved oxygen and nutrient distribution in the East Basin.

For flow similarity comparisons, Figures 60 and 61 give flow trajectories and depth-averaged tidal currents in Batiquitos Lagoon with the *Chang-channel* alternative for maximum flood and ebb flow during spring tides. Figures 60 & 61 display many similar flow structures to the mean range tide simulations in Figures 58 & 59. Figure 60 reveals maximum currents in the inlet channel reach 1.2 m/sec or 3.94 ft/sec. The flood tide jet through the West Basin sustains speeds of between 0.8 m/s (2.62 ft/sec) to 0.9 m/sec (2.95 ft/sec), well above the threshold of motion of the fine-grained beach sand on the bar in the West Basin and more than sufficient to induce scour and erosion of those sands. The eddy in the Central Basin spins at as much as 0.3 m/sec (0.98 ft/sec), but the middle portion over the bar remains near stagnation, again providing ideal conditions for entrained beach sediment to settle and deposit. Flooding spring tide currents speed back up to 0.4 m/sec (1.3 ft/sec) through the Chang-channel under the I-5 bridge before diverging into a complex set of rather vigorous set of eddies that populate the East Basin. The more organized eddy system during flooding mean range tides in Figure 44 is still apparent in the East Basin during spring flooding tides. East Basin eddy speeds are on the order of at 0.1 m/sec (0.3 ft/sec). The high marsh area at the east end of the East Basin exhibits a disorganized meandering flow system during flooding spring tides. During ebbing spring tides (Figure 61), the East Basin creeping flows at -0.05 m/sec to -0.1 m/sec are more rectilinear, while the flow through the Chang-channel at the I-5 bridge, spreads into the Central Basin as a fairly uniform jet with velocities of about -0.5 m/sec (-1.6 ft/sec), indicating that the flood tide dominance of tidal flow under the I-5 bridge has been greatly eliminated by the Chang-channel. The linear structures in I-5 ebb flow jet and the absence of significant swirl and turbulence indicate reduced drag and higher volume fluxes from the East Basin with more complete drainage.

Drag reduction achieved by the Chang-channel + flow fence expansion section in Figures 58-61 ultimately reduce the East Basin phase lag and thereby achieve more complete drainage of the East Basin during low tide. Figure 62 compares long term simulations of the daily low water levels in the East Basin with the existing I-5 bridge (black), the proposed I-5 bridge (red) and the proposed I-5 bridge + flow fences (cyan) and Chang-channel + flow fences (orange) and the Chang-channel in green. The Chang-channel + flow fences reduces the maximum daily lower low water levels to η_{LLW} = 2.24 ft MLLW

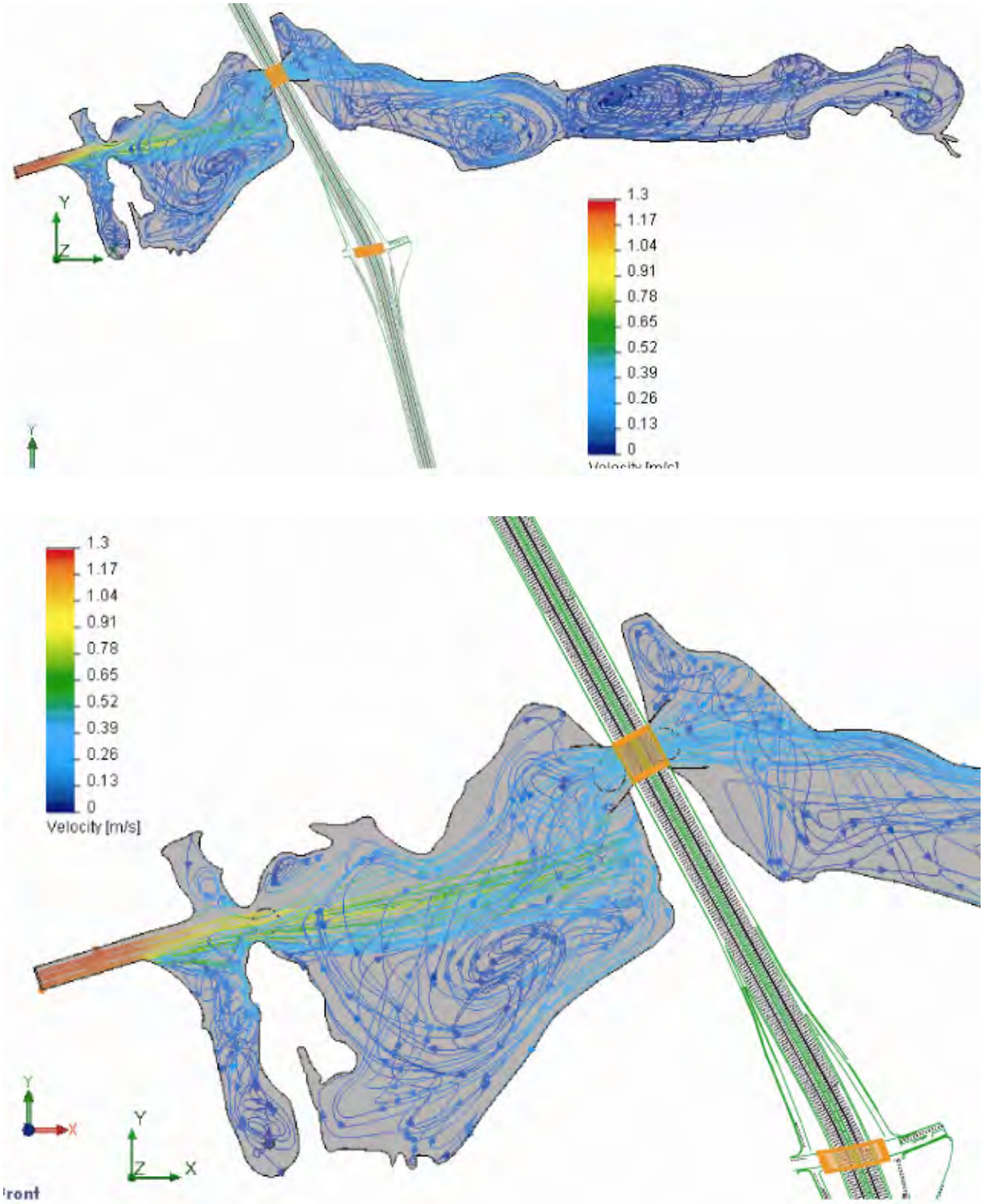

Figure 60: Hydrodynamic simulation of maximum flood flow during spring tides at Batiquitos Lagoon with the *Chang-channel + flow fences* alternative for the replacement bridge of North Coast Corridor Project.

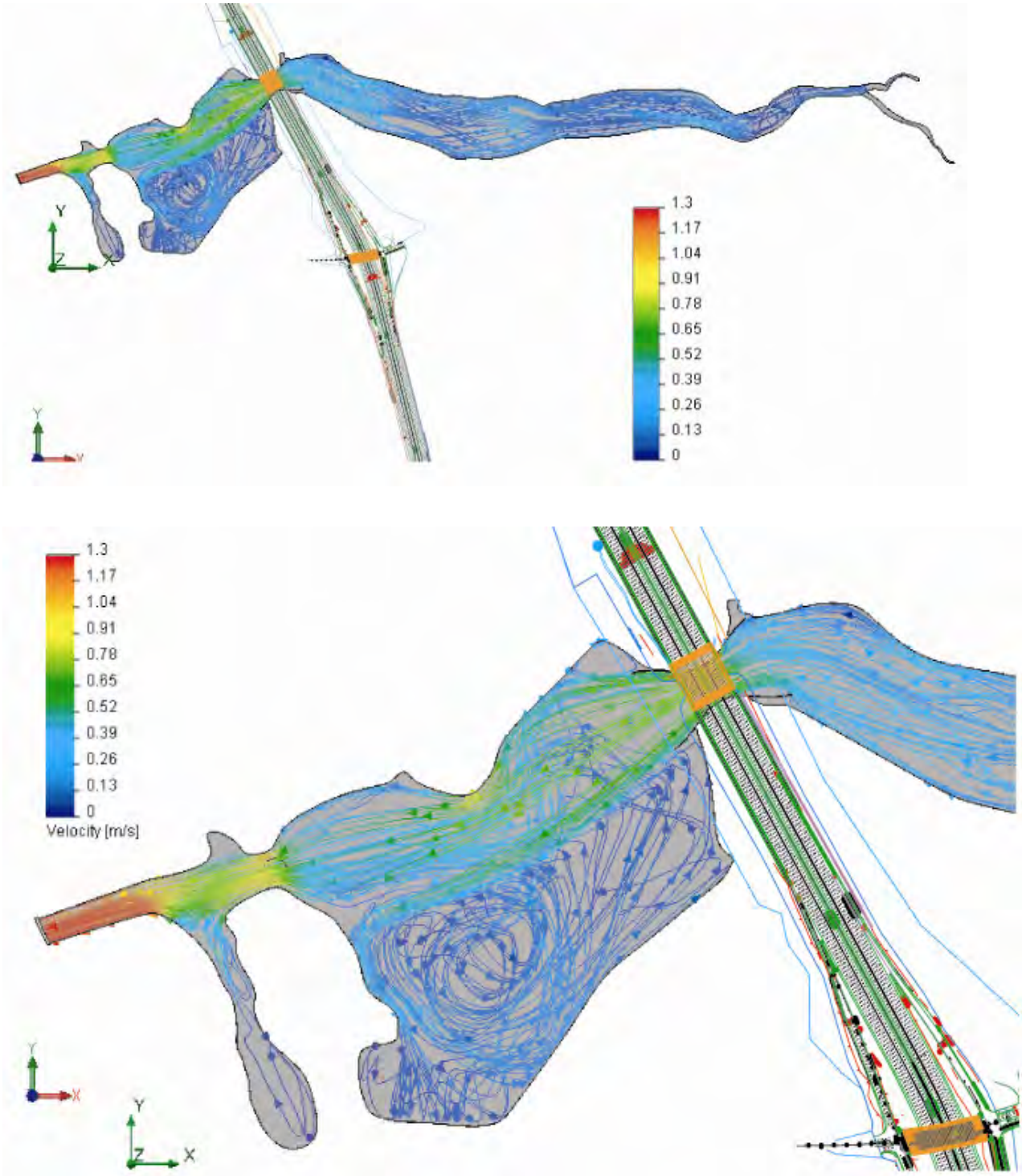

Figure 61: Hydrodynamic simulation of maximum ebb flow during spring tides at Batiquitos Lagoon with the *Chang-channel + flow fences* alternative for the replacement bridge of North Coast Corridor Project.

from η_{LLW} = 2.5 ft MLLW for the existing I-5 bridge; and, reduces average daily lowest water levels to $\overline{\eta}_{LLW}$ = 1.07 ft MLLW from the existing average of $\overline{\eta}_{LLW}$ = 1.58 ft MLLW. The minimum daily low water level achieved by the Chang-channel + flow fences is lowered most significantly to +0.17 ft MLLW, down from 0.9 ft MLLW for existing conditions (cf. Table 4.1).

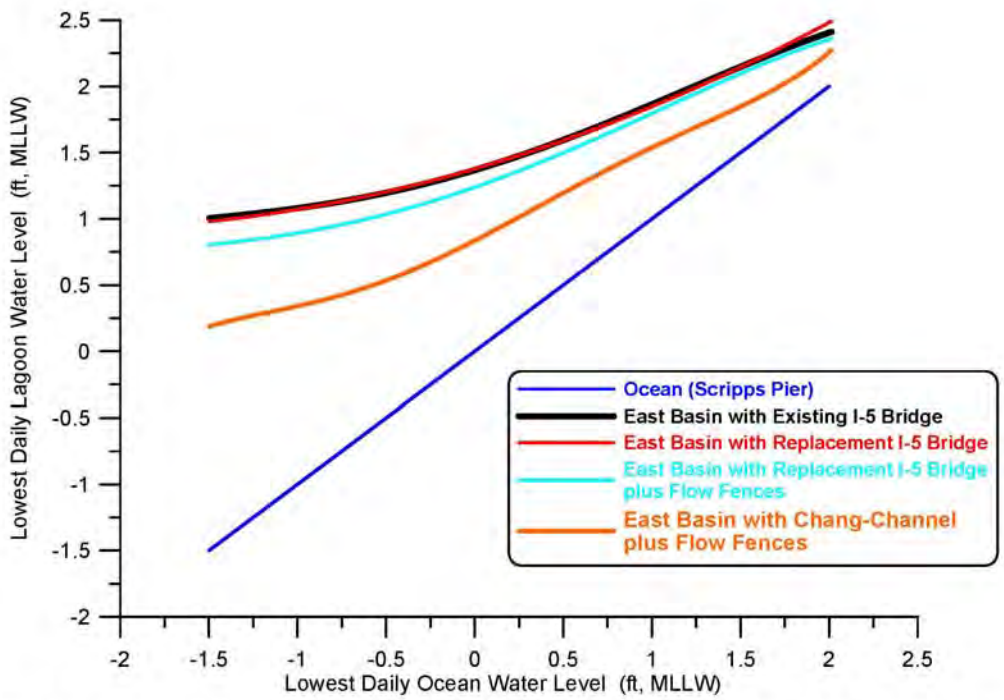

Figure 62. Comparison of daily lowest water level in east basin of Batiquitos Lagoon for existing I-5 bridge (black) and the proposed replacement I-5 bridge (red), the proposed replacement bridge with flow fences (cyan) vs the Chang Channel + Flow Fence alternative (orange). All shown as functions of daily lowest water level in the local ocean per Scripps Pier tide gage.

East Basin phase lags are substantially diminished with the Chang-channel + flow fences alternative. Figure 63 shows that in long term simulation the maximum East Basin phase lag is reduced from $\theta_{\max}$ = 186 minutes with the existing I-5 bridge to $\theta_{\max}$ = 120 minutes with the Chang-channel + flow fences alternative. Average East Basin phase lags are reduced from $\overline{\theta}$ = 117 minutes with the existing I-5 bridge to $\overline{\theta}$ = 68 minutes with the Chang-channel + flow fence alternative. The minimum phase lag for East Basin tides remains unchanged with the Chang-channel + flow fences alternative at 31 minutes, as this minimum occurs during neap tides with the choke points at the inlet channel and railroad bridge retaining ultimate hydraulic control for these small range tidal events.

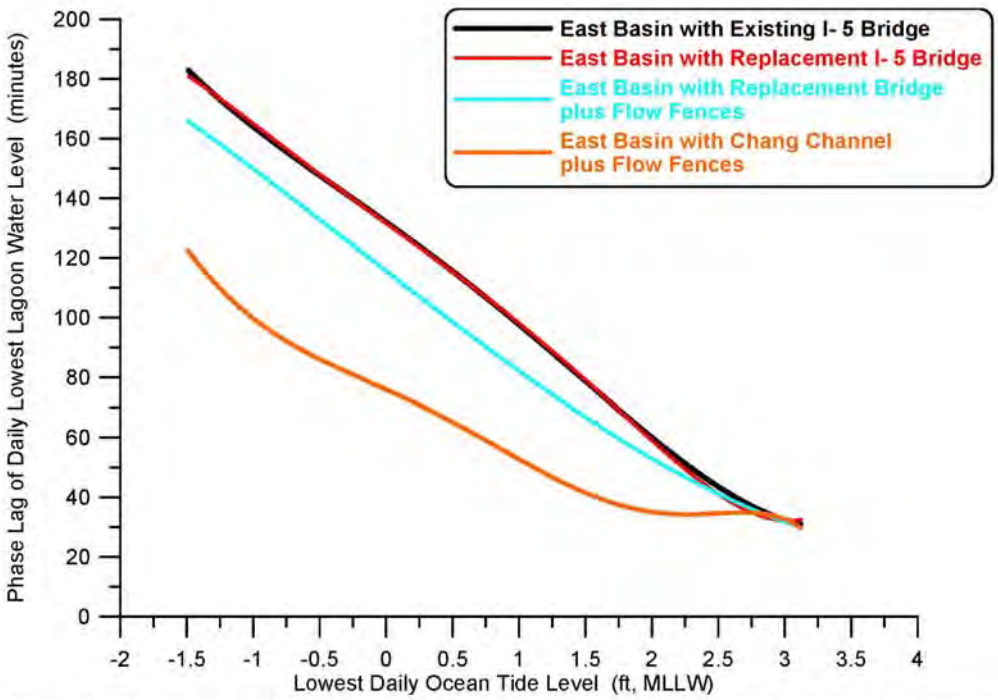

Figure 63. Comparison of the phase lag of lowest low water level in east basin of Batiquitos Lagoon for existing I-5 bridge (black), the proposed replacement I-5 bridge (red), the proposed replacement bridge + flow fences (cyan) versus the Chang Channel + flow fences (orange). All shown as functions of daily lowest water level in the local ocean.

The reductions in flow speeds and phase lags due to the Chang-channel + flow fences waterway alternative results in more complete conversion of velocity into potential energy of water elevation, thereby increasing the tidal range in the east basin of Batiquitos Lagoon. Table 4.9 gives a summary of the water level elevations calculated for Batiquitos Lagoon with the Chang-channel + flow fences I-5 bridge alternative based on long-term tidal simulations using historic ocean water level forcing for the 2008 period of record. Comparing Table 4.9 against existing conditions in Table 4.1, we find that both the mean and maximum diurnal tidal ranges in the East Basin are substantially increased with the Chang-channel + flow fences alternative. MHHW in the East Basin has been raised to +6.2 ft MLLW with the Chang-channel + flow fence alternative, while MLLW in the East Basin has been lowered to +1.07 ft MLLW, producing a mean diurnal tidal range of 5.13 ft, an increase of 0.63 ft over existing conditions. While extreme high water levels in the East Basin remain unchanged with the Chang-channel + flow fences

Table 4.9: Water Levels for Batiquitos Lagoon with Chang-channel + flow fences Alternative I-5 Bridge

Elevations Feet MLLW	Ocean	West Basin	Central Basin	East Basin
MEAN HIGHER HIGH WATER (MHHW)	5.7	5.8	6.0	6.2
MEAN HIGH WATER (MHW)	5.0	5.0	5.2	5.3
MEAN LOW WATER (MLW)	1.3	1.6	1.8	1.8
MEAN LOWER LOW WATER (MLLW)	0.4	0.9	1.05	1.07
EXTREME LOW WATER LEVEL (ELW)	-1.5	-0.2	0.15	0.15
EXTREME HIGH WATER LEVEL (EHW)	7.4	7.3	7.4	7.6
MAXIMUM TIDAL RANGE	8.9	7.5	7.2	7.4

alternative, extreme low water levels are lowered to +0.15 ft MLLW, resulting in a maximum tidal range of 7.45 ft, an increase of 0.75 ft over existing conditions. More complete drainage of the East Basin with the Chang-channel + flow fences alternative also makes a small improvement in the Central Basin, where MLW is lowered by 0.1 ft to +1.8 ft MLLW, MLLW is lowered by 0.15 ft to +1.05 ft MLLW; ELW is lowered by 0.15 ft to +0.15 ft MLLW; and the maximum tidal range is increased by 0.1 ft to 7.2 ft.

Figure 64 overlays the new MHHW and MLLW levels with the Chang-channel + flow fences bridge waterway alternative on the East Basin stage area function, producing an average of 211.2 intertidal acres in the East Basin, or a net gain of 19.8 intertidal acres over existing conditions (cf. Figure 21) and a net gain of 0.8 intertidal acres over the double-wide alternative. However most of this gain has resulted from conversion of sub-tidal to intertidal habitat, as the mean area of tidal inundation in the East Basin has increased by only 5.9 acres over existing conditions (and 0.5 acres more than the double-wide alternative). A complete accounting of this conversion of sub-tidal to intertidal area and the realignment of the expanded intertidal area is revealed by the hydroperiod function in Figure 65 based on 1980-2010 ocean water level forcing. Comparing the new habitat breaks for the hydroperiod function of the Chang-channel + flow fences I-5 bridge alternative in Figure 65 against those for existing conditions in Figure 36, we find that the improved drainage of the east basin promoted by the Chang-channel + flow fences lowers the zonation of mud flats and thereby allows vertical expansion of the low, mid and high

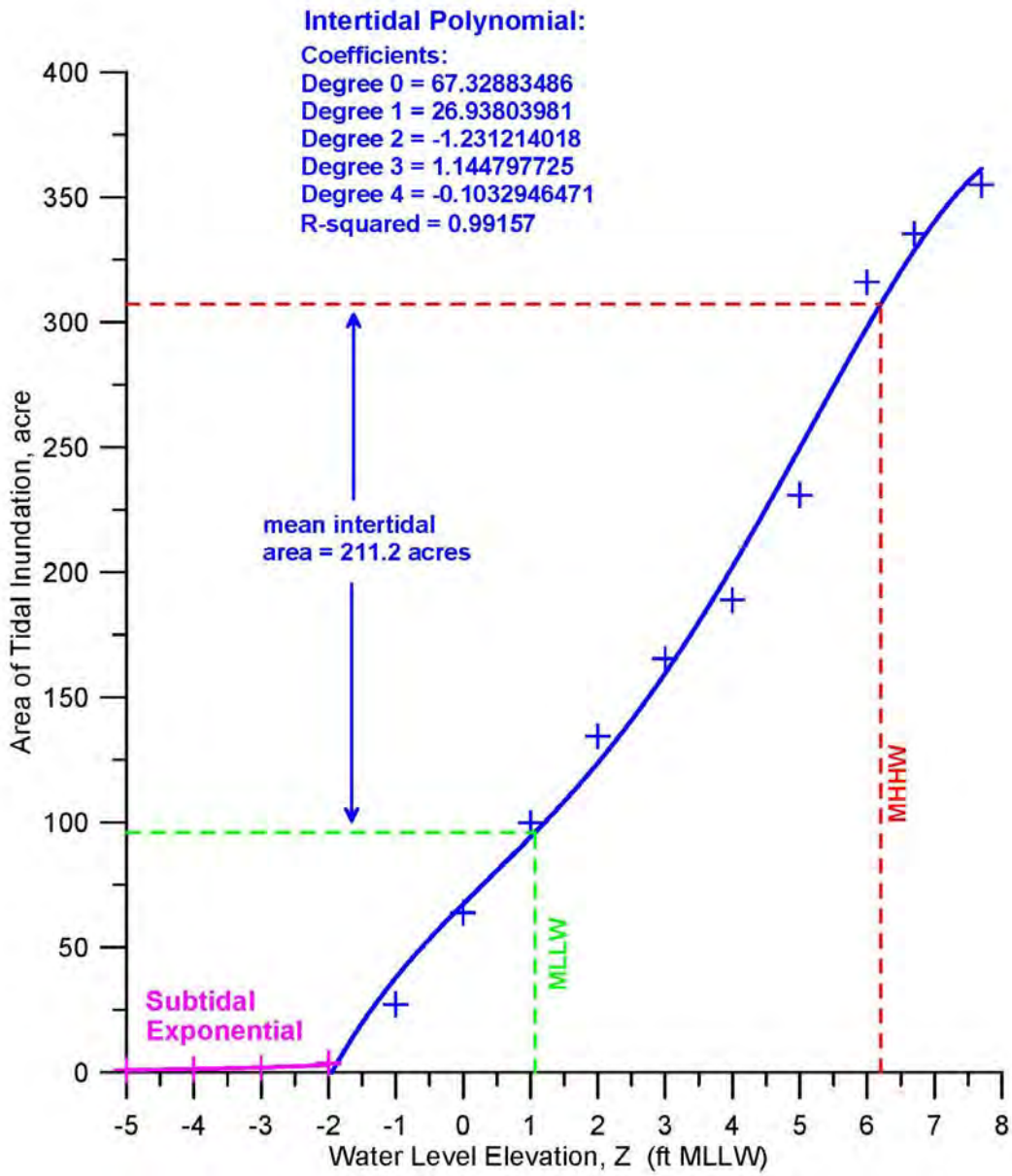

Figure 64. Area of tidal inundation in the east basin of Batiquitos Lagoon as a function of water level elevation for the Chang - Channel + Flow Fence alternative. Mean water levels from 2008 tidal forcing.

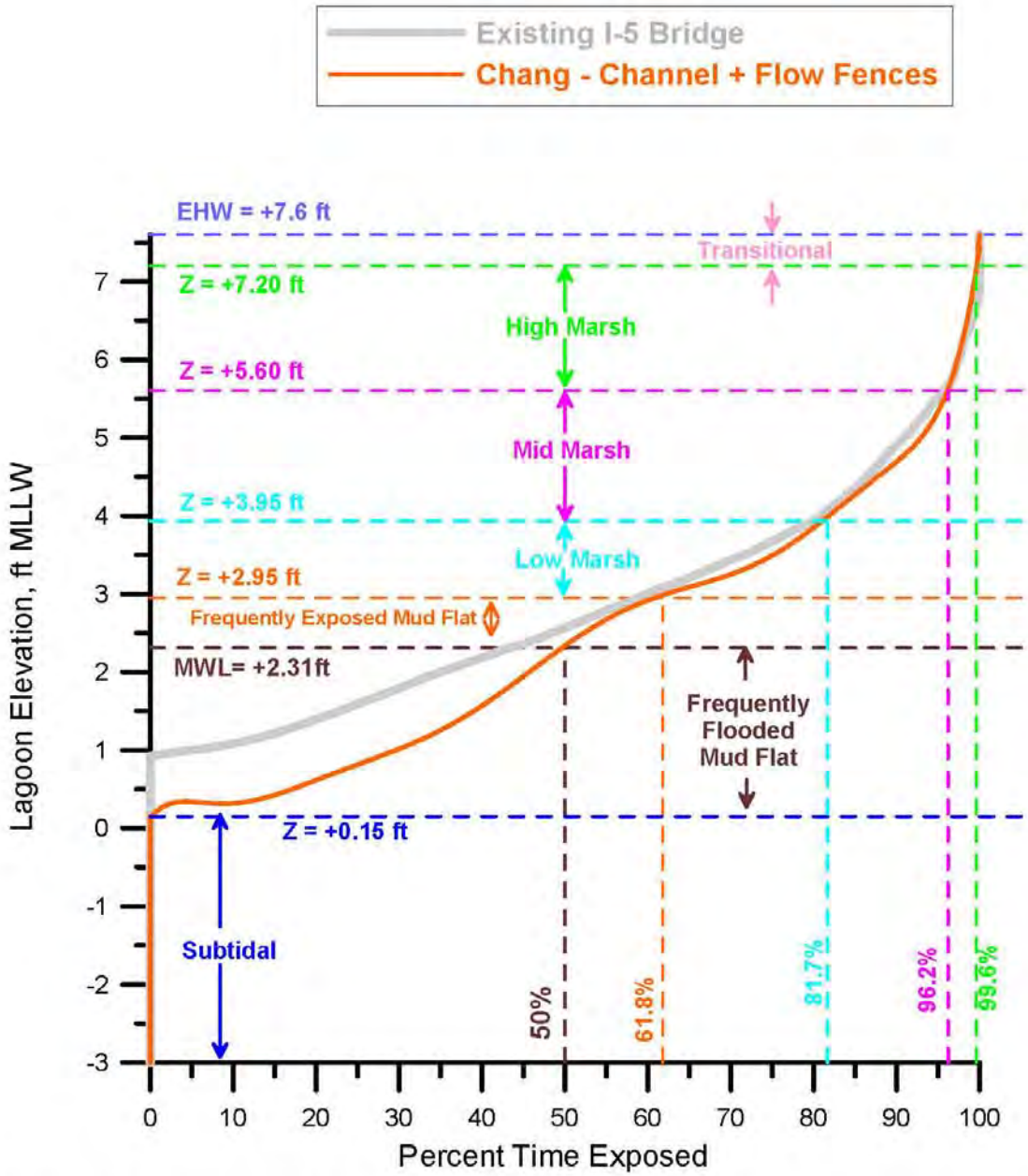

Figure 65. Hydroperiod function for the East Basin of Batiquitos Lagoon due to the Chang - Channel + Flow Fence alternative. Based on hydrodynamic simulation of East Basin water levels in response to tidal forcing from the Scripps Pier tide gage (NOAA # 941-0230). Habitat breaks based on habitat delineation from Josselyn and Whelchel (1999).

Table 4.10: East Basin Habitat Area Distribution from Hydroperiod and Stage Area Functions with Existing Bridge vs. Chang-channel + Flow Fences Alternative

East Basin Habitat Areas	Existing I-5 Bridge	Chang-channel + Flow Fences Alternative
Perpetual Sub-Tidal (acres)	91.3	71.8
Mean Sub-Tidal (acres)	111.3	96.5
Frequently Flooded Mud Flat (acres)	58.6	65.7
Frequently Exposed Mud Flat (acres)	13.6	20.6
Low Salt Marsh (acres)	42.3	42.3
Mid Salt Marsh (acres)	77.0	79.1
High Salt Marsh (acres)	45.8	68.1
Transitional Habitat (acres)	30.2	11.7
Maximum Intertidal Area (acres)	267.6	287.6
Maximum Area of Salt Water Inundation (acres)	358.9	359.4
Mean Intertidal Area (acres)	191.4	211.2
Mean Area of Salt Water Inundation (acres)	302.7	307.7

marsh habitat. This is shown in Table 4.10 where the elevations of the habitat breaks of the hydroperiod function in Figure 65 have been mapped against the stage area function (Figure 21) and used to estimate the sub-tidal and intertidal areas.

Table 4.10 shows that the perpetual sub-tidal area of the East Basin decreases by 19.5 acres to 71.8 acres with the Chang-channel + flow fences alternative, from 91.3 acres for the existing bridge, while the mean sub-tidal area with the Chang-channel + flow fences alternative decreases by 14.8 acres to 96.5 acres, from 111.3 acres for the existing bridge; frequently flooded mud flat is increased by 7.1 acres, from 58.6 acres for the existing bridge to 65.7 acres for the Chang-channel + flow fences alternative; frequently exposed mud flat is increased by 7.0 acres, from 13.6 acres for the existing bridge to 20.6 acres for the Chang-channel + flow fences alternative; low salt marsh is unchanged from 42.3

acres for the existing bridge; mid salt marsh is increased by only 2.1 acres, from 77.0 acres for the existing bridge to 79.1 acres for the Chang-channel + flow fences alternative; high salt marsh is increased considerably by 22.3 acres, from 45.8 acres for the existing bridge to 68.1 acres for the Chang-channel + flow fences alternative replacement bridge; some of the transitional habitat is converted into high salt marsh, reducing transitional habitat by 18.5 acres from 30.2 acres for the existing bridge to 11.7 acres for the Chang-channel + flow fences alternative. Maximum intertidal habitat is increased by 20.0 acres to 287.6 acres with the Chang-channel + flow fences alternative as compared to 267.6 acres for existing conditions and 286.8 acres for the double-wide alternative; and the mean area experiencing tidal inundation up to MHHW is increased by 5.0 acres from 302.7 acres for the existing bridge to 307.7 acres for the Chang-channel + flow fences alternative resulting in an average 211.2 acres of intertidal habit, an increase of 19.8 acres over existing conditions.

Generally, Figure 65 and Table 4.10 indicate that the Chang-channel + flow fences alternative is roughly comparable in performance to the double-wide alternative without the added cost of doubling the span of the replacement bridge. The Chang-channel + flow fences alternative will create 14.1 acres of new mud flats (1.3 acres more than the double-wide alternative) and both will increase the exposure time of existing mud flats; a benefit to shorebird foraging and a feature of the East Basin that has been lacking to some degree. It will also reduce the compression of present intertidal habitat by lowering the zonation of low mid and high marsh vegetation allowing for some expansion of the cordgrass currently in the lagoon and providing some improved habitat for clapper rail. The new hydroperiod function promoted by the Chang-channel + flow fences alternative in Figure 65 brings the functionality of the east basin of Batiquitos in closer alignment with its original restoration goals (see Merkel, 2008).

5) Tidal Hydraulics Impacts of Replacing and Widening the I-5 Bridge at Agua Hedionda Lagoon:

The I-5 bridge over the tidal channel of Agua Hedionda Lagoon will be replaced and widened under the current plans for the North Coast Corridor Project; and increases in span lengths may be a viable option if cost effective by comparison to conventional wetlands construction or restoration. The present specifications for the replacement I-5 bridge span at Agua Hedionda Lagoon (referred to as 10+4 buffer) are as follows:

Length of proposed bridge span, along I-5 (from piles, lines EB - BB): 52 m (170.61 ft)
Length of proposed bridge span (from edges of structure): 70.1 m (230 ft)

Width of existing bride deck, across I-5: (157.5 ft)
Width of proposed bridge deck: 77 m (252.9 ft)
Seven bridge spans.
Rows of piles decreased from 4 rows (existing) to 2 rows (replacement)
Number of piles in each row decreased from 32 (existing) to 16 (replacement)
Bridge low chard elevation: 27.2 feet at south end, 21.1 feet at north end
Elevation of armored bed: -6.56 m (-21.52 ft NGVD)
Bed width of trapezoidal channel, at hard bottom: 32.3 ft; at sediment fill: 75.9 ft
Side slope of trapezoidal channel: 1.5 to 1

5.1) Model Input: The TIDE_FEM model was gridded for the Agua Hedionda Lagoon bathymetry, based on the most resent lagoon soundings taken in 2007 by Cabrillo Power LLC. The most recent lagoon maintenance dredging was completed in April 2007 using differential GPS for precision ranging in conjunction with 40-200 KHz variable frequency fathometers. The 2007 survey did not provide bathymetric information above -2 ft MLLW; so consequently those data had to be merged with other survey data to obtain a complete picture of the lagoon over the entire tidal range. We began this merging exercise by building a bathymetric contour map from the 2007 survey data, obtaining bathymetric detail between -25 ft MLLW and – 2 ft MLLW. To fill in the upper sub-tidal and low-marsh intertidal regions, bathymetric contours from the April 1997 survey were stitched into the 2007 survey contours. The mid-marsh and high marsh contours were obtained from field surveys conducted by WRA for the City of Carlsbad that were overlaid on a 3D terrain map to determine the elevation of each point. There was some variation in the elevations of these points from different transects (due primarily to the limitations in accuracy of both the GPS data and the original 1' contours). To compensate for this and to determine the appropriate MHW elevation for the lagoon, WRA took the mean elevation of all of the MHW points. WRA repeated this averaging procedure to create the 0.5 ft, 1 ft, 1.5 ft and 2 ft above MHW contour lines. While this procedure worked quite well throughout much of the lagoon, when creating a 3D model of the terrain in very flat (or topographically complex) portions of the lagoon the software encountered data gaps that resulted in fairly erroneous topographic data in these areas. This could not be avoided when using 1 ft contours. There were relatively few regions of error, and based on fairly straightforward vegetative signatures on the aerials; and using this vegetation data, WRA was able to manually correct the topography.

Upon completion of vetting the topographic data using vegetation types for co-registration, the six mid and high marsh contours between + 2 ft MLLW and extreme high water at + 7.7 ft MLLW were stitched into the master bathymetric file for Agua Hedionda Lagoon, producing the bathymetric map shown in Figure 66. The TIDE_FEM

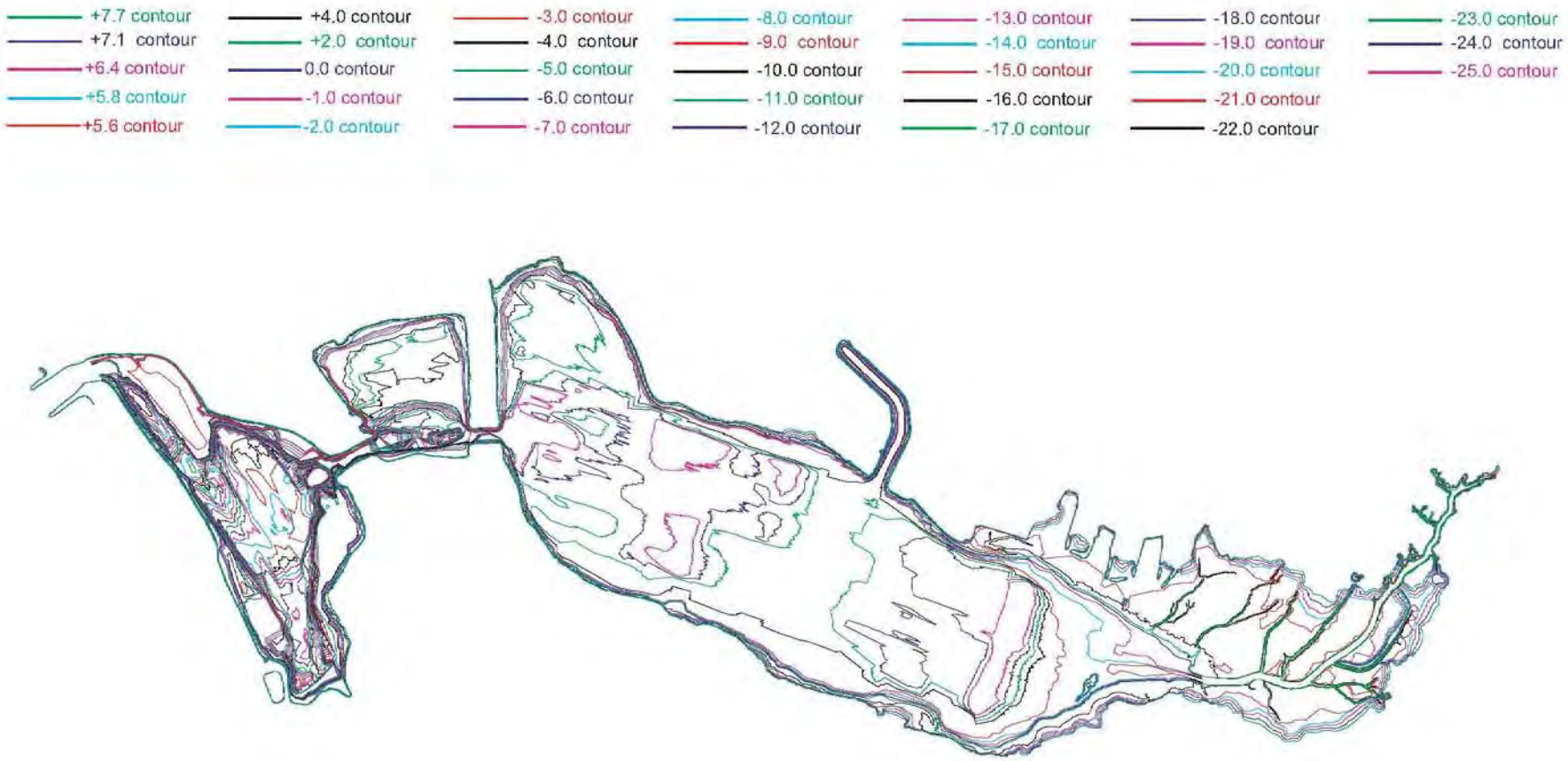

Figure 66. Agua Hedionda bathymetry in ft. MLLW, based on 2007 survey for -25 ft thru -2 ft; 1997 survey for -2.0 thru +2 ft; and on the WRA 2010 topographic survey for +2.0 thru +7.7.

tidal hydraulics model presented in Jenkins and Inman (1999) was gridded based on Figure 66. Of particular interest to the finite element mesh are the *hydraulic friction slope coefficients*, S_{fj}, providing tidal muting effects. Two separate formulations are used. One is given for the 3-node triangular elements situated in the interior of the mesh which do not experience successive wetting and drying during each tide cycle. The other formulation is for the elements situated along the wet and dry boundaries of the lagoon. These have been formulated as 3-node triangular elements with one curved side based upon the cubic-spline matrices developed by Weiyan (1992). These two sets of elements were assembled into a computational mesh of the lagoon conforming to the lagoon extreme high waterline in Figure 66. The wet-dry boundary coordinates of the curved waterline, (x', y'), are linearly interpolated for any given water elevation from the contours stored in the lagoon bathymetry file. The Figure 66 bathymetry features an inlet bar in the West Basin typical of that mapped during the October 2002 condition sounding. The post-dredging surveys indicated uniform deep water throughout the West Basin with depths ranging from -20 ft MLLW to – 25ft MLLW, similar to that found in Figure 2-2 of Elwany, et al (2005).

We consider five sub-sets of lagoon bathymetry for the alternative tidal hydraulics simulations: 1) The existing lagoon bathymetry using the proposed 230 ft replacement bridge span (Figure 67a) with its associated hard-bottom rip-rap lined channel at -19.22 ft MLLW (-21.52 ft NGVD) with sediment fill at -5 ft MLLW (-7.3 ft NGVD); 2) The existing lagoon bathymetry using the proposed 230 ft replacement bridge span with flow fences (Figure 68a, blue) retrofitted to the existing hard-bottom channel; 3) Slight modification to existing lagoon bathymetry by removal of a portion of the road bed fill to accommodate doubling the width of the existing channel along existing grade with hard bottom at -19.22 ft MLLW. This alternative requires doubling the replacement bridge span to 460 ft (*double-wide* alternative); 4) Slight modification to existing lagoon bathymetry by removal of a portion of the road bed fill to increase the bed width of the hard bottom channel to 99.1 ft while maintaining the existing depth of the hard bottom channel at -19.22 ft MLLW (-21.52 ft NGVD) along 1 on 1 side slopes (*Chang-channel*, Figure 68b). This alternative allows the replacement bridge span to remain at 230 ft; and 5) The slightly modified lagoon bathymetry with the Chang-channel and flow fences (Figure 68a, red) using the proposed 230 ft replacement bridge span (Figure 68b).

The theory behind the double-wide channel alternative (alternative 3) is to remediate tidal muting effects of the narrow bridge waterway at the Agua Hedionda I-5 bridge choke point. The double-wide channel alternative would double the width of the tidal channel along the existing grade of the north bank and require increasing the span of the North Coast Corridor Project from 230 ft (70.1) m to 460 ft (140.2 m). Channel width increases

effect only the north bank because the present tidal channel runs along the south bank of the Central Basin, and there is no free basin space to expand the channel to the south. Due to buried infrastructure concerns, the double-wide concept retains the hard channel bottom feature at -19.22 ft MLLW (-21.52 ft NGVD) with sediment fill at -5 ft MLLW (-7.3 ft NGVD).

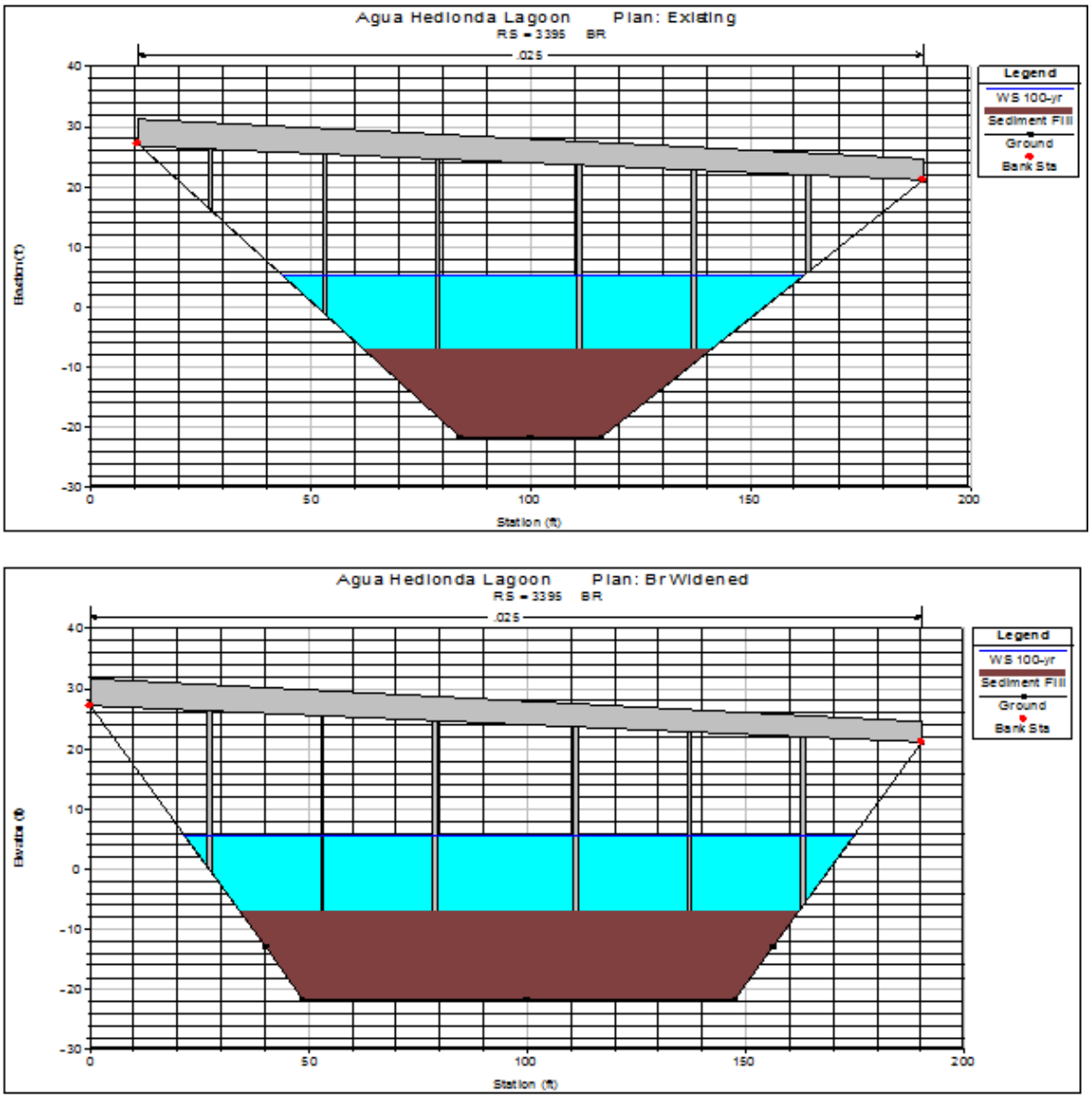

Figure 67: Bridge and Channel Cross Sections: a) proposed I-5 replacement span and existing bridge waterway channel cross section (upper panel); b) proposed I-5 replacement span with increased bridge waterway channel cross section (lower panel), referred to as the *Chang-channel* (lower panel). All elevations are in feet NGVD.

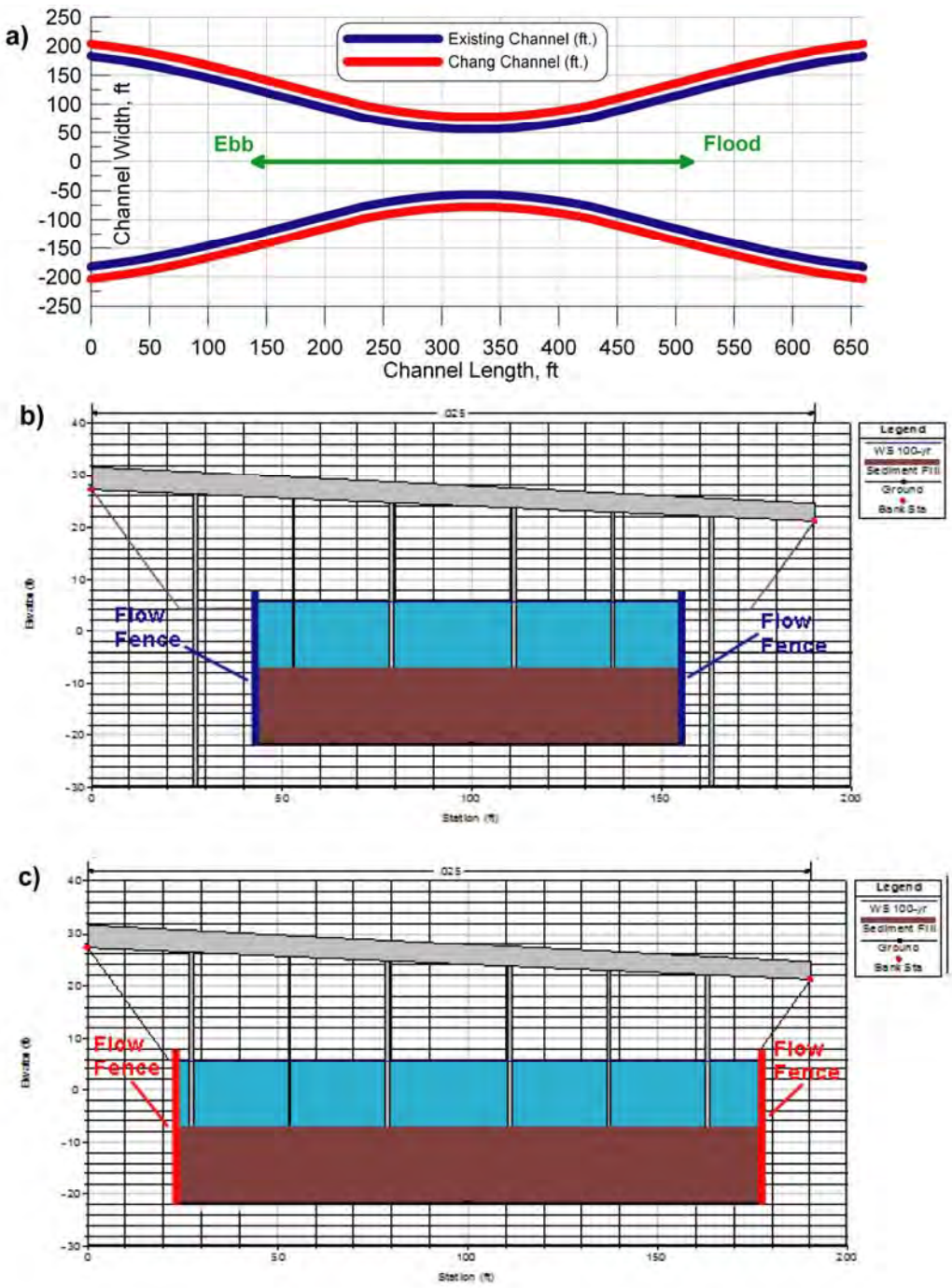

Figure 68. Agua Hedionda: a) Flow Fence design for pressure recover of velocity head through I-5 bridge waterway; b) existing channel cross section with flow fence; c) Chang channel cross section with flow fence. All elevations are in ft NGVD.

The theory behind the Chang-channel was to increase the cross section the bridge waterway channel without requiring an increase in the span of the replacement bridge. The specifications for the Chang-channel alternative in Figure 68 b are (all elevations are based on the NGVD datum):

Length of proposed bridge span, along I-5 (from piles, lines EB - BB): 52 m (170.61 ft)
Length of proposed bridge span (from edges of structure): 70.1 m (230 ft)
Width of existing bridge deck, across I-5: (157.5 ft)
Width of proposed bridge deck: 77 m (252.9 ft)
Elevation of existing armored bed: -6.56 m (-21.52 ft NGVD)
Bed width of proposed trapezoidal channel at hard bottom: (99.1 ft)
Bed width of proposed trapezoidal channel at sediment fill: (128 ft)
Side slope of existing trapezoidal channel: 1.5 to 1
Side slope of proposed trapezoidal channel: 1 to 1
Seven bridge spans with six sets of cylindrical piers.

The concept behind the flow fence is to achieve more complete pressure recovery of the velocity head through the narrowest portion of the bridge waterway channel (choke point). These flow fences are typically constructed of vertically driven sheet pile and are referred to as the “Stratford Fence” because they are based on the optimal turbulent pressure recovery relations due to Stratford (1959 a and b). B.S. Stratford developed an analytic solution for a pressure recovery distribution in a turbulent flow which both avoids flow separation while maintaining zero wall friction over the entire pressure recovery length. This solution is now widely regarded as a universal law for the minimum energy dissipation in a turbulent flow. It has been used to optimize turbine blades, lifting bodies, aircraft wings, ground effects tunnels and wings for race cars, flow nozzles and diffusers (see Liebeck, 1976; Smith, 1974; Wortmann, 1974; and McCormick, 1979). The present application of the Stratford pressure recovery to tidal channel choke points is very similar to the prior applications to flow nozzles. The primary distinction is that tidal flow through a choke point is bi-directional, whereas prior nozzle applications have been made for unidirectional flows.

Stratford recovery is sometimes referred to as "imminent separation recovery" because it works by keeping the flow on the verge of separation throughout the entire deceleration without actually separating. This principle works by keeping the flows downstream of the choke point on the verge of separation without actually separating. In this condition, vortex formation is prevented while velocity shear at the wall is close to zero; and, consequently, the friction nearly vanishes. While this occurs, kinetic energy of the velocity head is

reconverted into pressure as the local flow decelerates into the receiving basin, hence the notion of pressure recovery. To avoid dependence on the exact pressure and velocity of a particular flow, the pressure recovery is expressed in terms of pressure coefficient, $\overline{C}_P$, and local Reynolds number $R_{e\sigma_0}$ defined as

$$\overline{C}_p = \frac{p - p_0}{1/2\rho v_0^2}\ , \qquad R_{e\sigma_0} = \frac{v_0 \sigma_0}{\nu} \tag{5}$$

Here $v = v_0$ is the maximum local velocity of the flow at a point $\sigma = \sigma_0$ where the pressure recovery is initiated; p_0 is the static pressure at $\sigma = \sigma_0$; and p is the local static pressure at any point along the pressure recovery length $\sigma > \sigma_0$. The canonical coordinate, σ, is a non-dimensional form of the curvilinear coordinate s that is measured along the surface of the flow fence from the upstream stagnation point at $s = s_p$; and σ_0 corresponds to the location of the choke point at $s = s_0$. To maximize the expanse of low drag laminar boundary layers along the flow fence , Liebeck (1973) has shown that the optimal placement of the choke point channel half-width, *t*, is given by:

$$\sigma_0 = 38.2\left(R_{e\sigma_0}\right)^{-3/8}\left[\int_{s_p}^{s_o}\left(\frac{v}{v_0}\right)^5 d\left(\frac{s}{s_0 - s_p}\right)\right]^{-5/8} \tag{6}$$

When $\overline{C}_P = 0$ the flow is at its maximum velocity, v_0, and is about to convert the velocity head, $1/2\rho v_0{}^2$, back into pressure, whence $\overline{C}_P > 0$. If the flow reconverts all of its velocity head into pressure (total pressure recovery), then the flow would be brought to rest or $v = 0$ at $\sigma = 1.0$. This is a condition known as stagnation for which the pressure coefficient has a maximum value of $\overline{C}_P = 1.0$.

In the design of our flow fences we use an analytic formulation to specify the pressure recovery distribution in terms of $\overline{C}_P$ versus σ, and then solve the inverse problem for the physical shape of a given thickness that produces that pressure distribution. The analytic relation for the pressure recovery distribution is in the public domain and was

published by Stratford, (1959 a & b). It is given by:

$$\overline{C}_P = 0.49\left\{\left(R_{e\sigma_0}\right)^{1/5}\left[\left(\frac{\sigma}{\sigma_0}\right)^{1/5} - 1.0\right]\right\}^{1/3} \qquad \text{for} \quad \overline{C}_P \le \frac{4}{7} \tag{7a}$$

Or:

$$\overline{C}_P = 1.0 - \frac{t}{\left[\frac{\sigma}{\sigma_0} + c\right]^{1/2}} \qquad \text{for} \quad \overline{C}_P > \frac{4}{7} \tag{7b}$$

The pressure recovery relations in (7a & 7b) produce an initial sharp increase in $\overline{C}_P$ (deceleration) immediately after the pressure recovery begins at $\sigma = \sigma_0$. This places the flow on the verge of separation; but the initial flow deceleration is not made so large as to actually induce separation. Further flow deceleration and increases in $\overline{C}_P$ are made progressively more and more gradual in the downstream direction. This produces a concave pressure recovery distribution known as a "pressure recovery bucket." Stratford proved that the concave pressure recovery distribution had a stabilizing influence on a decelerating flow that was close to separation. The use of these pressure recovery relations gives our flow fence plan view contours in Figure 68a their distinctive concave expansion section. With this expansion section, eddy formation is prevented while velocity shear at the wall is close to zero; and, consequently, the turbulent wall friction nearly vanishes. This is how most of the energy dissipation is avoided and how most of the kinetic energy of the velocity head is reconverted into pressure. These relations specify a change in flow velocity with distance along the waterway channel axis that allows for maximum conversion of velocity head in the channel to pressure head once the channel empties into the tidal basin. Examples of the optimal velocity curves in the plan-view channel space of the I-5 bridge at Agua Hedionda Lagoon are shown in Figure 68a when retrofitted to the existing bridge waterway channel (red) and the Chang-channel (blue). This optimal velocity curve is constrained by existing depths of the tidal basins and by the width of the

bridge waterway, and is used to solve the inverse problem for the physical shape of either a flow fence or a contoured hard bottom.

Aside from gridding the TIDE_FEM tidal model, stage area and storage rating functions were calculated from the bathymetric contours of Figure 66. Figure 69 gives the stage area function of the East Basin in isolation. From calculations of the historic MHHW and MLLW water levels in the East Basin (Elwany, et. al., 2005), Agua Hedionda Lagoon presently supports an average of 59.8 acres of intertidal habitat east of the I-5 bridge, or about 30% of the mean intertidal area found in the present East Basin of Batiquitos Lagoon. Agua Hedionda was clearly designed as more of an open-water, sub-tidal lagoon for the purpose of providing a cooling water reservoir for the power plant rather than as a balanced wetland system. Sub-tidal habitat presently comprises an average of 191 acres of the 251 acres of East Basin habitat that receives tidal inundation to MHHW. During spring tides the East basin of Agua Hedionda experiences salt water inundation over about 266 acres under existing conditions.

Figure 70 gives the storage rating function of the entire Agua Hedionda system. The 2007 post-dredging survey indicates the lagoon stores a minimum of 1,410 acre ft of sub-tidal water volume and has a maximum tidal prism during spring tides of about 2,190 acre ft. Between MHHW and MLLW, the lagoon has a mean tidal prism of 1,620 acre-ft and an average sub-tidal volume of 1,750 acre-ft. This compares with a mean diurnal tidal prism in Batiquitos Lagoon of 1,515 acre-ft. These values are based on water levels in Agua Hedionda Lagoon measured by Elwany, et al, (2005). The stage area functions of each basin were integrated vertically to compute polynomial coefficients for the storage rating function of the entire system, as plotted in Figure 70. The polynomial derived from Figure 70 is also required in the initialization of the TIDE_FEM tidal hydraulics model.

5.1.1 Power Plant Flow Rates: The present day Agua Hedionda Lagoon is not a natural geomorphic structure; rather, it is a construct of modern dredging. Its West Tidal Basin (Figure 66) is unnaturally deep (-20 to – 25 ft MLLW) and the utilization of lagoon water for once-through cooling by the Encina Power Station renders Agua Hedionda's hydraulics distinctly different from any other natural tidal lagoon. Power plant cooling water uptake (Q_{plant}) acts as a kind of "negative river." Whereas natural lagoons have a river or stream adding water to the lagoon, causing a net outflow at the ocean inlet, the

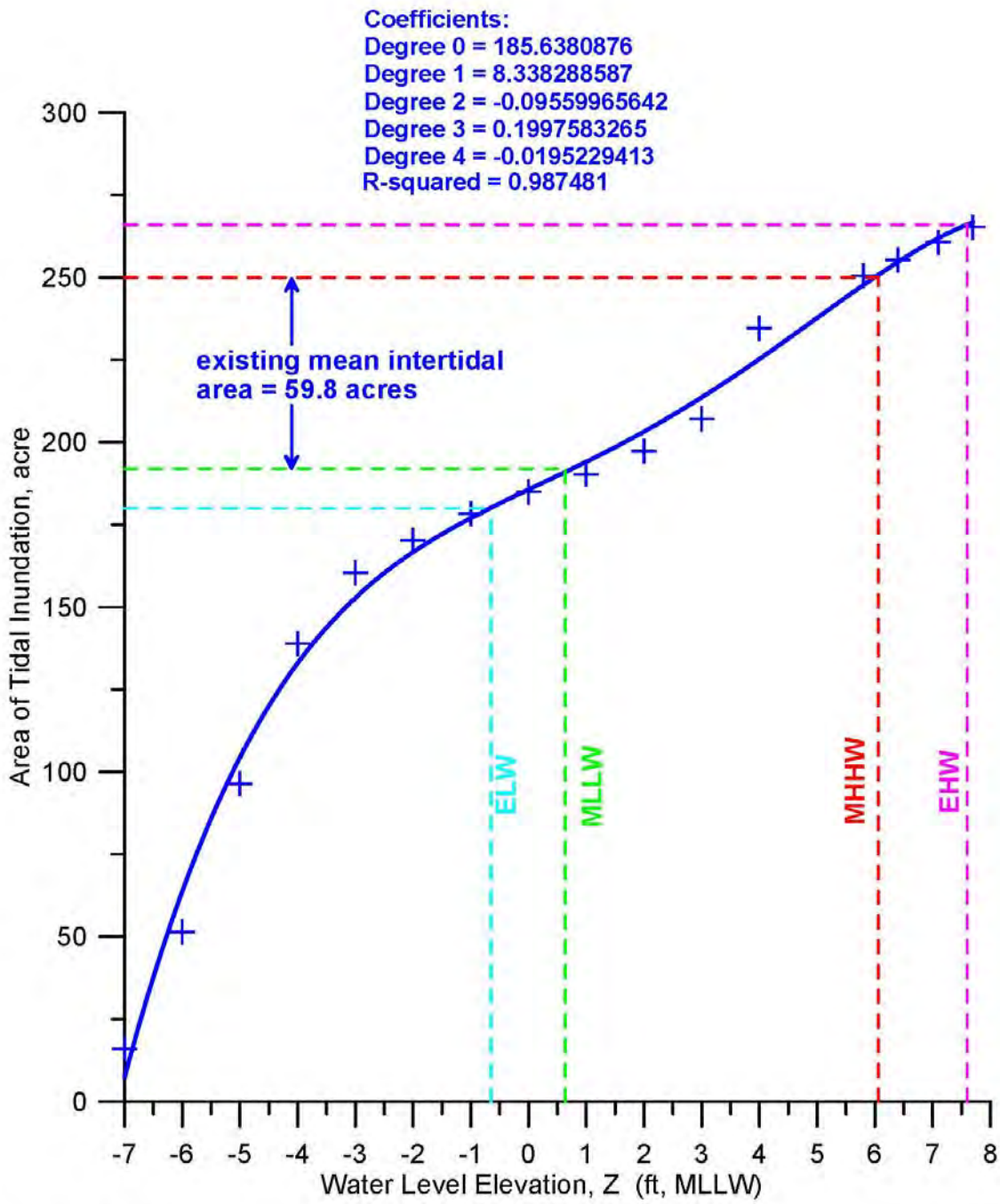

Figure 69. Area of tidal inundation in the east basin of Agua Heionda Lagoon as a function of water level elevation (stage area function from 2007 soundings). Water levels for existing conditions from Elwany et al, 2005.

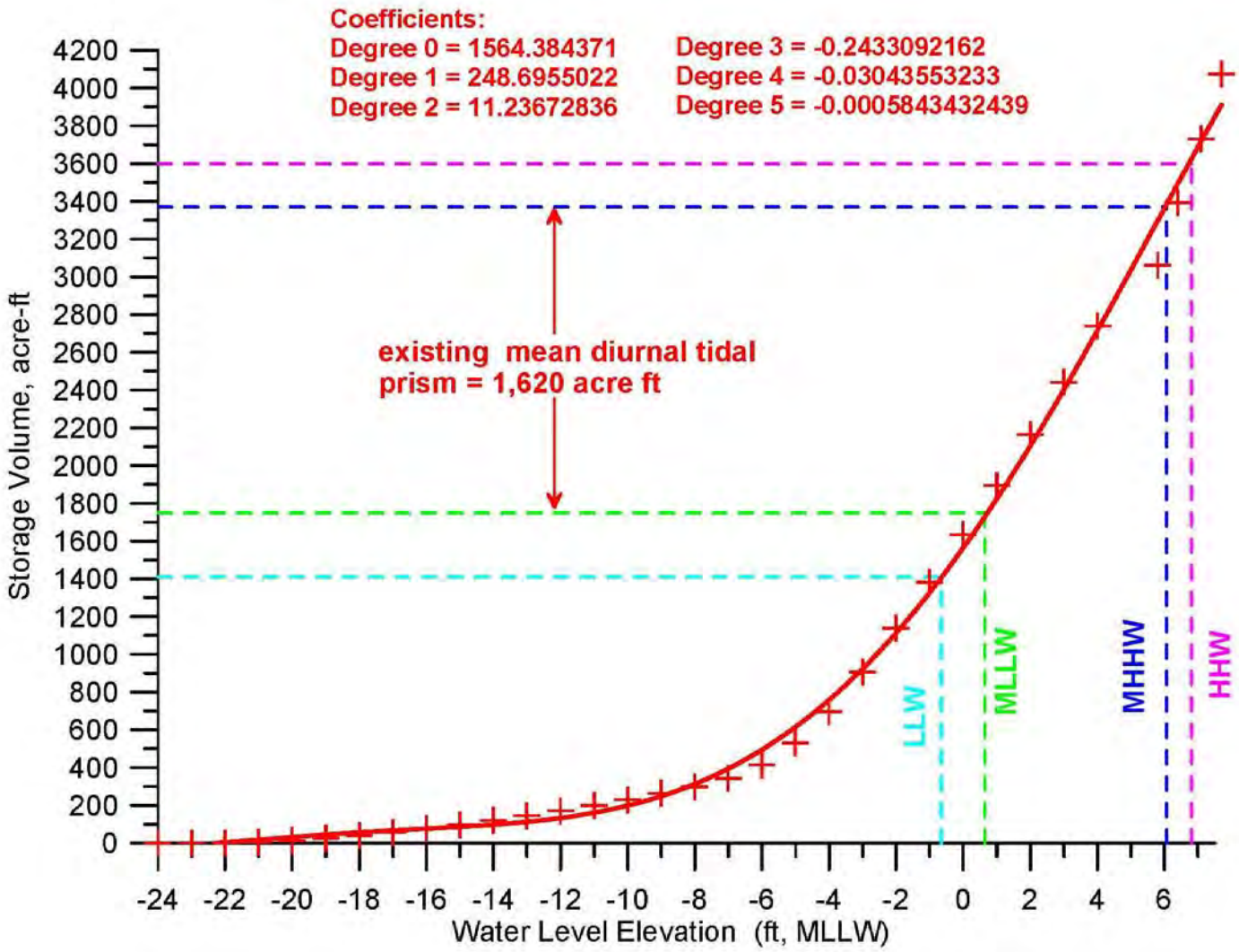

Figure 70. Storage rating function for Agua Hedionda Lagoon, based on 2007 sounding. Water levels for existing conditions from Elwany et al, 2005.

power plant infall removes water from Agua Hedionda Lagoon, resulting in a net inflow of water through the ocean inlet. This net inflow has several consequences for sediment transport into and out of the lagoon: 1) it draws nutritive particulate and suspended sediment from the surf zone into the lagoon, the latter forming bars and shoals (Figure 2) that subsequently restrict the tidal circulation, and 2) the net inflow of water diminishes or at times cancels the ebb flow velocities out of the inlet, and provides an artificial suction head on the Central and East Basins that helps to drain those water bodies on ebbing tide. Therefore, the plant demand for lagoon water strongly controls the tidal circulation of the lagoon.

The existing cascade of circulation and service water pumps available at Encina Power Station can provide a maximum once-through flow rate of 808 mgd, but has averaged about 508 mgd over the long term (see Figure 71). Generating Units 1, 2, and 3 each have two cooling water (CW) pumps providing 34.56 mgd each. In addition, Units 1 and 2 each have one salt water service pumps (SWSP) producing 4.32 mgd each. Unit 3 has two SWSP at 4.32 mgd each; Unit 4 has two CW pumps at 144 mgd each and two SWSP at 9.36 mgd each; and, Unit 5 has two CW pumps at 149.76 mgd each and two SWSP at 13.104 mgd each. Each generating unit needs at least one CW pump to operate, and usually employs two. The SWSP combinations can vary dramatically since the salt water service water system is interconnected. Should Encina repower, then Units 1, 2, and 3 will be retired, but their SWSP's may still be utilized.

Plant flow rate data was provided in daily average increments by Cabrillo Power I LLC for the period 1999 -2010, and plotted in Figure 71. However, the hydrodynamic simulation was ended at the completion of the last maintenance dredge cycle in April 2007. Flow rate data prior to 1999 was obtained from SDG&E. During peak user demand months for power (summer), plant flow rates are typically between 635 and 670 mgd, but it is not uncommon for flow rates to spike to peak flow rate capacity (808 mgd) for several days to a week at a time during summer heat waves (see Figure 3). However, When the 550 MW Palomar cogeneration facility in Escondido, CA came on-line in 2006, there has been a dramatic downturn in the consumption of Agua Hedionda Lagoon water for cooling. This is shown by the cumulative residual analysis of daily flow rates in Figure 3b. Prior to April 2006, the daily flow rates exceeded the 11-year mean of 508 mgd and the cumulative residual increased almost monotonically. After April 2006, the daily flow rates were systematically less than the long-term mean, (with some brief exceptions) and the cumulative residual progressively declined. Figure 3 shows that this decline in cumulative residual involves 125 no -flow days in a three year period as a consequence of no demand for Encina power. Recently the CW pumps are operated at

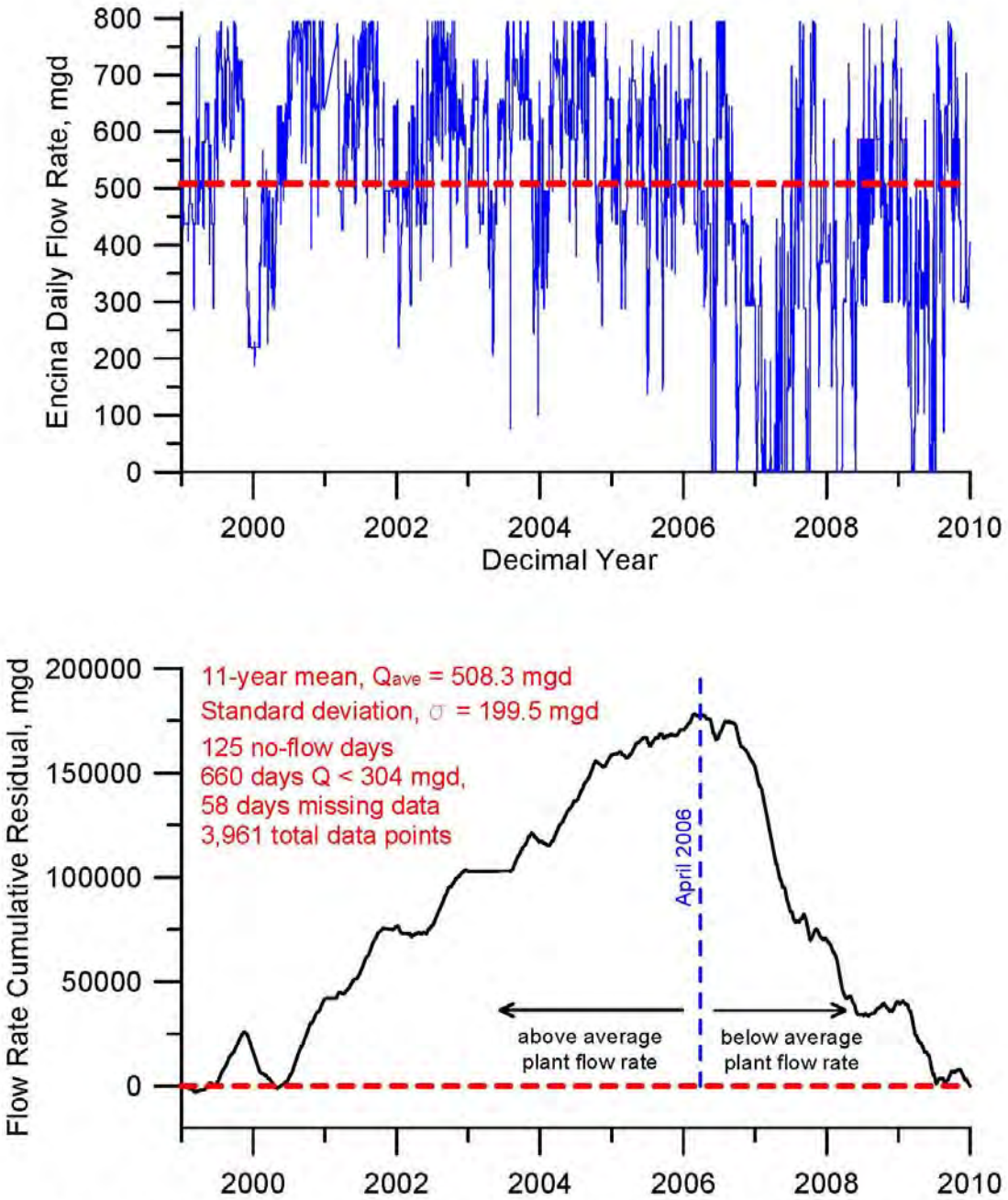

Figure 71. Once-through flow rate at Encina Power Station, Carlsbad, CA, for the period 1999 - 2010: a) daily flow rate history; b) cumulative residual of daily flow rate (accumulated departure from mean).

least once a week to inject sodium hypochlorite into the condensers; but in general consumption of Agua Hedionda Lagoon water for cooling has been running well under the long term mean in recent years.

The recent completion of environmental permitting for the 50 mgd Carlsbad Desalination Project will set a lower limit on daily consumption of Agua Hedionda Lagoon water at 304 mgd, as this is the minimum flow required to produce 50 mgd of product water while maintaining sufficient initial in-the-pipe dilution of 50 mgd of brine to be discharged into near shore waters on the open coast. Thus the flow rates passing through the Encina facility during stand-alone desalination operations would be about 40% less than the present average when power generation is occurring, and 62% less than the peak flow rate capability.

5.2) Model Calibration and Assessment of Existing Conditions: Spring, neap and mean tidal range simulations of the hydraulics of Agua Hedionda Lagoon were performed using astronomic tidal forcing functions at = 2 sec time step intervals for the period 2005-2008. Computed water surface elevations and depth-averaged velocities from the global solution matrix were converted to lagoon waterline contours and flow trajectories. Calibrations for determining the appropriate Manning factors and eddy viscosities were performed by running the TIDE_FEM model on the Figure 14 bathymetry file and comparing calculated water surface elevations in the East Basin and inlet channel velocities against measurements by Elwany et al. (2005) during a complete spring-neap cycle of 13 -30 June 2005. Plant flow rates during this lagoon monitoring period were input to TIDE_FEM according to Figure 3, daily recordings by Cabrillo LLC. Iterative selection of Manning factor n_0 = 0.03011 and an eddy viscosity of ε = 6.929 ft^2/sec gave calculations of water surface elevation and inlet channel velocities that reproduced the measured values to within 2% over the 18 day spring-neap monitoring cycle.

Figure 72 provides a quantitative assessment of the accuracy of the calibrated TIDE_FEM model over the entire 18 day calibration period of 13-30 June 2005. Here we compare East Basin water level variations predicted by the model (purple trace) with the actual water level measurements (black crosses) by Elwany et. al., (2005). The East Basin water level variations in purple are found to lag the ocean water levels by as much as 50 minutes during the spring tides on 21 June 2005, and this phase lag averages 39 minutes over the entire 18 day spring-neap cycle. The amplitudes and degree of non-linearity in the East Basin water level time series simulated by the model closely duplicate that observed in the measured lagoon tides. The maximum error in simulating the low tide

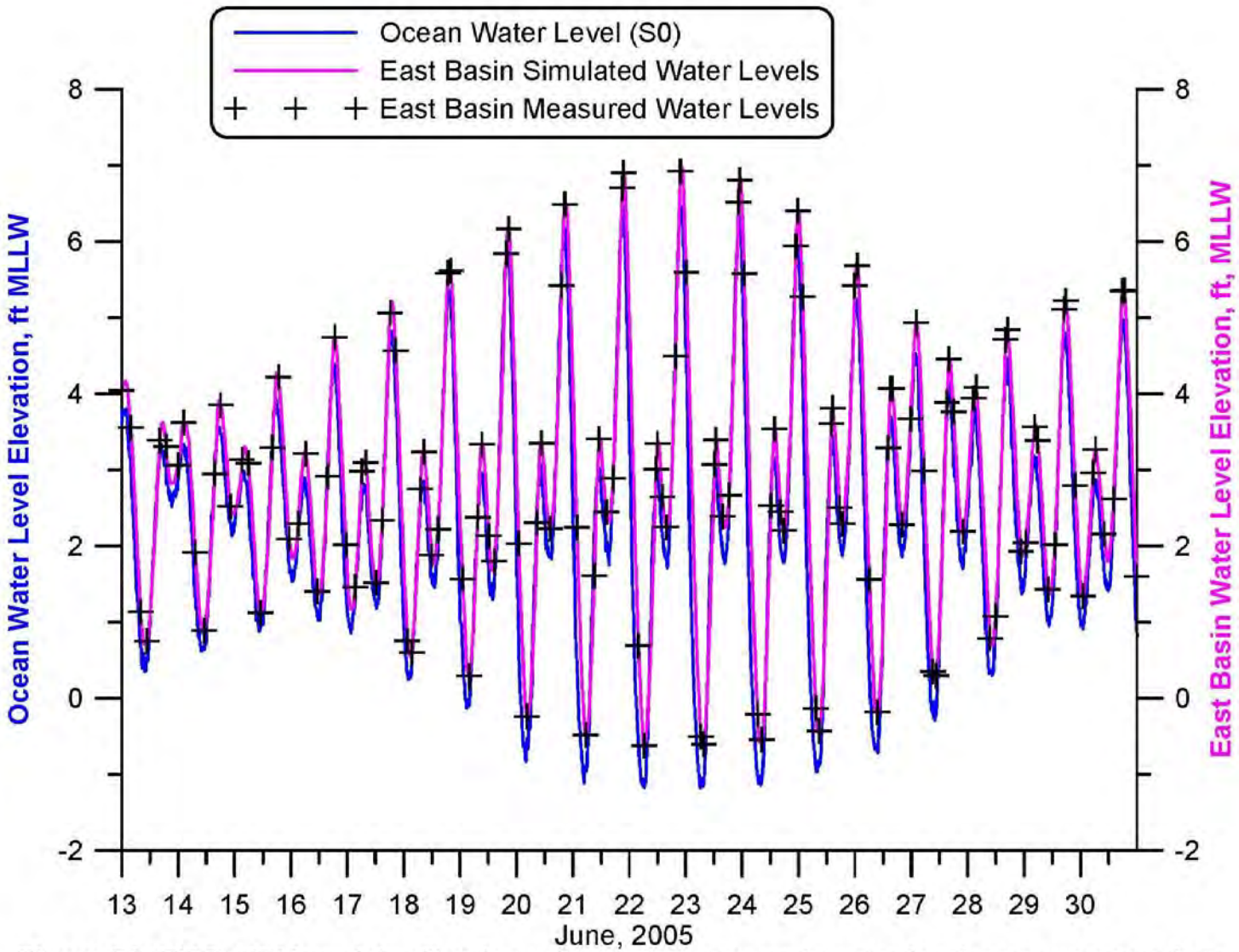

Figure 72: TIDE_FEM model calibration using spring-neap cycle water level measurements from Elwany, et al. 2005. Ocean water levels (S0) indicated in blue; hydrodynamic simulation of east basin water levels shown in purple, east basin water level measurements (S3) shown as black crosses.

elevations was found to be ε_L = +0.1 ft. The maximum high tide error in the model simulation relative to observations was found to be ε_H = -0.05 ft. Consequently, the calibration error appears to exhibit a systematic tendency. When amplitude errors occur they tend to over estimate the water elevation of the LLW tidal stage, and under estimate the water elevation of the HHW tidal stage. Although these errors are quite small and may be considered high predictive skill, this error mode would be consistent with *bathymetry errors* in which depth has been under estimated, Weiyan (1992). Bathymetry errors are the most common cause of modeling errors. Other sources of errors include:

ELEMENT INTERPOLATION ERROR: Due to the degree of the polynomial used to specify shape function, N_i.

DISCRETIZATION ERRORS: Due to mesh coarseness and approximating the curved wet/dry boundary side of an element with a quadratic spline.

QUADRATURE ERRORS: Due to reducing the weighted residual integrals with the influence coefficient matrices.

ITERATION ERRORS: Due to solving the system of algebraic equations reduced from the Galerkin Equations.

ROUNDOFF ERRORS: Due to time integration by the trapezoidal rule.

SEA LEVEL ANOMALIES: Due to discrepancies between the astronomic tides and the actual observed water levels in the ocean.

INSUFFICIENT CALIBRATION DATA: Due to limitations in the period of record.

Power (auto-) spectra are useful tools for determining how the energy in complex time series like Figure 73 is distributed among various frequencies of oscillation. The predominant frequencies, where most of the current energy appears (spectral peaks), can give clues that identify the mechanisms that predominate in the local tidal system. In Figure 73, auto spectra of the ocean tides (blue, upper panel) shows the predominant energy is centered on a diurnal frequency 10^{-5} Hz of the K1 lunar-solar diurnal tidal constituent at $f_{K1} = 1.16079$ x 10^{-5} Hz. The energy in this peak is disproportionately high relative to the next largest spectral peak occurring at the M2 principal lunar semi-diurnal tidal constituent, $f_{M2} = 2.2365$ x 10^{-5} Hz. The excess energy at diurnal frequencies is believed to be non-tidal and attributable to a wind-driven current component that has a diurnal fluctuation in response to daily heating of the land. With the onset of summer heating of the inland deserts, this diurnal sea breeze component would be strengthening in the June time frame of the 2005 lagoon monitoring. Other less energetic tidal peaks are also found in the spectra of Figure 73 including one believed to be a baroclinic *shelf resonance* formed by a resonant *triad* at the sum of the frequencies of the K1 and M2

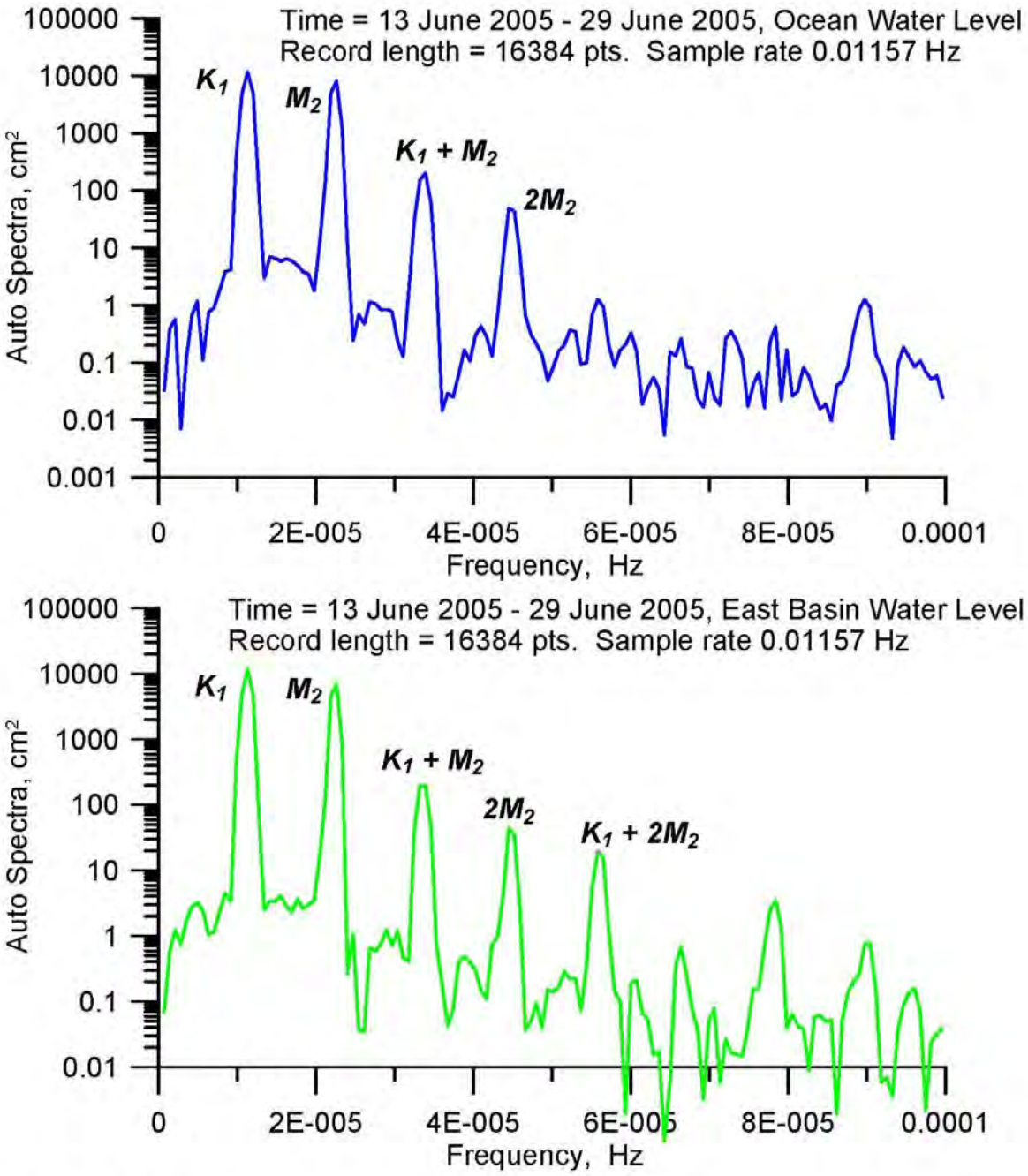

Figure 73 . a) Ocean water level spectra; b) Agua Hedionda East Basin water level spectra, 13 - 29 June 2005.

barotropic tides, ie a diurnal third harmonic at a frequency $f_3 = f_{K1} + f_{M2} = 3.3973$ x 10^{-5} Hz. This diurnal third harmonic is a baroclinic tide excited by the barotropic K1 and M2 tides interacting with the bottom topography, in particular the Carlsbad Submarine Canyon. Another baroclinic shelf resonance apparent in the spectra of the ocean tides in Figure 73 is a second harmonic of the barotropic M2 tide appearing at a frequency of $2f_{M2} =$ 4.4730 x 10^{-5} Hz. The auto spectra of the east basin tides shown in green in the lower panel of Figure 73 exhibits the same primary barotropic and baroclinic tidal peaks as the ocean tides in the upper panel; with one exception; an additional non-linear resonance appears as a triad formed by the sum of the K1 barotropic mode and the baroclinic second harmonic of the M2 tide, $f_{K1} + 2f_{M2} =$ 5.6338 x 10^{-5} Hz. Apparently this mode is excited by non-linear tidal interaction with the lagoon bathymetry.

The other quantitative data used to assess the accuracy of the calibrated TIDE_FEM model are the inlet channel currents, measured by Elwany et. al., (2005) during the lagoon monitoring period of 13-30 June 2005. Figure 74 compares the TIDE_FEM model simulations of inlet channel currents (green) against inlet velocity measurements (black crosses). For reference, the ocean tides are indicated in blue. The flood and ebb current maximums and minimums in the inlet channel are found to lead the high and low ocean water levels by as much as 13.7 hours during the spring tides on 21 June 2005. Maximum flood tide currents on this day were 5.16 ft/sec, while maximum ebb tide currents were -2.87 ft/sec; the flood tide dominance due to the scavenging effect of the power plant intake rate on the available lagoon water volume which was operating at 501 mgd. Throughout the 18 day monitoring period, average flood tide currents in the inlet channel were 1.91 ft/sec while average ebb tide currents were -0.91 ft/sec while the power plant averaged an intake flow rate of 430.97 mgd. The amplitudes and degree of non-linearity in the inlet current time series simulated by the model closely duplicate that observed in the measured currents. The maximum error in simulating the ebb tide currents was found to be ε_L = +0.1 ft/sec. The maximum flood tide error in the modeled currents relative to observations was found to be ε_H = -0.05 ft/sec. Again, this type of systematic simulation error is characteristic of bathymetry errors in the model input file; however, the size of these errors is well within what is considered to be high predictive skill.

Figure 75 compares the auto spectra of the inlet channel currents in green in the lower panel against the ocean tidal spectra from Figure 73 in blue in the upper panel. Spectral peaks in the ocean tides are all found in the spectra of the inlet channel currents but some of the higher harmonics are disproportionately large and there are also additional higher harmonics not found in the ocean tides. In particular, the M2 tidal peak in the spectra of

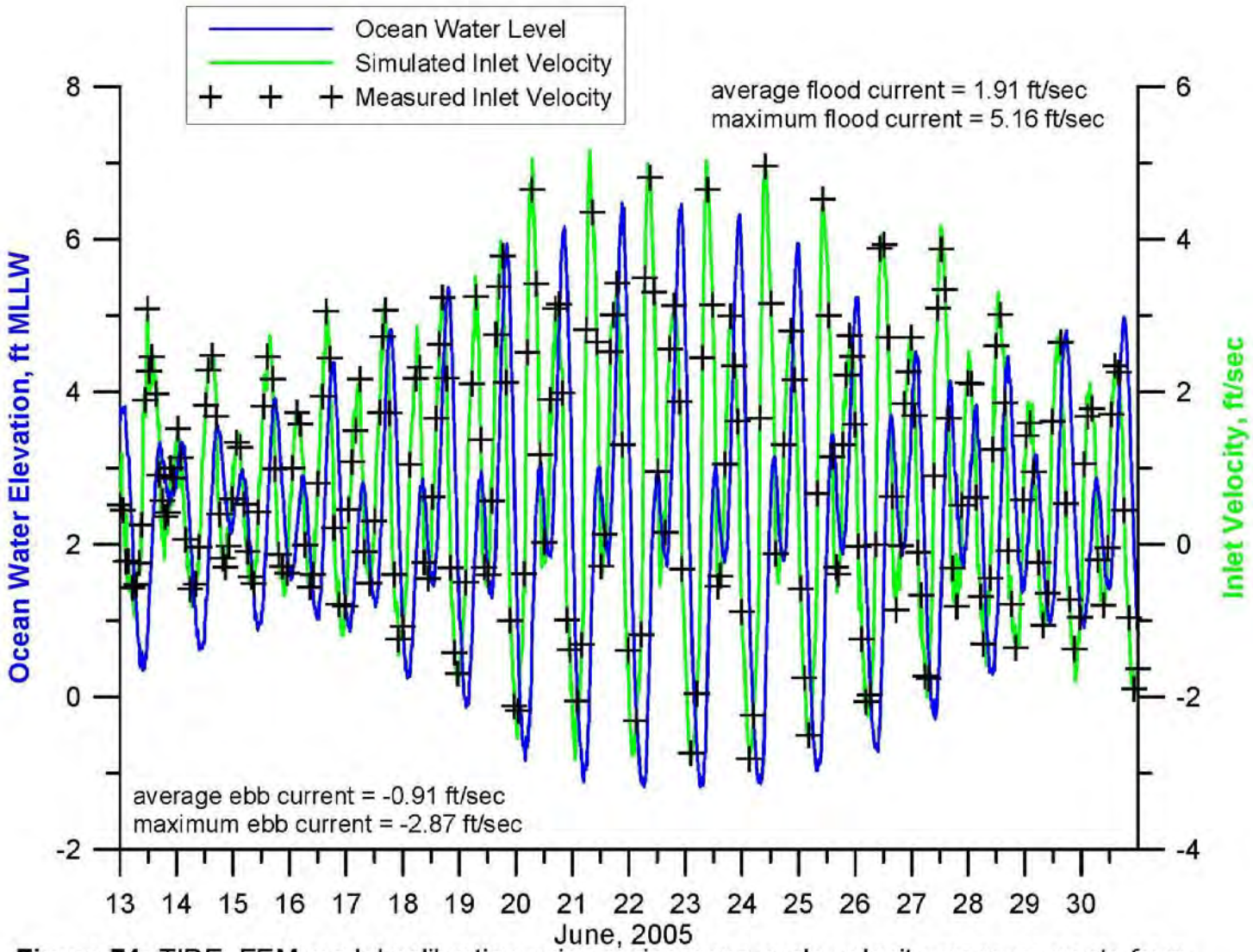

Figure 74: TIDE_FEM model calibration using spring-neap cycle velocity measurements from Elwany, et al. 2005. Ocean water levels (S0) indicated in blue; hydrodynamic simulation of inlet velocity shown in green, inlet velocity measurements (S0) shown as black crosses.

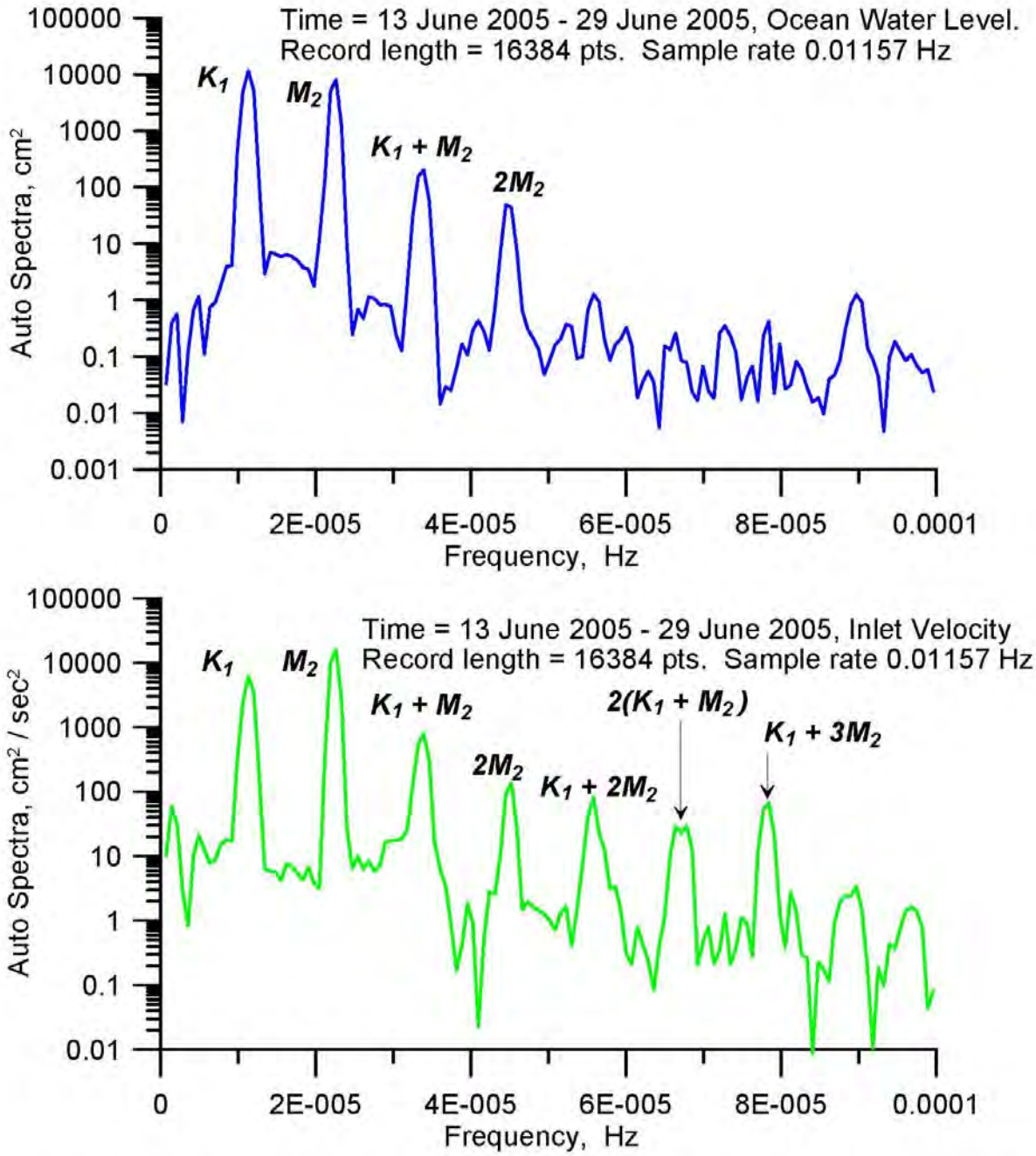

Figure 75. a) Ocean water level spectra; b) Agua Hedionda inlet velocity spectra, 13 - 29 June 2005.

the inlet channel currents has more energy than the K1 peak. This is probably indicative of non-linear friction effects on the inlet channel currents, producing a second harmonic of the diurnal K1 component that overlays on the semidiurnal M2. The diurnal third harmonic is present in the inlet channel currents at the sum of the frequencies of the K1 and M2 barotropic tides, as well as the second harmonic of the M2 tides. But we also find in the inlet channel current spectra the triad observed in the East Basin water level spectra (Figure 73) formed by the sum of the K1 barotropic mode and the baroclinic second harmonic of the M2 tide; so apparently that non-linear bathymetric mode was excited at the inlet. Further evidence of non-linear friction interacting with bathymetry is the presence of additional triads at higher harmonics of the inlet channel current spectra. These harmonics are not present with significant energy in the East Basin water level spectra of Figure 32. These frictionally generated harmonics include a second harmonic of the triad formed by the sum of the K1 barotropic mode and the baroclinic second harmonic of the M2 tide, $2\,(f_{K1} + f_{M2}) =$ 6.7946 x 10^{-5} Hz; and a triad formed by the sum of the K1 barotropic mode and the baroclinic third harmonic of the M2 tide, $f_{K1} + 3 f_{M2} =$ 7.8703 x 10^{-5} Hz. The presence of these non-linear higher harmonics in the inlet channel currents exert a strong influence on the transport of sand into the West Basin, as sediment transport is proportional to the cube of the inlet channel velocity.

Table 5.1 gives a summary of the water level elevations calculated by the calibrated model for Agua Hedionda Lagoon with the existing I-5 bridge, based long term forcing for 2005-2008 period of record using calibration from lagoon monitoring period of 13-30 June 2005 after Elwany et. al., (2005). A quantitative assessment of the predictive skill of the calibrated model over the entire period of monitoring 13-30 June 2005 is provided by Figure 76 for lowest daily water levels in the East Basin, and East Basin phase lag in Figure 77. The coefficient of determination of model predictions of daily lowest water level in Figure 26 for the East Basin is found to be R-squares = 0.984, while R-squares = 0.639 for the East Basin phase lag, with the preponderance of phase lags occurring between 30 minutes and 50 minutes, consistent with the phase lags observed during the spring/neap cycle of the calibration period 13-30 June 2005 (Figure 72). With the existing I-5 bridge, maximum daily lower low water level in the East Basin is η_{LLW} = 2.13 ft MLLW; the average daily lowest water level is $\overline{\eta}_{LLW}$ = 0.64 ft MLLW; and the minimum daily low water level is η_{LLW} = -0.65 ft MLLW, significantly lower than the minimum daily low water level at Batiquitos Lagoon where η_{LLW} = +1.6 ft MLLW. Maximum East Basin phase lag is $\theta_{\max}$ = 80.1 minutes, about 100 minutes less than occurs in the East Basin of Batiquitos Lagoon. Average East Basin phase lags in Agua Hedionda Lagoon are only $\overline{\theta}$ = 40 minutes with the existing I-5 bridge, or 77 minutes less than occurs in the

Table 5.1: Water Levels for Agua Hedionda Lagoon with Existing I-5 Bridge, based on long term forcing for 2005-2008 period of record.

Elevations Feet MLLW	Ocean	East Basin
MEAN HIGHER HIGH WATER (MHHW)	5.7	6.06
MEAN HIGH WATER (MHW)	5.0	5.36
MEAN LOW WATER (MLW)	1.3	1.68
MEAN LOWER LOW WATER (MLLW)	0.4	0.64
LOWEST OBSERVED WATER LEVEL (MLLW)	-1.5	-0.65
HIGHEST OBSERVED WATER LEVEL (MLLW)	7.4	7.6
MAXIMUM TIDAL RANGE	8.9	8.26

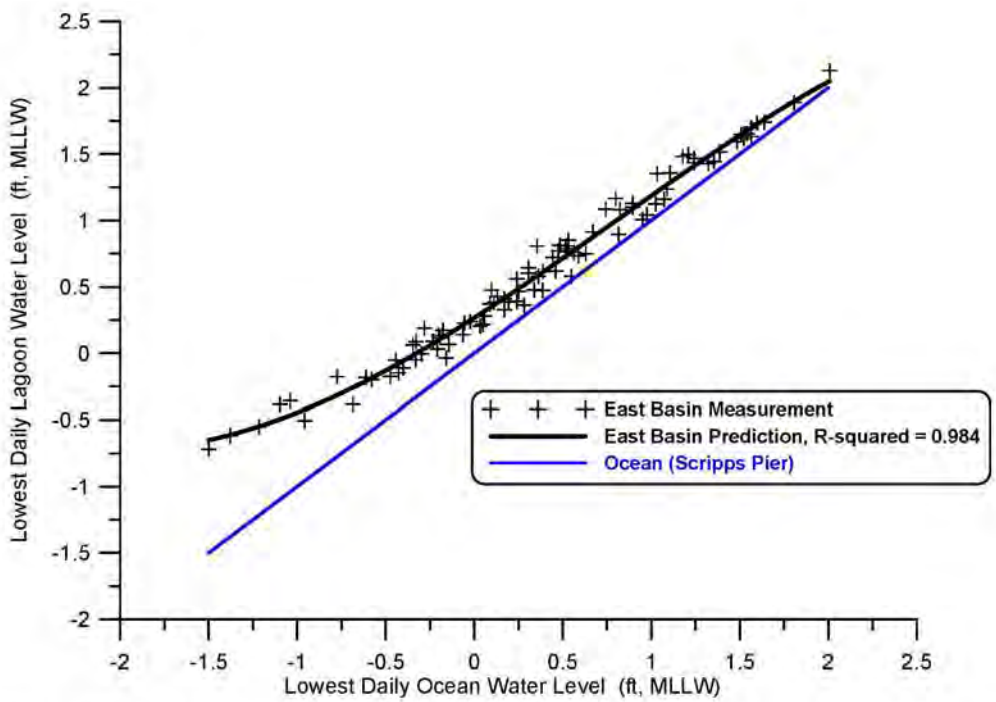

Figure 76. Daily lowest water level in Agua Hedionda Lagoon versus daily lowest water level in the local ocean as measured at the Scripps Pier tide gage (NOAA #941- 0230). Measured values indicated by crosses, model predictions according to black line. Water level data after Elwany, et. al., (2005).

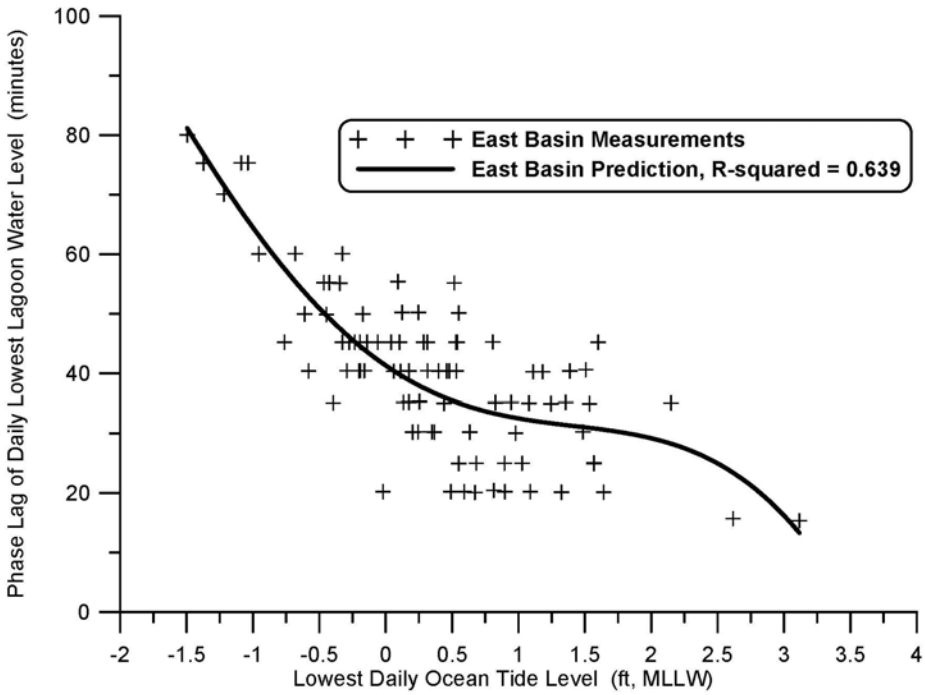

Figure 77. Phase lag of daily lowest water level in Agu Hedionda Lagoon relative to daily lowest water level in the local ocean as measured at the Scripps Pier tide gage (NOAA #941- 0230). Measured values indicated by crosses, model predictions according to black line. Water level data after Elwany, et. al., (2008)

east basin of Batiquitos Lagoon. The minimum phase lag for east basin of Agua Hedionda Lagoon is $\theta_{\min}$ = 15.3 minutes, about one-half the minimum phase lags occuring in the east basin of Batiquitos Lagoon. Figures 76 and 77 serve to emphasize how remarkably little tidal muting occurs at Agua Hedionda Lagoon, despite the fact that on average nearly the same mean tidal prism is exchanged with the ocean as Batiquitos Laggoon, where East Basin tidal muting and phase lags are four to six times greater. This difference is attributable to the controlling effects of the power plant whose suction induced horsepower from its seawater circulation pumps acts as an “iron lung” in helping the east basin of Agua Hedionda to more effectively drain on ebbing tide. This reduces the opportunity to achieve habitat gains and expansion of the intertidal zone with better I-5 bridge waterway alternatives at Agua Hedionda Lagoon, although in Section 5.3.1 we will explore possible alternative bridge waterway channels and road bed fill removal options for improving the residual choke point constraints of I-5 replacement bridges.

Figure 78 gives the hydroperiod function for the east basin of Agua Hedionda lagoon with the existing I-5 bridge, based on the relationships between habitat breaks and exposure used for San Dieguito Lagoon, as discussed in Section 3.3, Figure 17. The hydroperiod function in Figure 78 is based on tidal forcing using the Scripps Pier 1980-

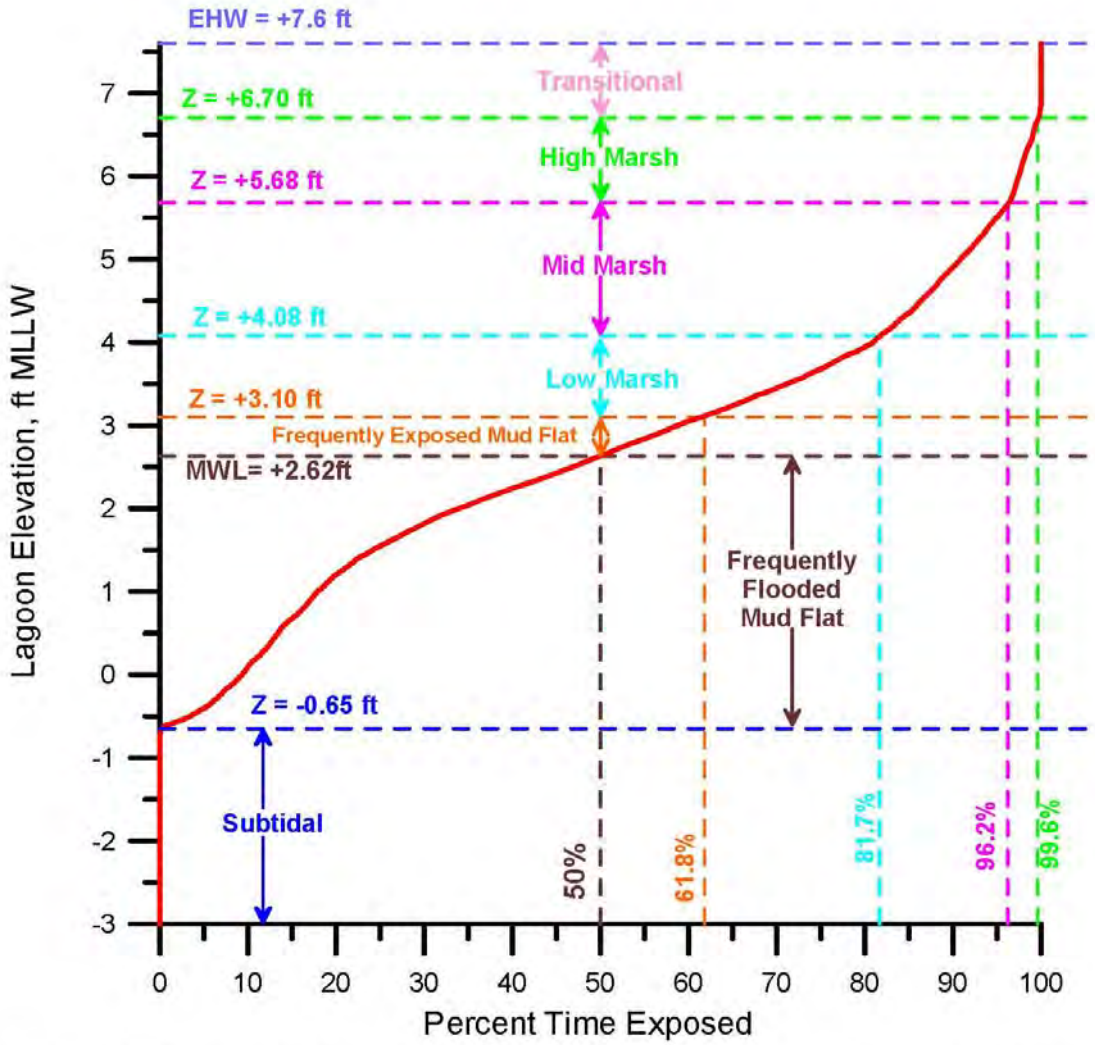

Figure 78. Hydroperiod function for the East Basin of Agua Hedionda Lagoon with existing I-5 bridge and bathymetry. Based on hydrodynamic simulation of East Basin water levels in response to tidal forcing from the Scripps Pier tide gage (NOAA # 941-0230). Habitat breaks based on habitat delineation from Josselyn and Whelchel (1999).

2010 ocean water level measurements in order to capture long-term water level extremes. Comparing Figure 78 with the hydroperiod function for San Dieguito Lagoon in Figure 17, it is apparent how the relatively short phase lag in the east basin of Agua Hedionda lagoon and its ability to fully drain on lower low water stages due to the power plant suction head has decompressed the present intertidal habitat and lowered the zonation of low mid and high marsh vegetation, even though the preponderance of the east basin of Agua Hedionda is (by design) sub-tidal. This promotes exposure of mud flats (particularly in the east end of the East Basin) and helps to support bird habitat. Given these favorable exposures at Agua Hedionda Lagoon across a rather broad vertical intertidal excursion, it will be difficult to achieve the degree of intertidal habitat expansion and improvement through alternative bride designs that were obtained for Batiquitos Lagoon in Section 4.3.

To establish a quantitative baseline for determining the degree to which some amount of habitat expansion can be met at Agua Hedionda Lagoon by various I-5 replacement bridge alternatives, we can map the elevations of the habitat breaks of the hydroperiod function in Figure 78 against the stage area function Figure 69 to estimate the proportions of habitat types of the East Basin with the existing I-5 bridge. This procedure gives the minimum sub-tidal and maximum intertidal habitat types since the hydroperiod function is based on the full range of water level variation over long periods of time (2005-2008 period of record). By that procedure, the minimum (perpetual) sub-tidal area of the East Basin is 180.1 acres; there are maximum of 30.3 acres of frequently flooded mud flat; 4.3 acres of frequently exposed mud flat; 11.5 acres of low salt marsh; 20.0 acres of mid salt marsh; 11.7 acres of high salt marsh; and 8.1 acres of transitional habitat. The maximum area inundated by salt water at extreme high water is 266.0 acres with at most 85.9 acres of intertidal habitat that experiences tidal inundation at least once in the period of record. An average of 250.8 acres experiences tidal inundation up to MHHW resulting in an average of 59.8 acres of intertidal habitat and 191.0 acres of sub-tidal habitat.

5.3) Simulated Tidal Hydraulics Impacts from I-5 Bridge Replacement and Widening at Agua Hedionda Lagoon

In this section we consider five possible alternatives for the replacement I-5 bridge at Agua Hedionda Lagoon: In Section 5.3.1, the proposed 230 ft replacement bridge span (Figure 67a) with its associated hard-bottom rip-rap lined channel at -19.22 ft MLLW (-21.52 ft NGVD) with sediment fill at -5 ft MLLW (-7.3 ft NGVD); In Section 5.3.2, removal of a portion of the road bed fill to accommodate doubling the width of the existing channel along existing grade with hard bottom at -19.22 ft MLLW. This alternative requires doubling the replacement bridge span to 460 ft (*double-wide* alternative). In Section 5.3.3, removal of a portion of the road bed fill to increase the bed width of the hard bottom channel to 99.1 ft while maintaining the existing depth of the hard bottom channel at -19.22 ft MLLW (-21.52 ft NGVD) along 1 on 1 side slopes (*Chang-channel*, Figure 68b). This alternative allows the replacement bridge span to remain at 230 ft. In Section 5.3.4, the proposed 230 ft replacement bridge span with flow fences (Figure 68a, blue) retrofitted to the existing hard-bottom channel. In Section 5.3.5, the Chang-channel and flow fences (Figure 68a, red) using the proposed 230 ft replacement bridge span (Figure 68b).

5.3.1) Tidal Hydraulics Impacts of the Proposed I-5 Bridge Replacement: Here we evaluate possible hydrodynamic impacts of the proposed replacement I-5 bridge design on the tidal exchange of the east basin of Agua Hedionda Lagoon. The potential source of any such impacts is the reduction of the numbers of bridge piles associated with the replacement span relative to existing conditions. Fewer piles create less drag and turbulence in the high-speed channel flow under the bridge.

Figure 79 gives the flow trajectories and depth-averaged tidal currents computed by the calibrated TIDE_FEM model during spring flooding tides on 21 June 2005 of the monitoring period from Elwany et al (2005) using the proposed replacement bridge. The model was initialized with a plant flow rate of 501.1 mgd as reported by Cabrillo Power LLC in Figure 71. This flow rate is roughly equivalent to the long-term mean in Figure 71. Maximum currents in the inlet channel reached 1.5 m/sec or 4.9 ft/sec. Flood tide currents in the West Basin form a well defined jet along the north bank at speeds of between 0.9 m/s (2.9 ft/sec) to 1.2 m/sec (3.9 ft/sec), sufficient to scour and transport fine sand in the 120-210 micron size regime. A sluggish eddy persists in the central portion of the West Basin while the middle portion of the recharge zone is near stagnation, ideal conditions for fine sand to settle in deep water post dredging bathymetry. A feeder current of about -0.4 m/sec (-1.3 ft/sec) spins off the southeast flank of the West Basin eddy, and flows toward the plant intake, thereby supplying feed water at a rate of 501

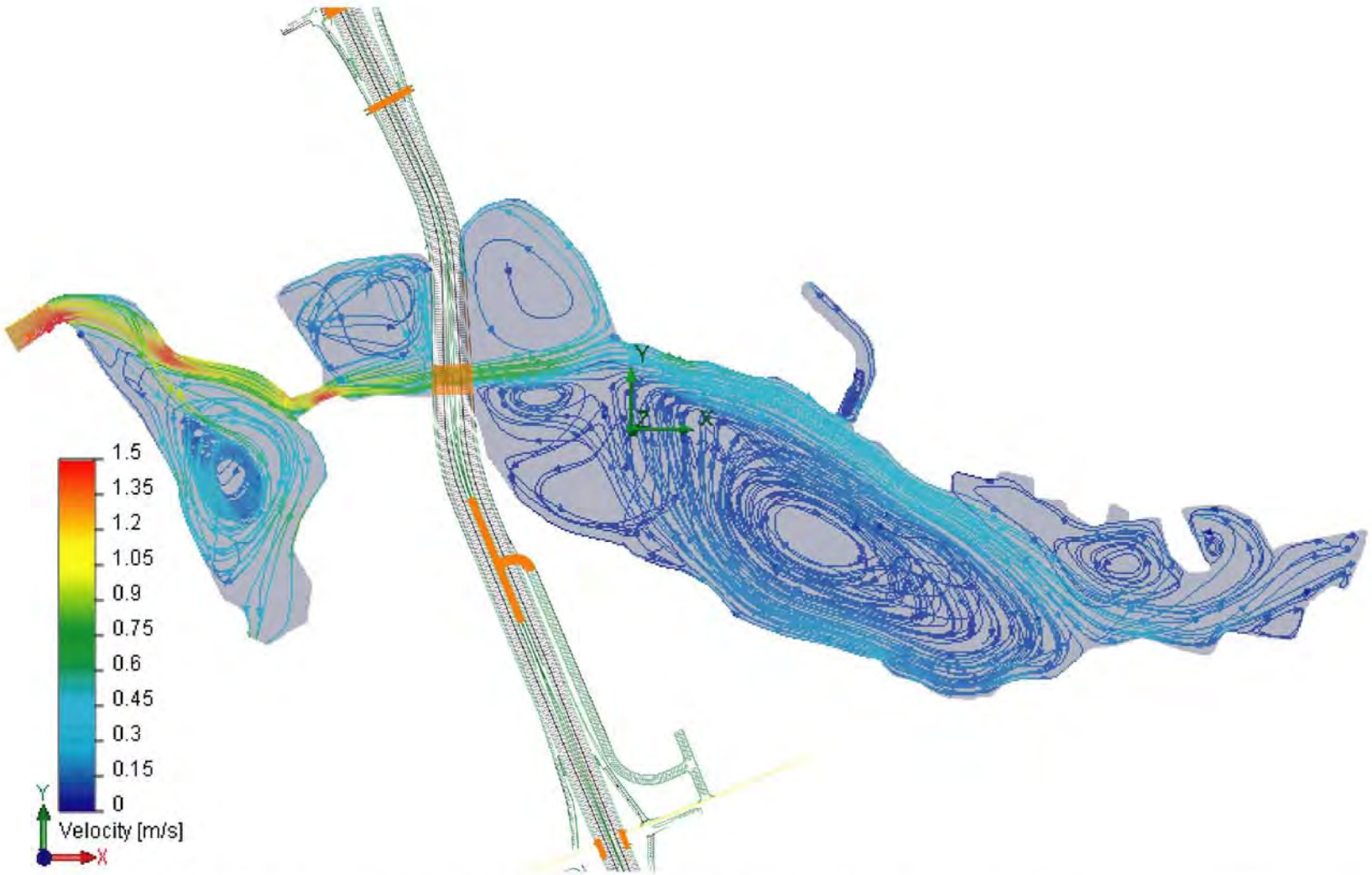

Figure 79. Hydrodynamic simulation of tidal flow into Agua Hedionda Lagoon with proposed replacement I-5 bridge during spring flooding tides.

mgd to the plant. The flood tide jet along the north bank of the West Basin speeds back up to as high as 1.5 m/sec (4.9 ft/sec) as it passes through the hardened channel under the rail road bridge and then losses energy as it diverges into the Central Basin, spinning up a somewhat disorganized Central Basin eddy. The core of the Central Basin eddy is at stagnation, again providing ideal conditions for suspended sediment to settle and deposit. Consequently, a bar forms here that was removed during the 1997-98 inner basin restoration dredging performed by SDG&E (Jenkins and Wasyl, 1998). Spring flood tide currents speed back up to 0.8-0.9 m/sec (2.6-2.9 ft/sec) through the hardened channel under the I-5 bridge before diverging into a complex set of counter rotating eddies that populate the East Basin. East Basin eddy speeds are on the order of 0.1 m/sec (0.3 ft/sec), insufficient to transport fine sand but an important stirring mechanism for mixing the East Basin water mass to maintain high oxygen levels and to maintain silt and clay sized sediment particles in suspension.

Figure 80 plots the TIDE_FEM simulation of ebbing spring tidal flows in the lagoon on 21 June 2005. The wetted area of the lagoon is significantly reduced relative to the flood tide area in Figure 79, due to the lower water levels acting on the stage area curve in Figure 69. A creeping flow with complex structure on the order of -0.1 m/sec (-0.3 ft/sec) evacuates the East Basin and accelerates to -0.8 m/sec (-2.6 ft/sec) as it passes through the hardened channel under the I-5 bridge. A vigorous well-ordered Central Basin eddy is spun up by an ebb-tide jet flowing along the southern bank of the Central Basin. This jet accelerates to -2m/sec (-6.6 ft/sec) as it passes through the hardened channel under the rail road bridge; and then splits into a south branch current and a north branch current as it diverges into the West Basin. The south branch current flows along the west bank of the West Basin and feeds the power plant source water at a rate of about -0.6 m/sec (-2.0 ft/sec). The north branch current also flows along the west bank of the West Basin and exits the lagoon through the ocean inlet. Maximum ebb flow currents in the inlet channel are only -0.8 m/sec (2.6 ft/sec) as the ebb flow volume flux is divided between the power plant intake and the ocean inlet. This is sufficient to flush the finer grain sizes from the bar in the recharge zone but not the coarser fractions in the 200 micron range.

Hydrodynamic simulations of flooding and ebbing neap tide currents on 14 June 2005 are plotted in Figures 81 & 82, respectively. The plant flow rate on this date remained at 501.1 mgd, (cf. Figure 71). The neap tide simulations show very similar flow structures as the spring tide simulations in Figures 81 & 82, only more sluggish and with less contrast in wetted lagoon area between flood and ebb due to the small tidal range during neap tides. Eddy systems remain well organized in the East Basin during flooding neap

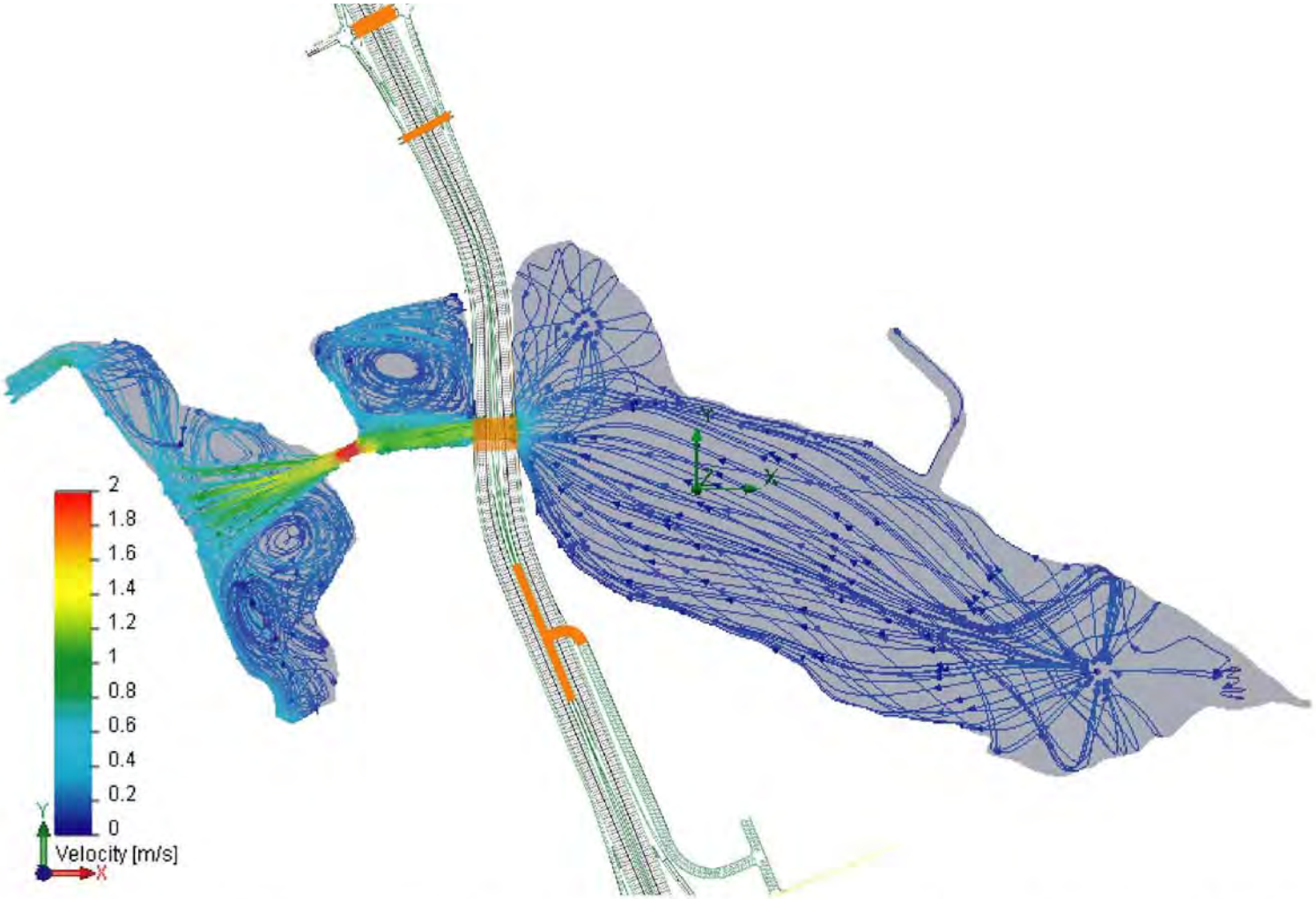

Figure 80. Hydrodynamic simulation of tidal flow out of Agua Hedionda Lagoon with proposed replacement I-5 bridge during spring ebbing tides.

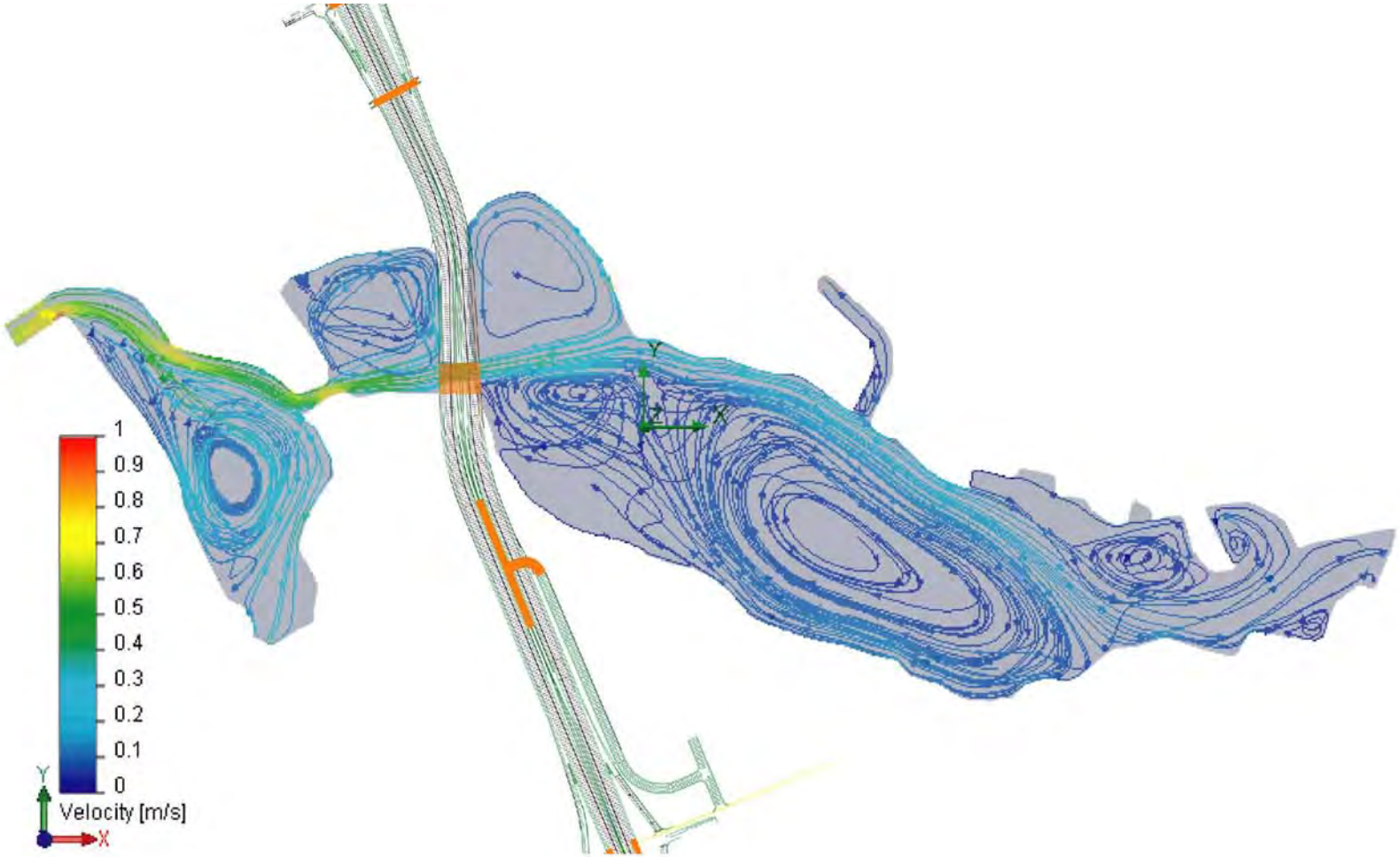

Figure 81. Hydrodynamic simulation of tidal flow into Agua Hedionda Lagoon with proposed replacement I-5 bridge during neap flooding tides.

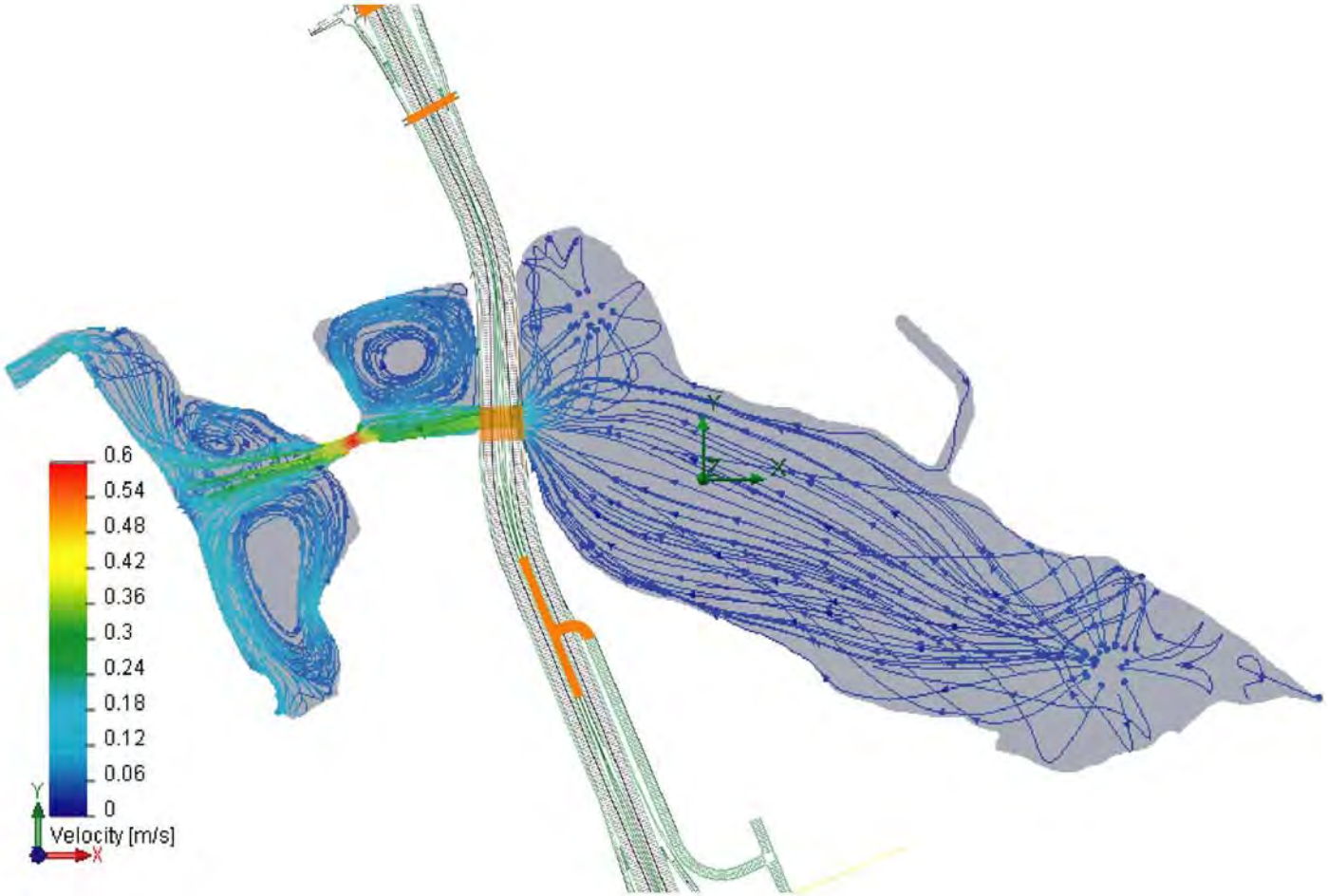

Figure 82. Hydrodynamic simulation of tidal flow out of Agua Hedionda Lagoon with proposed replacement I-5 bridge during neap ebbing tides.

tides (Figure 81) and a weak boundary current (0.2 m/sec or 0.6 m/sec) flows along the north bank, helping to stir the East Basin water mass in spite of the relatively low energy of the system. Maximum currents under the I-5 bridge reach 0.3 m/sec (0.98 ft/sec) during flooding neap tides (Figure 81), less than half the I-5 bridge waterway channel speeds as occurred during flooding spring tides at equivalent plant flow rate in Figure 79. Maximum I-5 bridge channel currents during ebbing neap tide (Figure 82) drop to only -0.4 m/sec (-1.3 ft/sec), stringer than flood tide currents due to the suction effect of the power plant combining with the tidal induced flow.

TIDE_FEM simulations of flooding and ebbing currents during mean tidal ranges on 30 June 2005 are plotted in Figures 83 & 84, respectively. For baseline comparisons with other bridge alternatives plant flow rates for mean range tides will be assumed to be the long-term minimum flow rate of 304 mgd, as required for stand-alone operations for the Carlsbad Desalination Project (cf. Figure 71). Again, the mean tide simulations show similar flow structures as the spring tide simulations in Figures 79 & 80, and although a bit more sluggish the wetted lagoon areas during flood and ebb and ebb are somewhat comparable to the spring tide cases. The south branch ebb current in the West Basin is significantly diminished due to the low plant flow rate, reaching only -0.2 m/sec (-0.6 ft/sec). The significant distinction of these mean tide simulations in Figures 83 & 84 is how the reduced plant flow rate has muted the flood flow currents in the inlet channel and I-5 bridge channel and allowed the ebb flow currents to be nearly comparable to spring tides and above threshold speed for the finer grain size fractions on the bar in the recharge zone. Maximum flood flow currents in the bridge waterway channel during mean tides (Figure 83) reach 0.7 m/sec (2.3 ft/sec), while maximum ebbing currents in the bridge waterway channel during mean tides (Figure 84) remain at -0.7 m/sec (-2.3 ft/sec), no longer showing the ebb dominance that was displayed at higher plant flow rates during the spring and neap ebb simulations in Figures 80 & 82.

Flow similitude between the existing and replacement bridge designs is born out in Figures 85 and 86 giving comparisons of the lowest low water level and phase lag in the East Basin. In both figures, the replacement bridge in red gives nearly the same East Basin response as the existing bridge in black, with relatively minor variance between the two at the upper and lower end of ocean low water levels. Although these small differences do not appear significant, they are due to fewer numbers of piles used in the replacement bridge design (where piles are increased from 32 in each row for existing, to 16 piles per row for the replacement design, while the numbers of rows are cut in half). Fewer numbers of piles reduce velocity head loss to turbulence and form drag with some improvement on the drainage ability of the East Basin. While the average daily lowest water level remains unchanged $\overline{\eta}_{LLW}$ = 0.64 ft MLLW, the minimum daily low water

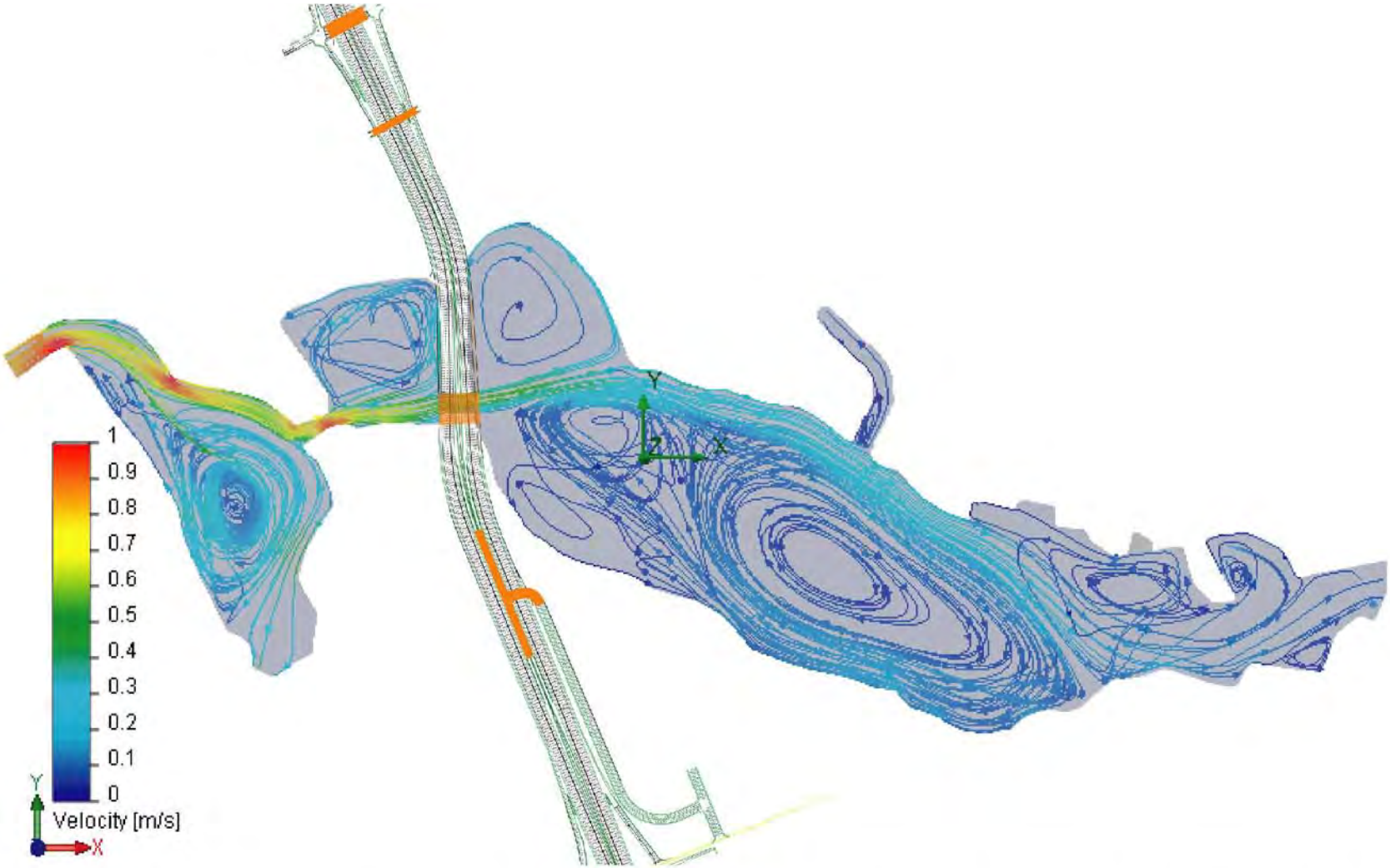

Figure 83. Hydrodynamic simulation of tidal flow into Agua Hedionda Lagoon with proposed replacement I-5 bridge during mean flooding tides.

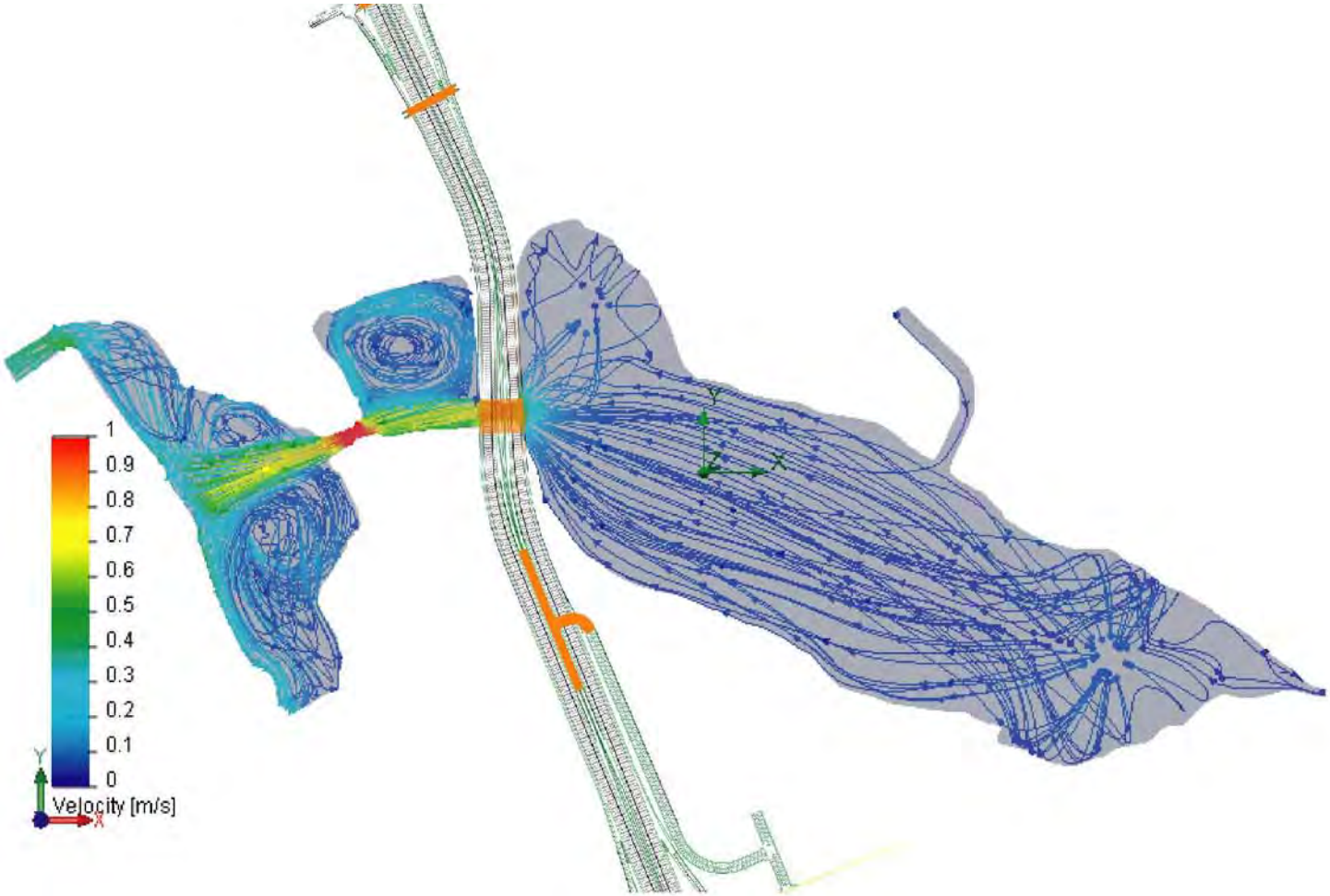

Figure 84. Hydrodynamic simulation of tidal flow out of Agua Hedionda Lagoon with proposed replacement I-5 bridge during mean ebbing tides.

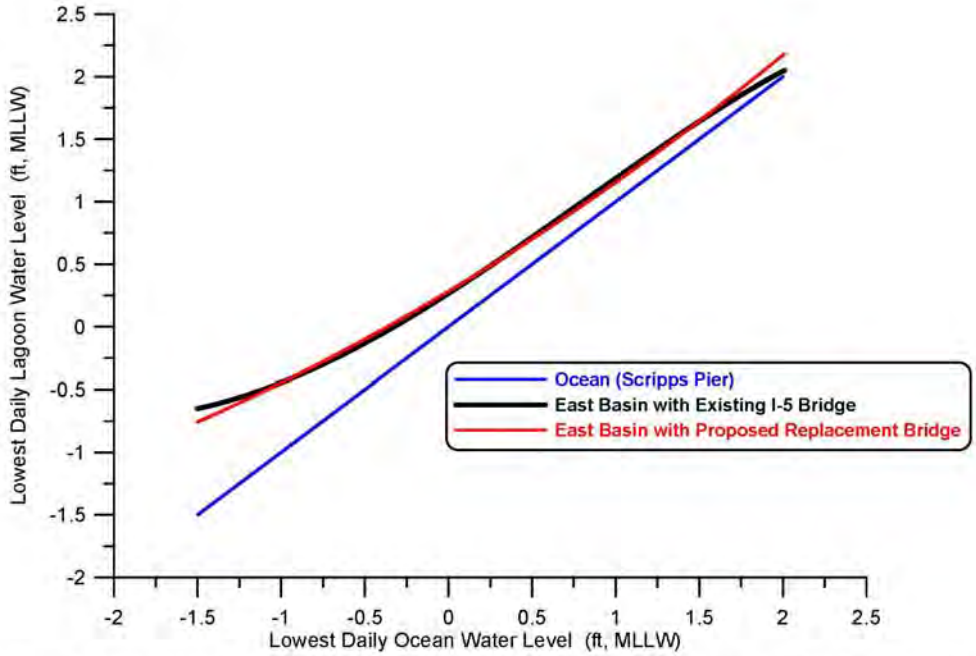

Figure 85. Comparison of daily lowest water level in east basin of Agua Hedionda Lagoon for existing I-5 bridge (black) versus the proposed replacement I-5 bridge (red). Both shown as functions of daily lowest water level in the local ocean as measured at the Scripps Pier tide gage (NOAA #941- 0230).

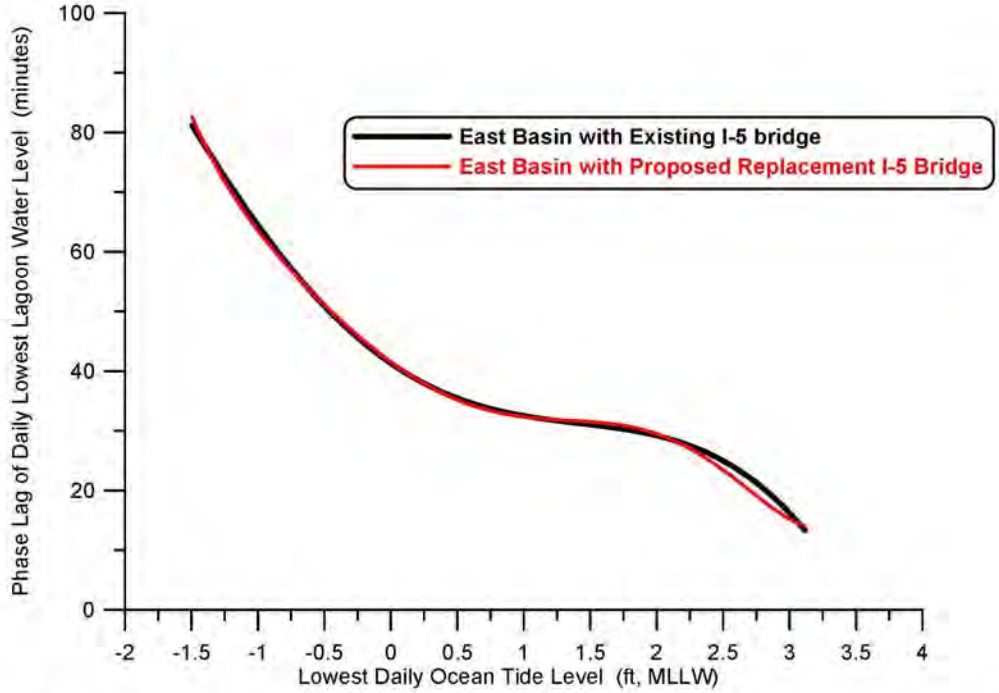

Figure 86. Comparison of the phase lag of lowest low water level in east basin of Agua Hedionda Lagoon for existing I-5 bridge (black) versus the proposed replacement I-5 bridge (red). Both shown as functions of daily lowest water level in the local ocean as measured at the Scripps Pier tide gage (NOAA #941- 0230).

level is lowered from η_{LLW} = -0.65 ft MLLW for the existing bridge to η_{LLW} = -0.78 ft MLLW for the replacement bridge. Mean higher high water is raised slightly from η_{MHHW} = +6.06 ft MLLW for the existing bridge to η_{MHHW} = +6.08 ft MLLW for the replacement bridge. Maximum and average East Basin phase lags remain unchanged with the replacement bridge at $\theta_{\max}$ = 80.1 minutes, and $\bar{\theta}$ = 40 minutes, respectively. A summary of the East Basin water level datum with the proposed replacement bridge is given tin Table 5.2.

Table 5.2: Water Levels for Agua Hedionda Lagoon With Proposed Replacement I-5 Bridge, based on long term forcing for 2005-2008 period of record.

Elevations Feet MLLW	Ocean	East Basin
MEAN HIGHER HIGH WATER (MHHW)	5.7	6.08
MEAN HIGH WATER (MHW)	5.0	5.38
MEAN LOW WATER (MLW)	1.3	1.72
MEAN LOWER LOW WATER (MLLW)	0.4	0.64
LOWEST OBSERVED WATER LEVEL (MLLW)	-1.5	-0.78
HIGHEST OBSERVED WATER LEVEL (MLLW)	7.4	7.6
MAXIMUM TIDAL RANGE	8.9	8.38

The slight reduction of East Basin tidal muting achieved by the replacement bride (as a consequence of a significant number of piles in the bridge waterway channel), slightly expands the intertidal habitat zonation, increases the exposure of mud flats to a small degree, while making a small reduction in the sub-tidal habitat. This is revealed by comparing the primary water level datum for the replacement bridge in Table 5.2 with those for the existing bridge in Table 5.1. With the replacement bridge, higher-high and high water levels are raised by a few hundredths of a foot while lower-low and low water levels are lowered by a by several hundredths to a tenth of a foot. Hydroperiod function comparisons in Figure 87 give a similar result, where the existing bridge is shown in red

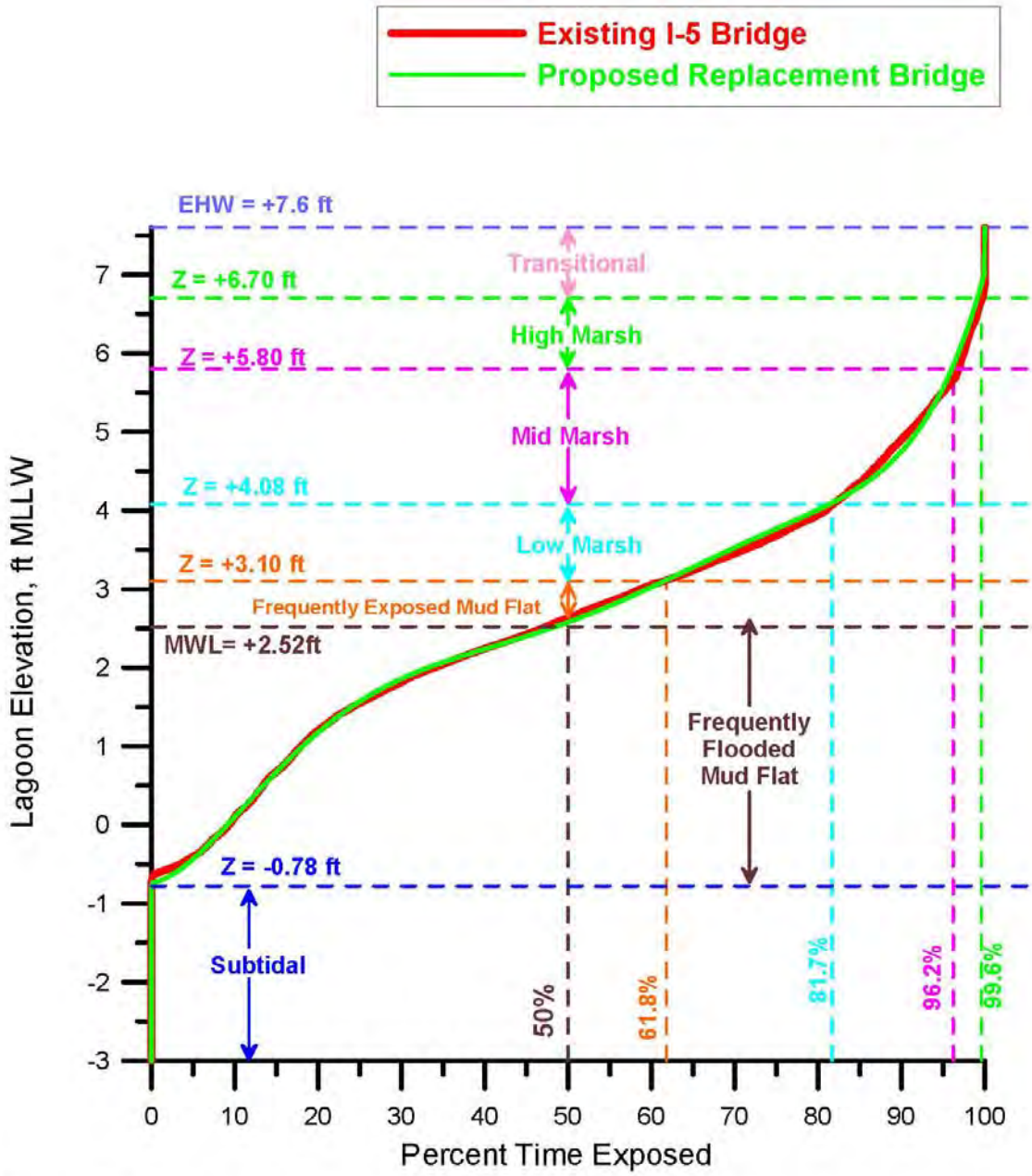

Figure 87. Hydroperiod function for the East Basin of Agua Hedionda Lagoon comparing existing I-5 bridge (red) against the proposed replacement I-5 bridge (green). Based on hydrodynamic simulation of East Basin water levels in response to tidal forcing from the Scripps Pier tide gage (NOAA # 941-0230). Habitat breaks based on habitat delineation from Josselyn and Whelchel (1999).

versus the replacement bridge in green. The elevations of the habitat breaks in Figure 87 can be mapped against the East Basin stage area function (Figure 69) and used to estimate the sub-tidal and intertidal habitat types for both the existing and replacement bridges. By that procedure Table 5.3 shows that the minimum (perpetual) sub-tidal area of the East Basin decreases by 1.1 acres with the replacement bridge, to 179.0 acres vs 180.1 acres for the existing bridge; the areas of frequently flooded mud flats remain unchanged at 30.3 acres; while frequently exposed mud flats are increased by 1.2 acres, from 4.3 acres for the existing bridge to 5.5 acres for the replacement bridge; low salt marsh remain unchanged at 11.5 acres; mid salt marsh increases by 1.4 acres, from 20.0 acres for the existing bridge to 21.4 acres for the replacement bridge; high salt marsh is reduced by 1.4 acres, from 11.7 acres for the existing bridge to 10.3 acres for the replacement bridge; and transitional habitat is unchanged at 8.1 acres. The maximum area inundated by salt water at extreme high water is unchanged at 266.0 acres, but the maximum the intertidal habitat is increased by 1.1 acres with the replacement bridge; and the mean area experiencing tidal inundation up to MHHW is increased slightly from 250.8 acres for the existing bridge to 251.0 acres with an average 60.0 acres of intertidal habit (an increase of 0.2 acres over existing conditions), while the mean sub-tidal habitat remains unchanged at 191 acres for both the existing bridge and the replacement bridge. These deviations in the distributions of areas among sub-tidal and intertidal habitat types are less than what replacement bridges caused at Batiquitos, because the preponderance of habitat at Agua Hedionda is one type, namely, sub-tidal. These small changes of a couple of acres or less are not considered as being a significant impact of the replacement bridge since the aggregate totals of habitat and their split between intertidal and sub-tidal remain essentially unchanged. The small deviations in intertidal habitat splits in Table 5.2 and Figure 87 are likely due to reductions in turbulence and drag effects associated with fewer numbers of piles in the waterway channel of the replacement bridge.

Table 5.3: Agua Hedionda East Basin Habitat Area Distribution from Hydroperiod & Stage Area Functions with Existing Bridge vs. Proposed Replacement Bridge

East Basin Habitat Areas	Existing I-5 Bridge	Replacement I-5 Bridge
Perpetual Sub-Tidal (acres)	180.1	179.0
Mean Sub-Tidal (acres)	191.0	191.0
Frequently Flooded Mud Flat (acres)	30.3	30.3
Frequently Exposed Mud Flat (acres)	4.3	5.5
Low Salt Marsh (acres)	11.5	11.5
Mid Salt Marsh (acres)	20.0	21.4
High Salt Marsh (acres)	11.7	10.3
Transitional Habitat (acres)	8.1	8.1
Maximum Intertidal Area (acres)	85.9	87.0
Maximum Area of Salt Water Inundation (acres)	266.0	266.0
Mean Intertidal Area (acres)	59.8	60.0
Mean Area of Salt Water Inundation (acres)	250.8	251.0

5.3.2) Tidal Hydraulics Impacts of I-5 Bridge Replacement with Fill Removal (*Double-Wide Alternative*): Here we evaluate the *double-wide* alternative that would require removal of a portion of the road bed fill to accommodate doubling the width of the tidal channel along the existing grade of the north bank and increasing the span of the replacement bridge from 230 ft (70.1 m) to 460 ft (140.2 m). Doubling of the span also places two additional rows of 16 piles each in the active transport region of the channel, but increases channel cross sectional two-fold. Channel width increases effect only the north bank because the present tidal channel runs along the south bank of the Central Basin, and there is no free basin space to expand the channel to the south. Due to buried infrastructure concerns, the double-wide concept retains the hard channel bottom feature at -19.22 ft MLLW (-21.52 ft NGVD) with sediment fill at -5 ft MLLW (-7.3 ft NGVD). Figure 88 compares the existing and double-wide channel bottom profiles on both the west side (Section 9) and the east side (Section 10) of the I-5 bridge.

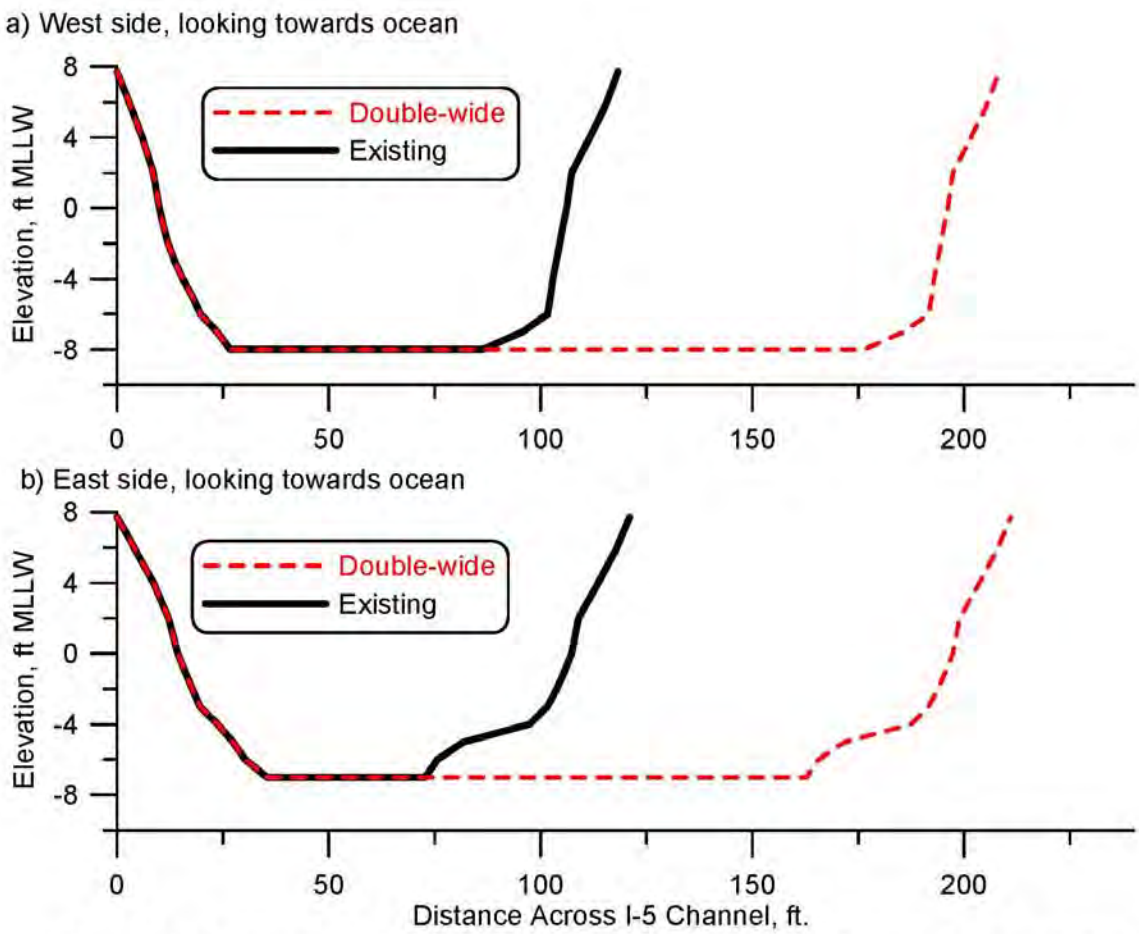

Figure 88: Comparison of existing vs. double-wide I-5 bridge channel at Agua Hedionda Lagoon: a) cross section west side of bridge, b) cross section east side of bridge.

Figure 89 gives flow trajectories and depth-averaged tidal currents in Agua Hedionda Lagoon with the double-wide alternative for maximum flood flow during mean range tides. Note the replacement bridge span has been doubled to accommodate the wider bridge waterway channel. This wider bridge waterway reduces the velocities of the flow exiting the hard bottom section of the channel to 0.34 m/sec (1.1 ft/sec) during maximum flood flow, down from 0.7 m/sec (2.3 ft/sec) for the proposed replacement bridge in Figure 83. In Figure 90, velocities of the flow exiting the hard bottom section of the channel are reduced to -0.34 m/sec (-1.1 ft/sec) during maximum ebbing flow, or about half the maximum channel velocity found for ebb flow with the proposed replacement bridge in Figure 84. Both of these examples are less than the threshold of incipient motion of the sediments that have in-filled the existing hard bottom channel in Figure 67a, and insufficient to cause scour of the East Basin sediments immediately east of the I-5 bridge. These sub-scour threshold channel velocities are insufficient to maintain the scour holes that presently exist on either side of the I-5 bridge (Figure 18); and consequently these holes will in-fill over time, further reducing losses of tidal energy to form drag.

Eddy structures and jets elsewhere in the East, Central and West Basins are similar in the case of the double-wide channel but not identical to those found for the existing and replacement spans on mean range flooding and ebbing tides in Figure 83 & 84. Maximum flood currents in the inlet channel reach 1.0 m/sec or (3.28 ft/sec) with the double-wide alternative; while maximum ebb flow currents in the inlet channel are -0.63 m/sec (-2.07 ft/sec) slightly more the proposed replacement spans in Figures 83 & 84 but the inlet is still strongly flood tide dominated due to the consumption of lagoon water by the power plant. Eddy structures in the Central Basin are a bit more vigorous with the double-wide channel, possibly because of slightly more volume flow in and out of the East Basin.

Drag reduction achieved by the double-wide channel cross section in Figure 88 ultimately reduces the East Basin phase lag and thereby achieving more complete drainage of the East Basin during low tide. Figure 91 compares long term simulations of the daily low water levels in the East Basin with the existing I-5 bridge (black), the proposed I-5 bridge (red) and the double-wide alternative (purple) with its double-wide channel cross section from Figure 88. The double-wide channel reduces average daily lowest water levels to $\overline{\eta}_{LLW}$ = +0.547 ft MLLW from the average for the existing bridge of $\overline{\eta}_{LLW}$ = +0.64 ft MLLW. The minimum daily low water level achieved by the double-wide channel is lowered to -0.91 ft MLLW, down from -0.65 ft MLLW for existing conditions (cf. Table 5.1). The maximum daily lower low water level with the double-wide alternative

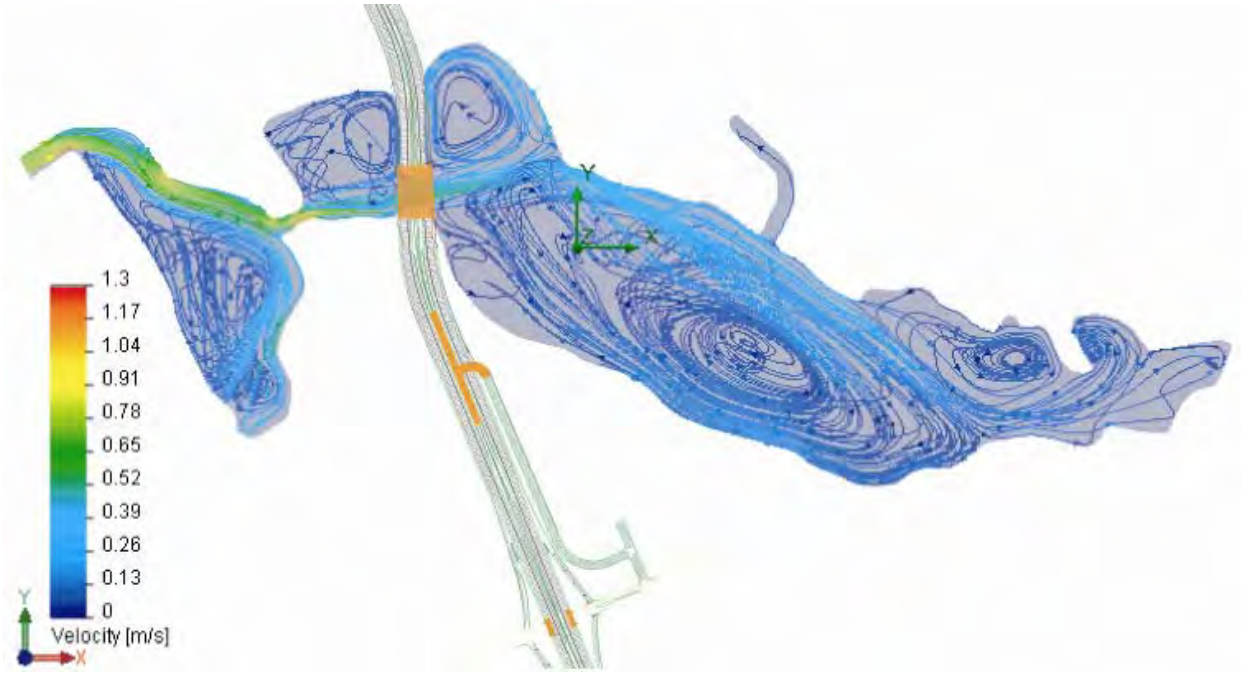

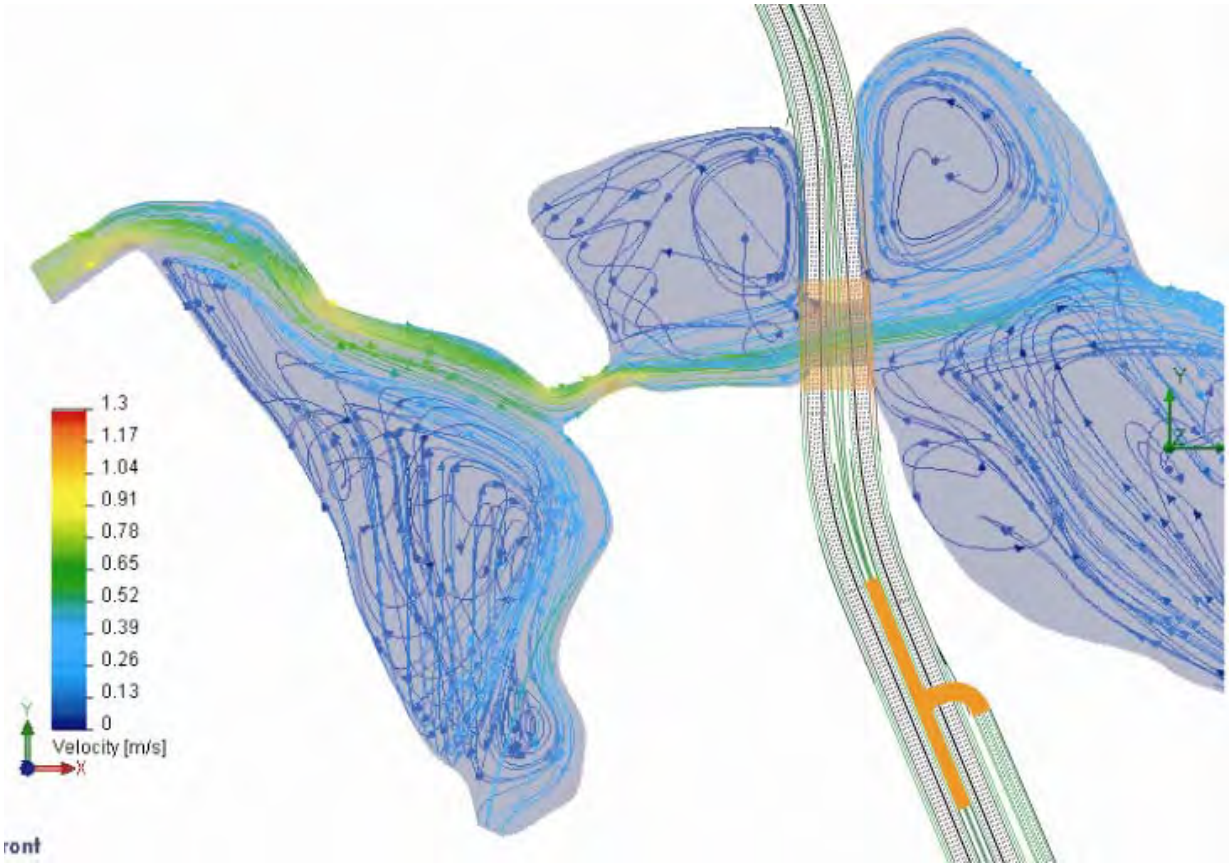

Figure 89: Hydrodynamic simulation of maximum flood flow during mean range tides at Agua Hedionda Lagoon with the *double-wide* alternative for the replacement bridge of North Coast Corridor Project. Power plant flow rate set at 304 mgd.

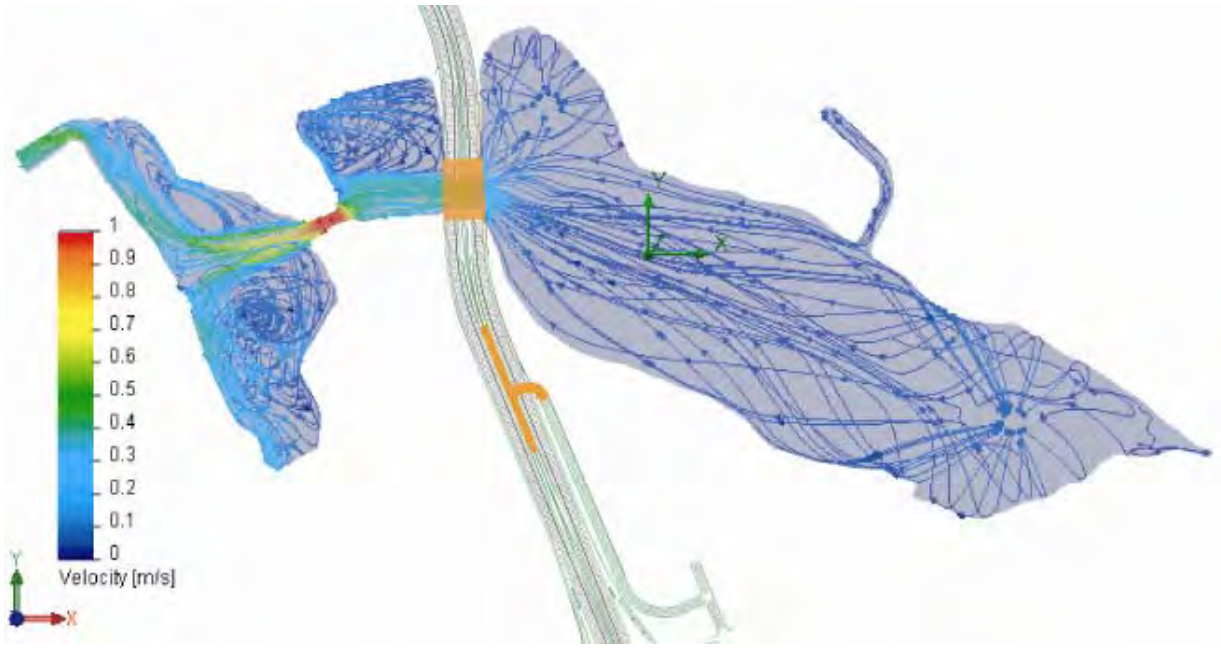

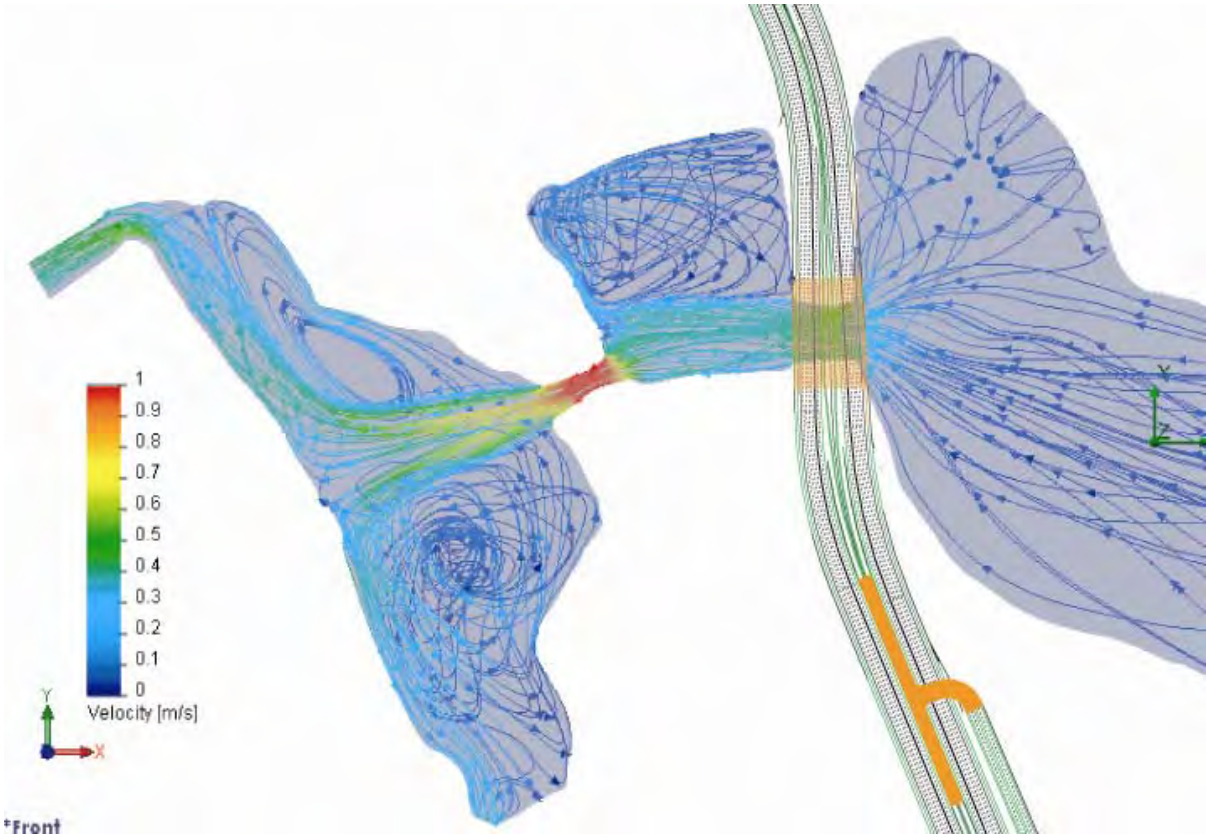

Figure 90: Hydrodynamic simulation of maximum ebb flow during mean range tides at Agua Hedionda Lagoon with the *double-wide* alternative for the replacement bridge of North Coast Corridor Project. Power plant flow rate set at 304 mgd.

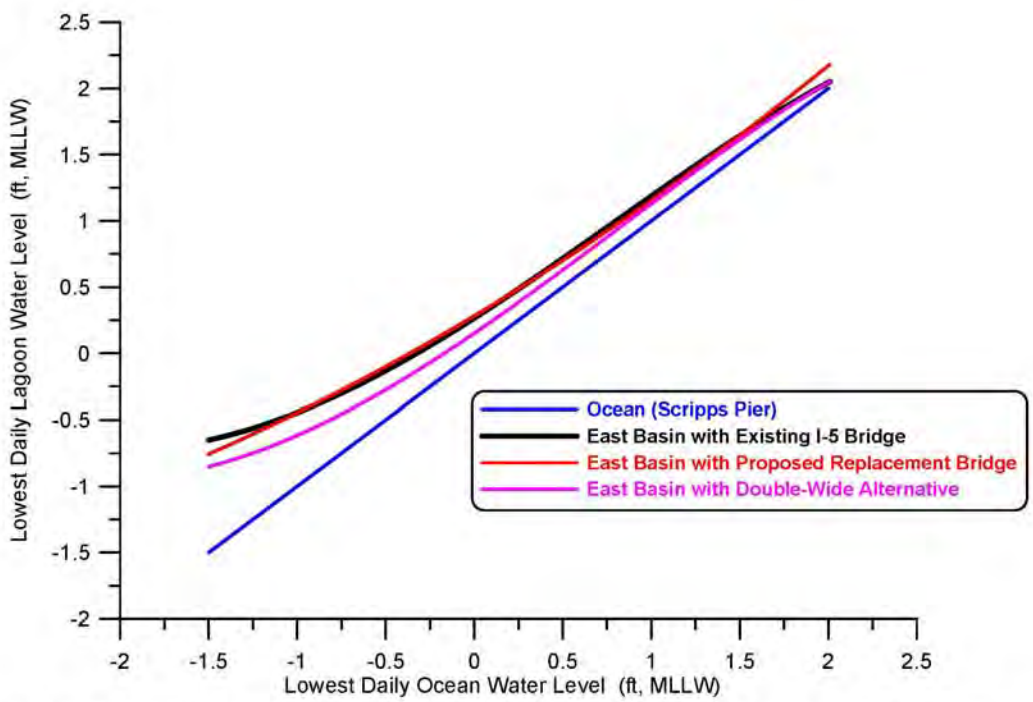

Figure 91. Comparison of daily lowest water level in east basin of Agua Hedionda Lagoon for existing I-5 bridge (black), proposed replacement I-5 bridge (red), versus the doubel-wide alternative (purple). All shown as functions of daily lowest water level measured at the Scripps Pier tide gage.

is unchanged from existing conditions, at η_{LLW} = +2.13 ft MLLW. As Figure 91 indicates, the incremental reduction in daily low water levels achieved for the East Basin by the double-wide alternative are most significant at the lower-low end of the scale and in any case represent relatively modest improvements in ebb-tide drainage over existing conditions. Similarly, East Basin phase lags are modestly diminished with the double-wide alternative. Figure 92 shows that in long term simulation the maximum East Basin phase lag is reduced from $\theta_{\max}$ = 80.1 minutes with the existing I-5 bridge to $\theta_{\max}$ = 61.6 minutes with the double-wide alternative. Average East Basin phase lags are reduced from $\bar{\theta}$ = 40.1 minutes with the existing I-5 bridge to $\bar{\theta}$ = 30.1 minutes with the double-wide alternative. The minimum phase lag for East Basin tides remains unchanged with the double-wide alternative at 15.3 minutes, as this minimum occurs during neap tides when the choke points at the inlet channel and railroad bridge retain ultimate hydraulic control for these small range tidal events.

The reductions in flow speeds and phase lags due to the double-wide waterway alternative results in more complete conversion of velocity head into potential energy of water elevation, thereby increasing the tidal range in the east basin of Agua Hedionda

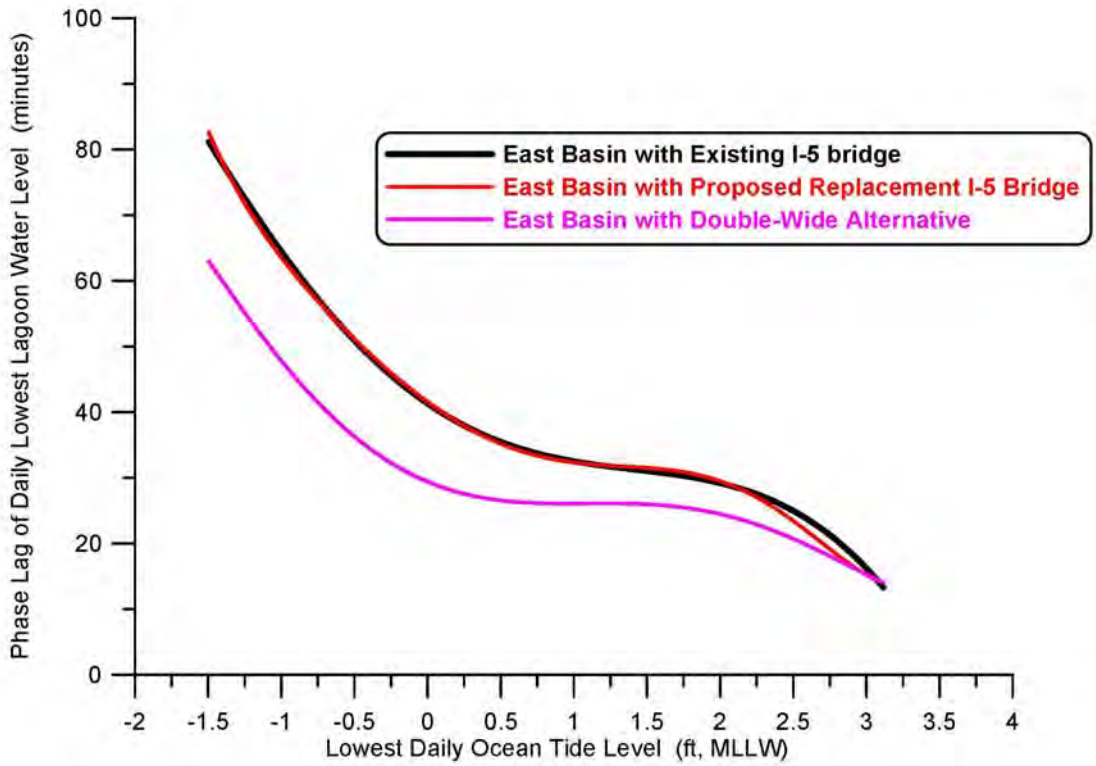

Figure 92. Comparison of phase lags in the east basin of Agua Hedionda Lagoon for existing I-5 bridge (black), proposed replacement I-5 bridge (red), versus the doubel-wide alternative (purple). All shown as functions of daily lowest water level measured at the Scripps Pier tide gage.

Lagoon. Table 5.4 gives a summary of the water level elevations calculated for Agua Hedionda Lagoon with the double-wide I-5 bridge alternative based on long-term tidal simulations using historic ocean water level forcing for the 2005-2008 period of record. Comparing Table 5.4 against existing conditions in Table 5.1, we find that both the mean and maximum diurnal tidal ranges in the East Basin are slightly increased with the double-wide alternative. MHHW in the East Basin has been raised to +6.13 ft MLLW with the double-wide alternative, while MLLW in the East Basin has been lowered to +0.55 ft MLLW, producing a mean diurnal tidal range of 5.58 ft, an increase of 0.16 ft over existing conditions. While extreme high water levels in the East Basin remain unchanged with the double-wide alternative, extreme low water levels are lowered to -0.91 ft MLLW, resulting in a maximum tidal range of 8.51 ft, an increase of 0.25 ft over existing conditions.

The 1980-2010 period of record of ocean tides from Scripps Pier tide gage were fed into the calibrated TIDE_FEM model configured for the double-wide alternative to give a long term output of East Basin water levels from which the hydroperiod function was

Table 5.4: Water Levels for Agua Hedionda Lagoon With Double-Wide Alternative Bridge Channel, based on long term forcing for 2005-2008 period of record.

Elevations Feet MLLW	Ocean	East Basin with Double-Wide Alternative
MEAN HIGHER HIGH WATER (MHHW)	5.7	6.13
MEAN HIGH WATER (MHW)	5.0	5.41
MEAN LOW WATER (MLW)	1.3	1.65
MEAN LOWER LOW WATER (MLLW)	0.4	0.55
LOWEST OBSERVED WATER LEVEL (MLLW)	-1.5	-0.91
HIGHEST OBSERVED WATER LEVEL (MLLW)	7.4	7.6
MAXIMUM TIDAL RANGE	8.9	8.51

calculated in Figure 93 (green) and compared against existing conditions shown in gray. Despite noticeable changes in the hydroperiod function with the double-wide alternative, those changes do not map into appreciable changes in habitat areas when factored against the stage area function in Figure 69. This is due to the fact that the preponderance of the East Basin habitat is sub-tidal, while the more significant changes in the hydroperiod function involve the intertidal habitat that comprises a relatively minor constituent. The mapping of habitat breaks from the hydroperiod function in Figure 93 into the stage area function in Figure 69 produces the habitat area distributions summarized in Table 5.5

Table 5.5 shows that the perpetual sub-tidal area of the East Basin decreases by 1.5 acres to 178.6 acres with the double-wide alternative, from 180.1 acres for the existing bridge while the mean sub-tidal area with the double-wide alternative is unchanged, equal to 191.0 acres, same as for the existing bridge; frequently flooded mud flat is increased by 0.3 acres, from 30.3 acres for the existing bridge to 30.6 acres for the double-wide alternative; frequently exposed mud flat is increased by 2.2 acres, from 4.3 acres for the existing bridge to 6.5 acres for the double-wide alternative; low salt marsh is increased by 1.2 acres, from 11.5 acres for the existing bridge to 12.7 acres for the double-wide alternative; mid salt marsh is increased by 1.6 acres, from 20.0 acres for the existing

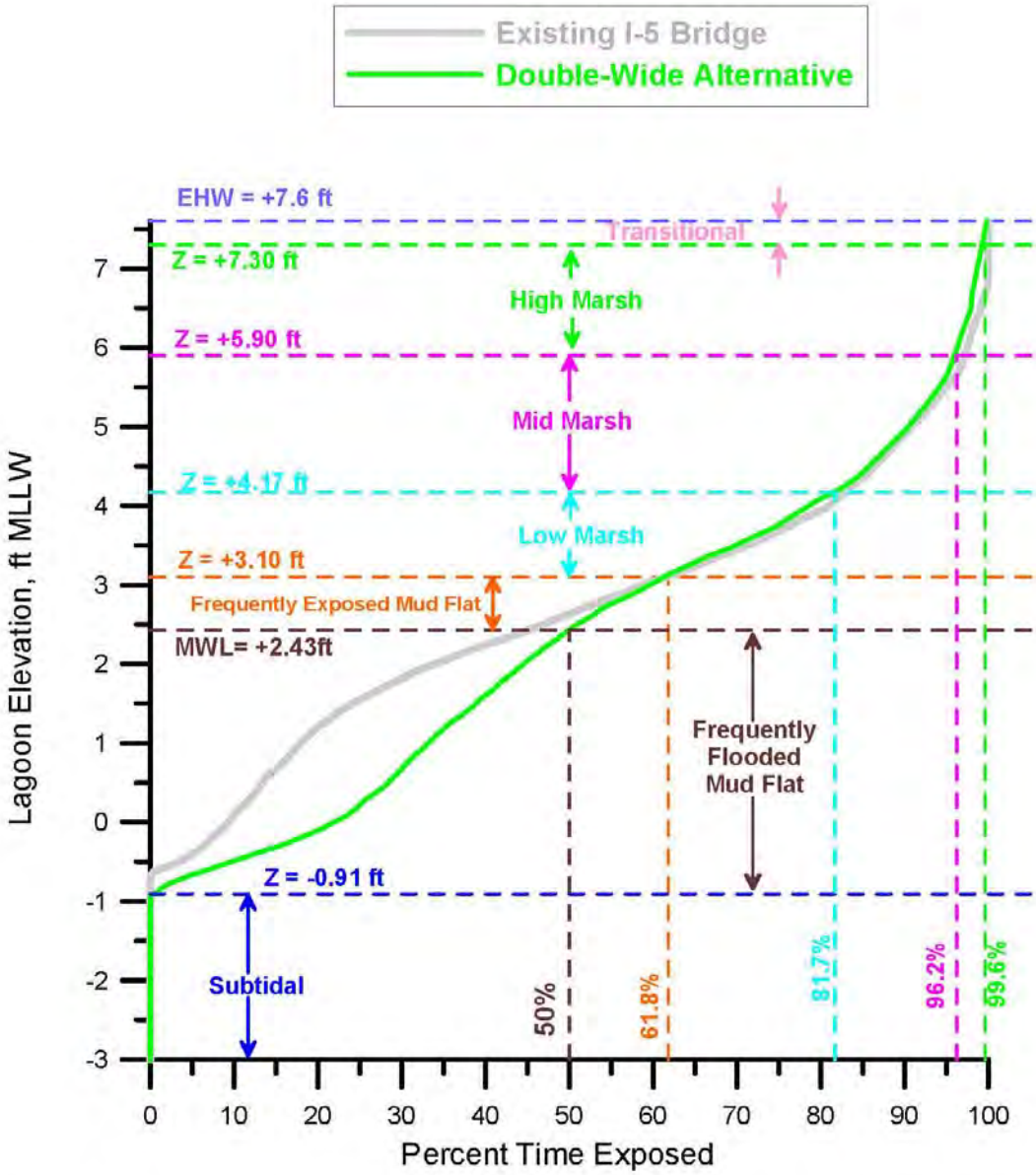

Figure 93. Hydroperiod function for the East Basin of Agua Hedionda Lagoon with existing I-5 bridge vs. double-wide alternative. Based on hydrodynamic simulation of East Basin water levels in response to tidal forcing from the Scripps Pier tide gage (NOAA # 941-0230). Habitat breaks based on habitat delineation from Josselyn and Whelchel (1999).

Table 5.5: East Basin Habitat Area Distribution from Agua Hedionda Hydroperiod and Stage Area Functions with Existing Bridge vs. Double-Wide Alternative

East Basin Habitat Areas	Existing I-5 Bridge	Double-Wide Alternative
Perpetual Sub-Tidal (acres)	180.1	178.6
Mean Sub-Tidal (acres)	191.0	191.0
Frequently Flooded Mud Flat (acres)	30.3	30.6
Frequently Exposed Mud Flat (acres)	4.3	6.5
Low Salt Marsh (acres)	11.5	12.7
Mid Salt Marsh (acres)	20.0	21.6
High Salt Marsh (acres)	11.7	14.9
Transitional Habitat (acres)	8.1	2.4
Maximum Intertidal Area (acres)	85.9	88.7
Maximum Area of Salt Water Inundation (acres)	266.0	267.3
Mean Intertidal Area (acres)	59.8	61.8
Mean Area of Salt Water Inundation (acres)	250.8	252.8

bridge to 21.6 acres for the double-wide alternative; high salt marsh is increased proportionately the largest increment, by 3.2 acres, from 11.7 acres for the existing bridge to 14.9 acres for the double-wide alternative replacement bridge; much of the transitional habitat is converted into salt marsh habitat, reducing transitional habitat by 5.7 acres from 8.1 acres for the existing bridge to 2.4 acres for the double-wide alternative. Altogether, net habitat gains and conversions to higher quality intertidal habitats are meager with the double-wide alternative. Maximum intertidal habitat is increased by 2.8 acres to 88.7 acres with the double-wide alternative as compared to 85.9 acres for existing conditions; while the mean area experiencing tidal inundation up to MHHW is increased by 2.0 acres from 250.8 acres for the existing bridge to 252.8 acres for the double-wide alternative resulting in an average 61.8 acres of intertidal habit, an increase of 2.0 acres over existing conditions.

Generally, Figure 94 and Table 5.5 indicate that the double-wide channel will create 2.5 acres of new mud flats and increase the exposure time of existing mud flats; a benefit to shorebird foraging and a feature of the East Basin. It will also reduce the compression of present intertidal habitat by lowering the zonation of low mid and high marsh vegetation, but that habitat type makes up only a minor fraction of the existing East Basin habitat, 77% of which is sub-tidal based on mean ranges of tidal inundation. Of the 2.0 acres of intertidal area created on average by the double-wide alternative, al of it (2.0 acres) represents net wetland habitat gain. Because of the “iron-lung” effect that the power plant exerts on tidal ventilation of the east basin of Agua Hedionda, it is difficult to achieve substantial habitat gains or conversions through improved bridge designs, even one involving rather significant removal of I-5 road bed fill such as the double-wide alternative.

5.3.3) Tidal Hydraulics Impacts of I-5 Bridge Replacement with Reduced Fill Removal (*Chang-channel Alternative*): Here we evaluate the *Chang-channel* alternative as a means to remediate tidal muting effects of the existing narrow bridge waterway at Agua Hedionda I-5 bridge. The *Chang-channel* alternative (Figure 67b) would require removal of a smaller portion of the road bed fill than the double-wide alternative in Section 5.3.2, and would not require doubling the span of the replacement, thereby providing a significant cost advantage. Channel width increases associated with the *Chang-channel* alternative increase the bed width of the hard bottom channel to 99.1 ft while maintaining the existing depth of the hard bottom channel at -19.22 ft MLLW (-21.52 ft NGVD) along 1 on 1 side slopes**.** While the double-wide alternative increases the channel cross section by a factor of 2 over existing conditions, the *Chang-channel* alternative provides an increase by a factor of 1.4.

Figure 95 gives flow trajectories and depth-averaged tidal currents in Agua Hedionda Lagoon with the *Chang-channel* alternative for maximum flood flow during mean range tides. With 40% more channel cross section than the existing bridge waterway, this alternative reduces the velocities of the flow exiting the hard bottom section of the channel to 0.5 m/sec (1.6 ft/sec) during maximum flood flow, down from 0.7 m/sec (2.3 ft/sec) for the replacement bridge (cf Figure 83). In Figure 96, velocities of the flow exiting the hard bottom section of the channel are reduced to -0.5 m/sec (0.98 ft/sec) during maximum ebbing flow. These flood and ebb velocities under the I-5 bridge with the Chang-channel are about 47% greater than with the double-wide alternative, but about 40% less than for the proposed replacement bridge. With lower velocity head, the Chang Channel has less drag and more pressure recovery than the proposed replacement bridge.

Eddy structures and jets in the East, Central and West Basins with the Chang-channel are similar to those for the double-wide channel but not identical to those found for the existing and replacement spans on mean range flooding and ebbing tides in Figure 83 & 84. Maximum flood currents in the inlet channel reach 0.99 m/sec or (3.25 ft/sec) with the Chang-channel alternative; while maximum ebb flow currents in the inlet channel are -0.5 m/sec (-0.98 ft/sec) slightly less than the double-wide alternative that moves more water through the system; but slightly more the proposed replacement spans in Figures 83 & 84 that move less water. Regardless, the inlet is remains strongly flood tide dominated due to the consumption of lagoon water by the power plant. Eddy structures in the East Basin during flooding tide similar to the double-wide channel or existing channel.

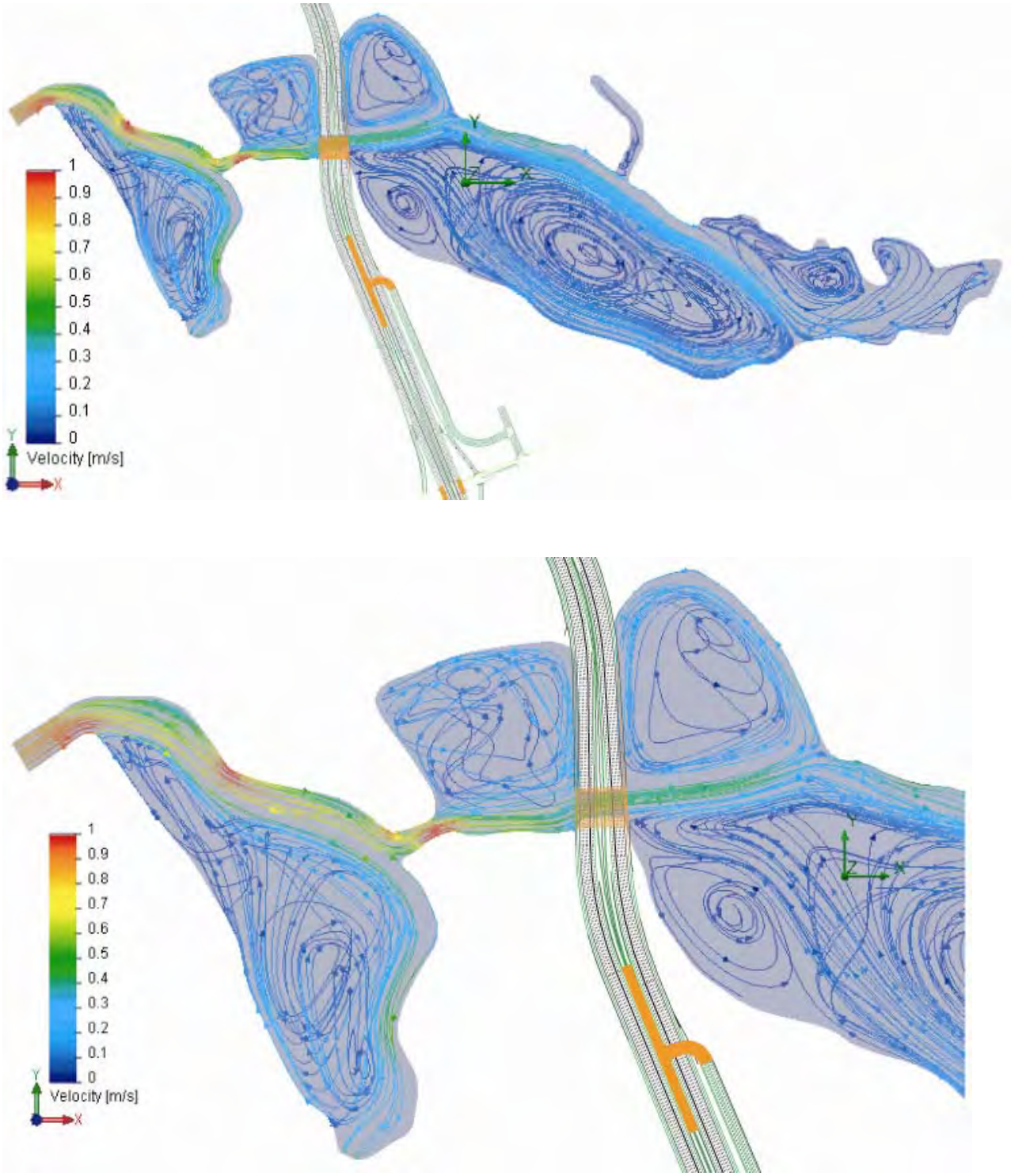

Figure 94: Hydrodynamic simulation of maximum flood flow during mean range tides at Agua Hedionda Lagoon with the *Chang-channel* alternative for the replacement bridge of North Coast Corridor Project. Power plant flow rate set at 304 mgd.

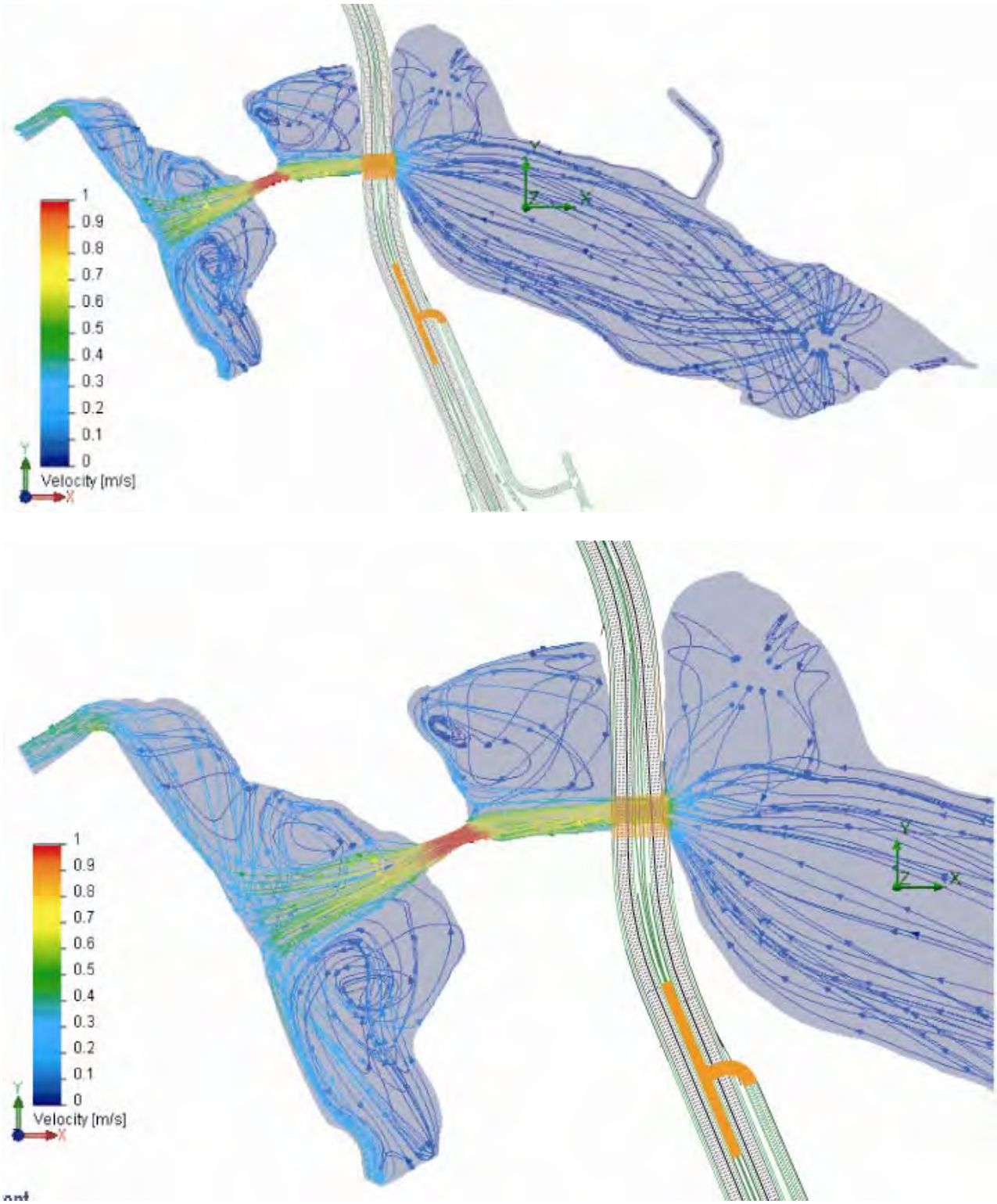

Figure 95: Hydrodynamic simulation of maximum ebb flow during mean range tides at Agua Hedionda Lagoon with the *Chang-channel* alternative for the replacement bridge of North Coast Corridor Project. Power plant flow rate set at 304 mgd.

Figure 96 compares long term simulations (2005-2008) of the daily low water levels in the East Basin with the existing I-5 bridge (black), the proposed I-5 bridge (red) and the Chang-channel alternative (purple) and the Chang-channel in green. The Chang-channel makes no change to the maximum daily lower low water levels, maintaining η_{LLW} = 2.13 ft MLLW, same as for the existing I-5 bridge; but, reduces average daily lowest water levels to $\overline{\eta}_{LLW}$ = +0.60 ft MLLW from the existing average of $\overline{\eta}_{LLW}$ = +0.64 ft MLLW. The minimum daily low water level achieved by the Chang-channel is lowered most to -0.80 ft MLLW, down from -0.65 ft MLLW for existing conditions (cf. Table 5.1).

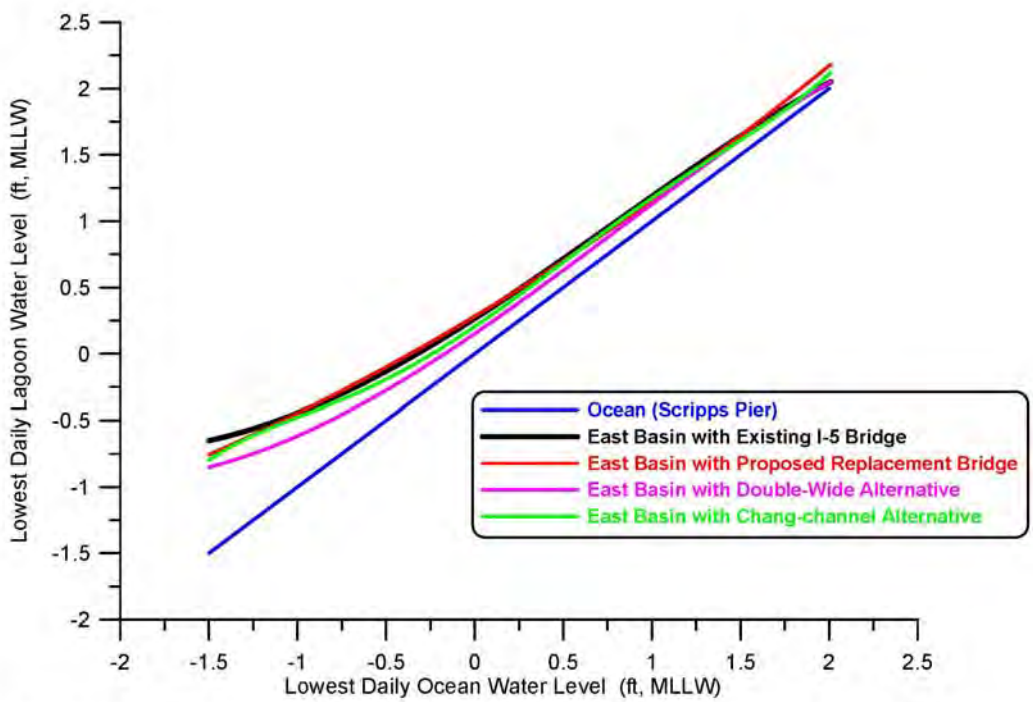

Figure 96. Comparison of daily lowest water level in east basin of Agua Hedionda Lagoon for existing I-5 bridge (black) and the proposed replacement I-5 bridge (red), the double-wide (purple), versus the Chang Channel (green). All shown as functions of daily lowest water level from the Scripps Pier tide gage.

East Basin phase lags are modestly diminished with the Chang-channel alternative. Figure 97 shows that in long term simulation the maximum East basin phase lag is reduced from $\theta_{\max}$ = 80.1 minutes with the existing I-5 bridge to $\theta_{\max}$ = 70.8 minutes with the Chang-channel alternative. Average East Basin phase lags are reduced from $\overline{\theta}$ = 40.1 minutes with the existing I-5 bridge to $\overline{\theta}$ = 34.7 minutes with the Chang-channel alternative. The minimum phase lag for East Basin tides is slightly increased with the Chang-channel alternative to 16.7 minutes, although this minimum occurs during neap

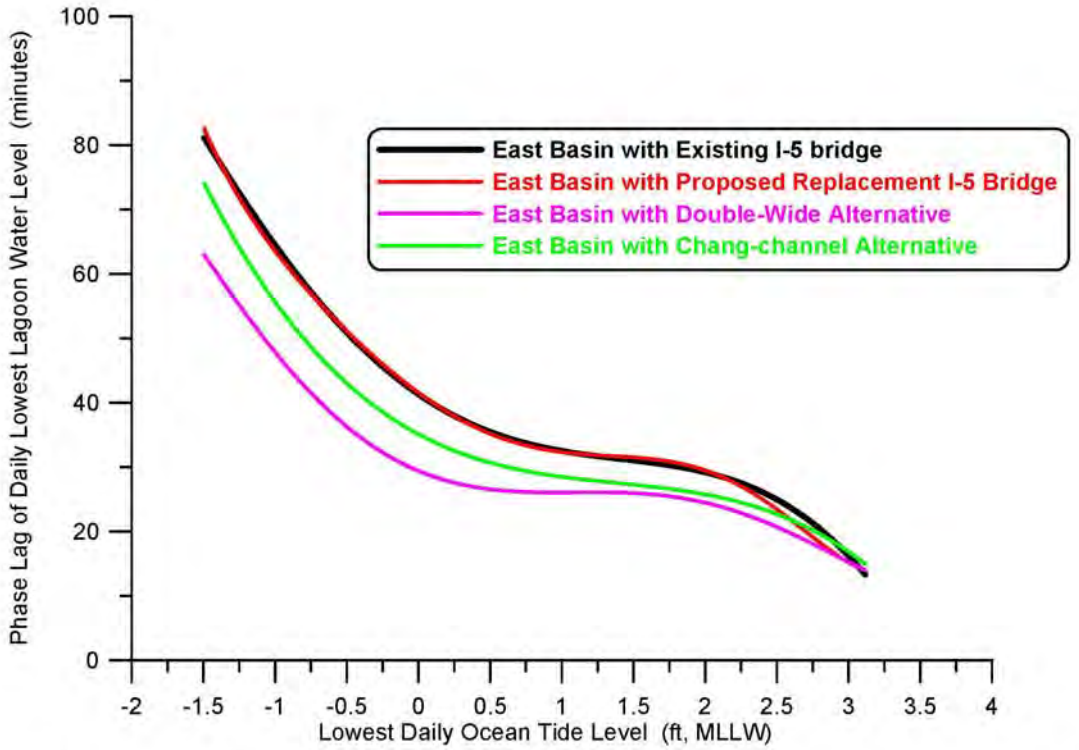

Figure 97. Comparison of the phase lag of lowest low water level in east basin of Agua Hedionda Lagoon for existing I-5 bridge (black), the proposed replacement I-5 bridge (red), the double-wide alternative (purple), versus the Chang-Channel (green). All shown as functions of daily lowest water level in the local ocean.

tides when the choke points at the inlet channel and railroad bridge retain ultimate hydraulic control for these small range tidal events.

Somewhat more complete conversion of velocity head into potential energy of water elevation is achieved by the 30% reductions in bridge waterway flow speeds and East Basin phase lags due to the Chang-channel waterway alternative, thereby modestly increasing the tidal range in the east basin of Agua Hedionda, although not to the extent achieved by the double-wide alternative. Table 5.6 gives a summary of the water level elevations calculated for Agua Hedionda Lagoon with the Chang-channel I-5 bridge alternative based on long-term tidal simulations using historic ocean water level forcing for the 2005-2008 period of record. Comparing Table 5.6 against existing conditions in Table 5.1, we find that both the mean and maximum diurnal tidal ranges in the East Basin are slightly increased with the Chang-channel alternative. MHHW in the East Basin has been raised to +6.10 ft MLLW with the Chang-channel alternative, while MLLW in the east basin has been lowered to +0.60 ft MLLW, producing a mean diurnal tidal range of 5.50 ft, an increase of 0.08 ft over existing conditions. While extreme high water levels

Table 5.6: Water Levels for Agua Hedionda Lagoon with Chang-channel Alternative, based on long term forcing for 2005-2008 period of record.

Elevations Feet MLLW	Ocean	East Basin with Chang-channel Alternative
MEAN HIGHER HIGH WATER (MHHW)	5.7	6.10
MEAN HIGH WATER (MHW)	5.0	5.39
MEAN LOW WATER (MLW)	1.3	1.66
MEAN LOWER LOW WATER (MLLW)	0.4	0.60
LOWEST OBSERVED WATER LEVEL (MLLW)	-1.5	-0.80
HIGHEST OBSERVED WATER LEVEL (MLLW)	7.4	7.6
MAXIMUM TIDAL RANGE	8.9	8.40

in the East Basin remain unchanged with the Chang-channel alternative, extreme low water levels are lowered to -0.80 ft MLLW, resulting in a maximum tidal range of 8.40 ft, an increase of 0.14 ft over existing conditions.

Hydroperiod function calculations for the East Basin with the Chang-channel alternative were calculated in Figure 98 from the 1980-2010 period of record of ocean tides from Scripps Pier tide and compared against existing conditions. Despite noticeable changes in the hydroperiod function with the Chang-channel alternative, those changes do not map into appreciable changes in habitat areas when factored against the stage area function in Figure 69. This is due to the fact that the preponderance of the East Basin habitat is sub-tidal, while the more significant changes in the hydroperiod function involve the intertidal habitat that comprises a relatively minor constituent. The mapping of habitat breaks from the hydroperiod function in Figure 98 into the stage area function in Figure 69 produces the habitat area distributions summarized in Table 5.7

Table 5.7 shows that the perpetual sub-tidal area of the East Basin decreases by 1.1 acres to 179.0 acres with the Chang-channel alternative, from 180.1 acres for the existing bridge while the mean sub-tidal area with the Chang-channel alternative decreases by 0.1 acres to 190.9 acres, from 191.0 acres for the existing bridge; frequently flooded mud flat

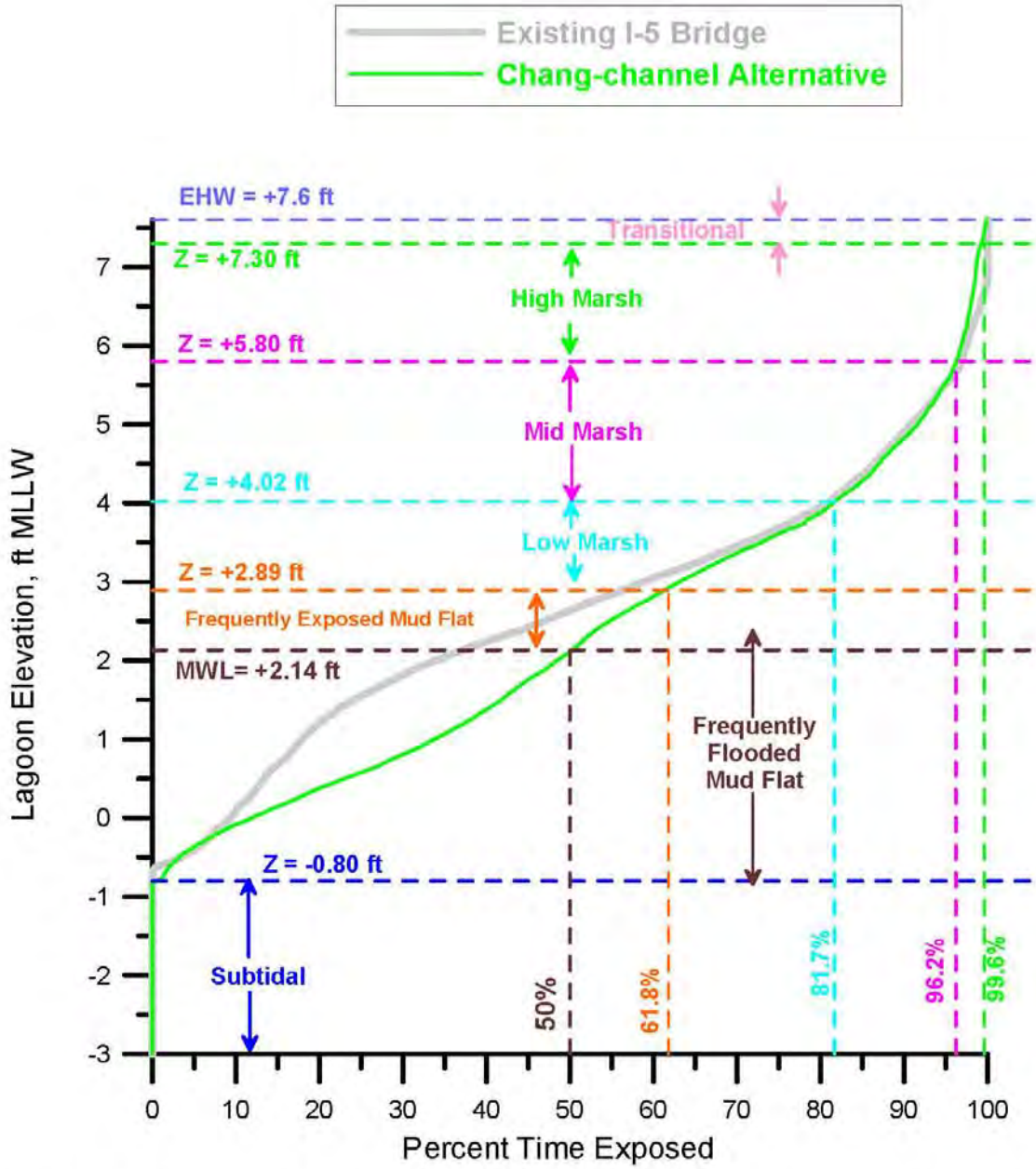

Figure 98. Hydroperiod function for the East Basin of Agua Hedionda Lagoon with existing I-5 bridge vs. Chang-channel alternative. Based on hydrodynamic simulation of East Basin water levels in response to tidal forcing from the Scripps Pier tide gage (NOAA # 941-0230). Habitat breaks based on habitat delineation from Josselyn and Whelchel (1999).

Table 5.7: East Basin Habitat Area Distribution from Agua Hedionda Hydroperiod and Stage Area Functions with Existing Bridge vs. Chang-channel Alternative

East Basin Habitat Areas	Existing I-5 Bridge	Chang-channel Alternative
Perpetual Sub-Tidal (acres)	180.1	179.0
Mean Sub-Tidal (acres)	191.0	190.9
Frequently Flooded Mud Flat (acres)	30.3	26.2
Frequently Exposed Mud Flat (acres)	4.3	7.4
Low Salt Marsh (acres)	11.5	13.1
Mid Salt Marsh (acres)	20.0	22.2
High Salt Marsh (acres)	11.7	16.0
Transitional Habitat (acres)	8.1	2.4
Maximum Intertidal Area (acres)	85.9	87.3
Maximum Area of Salt Water Inundation (acres)	266.0	266.3
Mean Intertidal Area (acres)	59.8	60.6
Mean Area of Salt Water Inundation (acres)	250.8	251.5

is decreased by 4.1 acres, from 30.3 acres for the existing bridge to 26.2 acres for the Chang-channel alternative; frequently exposed mud flat is increased by 3.1 acres, from 4.3 acres for the existing bridge to 7.4 acres for the Chang-channel alternative; low salt marsh is increased by 1.6 acres, from 11.5 acres for the existing bridge to 13.1 acres for the Chang-channel alternative; mid salt marsh is increased by 2.2 acres, from 20.0 acres for the existing bridge to 22.2 acres for the Chang-channel alternative; high salt marsh is increased proportionately the largest increment, by 4.3 acres, from 11.7 acres for the existing bridge to 16.0 acres for the Chang-channel alternative replacement bridge; much of the transitional habitat is converted into salt marsh habitat, reducing transitional habitat by 5.7 acres from 8.1 acres for the existing bridge to 2.4 acres for the Chang-channel alternative. Altogether, net habitat gains and conversions to higher quality intertidal habitats are meager with the Chang-channel alternative. Maximum intertidal habitat is increased by 1.4 acres to 87.3 acres with the Chang-channel alternative as compared to 85.9 acres for existing conditions; while the mean area experiencing tidal inundation up to MHHW is increased by only 0.7 acres from 250.8 acres for the existing bridge to 251.5

acres for the Chang-channel alternative resulting in an average 60.6 acres of intertidal habit, an increase of 0.8 acres over existing conditions.

Generally, Figure 98 and Table 5.7 indicate that the Chang-channel will result in the loss of 1.0 acres of new mud flats but increase the exposure time of existing mud flats; a bit of a wash in terms of net benefit to foraging birds. But, it will reduce the compression of present intertidal habitat to a certain degree by lowering the zonation of low mid and high marsh vegetation, although that habitat type makes up only a minor fraction of the existing East Basin habitat, 77% of which is sub-tidal based on mean ranges of tidal inundation. Of the 0.8 acres of intertidal area created on average by the Chang-channel alternative, 0.5 acres represents net wetland habitat gain. Again, the “iron-lung” effect that the power plant exerts on tidal ventilation of the East Basin makes it difficult to achieve substantial habitat gains or conversions through by removal of I-5 road bed fill as attempted with the Chang-channel alternative.

5.3.4) Tidal Hydraulics Impacts of the Proposed I-5 Bridge Replacement + Flow Fences: Here we evaluate potential remediation of tidal range muting in the east basin of Agua Hedionda Lagoon by retrofitting Stratford flow fencing as shown in blue in Figure 68a to the proposed replacement I-5 bridge design with its 70.1 m (230 feet) bridge span. The *flow fence* alternative (Figure 68a) would have negligible footprint over existing lagoon habitat as it is envisioned as being constructed from vertical inter-locking sheet pile members driven into the lagoon and existing bridge waterway along the blue contours shown in Figure 68a. It would be constructed in phases, with the sheet piles driven immediately after the removal of sections of the existing bridge and prior to the construction of the replacement sections. It has been sized to adapt to the + 4 ft MLLW contours of the existing channel under the I-5 bridge with a bed width of 113 ft (Figure 68b) comprised of rip rap at a depth of -19.22 ft MLLW (-21.52 ft NGVD) with sediment fill to a depth of -5 ft MLLW (-7.3 ft NGVD).

Figure 99 and 100 give flow trajectories and depth-averaged tidal currents in Agua Hedionda Lagoon with the *replacement bridge + flow fence* alternative for maximum flood and ebb flow during mean range tides. With its hydrodynamic efficient channel expansion sections, this alternative reduces velocities in the bridge waterway channel by about 0.1 ft/sec for both flood and ebb flow and also reduces the swirl in the flanking sections of the receiving basins. Both actions result in more complete recovery of velocity head in the channel into pressure and tidal elevation of the receiving basin. The flood flow entering the East Basin through the hard bottom expansion section of the channel and flow fence reaches a maximum of 0.6 m/sec (1.97 ft/sec) during maximum flood flow (Figure 99), down from 0.7 m/sec (2.3 ft sec) for the replacement bridge without the flow fence (Figure 83). In Figure 100, velocities of the ebb flow exiting the hard bottom expansion section form a very uniform jet into the Central Basin with maximum speeds of -0.6 m/sec (-1.97 ft/sec) with very little swirl, thereby reducing drag that would otherwise retard the ability of the East Basin to drain. Although the flow fence has cleaned up the structure of the tidal jets under the I-5 bridge, the velocities in those jets remain about 76% higher than what was achieved with the larger channel cross sections of the double–wide alternative, and about 20% higher than what was achieved with the Chang-channel alternative. With more velocity head to convert into pressure, the flow fence does not produce as much pressure and tidal elevation recovery in the receiving basins as the double–wide or Chang-channel alternatives.

Drag reduction and improved ebb flow structures achieved by the Stratford flow fence cross section in Figure 67 ultimately reduce the East Basin phase lag and thereby achieve more complete drainage of the East Basin during low tide. Figure 101 compares long

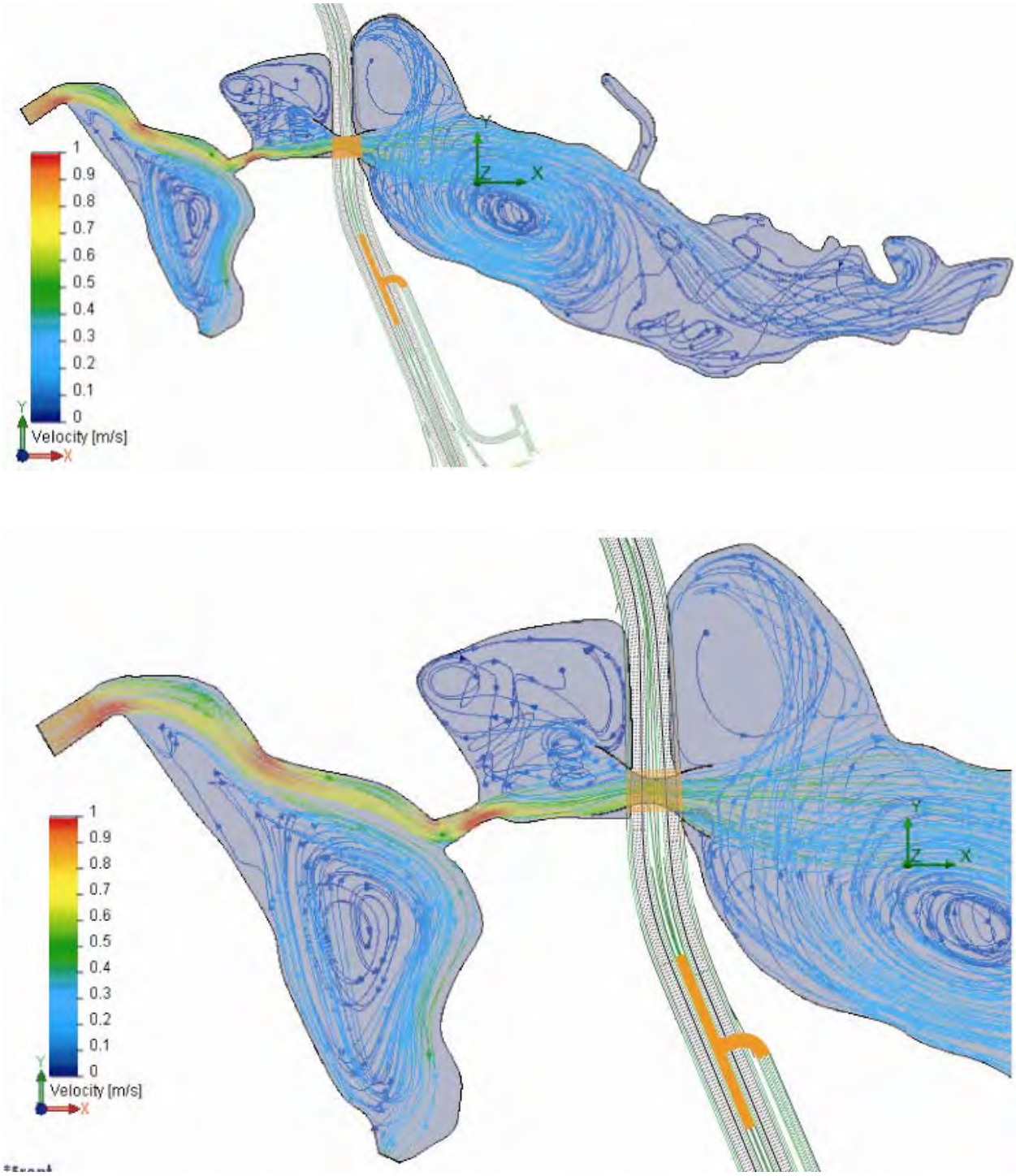

Figure 99: Hydrodynamic simulation of maximum flood flow during mean range tides at Agua Hedionda Lagoon with the proposed I-5 replacement bridge plus flow fences for the North Coast Corridor Project. Power Plant flow rate set at 304 mgd.

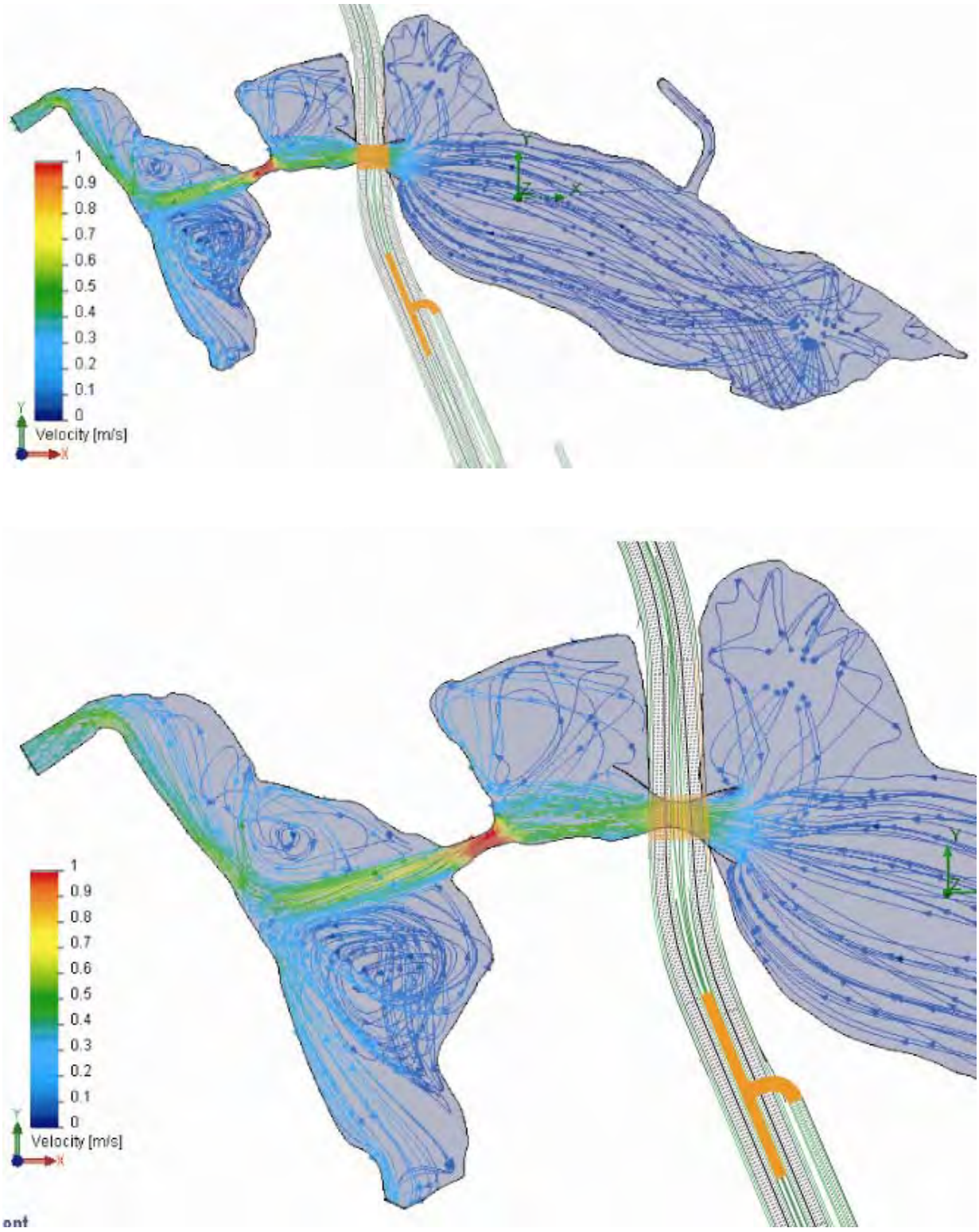

Figure 100: Hydrodynamic simulation of maximum ebb flow during mean range tides at Agua Hedionda Lagoon with the proposed I-5 replacement bridge plus flow fences for the North Coast Corridor Project. Power Plant flow rate set at 304 mgd.

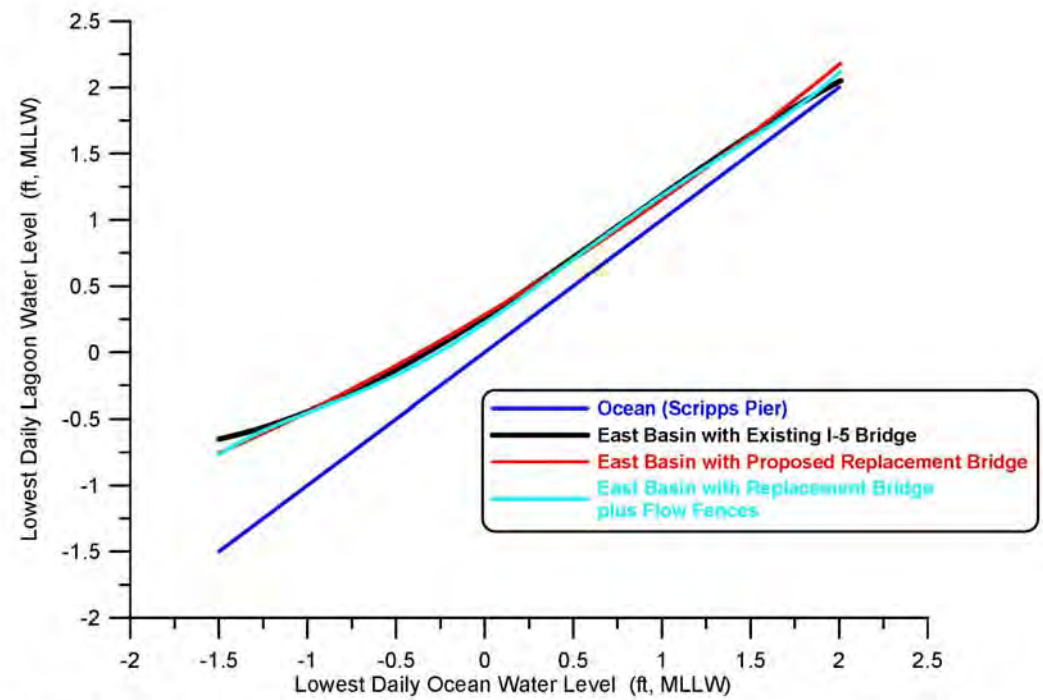

Figure 101. Comparison of daily lowest water level in east basin of Agua Hedionda Lagoon for existing I-5 bridge (black), the proposed replacement I-5 bridge (red) vs. the proposed replacement bridge with flow fence (cyan). All shown as functions of daily lowest water level at the Scripps Pier tide gage.

term simulations of the daily low water levels in the East Basin with the existing I-5 bridge (black), the proposed I-5 bridge (red) and the flow fence retrofit to the proposed I-5 bridge (cyan). The flow fence makes no change to the maximum daily lower low water level, remaining at η_{LLW} = 2.13 ft MLLW as for both the existing and replacement I-5 bridges. The flow fence reduces average daily lowest water levels to $\overline{\eta}_{LLW}$ = +0.62 ft MLLW from the existing average of $\overline{\eta}_{LLW}$ = +0.64 ft MLLW. The minimum daily low water level achieved by the flow fences is lowered to -0.79 ft MLLW, down from -0.65 ft MLLW for existing conditions and -0.78 ft for the replacement bridge, (cf. Table 5.1). Thus the flow fence in combination with the proposed replacement bridge is only able to achieve a very minor improvement of East Basin drainage.

East Basin phase lags are diminished by the addition of the Stratford flow fence to the proposed replacement bridge. Figure 102 shows that in long term simulation the maximum East basin phase lag is reduced from $\theta_{\max}$ = 80.1 minutes with the existing I-5 bridge to $\theta_{\max}$ = 75.4 minutes with the flow fences. Average East Basin

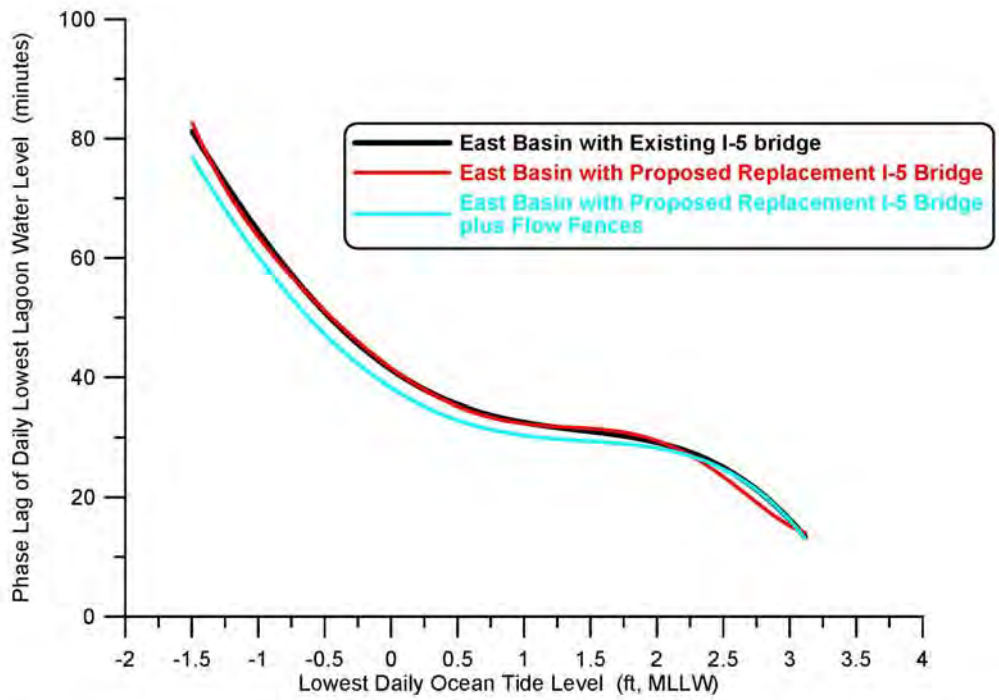

Figure 102. Comparison of phase lags in the east basin of Agua Hedionda Lagoon for existing I-5 bridge (black), the proposed replacement I-5 bridge (red) vs. the proposed replacement bridge with flow fence (cyan). All shown as functions of daily lowest water level at the Scripps Pier tide gage.

phase lags are reduced from $\overline{\theta}$ = 40.1 minutes with the existing I-5 bridge to $\overline{\theta}$ = 37.4 minutes with the the flow fences. The minimum phase lag for East Basin tides remains unchanged with the double-wide alternative at 15.3 minutes, as this minimum occurs during neap tides when the choke points at the inlet channel and railroad bridge retain ultimate hydraulic control for these small range tidal events.

The reductions in flow speeds and phase lags due to the flow fence waterway are not as significant as found with the double-wide and Chang-channel alternatives because the smaller channel cross section of the proposed replacement bridge still produces more velocity head that must ultimately be recovered into potential energy of water elevation. Consequently, the flow fence by itself, although a slight improvement on the proposed replacement bridge, can not achieve as much of the benefits of the double-wide or Chang-channel alternatives. This is apparent in Table 5.8, which gives a summary of the water level elevations calculated for Agua Hedionda Lagoon with the I-5 replacement bridge and flow fencing based on long-term tidal simulations using historic ocean water level forcing for the 2005-2008 period of record. Comparing Table 5.8 against existing conditions in Table 5.1, we find that both the mean and maximum diurnal tidal ranges in

Table 5.8: Water Levels for Agua Hedionda Lagoon with the proposed Replacement Bridge + Flow Fence, based on long term forcing for 2005-2008 period of record.

Elevations Feet MLLW	Ocean	Replacement Bridge + Flow Fence
MEAN HIGHER HIGH WATER (MHHW)	5.7	6.09
MEAN HIGH WATER (MHW)	5.0	5.39
MEAN LOW WATER (MLW)	1.3	1.67
MEAN LOWER LOW WATER (MLLW)	0.4	0.62
LOWEST OBSERVED WATER LEVEL (MLLW)	-1.5	-0.79
HIGHEST OBSERVED WATER LEVEL (MLLW)	7.4	7.6
MAXIMUM TIDAL RANGE	8.9	8.39

the East Basin are slightly increased with the flow fence waterway alternative. MHHW in the East Basin has been raised to +6.09 ft MLLW with the flow fence waterway, while MLLW in the east basin has been lowered to +0.62 ft MLLW, producing a mean diurnal tidal range of 5.47 ft, an increase of 0.05 ft over existing conditions. While extreme high water levels in the East Basin remain unchanged with the flow fence waterway, extreme low water levels are lowered to -0.79 ft MLLW, resulting in a maximum tidal range of 8.39 ft, an increase of 0.13 ft over existing conditions.

Hydroperiod function calculations for the East Basin with the flow fence waterway were calculated in Figure 103 from the 1980-2010 period of record of ocean tides from Scripps Pier tide and compared against existing conditions. Despite noticeable changes in the hydroperiod function with the flow fence waterway, those changes do not map into appreciable changes in habitat areas when factored against the stage area function in Figure 69. This is due to the fact that the preponderance of the East Basin habitat is sub-tidal, while the more significant changes in the hydroperiod function involve the intertidal habitat that comprises a relatively minor constituent. The mapping of habitat breaks from the hydroperiod function in Figure 103 into the stage area function in Figure 69 produces the habitat area distributions summarized in Table 5.9.

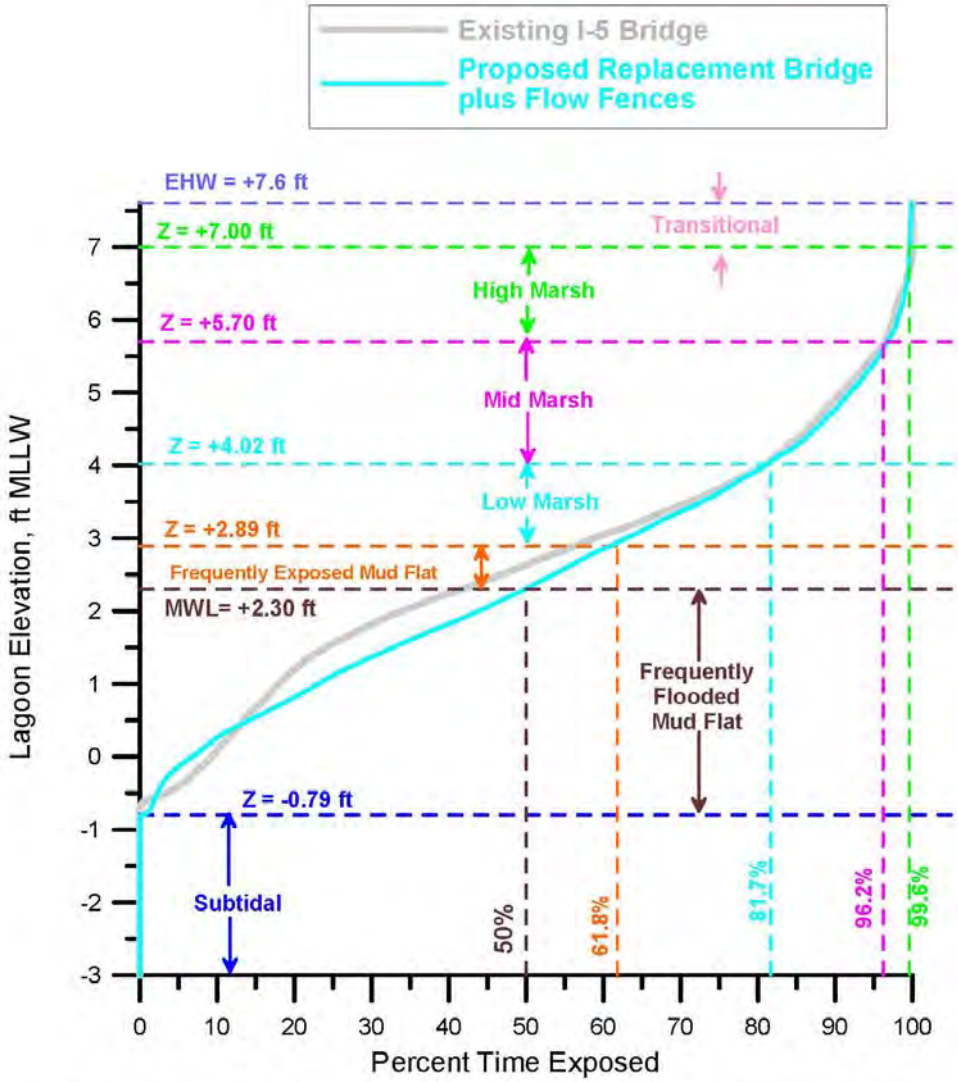

Figure 103. Hydroperiod function for the East Basin of Agua Hedionda Lagoon with existing I-5 bridge vs. proposed replacment bridge + flow fences. Based on hydrodynamic simulation of East Basin water levels in response to tidal forcing from the Scripps Pier tide gage (NOAA # 941-0230). Habitat breaks based on habitat delineation from Josselyn and Whelchel (1999).

Table 5.9: East Basin Habitat Area Distribution at Agua Hedionda Lagoon from Hydroperiod & Stage Area Functions for Existing Bridge vs. Proposed Replacement Bridge plus Flow Fences

East Basin Habitat Areas	Existing I-5 Bridge	Replacement Bridge + Flow Fences
Perpetual Sub-Tidal (acres)	180.1	178.9
Mean Sub-Tidal (acres)	191.0	190.8
Frequently Flooded Mud Flat (acres)	30.3	27.8
Frequently Exposed Mud Flat (acres)	4.3	5.7
Low Salt Marsh (acres)	11.5	13.1
Mid Salt Marsh (acres)	20.0	20.9
High Salt Marsh (acres)	11.7	14.5
Transitional Habitat (acres)	8.1	5.1
Maximum Intertidal Area (acres)	85.9	87.1
Maximum Area of Salt Water Inundation (acres)	266.0	266.0
Mean Intertidal Area (acres)	59.8	60.3
Mean Area of Salt Water Inundation (acres)	250.8	251.1

Table 5.9 shows that the perpetual sub-tidal area of the East Basin decreases by 1.2 acres to 178.9 acres with the double-wide alternative, from 180.1 acres for the existing bridge while the mean sub-tidal area with the flow fence waterway decreases by 1.3 acres to 190.8 acres, from 192.1 acres for the existing bridge; frequently flooded mud flat is decreased by 2.5 acres, from 30.3 acres for the existing bridge to 27.8 acres for the flow fence waterway retrofit; frequently exposed mud flat is increased by 1.4 acres, from 4.3 acres for the existing bridge to 5.7 acres for the flow fence waterway retrofit; low salt marsh is increased by 1.6 acres, from 11.5 acres for the existing bridge to 13.1 acres for the flow fence waterway retrofit; mid salt marsh is increased by 0.9 acres, from 20.0 acres for the existing bridge to 20.9 acres for the flow fence waterway retrofit; high salt marsh is increased by 2.8 acres, from 11.7 acres for the existing bridge to 14.5 acres for the flow fence waterway retrofit; some of the transitional habitat is converted into salt

marsh habitat, reducing transitional habitat by 3.0 acres from 8.1 acres for the existing bridge to 5.1 acres for the flow fence waterway retrofit. Altogether, net habitat gains and conversions to higher quality intertidal habitats are meager with the flow fence waterway retrofit. Maximum intertidal habitat is increased by 1.2 acres to 87.1 acres with the flow fence waterway retrofit as compared to 85.9 acres for existing conditions; while the mean area experiencing tidal inundation up to MHHW is increased by only 0.3 acres from 250.8 acres for the existing bridge to 251.1 acres for the flow fence waterway retrofit resulting in an average 60.3 acres of intertidal habit, an increase of 0.5 acres over existing conditions.

Generally, Figure 103 and Table 5.9 indicate that the flow fence retrofit will create small amounts of new East Basin habitat with small reduction of the compression of present intertidal habitat by lowering the zonation of low mid and high marsh vegetation. These benefits are modest by comparison to what was achieved by expanding the bridge waterway channel cross section with the double-wide or Chang-channel alternatives.

5.3.5) Tidal Hydraulics Impacts of the Chang-channel Alternative + Flow Fences: Here we evaluate potential remediation of tidal range muting in the east basin of Agua Hedionda Lagoon by retrofitting Stratford flow fencing as shown in red in Figure 68a to the Chang-channel I-5 bridge waterway with its 70.1 m (230 feet) bridge span. The Chang-channel + flow fences alternative (Figure 68a) would have negligible footprint over existing lagoon habitat as it is envisioned as being constructed from vertical inter-locking sheet pile members driven into the lagoon and existing bridge waterway along the red contours shown in Figure 68a. It would be constructed in phases, with the sheet piles driven immediately after the removal of sections of the existing bridge and prior to the construction of the replacement sections. It has been sized to adapt to the Chang-channel +4 ft MLLW contours under the I-5 bridge using a bed width of 156 ft comprised of rip rap at a depth of -19.22 ft MLLW (-21.52 ft NGVD) with sediment fill to a depth of -5 ft MLLW (-7.3 ft NGVD).

Figure 104 gives flow trajectories and depth-averaged tidal currents in Agua Hedionda Lagoon with the *Chang-channel + flow fences* alternative for maximum flood flow during mean range tides. With 80% more channel cross section than the existing bridge waterway in combination with an efficient flow fence expansion section for optimal pressure recovery, this alternative reduces the velocities of the flow exiting the hard bottom section of the channel from 0.7 m/s (2.3 ft/sec) for the existing bridge to 0.4 m/sec (1.3 ft/sec) during maximum flood flow. In Figure 105, velocities of the ebb flow exiting the hard bottom expansion section form a very uniform jet across the Central Basin, greatly reducing eddying in the Central Basin (cf. Figure 84), thereby reducing drag that would otherwise retard the ability of the East Basin to drain. Ebbing flow velocities exiting the hard bottom section of the channel are also reduced to 0.4 m/sec (1.3 ft/sec). While these flood and ebb velocities under the I-5 bridge are nearly comparable to the double-wide alternative, they remain less than the threshold of incipient motion of the resident East Basin and Central Basin sediments, and thereby insufficient to cause significant scour. These sub-scour threshold channel velocities are insufficient to maintain the scour holes that presently exist on either side of the I-5 bridge (Figure 18); and consequently these holes will in-fill over time, further reducing losses of tidal energy to form drag.

Eddy structures and jets in the East, Central and West Basins with the Chang-channel + flow fences alternative are similar to those for the double-wide channel but display less swirl in the tidal streams exiting the expansion section of the flow fence, resulting in nearly uniform streams across large expanses of the receiving basins. Maximum flood currents in the inlet channel reach 1.0 m/sec or (3.28 ft/sec) with the Chang-channel + flow fences alternative; while maximum ebb flow currents in the inlet channel are

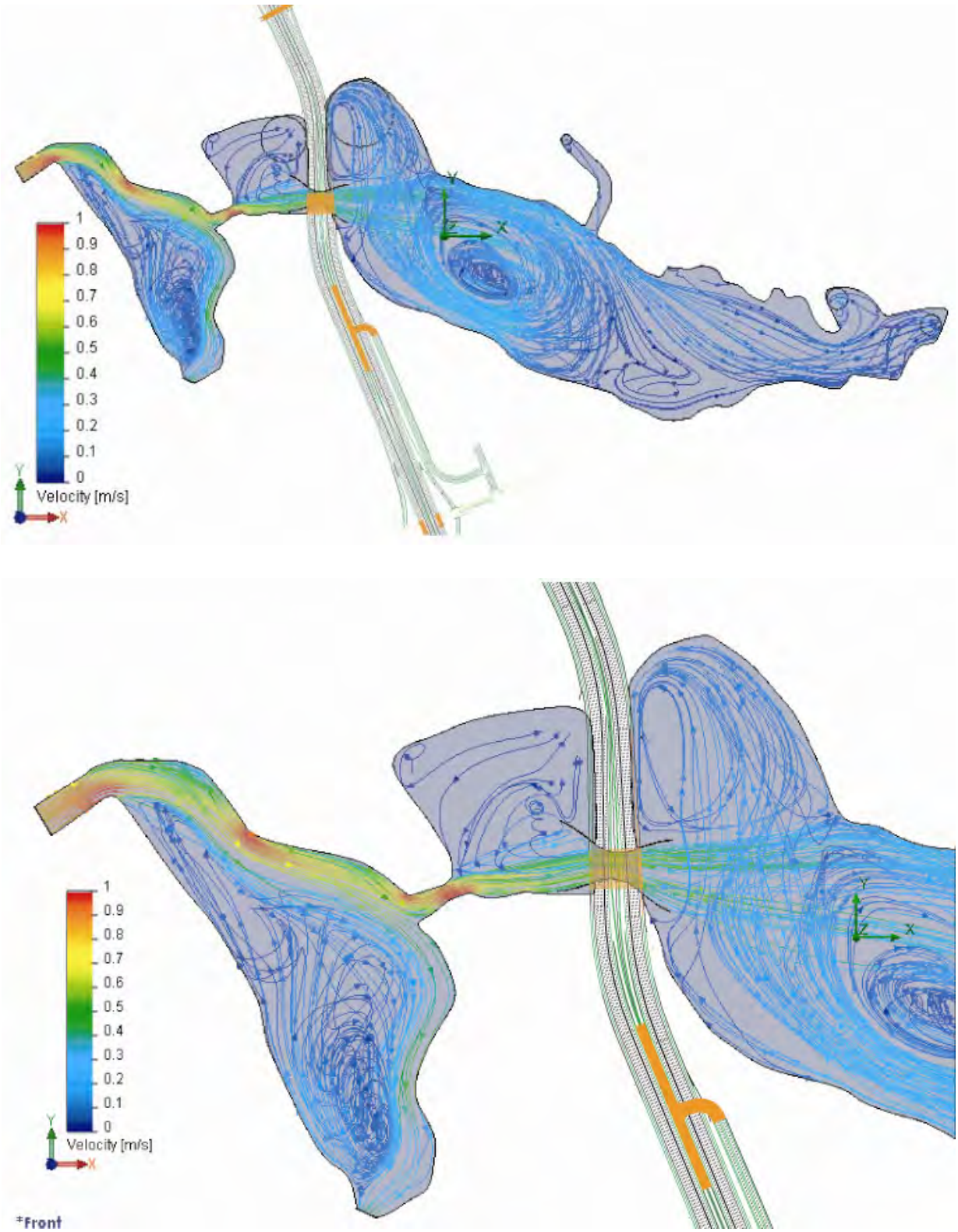

Figure 104: Hydrodynamic simulation of maximum flood flow during mean range tides at Agua Hedionda Lagoon with the *Chang-channel +flow fences* alternative for the replacement bridge of North Coast Corridor Project. Power plant flow rate set at 304 mgd.

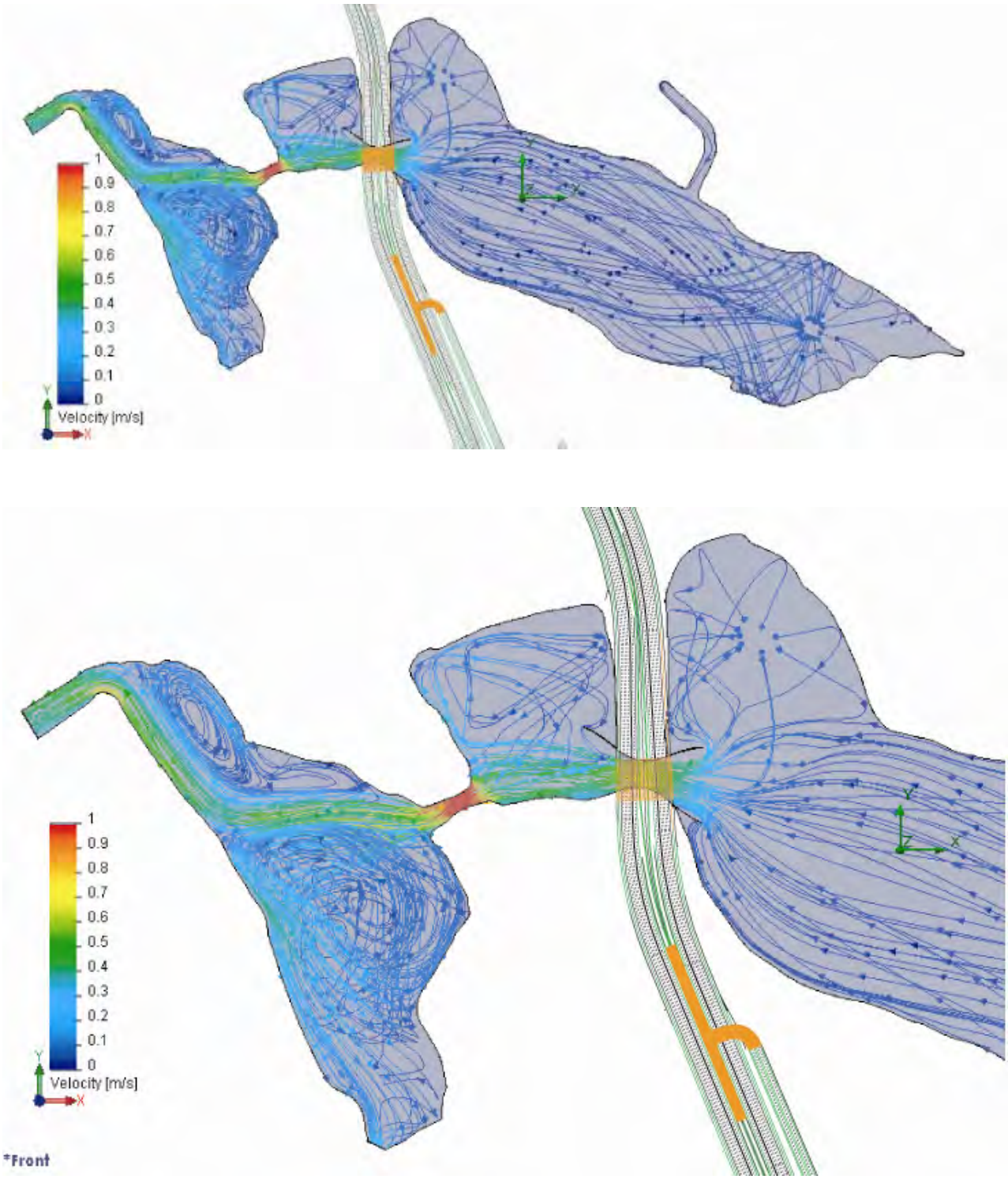

Figure 105: Hydrodynamic simulation of maximum flood flow during mean range tides at Agua Hedionda Lagoon with the *Chang-channel +flow fences* alternative for the replacement bridge of North Coast Corridor Project. Power plant flow rate set at 304 mgd.

0.63 m/sec (-2.07 ft/sec) comparable to the double-wide alternative, indicating a comparable volume of water is being tidally transported.

Eddy structures in the East Basin during flooding tide are better well-organized than with either the double-wide channel or existing channel. This is attributable to the swirl-free tidal stream exiting the expansion section of the flow fence, creating a boundary jet along the north bank of the East Basin during flooding tide that drives a system of counter rotating eddies throughout the East Basin. This stirring action should be beneficial to dissolved oxygen and nutrient distribution in the East Basin.

Drag reduction achieved by the Chang-channel + flow fence expansion section reduce the East Basin phase lag and thereby achieve more complete drainage of the East Basin during low tide. Figure 106 compares long term simulations of the daily low water levels in the East Basin with the existing I-5 bridge (black), the proposed I-5 bridge (red) and the proposed I-5 bridge + flow fences (cyan) and Chang-channel + flow fences (orange) and the Chang-channel in green. The Chang-channel + flow fences reduces average daily lowest water levels to $\overline{\eta}_{LLW}$ = +0.54 ft MLLW from the average for the existing bridge

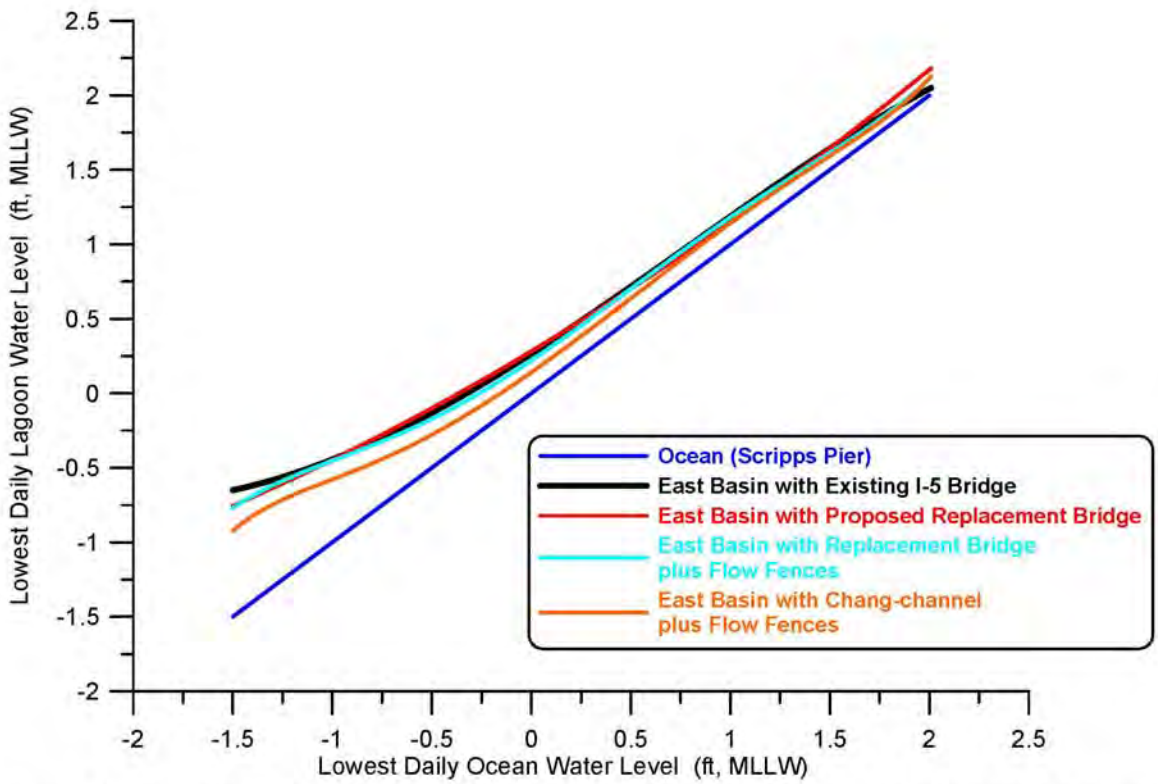

Figure 106. Comparison of daily lowest water level in east basin of Agua Hedionda Lagoon for existing I-5 bridge (black), the proposed replacement I-5 bridge (red), the proposed replacement bridge with flow fence (cyan) vs the Chang-channel + flow fences (orange). All shown as functions of daily lowest water level at the Scripps Pier tide gage.

of $\overline{\eta}_{LLW}$ = +0.64 ft MLLW. The minimum daily low water level achieved by the Chang-channel + flow fences is lowered to -0.93 ft MLLW, down from -0.65 ft MLLW for existing conditions (cf. Table 5.1). The maximum daily lower low water level with the Chang-channel + flow fences alternative remained unchanged from existing conditions, at η_{LLW} = +2.13 ft MLLW. As Figure 106 indicates, the incremental reduction in daily low water levels achieved for the East Basin by the Chang-channel + flow fences alternative are most significant at the lower-low end of the scale, and in any case, represent relatively modest improvements in ebb-tide drainage over existing conditions. Similarly, East Basin phase lags are modestly diminished with the Chang-channel + flow fences alternative. Figure 107 shows that in long term simulation the maximum East basin phase lag is reduced from $\theta_{\max}$ = 80.1 minutes with the existing I-5 bridge to $\theta_{\max}$ = 59.0 minutes with the Chang-channel + flow fences alternative. Average East Basin phase lags are reduced from $\overline{\theta}$ = 40.1 minutes with the existing I-5 bridge to $\overline{\theta}$ = 28.6 minutes with the Chang-channel + flow fences alternative. The minimum phase lag for East Basin tides remains unchanged with the double-wide alternative at 15.3 minutes, as

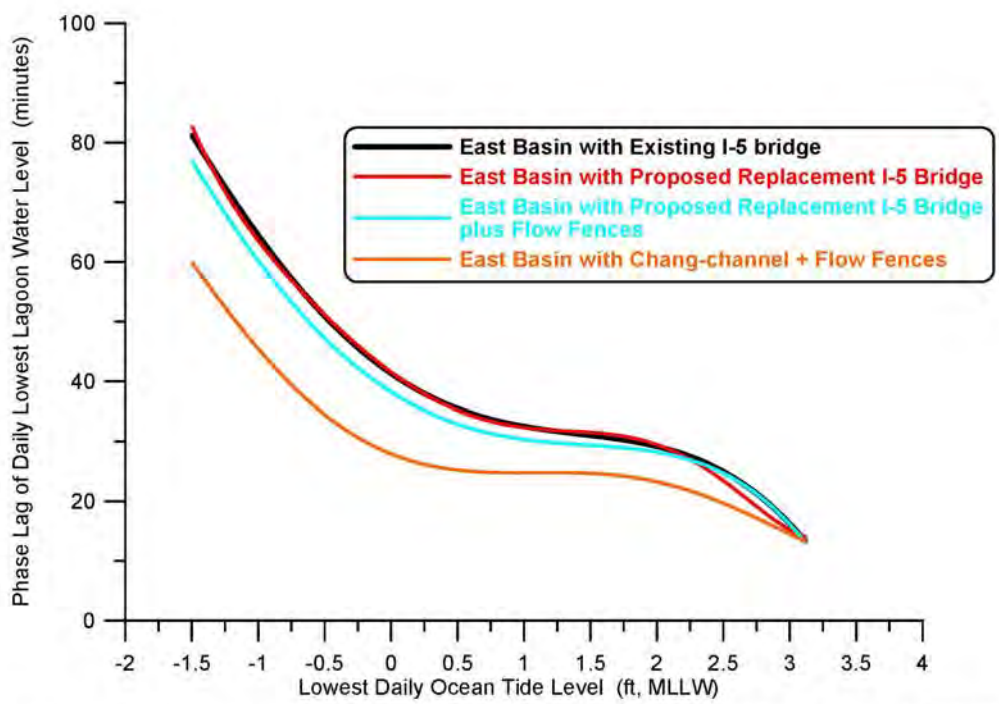

Figure 107. Comparison of daily phase lags in the east basin of Agua Hedionda Lagoon for existing I-5 bridge (black), the proposed replacement I-5 bridge (red), the proposed replacement bridge with flow fence (cyan) vs the Chang-channel + flow fences (orange). All shown as functions of daily lowest water level at the Scripps Pier tide gage.

this minimum occurs during neap tides when the choke points at the inlet channel and railroad bridge retain ultimate hydraulic control for these small range tidal events.

The reductions in flow speeds and phase lags due to the Chang-channel + flow fences alternative results in more complete conversion of velocity head into potential energy of water elevation, thereby increasing the tidal range in the east basin of Agua Hedionda Lagoon. Table 5.10 gives a summary of the water level elevations calculated for Agua Hedionda Lagoon with the Chang-channel + flow fences alternative based on long-term tidal simulations using historic ocean water level forcing for the 2005-2008 period of record. Comparing Table 5.10 against existing conditions in Table 5.1, we find that both the mean and maximum diurnal tidal ranges in the East Basin are slightly increased with the Chang-channel + flow fences alternative. MHHW in the East Basin has been raised to +6.12 ft MLLW with the double-wide alternative, while MLLW in the East Basin has been lowered to +0.54 ft MLLW, producing a mean diurnal tidal range of 5.58 ft, an increase of 0.16 ft over existing conditions. While extreme high water levels in the East Basin remain unchanged with the Chang-channel + flow fences alternative, extreme low water levels are lowered to -0.93 ft MLLW, resulting in a maximum tidal range of 8.53 ft, an increase of 0.27 ft over existing conditions.

Table 5.10: Water Levels for Agua Hedionda Lagoon with Chang-channel + Flow Fences Alternative, based on long term forcing for 2005-2008 period of record.

Elevations Feet MLLW	Ocean	East Basin with Chang-channel + Flow Fences Alternative
MEAN HIGHER HIGH WATER (MHHW)	5.7	6.12
MEAN HIGH WATER (MHW)	5.0	5.40
MEAN LOW WATER (MLW)	1.3	1.65
MEAN LOWER LOW WATER (MLLW)	0.4	0.54
LOWEST OBSERVED WATER LEVEL (MLLW)	-1.5	-0.93
HIGHEST OBSERVED WATER LEVEL (MLLW)	7.4	7.6
MAXIMUM TIDAL RANGE	8.9	8.53

The 1980-2010 period of record of ocean tides from Scripps Pier tide gage were fed into the calibrated TIDE_FEM model configured for the Chang-channel + flow fences alternative to give a long term output of East Basin water levels from which the hydroperiod function was calculated in Figure 108 (orange) and compared against existing conditions shown in gray. Despite noticeable changes in the hydroperiod function with the Chang-channel + flow fences alternative, those changes do not map into appreciable changes in habitat areas when factored against the stage area function in Figure 69. This is due to the fact that the preponderance of the East Basin habitat is sub-tidal, while the more significant changes in the hydroperiod function involve the intertidal habitat that comprises a relatively minor constituent. The mapping of habitat breaks from the hydroperiod function in Figure 108 into the stage area function in Figure 69 produces the habitat area distributions summarized in Table 5.11

Table 5.11 shows that the perpetual sub-tidal area of the East Basin decreases by 2.0 acres to 178.1 acres with the Chang-channel + flow fences alternative, from 180.1 acres for the existing bridge while the mean sub-tidal area with the Chang-channel + flow fences alternative decreases by 0.3 acres to 190.7 acres, from 191.0 acres for the existing bridge; frequently flooded mud flat is increased by 0.3 acres, from 30.3 acres for the existing bridge to 30.6 acres for the Chang-channel + flow fences alternative; frequently exposed mud flat is increased by 2.2 acres, from 4.3 acres for the existing bridge to 6.5 acres for the Chang-channel + flow fences alternative; low salt marsh is increased by 1.1 acres, from 11.5 acres for the existing bridge to 12.6 acres for the Chang-channel + flow fences alternative; mid salt marsh is increased by 0.3 acres, from 20.0 acres for the existing bridge to 20.3 acres for the Chang-channel + flow fences alternative; high salt marsh is increased proportionately the largest increment, by 3.4 acres, from 11.7 acres for the existing bridge to 15.1 acres for the Chang-channel + flow fences alternative; much of the transitional habitat is converted into salt marsh habitat, reducing transitional habitat by 4.9 acres from 8.1 acres for the existing bridge to 3.2 acres for the Chang-channel + flow fences alternative. Altogether, net habitat gains and conversions to higher quality intertidal habitats are meager with the Chang-channel + flow fences alternative. Maximum intertidal habitat is increased by 2.5 acres to 88.4 acres with the Chang-channel + flow fences alternative as compared to 85.9 acres for existing conditions; while the mean area experiencing tidal inundation up to MHHW is increased by only 1.2 acres from 250.8 acres for the existing bridge to 252.0 acres for the Chang-channel + flow fences alternative resulting in an average 61.3 acres of intertidal habit, an increase of 1.5 acres over existing conditions.

Generally, Figure 108 and Table 5.11 indicate that the Chang-channel + flow fences will create 2.5 acres of new mud flats and increase the exposure time of existing mud flats; a

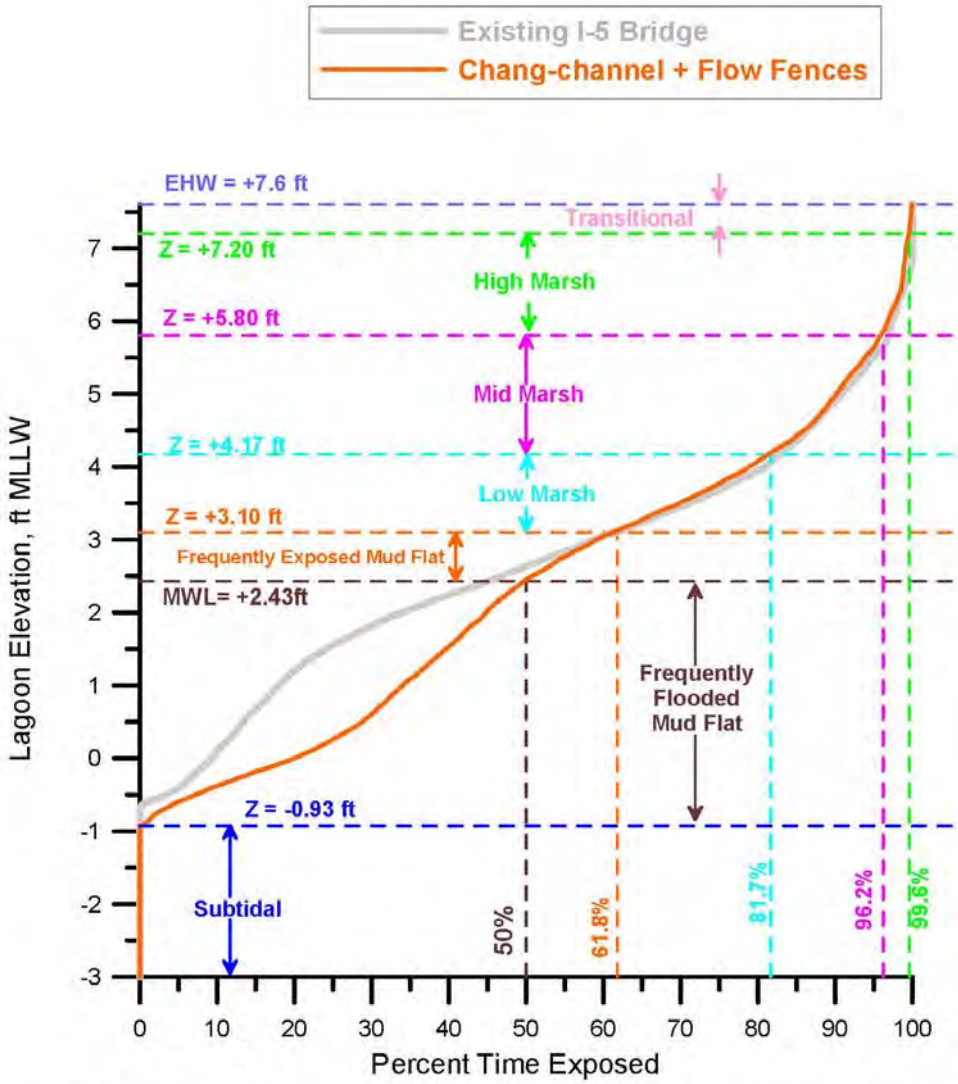

Figure 108. Hydroperiod function for the East Basin of Agua Hedionda Lagoon with existing I-5 bridge vs. Chang-channel + flow fences. Based on hydrodynamic simulation of East Basin water levels in response to tidal forcing from the Scripps Pier tide gage (NOAA # 941-0230). Habitat breaks based on habitat delineation from Josselyn and Whelchel (1999).

Table 5.11: East Basin Habitat Area Distribution from Agua Hedionda Hydroperiod and Stage Area Functions with Existing Bridge vs. Chang-channel + Flow Fences

East Basin Habitat Areas	Existing I-5 Bridge	Chang-channel + Flow Fences
Perpetual Sub-Tidal (acres)	180.1	178.1
Mean Sub-Tidal (acres)	191.0	190.7
Frequently Flooded Mud Flat (acres)	30.3	30.6
Frequently Exposed Mud Flat (acres)	4.3	6.5
Low Salt Marsh (acres)	11.5	12.6
Mid Salt Marsh (acres)	20.0	20.3
High Salt Marsh (acres)	11.7	15.1
Transitional Habitat (acres)	8.1	3.2
Maximum Intertidal Area (acres)	85.9	88.4
Maximum Area of Salt Water Inundation (acres)	266.0	266.5
Mean Intertidal Area (acres)	59.8	61.3
Mean Area of Salt Water Inundation (acres)	250.8	252.0

benefit to shorebird foraging and a feature of the East Basin. It will also reduce the compression of present intertidal habitat by lowering the zonation of low mid and high marsh vegetation, but that habitat type makes up only a minor fraction of the existing East Basin habitat, 77% of which is sub-tidal based on mean ranges of tidal inundation. Of the 1.5 acres of intertidal area created on average by the Chang-channel + flow fences alternative, 1.2 acres represents net wetland habitat gain. The “iron-lung” effect that the power plant exerts on lagoon tidal exchange, and the preponderance of East Basin area that is comprised of sub-tidal habitat, make substantial habitat gains or conversions through improved bridge designs difficult to attain, even one involving rather significant structural amendments to bridge under-works as the Chang-channel + flow fences alternative.

6.0) Sea level Rise Effects

In Section 2.1 we considered the envelope of variability in predicted sea level rise over the next century from six independent global climate models. The mean of these six predictions calls for 0.41 m (16 in) of sea level rise by 2100, while the most aggressive prediction calls for that amount of sea level rise by 2050. In this section, we will apply this predicted sea level rise to the tidal hydraulics model and resolve the potential effects on tidal exchange and habitat mix for both replacement bridges with existing bathymetric conditions and with the Chang Channel + flow fence I-5 bridge alternative. We chose the latter as it was found to be the most cost effective of the alternatives considered.

At the outset it would appear that sea level rise might have a favorable effect on tidal exchange, tidal prism, and area of salt water inundation within the wetland domains, as well as increase the percentage of sub-tidal habitat. However this intuition is based on an implicit assumption of rigid boundaries and stationary bathymetry, which certainly is not the case. Sea level rise will drown the beaches, reducing beach widths and making beach sands more mobile in the neighborhood of the ocean inlets. The latter will likely increase the influx of littoral sediment into the wetland systems because transport into these systems has be shown to be flood tide dominant owing to the fact that the majority portion of the tidal prism is above mean sea levels. We will not attempt to quantify beach impacts on the lagoon tidal hydraulics in the following analysis due to the numerous assumptions that must be made on future beach sand supplies in such an analysis. Instead we shall assume rigid boundaries and stationary bathymetry in the following analysis of impacts on lagoon tidal hydraulics due to predicted sea level rise as anticipated from Figure 1.

6.1) Sea level Rise Effects at Batiquitos Lagoon for Replacement Bridges: Here we evaluate sea level rise impacts on the tidal exchange of the East Basin of Batiquitos Lagoon with the proposed replacement I-5 bridge design in place. We will utilize the mean rise prediction of 0.41 m (1.33 ft) by 2100, which is the same as the most rapid rise prediction for 2050 (see Figure 1).

Figure 109 (upper panel) gives the flow trajectories and depth-averaged tidal currents computed by the calibrated TIDE_FEM model for the proposed replacement bridge during the mean range flooding tides with 0.41 m (16 inches) of sea level rise. Figure 109 (lower panel) shows fine scale flow details in the tidal channel near the proposed replacement I-5 bridge. The examples shown in Figure 109 use the existing hard bottom bridge waterway channel at -3 ft MLLW. Streamline patterns, flow trajectories and

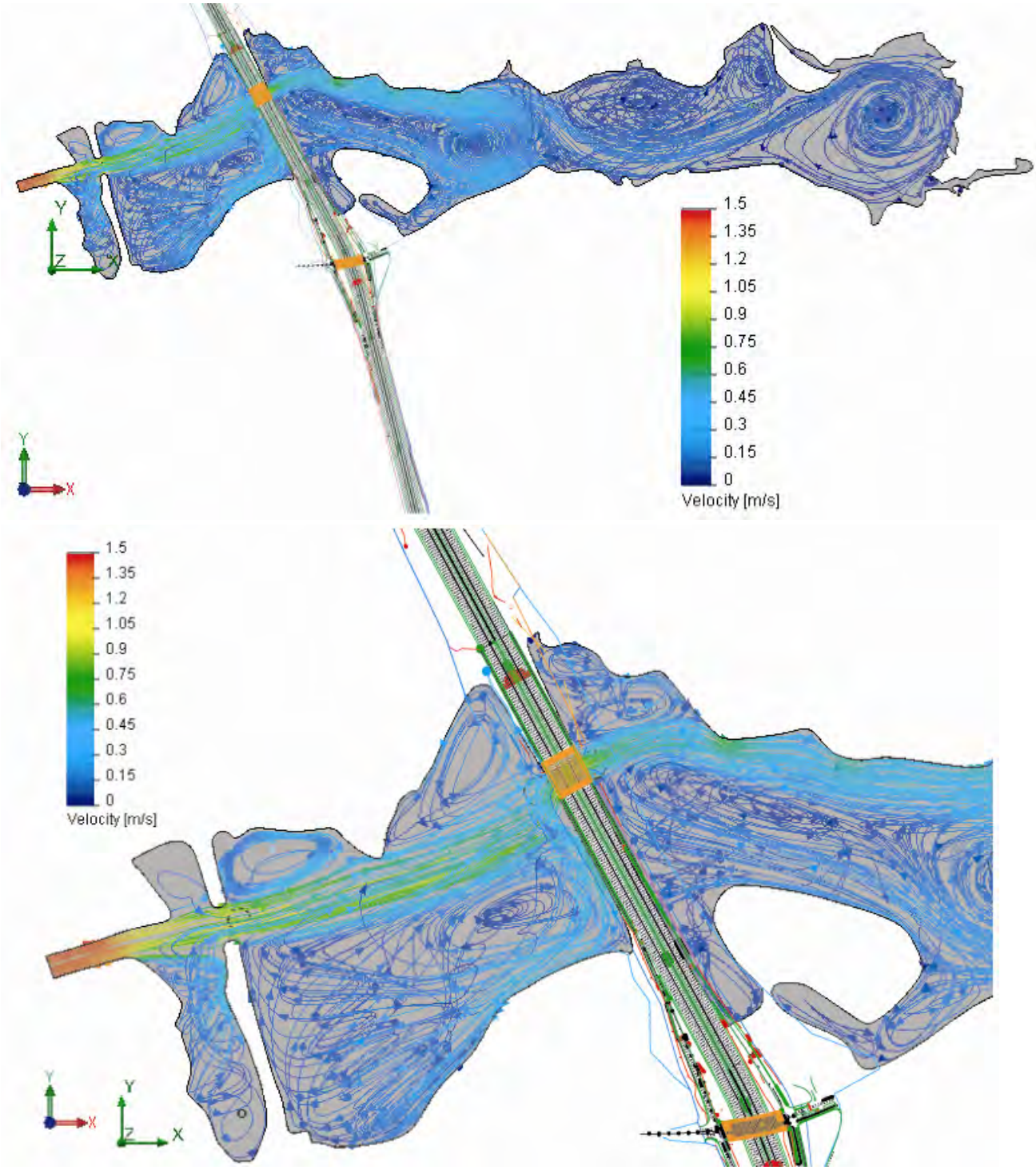

Figure 109: Hydrodynamic simulation of maximum flood flow during mean range tides at Batiquitos Lagoon superimposed on sea level rise with the proposed I-5 replacement bridge for the North Coast Corridor Project. Sea level rise set at 16 inches (1.33 ft) per the mean of six climate model prediction for 2100 (cf. Figure 1).

velocities are indistinguishable from those found for the narrower, present day I-5 bridge using the same amount of sea level rise. Note the significantly larger area of sea water inundation in Figure 109 as compared to the flood tide simulation in Figure 31 for present day sea levels. With both existing and replacement bridges, maximum flood currents in the inlet channel during future sea levels reach 1.35 m/sec (4.43 ft/sec), significantly greater than the 0.97 m/sec (3.18 ft/sec) inlet channel currents simulated in Figure 31 for present day sea level. The higher inlet channel currents in combination with the drowning of adjacent beaches during sea level rise will significantly increase sand influx rates into the West Basin, and accelerate the growth of the sand bars in the West and Central Basins (Figure 110). This in turn would raise the inlet sill and reduce the ability of the entire lagoon system to drain. However these sediment dynamics are merely inferred from the current speeds over existing bathymetry and are not explicitly resolved in the present modeling exercise which is based on rigid boundaries and stationary bathymetry.

In Figure 109, flood tide currents entering the lagoon form a well-defined jet through the West Basin and into the Central Basin at speeds of roughly 0.9 m/sec (2.95 ft/sec) as compared to 0.6 m/s (1.96 ft/sec) for the present day sea level simulation in Figure 31. These Central Basin current speeds during the sea level rise scenario are sufficient to transport beach sand in the 120-210 micron size regime through the Central Basin. The Central Basin flood tide jet in Figure 109 will likely scour an equilibrium channel through the north bank of the present Central Basin sand bar shown in Figure 110. Flood tide currents in Figure 109 accelerate to 1.05 m/sec (3.44 ft/sec) through the hardened channel under the both the existing and replacement I-5 bridge before diverging into a complex set of swirls and counter rotating eddies that populate the East Basin. Hence current speeds remain above the threshold of sediment motion from the ocean inlet all the way through to the East Basin. Consequently, littoral sands which form shoals and sand bars in the West and Central Basins under present sea levels (Figure 110) are likely to scour and move on into the East Basin under future sea level rise, forming East Basin sand bars that could shoal sufficiently to restrict tidal exchange in the East Basin. East Basin swirl and eddy speeds in Figure 109 are as high as 0.45 m/sec 1.47 ft/sec along the north bank in the western one-third of the East Basin under higher sea levels, sufficient to transport fine sand and cause scour and erosion of portions of the bottom of the East Basin. In contrast, these swirls under existing condition in Figure 31 are only 0.1 m/sec (0.3 ft/sec), and simply stir the East Basin water mass. Thus rapidly shoaling sand bars and localized scour and erosion are likely to occur under future high sea levels in all three basins of Batiquitos Lagoon with either the existing or proposed replacement bridges.

Figure 110: Flood tide shoals and sand bars in the West and Central Basins of Batiquitos Lagoon at present sea level, (from Merkel, 2008).

Figure 111 gives the hydroperiod function for the east basin of Batiquitos Lagoon at 0.41m (16 in) of sea level rise (the mean of these six predictions by 2100, cf. Figure 1) with the proposed replacement I-5 bridge. Elevations in Figure 111 are in terms of present day MLLW datum based on the 1983-2001 tidal epoch. This calculation is based on a linear superposition of the Scripps Pier 1980-2010 ocean water level measurements onto this predicted sea level rise; and on the relationships between habitat breaks and exposure used for San Dieguito Lagoon, as discussed in Section 3.3, Figure 17. Comparing the hydroperiod function in Figure 111 with that for existing conditions in Figure 30 indicates that future sea level rise could result in significant deepening of the sub-tidal zone (in the absence of hyper-sedimentation) by raising its upper limit to +2.23 ft MLLW, as well as significant vertical displacement of the mud flat and salt marsh habitat. When mapped onto the stage area function in Figure 23, sea level rise results in significant increases in tidally inundated areas. These increases are summarized in Table 6.1.

If sea level rises 0.41 m (1.33 ft.) above present eustatic sea level, then the minimum (perpetual) sub-tidal area of the East Basin with the replacement bridge in place will increase by 39.5 acres, to 131.4 acres versus 91.9 acres for the replacement bridge at present sea level; frequently flooded mud flat is increased by 10.8 acres, from 58.1 acres at present sea level to 68.9 acres for the replacement bridge at future sea level; frequently exposed mud flat is increased by 12.3 acres, from 9.6 acres for the replacement bridge at

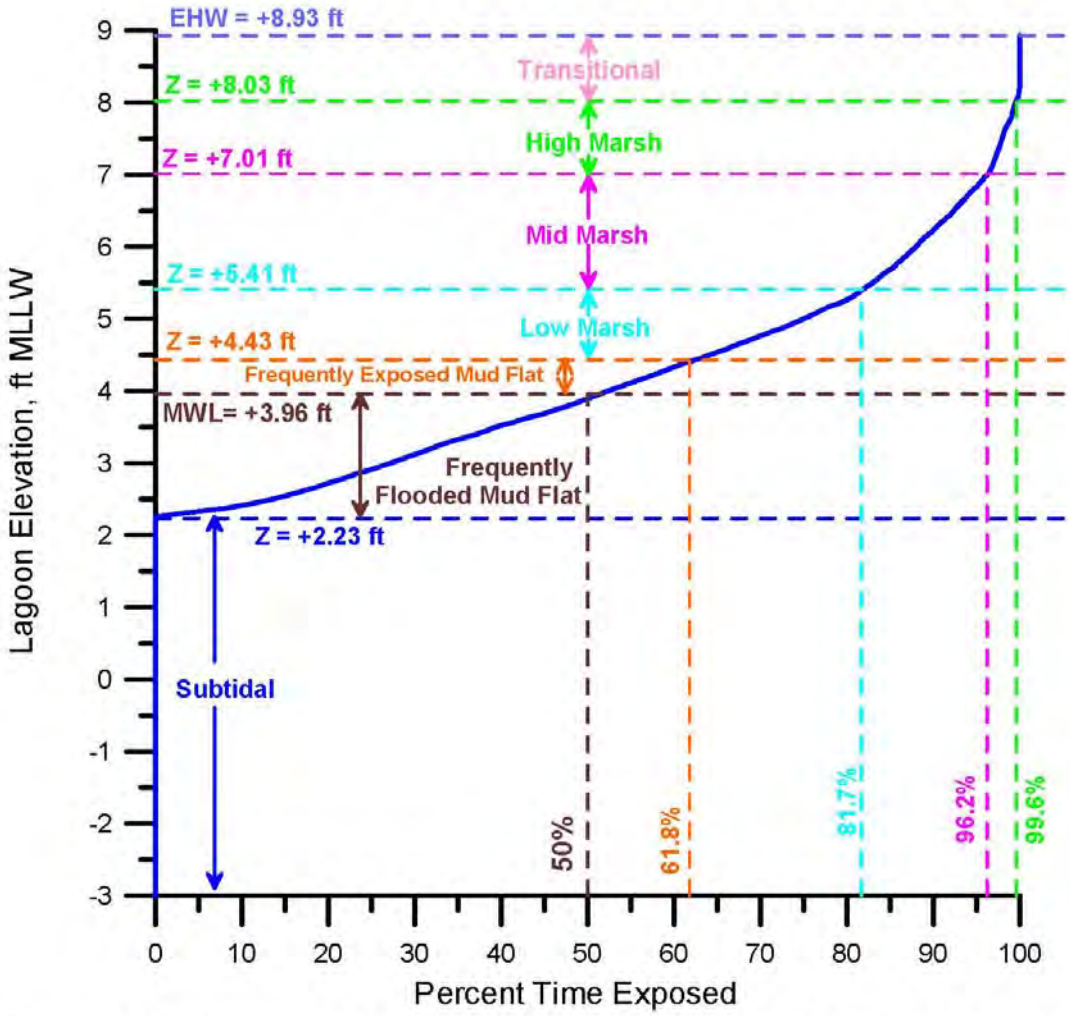

Figure 111. Hydroperiod function for the replacement I-5 bridge at Batiquitos Lagoon with 1.33 ft. of sea level rise over existing bathymetry. Based on hydrodynamic simulation of East Basin water levels in response to tidal forcing from the Scripps Pier tide gage (NOAA # 941-0230). Habitat breaks based on habitat delineation from Josselyn and Whelchel (1999). Elevations based on MLLW datum for the 1983-2001 tidal epoch.

Table 6.1: Batiquitos East Basin Habitat Area Distribution from Hydroperiod & Stage Area Functions with Existing Bridge vs. Proposed Replacement Bridge with +0.41 m (1.33 ft) Sea Level Rise

East Basin Habitat Areas	Existing I-5 Bridge Present Sea Level	Replacement I-5 Bridge Present Sea Level	Replacement I-5 Bridge Future Sea Level
Perpetual Sub-Tidal (acres)	91.3	91.9	131.4
Mean Sub-Tidal (acres)	111.3	111.3	157.3
Frequently Flooded Mud Flat (acres)	58.6	58.1	68.9
Frequently Exposed Mud Flat (acres)	13.6	9.6	21.9
Low Salt Marsh (acres)	42.3	50.9	47.6
Mid Salt Marsh (acres)	77.0	77.2	70.8
High Salt Marsh (acres)	45.8	41.0	26.9
Transitional Habitat (acres)	30.2	30.2	0.5
Maximum Intertidal Area (acres)	267.6	267.0	236.7
Maximum Area of Salt Water Inundation (acres)	358.9	358.9	368.1
Mean Intertidal Area (acres)	191.4	191.4	197.0
Mean Area of Salt Water Inundation (acres)	302.7	302.7	354.3

present sea level to 21.9 acres at future sea level;. However, low salt marsh is reduced by 3.3 acres, from 50.9 acres for the replacement bridge at present sea level to 47.6 acres at future sea level; mid salt marsh is also reduced by 6.4 acres at future sea level, from 77.2 acres for the replacement bridge at present sea level to 70.8 acres at future sea level; similarly, high salt marsh is reduced by 14.1 acres, from 41.0 acres for the replacement bridge at present sea level to 26.9 acres at future sea level; and, transitional habitat is significantly reduced by 29.7 acres at future sea level, from 30.2 acres for the replacement bridge at present sea level to only 0.5 acres at future sea level. Despite the

0.41 m (1.33 ft.) increase in elevations of salt water inundation at future sea levels, the maximum area inundated by salt water at extreme high water is increased by only 9.2 acres, from 358.9 acres for the replacement bridge at present sea level to 368.1 acres at future sea level. While the sub-tidal and mud flat habitats increase significantly at future sea levels, maximum the intertidal habitat is reduced by 30.3 acres, from 267.0 acres for the replacement bridge at present sea level to 236.7 acres at future sea level with the replacement bridge. The mean area experiencing tidal inundation up to MHHW at future sea level is substantially increased by 51.6 acres to 354.3 acres from 302.7 acres at present sea level with the replacement bridge; but again this increase is primarily sub-tidal in nature as the mean intertidal habit increases by only 5.6 acres to 197.0 with replacement bridge at future sea level versus 191.4 acres at present sea levels. The increase in mean sub-tidal area at future sea level is 46 acres, from 111.3 acres at present sea level to 157.3 acres at future sea level.

6.2) Sea level Rise Effects at Batiquitos Lagoon for Chang-channel + Flow Fences

Next we evaluate sea level rise impacts on the tidal exchange of the East Basin of Batiquitos Lagoon with the Chang-channel + flow fences alternative adapted to the proposed replacement I-5 bridge per Figure 20 a & 20c. Again, we will utilize the mean rise prediction of 0.41 m (1.33 ft) by 2100, which is equivalent to the most rapid rise prediction for 2050 per Figure 1.

Figure 112 (upper panel) gives the flow trajectories and depth-averaged tidal currents computed by the calibrated TIDE_FEM model for the Chang-channel + flow fences alternative during the mean range flooding tides superimposed on 0.41 m (16 inches) of sea level rise. Figure 112 (lower panel) shows fine scale flow details through the convergence and expansion sections of the flow fences. With 80% more channel cross section than the proposed replacement bridge waterway, this alternative reduces the velocities of the flow exiting the hard bottom section of the channel to 0.6 m/sec (1.96 ft/sec) during flood flow, as compared to 1.05 m/sec (3.44 ft/sec) for the proposed replacement bridge in Figure 109. While flood flow velocities during these mean range tides at higher sea levels are reduced by the Chang-channel & flow fence structures in Figure 112, they remain greater than the spring tide velocities at present sea level in Figure 60 that were in the range of 0.4 m/sec (1.31 ft/sec). Thus, the Chang-channel & flow fence structures can not prevent flood flows at higher sea levels from exceeding the threshold of incipient motion of the local relict San Marcos Creek sediments; and

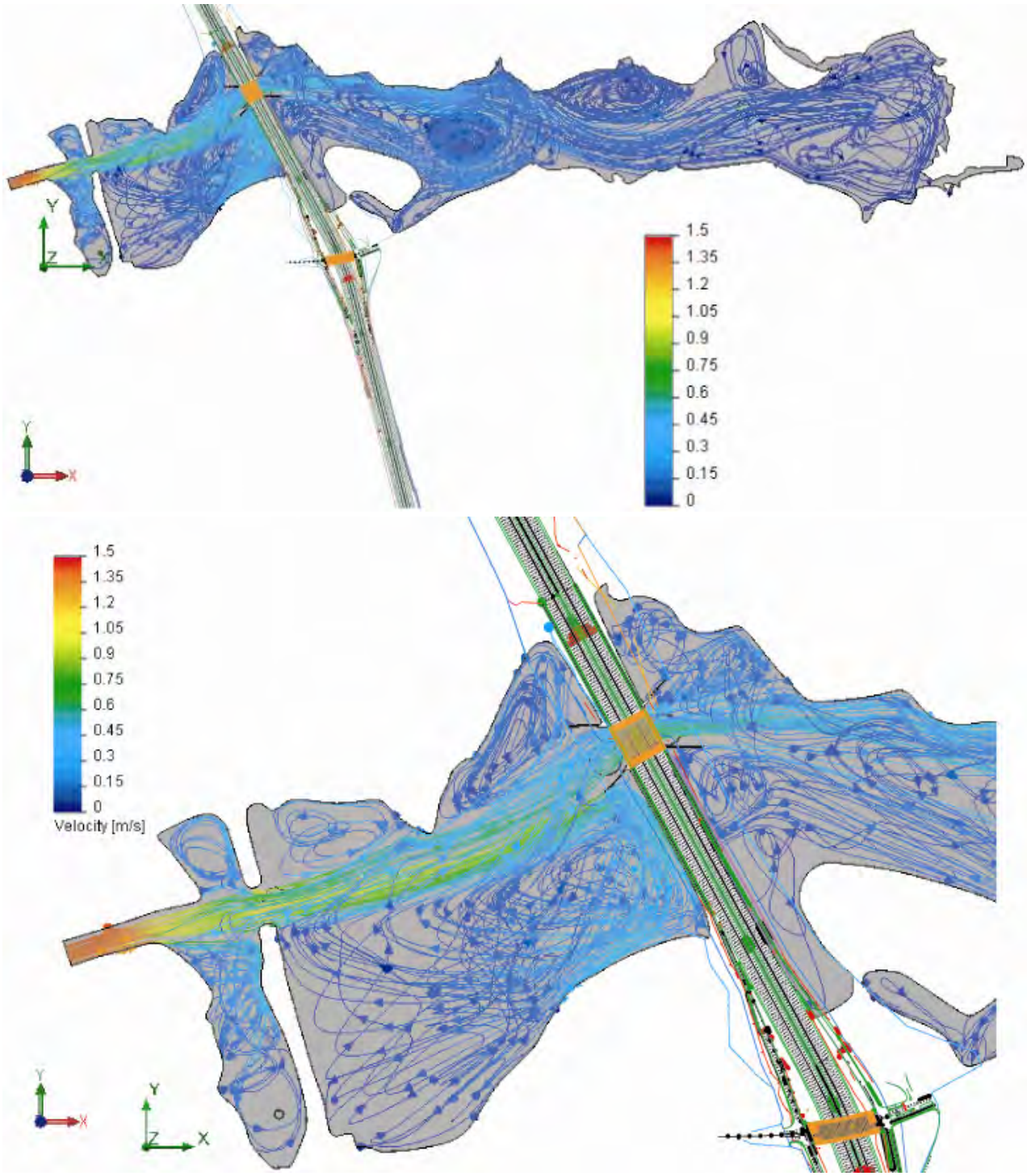

Figure 112: Hydrodynamic simulation of maximum flood flow during mean range tides at Batiquitos Lagoon superimposed on sea level rise with the Chang-channel + flow fences replacement bridge alternative for the North Coast Corridor Project. Sea level rise set at 16 inches (1.33 ft) per the mean of six climate model prediction for 2100 (cf. Figure1).

consequently scour and transport of sediment through the Chang-channel and flow fences will continue into the East Basin and induce progressive shoaling there over time.

Eddy structures and jets in the East, Central and West Basins with the Chang-channel + flow fences (Figure 112) are similar to those for the replacement bridges at higher sea levels in Figure 109. Maximum flood currents in the inlet channel in Figure 112 reach 1.4 m/sec or (4.59 ft/sec) as compared to 1.35 m/sec (4.43 ft/sec) for the replacement bridge at higher sea level (Figure 109), indicating the higher efficiency of the Chang-channel + flow fences allows for larger flow volumes into the tidal system. In Figure 112, flood tide currents entering the lagoon form a well defined jet through the West Basin and into the Central Basin having the same structure as found for the high sea level flow patterns with the replacement bridge in Figure 109, with speeds of roughly 0.9 m/sec (2.95 ft/sec) as compared to 0.6 m/s (1.96 ft/sec) for the present day sea level simulation in Figure 31. The Central Basin jet cuts across the north bank of the large sand bar shown in Figure 110 with sufficient speed during the sea level rise scenario to scour a channel that directly feeds the convergence section of the flow fence in Figure 112. Because speeds remain above the threshold of sediment motion the entire distance from the ocean inlet all the way through to the East Basin in Figure 112, the Chang-channel + flow fences alternative will not prevent littoral sand bars from forming in the East Basin under higher sea level conditions that could shoal sufficiently to restrict tidal exchange in the East Basin. East Basin swirl and eddy speeds in Figure 112 are a bit less with the Chang-channel + flow fences alternative, on the order of 0.3 m/sec (0.98 ft/sec) along the north bank in the western one-third of the East Basin under higher sea levels, but still sufficient to transport fine sand or silt and cause scour and erosion of portions of the sand/silt bottom of the East Basin. Thus rapidly shoaling sand bars and localized scour and erosion are likely to occur under future high sea levels in all three basins of Batiquitos Lagoon with either the proposed replacement bridges or with the Chang-channel + flow fences alternative.

When the Chang-channel + flow fences alternative is overlaid on a linear superposition of the Scripps Pier 1980-2010 ocean water level measurements and the predicted sea level rise 0.41m (16 in), we get the hydroperiod function for the east basin of Batiquitos Lagoon shown in Figure 113. Elevations in Figure 113 are in terms of present day MLLW datum based on the 1983-2001 tidal epoch. Comparing the hydroperiod function in Figure 113 with that for the replacement bridge in Figure 111 reveals the Chang-channel + flow fences alternative promotes less raising of sub-tidal zone and less compression of the intertidal zone under future sea level rise than would result with the proposed replacement bridge. With the Chang-channel + flow fences alternative the sub-tidal zone has an upper limit of +1.48 ft MLLW, 0.75 ft less super elevation than found

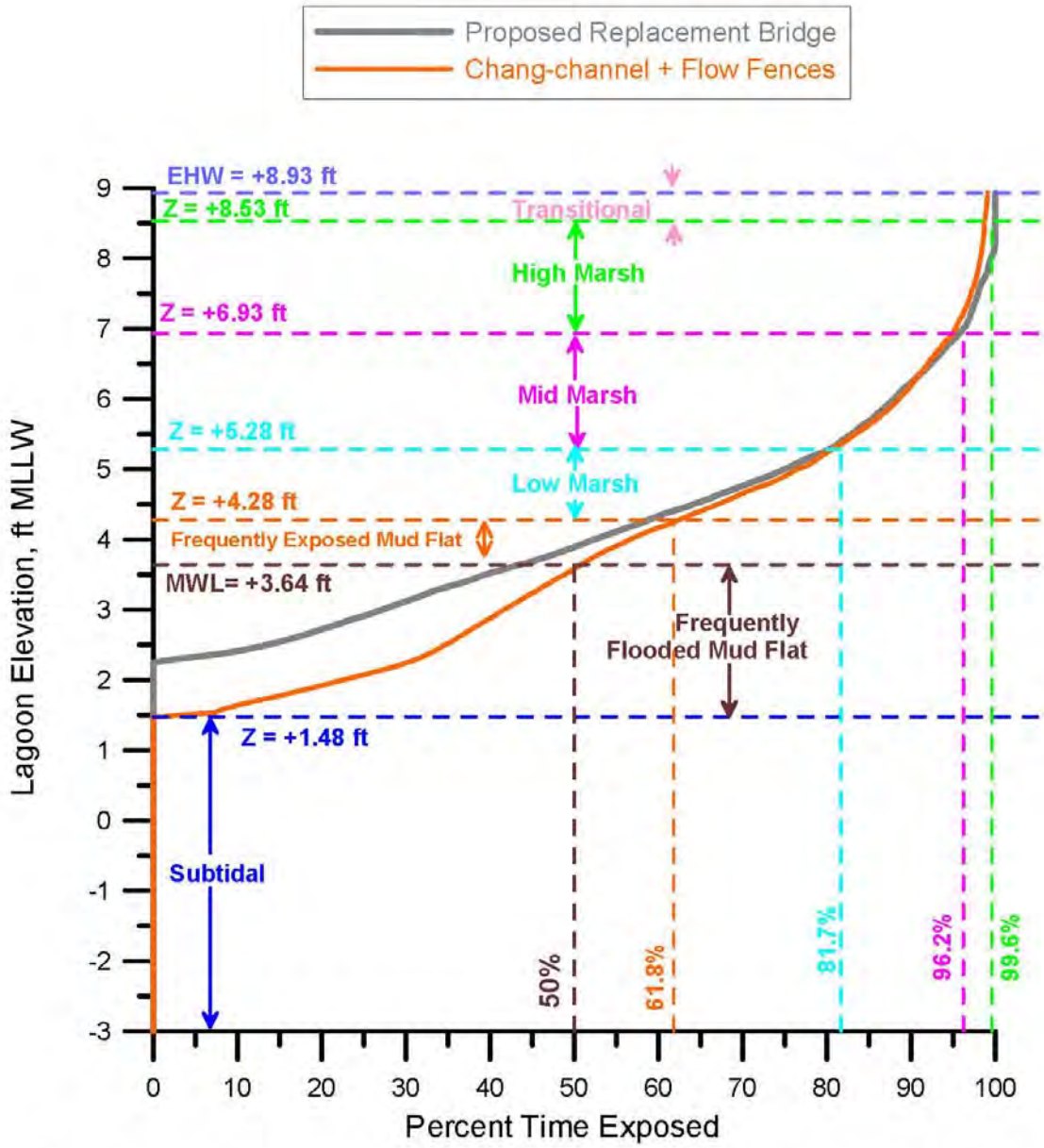

Figure 113. Hydroperiod function for the Chang-channel + flow fences alternative at Batiquitos Lagoon with 1.33 ft. of sea level rise over existing bathymetry. Based on hydrodynamic simulation of East Basin water levels in response to tidal forcing from the Scripps Pier tide gage (NOAA # 941-0230). Habitat breaks based on habitat delineation from Josselyn and Whelchel (1999). Elevations based on MLLW datum for the 1983-2001 tidal epoch.

Table 6.2: Batiquitos East Basin Habitat Area Distribution from Hydroperiod & Stage Area Functions with Proposed Replacement Bridge vs Chang-channel + flow fences alternative with +0.41 m (1.33 ft) of Sea Level Rise

East Basin Habitat Areas	Replacement I-5 Bridge Present Sea Level	Replacement I-5 Bridge Future Sea Level	Chang-channel+flow fences Future Sea Level
Perpetual Sub-Tidal (acres)	91.9	131.4	108.2
Mean Sub-Tidal (acres)	111.3	157.3	137.2
Frequently Flooded Mud Flat (acres)	58.1	68.9	78.4
Frequently Exposed Mud Flat (acres)	9.6	21.9	29.0
Low Salt Marsh (acres)	50.9	47.6	48.3
Mid Salt Marsh (acres)	77.2	70.8	74.2
High Salt Marsh (acres)	41.0	26.9	30.2
Transitional Habitat (acres)	30.2	0.5	0.3
Maximum Intertidal Area (acres)	267.0	236.7	263.8
Maximum Area of Salt Water Inundation (acres)	358.9	368.1	368.6
Mean Intertidal Area (acres)	191.4	197.0	219.8
Mean Area of Salt Water Inundation (acres)	302.7	354.3	357.0

for the replacement bridge in Figure 111, allowing an equivalent vertical expansion in the mud flat and salt marsh habitat. When mapped onto the stage area function in Figure 23, tides and sea level rise result in the habitat distributions summarized in Table 6.2 and net changes in habitat distributions are summarized in Table 6.3

Inspection of Table 6.2 reveals that even at higher sea levels, the Chang-channel + flow fences alternative delivers benefits over the replacement bridges in terms of East Basin habitat gains and diversity. Table 6.2 shows that the perpetual sub-tidal area of the East Basin at higher sea level decreases by 23.2 acres to 108.2 acres with the Chang-channel +

Table 6.3: Net Change in East Basin Habitat Area Distributions in Batiquitos Lagoon due to 1.33 ft of Sea Level Rise. Results Calculated from Hydroperiod & Stage Area Functions with Proposed Replacement Bridge vs Chang-channel + Flow Fences alternative

East Basin Habitat Areas	Net Change in Habitat Distribution Replacement I-5 Bridge Future Sea Level vs. Replacement I-5 Bridge Present Sea Level	Net Change in Habitat Distribution Chang-channel + Flow Fences Future Sea Level vs. Replacement I-5 Bridge Present Sea Level	Net Change in Habitat Distribution Chang-channel + Flow Fences Future Sea Level vs. Replacement I-5 Bridge Future Sea Level
Perpetual Sub-Tidal (acres)	+39.5	+16.3	-23.2
Mean Sub-Tidal (acres)	+46.0	+25.9	-20.1
Frequently Flooded Mud Flat (acres)	+10.8	+20.3	+9.5
Frequently Exposed Mud Flat (acres)	+12.3	+19.4	+7.1
Low Salt Marsh (acres)	-3.3	-2.6	+0.7
Mid Salt Marsh (acres)	-6.4	-3.0	+3.4
High Salt Marsh (acres)	-14.1	-10.8	+3.3
Transitional Habitat (acres)	-29.7	-29.9	-0.2
Maximum Intertidal Area (acres)	-30.3	-3.2	+27.1
Maximum Area of Salt Water Inundation (acres)	+9.2	+9.7	0.5
Mean Intertidal Area (acres)	+5.6	+28.4	+22.8
Mean Area of Salt Water Inundation (acres)	+51.6	+54.3	+2.7

flow fences alternative, from 131 acres for the replacement bridge, but still 15.8 acres more sub-tidal habitat than for present sea level. The mean sub-tidal area with the Chang-channel + flow fences alternative decreases by 20.1 acres to 137.2 acres, from 157.3 acres for the replacement bridge; but still 25.9 acres more of sub-tidal habitat on average than for present sea level. Frequently flooded mud flat is increased by 9.5 acres, from 68.9 acres for the replacement bridge at future sea level to 78.4 acres for the Chang-channel + flow fences alternative, 20.3 acres more than for present sea level. Frequently exposed mud flat is increased by 7.1 acres, from 21.9 acres for the replacement bridge at future sea level to 29.0 acres for the Chang-channel + flow fences alternative and 19.4 acres more than for present sea level. Low salt marsh changes only slightly, from 47.6 acres for the replacement bridge at future sea level to 48.3 acres for the Chang-channel + flow fences alternative but 2.6 acres less than for present sea level. Mid salt marsh is increased by 3.4 acres, from 70.8 acres for the replacement bridge at future sea level to 74.2 acres for the Chang-channel + flow fences alternative, but 3.0 acres less than for present sea level. High salt marsh is increased by 3.3 acres, from 26.9 acres for the replacement bridge at future sea level to 30.2 acres for the Chang-channel + flow fences alternative but 10.8 acres less than for present sea level. A fraction of the transitional habitat is converted into high salt marsh, reducing transitional habitat by 0.2 acres from 0.5 acres for the replacement bridge at future sea level to 0.3 acres for the Chang-channel + flow fences alternative. In either case there is little transitional habitat at higher sea levels because the upper limits of salt water inundation have nearly reached the day light contour of the upper limit of grading during the restoration project. Maximum intertidal habitat is increased by 27.1 acres to 263.8 acres with the Chang-channel + flow fences alternative as compared to 236.7 acres for the replacement bridge at future sea level and 267.0 acres for the present sea level conditions. The mean area experiencing tidal inundation up to MHHW is increased by 2.7 acres from 354.3 acres for the replacement bridge at future sea level to 357.0 acres for the Chang-channel + flow fences alternative, 54.3 acres more than for present sea level and resulting in an average 219.8 acres of intertidal habit, an increase of 22.8 acres over the replacement bridge at future sea level and 28.4 acres more than at present sea level.

As expected, the general impact from sea level rise was found to be an increase in both the maximum and average areas of salt water inundation in the East Basin of Batiquitos Lagoon, and this result held for both the proposed replacement bridge and the Chang-channel + flow fences alternative. However, these increases involved significant expansion in areas of sub tidal habitat and mud flats while producing moderate reductions in low and mid salt marsh and significant reductions in high salt marsh habitat. The incremental increases in tidally inundated habitat in response to sea level rise were moderately greater for the Chang-channel + flow fences alternative than for the proposed

replacement bridge. The unbalanced habitat shift away from salt marsh induced by sea level rise was less for the Chang-channel + flow fences alternative than for the proposed replacement bridge. The transitional habitat was nearly eliminated in the East Basin by sea level rise, with less than an acre remaining for both the proposed replacement bridge and the Chang-channel + flow fences alternative.

6.3) Sea level Rise Effects at Agua Hedionda Lagoon for Replacement Bridges:

Next we evaluate sea level rise impacts on the tidal exchange of the east basin of Agua Hedionda Lagoon with the proposed replacement I-5 bridge design in place. We will utilize the mean rise prediction of 0.41 m (1.33 ft) by 2100, which is the same as the most rapid rise prediction for 2050 (see Figure 1).

Figure 114 gives the flow trajectories and depth-averaged tidal currents computed by the calibrated TIDE_FEM model for the proposed replacement bridge during the mean range flooding tides with 0.41 m (16 inches) of sea level rise. Figure 114 displays many similar flow structures to the mean tide flood flow simulation in Figure 83 at present sea level, although the wetted footprint of the lagoon is significantly larger and more complex during the higher sea level. To facilitate comparisons with Figure 83, the future sea level simulation in Figure 83 is based on an equivalent plant flow rate of 304 mgd, the long term minimum based on stand alone desalination operations at Encina Power Station. Figure 114 reveals maximum currents in the inlet channel reach 2.2 m/sec or 7.2 ft/sec. The flood tide jet along the north bank of the West Basin sustains speeds of between 1.5 m/s (4.9 ft/sec) to 2.0 m/sec (6.5 ft/sec), well above the threshold of motion of the fine sand on the bar in the West Basin and more than sufficient to induce scour and erosion of those sands. The eddy in the central portion of the West Basin spins at 0.4 m/sec (1.3 ft/sec) but the middle portion remains near stagnation. The feeder current toward the plant intake runs at about -0.4 m/sec (-1.3 ft/sec), the same as in the simulation at present sea level in Figure 83 since both simulations are using the same plant flow rate, and circulation in the southern end of the West Basin is largely driven by plant flow rate. The flood tide jet along the north bank of the West Basin speeds back up to as high as 1.8 m/sec (5.9 ft/sec) as it passes through the hardened channel under the rail road bridge and then spins up a somewhat more orderly Central Basin eddy. The core of the Central Basin eddy remains at stagnation, again providing ideal conditions for suspended sediment to settle and deposit. Flood tide currents during future sea level speed back up to 1.1 m/sec (3.2 ft/sec) through the hardened channel under the I-5 bridge before diverging into a complex set of rather vigorous counter rotating eddies that populate the East Basin. This eddy structure includes 5 counter rotating eddies in the East Basin, two more than found for the simulation in Figure 83 for present sea level. East Basin eddy speeds are on the

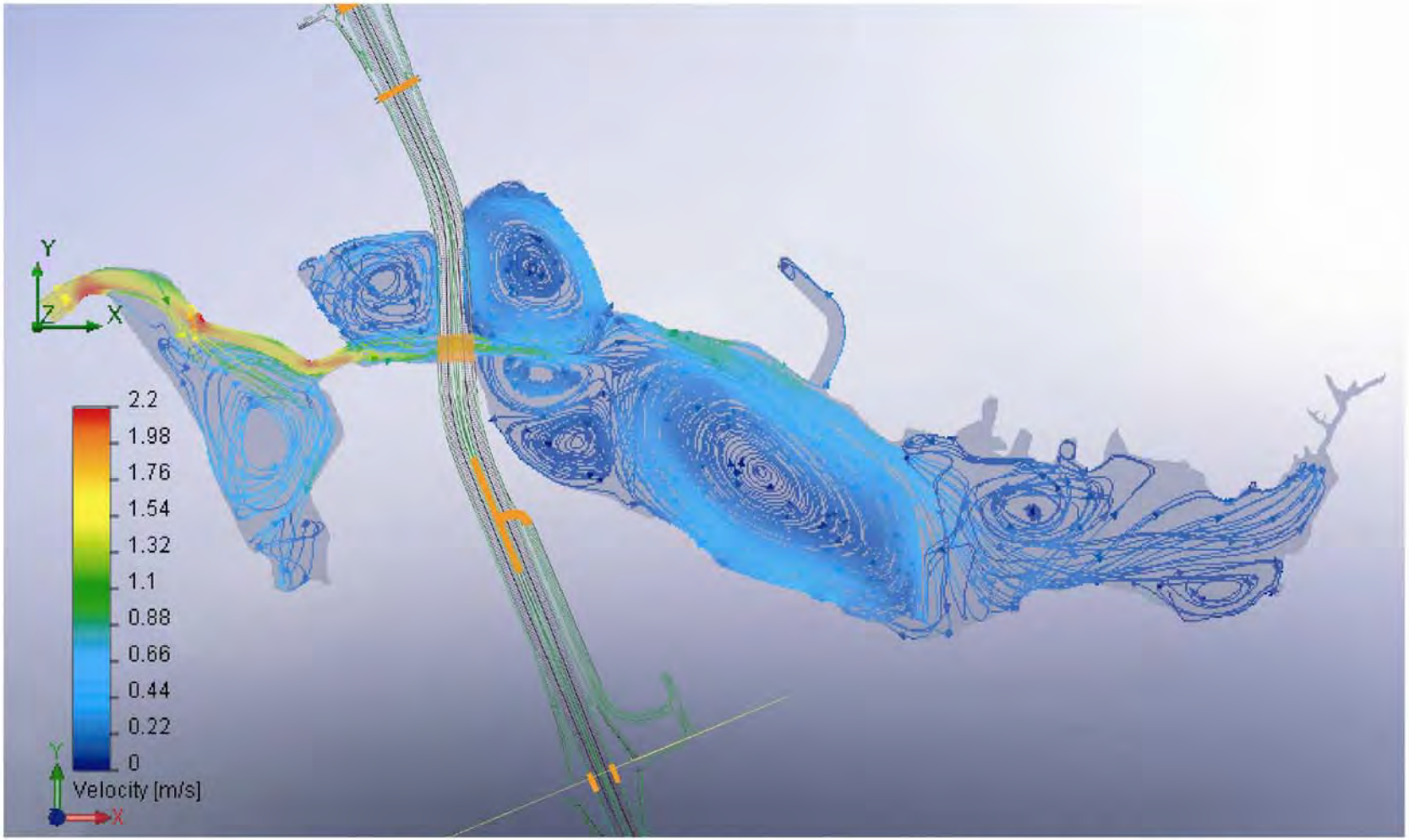

Figure 114. Hydrodynamic simulation of maximum flood flow during mean range tides at Agua Hedionda Lagoon superimposed on sea level rise with the proposed I-5 replacement bridge for the North Coast Corridor Project. Sea level rise set at 16 inches (1.33 ft) per the mean of six climate model prediction for 2100 (cf. Figure 1).

order of at 0.4 m/sec (1.3 ft/sec), four times stronger than for the simulation at present sea level in Figure 25. The high marsh area at the east end of the East Basin exhibits a disorganized meandering flow system during future sea level. From this collection of scenarios, we conclude that, as with Batiquitos Lagoon, current speeds at elevated sea level in Agua Hedionda Lagoon remain above the threshold of sediment motion the entire distance from the ocean inlet all the way through to the East Basin; and East Basin swirl and eddy speeds under higher sea levels are sufficient to transport fine sand and cause scour and erosion of portions of the bottom of the East Basin. Thus rapidly shoaling sand bars and localized scour and erosion are likely to occur under future high sea levels in all three basins of Agua Hedionda Lagoon with either the existing or proposed replacement bridges.

Figure 115 gives the hydroperiod function for the East Basin of Agua Hedionda lagoon at 0.41m (16 in) of sea level rise (the mean of these six predictions by 2100, cf. Figure 1) with the proposed replacement I-5 bridge. Elevations in Figure 115 are in terms of present day MLLW datum based on the 1983-2001 tidal epoch. This calculation is based on a linear superposition of the Scripps Pier 1980-2010 ocean water level measurements onto this predicted sea level rise; and on the relationships between habitat breaks and exposure used for San Dieguito Lagoon, as discussed in Section 3.3, Figure 17. Comparing the hydroperiod function in Figure 115 with that for existing conditions in Figure 78 indicates that future sea level rise could result in significant deepening of the sub-tidal zone (in the absence of hyper-sedimentation) by raising its upper limit to +0.55 ft MLLW, as well as vertical displacement of the mud flat and salt marsh habitat. When mapped onto the stage area function in Figure 69, sea level rise results in significant increases in tidally inundated areas. These increases are summarized in Table 6.4.

If sea level rises 0.41 m (1.33 ft.) above present eustatic sea level, then the minimum (perpetual) sub-tidal area of the East Basin with the replacement bridge in place will increase by 11.3 acres, to 190.3 acres versus 179.0 acres for the replacement bridge at present sea level; frequently flooded mud flat is increased by 2.9 acres, from 30.3 acres at present sea level to 33.2 acres for the replacement bridge at future sea level; frequently exposed mud flat is increased by 1.6 acres, from 5.5 acres for the replacement bridge at present sea level to 7.1 acres at future sea level;. However low salt marsh is increased slightly by 0.8 acres, from 11.5 acres for the replacement bridge at present sea level to 12.3 acres at future sea level; mid salt marsh is reduced by 2.1 acres at future sea level, from 21.4 acres for the replacement bridge at present sea level to 19.3 acres at future sea level; similarly, high salt marsh is reduced by 3.8 acres, from 10.3 acres for the replacement bridge at present sea level to 6.5 acres at future sea level; and, transitional

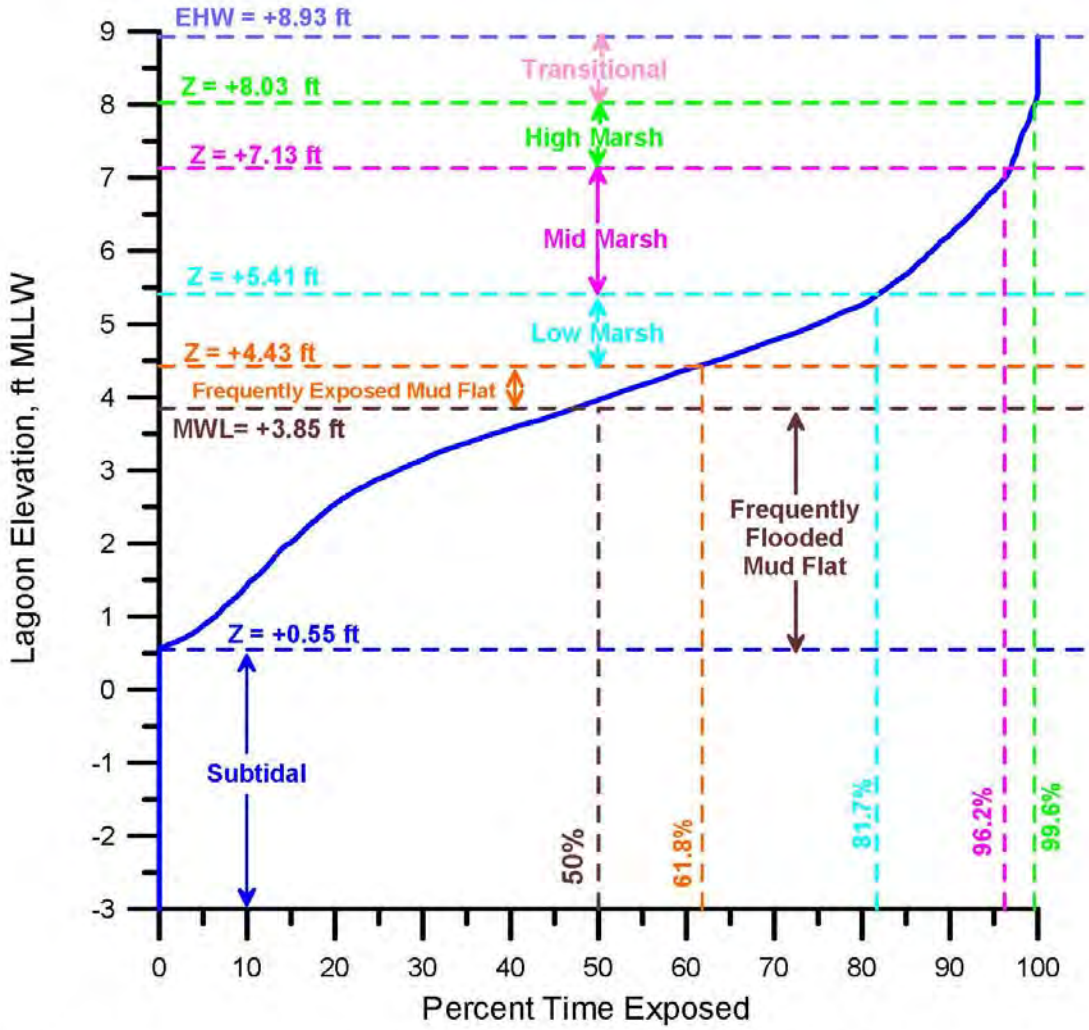

Figure 115. Hydroperiod function for the replacement I-5 bridge at Agua Hedionda Lagoon with 1.33 ft. of sea level rise over existing bathymetry. Based on hydrodynamic simulation of East Basin water levels in response to tidal forcing from the Scripps Pier tide gage (NOAA # 941-0230). Habitat breaks based on habitat delineation from Josselyn and Whelchel (1999). Elevations based on MLLW datum for the 1983-2001 tidal epoch.

Table 6.4: Agua Hedionda East Basin Habitat Area Distribution from Hydroperiod & Stage Area Functions with Existing Bridge vs. Proposed Replacement Bridge with +0.41 m (1.33 ft) Sea Level Rise.

East Basin Habitat Areas	Existing I-5 Bridge Present Sea Level	Replacement I-5 Bridge Present Sea Level	Replacement I-5 Bridge Future Sea Level
Perpetual Sub-Tidal (acres)	180.1	179.0	190.3
Mean Sub-Tidal (acres)	191.0	191.0	202.9
Frequently Flooded Mud Flat (acres)	30.3	30.3	33.2
Frequently Exposed Mud Flat (acres)	4.3	5.5	7.1
Low Salt Marsh (acres)	11.5	11.5	12.3
Mid Salt Marsh (acres)	20.0	21.4	19.3
High Salt Marsh (acres)	11.7	10.3	6.5
Transitional Habitat (acres)	8.1	8.1	1.9
Maximum Intertidal Area (acres)	85.9	87.0	80.3
Maximum Area of Salt Water Inundation (acres)	266.0	266.0	270.6
Mean Intertidal Area (acres)	59.8	60.0	61.7
Mean Area of Salt Water Inundation (acres)	250.8	251.0	264.6

habitat is reduced by 6.2 acres at future sea level, from 8.1 acres for the replacement bridge at present sea level to only 1.9 acres at future sea level. Despite the 0.41 m (1.33 ft.) increase in elevations of salt water inundation at future sea levels, the maximum area inundated by salt water at extreme high water is increased by only 4.6 acres, from 266.0 acres for the replacement bridge at present sea level to 270.6 acres at future sea level. While the sub-tidal and mud flat habitats increase significantly at future sea levels, maximum the intertidal habitat is reduced by 6.7 acres, from 87.0 acres for the replacement bridge at present sea level to 80.3 acres at future sea level with the replacement bridge. The mean area experiencing tidal inundation up to MHHW at future sea level is increased by 13.6 acres to 264.6 acres from 251.0 acres at present sea level

with the replacement bridge; but this increase is primarily sub-tidal in nature as the mean intertidal habit increases by only 1.7 acres to 61.7 acres with replacement bridge at future sea level versus 60.0 acres at present sea levels. The increase in mean sub-tidal area at future sea level is 11.9 acres, from 191.0 acres at present sea level to 202.9 acres at future sea level.

In general, sea level rise effects in the East Basin of Agua Hedionda are less pronounced than what was found for the East Basin of Batiquitos Lagoon in Section 6.1. Net gains in areas of tidal inundation are significantly less at Agua Hedionda, and losses of salt marsh habitat are also less. This is due to the differences in grading designs between the two lagoons. These differences are especially apparent in the in the steepness of the stage area functions in the upper portions of Figures 21 & 69. The east basin of Batiquitos Lagoon was designed to be a wetland restoration with shallow marsh slopes in the upper intertidal zone, whereas Agua Hedionda Lagoon was designed to be a cooling water reservoir with predominant sub-tidal area and steep slopes in the upper intertidal zone. Consequently sea level rise impacts on salt marsh are substantially less at Agua Hedionda Lagoon because that lagoon was designed with substantially less of that habitat type.

6.4) Sea level Rise Effects at Agua Hedionda Lagoon for Chang-channel + Flow Fences

Finally, we evaluate sea level rise impacts on the tidal exchange of the east basin of Agua Hedionda Lagoon with the Chang-channel + flow fences alternative adapted to the proposed replacement I-5 bridge per Figure 68a & 68c. Again, we will utilize the mean rise prediction of 0.41 m (1.33 ft) by 2100, which is equivalent to the most rapid rise prediction for 2050 per Figure 1.

Figure 116 (upper panel) gives the flow trajectories and depth-averaged tidal currents computed by the calibrated TIDE_FEM model for the Chang-channel + flow fences alternative during the mean range flooding tides superimposed on 0.41 m (16 inches) of sea level rise. Figure 116 (lower panel) shows fine scale flow details through the convergence and expansion sections of the flow fences. With more channel cross section than the proposed replacement bridge waterway, this alternative reduces the velocities of the flow exiting the hard bottom section of the channel to 0.8 m/sec (2.62 ft/sec) during flood flow, as compared to 1.1 m/sec (3.61 ft/sec) for the proposed replacement bridge in Figure 114. While flood flow velocities during these mean range tides at higher sea levels are reduced by the Chang-channel & flow fence structures in Figure 116, they remain greater than the spring tide velocities at present sea level in Figure 104 that were in the range of 0.4 m/sec (1.31 ft/sec). Thus, the Chang-channel & flow fence structures can not

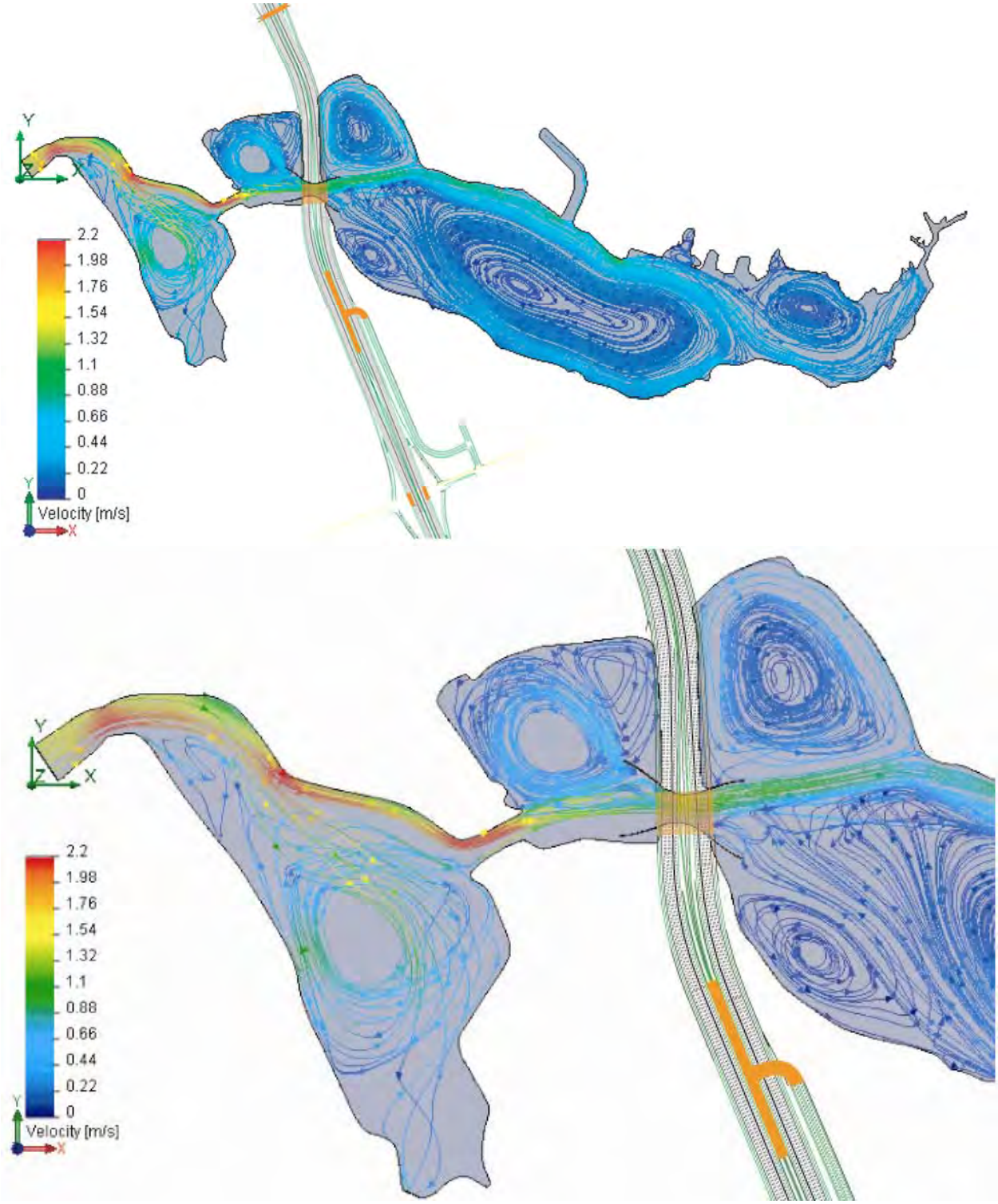

Figure 116: Hydrodynamic simulation of maximum flood flow during mean range tides at Agua Hedionda Lagoon superimposed on sea level rise with the Chang-channel + flow fences replacement bridge alternative for the North Coast Corridor Project. Sea level rise set at 16 inches (1.33 ft) per the mean of six climate model prediction for 2100 (cf. Figure1).

prevent flood flows at higher sea levels from exceeding the threshold of incipient motion of the littoral sediments; and consequently scour and transport of sediment through the Chang-channel and flow fences will continue into the East Basin and induce progressive shoaling there over time.

Eddy structures and jets in the East, Central and West Basins with the Chang-channel + flow fences (Figure 116) are similar to those for the replacement bridges at higher sea levels in Figure 114. Maximum flood currents in the inlet channel in Figure 112 reach 2.2 m/sec or (7.2 ft/sec) as comparable to the replacement bridge at higher sea level (Figure 114), indicating the Chang-channel + flow fences are not allowing significantly larger flow volumes into the tidal system. In Figure 116, flood tide currents entering the lagoon form a well defined jet along the north bank of the West Basin and into the Central Basin having the same structure as found for the high sea level flow patterns with the replacement bridge in Figure 114, with speeds of roughly 1.8 m/sec (5.91 ft/sec) as compared to 0.9 m/s (2.95 ft/sec) for the present day sea level simulation in Figure 104. The Central Basin jet cuts across the south bank of the large Central Basin sand bar with sufficient speed during the sea level rise scenario to scour a channel that directly feeds the convergence section of the flow fence in Figure 116. Because speeds remain above the threshold of sediment motion the entire distance from the ocean inlet all the way through to the East Basin in Figure 116, the Chang-channel + flow fences alternative will not prevent littoral sand bars from forming in the East Basin under higher sea level conditions that could shoal sufficiently to restrict tidal exchange in the East Basin. East Basin swirl and eddy speeds in Figure 116 are a bit less with the Chang-channel + flow fences alternative, on the order of 0.4 m/sec (1.3 ft/sec) along the north bank in the western two-thirds of the East Basin under higher sea levels, but still sufficient to transport fine sand or silt and cause scour and erosion of portions of the sand/silt bottom of the East Basin. The high marsh area at the east end of the East Basin exhibits well organized eddy with the Chang-channel + flow fences (Figure 116) that is not present in the simulation of the replacement bridge at future sea level in Figure 114. Circulation in this eddy is also in the range of 0.4 m/sec (1.3 ft/sec) and may cause erosion of the mud flats at the mouth of Agua Hedionda Creek. Thus rapidly shoaling sand bars and localized scour and erosion are likely to occur under future high sea levels in all three basins of Agua Hedionda Lagoon with either the proposed replacement bridges or with the Chang-channel + flow fences alternative.

When the Chang-channel + flow fences alternative is overlaid on a linear superposition of the Scripps Pier 1980-2010 ocean water level measurements and the predicted sea level rise 0.41m (16 in), we get the hydroperiod function for the East Basin of Agua Hedionda lagoon shown in Figure 117. Elevations in Figure 117 are in terms of present day MLLW

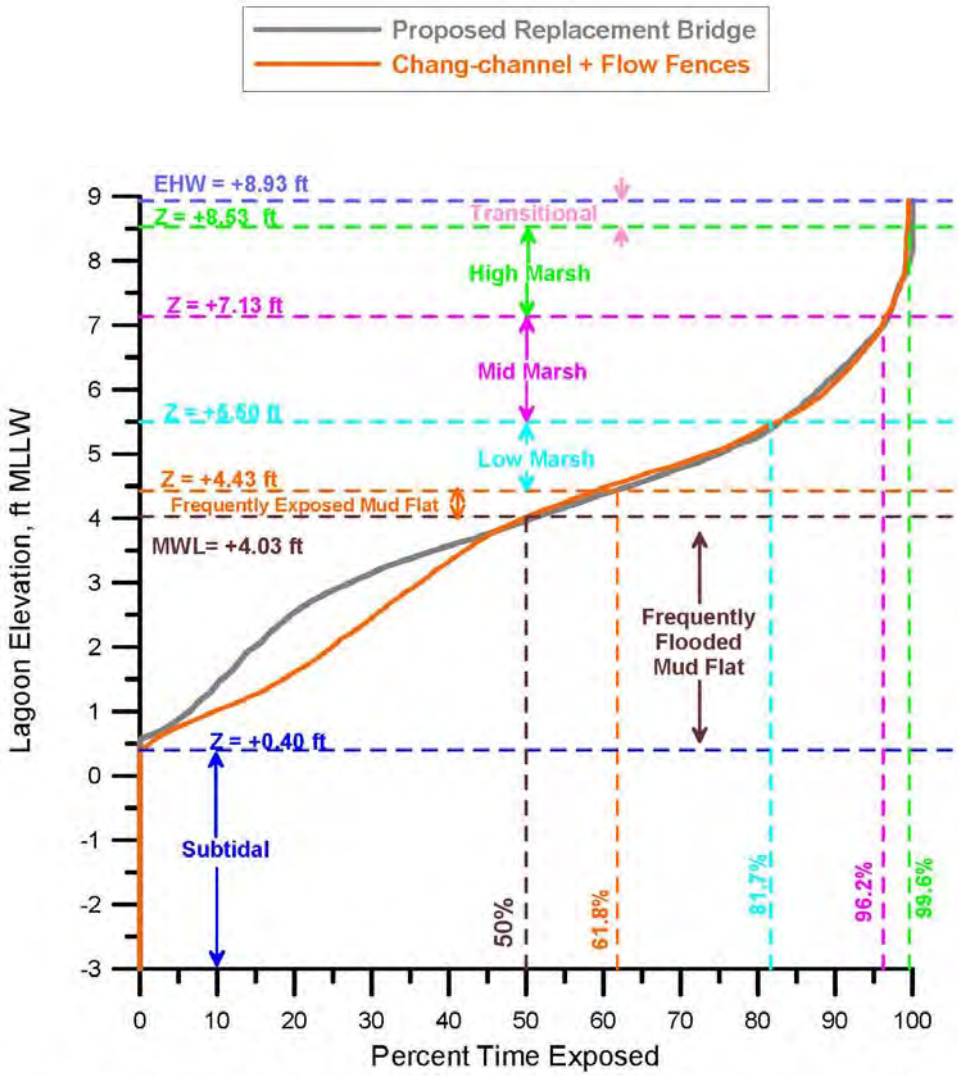

Figure 117. Hydroperiod function for the Chang-channel + flow fences alternative at Agua Hedionda Lagoon with 1.33 ft. of sea level rise over existing bathymetry. Based on hydrodynamic simulation of East Basin water levels in response to tidal forcing from the Scripps Pier tide gage (NOAA # 941-0230). Habitat breaks based on habitat delineation from Josselyn and Whelchel (1999). Elevations based on MLLW datum for the 1983-2001 tidal epoch.

datum based on the 1983-2001 tidal epoch. Comparing the hydroperiod function in Figure 117 with that for the replacement bridge in Figure 115 reveals the Chang-channel + flow fences alternative promotes less raising of sub-tidal zone and less compression of the intertidal zone under future sea level rise than would result with the proposed replacement bridge. With the Chang-channel + flow fences alternative the sub-tidal zone has an upper limit of +0.40 ft MLLW, 0.15 ft less super elevation than found for the replacement bridge in Figure 115, allowing for slight vertical expansion in the mud flat and salt marsh habitat. When mapped onto the stage area function in Figure 23, tidal superposition and sea level rise result in the habitat distributions summarized in Table 6.5 and net changes in habitat distributions are summarized in Table 6.6.

Inspection of Table 6.5 reveals that at higher sea levels, the Chang-channel + flow fences alternative delivers only minor benefits over the replacement bridges in terms of East Basin habitat gains and diversity. Tables 6.5 shows that the perpetual sub-tidal area of the East Basin at higher sea level decreases by 0.9 acres to 189.4 acres with the Chang-channel + flow fences alternative, from 190.3 acres for the replacement bridge, but still 9.9 acres more sub-tidal habitat than for present sea level. The mean sub-tidal area with the Chang-channel + flow fences alternative decreases by 0.9 acres to 202.0 acres, from 202.9 acres for the replacement bridge; but still 11.0 acres more sub-tidal habitat on average than for present sea level. Frequently flooded mud flat is increased by 0.4 acres, from 33.2 acres for the replacement bridge at future sea level to 33.6 acres for the Chang-channel + flow fences alternative, 3.3 acres more than for present sea level. Frequently exposed mud flat is decreased by 2.2 acres, from 7.1 acres for the replacement bridge at future sea level to 4.9 acres for the Chang-channel + flow fences alternative and 0.6 acres less than for present sea level. Low salt marsh changes only slightly, increasing by 1.1 acres from 12.3 acres for the replacement bridge at future sea level to 13.4 acres for the Chang-channel + flow fences alternative and 1.9 acres more than for present sea level. Mid salt marsh is decreased by 1.1 acres, from 19.3 acres for the replacement bridge at future sea level to 18.2 acres for the Chang-channel + flow fences alternative, and 3.2 acres less than for present sea level. High salt marsh is increased by 1.7 acres, from 6.5 acres for the replacement bridge at future sea level to 8.2 acres for the Chang-channel + flow fences alternative but 2.1 acres less than for present sea level. Most of the transitional habitat is converted into high salt marsh, reducing transitional habitat by 1.8 acres from 1.9 acres for the replacement bridge at future sea level to 0.1 acres for the Chang-channel + flow fences alternative. In either case there is little transitional habitat at higher sea levels because the upper limits of salt water inundation have nearly reached the day light contour of the upper limit of grading during the lagoon excavation in 1955. Maximum intertidal habitat is increased by 1.4 acres to 81.7 acres with the Chang-channel + flow fences alternative as compared to 80.3 acres for the replacement bridge at

Table 6.5: Agua Hedionda East Basin Habitat Area Distribution from Hydroperiod & Stage Area Functions with Proposed Replacement Bridge vs Chang-channel + flow fences alternative with +0.41 m (1.33 ft) of Sea Level Rise

East Basin Habitat Areas	Replacement I-5 Bridge Present Sea Level	Replacement I-5 Bridge Future Sea Level	Chang-channel+flow fences Future Sea Level
Perpetual Sub-Tidal (acres)	179.0	190.3	189.4
Mean Sub-Tidal (acres)	191.0	202.9	202.0
Frequently Flooded Mud Flat (acres)	30.3	33.2	33.6
Frequently Exposed Mud Flat (acres)	5.5	7.1	4.9
Low Salt Marsh (acres)	11.5	12.3	13.4
Mid Salt Marsh (acres)	21.4	19.3	18.2
High Salt Marsh (acres)	10.3	6.5	8.2
Transitional Habitat (acres)	8.1	1.9	0.1
Maximum Intertidal Area (acres)	87.0	80.3	81.7
Maximum Area of Salt Water Inundation (acres)	266.0	270.6	271.1
Mean Intertidal Area (acres)	60.0	61.7	62.9
Mean Area of Salt Water Inundation (acres)	251.0	264.6	264.9

future sea level but 5.3 acres less than for the present sea level conditions. The mean area experiencing tidal inundation up to MHHW is increased by only 0.3 acres from 264.6 acres for the replacement bridge at future sea level to 264.9 acres for the Chang-channel + flow fences alternative, 13.9 acres more than for present sea level and resulting in an average 62.9 acres of intertidal habit, an increase of 1.2 acres over the replacement bridge at future sea level and 2.9 acres more than at present sea level. Therefore, the modest gains in intertidal habitat by the Chang-channel + flow fences alternative at present sea level are reduced to only meager gains at future sea levels.

Table 6.6: Net Change in Agua Hedionda East Basin Habitat Area Distribution due to +0.41 m (1.33 ft) of Sea Level Rise. Results from Hydroperiod & Stage Area Functions with Proposed Replacement Bridge vs Chang-channel + Flow Fences alternative .

East Basin Habitat Areas	Net Change in Habitat Distribution Replacement I-5 Bridge Future Sea Level vs. Replacement I-5 Bridge Present Sea Level	Net Change in Habitat Distribution Chang-channel + Flow Fences Future Sea Level vs. Replacement I-5 Bridge Present Sea Level	Net Change in Habitat Distribution Chang-channel + Flow Fences Future Sea Level vs. Replacement Bridge Future Sea Level
Perpetual Sub-Tidal (acres)	+11.3	+10.4	-0.9
Mean Sub-Tidal (acres)	+11.9	+11.0	-0.9
Frequently Flooded Mud Flat (acres)	+2.9	+3.3	+0.4
Frequently Exposed Mud Flat (acres)	+1.6	-0.6	-2.2
Low Salt Marsh (acres)	+0.8	+1.9	+1.1
Mid Salt Marsh (acres)	-2.1	-3.2	-1.1
High Salt Marsh (acres)	-3.8	-2.1	+1.7
Transitional Habitat (acres)	-6.2	-8	-1.8
Maximum Intertidal Area (acres)	-6.7	-5.3	+1.4
Maximum Area of Salt Water Inundation (acres)	+4.6	+5.1	0.5
Mean Intertidal Area (acres)	+1.7	+2.9	+1.2
Mean Area of Salt Water Inundation (acres)	+13.6	+13.9	+0.3

7.0) Conclusions

7.1) San Dieguito Lagoon: The study begins in Section 3 with a hydrodynamic evaluation of potential tidal exchange effects from widening the I-5 Bridge at San Dieguito Lagoon; and the potential mitigation credits that may be derived for the North Coast Corridor Project by constructing a new tidal basin east of the I-5 Bridge referred to as Basin W-19. The I-5 Bridge over the tidal/river channel of San Dieguito Lagoon will not be replaced under the current plans for the North Coast Corridor Project; but rather will be widened in place using the existing span. We conclude that the effect of the W-19 tidal basin on tidal inundation overwhelms potential changes in the San Dieguito Lagoon system; and that no significant impact from bridge width changes can be found in the model results. Hydroperiod computations indicate that the habitat breaks of the lagoon system are not materially altered by the wider I-5 bridge. Regardless of whether the hydroperiod is calculated for the existing bridge or the widened bridge, we find that W-19 will create the following mix of wetland habitat: a) 4.84 acres of sub-tidal (fish) habitat; b) 5.09 acres of frequently flooded mud flat; c) 4.98 acres of frequently exposed mud flat; d) 12.24 acres of low salt marsh; e) 9.92 acres of mid salt marsh; f) 1.94 acres of high salt marsh; and, g) 0.24 acres of transitional habitat. This mix of habitat adds up to 39.25 acres of new wetlands habitat created by the W-19 basin at San Dieguito Lagoon. In considering patterns of tidal flow, water level, areas of tidal inundation and hydroperiod in total, it is concluded that the proposed widening of the I-5 bridge results in no significant changes to tidal exchange and habitat divisions relative to existing conditions in San Dieguito Lagoon. This finding was expected since neither the existing nor the widened I-5 bridges have any structural footprint (eg. support piles) located in the active tidal channel under the I-5 bridge. Due to the long bridge span at San Dieguito lagoon (209 m or 686 ft), both the existing and widened bridges are transparent to the tidal circulation.

The study proceeds to evaluate potential impacts to tidal circulation from replacement I-5 bridges at Batiquitos Lagoon in Section 4 and at Agua Hedionda Lagoon in Section 5. In both sections, tidal hydraulics of these lagoons are first evaluated in detail for existing conditions to establish a comparative baseline, and then re-evaluated for the proposed replacement bridges. The replacement bridges are wider and have a different structural footprint in the tidal channel under the bridge (bridge waterway) as compared to the existing bridges; with the replacement bridge at Batiquios Lagoon having double the number of piles as the existing bridge, while at Agua Hedionda Lagoon the replacement bridge has one-half the number of piles as the existing bridge. Evaluation of the existing and replacement bridge tidal hydraulics provides a comparative baseline for assessing

potential wetland habitat gains and improvements from replacement bridges and bridge waterway alternatives.

The first generic class of alternatives that was considered is referred to as *soft-alternatives,* and involves reductions of fill and earth works along transportation crossings in order to increase the cross sectional area of the tidal channel under the bridges. This alternative is referred to herein as the "double-wide" alternative and involves the excavation of a wider tidal channel along the existing grade. It also requires doubling of the replacement bridge spans.

The second generic class of bridge waterways that were studied is based on fixed, hardened channels beneath the bridges whose geometries and dimensions are optimized for rigid boundary flow conditions. There are three basic types of these *hardened-alternatives* that were studied: 1) increasing the choke point channel cross section of the bridge waterway, referred to herein as the *Chang-channel* concept; 2) adding structural amendments to the present bridge waterway configurations that provide high hydrodynamic efficiency; referred to as *flow-fences,* and 3) a combination of Chang-channel geometry and flow fences.

7.2) Batiquitos Lagoon: Table 7.1 summarizes the habitat distributions in the east basin of Batiquitos Lagoon resolved from the hydrodynamic simulations for the existing and replacement bridge baselines, and compares them against the soft and hard replacement bridge waterway alternatives. Table 7.2 summarizes the net changes in habitat distributions arising from these replacement bridge waterway alternatives.

We find the proposed replacement bridge at Batiquitos Lagoon does have a minor effect on the tidal elevations, phase lags and hydroperiod function of the East Basin. Minimum (perpetual) sub-tidal area of the East Basin increases by 0.6 acres with the replacement bridge, to 91.9 acres vs 91.3 acres for the existing bridge; frequently flooded mud flat is reduced by 0.5 acres, from 58.6 acres for the existing bridge to 58.1 acres for the replacement bridge; frequently exposed mud flat is reduced by 4.0 acres, from 13.6 acres for the existing bridge to 9.6 acres for the replacement bridge; low salt marsh is increased by 8.6 acres, from 42.3 acres for the existing bridge to 50.9 acres for the replacement bridge; mid salt marsh is relatively unchanged, increasing by only 0.2 acres, from 77.0 acres for the existing bridge to 77.2 acres for the replacement bridge; high salt marsh is reduced by 4.8 acres, from 45.8 acres for the existing bridge to 41.0 acres for the replacement bridge; transitional habitat is unchanged at 30.2 acres. Because the maximum area inundated by salt water at extreme high water is unchanged at 358.9, the maximum intertidal habitat is reduced by only 0.6 with the replacement bridge; and the

Table 7.1: East Basin Habitat Area Distribution for I-5 Bridge Alternatives at Batiquitos Lagoon.

East Basin Habitat Areas	Existing I-5 Bridge	Replacement I-5 Bridge	Replacement I-5 Bridge + Flow Fences	Double-Wide Alternative	Chang-Channel Alternative	Chang-Channel +Flow Fences
Perpetual Sub-Tidal (acres)	91.3	91.9	87.3	73.4	78.2	71.8
Mean Sub-Tidal (acres)	111.3	111.3	107.4	97.7	99.9	96.5
Frequently Flooded Mud Flat (acres)	58.6	58.1	53.8	64.5	63.2	65.7
Frequently Exposed Mud Flat (acres)	13.6	9.6	16.6	20.6	16.6	20.6
Low Salt Marsh (acres)	42.3	50.9	40.0	40.1	36.9	42.3
Mid Salt Marsh (acres)	77.0	77.2	76.5	84.4	79.7	79.1
High Salt Marsh (acres)	45.8	41.0	58.5	71.7	79.2	68.1
Transitional Habitat (acres)	30.2	30.2	26.2	5.5	5.5	11.7
Maximum Intertidal Area (acres)	267.6	267.0	271.6	286.8	281.1	287.6
Maximum Area of Salt Water Inundation (acres)	358.9	358.9	358.9	360.2	359.3	359.4
Mean Intertidal Area (acres)	191.4	191.4	196.6	210.6	207.6	211.2
Mean Area of Salt Water Inundation (acres)	302.7	302.7	304.0	308.3	307.5	307.7

Table 7.2: Net Change of East Basin Habitat Areas Resulting from I-5 Bridge Alternatives at Batiquitos Lagoon.

Changes in East Basin Habitat Areas	Replacement I-5 Bridge	Replacement I-5 Bridge + Flow Fences	Double-Wide Alternative	Chang-Channel Alternative	Chang-Channel +Flow Fences
Perpetual Sub-Tidal (acres)	0.6	-4.0	-17.9	-13.1	-19.5
Mean Sub-Tidal (acres)	0.0	-3.9	-13.6	-11.4	-14.8
Frequently Flooded Mud Flat (acres)	-0.5	-4.8	5.9	4.6	7.1
Frequently Exposed Mud Flat (acres)	-4.0	3.0	7.0	3.0	7.0
Low Salt Marsh (acres)	8.6	-2.3	-2.2	-5.4	0.0
Mid Salt Marsh (acres)	0.2	-0.5	7.4	2.7	2.1
High Salt Marsh (acres)	-4.8	12.7	25.9	33.4	22.3
Transitional Habitat (acres)	0.0	-4.0	-24.7	-24.7	-18.5
Maximum Intertidal Area (acres)	-0.6	4.0	19.2	13.5	20.0
Maximum Area of Salt Water Inundation (acres)	0.0	0.0	1.3	0.4	0.5
Mean Intertidal Area (acres)	0.0	5.2	19.2	16.2	19.8
Mean Area of Salt Water Inundation (acres)	0.0	1.3	5.6	4.8	5.0

mean area experiencing tidal inundation up to MHHW is unchanged at 302.7 acres with an average of 191.4 acres of intertidal habit, and a mean sub-tidal habitat of 111.3 acres for both existing and replacement bridges. Therefore, the small deviations in the distributions of areas among intertidal habitat types are not considered as being a significant impact of the replacement bridge since the aggregate totals of habitat and their split between intertidal and sub-tidal remain essentially unchanged. The small deviations in intertidal habitat splits are likely due to the turbulence and drag effects associated with the increase in numbers of piles on the replacement bridge. Maximum intertidal habitat is increased by 18.6 acres with the double-wide alternative.

The addition of *flow fences* to the replacement bridge would have negligible footprint over existing lagoon habitat, as it is envisioned as being constructed from vertical inter-locking sheet pile members driven into the lagoon and existing bridge waterway along a hydrodynamic efficient arc computed from Stratford turbulent pressure recovery relations. It would be constructed in phases, with the sheet piles driven immediately after the removal of sections of the existing bridge and prior to the construction of the replacement sections. It has been sized to adapt to the + 4 ft MLLW contours of the existing channel under the I-5 bridge, maintaining the existing channel bed at -3 ft MLLW. Generally, we find that the flow fence retrofit to the replacement bridge will create small amounts of new East Basin habitat with small reduction of the compression of present intertidal habitat. The flow fence retrofit to the proposed replacement bridge produces an average of 196.6 intertidal acres in the East Basin, or a net gain of 5.2 intertidal acres over existing conditions. Most of this gain has resulted from conversion of sub-tidal to intertidal habitat, as the mean area of tidal inundation in the East Basin has increased by only 1.3 acres over existing conditions. Maximum intertidal habitat is increased by 4.0 acres to 271.6 acres with the flow fence retrofit, as compared to 267.6 acres for existing conditions. These benefits are modest by comparison to what was achieved by expanding the bridge waterway channel cross section with the double-wide or Chang-channel alternatives.

To remediate tidal muting effects of the narrow bridge waterway at the Batiquitos Lagoon I-5 bridge, we first pose the *double-wide* alternative that would require removal of a portion of the road bed fill to accommodate doubling the width of the tidal channel along the existing grade of the south bank and increasing the span of the replacement bridge from 246 ft (78 m) to 492 ft (156 m). Doubling of the span also places two additional rows of 12 piles each in the active transport region of the channel, but increases channel cross section two-fold. Channel width increases effect only the south bank because the I-5 grades upward to higher ground toward the north (requiring more fill and longer bridge spans if the channel were widened in that direction), and grades

downward toward the south. Also, most of the vegetation around the bridge footings and road bed on the south side of the channel appears to be ruderal. The double-wide concept retains the hard channel bottom feature at -3 ft MLLW.

The reductions in flow speeds and phase lags due to the double-wide waterway alternative results in more complete conversion of velocity into potential energy of water elevation, thereby increasing the tidal range in the east basin of Batiquitos Lagoon. MHHW in the East Basin has been raised to +6.2 ft MLLW with the double-wide alternative, while MLLW in the East Basin has been lowered to +1.1 ft MLLW, producing a mean diurnal tidal range of 5.1 ft, an increase of 0.6 ft over existing conditions. The double-wide channel eliminates nearly all tidal muting due to the I-5 choke point, but some tidal muting still remains in the system from the seaward choke points at the railroad and PCH bridges. Regardless, substantial habitat gains and improvements are achieved in the East Basin. Maximum intertidal habitat is increased by 19.2 acres to 286.8 acres with the double-wide alternative as compared to 267.6 acres for existing conditions; and the mean area experiencing tidal inundation up to MHHW is increased by 5.6 acres from 302.7 acres for the existing bridge to 308.3 acres for the double-wide alternative, resulting in an average 210.6 acres of intertidal habit, an increase of 19.2 acres over existing conditions. The double-wide channel will create 12.9 acres of new mud flats and increase the exposure time of existing mud flats; a benefit to shorebird foraging and a feature of the East Basin that has been lacking to some degree. It will also reduce the compression of present intertidal habitat by lowering the zonation of low, mid, and high marsh vegetation allowing for some expansion of the cordgrass currently in the lagoon and providing some improved habitat for clapper rail. The new hydroperiod function promoted by the double-wide alternative brings the functionality of the east basin of Batiquitos Lagoon in closer alignment with its original restoration goals.

Under existing conditions, depth constrictions under the railroad bridge are the leading order cause of limited ebb tide drainage out of the central basin of Batiquitos Lagoon, which in turn limits further drainage from the East Basin, even with the double-wide channel improvements in place. About 76% of the tidal muting of the East Basin of Batiquitos Lagoon is attributable to the combination of choke points at the PCH and railroad bridges. Attempts to relieve these choke points through application of a double-wide type of concept would be problematic, and attempts to eliminate them altogether are probably infeasible. The depth of the channel under the railroad bridge is hardened at only -3 ft to -4 ft MLLW. Removal of fill at the rail road bridge to widen the channel would have constraints with respect to fill disposal and removal of large stone, as the bed fill is armored by rip rap and could have contaminant issues. Attempts to convert the footprint of this fill into functioning wetland would suffer degradation from shading. The

remaining constriction at the ocean inlet is due to the West Basin inlet bar, which in turn, is a consequence of failure to perform timely and adequate maintenance dredging. Attempts to recover the footprint of the PCH road bed fill for restorative improvement would make the entire West Basin vulnerable to sand infilling by wave overtopping of the beach berm, as the PCH road bed fill functions as a sea wall to protect the West Basin of the lagoon. In spite of these concerns, if the constrictions at the railroad bridge, the West Basin inlet bar, and the PCH bridge were remediated, the double-wide alternative for the I-5 bridge would function optimally as it was sized to convey the entire potential tidal prism of the East Basin.

The *Chang-channel* alternative would require removal of a smaller portion of the road bed fill than the double-wide alternative, and would not require doubling the span of the replacement, thereby providing a significant cost advantage. Channel width increases associated with the *Chang-channel* alternative are symmetric with respect to existing conditions, but the channel is deepened from -3 ft MLLW to -4.7 ft MLLW. While the double-wide alternative provided a 100% increase in channel cross section over existing conditions, the *Chang-channel* alternative provides an 80% increase. Maximum intertidal habitat is increased by 13.5 acres to 281.1 acres with the Chang-channel alternative as compared to 267.6 acres for existing conditions; and the mean area experiencing tidal inundation up to MHHW is increased by 4.8 acres from 302.7 acres for the existing bridge to 307.5 acres for the Chang-channel alternative, resulting in an average 207.6 acres of intertidal habit, an increase of 16.2 acres over existing conditions. The Chang-channel will create 7.6 acres of new mud flats and increase the exposure time of existing mud flats. Although this gain is slightly less than achieved by the double-wide alternative, it is, none the less, still a benefit to shorebird foraging.

Combining the Stratford flow fences with the Chang-channel produces tidal inundation in the east basin of Batiquitos Lagoon that is roughly comparable in hydraulic performance to the double-wide alternative without the added cost of doubling the span of the replacement bridge. The Chang-channel + flow fences alternative will create 14.1 acres of new mud flats (1.3 acres more than the double-wide alternative). Maximum intertidal habitat is increased by 20.0 acres to 287.6 acres with the Chang-channel + flow fences alternative as compared to 267.6 acres for existing conditions and 286.8 acres for the double-wide alternative; and the mean area experiencing tidal inundation up to MHHW is increased by 5.0 acres from 302.7 acres for the existing bridge to 307.7 acres for the Chang-channel + flow fences alternative, resulting in an average 211.2 acres of intertidal habit, an increase of 19.8 acres over existing conditions.

7.3) Agua Hedionda Lagoon: The utilization of lagoon water for once-through cooling by the Encina Power Station renders Agua Hedionda's hydraulics distinctly different from any other natural tidal lagoon. Power plant cooling water uptake acts as a kind of "negative river." Whereas natural lagoons have a river or stream adding water to the lagoon, causing a net outflow at the ocean inlet, the power plant infall removes water from Agua Hedionda Lagoon, resulting in a net inflow of water through the ocean inlet. This net inflow has several consequences for sediment transport into and out of the lagoon: 1) it draws nutritive particulate and suspended sediment from the surf zone into the lagoon, the latter forming bars and shoals that subsequently restrict the tidal circulation, and 2) the net inflow of water diminishes or at times cancels the ebb flow velocities out of the inlet, and provides an artificial suction head on the Central and East Basins that helps to drain those water bodies on ebbing tide. Therefore, the plant demand for lagoon water strongly controls the tidal circulation of the lagoon.

Remarkably little tidal muting occurs under existing conditions at Agua Hedionda Lagoon, despite the fact that on average nearly the same mean tidal prism is exchanged with the ocean as at Batiquitos Lagoon, where East Basin tidal muting and phase lags are four to six times greater. This difference is attributable to the controlling effects of the power plant whose suction-induced horsepower from its seawater circulation pumps acts as an "iron lung" in helping the east basin of Agua Hedionda to more effectively drain on ebbing tide. This reduces the opportunity to achieve habitat gains and expansion of the intertidal zone with more efficient I-5 bridge waterway alternatives at Agua Hedionda Lagoon. The other limiting aspect for achieving significant habitat gains at Agua Hedionda Lagoon is that these bridge waterway alternatives essentially work only on the intertidal zone by improving tidal exchange. However, that habitat type makes up only a minor fraction of the existing East Basin habitat, 77% of which is sub-tidal based on mean ranges of tidal inundation.

Table 7.3 summarizes the habitat distributions in the east basin of Agua Hedionda Lagoon resolved from the hydrodynamic simulations for the existing and replacement bridge baselines, and compares them against the soft and hard replacement bridge waterway alternatives. In the simulations of these alternatives, power plant flow rates were set at 304 mgd, the expected future consumption rate for the Carlsbad Desalination Project that is expected to take over operations of the Encina sea water circulation system once Cabrillo Power LLC repowers the generating facility using air cooling systems. Table 7.4 summarizes the net changes in habitat distributions arising from these replacement bridge waterway alternatives. Comparing Table 7.4 with Table 7.2, it is apparent how limited the habitat gains and improvements at Agua Hedionda Lagoon are

in comparison to those achieved at Batiquitos Lagoon using the same soft and hard bridge waterway alternatives.

Table 7.3 indicates that the slight reductions of East Basin tidal muting achieved by the Agua Hedionda replacement bride (as a consequence of a significant number of piles in the bridge waterway channel), will slightly expand the intertidal habitat zonation and increase the exposure of mud flats to a small degree, while making a small reduction in the sub-tidal habitat. Table 7.3 shows that the minimum (perpetual) sub-tidal area of the East Basin decreases by 1.1 acres with the replacement bridge, to 179.0 acres vs 180.1 acres for the existing bridge; the areas of frequently flooded mud flats remain unchanged at 30.3 acres; while frequently exposed mud flats are increased by 1.2 acres, from 4.3 acres for the existing bridge to 5.5 acres for the replacement bridge; low salt marsh remain unchanged at 11.5 acres; mid salt marsh increases by 1.4 acres, from 20.0 acres for the existing bridge to 21.4 acres for the replacement bridge; high salt marsh is reduced by 1.4 acres, from 11.7 acres for the existing bridge to 10.3 acres for the replacement bridge; and transitional habitat is unchanged at 8.1 acres. The maximum area inundated by salt water at extreme high water is unchanged at 266.0, but the maximum the intertidal habitat is increased by 1.1 acres with the replacement bridge; and the mean area experiencing tidal inundation up to MHHW is increased slightly from 250.8 acres for the existing bridge to 251.0 acres with an average 60.0 acres of intertidal habit (an increase of 0.2 acres over existing conditions), while the mean sub-tidal habitat remains unchanged at 191 acres for both the existing bridge and the replacement bridge. These deviations in the distributions of areas among sub-tidal and intertidal habitat types are less than what replacement bridges caused at Batiquitos, because the preponderance of habitat at Agua Hedionda is one type, namely, sub-tidal. These small changes of a couple of acres or less are not considered as being a significant impact of the replacement bridge since the aggregate totals of habitat and their split between intertidal and sub-tidal remain essentially unchanged. The small deviations in intertidal habitat splits in Table 7.3 and Figure 87 are likely due to reductions in turbulence and drag effects associated with fewer numbers of piles in the waterway channel of the replacement bridge.

The addition of *flow fences* to the replacement bridge at Agua Hedionda Lagoon would have a negligible footprint on existing lagoon habitat, as it is envisioned as being constructed from vertical inter-locking sheet pile members driven into the lagoon and existing bridge waterway along a hydrodynamic efficient arc computed from Stratford turbulent pressure recovery relations. It has been sized to adapt to the + 4 ft MLLW contours of the existing channel under the I-5 bridge with a bed width of 113 ft (Figure 68b) comprised of rip rap at a depth of -19.22 ft MLLW (-21.52 ft NGVD) with sediment

Table 7.3: East Basin Habitat Area Distribution for I-5 Bridge Alternatives at Agua Hedionda Lagoon.

East Basin Habitat Areas	Existing I-5 Bridge	Replacement I-5 Bridge	Replacement I-5 Bridge + Flow Fences	Double-Wide Alternative	Chang-Channel Alternative	Chang-Channel +Flow Fences
Perpetual Sub-Tidal (acres)	180.1	179.0	178.9	178.6	179.0	178.1
Mean Sub-Tidal (acres)	191.0	191.0	190.8	191.0	190.9	190.7
Frequently Flooded Mud Flat (acres)	30.3	30.3	27.8	30.6	26.2	30.6
Frequently Exposed Mud Flat (acres)	4.3	5.5	5.7	6.5	7.4	6.5
Low Salt Marsh (acres)	11.5	11.5	13.1	12.7	13.1	12.6
Mid Salt Marsh (acres)	20.0	21.4	20.9	21.6	22.2	20.3
High Salt Marsh (acres)	11.7	10.3	14.5	14.9	16.0	15.1
Transitional Habitat (acres)	8.1	8.1	5.1	2.4	2.4	3.2
Maximum Intertidal Area (acres)	85.9	87.0	87.1	88.7	87.3	88.4
Maximum Area of Salt Water Inundation (acres)	266.0	266.0	266.0	267.3	266.3	266.5
Mean Intertidal Area (acres)	59.8	60.0	60.3	61.8	60.6	61.3
Mean Area of Salt Water Inundation (acres)	250.8	251.0	251.1	252.8	251.5	252.0

Table 7.4: Net Change of East Basin Habitat Areas Resulting from I-5 Bridge Alternatives at Agua Hedionda Lagoon.

Changes in East Basin Habitat Areas	Replacement I-5 Bridge	Replacement I-5 Bridge + Flow Fences	Double-Wide Alternative	Chang-Channel Alternative	Chang-Channel +Flow Fences
Perpetual Sub-Tidal (acres)	-1.1	-1.2	-1.5	-1.1	-2.0
Mean Sub-Tidal (acres)	0	-0.2	0.0	-0.1	-0.3
Frequently Flooded Mud Flat (acres)	0	-2.5	0.3	-4.1	0.3
Frequently Exposed Mud Flat (acres)	1.2	1.4	2.2	3.1	2.2
Low Salt Marsh (acres)	0	1.6	1.2	1.6	1.1
Mid Salt Marsh (acres)	1.4	0.9	1.6	2.2	0.3
High Salt Marsh (acres)	-1.4	2.8	3.2	4.3	3.4
Transitional Habitat (acres)	0	-3	-5.7	-5.7	-4.9
Maximum Intertidal Area (acres)	1.1	1.2	2.8	1.4	2.5
Maximum Area of Salt Water Inundation (acres)	0	0	1.3	0.3	0.5
Mean Intertidal Area (acres)	0.2	0.5	2.0	0.8	1.5
Mean Area of Salt Water Inundation (acres)	0.2	0.3	2.0	0.7	1.2

fill to a depth of -5 ft MLLW (-7.3 ft NGVD). Despite noticeable changes in the hydroperiod function with the flow fence waterway, those changes do not map into appreciable changes in habitat areas when factored against the stage area function in of the East Basin. This is due to the fact that the preponderance of the East Basin habitat is sub-tidal, while the more significant changes in the hydroperiod function involve the intertidal habitat that comprises a relatively minor constituent. Altogether, net habitat gains and conversions to higher quality intertidal habitats are meager with the flow fence waterway retrofit. Maximum intertidal habitat is increased by 1.2 acres to 87.1 acres with the flow fence waterway retrofit as compared to 85.9 acres for existing conditions; while the mean area experiencing tidal inundation up to MHHW is increased by only 0.3 acres from 250.8 acres for the existing bridge to 251.1 acres for the flow fence waterway retrofit resulting in an average 60.3 acres of intertidal habit, an increase of 0.5 acres over existing conditions.

The *double-wide* bridge waterway alternative that gave significant gains in habitat amount and quality at Batiquitos Lagoon was also tested at Agua Hedionda Lagoon. Here the double-wide alternative would require removal of a portion of the road bed fill to accommodate doubling the width of the tidal channel along the existing grade of the north bank and increasing the span of the replacement bridge from 230 ft (70.1 m) to 460 ft (140.2 m). Doubling of the span also places two additional rows of 16 piles each in the active transport region of the channel, but increases channel cross sectional two-fold. Channel width increases effect only the north bank because the present tidal channel runs along the south bank of the Central Basin, and there is no free basin space to expand the channel to the south. Due to buried infrastructure concerns, the double-wide concept retains the hard channel bottom feature at -19.22 ft MLLW (-21.52 ft NGVD) with sediment fill at -5 ft MLLW (-7.3 ft NGVD).

The reductions in flow speeds and phase lags due to the double-wide waterway alternative results in more complete conversion of velocity head into potential energy of water elevation, thereby increasing the tidal range in the east basin of Agua Hedionda Lagoon. We find that both the mean and maximum diurnal tidal ranges in the East Basin are slightly increased with the double-wide alternative. MHHW in the East Basin has been raised to +6.13 ft MLLW with the double-wide alternative, while MLLW in the East Basin has been lowered to +0.55 ft MLLW, producing a mean diurnal tidal range of 5.58 ft, an increase of 0.16 ft over existing conditions. While extreme high water levels in the East Basin remain unchanged with the double-wide alternative, extreme low water levels are lowered to -0.91 ft MLLW, resulting in a maximum tidal range of 8.51 ft, an increase of 0.25 ft over existing conditions. With these increases in maximum and mean tidal ranges came small increases in intertidal habitat. Maximum intertidal habitat is increased

by 2.8 acres to 88.7 acres with the double-wide alternative as compared to 85.9 acres for existing conditions; while the mean area experiencing tidal inundation up to MHHW is increased by 2.0 acres from 250.8 acres for the existing bridge to 252.8 acres for the double-wide alternative resulting in an average 61.8 acres of intertidal habit, an increase of 2.0 acres over existing conditions. The double-wide channel will create 2.5 acres of new mud flats in the east basin of Agua Hedionda Lagoon and increase the exposure time of existing mud flats. These gains are about eight to nine times smaller than the gains achieved with the double-wide alternative at Batiquitos Lagoon. Because of the "iron-lung" effect that the power plant exerts on tidal ventilation of the east basin of Agua Hedionda, it is difficult to achieve substantial habitat gains or conversions through improved bridge designs, even one involving rather significant removal of I-5 road bed fill such as the double-wide alternative.

Implementing the *Chang-channel* alternative at Agua Hedionda Lagoon would also require removal of a smaller portion of the road bed fill than the double-wide alternative, and would not require doubling the span of the replacement, again providing a significant cost advantage. Channel width increases associated with the *Chang-channel* alternative increase the bed width of the hard bottom channel to 99.1 ft while maintaining the existing depth of the hard bottom channel at -19.22 ft MLLW (-21.52 ft NGVD) along 1 on 1 side slopes**.** While the double-wide alternative increases the channel cross section by a factor of 2 over existing conditions, the *Chang-channel* alternative provides an increase by a factor of 1.4. Maximum intertidal habitat is increased by 1.4 acres to 87.3 acres with the Chang-channel alternative as compared to 85.9 acres for existing conditions; while the mean area experiencing tidal inundation up to MHHW is increased by only 0.7 acres from 250.8 acres for the existing bridge to 251.5 acres for the Chang-channel alternative resulting in an average 60.6 acres of intertidal habit, an increase of 0.8 acres over existing conditions. The Chang-channel will result in the loss of 1.0 acres of new mud flats but increase the exposure time of existing mud flats; a bit of a wash in terms of net benefit to foraging birds. Of the 0.8 acres of intertidal area created on average by the Chang-channel alternative, 0.7 acres represents net wetland habitat gain. Again, the "iron-lung" effect that the power plant exerts on tidal ventilation of the East Basin makes it difficult to achieve substantial habitat gains or conversions through by removal of I-5 road bed fill as attempted with the Chang-channel alternative.

Combining the Stratford flow fences with the Chang-channel produces tidal inundation in the east basin of Agua Hedionda Lagoon that is slightly better in hydraulic performance than the double-wide alternative without the added cost of doubling the span of the replacement bridge. It has been sized to adapt to the Chang-channel +4 ft MLLW contours under the I-5 bridge using a bed width of 156 ft comprised of rip rap at a depth

of -19.22 ft MLLW (-21.52 ft NGVD) with sediment fill to a depth of -5 ft MLLW (-7.3 ft NGVD), and provides 80% more channel cross section than the existing bridge. The Chang-channel + flow fences alternative will increase the maximum intertidal habitat by 2.5 acres to 88.4 acres with the Chang-channel + flow fences alternative as compared to 85.9 acres for existing conditions; while the mean area experiencing tidal inundation up to MHHW is increased by only 1.2 acres from 250.8 acres for the existing bridge to 252.0 acres for the Chang-channel + flow fences alternative resulting in an average 61.3 acres of intertidal habit, an increase of 1.5 acres over existing conditions. The Chang-channel + flow fences will create 2.5 acres of new mud flats and increase the exposure time of existing mud flats. Of the 1.5 acres of intertidal area created on average by the Chang-channel + flow fences alternative, 1.2 acres represents net wetland habitat gain. The "iron-lung" effect that the power plant exerts on lagoon tidal exchange and the preponderance of East Basin area that is comprised of sub-tidal habitat make substantial habitat gains or conversions through improved bridge designs difficult to attain, even one involving rather significant structural amendments to bridge under-works as the Chang-channel + flow fences alternative.

7.4) Sea level Rise Effects : The mean of six climate model predictions calls for 0.41 m (1.33 ft) of sea level rise by 2100, while the most aggressive prediction calls for that amount of sea level rise by 2050. This predicted sea level rise was linearly combined with the historic ocean water level record and used to drive the tidal hydraulics model and thereby resolve the potential effects on tidal exchange and habitat mix for replacement bridges and the Chang Channel + flow fence I-5 bridge alternative, both using existing bathymetric conditions. Although sea level rise will undoubtedly erode neighboring beaches, we did not attempt to quantify beach impacts on the lagoon bathymetry and tidal hydraulics due to the numerous assumptions that must be made on future beach sand supplies in such an analysis. We chose the Chang Channel + flow fence alternative to make comparisons against the proposed replacement bridges because it was generally found to be the most cost effective of the alternatives considered.

Batiquitos Lagoon: Sea level rise effects on the east basin of Batiquitos Lagoon are summarized in Table 7.5. Despite the 0.41 m (1.33 ft.) increase in elevations of salt water inundation at future sea levels, the maximum area inundated by salt water at extreme high water is increased by only 9.2 acres, from 358.9 acres for the replacement bridge at present sea level to 368.1 acres at future sea level. While the sub-tidal and mud flat habitats increase significantly at future sea levels, maximum the intertidal habitat is reduced by 30.3 acres, from 267.0 acres for the replacement bridge at present sea level to 236.7 acres at future sea level with the replacement bridge. The mean area experiencing tidal inundation up to MHHW at future sea level is substantially increased by 51.6 acres

to 354.3 acres from 302.7 acres at present sea level with the replacement bridge; but this increase is primarily sub-tidal in nature as the mean intertidal habit increases by only 5.6 acres to 197.0 with replacement bridge at future sea level versus 191.4 acres at present sea levels. The increase in mean sub-tidal area at future sea level is 46 acres, from 111.3 acres at present sea level to 157.3 acres at future sea level.

Inspection of Table 7.5 reveals that even at higher sea levels, the Chang-channel + flow fences alternative delivers benefits over the replacement bridges in terms of East Basin habitat gains and diversity. Maximum intertidal habitat is increased by 27.1 acres to 263.8 acres with the Chang-channel + flow fences alternative as compared to 236.7 acres for the replacement bridge at future sea level and 267.0 acres for the present sea level conditions. The mean area experiencing tidal inundation up to MHHW is increased by 2.7 acres from 354.3 acres for the replacement bridge at future sea level to 357.0 acres for the Chang-channel + flow fences alternative, 54.3 acres more than for present sea level and resulting in an average 219.8 acres of intertidal habit, an increase of 22.8 acres over the replacement bridge at future sea level and 28.4 acres more than at present sea level.

As expected, the general impact from sea level rise was found to be an increase in both the maximum and average areas of salt water inundation in the East Basin of Batiquitos Lagoon, and this result held for both the proposed replacement bridge and the Chang-channel + flow fences alternative. However, these increases involved significant expansion in areas of sub-tidal habitat and mud flats while producing moderate reductions in low and mid salt marsh and significant reductions in high salt marsh habitat. The incremental increases in tidally inundated habitat in response to sea level rise were moderately greater for the Chang-channel + flow fences alternative than for the proposed replacement bridge. The unbalanced habitat shift away from salt marsh induced by sea level rise was less for the Chang-channel + flow fences alternative than for the proposed replacement bridge. The transitional habitat was nearly eliminated in the East Basin by sea level rise, with less than an acre remaining for both the proposed replacement bridge and the Chang-channel + flow fences alternative.

Other adverse consequences of sea level rise at Batiquitos Lagoon can be inferred from the tidal velocities predicted by the model. While the model assumes rigid boundaries and stationary, existing bathymetry, the flood tide currents at higher sea levels form jets and boundary streams that are significantly stronger than during spring tides at present sea level, and remain above the threshold of sediment motion the entire distance from the ocean inlet to the East Basin. Thus rapidly shoaling sand bars and localized scour and erosion are likely to occur under future high sea levels in all three basins of Batiquitos

Table 7.5: Batiquitos East Basin Habitat Area Distribution from Hydroperiod & Stage Area Functions with Proposed Replacement Bridge vs Chang-channel + flow fences alternative with +0.41 m (1.33 ft) of Sea Level Rise

East Basin Habitat Areas	Replacement I-5 Bridge Present Sea Level	Replacement I-5 Bridge Future Sea Level	Chang-channel+flow fences Future Sea Level
Perpetual Sub-Tidal (acres)	91.9	131.4	108.2
Mean Sub-Tidal (acres)	111.3	157.3	137.2
Frequently Flooded Mud Flat (acres)	58.1	68.9	78.4
Frequently Exposed Mud Flat (acres)	9.6	21.9	29.0
Low Salt Marsh (acres)	50.9	47.6	48.3
Mid Salt Marsh (acres)	77.2	70.8	74.2
High Salt Marsh (acres)	41.0	26.9	30.2
Transitional Habitat (acres)	30.2	0.5	0.3
Maximum Intertidal Area (acres)	267.0	236.7	263.8
Maximum Area of Salt Water Inundation (acres)	358.9	368.1	368.6
Mean Intertidal Area (acres)	191.4	197.0	219.8
Mean Area of Salt Water Inundation (acres)	302.7	354.3	357.0

Lagoon with either the proposed replacement bridges or with the Chang-channel + flow fences alternative.

Agua Hedionda Lagoon: Sea level rise effects on the east basin of Agua Hedionda Lagoon are summarized in Table 7.6. Despite 0.41 m (1.33 ft.) increases in elevations of salt water inundation at future sea levels, the maximum area inundated by salt water at extreme high water is increased by only 4.6 acres, from 266.0 acres for the replacement

bridge at present sea level to 270.6 acres at future sea level. While the sub-tidal and mud flat habitats increase significantly at future sea levels, maximum the intertidal habitat is reduced by 6.7 acres, from 87.0 acres for the replacement bridge at present sea level to 80.3 acres at future sea level with the replacement bridge. The mean area experiencing tidal inundation up to MHHW at future sea level is increased by 13.6 acres to 264.6 acres from 251.0 acres at present sea level with the replacement bridge; but this increase is primarily sub-tidal in nature as the mean intertidal habit increases by only 1.7 acres to 61.7 acres with replacement bridge at future sea level versus 60.0 acres at present sea levels. The increase in mean sub-tidal area at future sea level is 11.9 acres, from 191.0 acres at present sea level to 202.9 acres at future sea level.

Inspection of Table 7.6 reveals that at higher sea levels, the Chang-channel + flow fences alternative delivers only minor benefits over the replacement bridges in terms of East Basin habitat gains and diversity. Little transitional habitat at higher sea levels because the upper limits of salt water inundation have nearly reached the day light contour of the upper limit of grading during the lagoon excavation in 1955. Maximum intertidal habitat is increased by 1.4 acres to 81.7 acres with the Chang-channel + flow fences alternative as compared to 80.3 acres for the replacement bridge at future sea level but 5.3 acres less than for the present sea level conditions. The mean area experiencing tidal inundation up to MHHW is increased by only 0.3 acres from 264.6 acres for the replacement bridge at future sea level to 264.9 acres for the Chang-channel + flow fences alternative, 13.9 acres more than for present sea level and resulting in an average 62.9 acres of intertidal habit, an increase of 1.2 acres over the replacement bridge at future sea level and 2.9 acres more than at present sea level. Therefore, the modest gains in intertidal habitat by the Chang-channel + flow fences alternative at present sea level are reduced to only meager gains at future sea levels.

In general, sea level rise effects in the east basin of Agua Hedionda are less pronounced than what was found for the east basin of Batiquitos Lagoon. Net gains in areas of tidal inundation are significantly less at Agua Hedionda, and losses of salt marsh habitat are also less. This is due to the differences in grading designs between the two lagoons. The east basin of Batiquitos Lagoon was designed to be a wetland restoration with broad shallow sloping marsh plains in the upper intertidal zone, whereas Agua Hedionda Lagoon was designed to be a cooling water reservoir with predominant sub-tidal area and steep slopes in the upper intertidal zone. Consequently sea level rise impacts on salt marsh are substantially less at Agua Hedionda Lagoon because that lagoon was designed with substantially less of that habitat type. Sediment transport inferred from modeled tidal velocities indicate rapidly shoaling sand bars and localized scour and erosion are likely to occur under future high sea levels in all three basins of Agua Hedionda Lagoon

Table 7.6: Agua Hedionda East Basin Habitat Area Distribution from Hydroperiod & Stage Area Functions with Proposed Replacement Bridge vs Chang-channel + flow fences alternative with +0.41 m (1.33 ft) of Sea Level Rise

East Basin Habitat Areas	Replacement I-5 Bridge Present Sea Level	Replacement I-5 Bridge Future Sea Level	Chang-channel+flow fences Future Sea Level
Perpetual Sub-Tidal (acres)	179.0	190.3	189.4
Mean Sub-Tidal (acres)	191.0	202.9	202.0
Frequently Flooded Mud Flat (acres)	30.3	33.2	33.6
Frequently Exposed Mud Flat (acres)	5.5	7.1	4.9
Low Salt Marsh (acres)	11.5	12.3	13.4
Mid Salt Marsh (acres)	21.4	19.3	18.2
High Salt Marsh (acres)	10.3	6.5	8.2
Transitional Habitat (acres)	8.1	1.9	0.1
Maximum Intertidal Area (acres)	87.0	80.3	81.7
Maximum Area of Salt Water Inundation (acres)	266.0	270.6	271.1
Mean Intertidal Area (acres)	60.0	61.7	62.9
Mean Area of Salt Water Inundation (acres)	251.0	264.6	264.9

with either the proposed replacement bridges or with the Chang-channel + flow fences alternative.

REFERENCES

Coastal Environments, 2009, “2009 Monitoring Program for San Dieguito Lagoon: Topography, Hydrology, and Water Quality Surveys”, submitted to Southern California Edison Company, 134 pp + app.

Elwany, M. H. S., R. E. Flick, M. White, and K. Goodell, 2005, “Agua Hedionda Lagoon Hydrodynamic Studies,” prepared for Tenera Environmental, 39 pp. + appens.

EIR/EIS, 2000, Environmental Impact Report/Environmental Impact Statement (EIR/EIS) for the San Dieguito Wetland Restoration Project.

Houghton, J., 2004, *Global Warming; The Complete Briefing*, 3rd edition, Cambridge Univ. Press, 340 pp.

Flick, R. E. & D. R. Cayan, 1984, “Extreme sea levels on the coast of California,” Coastal Engineering 1984, *Proc. 19th Int. Conf. (Houston)*, Amer. Soc. Civil Eng., New York, p. 886-96.

Jenkins, S. A. and D. W. Skelly, 1988, "An Evaluation of the Coastal Data Base Pertaining to Seawater Diversion at Encina Power Plant Carlsbad, CA," submitted to San Diego Gas and Electric, Co., 56 pp.

Jenkins, S. A., D. W. Skelly, and J. Wasyl, 1989, "Dispersion and Momentum Flux Study of the Cooling Water Outfall at Agua Hedionda," submitted to San Diego Gas and Electric, Co., 36 pp. + appens.

Jenkins, S. A. and J. Wasyl, 1993, "Numerical Modeling of Tidal Hydraulics and Inlet Closures at Agua Hedionda Lagoon," submitted to San Diego Gas and Electric, Co., 91 pp.

Jenkins, S. A. and J. Wasyl, 1994, "Numerical Modeling of Tidal Hydraulics and Inlet Closures at Agua Hedionda Lagoon Part II: Risk Analysis," submitted to San Diego Gas and Electric, Co., 46 pp. + appens.

Jenkins, S. A. and J. Wasyl, 1995, "Optimization of Choke Point Channels at Agua Hedionda Lagoon using Stratford Turbulent Pressure Recovery," submitted to San Diego Gas and Electric, Co., 59 pp.

Jenkins, S. A. & J. Wasyl, 1996, Wave Transport Corrections to the Inlet Closure Problem of the San Dieguito Lagoon CA,, submitted to *Southern California Edison Co.*, 101 pp.

Jenkins, S. A. and J. Wasyl, 1997, "Analysis of inlet closure risks at Agua Hedionda Lagoon, CA and potential remedial measures, Part II," submitted to San Diego Gas and Electric, Co., 152 pp. + appens.

Jenkins, S. A. and J. Wasyl, 1998a, Analysis of Coastal Processes Effects Due to the San Dieguito Lagoon Restoration Project: Final Report, submitted to Southern California Edison Co., 333 pp.

Jenkins, S. A. and J. Wasyl, 1998b, Coastal Processes Analysis of Maintenance Dredging Requirements for Agua Hedionda Lagoon, submitted to San Diego Gas and Electric Co., 176 pp. + appens.

Jenkins, S. A. and D. L. Inman, 1999, “Sand transport mechanics for equilibrium in tidal inlets,” *Shore and Beach*, vol. 67, no. 1, pp. 53-58.

Jenkins, S. A., M. Josselyn & J. Wasyl, 1999, “Hydroperiod and residence time functions for habitat mapping of restoration alternatives for San Dieguito Lagoon,” submitted to Southern California Edison Company, 30 pp., + appen.

Jenkins, S. A. & J. Wasyl, 1999a, Performance and Optimization of the Mixed Habitat Plan in Long-Term Inundations Simulation, submitted to Southern *California Edison Co.*, 62 pp. + 8 appens.

Jenkins, S. A. & J. Wasyl, 1999b, Long-Term Inundation Simulations of Alternative Restoration Plans* for the San Dieguito Lagoon, CA, submitted to *Southern California Edison Co.*, 57 pp.

Jenkins, S. A. & J. Wasyl, 1999c, Long-Term Tidal Inundation Frequency Analysis for Credit Evaluation of the San Dieguito Lagoon Restoration Alternatives, submitted to *Southern California Edison Co.*, 10 pp. + 8 appens.

Jenkins, S. A., M. Josselyn & J. Wasyl, 1999, Hydroperiod and Residence Time Functions for Habitat Mapping of Restoration Alternatives for San Dieguito Lagoon, submitted to *Southern California Edison Co.*, 30 pp. + 1 appen.

Jenkins, S. A. and J. Wasyl, 2001, Agua Hedionda Lagoon North Jetty Resoration Project: Sand Influx Study, submitted to Cabrillo Power LLC., 178 pp. + appens.

Jenkins, S. A. and J. Wasyl, 2003, Sand Influx at Agua Hedionda Lagoon in the Aftermath of the San Diego Regional Beach Sand Project, submitted to Cabrillo Power LLC., 95 pp. + appens

Jenkins, S. A. and J. Wasyl, 2005, Hydrodynamic Modeling of Dispersion and Dilution of Concentrated Sea Water Produced by the Ocean Desalination Project at the Encina Power Plant, Carlsbad, CA. Part II: Saline Anomalies due to Theoretical Extreme Case Hydraulic Scenarios, submitted to Poseidon Resources, 97 pp.

Jenkins, S. A. and J. Wasyl, 2005, "Coastal evolution model," Scripps Institution of Oceanography, Tech.Rpt.No.58, 179pp.+appendices.
http://repositories.cdlib.org/sio/techreport/58/

Jenkins, S. A. and D. L. Inman, 2006, "Thermodynamic solutions for equilibrium beach profiles", *Jour. Geophys. Res.*, v.3, C02003, doi:10.1029, 21pp.

Josselyn, M. & A. Whelchel, 1999, "Determining the Upper Extent of Tidal Marsh Habitat San Dieguito Lagoon, submitted to *Southern California Edison Co.*, 16 pp.

Merkel, 2008, Batiquitos Lagoon Long-term Biological Monitoring Program Final Report, 2.0 Physical Evolution, submitted to Port of Los Angeles, 47 pp.

Leendertse, J. J., 1970, AA water quality model for well-mixed estuaries and coastal seas,@ vol. I, *Principles of Computation*, Memorandum RM-6230-RC, The Rand Corporation, Santa Monica, California, Feb. 1970.

Liebeck, R. H., 1976, "On the design of subsonic airfoils of high lift," paper no. 6463, McDonnell Douglas Tech. Report, 25 pp.Liebeck, R.H., and Ormsbee, A.I., "Optimization of Airfoils for Maximum Lift," *AIAA Journal of Aircraft*, v. 7, n. 5, Sept-Oct 1970.

McCormick, B., 1979, *Aerodynamics, Aeronautics and Flight Mechanics*, John Wiley & Sons, New York, 652 pp.

NOAA, 1998, "Verified/Historical Water Level Data"
http://www.opsd.nos.noaa.gov/data_res.html

SCE, 2005, “San Dieguito Wetlands Restoration Project, Final Restoration Plan” submitted to California Coastal Commission, prepared by Southern California Edison Company, November, 2005, 265 pp.

Stratford, B.S., 1959, The Prediction of Separation of the Turbulent Boundary Layer, *Jour. Fluid Mech.*, v. 5, pp. 1-15.

Stratford, B.S., 1959, An Experimental Flow with Zero Skin Friction Throughout its Region of Pressure Rise, *Jour. Fluid Mech.*, v. 5, pp. 16-23.

Appendix B

Chang Consultants. 2010. Hydraulic and Scour Studies for Proposed Interstate 5 Bridge Widening across Three Lagoons. Prepared by Chang Consultants PO Box 9492 Rancho Santa Fe, CA 92067 148 pp.

.

Hydraulic and Scour Studies for Proposed Interstate 5 Bridge Widening across Three Lagoons

Prepared for WRA
Environmental Consultants
San Rafael, CA 94901

Prepared by Howard H. Chang
Ph.D., P.E.
July 2010

CHANG Consultants

Hydraulic and Hydrologic Engineering
Erosion and Sedimentation

P.O. Box 9492
6001 Avenida Alteras
Rancho Santa Fe, CA 92067-4492
TEL: (858) 756-9050, (858) 692-0760
FAX: (858) 756-9460

This Page Left Intentionally Blank

TABLE OF CONTENTS

EXECUTIVE SUMMARY……. 1
I. INTRODUCTION…….. 3
Guidelines for Bridge Hydraulics …… 3
Effective Flow Area and Ineffective Flow Area …… 4

II. HYDRAULIC STUDY FOR INTERSTATE 5 BRIDGE ACROSS AGUA HEDIONDA LAGOON…….5
Hydrology…… 11
Hydraulic Analysis…….. 11
Water-Surface Profiles for Stream Channel …….. 11
Hydrologic Data Summary……. 24
Bridge Scour …….. 24

III. HYDRAULIC STUDY FOR INTERSTATE 5 BRIDGE ACROSS BATIQUITOS LAGOON…… 25
Geometric Features of I-5 Bridge across Batiquitos Lagoon …… 28
Hydrology…….. 33
Hydraulic Analysis……. 33
Water-Surface Profiles for Stream Channel …….. 33
Hydrologic Data Summary …… 42
Bridge Scour …….. 43

IV. HYDRAULIC STUDY FOR INTERSTATE 5 BRIDGE ACROSS SAN DIEGUITO RIVER……. 44
The I-5 Bridge on the San Dieguito River…….. 48
Hydrology of the San Dieguito River …… 51
Hydraulics for I-5 Bridge on the San Dieguito River …… 52
Hydrologic Data Summary …… 61

V. SCOUR STUDY FOR THE INTERSTATE 5 BRIDGE……. 63
Mathematical Model for General Scour……. 63
Selection of the Engelund-Hansen Formula …… 65
Engelund-Hansen Formula …… 65
Simulated Results on Scour …….. 66
Local Scour around Piers/Bents……. 67

REFERENCES…….. 68

APPENDIX A. HEC-RAS REPORT FOR THE HYDRAULIC STUDY…….70

APPENDIX B. INPUT/OUTPUT DESCRIPTIONS OF FLUVIAL-12……130

ATTACHMENTS. Computer files for FLUVIAL-12 and HEC-RAS

This Page Left Intentionally Blank

EXECUTIVE SUMMARY

Caltrans has made plans to widen the Interstate 5 Bridges in the County of San Diego. This report presents hydraulics studies have been performed for the bridges across Agua Hedionda Lagoon, Batiquitos Lagoon, and the San Dieguito River, covering the existing conditions and proposed bridge alternatvies. A scour study has also been made for the I-5 Bridge across the San Dieguito River. The project goal is to evaluate bridge alternatives and to achieve a bridge plan without adverse impacts on the stream channel while beneficial for the environment.

The studies performed for the hydraulic and scour studies are in accordance with the Caltrans Local Assistance Procedure Manual, the Army Corps of Engineers and the Federal Emergency Management Agency (FEMA) requirements. These studies provide bridge hydraulics as well as channel bed scour at the bridge footings. The information is essential for the design of bridge while providing evaluation of project impacts.

The objective of bridge alternatives is to achieve the maximum possible reduction in tidal muting. The largest incremental reduction in tidal muting occurs with the first few increments of widening of channel plane (free space) beneath the bridge. Thereafter, each additional increment of channel plane produces smaller and smaller reductions in tidal muting while the length of bridge free span and attendant cost increases.

Bridge modifications were made in consideration of several considerations. According to Caltrans, the channel bottom under the bridges can be lowered as long as it is not filled right back up by sediment deposition. The bed armoring may also be set at a new depth, if needed. Vertical side walls for the channel are permissible. A bench on each side of the channel is required for pedestrian trail and wildlife crossing. Adequate clearance between the bench and the bridge deck needs to be maintained. The bench should be at least 12 feet in width, but a 16-foot side bench is considered more desirable.

The alternatives for modification of bridges over Agua Hedionda Lagoon and Batiquitos Lagoon were made in consideration of the conditions stated above. The bridge openings for flow passage will be enlarged while the same bridge spans will be maintained. The detailed hydraulic geometries for the bridges are provided. Water-surface profiles and flow velocities for the bridges were computed using the HEC-RAS program for existing conditions and proposed bridge modifications using the 100-yr flood. The bridge modifications will lower the 100-yr flood level and at the same time improve the tidal flow. The two bridges have armored bottoms; therefore, the channel beds at these bridge crossings are not subject to scour.

For the I-5 Bridge on the San Dieguito River, bridge roadway will be widened for additional lanes but the bridge opening for flow passage will remain the same. For the proposed bridge design, studies have been made for bridge hydraulics and potential scour at the bridge crossing. The 50-yr and 100-yr flood were included in hydraulic computations for the existing channel conditions as well as the proposed conditions.

Bridge hydraulics consists of hydraulic calculations for flood levels and flow velocities under the 50-yr, 100-yr, and overtopping floods as required in the hydrologic data summary. Water-surface profiles and flow velocities for the bridge were computed using the HEC-RAS program for existing conditions and proposed bridge design. A goal of the project was to keep

the computed 100-yr water-surface elevations for the proposed design no higher than those for the existing conditions. Another goal was to avoid any adverse flooding effects on neighboring properties. At the same time, it is necessary to pass the design flood without overtopping. The results show that the proposed bridge design will not result in a rise of the flood level. The 100-yr water surface stays well below the bridge low chord, sufficient to pass the floating debris.

For the scour study, an erodible boundary model, FLUVIAL-12 (Chang, 1988) was used. The scour study is to provide the information on general scour and local scour to be used for the design of the bridge. The 100-yr flood was used to simulate sediment transport and stream channel changes for the lower San Dieguito River under the proposed bridge plan. Simulated results are presented in graphical forms showing the changes in channel cross section at the bridge crossing. The cross-sectional profile for maximum general scour at the bridge crossing is also shown. The minimum bed elevation reached by general scour during the 100-yr flood is simulated to reach the bed elevation of -5.2 feet. Local scour depths at the bridge piers (or bents) have also been computed for several pier widths (or diameters). The scour information is needed for bridge design.

Hydraulic and Scour Studies for Proposed Interstate 5 Bridge Widening across Three Lagoons

I. INTRODUCTION

Caltrans has made plans to widen the Interstate 5 Bridges in the County of San Diego. Such bridges cross the San Dieguito River, San Elijo Lagoon, Batiquitos Lagoon, Agua Hedionda Lagoon, Buena Vista Lagoon, and Los Penasquitos Lagoon. This report has been prepared to provide hydraulic and scour studies for the bridge alternatives for the proposed I-5 Bridge widening at selected locations. The studies were conducted for the San Dieguito River Bridge, the Batiquitos Lagoon Bridge, and Agua Hedionda Lagoon Bridge.

The work performed for the hydraulic and scour studies are in accordance with the Caltrans Local Assistance Procedure Manual, the Army Corps of Engineers and the Federal Emergency Management Agency (FEMA) requirements. The project goal is to evaluate project alternatives and to achieve a bridge plan without adverse impacts on the stream channel while beneficial for the environment. To be more specific, the project must meet the following conditions:

No increased bridge scour
No increase in flood plain elevation
No erosion of least tern islands or other in-place restoration features
No adverse affects on state and federal listed plants or animals
No net general scour or stream bed erosion
No reduction in conveyance of fluvial sediments through the lagoon
No increase in maintenance beyond what existing bridge waterways require
Accommodation of I-5 widening dimensions
Protection of existing Infrastructure (gas pipelines, power lines phone and fiber optic cables)
Favorable Cost/Benefit Ratio.

This study provides modeling of bridge hydraulics as well as channel bed scour at the bridge footings. The information is essential for the design of bridge widening while providing evaluation of project impacts.

Guidelines for Bridge Hydraulics - For bridge hydraulics, a computer model, such as HEC-2 or HEC-RAS is used to perform hydraulic computations to provide:

(1) Water-surface elevations,
(2) Flow velocities, and
(3) Overtopping flow.

For this project, water-surface profiles and flow velocities for the bridges are computed using the HEC-RAS program for existing conditions and proposed bridge widening. A goal of the project is to keep the computed 100-yr water-surface elevations for the proposed conditions no higher than those for the existing conditions. Another goal is to avoid any adverse flooding effects on neighboring properties. At the same time, it is necessary to pass the design flood without overtopping.

The selected design must meet the requirements, regulations, and policies set by FEMA and the Executive Order 11988 (Federal Policy on Floodplain Management), including:

(1) Conveyance of the base flood, Q_{100}.
(2) Backwater caused by the bridge encroachment with that caused by all other obstructions is limited to one foot above the surface of the base flood.

The design flood for the bridge was determined in accordance with Caltrans Local Assistance Manual, Chapter 11 "Design Standards", Caltrans Memorandum to Designers I-23, and the Highway Design Manual, Section 821.3 "Selection of Design Flood". The 100-yr flood was included in hydraulic computations for the existing channel conditions as well as the proposed conditions. The 50-yr food, if available, would also be used.

A general guideline for the hydraulic design of bridges is that they should pass the 50-yr flood with adequate freeboard to pass anticipated drift. Typically two feet of freeboard above the 50-yr water surface elevation is adequate for the area. The bridge should also be able to convey the 100-yr flood.

Effective Flow Area and Ineffective Flow Area -The I-5 Bridges across the lagoons in San Diego County usually have small spans in comparison to the large lagoon widths. Distribution of flow velocity in a lagoon near the bridge is not uniform, as illustrated in Figure 1. This velocity distribution was simulated using the two-dimensional hydrodynamic model FESWNS (Federal Highway Administration, 1992). Based on the velocity distribution, the broad floodplain or lagoon can be divided into an effective flow area and an ineffective flow area. The effective flow area has significant flow velocities and it contributes to the conveyance of most of the flow discharge. The ineffective flow area, on the other hand, has very small flow velocities and it does not contribute significantly to the conveyance of the flow discharge. The effective flow area as delineated using the FESWNS model is shown in the figure to be within the boundaries designated by dashed lines; it is along the main channel of the river and it passes through the bridge openings. The ineffective flow area is outside the effective flow area.

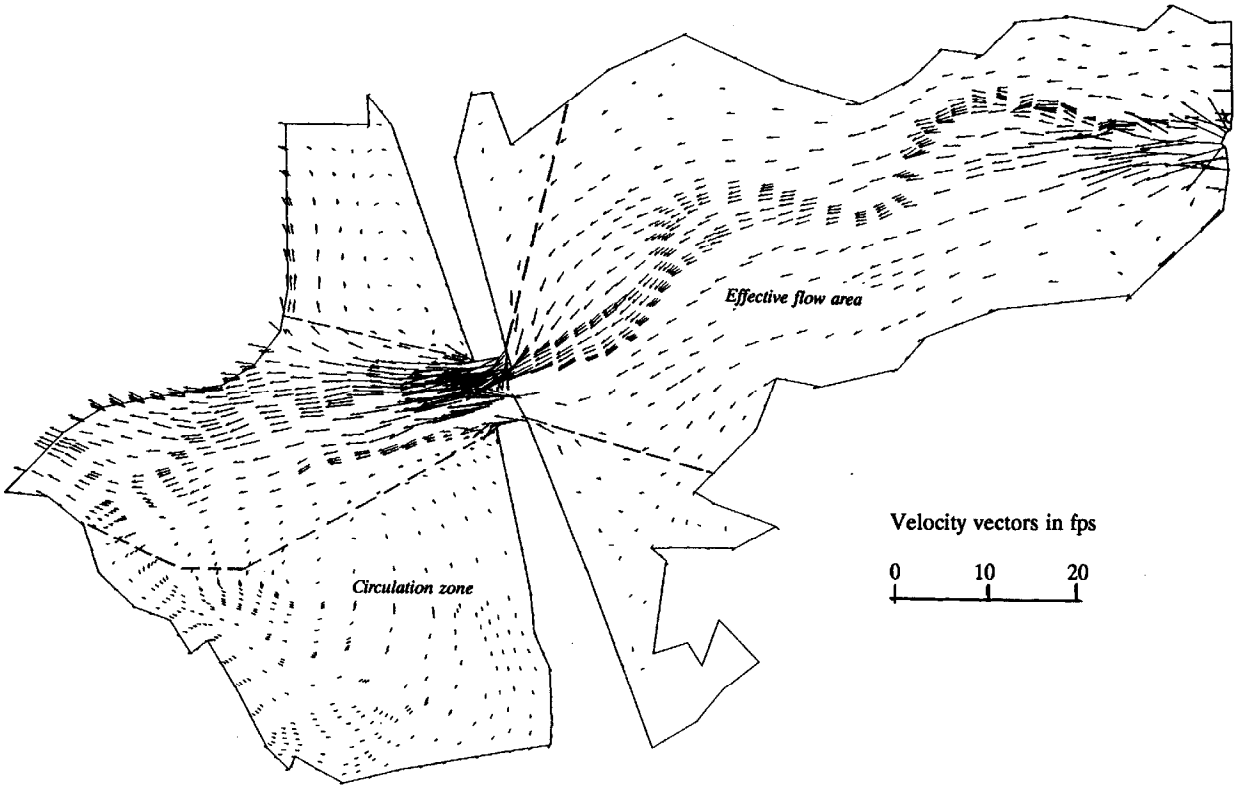

Figure 1. Sample two-dimensional velocity distribution in the floodplain showing effective and ineffective flow areas (Q = 20,000 cfs)

II. HYDRAULIC STUDY FOR INTERSTATE 5 BRIDGE ACROSS AGUA HEDIONDA LAGOON

Agua Hedionda Lagoon is at the downstream end of Agua Hedionda Creek and its tributary Calavera Creek. The lagoon has been improved for public fishing at the downstream end near Carlsbad Boulevard. The Interstate 5 Bridge crosses Agua Hedionda Lagoon 6.2 miles from the stream mouth. Figure 2 is a Google image of the lagoon. Figure 3 is the I-5 Bridge viewed toward downstream and Figure 4 is a view of the bridge toward upstream.

The Agua Hedionda Lagoon bathymetry as shown in Figure 5 was prepared from bathmetry data taken in the lagoon between 1997 and 2007. The 2007 survey data are for the bathymetry no higher than -2 ft NGVD. The 2004 data was used for the bathymetry between -2 ft NGVD and 0 ft NGVD. The 1997 survey was used to fill in the higher contours up to + 4 ft NGVD.

Figure 2. Google image of Agua Hedionda Lagoon

Figure 3. View of the I-5 Bridge toward downstream

Figure 4. View of the I-5 Bridge toward upstream

Plans from Caltrans planning study for the existing I-5 Bridge across Agua Hedionda Lagoon are shown in Figure 6. Many geometric features of the existing bridge are given in the plans. Specification for the I-5 Bridge are given in Caltrans drawings entitled "Planning Study, Agua Hedionda Creek Bridge (Replace)" designed by and drawn by Gary Hight, September 2004. A bridge modification is proposed for the purpose of improving tidal flow through the bridge opening in order to enhance the wetland in the east lagoon. The cross-sectional profiles for existing bridge and the proposed alternative are shown in Figures 7 and Figure 8, respectively. The specifications of the existing bridge and the proposed alternative for bridge modification are listed below: All elevations are based on the NGVD datum.

Length of proposed bridge span, along I-5 (from piles, lines EB - BB): 52 m (170.61 ft)
Length of proposed bridge span (from edges of structure): 70.1 m (230 ft)
Width of existing bridge deck, across I-5: (157.5 ft)
Width of proposed bridge deck: 77 m (252.9 ft)
Bridge low chord elevation: 27.2 feet at south end, 21.1 feet at north end
Elevation of existing armored bed: -6.56 m (-21.52 ft NGVD)
Elevation of proposed armored bed: -12.9 feet
Bed width of existing trapezoidal channel at bottom: (32.31 ft)
Bed width of proposed trapezoidal channel at bottom: (99.1 ft)
Bed width of proposed trapezoidal channel at sediment fill: close to 120 feet
Side slope of existing trapezoidal channel: 1.5 to 1
Side slope of proposed trapezoidal channel: 1 to 1
Seven bridge spans with six sets of cylindrical piers.

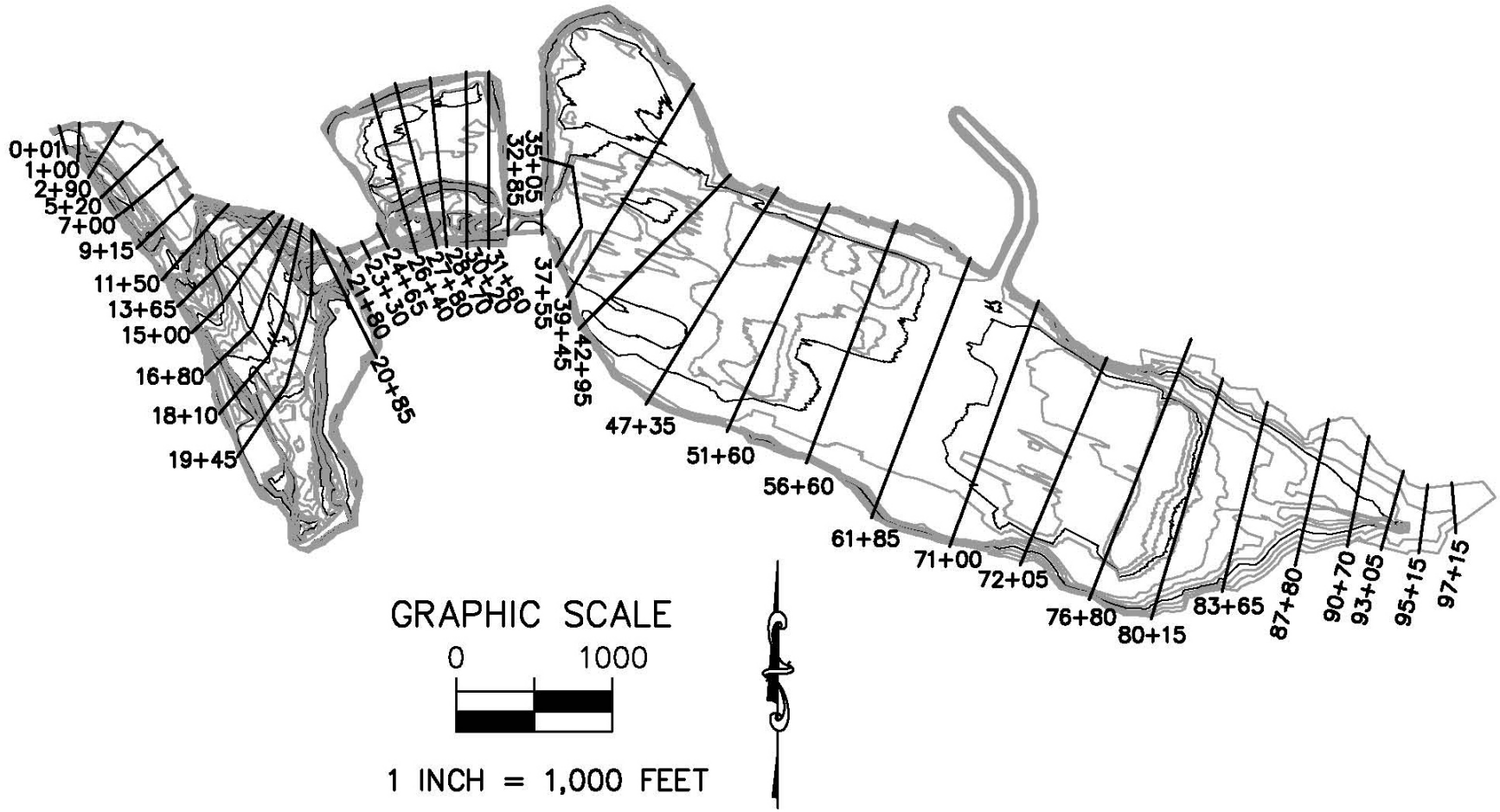

Figure 5. Bathymetry of Agua Hedionda Lagoon

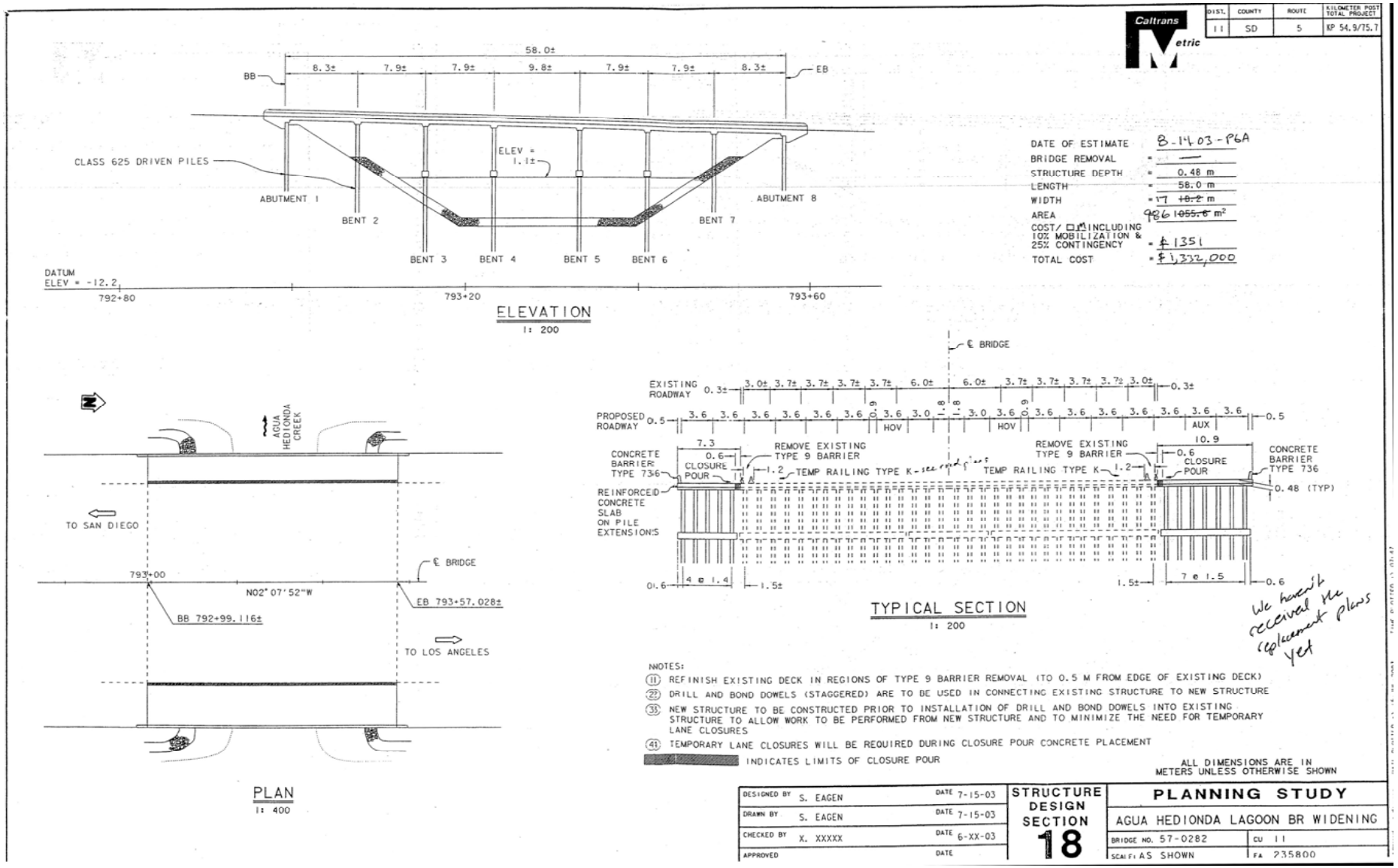

Figure 6. Plans for I-5 Bridge across Agua Hedionda Lagoon from Caltrans planning study

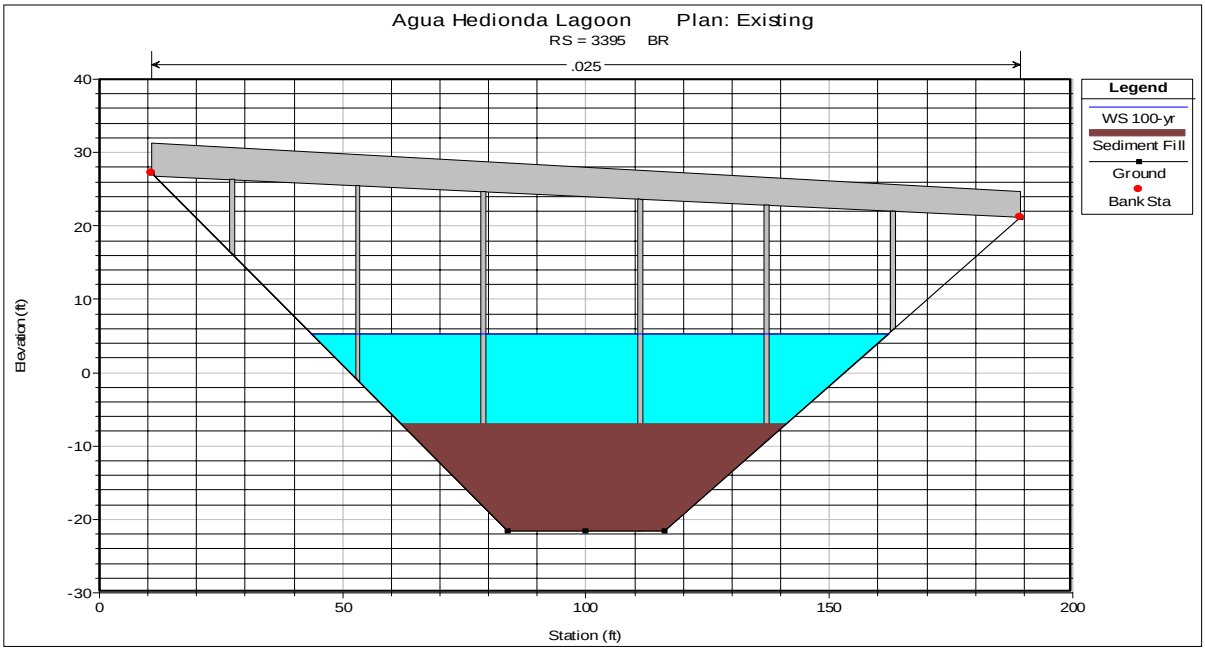

Figure 7. Cross-sectional profile of existing I-5 Bridge across Agua Hedionda Lagoon

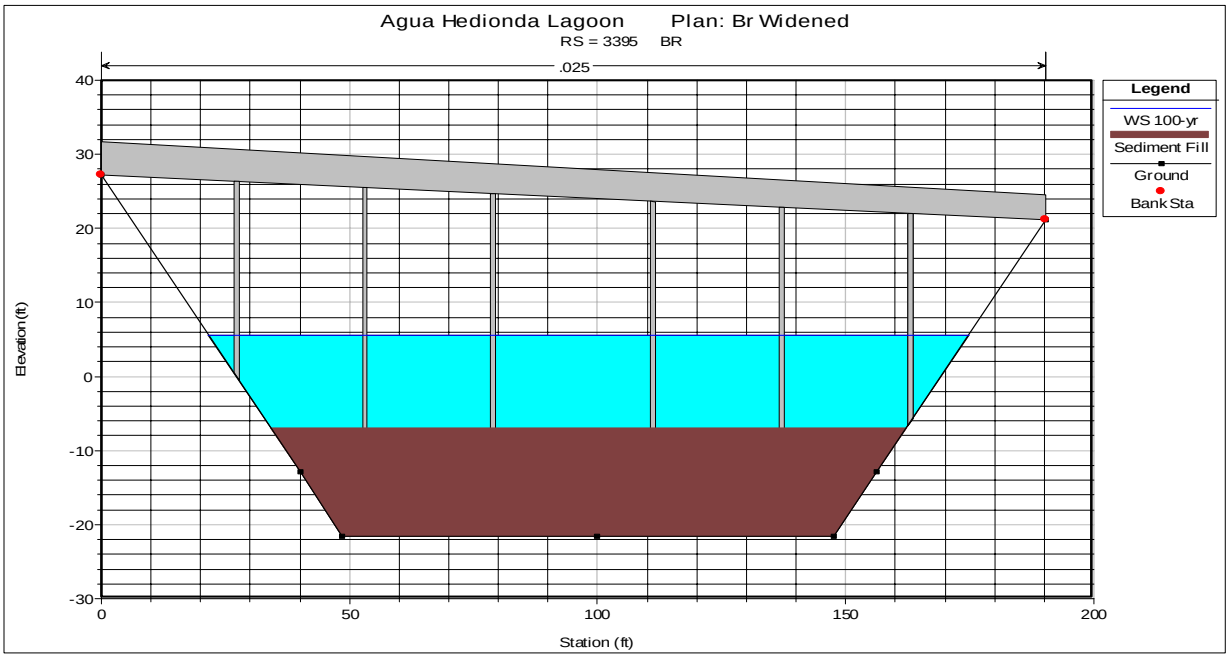

Figure 8. Cross-sectional profile of proposed alternative for bridge modification for I-5 Bridge across Agua Hedionda Lagoon

Hydrology – Agua Hedionda Creek drains a watershed area of 29 square miles. According to the report "Flood Insurance Study for San Diego County, California", 1999, by FEMA, the 100-yr discharge of Agua Hedionda Creek at El Camino Real is 9,850 cfs. According to the report "Flood Plain Information, Agua Hedionda Creek", 1973, by the U.S. Army Corps of Engineers, Los Angeles District, the 100-yr flood discharge for Agua Hedionda Lagoon is 10,500 cfs. The 50-yr flood for the lagoon is not available.

Hydraulic Analysis - The HEC-RAS computer program was used to compute water-surface profiles and velocities through the lagoon and the bridges for the existing conditions as well as the proposed conditions. Topographic map with the bathymetry of Agua Hedionda Lagoon is shown in Figure 5, which also has cross sections for the hydraulic analysis. Important locations and their respective channel stations are listed in Table 1.

Table 1. List of important locations along Agua Hedionda Lagoon

Points of interest	Location Feet
Lagoon mouth	0+01
Highway 101	1+00
Railroad Bridge	23+30
Interstate 5 Bridge	32+85 – 35+05
Upstream end of lagoon	97+15

The HEC-RAS study reach starts from downstream at station 0+01 and ends upstream at station 97+15. Results of the HEC-RAS computation are described below. A detailed hydraulic report is given in Appendix A.

Water-Surface Profiles for Stream Channel - Water-surface profiles for the existing and proposed conditions were computed using the 100-yr flood. The 50-yr flood was not used since it is not available. Results of the computation for the existing and proposed conditions are shown in Figure 9, which includes the longitudinal water-surface and channel-bed profiles. Figure 10 shows sample cross-sectional profiles of the lagoon with the computed water-surface profiles. In the cross-sectional profiles, the label "RS" is the River Station in feet. The roughness coefficient in terms of Manning's *n* is written above the picture frame.

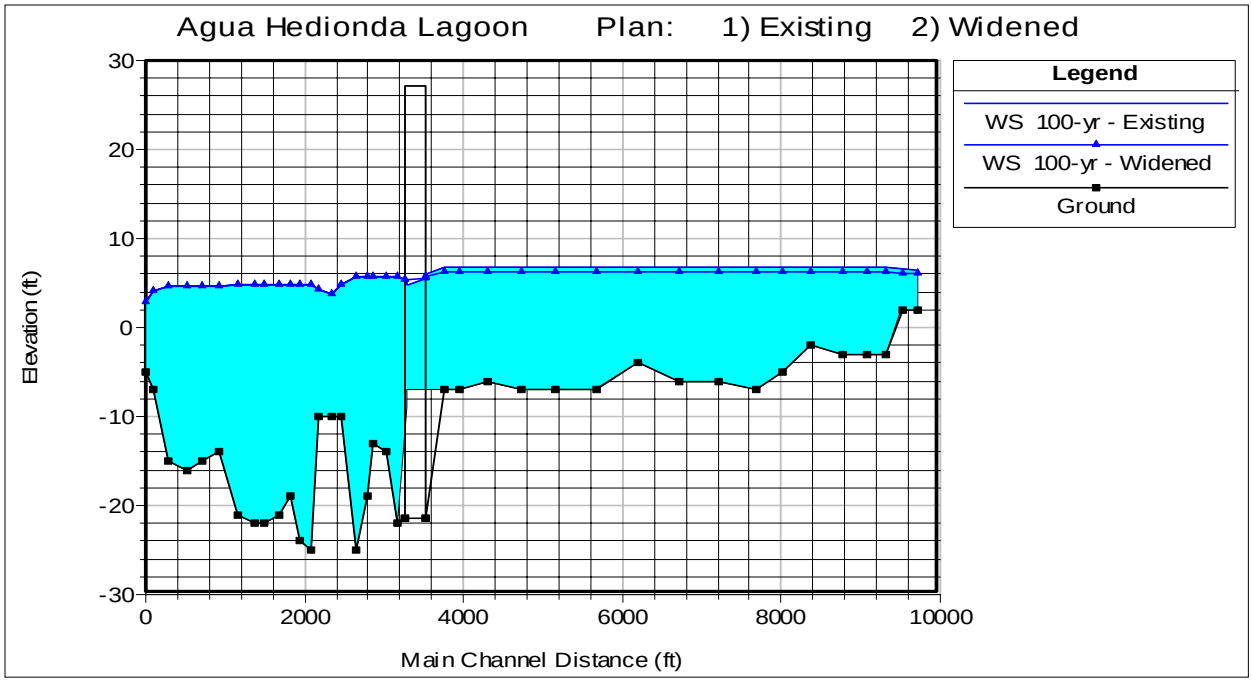

Figure 9. Water-surface and channel bed profiles for longtidinal section through Agua Hedionda Lagoon

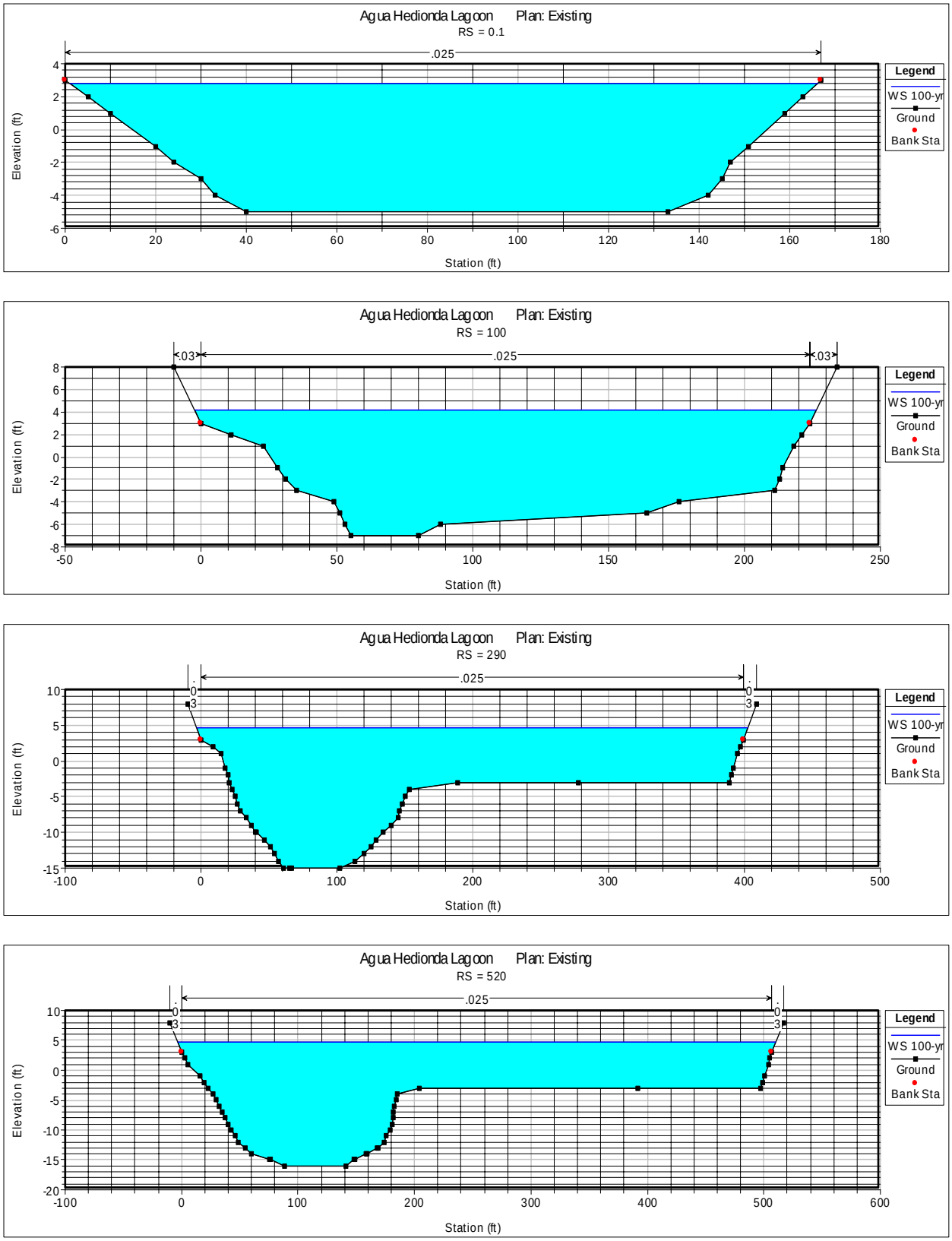

Figure 10. Cross-sectional profiles along Agua Hedionda Lagoon

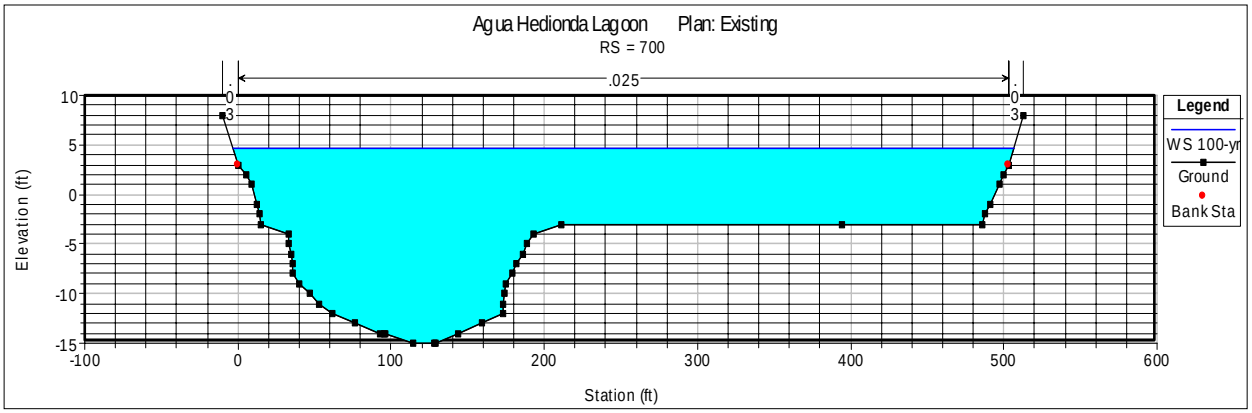

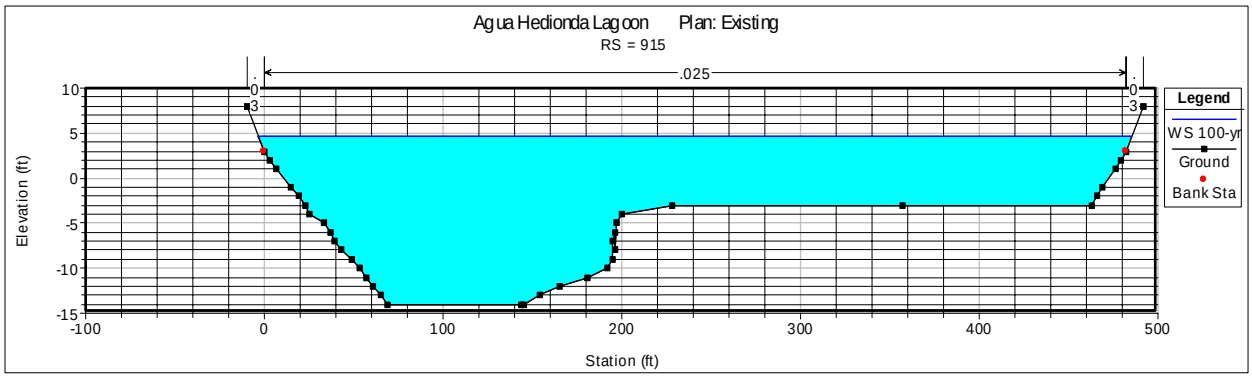

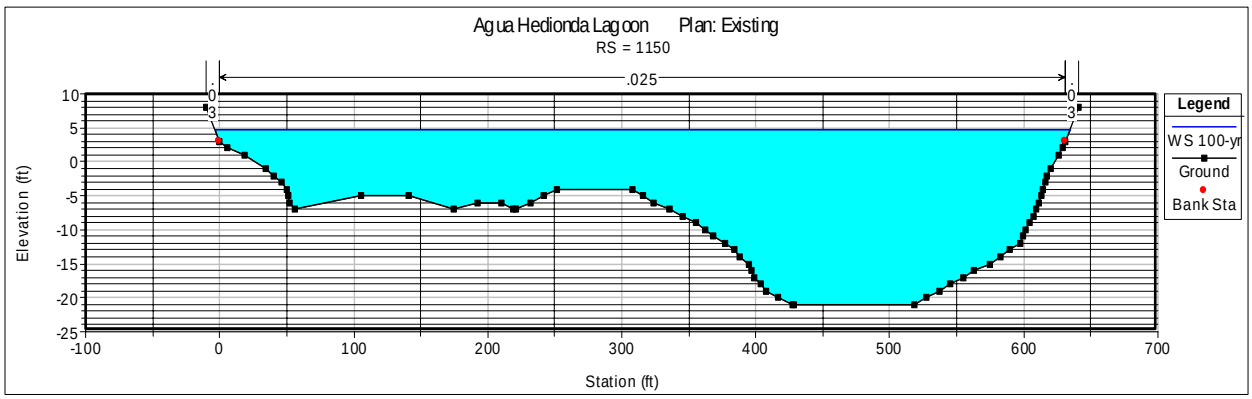

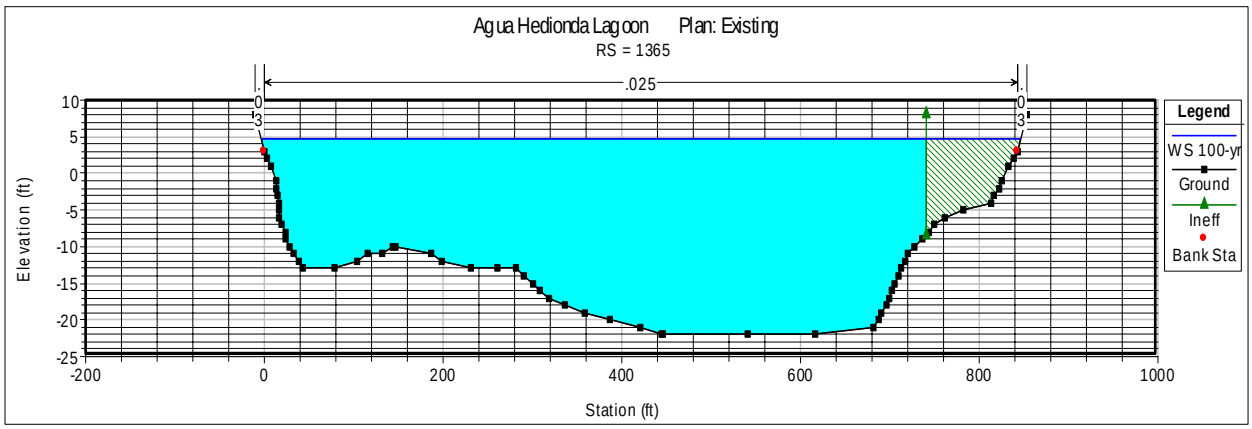

Figure 10 (continued). Cross-sectional profiles along Agua Hedionda Lagoon

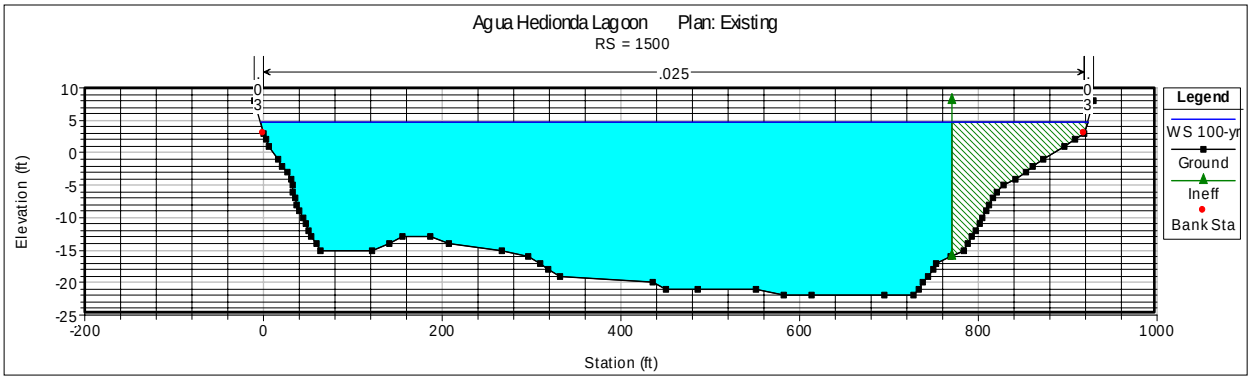

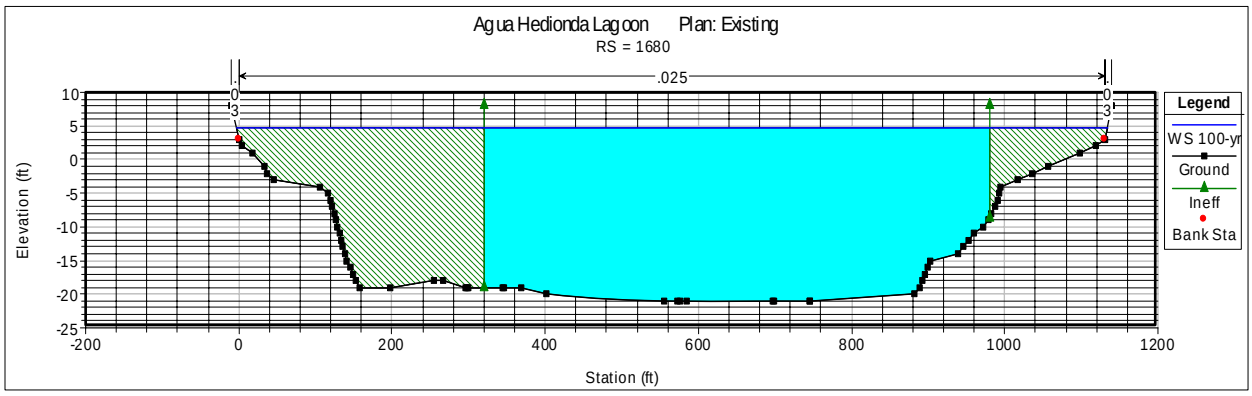

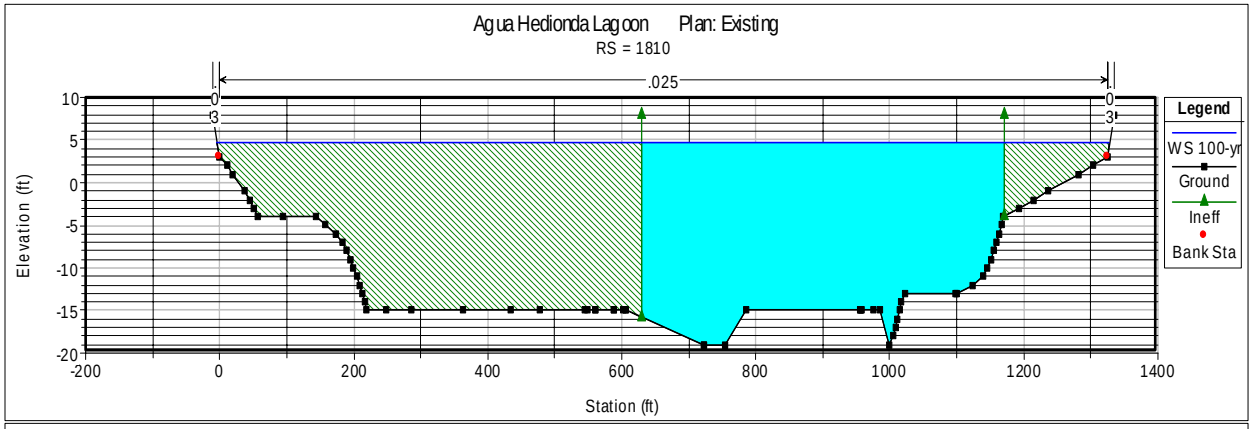

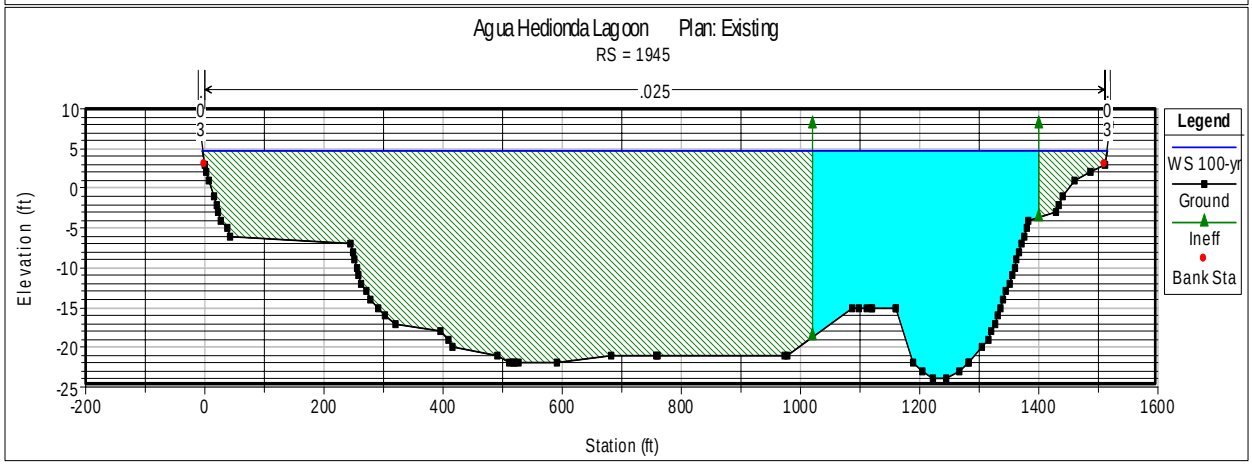

Figure 10 (continued). Cross-sectional profiles along Agua Hedionda Lagoon

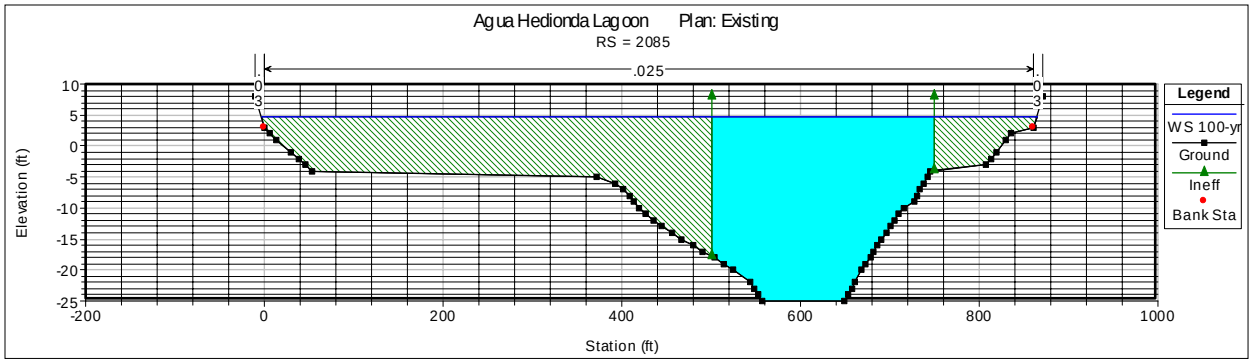

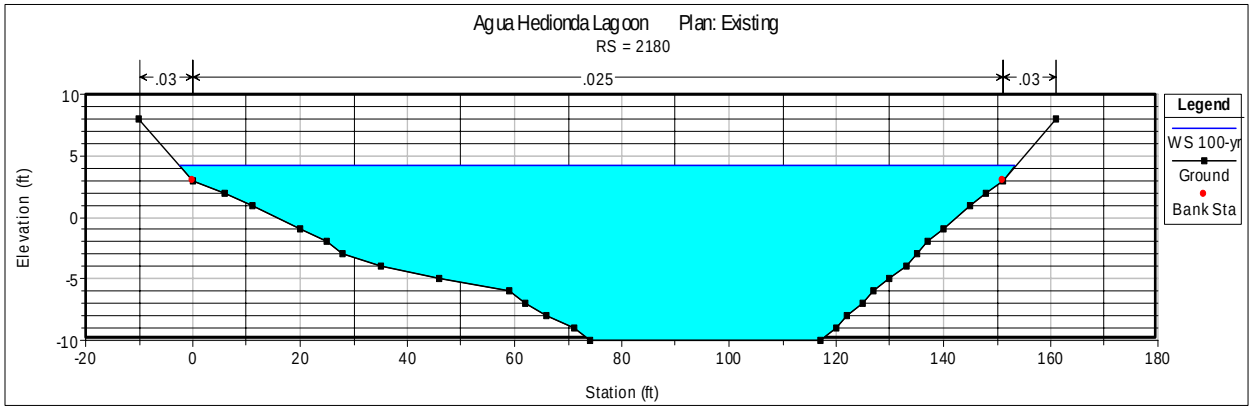

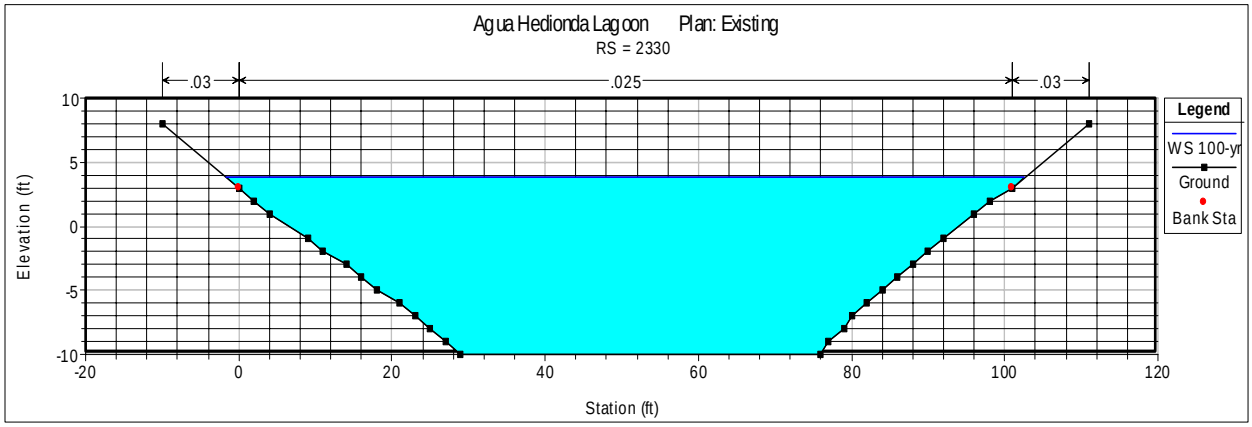

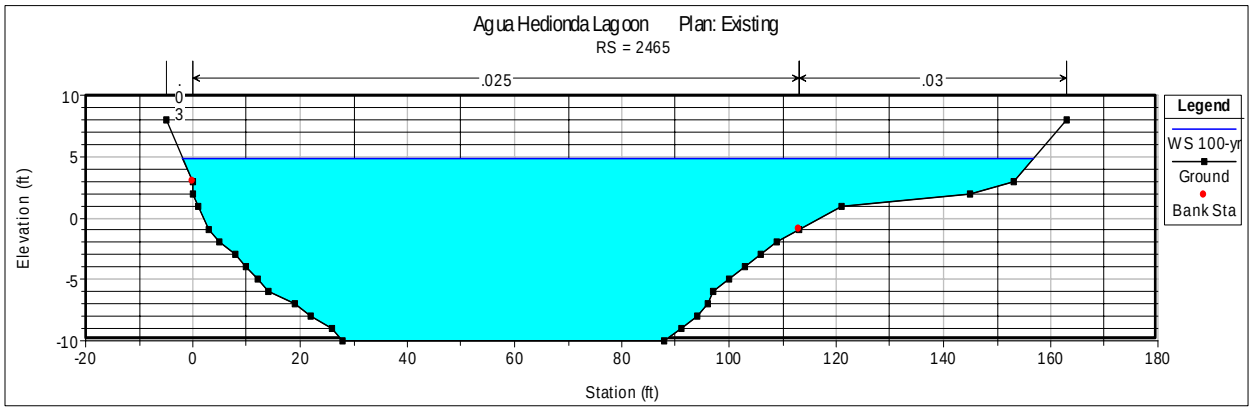

Figure 10 (continued). Cross-sectional profiles along Agua Hedionda Lagoon

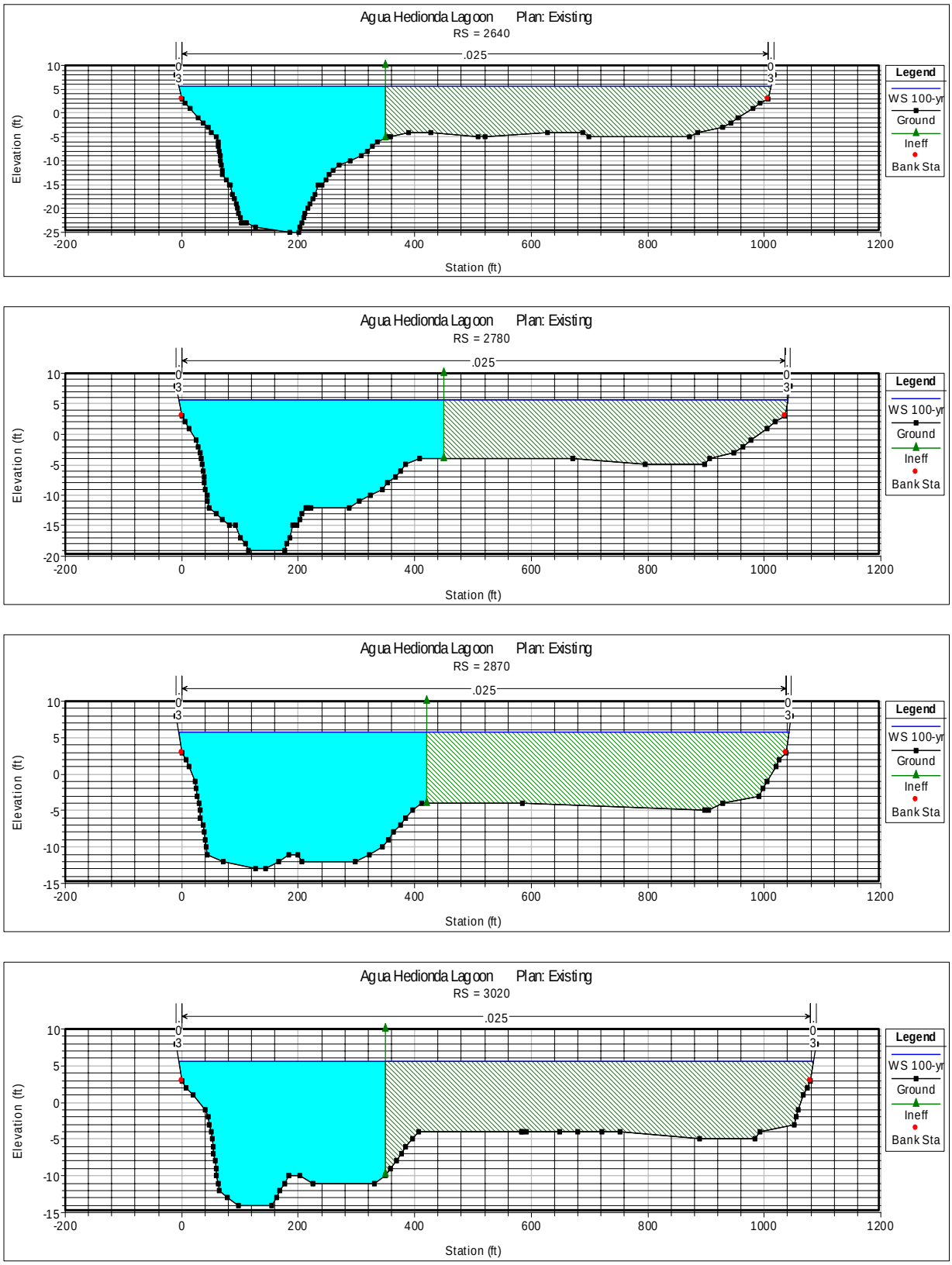

Figure 10 (continued). Cross-sectional profiles along Agua Hedionda Lagoon

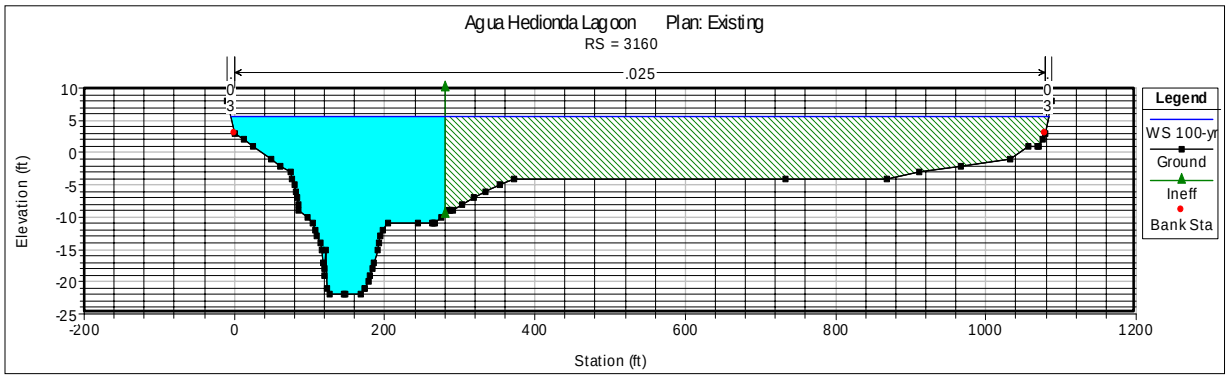

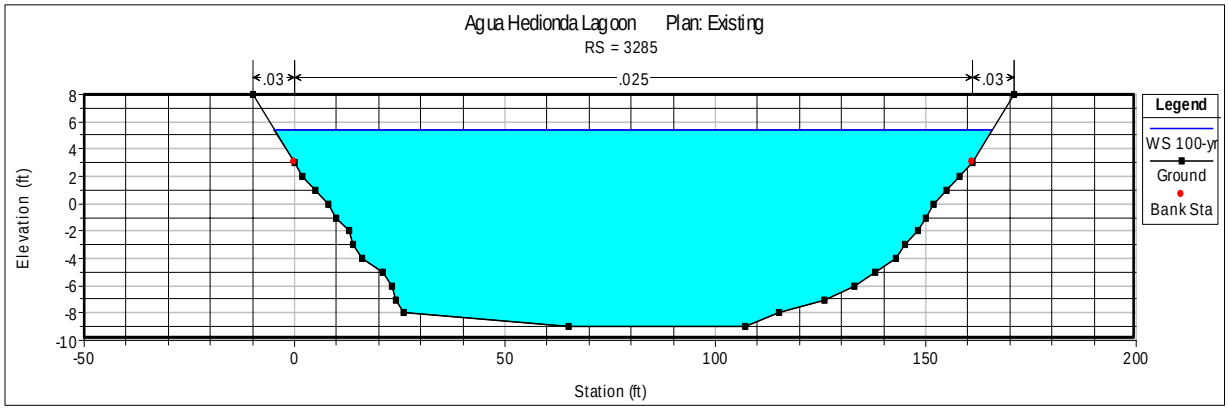

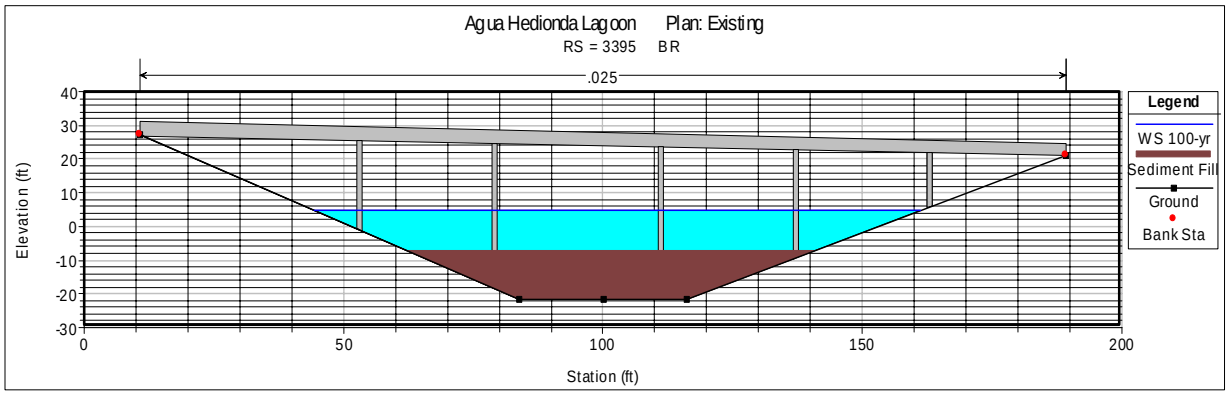

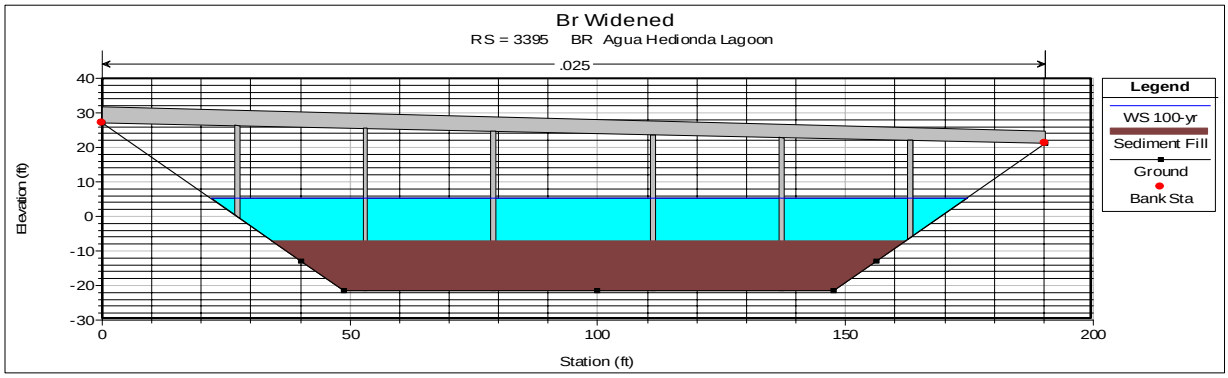

Figure 10 (continued). Cross-sectional profiles along Agua Hedionda Lagoon

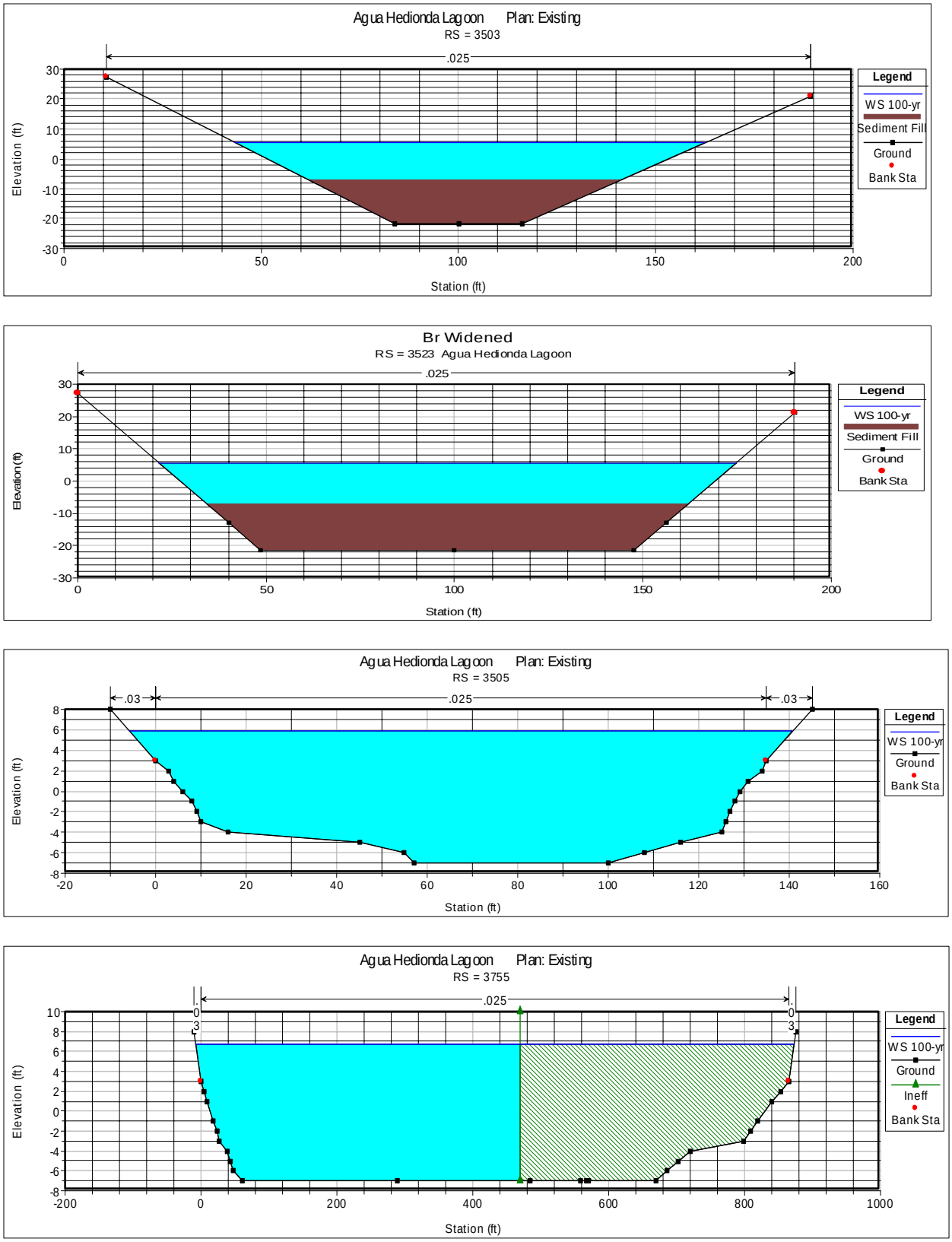

Figure 10 (continued). Cross-sectional profiles along Agua Hedionda Lagoon

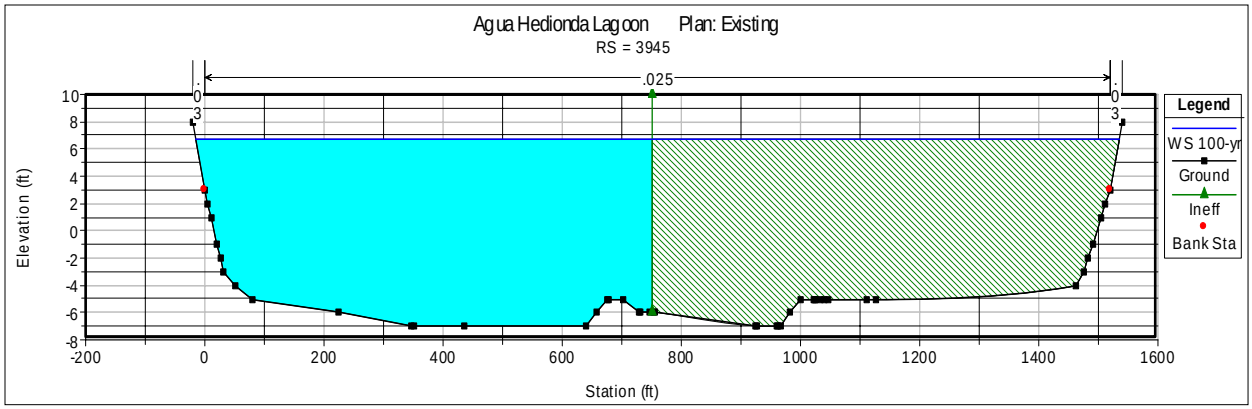

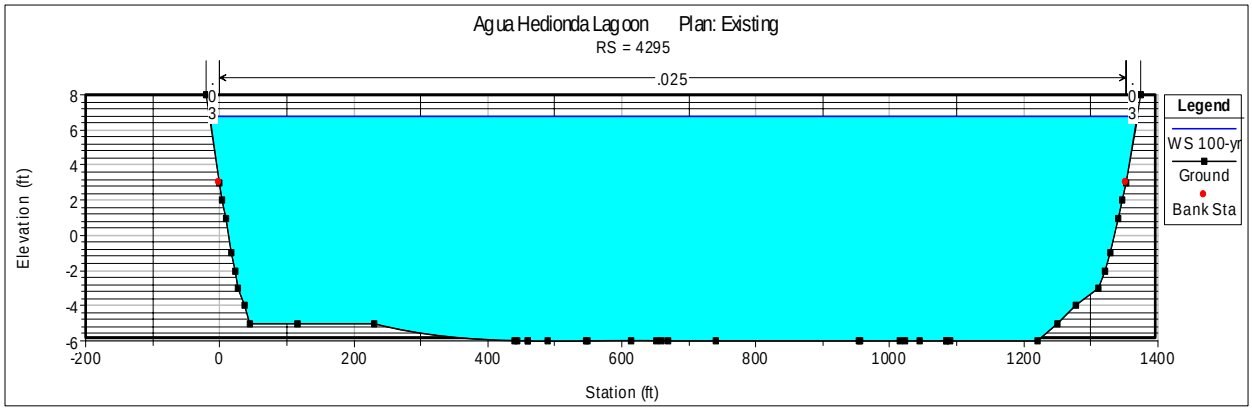

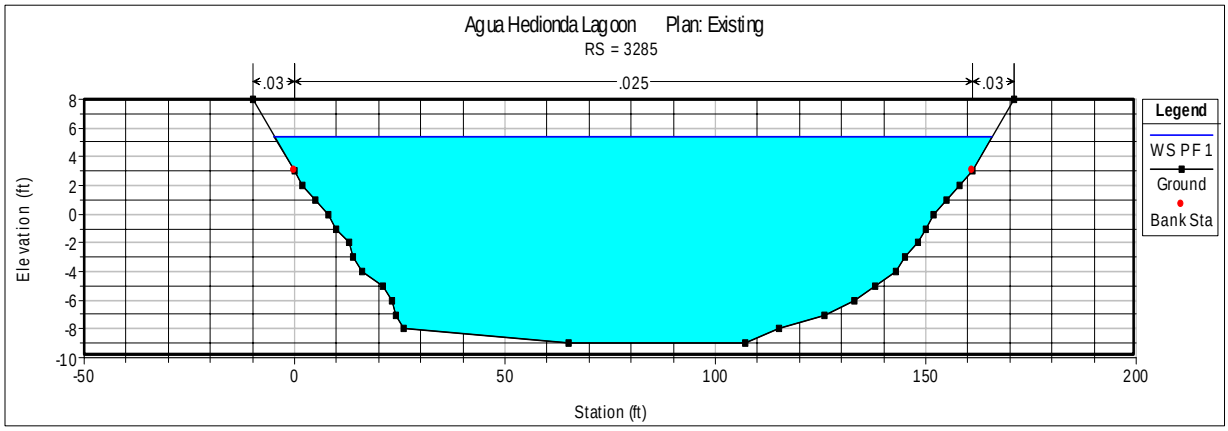

Figure 10 (continued). Cross-sectional profiles along Agua Hedionda Lagoon

Summary of the given and computed hydraulic parameters for the existing and proposed conditions are listed in Table 2. When the computed results for the existing and proposed conditions are compared, it can be seen that the proposed bridge alternative will not result in a rise of the 100-yr water-surface elevation.

Table 2. Summary of hydraulic parameters from hydraulic modeling

Sta	Profile	Plan	Q (cfs)	Bed El (ft)	W.S. (ft)	Vel (ft/s)	Width (ft)	Froude #
9715	100-yr	Existing	10500	2.00	6.21	10.44	306.23	0.95
9715	100-yr	Widened	10500	2.00	6.24	10.35	306.67	0.94
9515	100-yr	Existing	10500	2.00	6.40	6.22	437.08	0.54
9515	100-yr	Widened	10500	2.00	6.43	6.17	437.41	0.53
9305	100-yr	Existing	10500	-3.00	6.49	3.90	512.94	0.29
9305	100-yr	Widened	10500	-3.00	6.52	3.88	513.19	0.29
9070	100-yr	Existing	10500	-3.00	6.52	2.60	706.69	0.19
9070	100-yr	Widened	10500	-3.00	6.55	2.59	706.96	0.19
8780	100-yr	Existing	10500	-3.00	6.51	2.02	847.21	0.14
8780	100-yr	Widened	10500	-3.00	6.54	2.01	847.47	0.14
8365	100-yr	Existing	10500	-2.00	6.52	1.15	1211.90	0.07
8365	100-yr	Widened	10500	-2.00	6.55	1.15	1212.15	0.07
8015	100-yr	Existing	10500	-5.00	6.53	0.72	1572.23	0.04
8015	100-yr	Widened	10500	-5.00	6.56	0.72	1572.47	0.04
7680	100-yr	Existing	10500	-7.00	6.53	0.57	1618.23	0.03
7680	100-yr	Widened	10500	-7.00	6.56	0.57	1618.47	0.03
7205	100-yr	Existing	10500	-6.00	6.53	0.66	1408.20	0.03
7205	100-yr	Widened	10500	-6.00	6.56	0.65	1408.45	0.03
6705	100-yr	Existing	10500	-6.00	6.52	0.58	1638.10	0.03
6705	100-yr	Widened	10500	-6.00	6.55	0.58	1638.22	0.03
6185	100-yr	Existing	10500	-4.00	6.52	0.61	1735.17	0.03
6185	100-yr	Widened	10500	-4.00	6.55	0.60	1735.42	0.03
5660	100-yr	Existing	10500	-7.00	6.52	0.58	1614.16	0.03
5660	100-yr	Widened	10500	-7.00	6.55	0.58	1614.40	0.03

5160	100-yr	Existing	10500	-7.00	6.52	0.55	1541.15	0.03
5160	100-yr	Widened	10500	-7.00	6.55	0.55	1541.39	0.03
4735	100-yr	Existing	10500	-7.00	6.52	0.56	1583.13	0.03
4735	100-yr	Widened	10500	-7.00	6.55	0.56	1583.38	0.03
4295	100-yr	Existing	10500	-6.00	6.77	0.64	1384.65	0.03
4295	100-yr	Widened	10500	-6.00	6.26	0.67	1380.42	0.03
3945	100-yr	Existing	10500	-7.00	6.75	1.10	1549.76	0.05
3945	100-yr	Widened	10500	-7.00	6.25	1.15	1545.63	0.06
3755	100-yr	Existing	10500	-7.00	6.72	1.69	879.88	0.08
3755	100-yr	Widened	10500	-7.00	6.21	1.76	877.85	0.09
3523	100-yr	Widened	10500	-7.00	5.65	5.90	153.31	0.31
3505	100-yr	Existing	10500	-7.00	5.85	7.27	146.40	0.39
3503	100-yr	Existing	10500	-7.00	5.53	8.46	119.25	0.46
3395		Bridge						
3287	100-yr	Existing	10500	-7.00	4.84	9.05	117.05	0.51
3285	100-yr	Existing	10500	-9.00	5.40	5.55	170.59	0.29
3285	100-yr	Widened	10500	-9.00	5.40	5.55	170.59	0.29
3269	100-yr	Widened	10500	-7.00	5.33	6.07	152.66	0.32
3160	100-yr	Existing	10500	-22.0	5.66	2.32	1089.11	0.10
3160	100-yr	Widened	10500	-22.0	5.66	2.32	1089.11	0.10
3020	100-yr	Existing	10500	-14.0	5.68	1.92	1089.70	0.09
3020	100-yr	Widened	10500	-14.0	5.68	1.92	1089.70	0.09
2870	100-yr	Existing	10500	-13.0	5.68	1.60	1047.74	0.07
2870	100-yr	Widened	10500	-13.0	5.68	1.60	1047.74	0.07
2780	100-yr	Existing	10500	-19.0	5.69	1.41	1045.76	0.06
2780	100-yr	Widened	10500	-19.0	5.69	1.41	1045.76	0.06
2640	100-yr	Existing	10500	-25.0	5.68	1.52	1016.73	0.06
2640	100-yr	Widened	10500	-25.0	5.68	1.52	1016.73	0.06
2465	100-yr	Existing	10500	-10.0	4.87	7.13	158.62	0.35
2465	100-yr	Widened	10500	-10.0	4.87	7.13	158.62	0.35

2330	100-yr	Existing	10500	-10.0	3.81	10.24	104.25	0.57
2330	100-yr	Widened	10500	-10.0	3.81	10.24	104.25	0.57
2180	100-yr	Existing	10500	-10.0	4.22	7.28	155.88	0.42
2180	100-yr	Widened	10500	-10.0	4.22	7.28	155.88	0.42
2085	100-yr	Existing	10500	-25.0	4.76	1.74	868.04	0.06
2085	100-yr	Widened	10500	-25.0	4.76	1.74	868.04	0.06
1945	100-yr	Existing	10500	-24.0	4.77	1.27	1518.10	0.05
1945	100-yr	Widened	10500	-24.0	4.77	1.27	1518.10	0.05
1810	100-yr	Existing	10500	-19.0	4.78	0.99	1331.12	0.04
1810	100-yr	Widened	10500	-19.0	4.78	0.99	1331.12	0.04
1680	100-yr	Existing	10500	-21.0	4.79	0.66	1137.14	0.02
1680	100-yr	Widened	10500	-21.0	4.79	0.66	1137.14	0.02
1500	100-yr	Existing	10500	-22.0	4.79	0.61	926.14	0.02
1500	100-yr	Widened	10500	-22.0	4.79	0.61	926.14	0.02
1365	100-yr	Existing	10500	-22.0	4.78	0.67	850.14	0.03
1365	100-yr	Widened	10500	-22.0	4.78	0.67	850.14	0.03
1150	100-yr	Existing	10500	-21.0	4.77	1.14	638.08	0.05
1150	100-yr	Widened	10500	-21.0	4.77	1.14	638.08	0.05
915	100-yr	Existing	10500	-14.0	4.72	2.04	488.86	0.11
915	100-yr	Widened	10500	-14.0	4.72	2.04	488.86	0.11
700	100-yr	Existing	10500	-15.0	4.71	2.0	509.83	0.11
700	100-yr	Widened	10500	-15.0	4.71	2.0	509.83	0.11
520	100-yr	Existing	10500	-16.0	4.70	1.91	513.81	0.10
520	100-yr	Widened	10500	-16.0	4.70	1.91	513.81	0.10
290	100-yr	Existing	10500	-15.0	4.64	2.55	405.56	0.14
290	100-yr	Widened	10500	-15.0	4.64	2.55	405.56	0.14
100	100-yr	Existing	10500	-7.0	4.13	5.86	228.52	0.36
100	100-yr	Widened	10500	-7.0	4.13	5.86	228.52	0.36
0.1	100-yr	Existing	10500	-5.0	2.80	10.28	165.20	0.73
0.1	100-yr	Widened	10500	-5.0	2.80	10.28	165.20	0.73

Hydrologic Data Summary - The hydrologic data include characteristics of the design flood, the base flood, the flood of record, and the overtopping flood. The design flood is the peak discharge selected for the design of the bridge located within a base floodplain. By definition, through lanes will not be overtopped by the design flood. The base flood is the 100-yr flood for which the exceedance probability is one percent in any given year. The hydrologic data summary is given in Table 3. The table shows that the bridge with its low chord elevation at 21.1 feet will pass the 100-yr flood with a freeboard exceeding 7 feet. The record flood is the greatest recorded flood in the drainage basin; its value is not available. The overtopping flood is determined based on the minimum roadway elevation for the approach road embankments. For a discharge exceeding the design discharge, the roadway will be overtopped. For the I-5 Bridge across Agua Hedionda Lagoon, the roadway elevation is at least 9 feet above the base flood elevation. Because of the large freeboard, the overtopping flood would have to be extremely large, exceeding the 100-yr flood discharge.

Table 3. Hydrologic data summary for proposed I-5 Bridge across Agua Hedionda Lagoon in English units

Hydrologic Summary	Flood of Record	Design flood	Over-topping Flood	50-yr Flood
Frequency (Yrs.)	NA	100	NA	NA
Discharge (CFS)	NA	10,500	NA	NA
Water-Surface Elev. (Ft)	NA	5.65	NA	NA
Velocity (FPS)	NA	5.90	NA	NA

Bridge Scour – The channel bed at the I-5 Bridge crossing is armored. For this reason, bridge scour is not an issue here.

III. HYDRAULIC STUDY FOR INTERSTATE 5 BRIDGE ACROSS BATIQUITOS LAGOON

Batiquitos Lagoon is at the downstream end of San Marcos Creek. A Google aerial image of Batquitos Lagoon and Interstate 5 is shown in Figure 11. Pictures of the existing Interstate 5 Bridge across Batiquitos Lagoon are shown in Figure 12. Topographic map of the lagoon bathymetry based on the 2008 survey by Merkel and Associates is shown in Figure 13. Elevations for the lagoon bathymetry are based on the datum of MLLW. The latest offset between MLLW datum and NGVD datum is 0.70 meters or 2.30 ft. In order to covert to the NGVD datum, the difference of 2.3 feet needs to be added to the elevations in the original data.

Figure 11. Google image of Batiquitos Lagoon and Interstate 5

Figure 12. Views of I-5 Bridge across Batiquitos lagoon

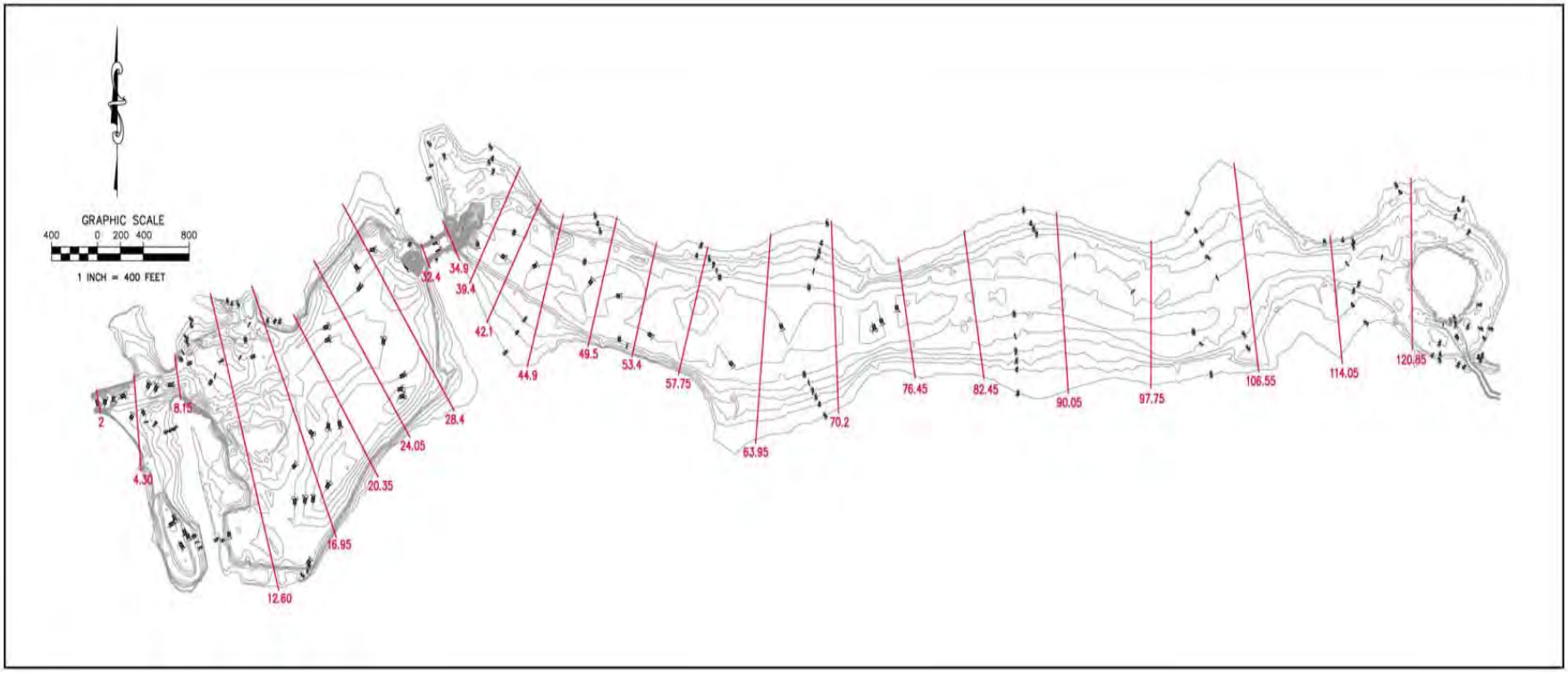

Figure 13. Bathymetry of Batiquitos Lagoon from 2008 survey

The channel bed at the existing I-5 Bridge crossing is armored and thus non-erodible. Tidal flow has caused severe scour on both sides of the bed armor as shown in Figure 14. The scour hole on the upstream sides has the minimum bed elevation of -24 feet; it is -21 feet on the downstream side.

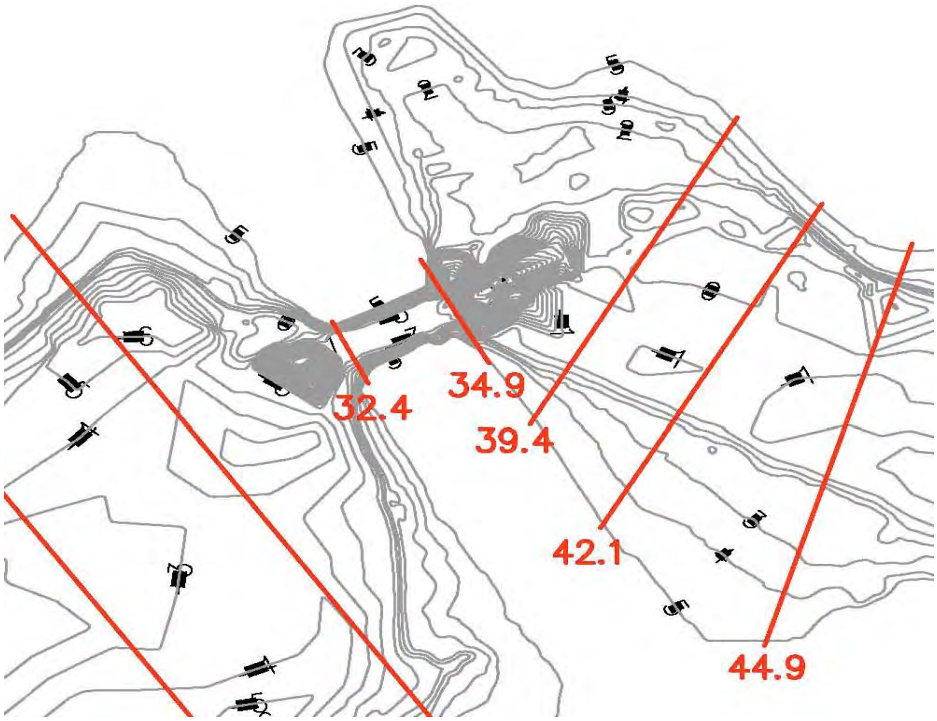

Fig. 14 Batiquitos Lagoon bathymetry near Interstate 5 Bridge. The channel bed at the existing bridge crossing is armored and thus non-erodible. Tidal flow has caused severe scour on both sides of the bed armor. The scour hole on the upstream sides has the minimum bed elevation of -24 feet; it is -21 feet on the downstream side.

Geometric Features of I-5 Bridge across Batiquitos Lagoon - Plans from Caltrans planning study for the I-5 Bridge are shown in Figure 15. Many geometric features of the bridge are given in the plans. Specification for the I-5 Bridge are given in Caltrans drawings entitled "Planning Study, Bridges Across Batiquitos Lagoon (Replace)", designed by and drawn by Gary Hight, September 2004. The specifications are listed below: All elevations are based on the NGVD datum.

Length of bridge span: 246 feet (75 meters)
Width of existing bridge deck: 154 feet
Width of proposed bridge deck: 229.3 ft (69.88 m)
Elevation of existing armored bed: -5.3 ft NGVD
Bed width of trapezoidal channel 127.1 ft.
Bridge low chard elevation: 15 feet at south end, 20 feet at north end
Three bridge spans with two sets of cylindrical piers.

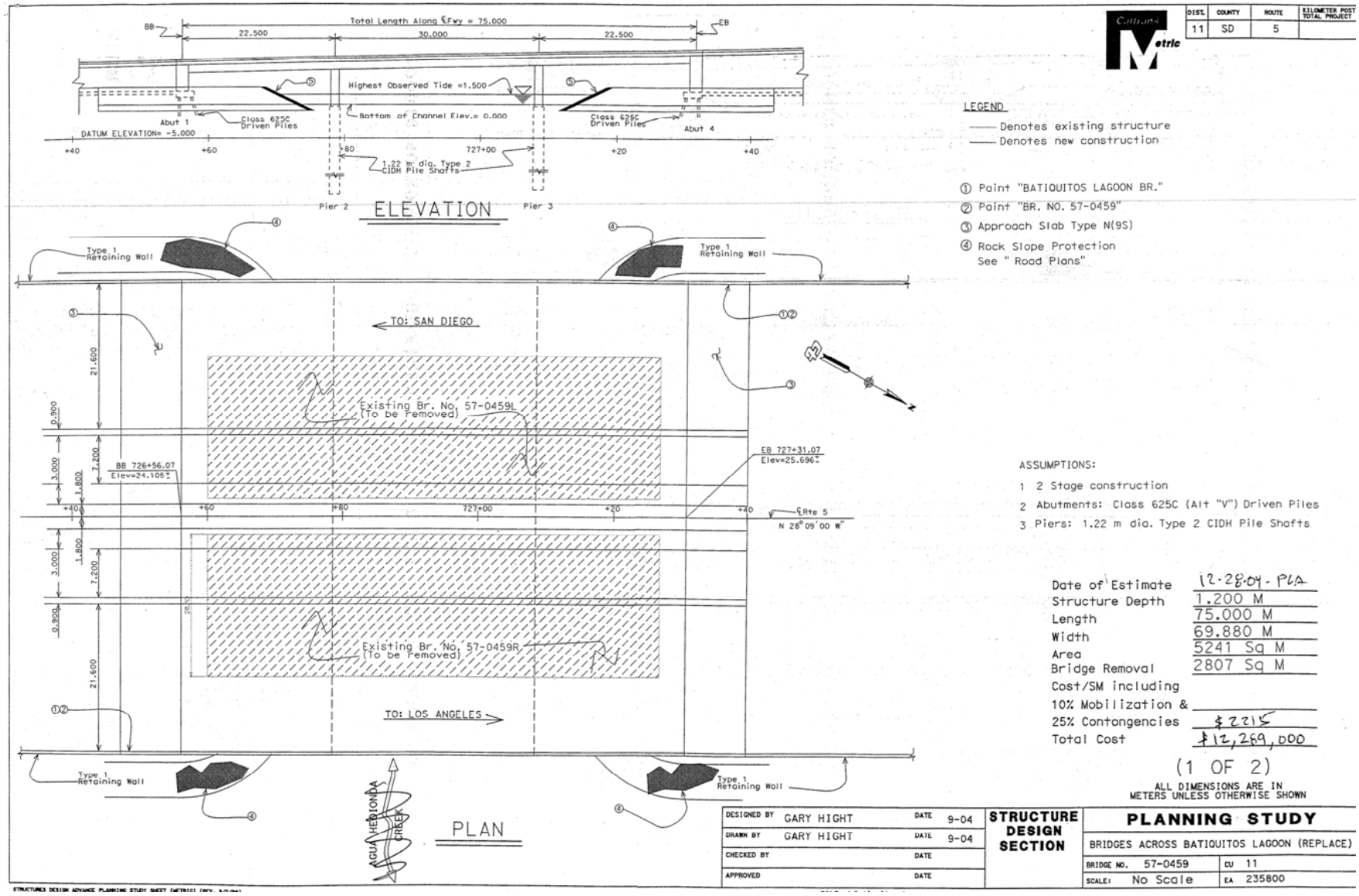

Figure 15. Plans for I-5 Bridge across Batiquitos Lagoon from Caltrans planning study

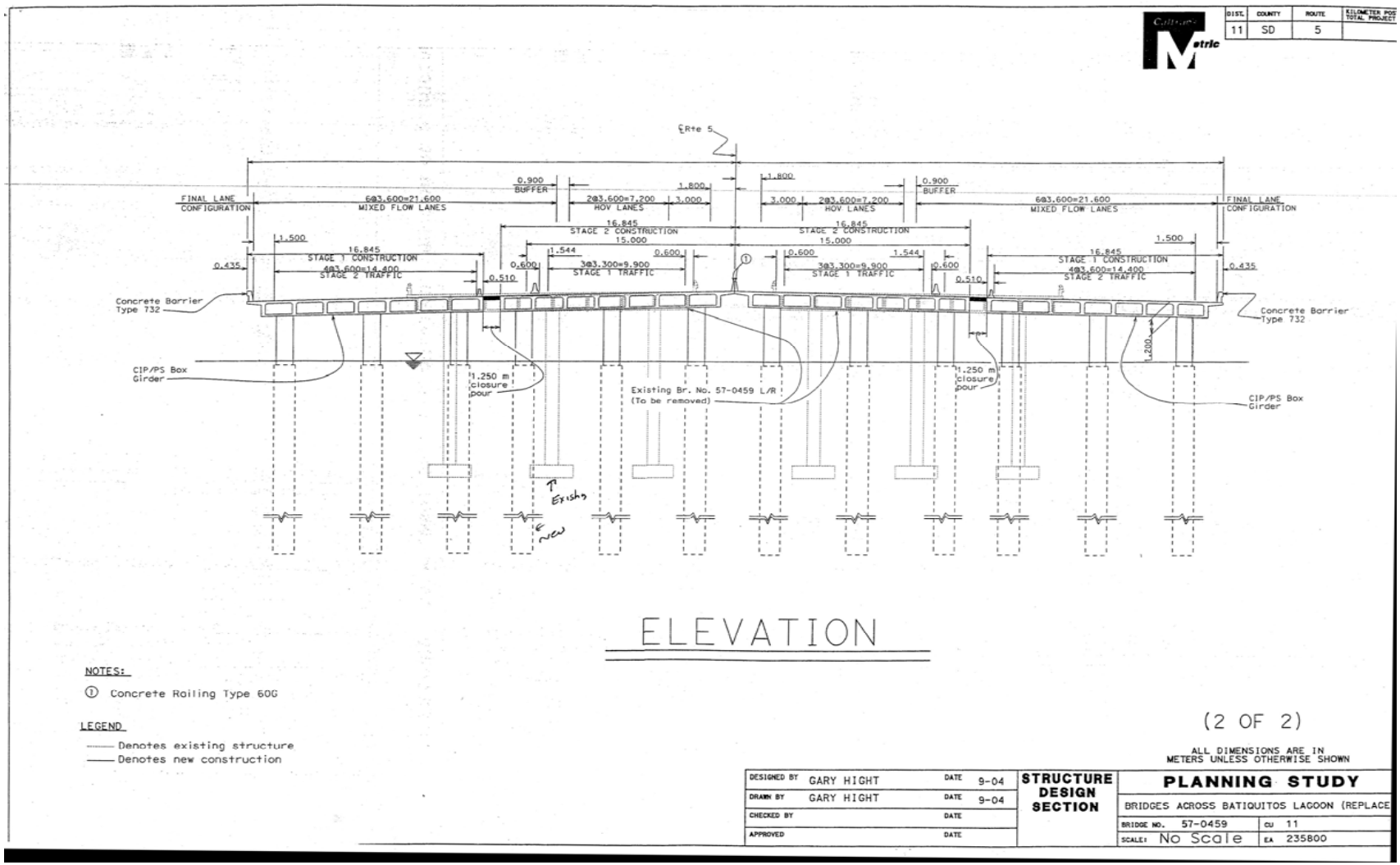

Figure 15 (continued). Plans for I-5 Bridge across Batiquitos Lagoon from Caltrans planning study

Bridge modification is proposed. The objective of bridge modification is to achieve the maximum possible reduction in tidal muting. The largest incremental reduction in tidal muting occurs with the first few increments of widening of channel plane (free space) beneath the bridge. Thereafter, each additional increment of channel plane produces smaller and smaller reductions in tidal muting while the length of bridge free span and attendant cost increases.

Bridge modification is subject to several considerations. According to Caltrans, the channel bottom under the bridges can be lowered as long as it is not filled right back up by sediment. The bed armoring may also be set at a new depth, if needed. Vertical side walls for the channel are permissible. A bench on each side of the channel is required for human trail and wildlife crossing. Adequate clearance between the bench and the bridge deck needs to be maintained. The bench should be at least 12 feet in width, but a 16-foot side bench is considered more desirable.

In consideration of the conditions stated above, different alternatives for bridge modification can be developed. The option as developed has the following features: All elevations are based on the NGVD datum.

(1) Bridge span: Use the existing bridge span of 75 m (246 feet) with no change.
(2) Bridge deck width: The planned new deck width of 229.3 feet is wider than the existing deck width of 154 feet.
(3) Channel bottom elevation: The existing bottom elevation will be lowered to the new bottom elevation of -7 feet, to be consistent with the adjacent channel bed.
(4) Armoring of the channel: The channel cross section at the bridge crossing will be armored to avoid excessive abutment scour.
(5) Channel bench: A 16-foot wide bench will be installed on each side of the channel. The bench has the top elevation of 8 feet in order to cover the pile caps supporting the bridge piers.
(6) Side slope of channel: The channel has the one-on-one side slope.
(7) Bed width of channel: The channel has the bed width of 180 feet.

The cross-sectional profile for the existing I-5 Bridge is shown in Figure 16. The cross-sectional of the I-5 Bridge for the proposed alternative is shown in Figure 17.

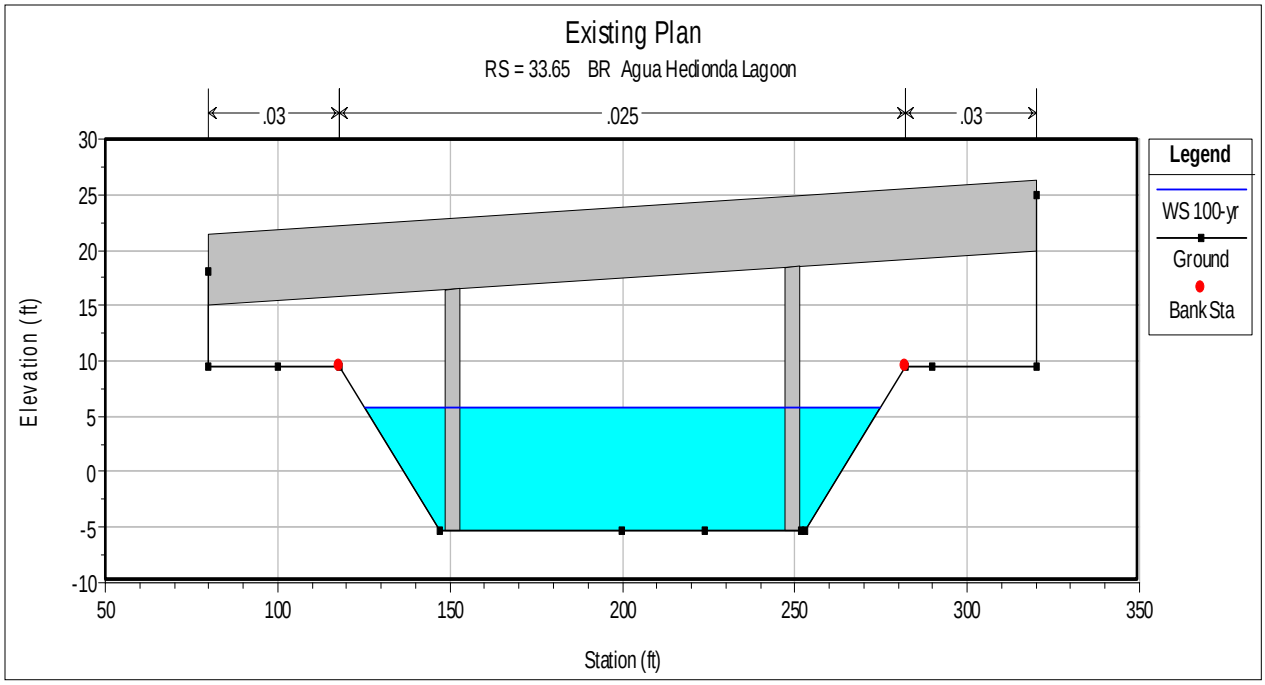

Figure 16. Cross sectional profile for the existing bridge

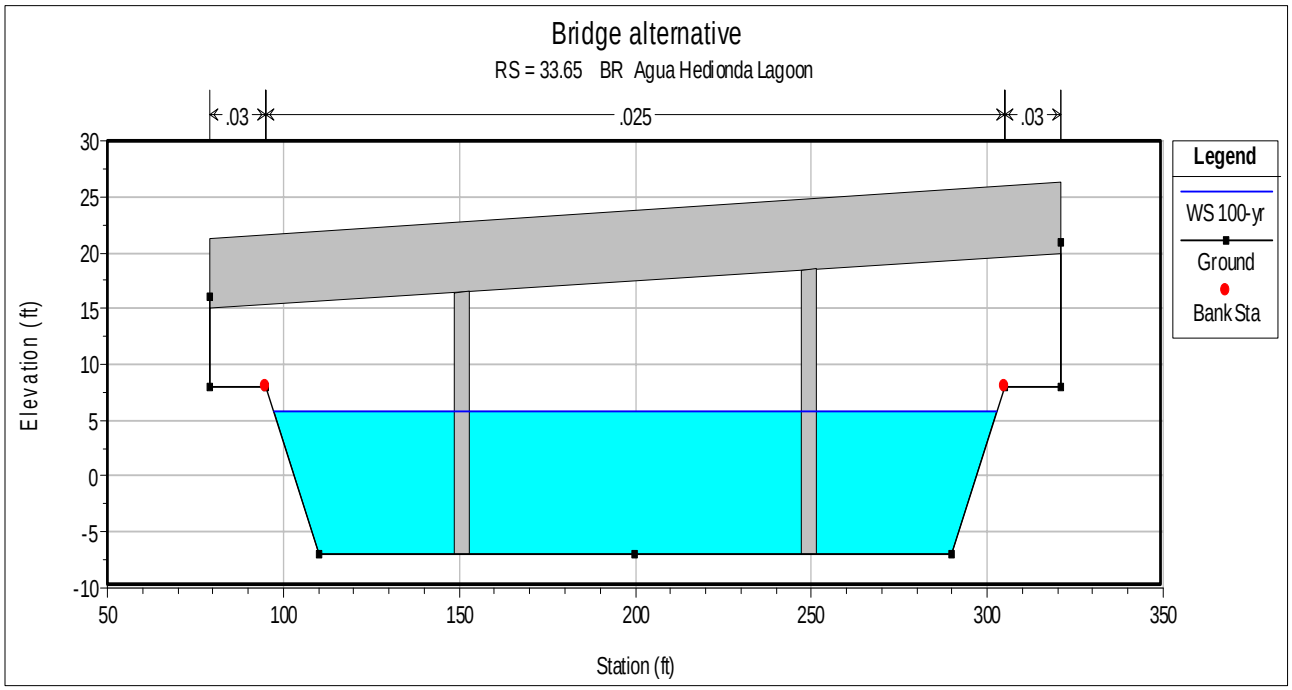

Figure 17. Cross-sectional profile for bridge alternative

Hydrology - The Interstate 5 Bridge crosses Batiquitos Lagoon, which is the lower reach of San Marcos Creek. According to the report "Flood Plain Information, San Marcos Creek", 1971, by the U.S. Army Crops of Engineers, Los Angeles District, the 100-yr flood has the peak discharge of 15,000 cfs at the mouth of San Marcos Creek into the Pacific Ocean.

Hydraulic Analysis - The HEC-RAS computer program was used to compute water-surface profiles and velocities in the stream channel for the existing conditions as well as the proposed conditions. The topographic map with the bathymetry of the lagoon as shown in Figure 18 also has cross sections used for the hydraulic analysis. Cross-sectional data for the channel reach were digitized from the topographic information. Important locations and their respective channel stations are listed in Table 4.

Table 4. List of important locations along Batiquitos Lagoon

Points of interest	Location Feet
Lagoon mouth	0+01
Highway 101	2+00
Railroad Bridge	8+15
Interstate 5 Bridge	32+40 – 34+90
Upstream end of lagoon	120+85

The HEC-RAS study reach starts from downstream at station 0+01 and ends upstream at station 120+85. Results of the HEC-RAS computation are described below. A detailed hydraulic report is given in Appendix A.

Water-Surface Profiles for Stream Channel - Water-surface profiles for the existing and proposed conditions were computed using the 100-yr floods. The 50-yr flood was not used since it is not available. Results of the computation for the existing and proposed conditions are shown in Figure 18, which includes the longitudinal water-surface and channel-bed profiles. Figure 19 shows sample cross-sectional profiles of the lagoon with the computed water-surface profiles. In the cross-sectional profiles, the label "RS" is the River Station in feet. The roughness coefficient in terms of Manning's *n* is written above the picture frame.

A summary of the given and computed hydraulic parameters for the existing and proposed conditions is listed in Table 5. When the computed results for the existing and proposed conditions are compared, it can be seen that the proposed bridge design will not result in a significant rise of the 100-yr water-surface elevation.

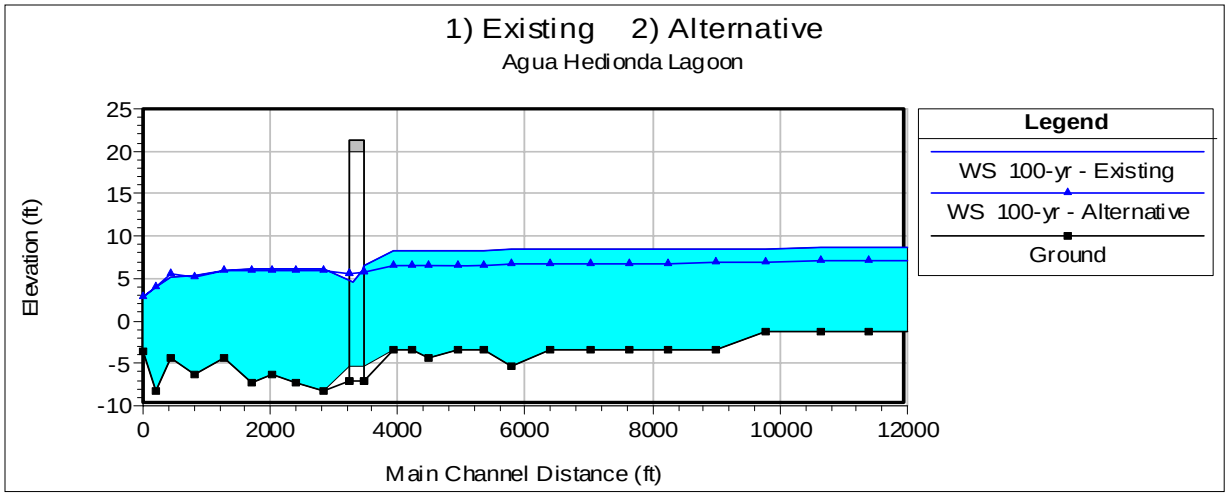

Figure 18. Water-surface and channel bed profiles for Batiquitos Lagoon for existing I-5 Bridge and proposed I-5 Bridge alternative

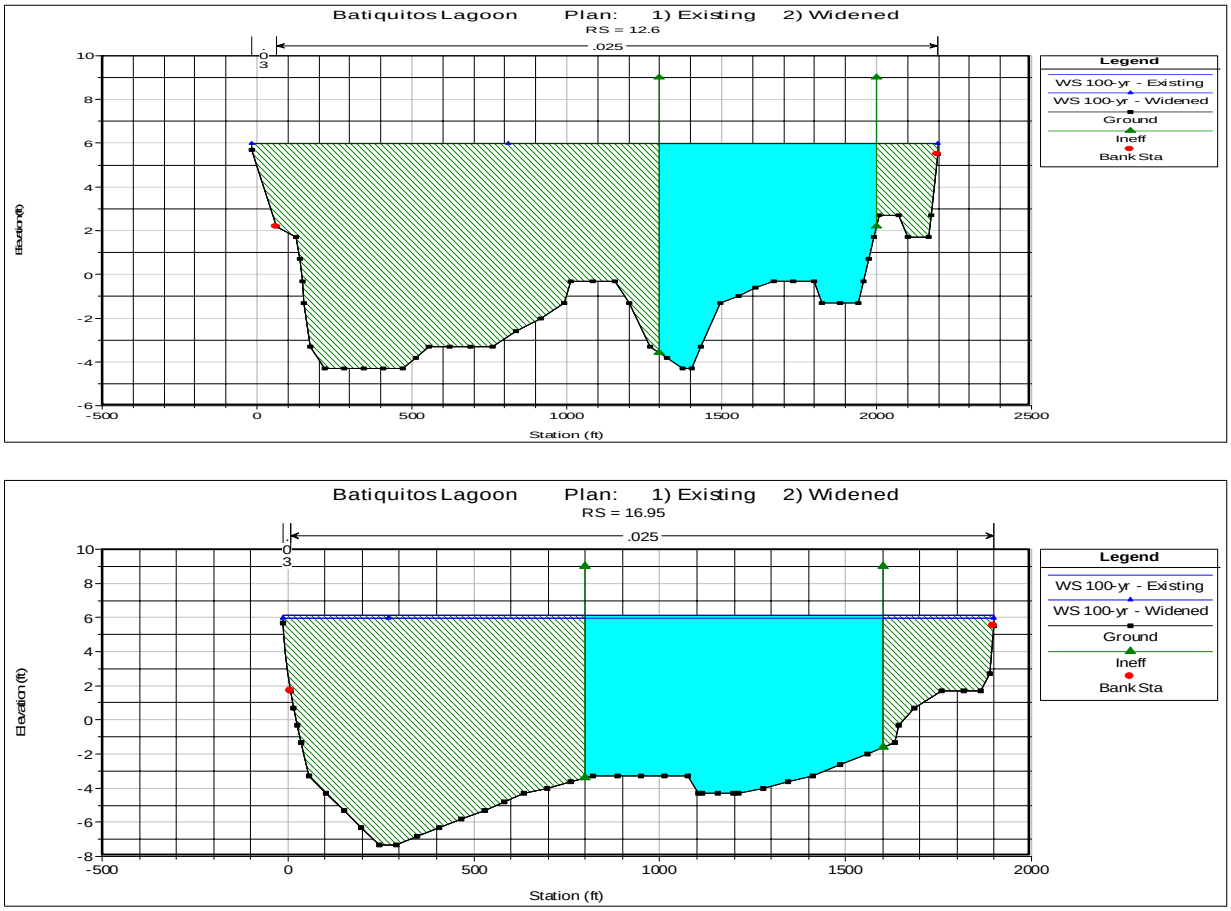

Figure 19. Sample cross-sectional profiles along Batiquitos Lagoon

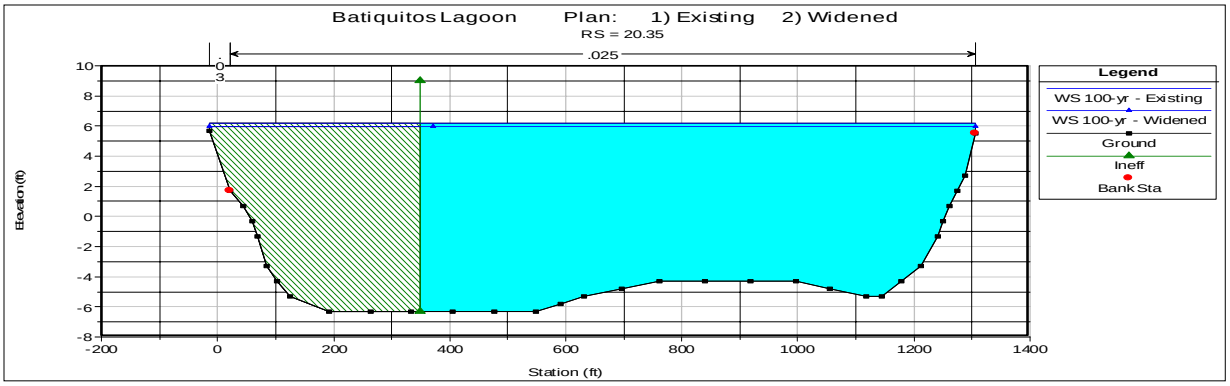

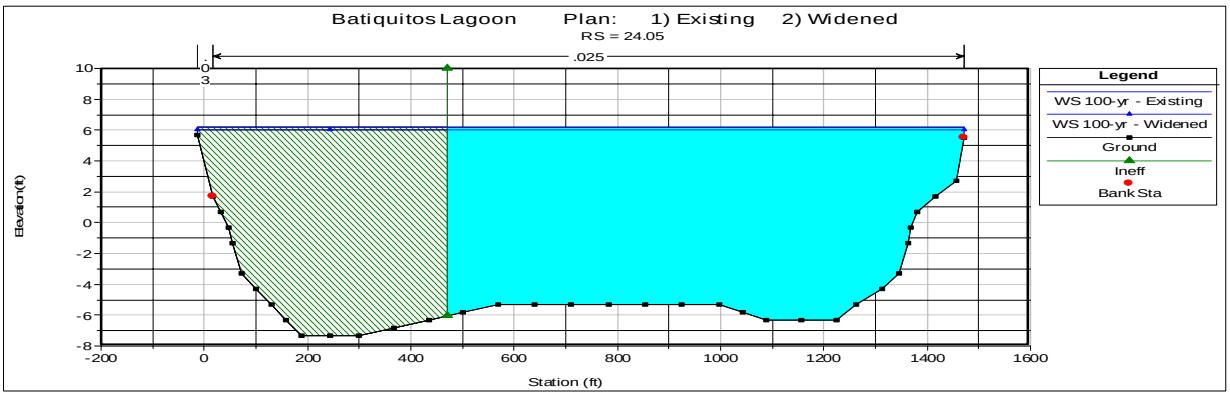

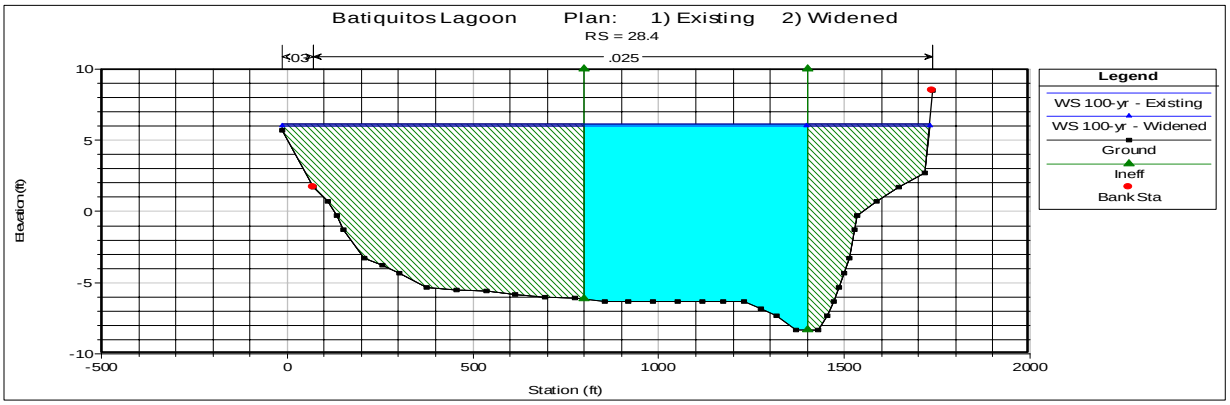

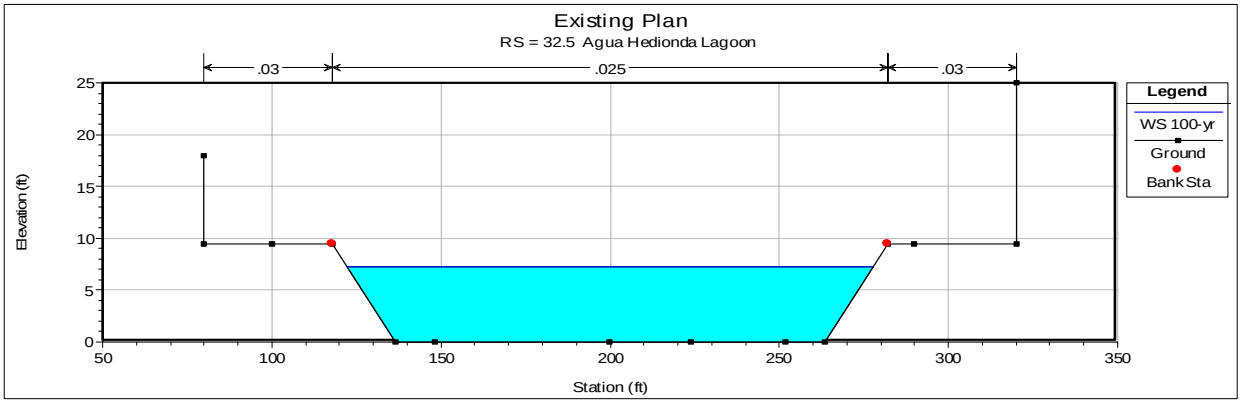

Figure 19 (continued). Sample cross-sectional profiles along Batiquitos Lagoon

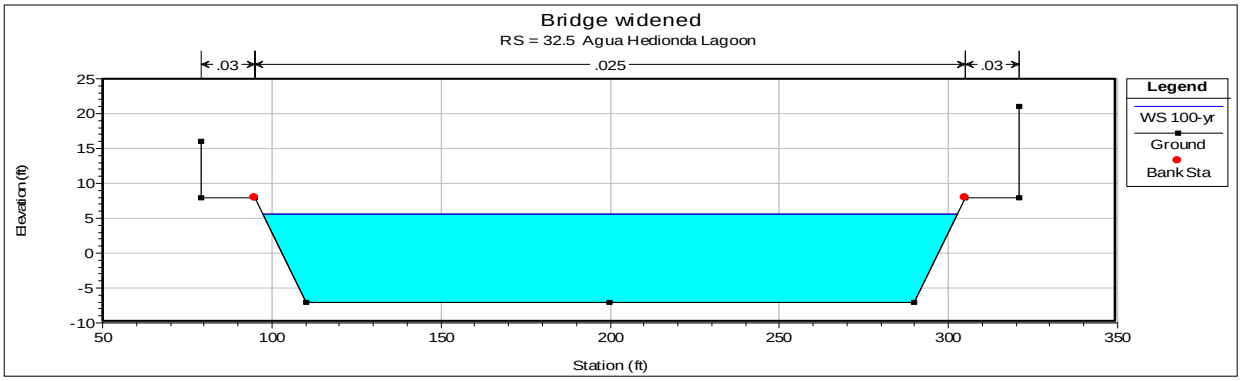

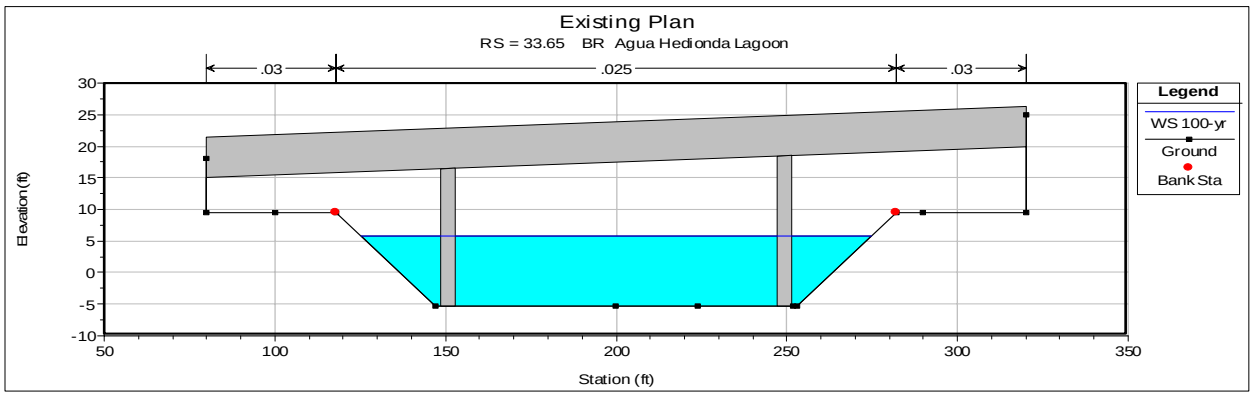

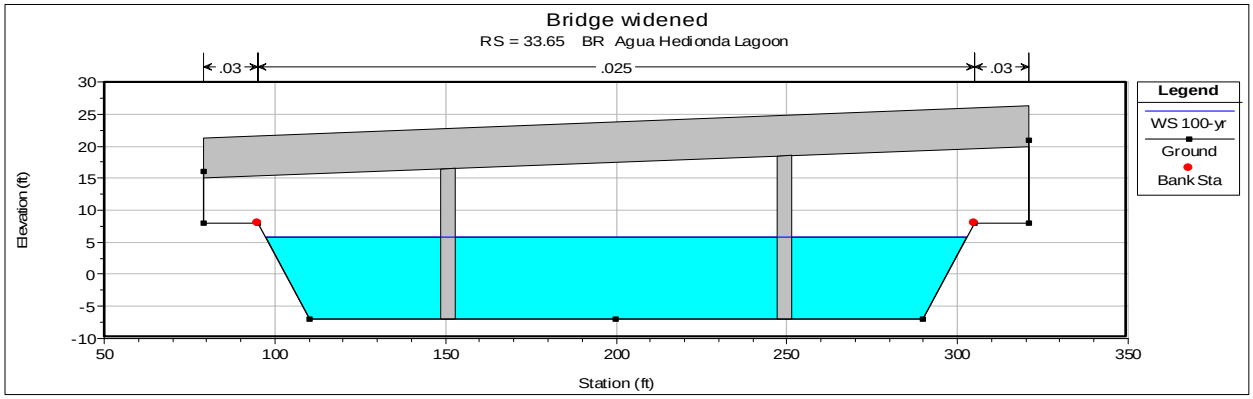

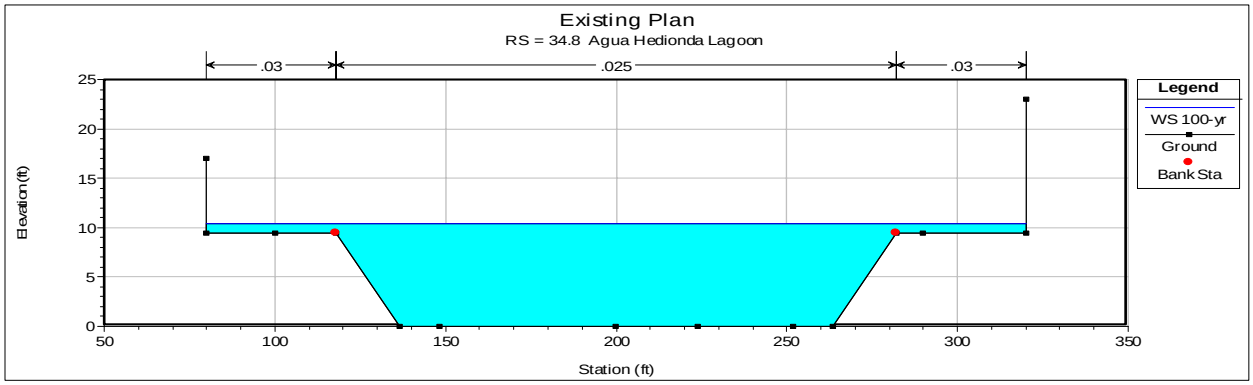

Figure 19 (continued). Sample cross-sectional profiles along Batiquitos Lagoon

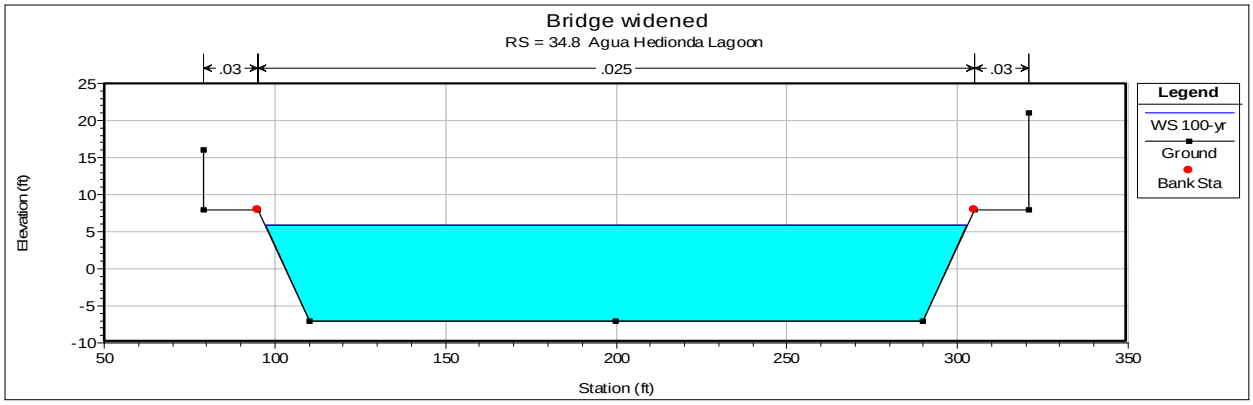

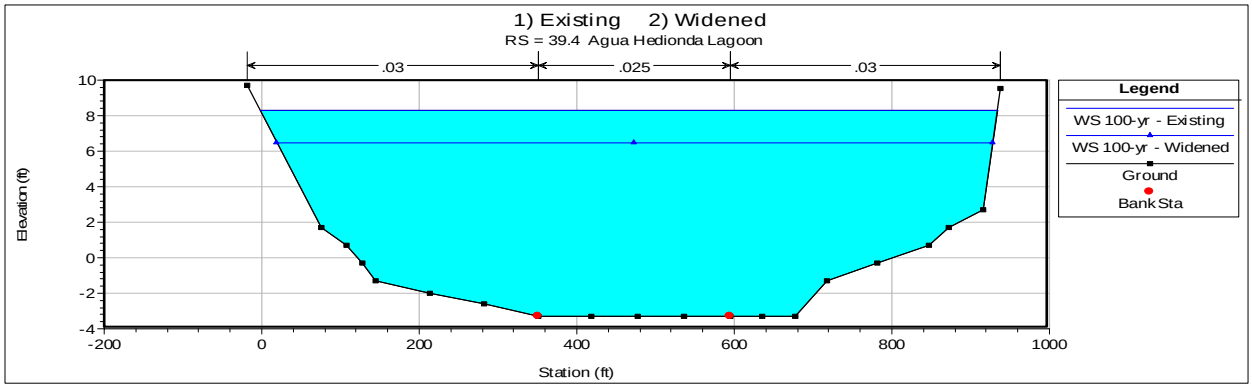

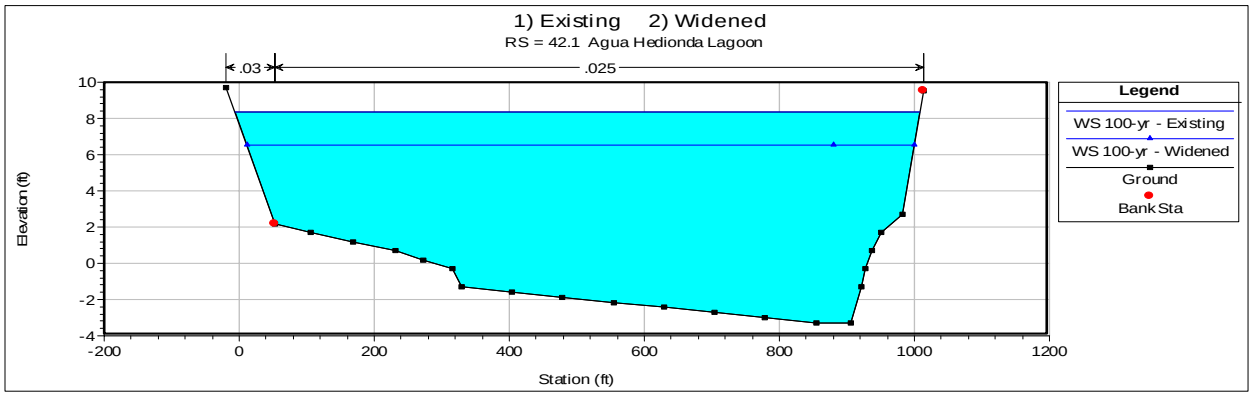

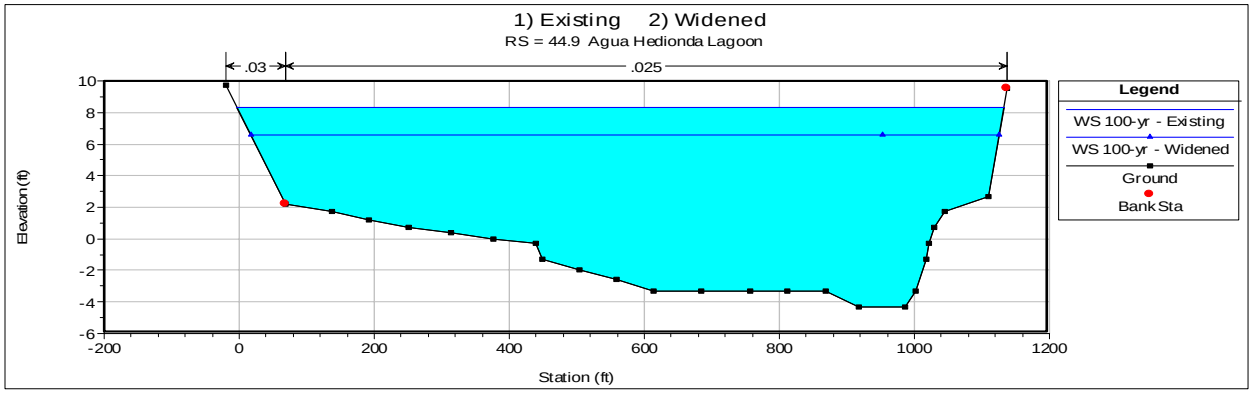

Figure 19 (continued). Sample cross-sectional profiles along Batiquitos Lagoon

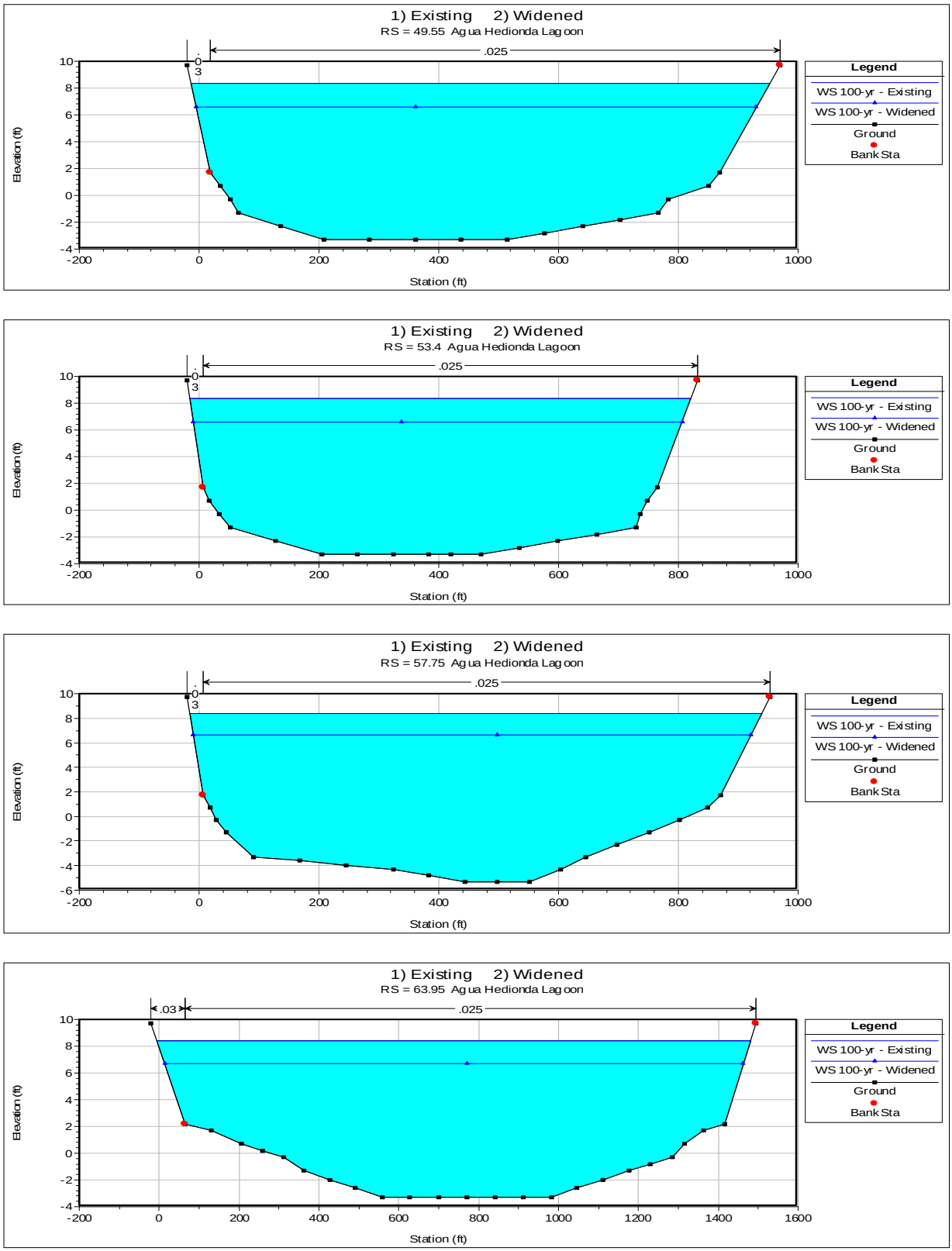

Figure 19 (continued). Sample cross-sectional profiles along Batiquitos Lagoon

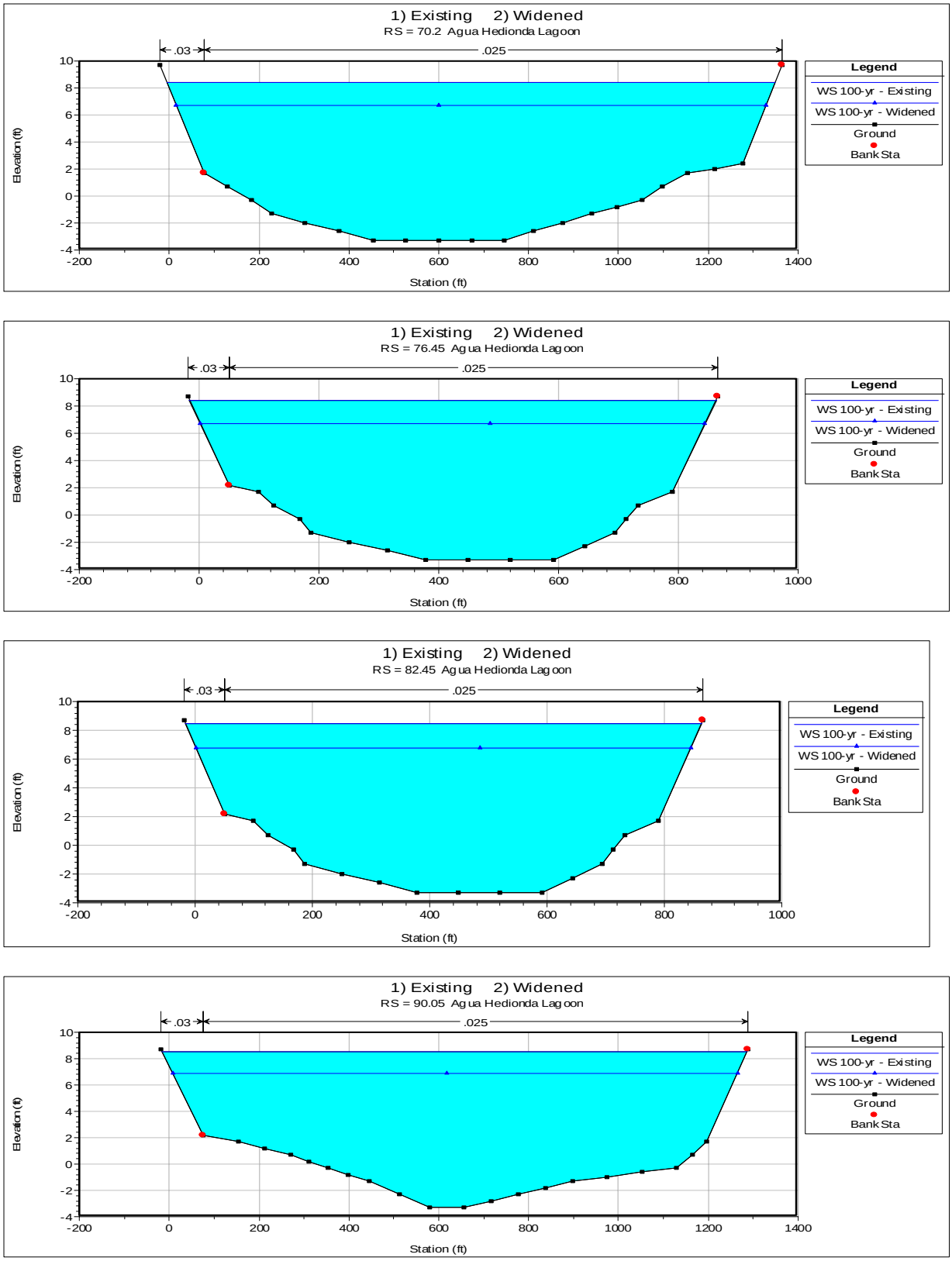

Figure 19 (continued). Sample cross-sectional profiles along Batiquitos Lagoon

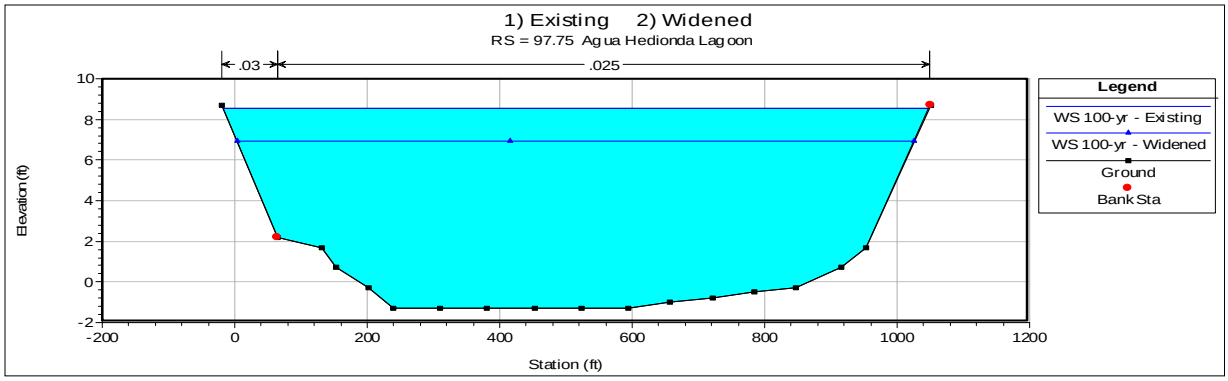

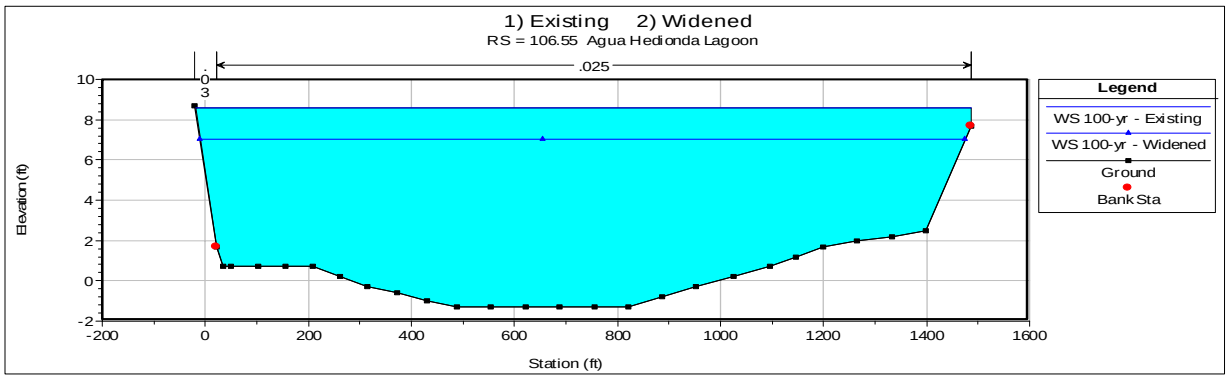

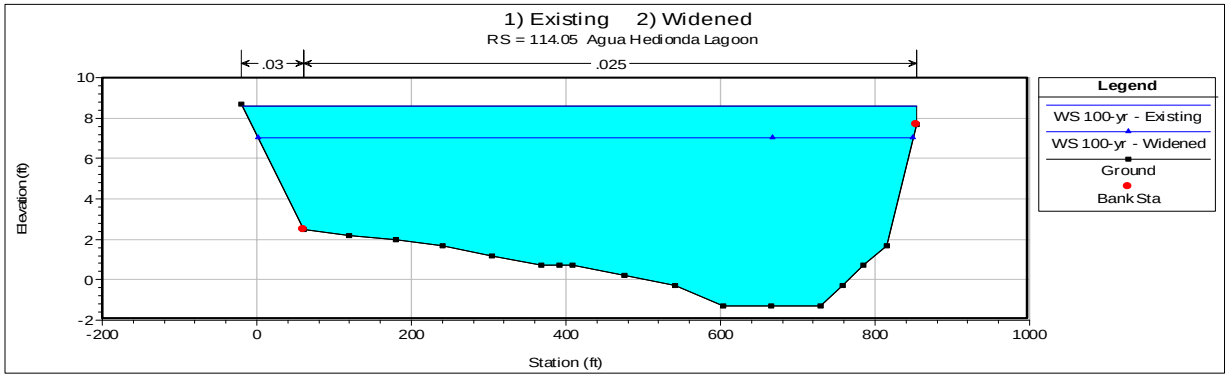

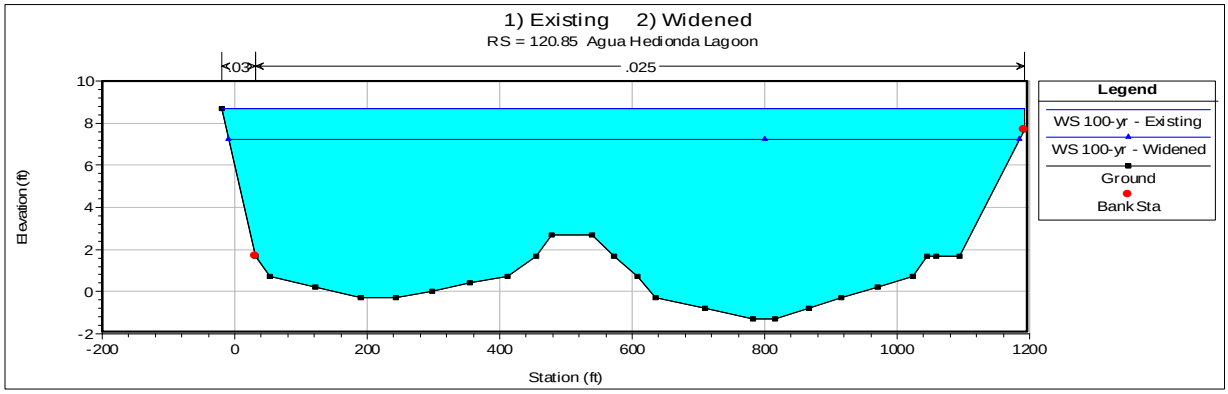

Figure 19 (continued). Sample cross-sectional profiles along Batiquitos Lagoon

Table 5. Summary of hydraulic parameters from hydraulic modeling

Sta	Profile	Plan	Q (cfs)	Bed El (ft)	W.S. (ft)	Vel (ft/s)	Width (ft)	Froude #
120.85	100-yr	Existing	15000	-1.30	8.70	1.60	1211.97	0.10
120.85	100-yr	Alternative	15000	-1.30	7.20	1.97	1192.89	0.14
114.05	100-yr	Existing	15000	-1.30	8.60	2.36	871.66	0.15
114.05	100-yr	Alternative	15000	-1.30	7.03	2.97	847.11	0.21
106.55	100-yr	Existing	15000	-1.30	8.61	1.23	1505.42	0.08
106.55	100-yr	Alternative	15000	-1.30	7.02	1.53	1484.41	0.10
97.75	100-yr	Existing	15000	-1.30	8.54	1.77	1065.80	0.11
97.75	100-yr	Alternative	15000	-1.30	6.92	2.19	1021.74	0.15
90.05	100-yr	Existing	15000	-3.30	8.53	1.36	1303.26	0.08
90.05	100-yr	Alternative	15000	-3.30	6.88	1.67	1257.33	0.11
82.45	100-yr	Existing	15000	-3.30	8.47	1.92	880.01	0.11
82.45	100-yr	Alternative	15000	-3.30	6.78	2.34	843.78	0.15
76.45	100-yr	Existing	15000	-3.30	8.44	1.93	879.32	0.11
76.45	100-yr	Alternative	15000	-3.30	6.72	2.36	842.47	0.15
70.2	100-yr	Existing	15000	-3.30	8.44	1.24	1353.51	0.07
70.2	100-yr	Alternative	15000	-3.30	6.72	1.52	1311.86	0.10
63.95	100-yr	Existing	15000	-3.30	8.43	1.10	1486.24	0.06
63.95	100-yr	Alternative	15000	-3.30	6.70	1.34	1448.38	0.08
57.75	100-yr	Existing	15000	-5.30	8.40	1.46	955.30	0.08
57.75	100-yr	Alternative	15000	-5.30	6.65	1.73	931.50	0.10
53.4	100-yr	Existing	15000	-3.30	8.37	1.79	836.34	0.10
53.4	100-yr	Alternative	15000	-3.30	6.60	2.17	815.56	0.13
49.55	100-yr	Existing	15000	-3.30	8.36	1.61	965.71	0.09
49.55	100-yr	Alternative	15000	-3.30	6.58	1.96	934.81	0.12
44.9	100-yr	Existing	15000	-4.30	8.35	1.47	1136.58	0.08
44.9	100-yr	Alternative	15000	-4.30	6.56	1.82	1108.45	0.12
42.1	100-yr	Existing	15000	-3.30	8.33	1.67	1014.47	0.10
42.1	100-yr	Alternative	15000	-3.30	6.52	2.08	988.89	0.13
39.4	100-yr	Existing	15000	-3.30	8.31	2.17	936.60	0.11
39.4	100-yr	Alternative	15000	-3.30	6.48	2.68	909.04	0.15

34.8	100-yr	Existing	15000	-5.30	6.50	9.85	152.23	0.55
34.8	100-yr	Alternative	15000	-7.00	5.81	6.07	205.62	0.31
33.65		Bridge						
32.5	100-yr	Existing	15000	-5.30	4.71	11.93	145.21	0.71
32.5	100-yr	Alternative	15000	-7.00	5.61	6.18	205.22	0.32
28.4	100-yr	Existing	15000	-8.30	6.17	1.96	1743.55	0.10
28.4	100-yr	Alternative	15000	-8.30	6.01	0.85	1742.97	0.05
28.4	100-yr	Existing	15000	-8.30	6.17	1.96	1743.55	0.10
28.4	100-yr	Alternative	15000	-8.30	6.01	0.85	1742.97	0.05
24.05	100-yr	Existing	15000	-7.30	6.17	1.38	1486.00	0.07
24.05	100-yr	Alternative	15000	-7.30	6.00	0.94	1486.00	0.05
20.35	100-yr	Existing	15000	-6.30	6.16	1.47	1321.00	0.08
20.35	100-yr	Alternative	15000	-6.30	5.99	1.10	1321.00	0.06
16.95	100-yr	Existing	15000	-7.30	6.12	1.98	1914.00	0.11
16.95	100-yr	Alternative	15000	-7.30	5.99	0.84	1914.00	0.05
12.6	100-yr	Existing	15000	-4.30	5.99	2.89	2213.00	0.19
12.6	100-yr	Alternative	15000	-4.30	5.98	0.91	2213.00	0.06
8.15	100-yr	Existing	15000	-6.30	5.29	6.26	307.94	0.39
8.15	100-yr	Alternative	15000	-6.30	5.24	6.30	307.59	0.39
4.3	100-yr	Existing	15000	-4.30	5.16	5.44	708.53	0.34
4.3	100-yr	Alternative	15000	-4.30	5.47	2.88	712.59	0.19
2	100-yr	Existing	15000	-8.30	4.03	9.01	172.50	0.50
2	100-yr	Alternative	15000	-8.30	4.03	9.01	172.50	0.50
0.01	100-yr	Existing	15000	-3.50	2.88	11.01	375.43	0.98
0.01	100-yr	Alternative	15000	-3.50	2.88	11.01	375.43	0.98

Hydrologic Data Summary - The hydrologic data include characteristics of the design flood, the base flood, the flood of record, and the overtopping flood. The design flood is the peak discharge selected for the design of the bridge located within a base floodplain. By definition, through lanes will not be overtopped by the design flood. The base flood is the 100-yr flood for which the exceedance probability is one percent in any given year. The hydrologic data summary is given in Table 6. The table shows that the bridge with its low chord elevation of 20.0 feet will pass the 100-yr flood with a freeboard exceeding 13 feet. The record flood is the greatest recorded flood in the drainage basin; its value is not available. The overtopping flood is determined based on the minimum roadway elevation for the approach road embankments. Under a discharge exceeding the design discharge, the roadway will be overtopped. For the I-5 Bridge across Batiquitos Lagoon, the roadway elevation is at least 14

feet above the base flood elevation. Because of the large freeboard, the overtopping flood would be very large and hence not considered.

Table 6. Hydrologic data summary for bridge alternative across Batiquitos Lagoon in English units

Hydrologic Summary	Flood of Record	Design flood	Over-topping Flood	50-yr Flood
Frequency (Yrs.)	NA	100	NA	NA
Discharge (CFS)	NA	15,000	NA	NA
Water-Surface Elev. (Ft)	NA	5.81	NA	NA
Velocity (FPS)	NA	6.07	NA	NA

Bridge Scour – The channel bed at the I-5 Bridge crossing is armored. For this reason, bridge scour is not an issue here.

IV. HYDRAULIC STUDY FOR INTERSTATE 5 BRIDGE ACROSS SAN DIEGUITO RIVER

Bridge widening is proposed for the I-5 Bridge on the San Dieguito River. A topographic map for the San Dieguito River is shown in Figure 20, which also has cross sections used for the hydraulic analysis. Topographic survey of the Sand Dieguito River was made in 2005 by Project Design Consultants for the Southern California Edison Company. The survey used for the project is based on the NGVD29 datum. Important locations and their respective channel stations are listed in Table 7.

Table 7. List of important locations along the San Dieguito River channel

Points of interest	Location River miles
River mouth	0
Highway 101	0.087 - 0.107
Railroad Bridge	0.293 – 0.299
Jimmy Durante Bridge	0.570 - 0.581
River bend	0.706
Interstate 5 Bridge	1.355 – 1.391
El Camino Real	2.806 – 2.813

A major environmental enhancement project sponsored by the Southern California Edison Company has recently been completed in the floodplain of the San Dieguito River. The project entitled San Dieguito Wetland Restoration Project includes the creation of open water lagoons and tidal wetlands that are shown in Figure 21 and the Google image in Figure 22. These features are separated from the main river channel by berms to keep the effective river flow and sediment transport in the main channel.

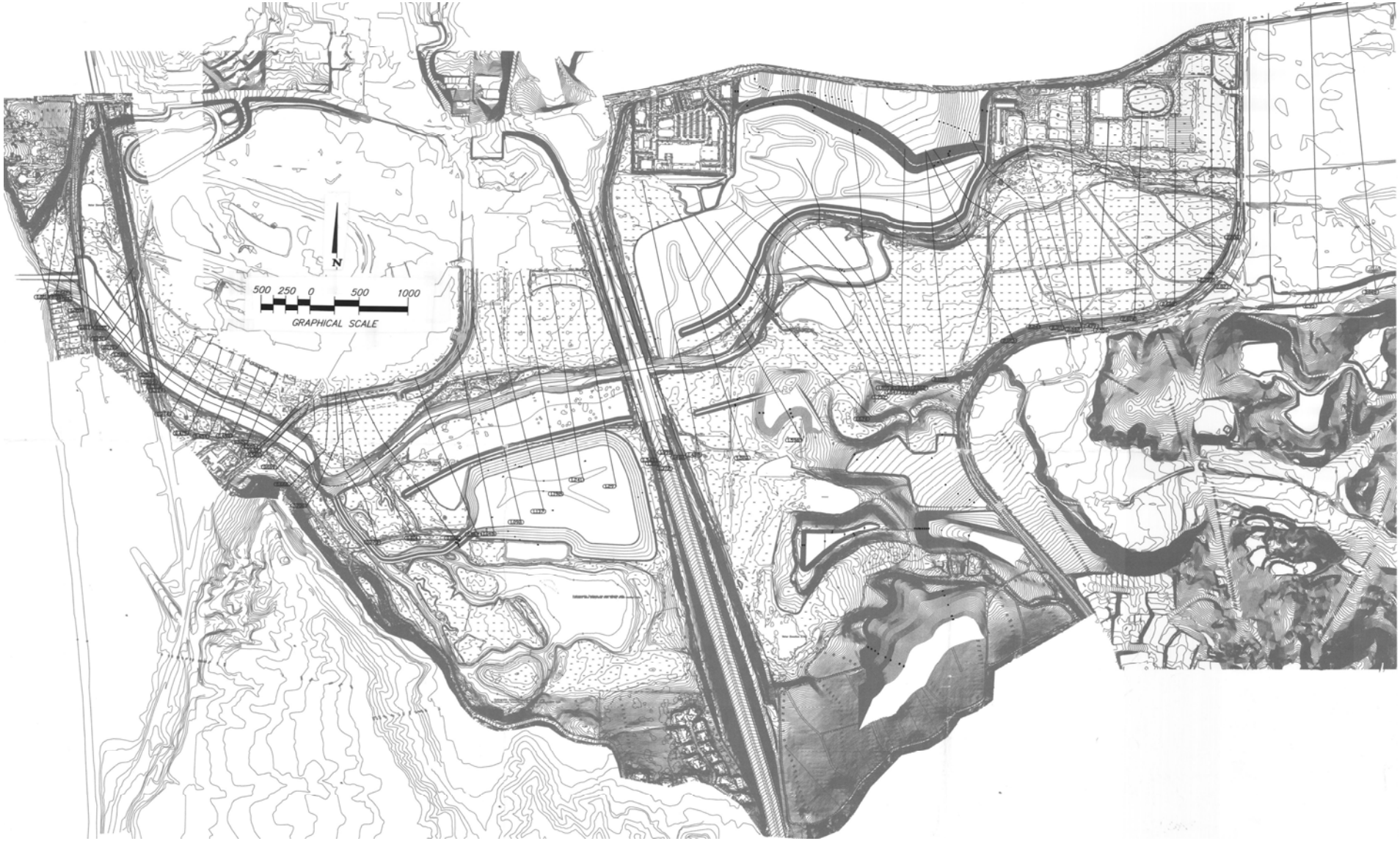

Figure 20. Topographic amp of the San Dieguito River

Figure 20 (continued). Topographic amp of the San Dieguito River

Figure 21. Plan for San Dieguito River Wetland Restoration Project

Figure 22. Google image of the San Dieguito River near I-5

The I-5 Bridge on the San Dieguito River – Pictures of the existing I-5 Bridge are shown in Figures 23 and 24. Figure 23 is a view of the bridge from downstream and Figure 24 is a view from upstream. Bridge widening is proposed for the project. Plans from the Caltrans planning study for the I-5 Bridge are shown in Figure 25. Many geometric features of the bridge are given in the plans. Specifications for the I-5 Bridge are listed below: All elevations are based on the NGVD datum.

Total bridge span length: 649.5 ft
Width of existing bridge deck: 179 ft (54.5 m)
Width of proposed/new bridge deck: 253 ft (77.1 m)
Side slope of channel: 2 to 1
Bridge low chard elevation: 23.3 feet at south end, 21.7 feet at north end

Purposes of current studies include the following:
(1) Bridge hydraulics - This consists of hydraulic calculations for flood levels and flow velocities under the 50-yr, 100-yr, and overtopping floods as required in the hydrologic data summary.
(2) Potential stream channel scour at the bridge crossing - This is to provide the information on general scour and local scour to be used for bridge design.

Two types of models were used in these studies. For bridge hydraulics, a fixed boundary model, HEC-RAS, developed by the U. S. Army Corps of Engineers was used. For the scour study, an erodible boundary model, FLUVIAL-12 (Chang, 1988) was used.

Figure 23. View of the I-5 Bridge from downstream

Figure 24. View of the I-5 Bridge from upstream

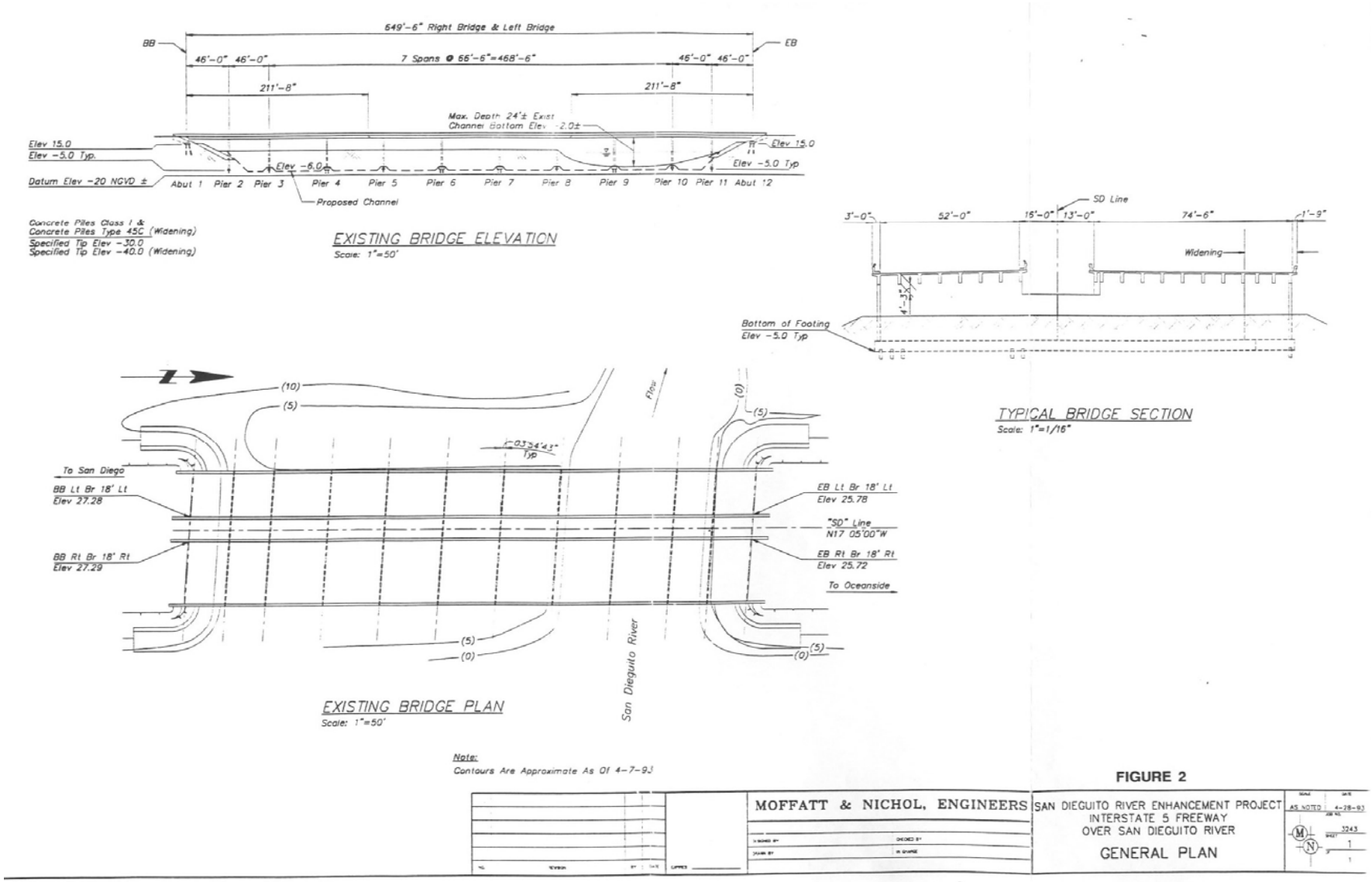

Figure 25 Plans from the Caltrans planning study for the I-5 Bridge

Hydrology of the San Dieguito River - The San Dieguito River has a total drainage area of 346.5 square miles, of which 303 square miles are above Lake Hodges. Since its completion in 1926, the dam has controlled 87.4 % of the drainage basin. Lake Hodges cuts off the surface runoff of small storms to the lower reach. The reservoir spills during larger storms. Significant spillage of the reservoir occurred in 26 years of the last 78 years (1926-2003). For larger storms, the upper basin above Lake Hodges supplies the discharge in the Lower San Dieguito River, but for smaller storms, the flow in the lower reach is only supplied by runoff from the lower river basin below Lake Hodges. A summary of peak discharges for representative return periods is given in Table 8. There is a lack of sufficient stream flow data for the river channel. The County of San Diego used hydrological simulation to determine the flood discharges. Peak discharges of other floods may be estimated based the assumption that the distribution of peak discharges follows a lognormal distribution. Since the completion of the Lake Hodges Dam in 1926, the largest recorded flood had the peak flow of 22,000 cfs when Lake Hodges spilled in 1980. Such a discharge is estimated to be a 35 year flood

Table 8. Flood discharges for the San Dieguito River

Flood event	Peak Discharge, cfs	
	Upstream of Jimmy Durante Br.	Upstream of I-5 Bridge
10-yr	5,800	5,900
50-yr	32,100	32,100
100-yr	42,400	42,800

In connection with the wetland restoration project, a part of the 100-yr flood discharge is diverted into the wetland on the north side of the river channel just upstream of the I-5 Bridge crossing. As a result of the flow diversion, the peak discharge for the 100-yr flood upstream of the bridge crossing in the main channel is reduced to 36,500 cfs. The hydrograph for the 100-yr flood is shown in Figure 26.

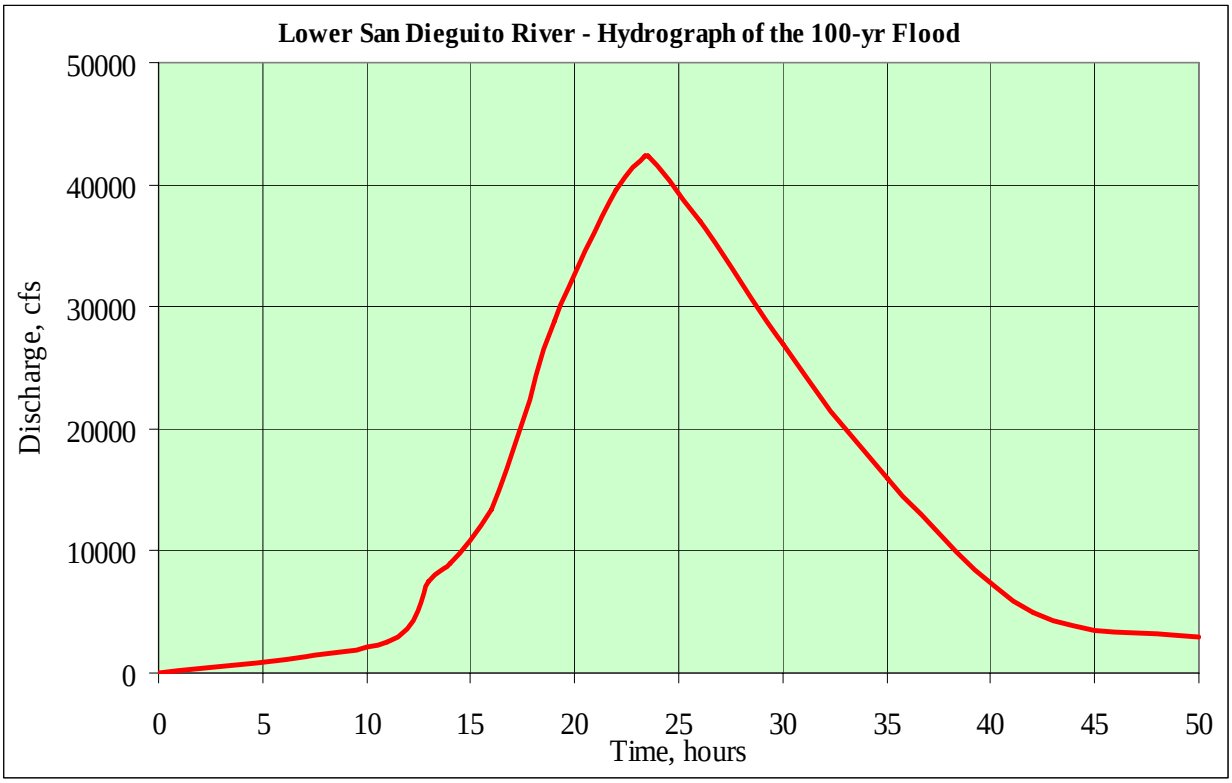

Figure 26. Hydrograph of the 100-yr flood

Hydraulics of I-5 Bridge on the San Dieguito River - For bridge hydraulics, the HEC-RAS model was used. Hydraulic computations were performed to provide:

(1) Water-surface elevations,
(2) Flow velocities, and
(3) Overtopping flow.

Water-surface profiles and flow velocities for the bridge were computed using the HEC-RAS program for existing conditions and proposed bridge widening. A goal of the project was to keep the computed 100-yr water-surface elevations for the proposed conditions no higher than those for the existing conditions. Another goal was to avoid any adverse flooding effects on neighboring properties. At the same time, it is necessary to pass the design flood without overtopping.

The selected design must meet the requirements, regulations, and policies set by FEMA, and the Executive Order 11988 (Federal Policy on Floodplain Management), including:

(3) Conveyance of the base flood, Q_{100}.
(4) Backwater caused by the bridge encroachment with that caused by all other obstructions is limited to one foot above the surface of the base flood.

The design flood for the bridge was determined in accordance with Caltrans Local Assistance Manual, Chapter 11 “Design Standards”, Caltrans Memorandum to Designers I-23, and the Highway Design Manual, Section 821.3 “Selection of Design Flood”. The 50-yr and

100-yr flood were included in hydraulic computations for the existing channel conditions as well as the proposed conditions.

A general guideline for the hydraulic design of bridges is that they should pass the 50-yr flood with adequate freeboard to pass anticipated drift. Typically two feet of freeboard above the 50-yr water surface elevation is adequate for the area. The bridge should also be able to convey the 100-yr flood.

Hydraulic modeling using the HEC-RAS model for the existing and proposed bridges has been made to study the impacts of bridge widening on the 100-year water-surface elevation. The hydraulic study also used the 50-yr flood, which is the design standard for the bridge. The computed water-surface profiles for the 50- and 100-yr floods of the river channel with the existing and proposed bridges are shown in Figures 27 and 28, respectively. In the cross-sectional profiles, the label "RS" is the River Station in feet. The roughness coefficient in terms of Manning's *n* is written above the picture frame. The 100-yr flood is also the base flood according the terminology used by FEMA.

The computed water-surface elevations at the bridge crossing and other adjacent channel cross sections are shown in Figure 29. Computed results for the existing and proposed bridges are summarized in Table 9. The results show that the proposed bridge alternaitive will not result in a rise of the flood level. The 100-yr water surface stays well below the bridge low chord.

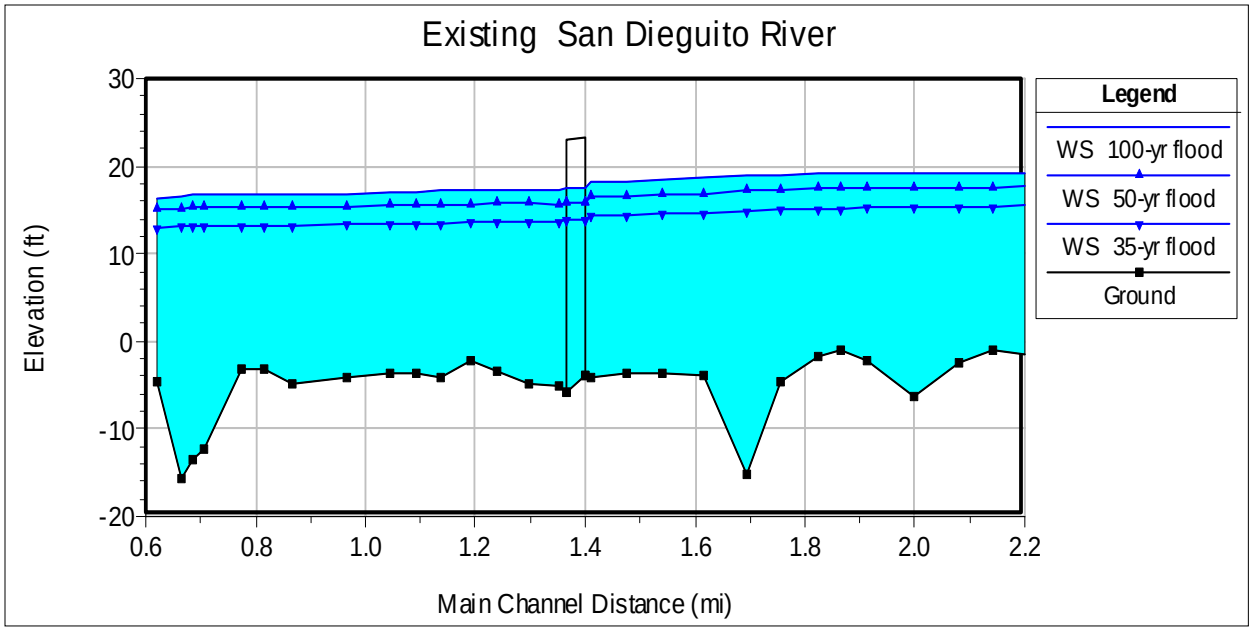

Figure 27. Computed longitudinal water-surface profiles of the river channel with the existing bridge

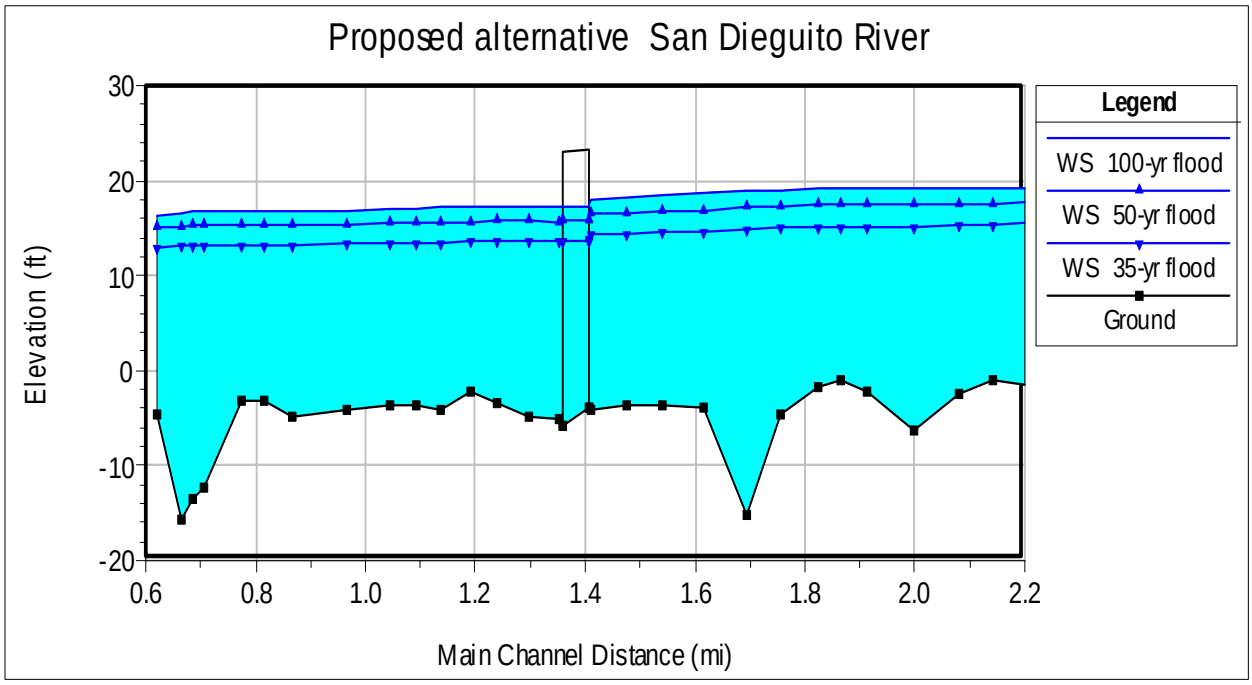

Figure 28. Computed longitudinal water-surface profiles of the river channel with the proposed bridge alternative

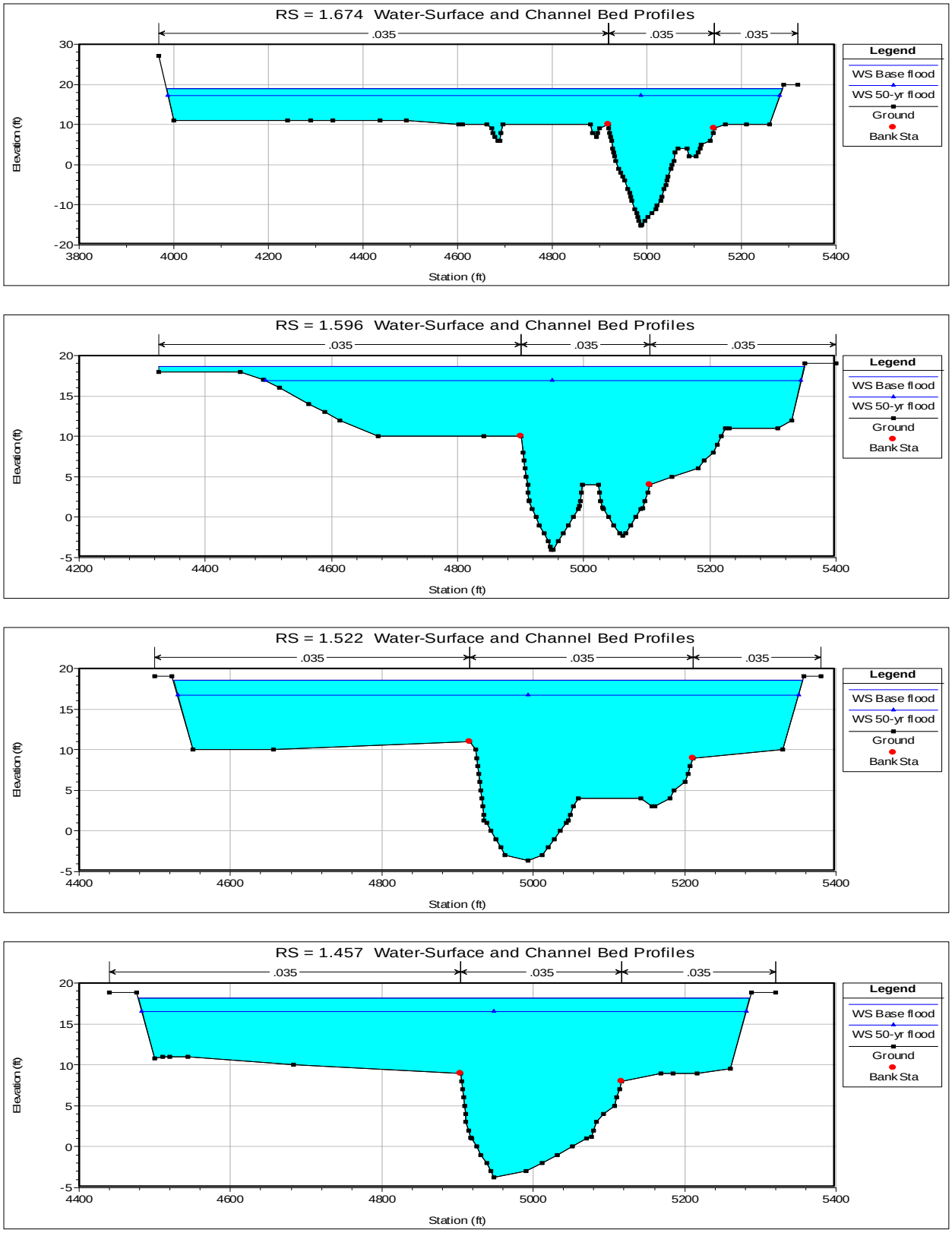

Figure 29. Cross-sectional profiles of the river channel near the I-5 Bridge crossing

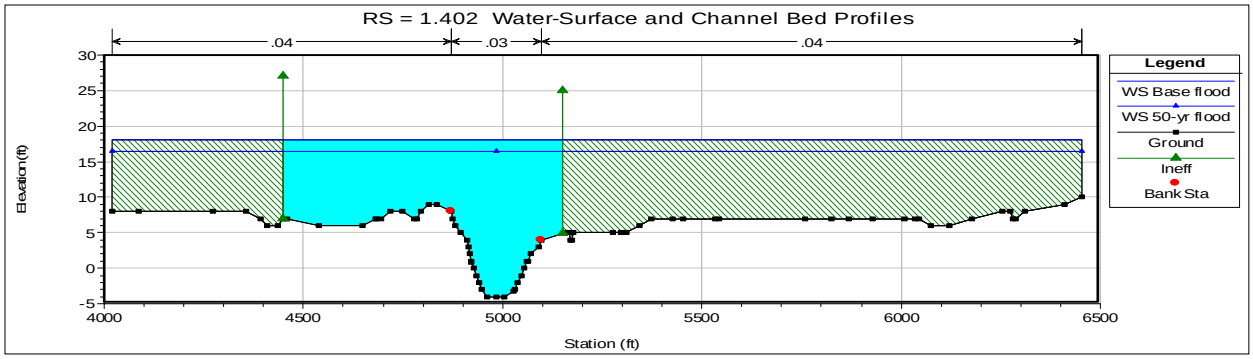

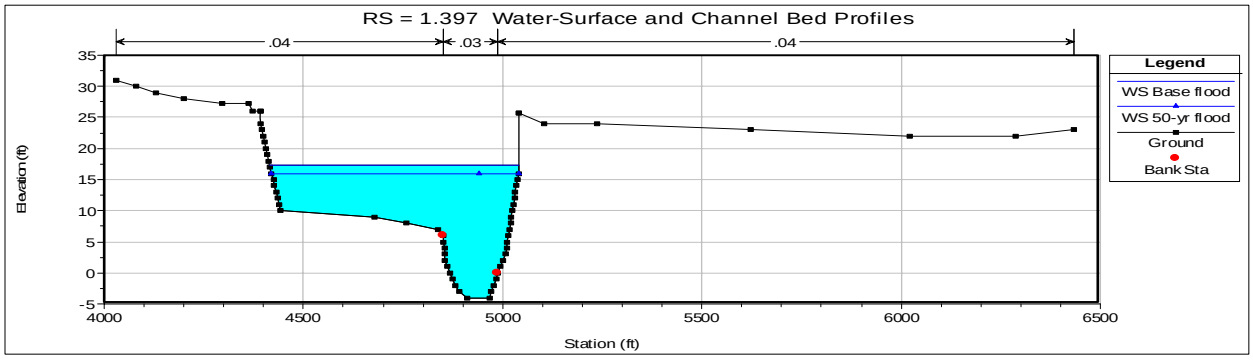

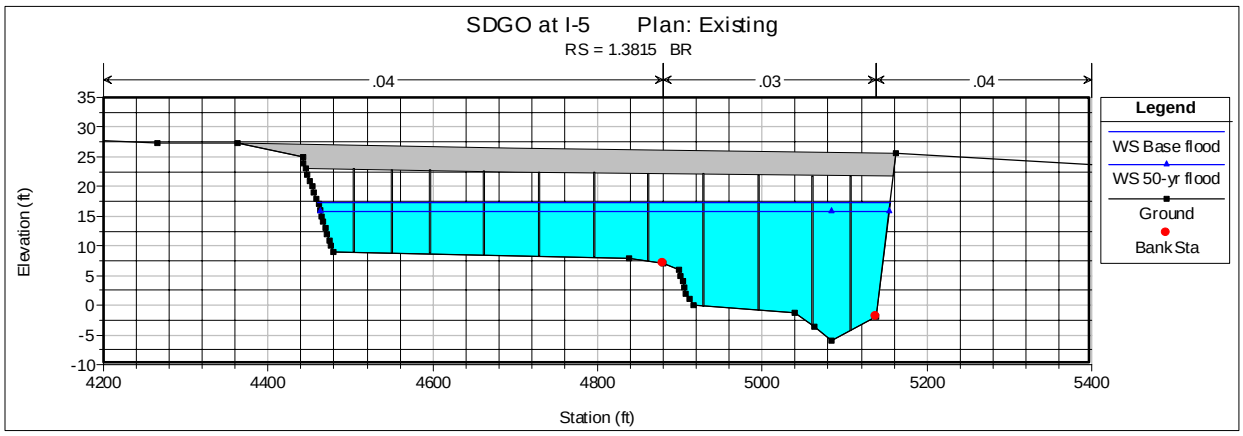

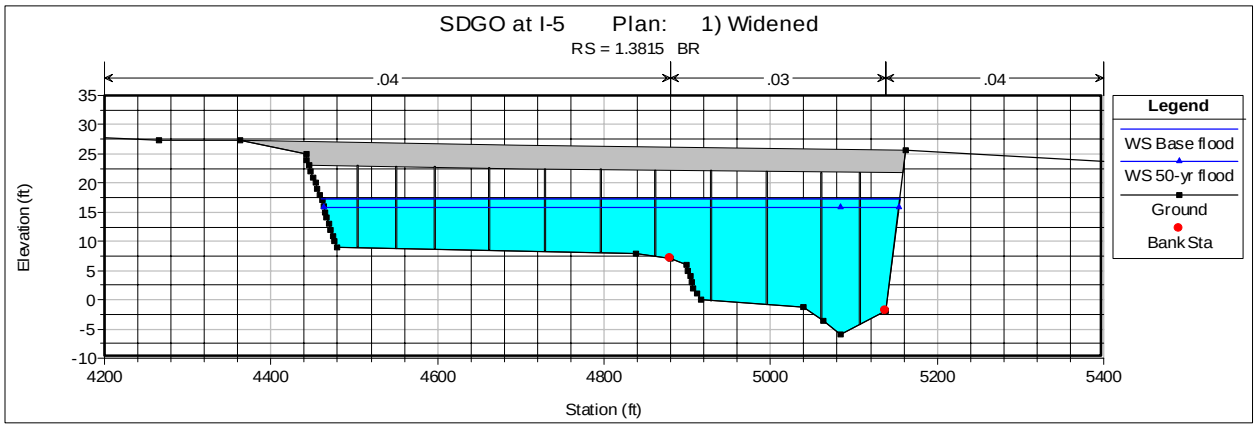

Figure 29 (continued). Cross-sectional profiles of the river channel near the I-5 Bridge crossing

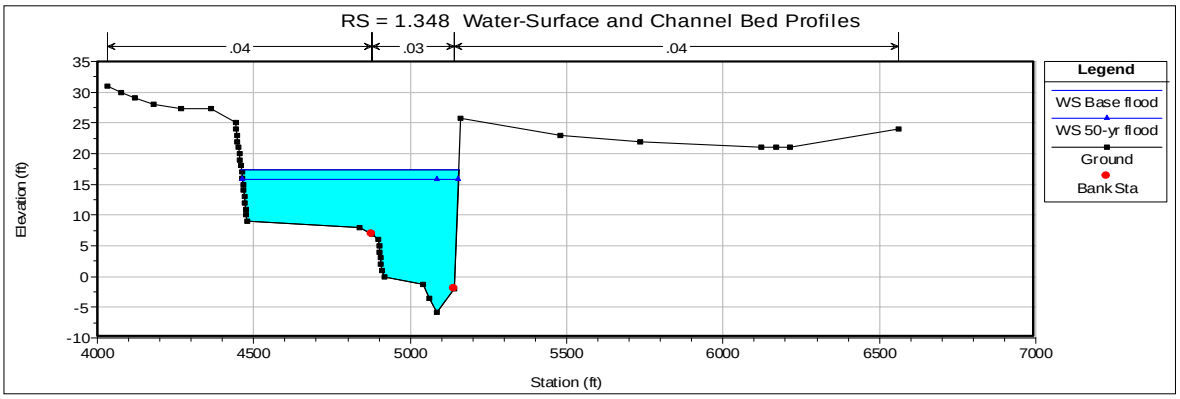

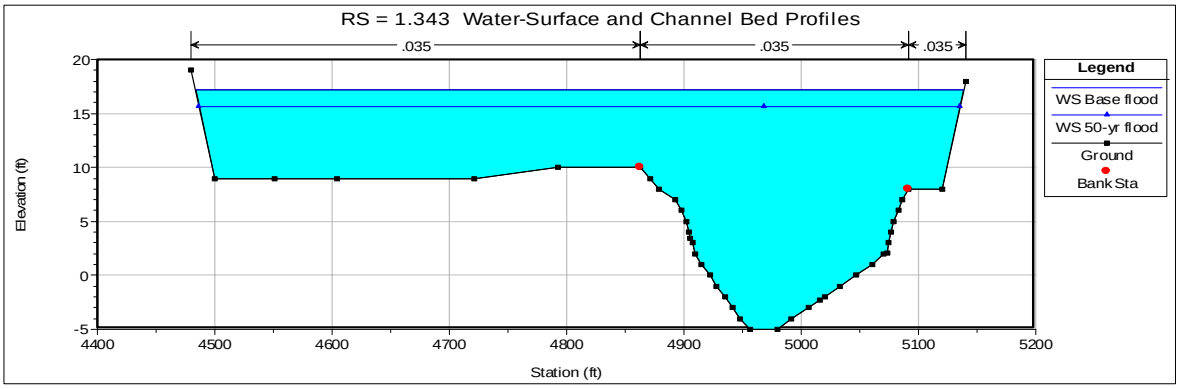

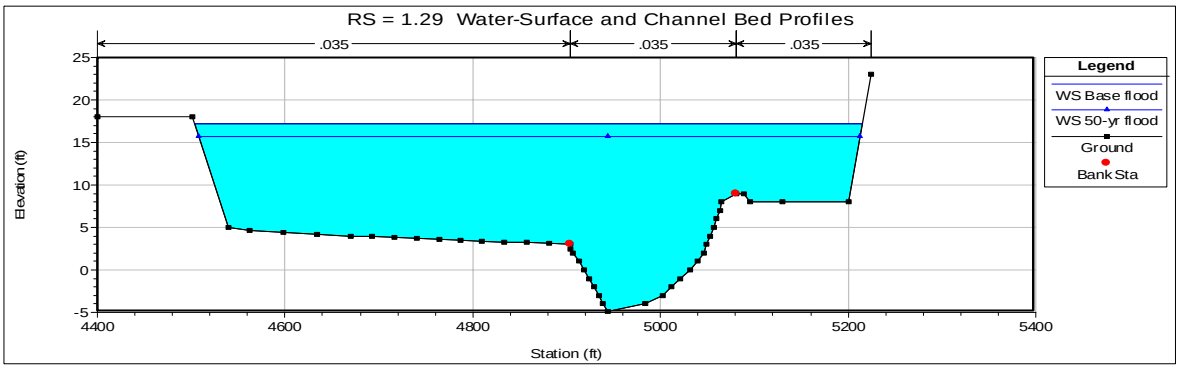

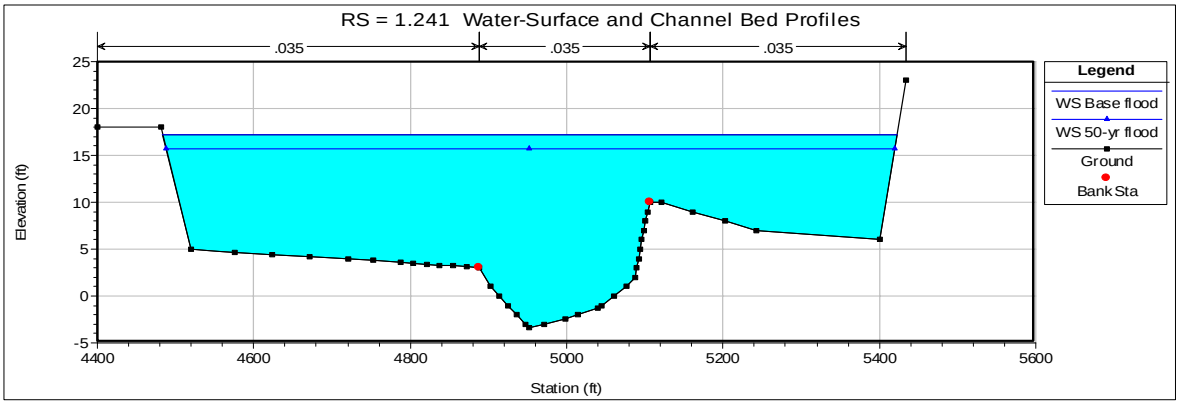

Figure 29 (continued). Cross-sectional profiles of the river channel near the I-5 Bridge crossing

Table 9. Summary of hydraulic parameters from hydraulic modeling

River Sta	Profile	Plan	Q (cfs)	Bed El (ft)	W.S. (ft)	Vel (ft/s)	Width (ft)	Froude #
2.24	Base flood	Existing	36500	-1.10	19.38	3.70	1568.30	0.15
2.24	Base flood	Alternative	36500	-1.10	19.38	3.70	1568.30	0.15
2.24	50-yr flood	Existing	32100	-1.10	17.82	4.09	1558.73	0.18
2.24	50-yr flood	Alternative	32100	-1.10	17.82	4.09	1558.73	0.18
2.183	Base flood	Existing	36500	-1.50	19.27	3.87	1341.84	0.16
2.183	Base flood	Alternative	36500	-1.50	19.27	3.87	1341.84	0.16
2.183	50-yr flood	Existing	32100	-1.50	17.67	4.20	1333.53	0.19
2.183	50-yr flood	Alternative	32100	-1.50	17.67	4.20	1333.53	0.19
2.122	Base flood	Existing	36500	-1	19.20	3.97	1523.71	0.17
2.122	Base flood	Alternative	36500	-1	19.20	3.97	1523.71	0.17
2.122	50-yr flood	Existing	32100	-1	17.57	4.46	1515.36	0.20
2.122	50-yr flood	Alternative	32100	-1	17.57	4.46	1515.36	0.20
2.062	Base flood	Existing	36500	-2.40	19.15	4.04	1609.45	0.16
2.062	Base flood	Alternative	36500	-2.40	19.15	4.04	1609.45	0.16
2.062	50-yr flood	Existing	32100	-2.40	17.49	4.62	1604.48	0.19
2.062	50-yr flood	Alternative	32100	-2.40	17.49	4.62	1604.48	0.19
1.979	Base flood	Existing	36500	-6.30	19.14	2.67	1907.91	0.11
1.979	Base flood	Alternative	36500	-6.30	19.14	2.67	1907.91	0.11
1.979	50-yr flood	Existing	32100	-6.30	17.48	2.92	1902.93	0.13
1.979	50-yr flood	Alternative	32100	-6.30	17.48	2.92	1902.93	0.13
1.895	Base flood	Existing	36500	-2.20	19.13	2.06	2027.39	0.09
1.895	Base flood	Alternative	36500	-2.20	19.13	2.06	2027.39	0.09
1.895	50-yr flood	Existing	32100	-2.20	17.47	2.20	2022.40	0.10
1.895	50-yr flood	Alternative	32100	-2.20	17.47	2.20	2022.40	0.10
1.847	Base flood	Existing	36500	-1	19.12	2.08	2083.37	0.09
1.847	Base flood	Alternative	36500	-1	19.12	2.08	2083.37	0.09
1.847	50-yr flood	Existing	32100	-1	17.46	2.22	2078.37	0.10
1.847	50-yr flood	Alternative	32100	-1	17.46	2.22	2078.37	0.10
1.805	Base flood	Existing	36500	-1.80	19.10	2.38	1983.61	0.10
1.805	Base flood	Alternative	36500	-1.80	19.10	2.38	1983.61	0.10
1.805	50-yr flood	Existing	32100	-1.80	17.43	2.57	1972.01	0.11
1.805	50-yr flood	Alternative	32100	-1.80	17.43	2.57	1972.01	0.11
1.737	Base flood	Existing	36500	-4.60	19.04	3.31	1723.20	0.13

1.737	Base flood	Alternative	36500	-4.60	19.04	3.31	1723.20	0.13
1.737	50-yr flood	Existing	32100	-4.60	17.35	3.69	1714.73	0.15
1.737	50-yr flood	Alternative	32100	-4.60	17.35	3.69	1714.73	0.15
1.674	Base flood	Existing	36500	-15.20	18.93	3.76	1302.63	0.14
1.674	Base flood	Alternative	36500	-15.20	18.93	3.76	1302.63	0.14
1.674	50-yr flood	Existing	32100	-15.20	17.20	4.03	1294.02	0.16
1.674	50-yr flood	Alternative	32100	-15.20	17.20	4.03	1294.02	0.16
1.596	Base flood	Existing	36500	-4	18.63	5.50	1023.88	0.23
1.596	Base flood	Alternative	36500	-4	18.63	5.50	1023.88	0.23
1.596	50-yr flood	Existing	32100	-4	16.88	5.69	849.52	0.25
1.596	50-yr flood	Alternative	32100	-4	16.88	5.69	849.52	0.25
1.522	Base flood	Existing	36500	-3.60	18.53	4.86	831.17	0.21
1.522	Base flood	Alternative	36500	-3.60	18.53	4.86	831.17	0.21
1.522	50-yr flood	Existing	32100	-3.60	16.74	5.14	820.42	0.24
1.522	50-yr flood	Alternative	32100	-3.60	16.74	5.14	820.42	0.24
1.457	Base flood	Existing	42400	-3.70	18.22	6.28	808.52	0.26
1.457	Base flood	Alternative	42400	-3.70	18.19	6.29	808.34	0.26
1.457	50-yr flood	Existing	32100	-3.70	16.54	5.68	798.42	0.25
1.457	50-yr flood	Alternative	32100	-3.70	16.51	5.70	798.26	0.25
1.402	Base flood	Existing	42400	-4.10	18.13	5.97	2435.00	0.25
1.402	Base flood	Alternative	42400	-4.10	18.10	5.99	2435.00	0.25
1.402	50-yr flood	Existing	32100	-4.10	16.48	5.18	2435.00	0.22
1.402	50-yr flood	Alternative	32100	-4.10	16.45	5.19	2435.00	0.22
1.397	Base flood	Alternative	42400	-4.00	17.39	9.40	624.75	0.37
1.397	50-yr flood	Alternative	32100	-4.00	15.87	8.25	619.06	0.34
1.391	Base flood	Existing	42400	-4.00	17.41	9.38	624.82	0.37
1.391	50-yr flood	Existing	32100	-4.00	15.88	8.24	619.17	0.34
1.3815		Bridge						
1.355	Base flood	Existing	42400	-5.90	17.39	6.48	695.28	0.27
1.355	50-yr flood	Existing	32100	-5.90	15.87	5.57	690.57	0.24
1.348	Base flood	Alternative	42400	-5.90	17.37	6.49	695.21	0.27
1.348	50-yr flood	Alternative	32100	-5.90	15.85	5.58	690.52	0.24
1.343	Base flood	Existing	42400	-5.00	17.18	7.34	654.72	0.32
1.343	Base flood	Alternative	42400	-5.00	17.18	7.34	654.72	0.32
1.343	50-yr flood	Existing	32100	-5.00	15.67	6.49	648.68	0.29

1.343	50-yr flood	Alternative	32100	-5.00	15.67	6.49	648.68	0.29
1.29	Base flood	Existing	42400	-4.90	17.25	5.31	712.19	0.22
1.29	Base flood	Alternative	42400	-4.90	17.25	5.31	712.19	0.22
1.29	50-yr flood	Existing	32100	-4.90	15.73	4.57	705.09	0.20
1.29	50-yr flood	Alternative	32100	-4.90	15.73	4.57	705.09	0.20
1.241	Base flood	Existing	42400	-3.40	17.26	4.27	939.28	0.18
1.241	Base flood	Alternative	42400	-3.40	17.26	4.27	939.28	0.18
1.241	50-yr flood	Existing	32100	-3.40	15.73	3.72	931.63	0.16
1.241	50-yr flood	Alternative	32100	-3.40	15.73	3.72	931.63	0.16
1.192	Base flood	Existing	42400	-2.20	17.21	3.96	965.20	0.17
1.192	Base flood	Alternative	42400	-2.20	17.21	3.96	965.20	0.17
1.192	50-yr flood	Existing	32100	-2.20	15.69	3.43	957.85	0.16
1.192	50-yr flood	Alternative	32100	-2.20	15.69	3.43	957.85	0.16
1.137	Base flood	Existing	42400	-4.10	17.16	4.03	1079.56	0.17
1.137	Base flood	Alternative	42400	-4.10	17.16	4.03	1079.56	0.17
1.137	50-yr flood	Existing	32100	-4.10	15.64	3.54	1072.82	0.16
1.137	50-yr flood	Alternative	32100	-4.10	15.64	3.54	1072.82	0.16
1.092	Base flood	Existing	42400	-3.70	17.09	4.28	1129.17	0.18
1.092	Base flood	Alternative	42400	-3.70	17.09	4.28	1129.17	0.18
1.092	50-yr flood	Existing	32100	-3.70	15.58	3.80	1121.87	0.17
1.092	50-yr flood	Alternative	32100	-3.70	15.58	3.80	1121.87	0.17
1.045	Base flood	Existing	42400	-3.60	17.02	4.50	1104.07	0.19
1.045	Base flood	Alternative	42400	-3.60	17.02	4.50	1104.07	0.19
1.045	50-yr flood	Existing	32100	-3.60	15.52	3.84	1041.14	0.17
1.045	50-yr flood	Alternative	32100	-3.60	15.52	3.84	1041.14	0.17
0.967	Base flood	Existing	42400	-4.20	16.89	4.61	905.67	0.19
0.967	Base flood	Alternative	42400	-4.20	16.89	4.61	905.67	0.19
0.967	50-yr flood	Existing	32100	-4.20	15.42	4	901.25	0.17
0.967	50-yr flood	Alternative	32100	-4.20	15.42	4	901.25	0.17
0.866	Base flood	Existing	42400	-4.90	16.83	4.04	1187	0.17
0.866	Base flood	Alternative	42400	-4.90	16.83	4.04	1187	0.17
0.866	50-yr flood	Existing	32100	-4.90	15.36	3.46	1118.09	0.15
0.866	50-yr flood	Alternative	32100	-4.90	15.36	3.46	1118.09	0.15
0.814	Base flood	Existing	42400	-3.20	16.82	3.16	1257.05	0.13
0.814	Base flood	Alternative	42400	-3.20	16.82	3.16	1257.05	0.13
0.814	50-yr flood	Existing	32100	-3.20	15.36	2.74	1254.30	0.12
0.814	50-yr flood	Alternative	32100	-3.20	15.36	2.74	1254.30	0.12

0.773	Base flood	Existing	42400	-3.20	16.81	3.08	1325.01	0.13
0.773	Base flood	Alternative	42400	-3.20	16.81	3.08	1325.01	0.13
0.773	50-yr flood	Existing	32100	-3.20	15.34	2.68	1323.68	0.11
0.773	50-yr flood	Alternative	32100	-3.20	15.34	2.68	1323.68	0.11
0.706	Base flood	Existing	42400	-12.30	16.71	4.10	1163.18	0.15
0.706	Base flood	Alternative	42400	-12.30	16.71	4.10	1163.18	0.15
0.706	50-yr flood	Existing	32100	-12.30	15.27	3.59	1159.05	0.14
0.706	50-yr flood	Alternative	32100	-12.30	15.27	3.59	1159.05	0.14
0.685	Base flood	Existing	42400	-13.50	16.70	3.38	1074.91	0.15
0.685	Base flood	Alternative	42400	-13.50	16.70	3.38	1074.91	0.15
0.685	50-yr flood	Existing	32100	-13.50	15.26	2.90	1072.29	0.14
0.685	50-yr flood	Alternative	32100	-13.50	15.26	2.90	1072.29	0.14
0.666	Base flood	Existing	42400	-15.60	16.57	5.03	870.47	0.18
0.666	Base flood	Alternative	42400	-15.60	16.57	5.03	870.47	0.18
0.666	50-yr flood	Existing	32100	-15.60	15.16	4.34	870.38	0.16
0.666	50-yr flood	Alternative	32100	-15.60	15.16	4.34	870.38	0.16
0.619	Base flood	Existing	42400	-4.70	16.36	5.67	718.24	0.23
0.619	Base flood	Alternative	42400	-4.70	16.36	5.67	718.24	0.23
0.619	50-yr flood	Existing	32100	-4.70	15	4.86	717.33	0.21
0.619	50-yr flood	Alternative	32100	-4.70	15	4.86	717.33	0.21

Hydrologic Data Summary - The hydrologic data include characteristics of the design flood, the base flood, the flood of record, and the overtopping flood. The design flood is the peak discharge selected for the design of the bridge located within a base floodplain. By definition, through lanes will not be overtopped by the design flood. The base flood is the 100-yr flood for which the exceedance probability is one percent in any given year. The hydrologic data summary is given in Table 10. The table shows that the bridge with its low chord elevation of 23.3 feet will pass the 100-yr flood with a freeboard of about 6 feet. The record flood is the greatest recorded flood in the drainage basin; its value is 22,000 cfs. The overtopping flood is determined based on the minimum roadway elevation for the approach road embankments. Under a discharge exceeding the design discharge, the roadway will be overtopped. For the I-5 Bridge on the San Dieguito River, the roadway elevation is about 8 feet above the base flood elevation. Because of the large freeboard, the overtopping flood would be very large and hence not considered.

Table 10. Hydrologic data summary for proposed I-5 Bridge across San Dieguito River in English units

Hydrologic Summary	Flood of Record	Design flood	Over-topping flood	100-yr Flood
Frequency (Yrs.)	35	50	NA	100
Discharge (CFS)	22,000	32,100	NA	42,400
Water-Surface Elev. (Ft)	13.8	15.9	NA	17.4
Velocity (FPS)	7.1	8.3	NA	9.4

V. SCOUR STUDY FOR THE INTERSTATE 5 BRIDGE

River channel scour at the I-5 Bridge crossing is related to flood flow, river channel geometry and the bed sediment characteristics. The study reach of the San Dieguito River is a sand bed river. Sediment samples were taken from the river bed at several locations. These samples were analyzed and their grain size distributions are shown in Figure 30. The bed material consists primarily of sand with small amounts of fines (silt and clay) and gravel.

Stream channel scour consists of general scour and local scour. General scour is related to the sediment supplied to and transported out of a channel reach. Local scour is due to a local obstruction to flow by a bridge pier/bent or abutment.

To determine general scour, it is necessary to consider the sediment supply by flow to the channel reach and sediment removal out of the reach. Sediment delivery in the stream channel and supply to the subject area is related to the flood hydrograph, channel geometry, and sediment characteristics, etc. To account for these factors, it requires mathematical simulation of the hydraulics of stream flow, sediment transport and stream channel changes.

Mathematical Model for General Scour - The FLUVIAL-12 model (Chang, 1988) is employed for this project. For a given flood hydrograph, the FLUVIAL model simulates spatial and temporal variations in water-surface elevation, sediment transport and channel geometry. Scour and fill of the streambed are coupled with width variation in the prediction of river channel changes. Computations are based on finite difference approximations to energy and mass conservation that are representative of open channel flow.

The model simulates the inter-related changes in channel-bed profile and channel width, based upon a stream's tendency to seek uniformities in sediment discharge and power expenditure. At each time step, scour and fill of the channel bed are computed based on the spatial variation in sediment discharge along the channel. Channel-bed corrections for scour and fill will reduce the non-uniformity in sediment discharge. Width changes are also made at each time step, resulting in a movement toward uniformity in power expenditure along the channel. Because the energy gradient is a measure of the power expenditure, uniformity in power expenditure also means a uniform energy gradient or linear water surface profile. A river channel may not have a uniform power expenditure or linear water-surface profile, but it is constantly adjusting itself toward that direction. The model was calibrated using 12 sets of field data. Such calibration studies are as listed in the Users Manual for FLUVIAL-12. Most of the calibration studies were peer-reviewed.

Grain size distributions of the bed material are required data for the modeling study. Such data for the San Dieguito River are shown in Figure 30.

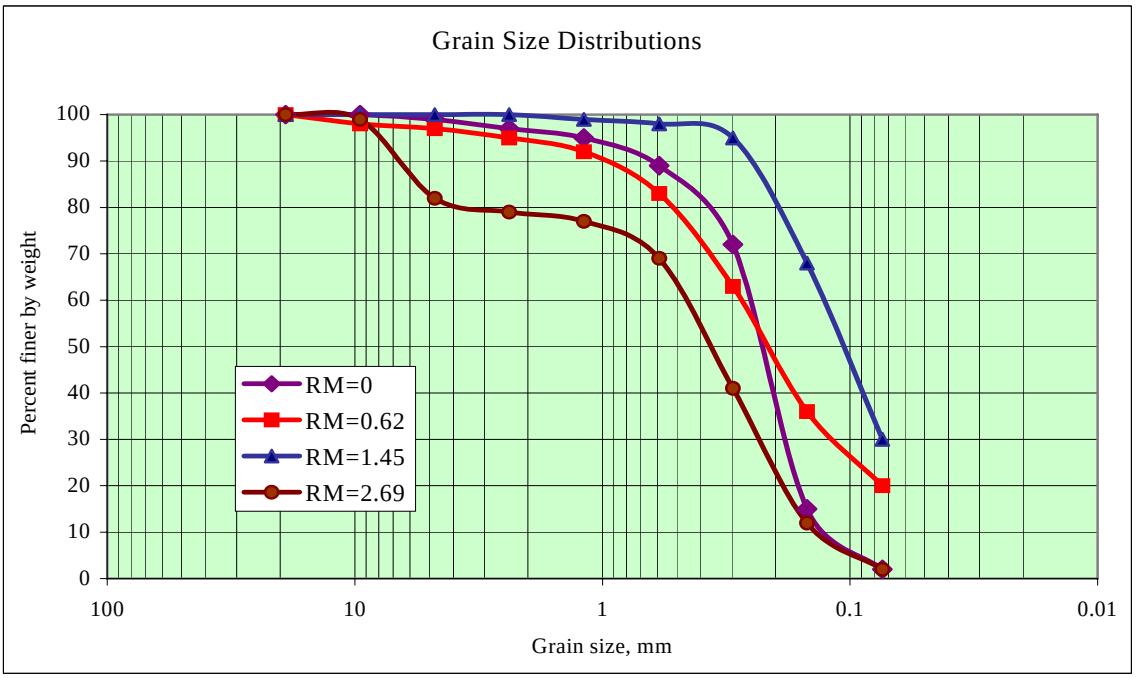

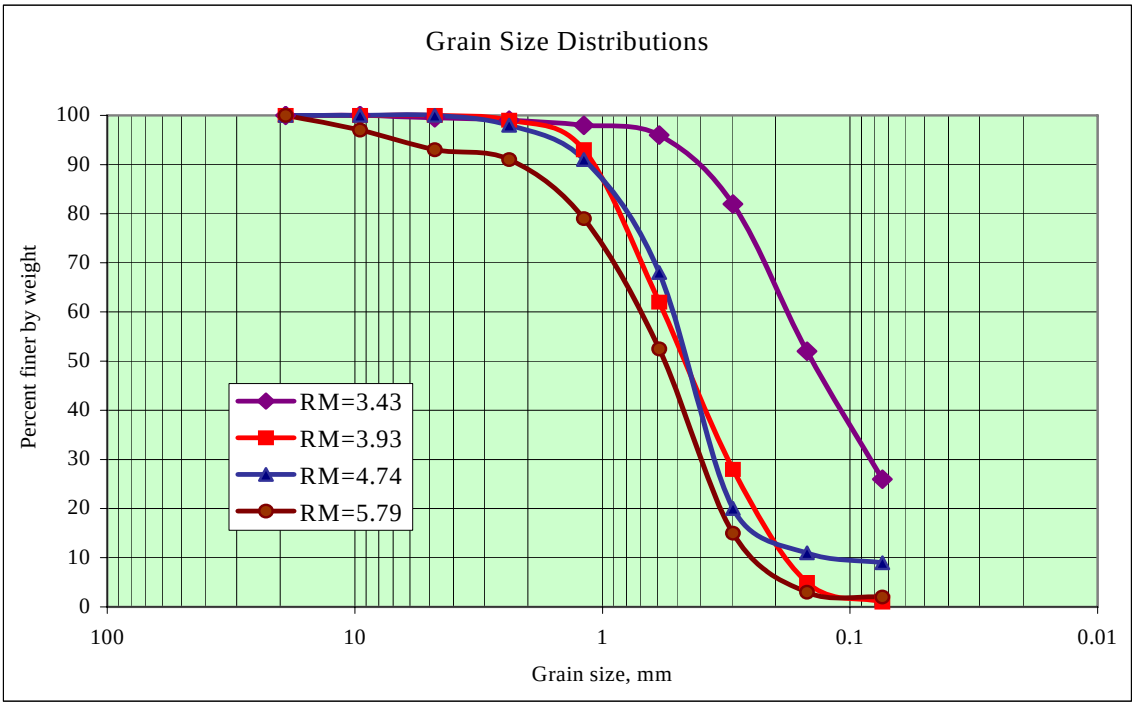

Figure 30. Grain size distributions of bed sediment

Selection of the Engelund-Hansen Formula — A sediment transport formula is employed in the model. The Engelund-Hansen formula for sediment transport was selected for the study for the following reasons:

(1) The selection was based on the most extensive evaluation of formulas made by Brownlie (see Figure 31); the Engelund-Hansen formula has the best correlation with field data.

(2) The Engelund-Hansen formula was used in many studies in this region. The results of these studies were verified by field data.

(3) In a calibration study of the FLUVIAL-12 model, the results generated by the Engelund-Hansen formula can be correlated with the measured channel changes in the San Dieguito River during the 1993 flood.

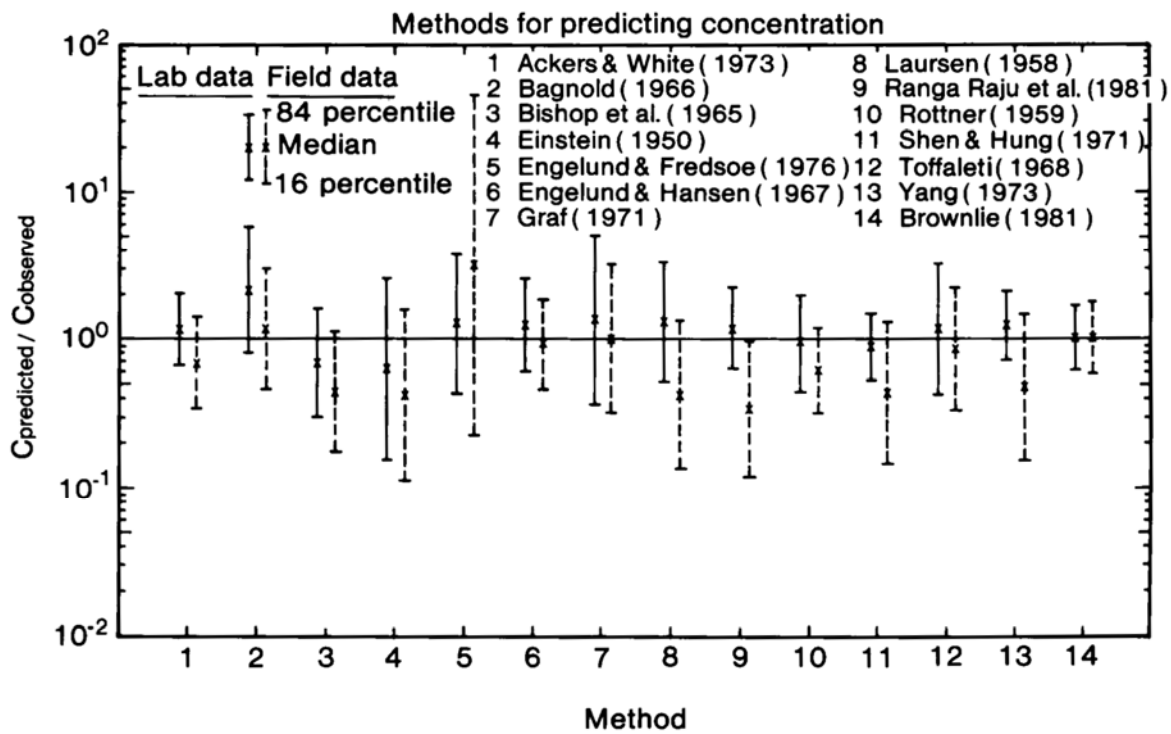

Figure 31. Evaluation of sediment transport formulas by Brownlie

Engelund-Hansen Formula - Engelund and Hansen applied Bagnold's stream power concept and the similarity principle to obtain their sediment transport equation:

$$f' \varphi = 0.1 (\tau_*)^{5/2} \tag{1}$$

with $$f' = \frac{2gRS}{U^2} \tag{2}$$

$$\varphi = \frac{q_s}{\gamma_s [(s - 1) gd^3]^{1/2}}, \qquad \tau_* = \frac{\tau_o}{(\gamma_s - \gamma) d} \tag{3}$$

where f' is the friction factor, d is the median fall diameter of the bed material, φ is the dimensionless sediment discharge, s is the specific gravity of sediment, and τ_* is the dimensionless shear stress or the Shields stress. Substituting Eqs. 2 and 3 into Eq. 1 yields

$$C_s = 0.05 \frac{s}{s - 1} \frac{US}{[(s - 1)gd]^{1/2}} \left[\frac{RS}{(s - 1)\, d}\right]^{1/2} \tag{4}$$

where C_s (= Q_s/Q) is the sediment concentration by weight. This equation relates sediment concentration to the *U-S* product (which is the rate of energy expenditure per unit weight of water) and the *R-S* product (which is the shear stress). Strictly speaking, the Engelund-Hansen formula should be applied to streams with a dune bed in accordance with the similarity principle. However, it can be applied to upper flow regime with particle size greater than 0.15 mm without serious error.

Simulated Results on Scour - The 100-yr flood was used to simulate sediment transport and stream channel changes for the lower San Dieguito River under the proposed bridge plan. Simulated results are presented in graphical forms, in Figures 32 and 33. Figure 32 shows the water-surface and channel bed profile changes of the adjacent river reach during the 100-yr flood; Figure 33 shows the changes in channel cross section at the bridge crossing. In each figure, the graphical results include those before the flood, at the peak flow, and at the end of flood. The cross-sectional profile for maximum general scour at the bridge crossing is also shown in Figure 33. The minimum bed elevation reached by general scour during the 100-yr flood is simulated to reach the bed elevation of -5.2 feet.

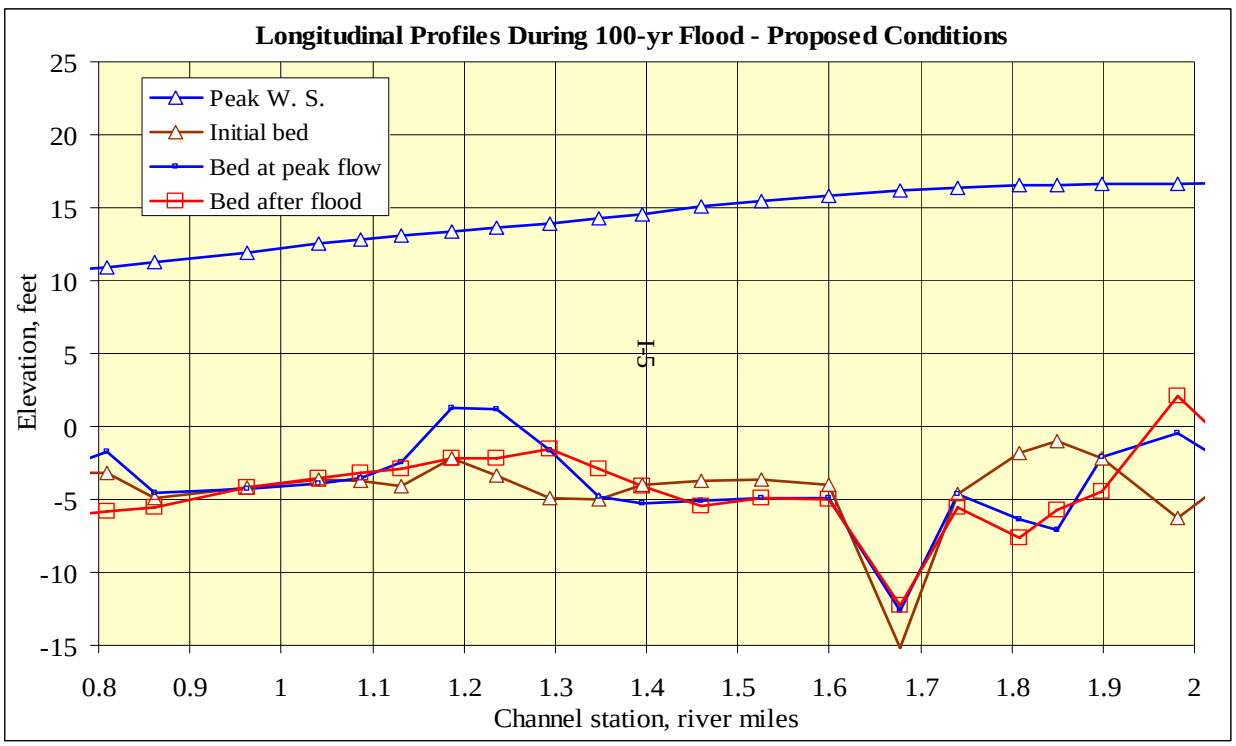

Figure 32. Water-surface and channel-bed profile changes during 100-yr flood for proposed conditions

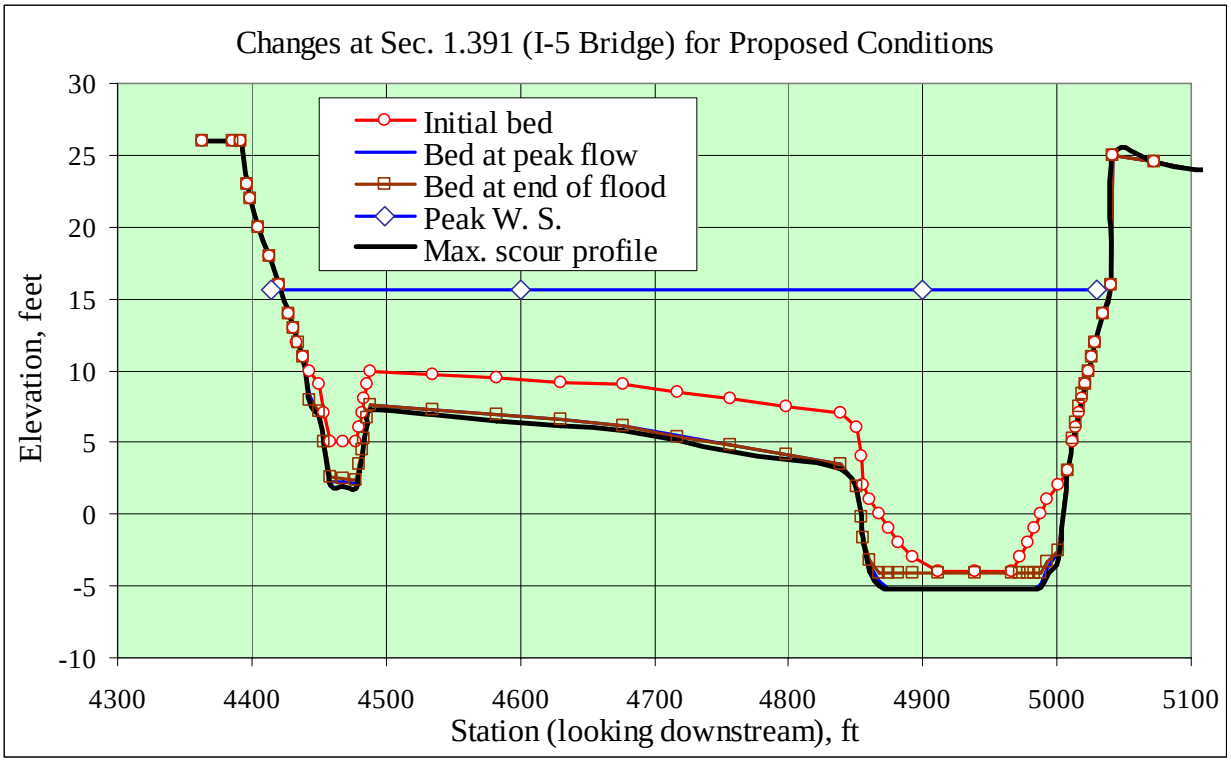

Figure 33. Changes in channel cross section at I-5 Bridge crossing during 100-yr flood for proposed conditions

Local Scour at Bridge Piers/Bents - For the piers of the bridge, the total scour is the general scour plus the local scour at the piers. The magnitude of local scour around bridge piers/bents may be estimated using certain established formulas. The Federal Highway Administration has adopted the following equation (see Hydraulic Engineering Circular No. 18 by FHWA, 2006) for round-nosed piers/bents or cylindrical piers/bents.

$$Y_s/Y_1 = 2.0\ K_1\ K_2\ (b/Y_1)^{0.65}\ \mathbf{F}^{0.43} \qquad (5)$$

where Y = depth of local scour measured from the mean bed elevation, in feet;
K_1 = correction for pier/bent nose shape, equal to 1 for circular piers/bents and 1.1 for rectangular piers/bents;
K_2 = correction factor for angle of attack, equal to 1 for zero skew;
b = projected pier/bent width;
Y_1 = approach flow depth;
$\mathbf{F}$ = Froude number = $V//gY_1$; and
V = velocity of approach flow.

The required hydraulic information for this equation is included in the FLUVIAL-12 output with the bridge in place. The value of Y_1 (approach flow depth) is 14.6 feet and the Froude number is 0.32.

The depths of local scour at the bridge piers were computed using Equation 5. For the proposed conditions, pertinent parameters for the bridge hydraulics are taken from the output listings of FLUVIAL-12 for the bridge crossing at the peak discharge. Since the pier width is

not yet selected, several pier widths were assumed. The computed results for local scour are listed in Table 11. The maximum total scour at the bridge piers is the general scour plus the local scour.

Table 11. Summary of computed local scour depths at bridge piers/bents

Pier width of diameter Feet	Local scour depth
0.5	2.0
1	3.1
1.5	4.1
2	4.9
2.5	5.7
3	6.4
4	7.1

The maximum total scour at the bridge piers is the general scour plus the local scour. The profile of maximum general scour is shown in Figure 33. If pile caps are used, they should be located below the elevation of total scour. The minimum bed elevation reached by total scour is the bed elevation reached by general scour of -5.2 feet minus the depth of local scour.

REFERENCES

Brownlie, W. R., "Prediction of Flow Depth and Sediment Discharge in Open Channels," Rept. No. KH-R-43A, W.M. Keck Laboratory of Hydraulics and Water Resources, California Institute of Technology, Pasadena, California, November 1981.

Chang, H. H., *Fluvial Processes in River Engineering*, John Wiley & Sons, New York, NY, 1988, 432 pp.

Engelund, F. and Hansen, E., A Monograph on Sediment Transport in Alluvial Streams, Teknisk Vorlag, Copenhagen, Denmark, 1967.

Federal Highway Administraion, “Hydrologic Engineeing Circular 18”, 2006.

U. S. Army Corps of Engineers, "Hydraulic Design of Flood Control Structures", EM 1110-2-1601, July 1970.

U.S. Army Crops of Engineers, Los Angeles District, “Flood Plain Information, Agua Hedionda Creek”, 1973.

U.S. Army Crops of Engineers, Los Angeles District, “Flood Plain Information, San Marcos Creek”, 1971.

APPENDIX A. HEC-RAS REPORT FOR THE HYDRAULIC STUDY

PART I. AGUA HEDIONDA LAGOON

```
                    HEC-RAS Version 4.1.0 Jan 2010
                         U.S. Army Corps of Engineers
                        Hydrologic Engineering Center
                              609 Second Street
                              Davis, California


            X     X  XXXXXX    XXXX        XXXX       XX      XXXX
            X     X  X        X    X       X   X     X  X    X
            X     X  X        X            X   X    X    X   X
            XXXXXXX  XXXX     X       XXX  XXXX     XXXXXX    XXXX
            X     X  X        X            X  X     X    X        X
            X     X  X        X    X       X   X    X    X        X
            X     X  XXXXXX    XXXX        X    X   X    X   XXXXX



PROJECT DATA
Project Title: Agua Hedionda Lagoon
Project File : AguaHedi.prj
Run Date and Time: 5/6/2010 1:47:42 PM

Project in English units

Project Description:
AGUA HEDIONDA, BATHYMETRY FROM JENKINS
    NGVD
    HOWARD H. CHANG,
APRIL 2010, Q100=15,000 cfs
    AGUA HEDIONDA, BATHYMETRY FROM JENKINS

NGVD
    HOWARD H. CHANG, APRIL 2010, Q100=15,000 cfs



PLAN DATA

Plan Title: Existing
Plan File : C:\HEC Data\RAS\AguaHedi.p03

           Geometry Title: Existing Geom
           Geometry File : C:\HEC Data\RAS\AguaHedi.g03

           Flow Title    : Imported Flow 03
           Flow File     : C:\HEC Data\RAS\AguaHedi.f03

Plan Summary Information:
Number of:  Cross Sections =   42    Multiple Openings  =    0
            Culverts       =    0    Inline Structures  =    0
            Bridges        =    1    Lateral Structures =    0

Computational Information
    Water surface calculation tolerance  =  0.01
    Critical depth calculation tolerance =  0.01
```

```
    Maximum number of iterations         =  20
    Maximum difference tolerance         =  0.3
    Flow tolerance factor                =  0.001

Computation Options
    Critical depth computed only where necessary
    Conveyance Calculation Method: At breaks in n values only
    Friction Slope Method:         Average Conveyance
    Computational Flow Regime:     Subcritical Flow




FLOW DATA

Flow Title: Imported Flow 03
Flow File : C:\HEC Data\RAS\AguaHedi.f03

Flow Data (cfs)

  River           Reach           RS                 100-yr
  RIVER-1         Reach-1         9715                10500


Boundary Conditions

  River           Reach           Profile                       Upstream
Downstream

  RIVER-1         Reach-1         100-yr
Known WS = 2.8




GEOMETRY DATA

Geometry Title: Existing Geom
Geometry File : C:\HEC Data\RAS\AguaHedi.g03

CROSS SECTION


RIVER: RIVER-1
REACH: Reach-1            RS: 9715

INPUT
Description: 97
Station Elevation Data    num=       6
     Sta    Elev     Sta    Elev     Sta    Elev     Sta    Elev     Sta    Elev
     -32       8       0       3      63       2      75       2     260       3
     300       8

Manning's n Values        num=       3
     Sta   n Val     Sta   n Val     Sta   n Val
     -32     .03       0    .025     260     .03

Bank Sta: Left   Right    Lengths: Left Channel   Right     Coeff Contr.   Expan.
             0     260              220     200     180             .1       .3

CROSS SECTION


RIVER: RIVER-1
```

```
REACH: Reach-1            RS: 9515

INPUT
Description: 95
Station Elevation Data    num=       6
     Sta    Elev     Sta    Elev     Sta    Elev     Sta    Elev     Sta    Elev
     -32       8       0       3      68       2     258       2     401       3
     422       8

Manning's n Values        num=       3
     Sta   n Val     Sta   n Val     Sta   n Val
     -32     .03       0    .025     401     .03

Bank Sta: Left   Right    Lengths: Left Channel   Right     Coeff Contr.   Expan.
             0     401              225     210     180             .1       .3

CROSS SECTION


RIVER: RIVER-1
REACH: Reach-1            RS: 9305

INPUT
Description: 93
Station Elevation Data    num=      14
     Sta    Elev     Sta    Elev     Sta    Elev     Sta    Elev     Sta    Elev
     -20       8       0       3      78       2     118       1     125      -1
     127      -2     130      -3     162      -3     170      -2     178      -1
     304       1     400       2     485       3     505       8

Manning's n Values        num=       3
     Sta   n Val     Sta   n Val     Sta   n Val
     -20     .03       0    .025     485     .03

Bank Sta: Left   Right    Lengths: Left Channel   Right     Coeff Contr.   Expan.
             0     485              225     235     245             .1       .3

CROSS SECTION


RIVER: RIVER-1
REACH: Reach-1            RS: 9070

INPUT
Description: 90
Station Elevation Data    num=      14
     Sta    Elev     Sta    Elev     Sta    Elev     Sta    Elev     Sta    Elev
     -20       8       0       3      27       2      54       1     119      -1
     142      -2     173      -3     187      -3     198      -2     210      -1
     443       1     542       2     675       3     700       8

Manning's n Values        num=       3
     Sta   n Val     Sta   n Val     Sta   n Val
     -20     .03       0    .025     675     .03

Bank Sta: Left   Right    Lengths: Left Channel   Right     Coeff Contr.   Expan.
             0     675              290     290     290             .1       .3

CROSS SECTION


RIVER: RIVER-1
REACH: Reach-1            RS: 8780
```

```
INPUT
Description: 87
Station Elevation Data    num=      14
     Sta    Elev     Sta    Elev     Sta    Elev     Sta    Elev     Sta    Elev
     -20       8       0       3      37       2      75       1     164      -1
     193      -2     206      -3     266      -3     295      -2     348      -1
     616       1     710       2     817       3     840       8

Manning's n Values        num=       3
     Sta   n Val     Sta   n Val     Sta   n Val
     -20     .03       0    .025     817     .03

Bank Sta: Left   Right    Lengths: Left Channel   Right     Coeff Contr.   Expan.
             0     817              415     415     415             .1       .3

CROSS SECTION


RIVER: RIVER-1
REACH: Reach-1            RS: 8365

INPUT
Description: 83
Station Elevation Data    num=      14
     Sta    Elev     Sta    Elev     Sta    Elev     Sta    Elev     Sta    Elev
     -20       8       0       3      19       2      38       1     130      -1
     224      -2     402      -2     476      -2     933      -2    1027      -1
    1083       1    1100       2    1183       3    1204       8

Manning's n Values        num=       3
     Sta   n Val     Sta   n Val     Sta   n Val
     -20     .03       0    .025    1183     .03

Bank Sta: Left   Right    Lengths: Left Channel   Right     Coeff Contr.   Expan.
             0    1183              370     350     330             .1       .3

CROSS SECTION


RIVER: RIVER-1
REACH: Reach-1            RS: 8015

INPUT
Description: 80
Station Elevation Data    num=      44
     Sta    Elev     Sta    Elev     Sta    Elev     Sta    Elev     Sta    Elev
     -20       8       0       3      24       2      58       1     116      -1
     164      -2     230      -3     397      -4     585      -4     593      -4
     604      -4     641      -4     645      -4     678      -4     683      -4
     687      -4     792      -5     800      -5     801      -5     802      -5
     808      -5     833      -5     992      -4     993      -4    1008      -4
    1016      -4    1036      -4    1055      -4    1057      -4    1061      -4
    1063      -4    1070      -4    1095      -4    1163      -4    1169      -4
    1172      -4    1205      -4    1253      -3    1338      -2    1406      -1
    1458       1    1484       2    1544       3    1564       8

Manning's n Values        num=       3
     Sta   n Val     Sta   n Val     Sta   n Val
     -20     .03       0    .025    1544     .03

Bank Sta: Left   Right    Lengths: Left Channel   Right     Coeff Contr.   Expan.
             0    1544              390     335     300             .1       .3

CROSS SECTION
```

RIVER: RIVER-1
REACH: Reach-1 RS: 7680

INPUT
Description: 76
Station Elevation Data num= 36

Sta	Elev	Sta	Elev	Sta	Elev	Sta	Elev	Sta	Elev
-20	8	0	3	7	2	15	1	31	-1
39	-2	47	-3	231	-4	241	-5	258	-6
637	-6	720	-6	728	-6	732	-6	735	-6
745	-6	814	-7	826	-7	827	-7	872	-7
879	-7	881	-7	901	-7	917	-7	931	-7
1294	-7	1314	-6	1334	-5	1355	-4	1394	-3
1454	-2	1482	-1	1531	1	1557	2	1590	3
1610	8								

Manning's n Values num= 3

Sta	n Val	Sta	n Val	Sta	n Val
-20	.03	0	.025	1590	.03

Bank Sta: Left	Right	Lengths: Left	Channel	Right	Coeff Contr.	Expan.
0	1590	475	475	475	.1	.3

CROSS SECTION

RIVER: RIVER-1
REACH: Reach-1 RS: 7205

INPUT
Description: 72
Station Elevation Data num= 26

Sta	Elev	Sta	Elev	Sta	Elev	Sta	Elev	Sta	Elev
-20	8	0	3	23	2	46	1	93	-1
116	-2	137	-3	153	-4	172	-5	202	-6
477	-6	484	-6	508	-6	722	-6	729	-6
882	-6	1251	-6	1292	-5	1315	-4	1330	-3
1346	-2	1356	-1	1368	1	1374	2	1380	3
1400	8								

Manning's n Values num= 3

Sta	n Val	Sta	n Val	Sta	n Val
-20	.03	0	.025	1380	.03

Bank Sta: Left	Right	Lengths: Left	Channel	Right	Coeff Contr.	Expan.
0	1380	480	500	520	.1	.3

CROSS SECTION

RIVER: RIVER-1
REACH: Reach-1 RS: 6705

INPUT
Description: 31
Station Elevation Data num= 25

Sta	Elev	Sta	Elev	Sta	Elev	Sta	Elev	Sta	Elev
-20		0	3	4	2	9	1	19	-1
25	-2	39	-3	295	-4	382	-5	389	-5
391	-5	395	-5	398	-5	413	-5	511	-6
577	-6	1455	-5	1488	-4	1558	-3	1564	-2
1572	-1	1589	1	1596	2	1604	3	1624	8

```
Manning's n Values        num=       3
     Sta   n Val     Sta   n Val     Sta   n Val
     -20     .03       0    .025    1604     .03

Bank Sta: Left   Right    Lengths: Left Channel   Right     Coeff Contr.   Expan.
             0    1604              520     520     520             .1       .3

CROSS SECTION


RIVER: RIVER-1
REACH: Reach-1            RS: 6185

INPUT
Description: 61
Station Elevation Data    num=      16
     Sta    Elev     Sta    Elev     Sta    Elev     Sta    Elev     Sta    Elev
     -20       8       0       3      15       2      30       1      60      -1
      75      -2      90      -3     296      -4    1575      -4    1674      -3
    1681      -2    1686      -1    1697       1    1703       2    1707       3
    1727       8

Manning's n Values        num=       3
     Sta   n Val     Sta   n Val     Sta   n Val
     -20     .03       0    .025    1707     .03

Bank Sta: Left   Right    Lengths: Left Channel   Right     Coeff Contr.   Expan.
             0    1707              525     525     525             .1       .3

CROSS SECTION


RIVER: RIVER-1
REACH: Reach-1            RS: 5660

INPUT
Description: 56
Station Elevation Data    num=      31
     Sta    Elev     Sta    Elev     Sta    Elev     Sta    Elev     Sta    Elev
     -20       8       0       3       6       2      12       1      24      -1
      29      -2      35      -3     118      -4     722      -5     884      -6
     934      -6     954      -6     955      -6    1016      -6    1029      -6
    1122      -6    1208      -7    1212      -7    1307      -7    1308      -7
    1381      -7    1392      -6    1399      -5    1408      -4    1518      -3
    1524      -2    1540      -1    1564       1    1576       2    1586       3
    1606       8

Manning's n Values        num=       3
     Sta   n Val     Sta   n Val     Sta   n Val
     -20     .03       0    .025    1586     .03

Bank Sta: Left   Right    Lengths: Left Channel   Right     Coeff Contr.   Expan.
             0    1586              540     500     460             .1       .3

CROSS SECTION


RIVER: RIVER-1
REACH: Reach-1            RS: 5160

INPUT
Description: 51
Station Elevation Data    num=      30
```

```
     Sta    Elev     Sta    Elev     Sta    Elev     Sta    Elev     Sta    Elev
     -20       8       0       3       3       2       7       1      12      -1
      14      -2      17      -3      51      -4     195      -5     252      -6
     268      -7     717      -7     718      -7    1148      -7    1155      -7
    1164      -7    1184      -7    1195      -7    1196      -7    1339      -7
    1353      -6    1363      -5    1411      -4    1481      -3    1487      -2
    1492      -1    1503       1    1508       2    1513       3    1533       8

Manning's n Values        num=       3
     Sta   n Val     Sta   n Val     Sta   n Val
     -20     .03       0    .025    1513     .03

Bank Sta: Left   Right    Lengths: Left Channel   Right     Coeff Contr.   Expan.
             0    1513              520     425     350             .1       .3

CROSS SECTION


RIVER: RIVER-1
REACH: Reach-1            RS: 4735

INPUT
Description: 47
Station Elevation Data    num=      24
     Sta    Elev     Sta    Elev     Sta    Elev     Sta    Elev     Sta    Elev
     -20       8       0       3       6       2      13       1      26      -1
      32      -2      39      -3      69      -4     225      -5     427      -5
     436      -5     684      -6    1035      -7    1387      -7    1392      -6
    1402      -5    1476      -4    1502      -3    1511      -2    1521      -1
    1541       1    1551       2    1555       3    1575       8

Manning's n Values        num=       3
     Sta   n Val     Sta   n Val     Sta   n Val
     -20     .03       0    .025    1555     .03

Bank Sta: Left   Right    Lengths: Left Channel   Right     Coeff Contr.   Expan.
             0    1555              600     440     300             .1       .3

CROSS SECTION


RIVER: RIVER-1
REACH: Reach-1            RS: 4295

INPUT
Description: 42
Station Elevation Data    num=      41
     Sta    Elev     Sta    Elev     Sta    Elev     Sta    Elev     Sta    Elev
     -20       8       0       3       4       2       9       1      18      -1
      23      -2      28      -3      38      -4      45      -5     116      -5
     230      -5     440      -6     444      -6     459      -6     460      -6
     490      -6     546      -6     549      -6     614      -6     651      -6
     659      -6     669      -6     741      -6     954      -6     955      -6
    1014      -6    1022      -6    1044      -6    1083      -6    1084      -6
    1090      -6    1221      -6    1249      -5    1278      -4    1311      -3
    1321      -2    1328      -1    1340       1    1347       2    1353       3
    1375       8

Manning's n Values        num=       3
     Sta   n Val     Sta   n Val     Sta   n Val
     -20     .03       0    .025    1353     .03

Bank Sta: Left   Right    Lengths: Left Channel   Right     Coeff Contr.   Expan.
             0    1353              250     350     450             .1       .3
```

CROSS SECTION

RIVER: RIVER-1
REACH: Reach-1 RS: 3945

INPUT
Description: 39
Station Elevation Data num= 46

Sta	Elev	Sta	Elev	Sta	Elev	Sta	Elev	Sta	Elev
-20	8	0	3	5	2	10	1	21	-1
26	-2	31	-3	50	-4	81	-5	225	-6
346	-7	350	-7	436	-7	640	-7	657	-6
676	-5	677	-5	703	-5	728	-6	732	-6
747	-6	754	-6	755	-6	925	-7	926	-7
961	-7	962	-7	967	-7	983	-6	1000	-5
1023	-5	1024	-5	1025	-5	1034	-5	1039	-5
1047	-5	1110	-5	1127	-5	1463	-4	1475	-3
1482	-2	1490	-1	1504	1	1512	2	1519	3
1540	8								

Manning's n Values num= 3

Sta	n Val	Sta	n Val	Sta	n Val
-20	.03	0	.025	1519	.03

Bank Sta: Left	Right	Lengths: Left	Channel	Right	Coeff Contr.	Expan.
0	1519	160	190	350	.1	.3

Ineffective Flow num= 1

Sta L	Sta R	Elev	Permanent
750	1540	10	F

CROSS SECTION

RIVER: RIVER-1
REACH: Reach-1 RS: 3755

INPUT
Description: 37
Station Elevation Data num= 27

Sta	Elev	Sta	Elev	Sta	Elev	Sta	Elev	Sta	Elev
-10	8	0	3	4	2	9	1	18	-1
23	-2	27	-3	39	-4	43	-5	48	-6
61	-7	289	-7	485	-7	558	-7	568	-7
571	-7	669	-7	686	-6	702	-5	720	-4
798	-3	809	-2	819	-1	840	1	853	2
865	3	875	8						

Manning's n Values num= 3

Sta	n Val	Sta	n Val	Sta	n Val
-10	.03	0	.025	865	.03

Bank Sta: Left	Right	Lengths: Left	Channel	Right	Coeff Contr.	Expan.
0	865	250	250	250	.1	.3

Ineffective Flow num= 1

Sta L	Sta R	Elev	Permanent
470	875	10	F

CROSS SECTION

RIVER: RIVER-1
REACH: Reach-1 RS: 3505

```
INPUT
Description: 35
Station Elevation Data    num=      24
     Sta    Elev     Sta    Elev     Sta    Elev     Sta    Elev     Sta    Elev
     -10       8       0       3       3       2       4       1       6       0
       8      -1       9      -2      10      -3      16      -4      45      -5
      55      -6      57      -7     100      -7     108      -6     116      -5
     125      -4     126      -3     127      -2     128      -1     129       0
     131       1     134       2     135       3     145       8

Manning's n Values        num=       3
     Sta   n Val     Sta   n Val     Sta   n Val
     -10     .03       0    .025     135     .03

Bank Sta: Left   Right    Lengths: Left Channel   Right     Coeff Contr.   Expan.
             0     135                2       2       2             .1       .3

CROSS SECTION


RIVER: RIVER-1
REACH: Reach-1            RS: 3503

INPUT
Description:
Station Elevation Data    num=       5
     Sta    Elev     Sta    Elev     Sta    Elev     Sta    Elev     Sta    Elev
   10.77    27.2   83.85  -21.52     100  -21.52  116.15  -21.52  189.23    21.1

Manning's n Values        num=       3
     Sta   n Val     Sta   n Val     Sta   n Val
   10.77     .03   10.77    .025  189.23     .03

Bank Sta: Left   Right    Lengths: Left Channel   Right     Coeff Contr.   Expan.
         10.77  189.23              216     216     216             .1       .3
Blocked Obstructions     num=       2
   Sta L   Sta R    Elev   Sta L   Sta R    Elev
   10.77       0      -8     190  189.23      -8
Sediment Elevation = -7

BRIDGE


RIVER: RIVER-1
REACH: Reach-1            RS: 3395

INPUT
Description:
Distance from Upstream XS =   29.25
Deck/Roadway Width        =   157.5
Weir Coefficient          =     2.6
Upstream  Deck/Roadway Coordinates
    num=       2
     Sta Hi Cord Lo Cord     Sta Hi Cord Lo Cord
       0    31.7    27.2   190.3    24.6    21.1

Upstream Bridge Cross Section Data
Station Elevation Data    num=       5
     Sta    Elev     Sta    Elev     Sta    Elev     Sta    Elev     Sta    Elev
   10.77    27.2   83.85  -21.52     100  -21.52  116.15  -21.52  189.23    21.1

Manning's n Values        num=       3
     Sta   n Val     Sta   n Val     Sta   n Val
```

```
   10.77     .03   10.77    .025  189.23     .03

Bank Sta: Left   Right    Coeff Contr.   Expan.
         10.77  189.23             .1       .3
Blocked Obstructions     num=       2
   Sta L   Sta R    Elev   Sta L   Sta R    Elev
   10.77       0      -8     190  189.23      -8
Sediment Elevation = -7

Downstream  Deck/Roadway Coordinates
    num=       2
     Sta Hi Cord Lo Cord     Sta Hi Cord Lo Cord
       0    31.7    27.2   190.3    24.6    21.1

Downstream Bridge Cross Section Data
Station Elevation Data    num=       5
     Sta    Elev     Sta    Elev     Sta    Elev     Sta    Elev     Sta    Elev
   10.77    27.2   83.85  -21.52     100  -21.52  116.15  -21.52  189.23    21.1

Manning's n Values        num=       3
     Sta   n Val     Sta   n Val     Sta   n Val
   10.77     .03   10.77    .025  189.23     .03

Bank Sta: Left   Right    Coeff Contr.   Expan.
         10.77  189.23             .1       .3
Blocked Obstructions     num=       2
   Sta L   Sta R    Elev   Sta L   Sta R    Elev
   10.77       0      -8     190  189.23      -8
Sediment Elevation = -7

Upstream Embankment side slope              =       0 horiz. to 1.0 vertical
Downstream Embankment side slope            =       0 horiz. to 1.0 vertical
Maximum allowable submergence for weir flow =     .98
Elevation at which weir flow begins         =
Energy head used in spillway design         =
Spillway height used in design              =
Weir crest shape                            = Broad Crested

Number of Piers =  7

Pier Data
Pier Station     Upstream=    27.2    Downstream=    27.2
Upstream     num=       2
    Width   Elev    Width   Elev
       1     -13       1      27
Downstream     num=       2
    Width   Elev    Width   Elev
       1 -27.213       1    27.2

Pier Data
Pier Station     Upstream=    53.1    Downstream=    53.1
Upstream     num=       2
    Width   Elev    Width   Elev
       1     -13       1      27
Downstream     num=       2
    Width   Elev    Width   Elev
       1     -13       1      27

Pier Data
Pier Station     Upstream=      79    Downstream=      79
Upstream     num=       2
    Width   Elev    Width   Elev
       1     -13       1      27
Downstream     num=       2
```

```
    Width   Elev    Width   Elev
       1     -13       1      27

Pier Data
Pier Station     Upstream=   111.2    Downstream=   111.2
Upstream     num=       2
    Width   Elev    Width   Elev
       1     -13       1      27
Downstream     num=       2
    Width   Elev    Width   Elev
       1     -13       1      27

Pier Data
Pier Station     Upstream=   137.1    Downstream=   137.1
Upstream     num=       2
    Width   Elev    Width   Elev
       1     -13       1      27
Downstream     num=       2
    Width   Elev    Width   Elev
       1     -13       1      27

Pier Data
Pier Station     Upstream=     163    Downstream=     163
Upstream     num=       2
    Width   Elev    Width   Elev
       1     -13       1      27
Downstream     num=       2
    Width   Elev    Width   Elev
       1     -13       1      27

Pier Data
Pier Station     Upstream=     163    Downstream=     163
Upstream     num=       2
    Width   Elev    Width   Elev
       1     -13       1      27
Downstream     num=       2
    Width   Elev    Width   Elev
       1     -13       1      27

Number of Bridge Coefficient Sets =  1

Low Flow Methods and Data
       Energy
Selected Low Flow Methods = Highest Energy Answer

High Flow Method
       Energy Only

Additional Bridge Parameters
       Add Friction component to Momentum
       Do not add Weight component to Momentum
       Class B flow critical depth computations use critical depth
           inside the bridge at the upstream end
       Criteria to check for pressure flow = Upstream energy grade line

CROSS SECTION


RIVER: RIVER-1
REACH: Reach-1            RS: 3287

INPUT
Description:
Station Elevation Data    num=       5
```

```
     Sta    Elev     Sta    Elev     Sta    Elev     Sta    Elev     Sta    Elev
   10.77    27.2   83.85  -21.52     100  -21.52  116.15  -21.52  189.23    21.1

Manning's n Values        num=       3
     Sta   n Val     Sta   n Val     Sta   n Val
   10.77     .03   10.77    .025  189.23     .03

Bank Sta: Left   Right    Lengths: Left Channel   Right     Coeff Contr.   Expan.
         10.77  189.23                 2       2       2             .1       .3
Blocked Obstructions     num=       2
   Sta L   Sta R    Elev   Sta L   Sta R    Elev
   10.77       0      -8     190  189.23      -8
Sediment Elevation = -7

CROSS SECTION


RIVER: RIVER-1
REACH: Reach-1            RS: 3285

INPUT
Description: 32
Station Elevation Data    num=      28
     Sta    Elev     Sta    Elev     Sta    Elev     Sta    Elev     Sta    Elev
     -10       8       0       3       2       2       5       1       8       0
      10      -1      13      -2      14      -3      16      -4      21      -5
      23      -6      24      -7      26      -8      65      -9     107      -9
     115      -8     126      -7     133      -6     138      -5     143      -4
     145      -3     148      -2     150      -1     152       0     155       1
     158       2     161       3     171       8

Manning's n Values        num=       3
     Sta   n Val     Sta   n Val     Sta   n Val
     -10     .03       0    .025     161     .03

Bank Sta: Left   Right    Lengths: Left Channel   Right     Coeff Contr.   Expan.
               0     161               125     125     125             .1       .3

CROSS SECTION


RIVER: RIVER-1
REACH: Reach-1            RS: 3160

INPUT
Description: 31
Station Elevation Data    num=      63
     Sta    Elev     Sta    Elev     Sta    Elev     Sta    Elev     Sta    Elev
     -10       8       0       3      12       2      24       1      49      -1
      61      -2      75      -3      76      -4      80      -5      82      -6
      83      -7      85      -8      86      -9      98     -10     105     -11
     108     -12     110     -13     114     -14     116     -15     118     -17
     119     -18     120     -19     121     -15     123     -21     126     -22
     145     -22     147     -22     169     -22     173     -21     174     -21
     178     -20     181     -19     183     -18     186     -17     190     -15
     192     -14     194     -13     197     -12     204     -11     245     -11
     264     -11     265     -11     266     -11     276     -10     285      -9
     287      -9     291      -9     303      -8     319      -7     334      -6
     353      -5     372      -4     734      -4     869      -4     911      -3
     966      -2    1032      -1    1056       1    1068       1    1071       1
    1076       2    1079       3    1088       8

Manning's n Values        num=       3
     Sta   n Val     Sta   n Val     Sta   n Val
```

```
     -10     .03       0    .025    1079     .03

Bank Sta: Left   Right    Lengths: Left Channel   Right     Coeff Contr.   Expan.
             0    1079               140     140     140             .1       .3
Ineffective Flow     num=       1
   Sta L   Sta R    Elev  Permanent
     280    1088      10       F

CROSS SECTION


RIVER: RIVER-1
REACH: Reach-1            RS: 3020

INPUT
Description: 30
Station Elevation Data    num=      51
     Sta    Elev     Sta    Elev     Sta    Elev     Sta    Elev     Sta    Elev
     -10       8       0       3       7       2      19       1      41      -1
      45      -2      48      -3      50      -4      52      -5      54      -6
      54      -7      57      -8      59      -9      60     -10      62     -11
      64     -12      79     -13      97     -14     154     -14     163     -13
     169     -12     176     -11     183     -10     184     -10     202     -10
     225     -11     331     -11     349     -10     358      -9     368      -8
     378      -7     385      -6     397      -5     407      -4     583      -4
     584      -4     591      -4     648      -4     679      -4     722      -4
     752      -4     889      -5     984      -5     993      -4    1052      -3
    1055      -2    1059      -1    1067       1    1073       2    1079       3
    1089       8

Manning's n Values        num=       3
     Sta   n Val     Sta   n Val     Sta   n Val
     -10     .03       0    .025    1079     .03

Bank Sta: Left   Right    Lengths: Left Channel   Right     Coeff Contr.   Expan.
             0    1079               140     150     160             .1       .3
Ineffective Flow     num=       1
   Sta L   Sta R    Elev  Permanent
     350    1089      10       F

CROSS SECTION


RIVER: RIVER-1
REACH: Reach-1            RS: 2870

INPUT
Description: 28
Station Elevation Data    num=      42
     Sta    Elev     Sta    Elev     Sta    Elev     Sta    Elev     Sta    Elev
     -10       8       0       3       7       2      13       1      23      -1
      25      -2      27      -3      30      -4      31      -5      32      -6
      36      -7      39      -8      40      -9      42     -10      44     -11
      71     -12     127     -13     144     -13     167     -12     183     -11
     200     -11     207     -12     298     -12     322     -11     344     -10
     354      -9     364      -8     376      -7     384      -6     396      -5
     412      -4     585      -4     898      -5     904      -5     928      -4
     990      -3     997      -2    1005      -1    1020       1    1026       2
    1037       3    1047       8

Manning's n Values        num=       3
     Sta   n Val     Sta   n Val     Sta   n Val
     -10     .03       0    .025    1037     .03
```

```
Bank Sta: Left   Right    Lengths: Left Channel   Right     Coeff Contr.   Expan.
             0    1037               80      90     110             .1       .3
Ineffective Flow     num=       1
   Sta L   Sta R    Elev  Permanent
     420    1047      10       F

CROSS SECTION


RIVER: RIVER-1
REACH: Reach-1            RS: 2780

INPUT
Description: 27
Station Elevation Data    num=      54
     Sta    Elev     Sta    Elev     Sta    Elev     Sta    Elev     Sta    Elev
     -10       8       0       3       6       2      13       1      25      -1
      28      -2      32      -3      34      -4      35      -5      37      -6
      38      -7      39      -8      40      -9      43     -10      44     -11
      48     -12      59     -13      70     -14      81     -15      92     -15
     101     -17     110     -18     115     -19     176     -19     180     -18
     185     -17     191     -15     197     -15     202     -14     206     -13
     213     -12     214     -12     217     -12     221     -12     287     -12
     304     -11     323     -10     345      -9     353      -8     367      -7
     376      -6     385      -5     408      -4     671      -4     795      -5
     897      -5     906      -4     948      -3     963      -2     977      -1
    1005       1    1018       2    1035       3    1045       8

Manning's n Values        num=       3
     Sta   n Val     Sta   n Val     Sta   n Val
     -10     .03       0    .025    1035     .03

Bank Sta: Left   Right    Lengths: Left Channel   Right     Coeff Contr.   Expan.
             0    1035               140     140     140             .1       .3
Ineffective Flow     num=       1
   Sta L   Sta R    Elev  Permanent
     450    1045      10       F

CROSS SECTION


RIVER: RIVER-1
REACH: Reach-1            RS: 2640

INPUT
Description: 26
Station Elevation Data    num=      70
     Sta    Elev     Sta    Elev     Sta    Elev     Sta    Elev     Sta    Elev
     -10       8       0       3       6       2      14       1      29      -1
      37      -2      45      -3      50      -4      59      -5      62      -6
      63      -7      64      -8      66      -9      66     -10      68     -11
      69     -12      70     -13      77     -14      81     -15      84     -15
      87     -17      91     -18      94     -19      96     -20      98     -21
     100     -22     102     -23     103     -23     109     -23     111     -23
     126     -24     185     -25     201     -25     203     -24     207     -23
     210     -22     212     -21     217     -20     220     -19     225     -18
     228     -17     234     -15     240     -15     247     -14     253     -13
     260     -12     270     -11     289     -10     308      -9     318      -8
     327      -7     335      -6     354      -5     358      -5     390      -4
     428      -4     508      -5     521      -5     628      -4     689      -4
     699      -5     871      -5     885      -4     929      -3     942      -2
     954      -1     980       1     993       2    1006       3    1016       8

Manning's n Values        num=       3
```

```
     Sta   n Val     Sta   n Val     Sta   n Val
     -10     .03       0    .025    1006     .03

Bank Sta: Left   Right    Lengths: Left Channel   Right     Coeff Contr.   Expan.
             0    1006              160     175     200             .1       .3
Ineffective Flow     num=       1
   Sta L   Sta R    Elev  Permanent
     350    1016      10       F

CROSS SECTION


RIVER: RIVER-1
REACH: Reach-1            RS: 2465

INPUT
Description: 24
Station Elevation Data    num=      28
     Sta    Elev     Sta    Elev     Sta    Elev     Sta    Elev     Sta    Elev
      -5       8       0       3       0       2       1       1       3      -1
       5      -2       8      -3      10      -4      12      -5      14      -6
      19      -7      22      -8      26      -9      28     -10      88     -10
      91      -9      94      -8      96      -7      97      -6     100      -5
     103      -4     106      -3     109      -2     113      -1     121       1
     145       2     153       3     163       8

Manning's n Values        num=       3
     Sta   n Val     Sta   n Val     Sta   n Val
      -5     .03       0    .025     113     .03

Bank Sta: Left   Right    Lengths: Left Channel   Right     Coeff Contr.   Expan.
             0     113              135     135     135             .1       .3

CROSS SECTION


RIVER: RIVER-1
REACH: Reach-1            RS: 2330

INPUT
Description: 23
Station Elevation Data    num=      28
     Sta    Elev     Sta    Elev     Sta    Elev     Sta    Elev     Sta    Elev
     -10       8       0       3       2       2       4       1       9      -1
      11      -2      14      -3      16      -4      18      -5      21      -6
      23      -7      25      -8      27      -9      29     -10      76     -10
      77      -9      79      -8      80      -7      82      -6      84      -5
      86      -4      88      -3      90      -2      92      -1      96       1
      98       2     101       3     111       8

Manning's n Values        num=       3
     Sta   n Val     Sta   n Val     Sta   n Val
     -10     .03       0    .025     101     .03

Bank Sta: Left   Right    Lengths: Left Channel   Right     Coeff Contr.   Expan.
             0     101              150     150     150             .1       .3

CROSS SECTION


RIVER: RIVER-1
REACH: Reach-1            RS: 2180

INPUT
```

```
Description: 21
Station Elevation Data    num=      28
     Sta    Elev     Sta    Elev     Sta    Elev     Sta    Elev     Sta    Elev
     -10       8       0       3       6       2      11       1      20      -1
      25      -2      28      -3      35      -4      46      -5      59      -6
      62      -7      66      -8      71      -9      74     -10     117     -10
     120      -9     122      -8     125      -7     127      -6     130      -5
     133      -4     135      -3     137      -2     140      -1     145       1
     148       2     151       3     161       8

Manning's n Values        num=       3
     Sta   n Val     Sta   n Val     Sta   n Val
     -10     .03       0    .025     151     .03

Bank Sta: Left   Right    Lengths: Left Channel   Right     Coeff Contr.   Expan.
             0     151               95      95      95             .1       .3

CROSS SECTION


RIVER: RIVER-1
REACH: Reach-1            RS: 2085

INPUT
Description: 20
Station Elevation Data    num=      56
     Sta    Elev     Sta    Elev     Sta    Elev     Sta    Elev     Sta    Elev
     -10       8       0       3       6       2      14       1      30      -1
      38      -2      46      -3      53      -4     372      -5     393      -6
     401      -7     409      -8     413      -9     419     -10     426     -11
     435     -12     445     -13     457     -14     467     -15     480     -16
     491     -17     503     -18     514     -19     525     -20     544     -22
     548     -23     553     -24     557     -25     649     -25     654     -24
     658     -23     661     -22     668     -20     673     -19     678     -18
     682     -17     686     -16     691     -15     696     -14     700     -13
     705     -12     710     -11     716     -10     727      -9     731      -8
     733      -7     738      -6     742      -5     745      -4     808      -3
     813      -2     819      -1     830       1     836       2     861       3
     871       8

Manning's n Values        num=       3
     Sta   n Val     Sta   n Val     Sta   n Val
     -10     .03       0    .025     861     .03

Bank Sta: Left   Right    Lengths: Left Channel   Right     Coeff Contr.   Expan.
             0     861              150     140     110             .1       .3
Ineffective Flow     num=       2
   Sta L   Sta R    Elev  Permanent
     -10     500       8       F
     750     871       8       F

CROSS SECTION


RIVER: RIVER-1
REACH: Reach-1            RS: 1945

INPUT
Description: 19
Station Elevation Data    num=      73
     Sta    Elev     Sta    Elev     Sta    Elev     Sta    Elev     Sta    Elev
     -10       8       0       3       3       2       7       1      15      -1
      19      -2      23      -3      27      -4      38      -5      43      -6
     245      -7     248      -8     251      -9     255     -10     258     -11
```

263	-12	271	-13	277	-14	290	-15	303	-16
321	-17	395	-18	408	-19	416	-20	491	-21
510	-22	518	-22	519	-22	526	-22	592	-22
683	-21	758	-21	761	-21	974	-21	978	-21
1086	-15	1097	-15	1110	-15	1119	-15	1120	-15
1159	-15	1160	-15	1189	-22	1204	-23	1222	-24
1244	-24	1267	-23	1282	-22	1283	-22	1305	-20
1315	-19	1321	-18	1326	-17	1331	-16	1336	-15
1341	-14	1345	-13	1351	-12	1355	-11	1359	-10
1363	-9	1367	-8	1371	-7	1375	-6	1379	-5
1383	-4	1428	-3	1434	-2	1441	-1	1461	1
1486	2	1511	3	1521	8				

Manning's n Values num= 3

Sta	n Val	Sta	n Val	Sta	n Val
-10	.03	0	.025	1511	.03

Bank Sta: Left	Right	Lengths: Left	Channel	Right	Coeff Contr.	Expan.
0	1511	160	135	100	.1	.3

Ineffective Flow num= 2

Sta L	Sta R	Elev	Permanent
-10	1020	8	F
1400	1521	8	F

CROSS SECTION

RIVER: RIVER-1
REACH: Reach-1 RS: 1810

INPUT
Description: 18
Station Elevation Data num= 70

Sta	Elev	Sta	Elev	Sta	Elev	Sta	Elev	Sta	Elev
-10	8	0	3	12	2	20	1	37	-1
45	-2	51	-3	57	-4	94	-4	143	-4
157	-5	173	-6	184	-7	190	-8	195	-9
200	-10	205	-11	209	-12	213	-13	216	-14
218	-15	249	-15	286	-15	363	-15	435	-15
477	-15	544	-15	549	-15	560	-15	561	-15
588	-15	589	-15	602	-15	605	-15	606	-15
722	-19	723	-19	755	-19	785	-15	955	-15
956	-15	957	-15	958	-15	976	-15	985	-15
1000	-19	1004	-18	1008	-17	1011	-16	1014	-15
1017	-14	1022	-13	1098	-13	1099	-13	1124	-12
1139	-11	1146	-10	1151	-9	1156	-8	1160	-7
1163	-6	1166	-5	1169	-4	1192	-3	1214	-2
1237	-1	1282	1	1303	2	1324	3	1334	8

Manning's n Values num= 3

Sta	n Val	Sta	n Val	Sta	n Val
-10	.03	0	.025	1324	.03

Bank Sta: Left	Right	Lengths: Left	Channel	Right	Coeff Contr.	Expan.
0	1324	155	130	100	.1	.3

Ineffective Flow num= 2

Sta L	Sta R	Elev	Permanent
-10	630	8	F
1170	1334	8	F

CROSS SECTION

RIVER: RIVER-1

REACH: Reach-1 RS: 1680

INPUT
Description: 16
Station Elevation Data num= 65

Sta	Elev	Sta	Elev	Sta	Elev	Sta	Elev	Sta	Elev
-10	8	0	3	4	2	17	1	33	-1
37	-2	45	-3	106	-4	116	-5	119	-6
122	-7	125	-8	127	-9	129	-10	131	-11
133	-12	135	-13	138	-14	141	-15	145	-16
149	-17	153	-18	157	-19	197	-19	255	-18
267	-18	296	-19	297	-19	300	-19	344	-19
347	-19	369	-19	402	-20	556	-21	572	-21
576	-21	584	-21	697	-21	698	-21	745	-21
746	-21	882	-20	889	-19	892	-18	896	-17
899	-16	903	-15	939	-14	946	-13	952	-12
959	-11	971	-10	979	-9	983	-8	987	-7
990	-6	992	-5	995	-4	1017	-3	1035	-2
1056	-1	1098	1	1118	2	1130	3	1140	8

Manning's n Values num= 3

Sta	n Val	Sta	n Val	Sta	n Val
-10	.03	0	.025	1130	.03

Bank Sta: Left	Right	Lengths: Left	Channel	Right	Coeff Contr.	Expan.
0	1130	220	180	130	.1	.3

Ineffective Flow num= 2

Sta L	Sta R	Elev	Permanent
-10	320	8	F
980	1140	8	F

CROSS SECTION

RIVER: RIVER-1
REACH: Reach-1 RS: 1500

INPUT
Description: 15
Station Elevation Data num= 62

Sta	Elev	Sta	Elev	Sta	Elev	Sta	Elev	Sta	Elev
-10	8	0	3	3	2	6	1	16	-1
21	-2	26	-3	31	-4	32	-5	33	-6
35	-7	37	-8	40	-9	44	-10	47	-11
51	-12	54	-13	59	-14	64	-15	122	-15
141	-14	155	-13	187	-13	207	-14	266	-15
296	-16	310	-17	318	-18	332	-19	435	-20
451	-21	486	-21	551	-21	582	-22	613	-22
695	-22	727	-22	733	-21	738	-20	743	-19
749	-18	752	-17	769	-16	784	-15	788	-14
792	-13	797	-12	801	-11	805	-10	809	-9
812	-8	816	-7	821	-6	828	-5	842	-4
853	-3	860	-2	872	-1	896	1	908	2
919	3	929	8						

Manning's n Values num= 3

Sta	n Val	Sta	n Val	Sta	n Val
-10	.03	0	.025	919	.03

Bank Sta: Left	Right	Lengths: Left	Channel	Right	Coeff Contr.	Expan.
0	919	180	135	120	.1	.3

Ineffective Flow num= 1

Sta L	Sta R	Elev	Permanent
770	929	8	F

CROSS SECTION

RIVER: RIVER-1
REACH: Reach-1 RS: 1365

INPUT
Description: 13
Station Elevation Data num= 65

Sta	Elev	Sta	Elev	Sta	Elev	Sta	Elev	Sta	Elev
-10	8	0	3	3	2	7	1	13	-1
13	-2	15	-3	16	-4	16	-5	17	-6
19	-7	23	-8	24	-9	28	-10	33	-11
38	-12	43	-13	79	-13	103	-12	116	-11
132	-11	143	-10	147	-10	186	-11	199	-12
231	-13	261	-13	282	-13	290	-14	301	-15
308	-16	318	-17	337	-18	359	-19	386	-20
420	-21	445	-22	446	-22	541	-22	616	-22
682	-21	687	-20	691	-19	696	-18	699	-17
702	-16	705	-15	709	-14	713	-13	717	-12
720	-11	727	-10	737	-9	744	-8	749	-7
761	-6	782	-5	813	-4	817	-3	822	-2
825	-1	833	1	838	2	843	3	853	8

Manning's n Values num= 3

Sta	n Val	Sta	n Val	Sta	n Val
-10	.03	0	.025	843	.03

Bank Sta: Left	Right	Lengths: Left	Channel	Right	Coeff Contr.	Expan.
0	843	210	215	230	.1	.3

Ineffective Flow num= 1

Sta L	Sta R	Elev	Permanent
740	853	8	F

CROSS SECTION

RIVER: RIVER-1
REACH: Reach-1 RS: 1150

INPUT
Description: 11
Station Elevation Data num= 65

Sta	Elev	Sta	Elev	Sta	Elev	Sta	Elev	Sta	Elev
-10	8	0	3	6	2	19	1	34	-1
40	-2	46	-3	50	-4	51	-5	52	-6
56	-7	105	-5	141	-5	175	-7	192	-6
210	-6	219	-7	221	-7	232	-6	242	-5
252	-4	308	-4	316	-5	324	-6	336	-7
345	-8	355	-9	362	-10	368	-11	377	-12
384	-13	388	-14	395	-15	397	-16	399	-17
404	-18	408	-19	417	-20	427	-21	428	-21
518	-21	527	-20	537	-19	545	-18	555	-17
563	-16	575	-15	582	-14	589	-13	597	-12
599	-11	601	-10	604	-9	607	-8	609	-7
611	-6	613	-5	614	-4	616	-3	617	-2
620	-1	626	1	629	2	631	3	641	8

Manning's n Values num= 3

Sta	n Val	Sta	n Val	Sta	n Val
-10	.03	0	.025	631	.03

Bank Sta: Left	Right	Lengths: Left	Channel	Right	Coeff Contr.	Expan.

```
             0     631              245     235     225             .1       .3

CROSS SECTION


RIVER: RIVER-1
REACH: Reach-1            RS: 915

INPUT
Description: 9
Station Elevation Data    num=      39
     Sta    Elev     Sta    Elev     Sta    Elev     Sta    Elev     Sta    Elev
     -10       8       0       3       3       2       7       1      15      -1
      19      -2      23      -3      25      -4      33      -5      37      -6
      39      -7      43      -8      49      -9      53     -10      57     -11
      61     -12      65     -13      69     -14     144     -14     145     -14
     154     -13     165     -12     181     -11     192     -10     195      -9
     195      -7     196      -6     196      -8     197      -5     200      -4
     228      -3     357      -3     463      -3     466      -2     469      -1
     476       1     479       2     482       3     492       8

Manning's n Values        num=       3
     Sta   n Val     Sta   n Val     Sta   n Val
     -10     .03       0    .025     482     .03

Bank Sta: Left   Right    Lengths: Left Channel   Right     Coeff Contr.   Expan.
             0     482              220     215     210             .1       .3

CROSS SECTION


RIVER: RIVER-1
REACH: Reach-1            RS: 700

INPUT
Description: 7
Station Elevation Data    num=      43
     Sta    Elev     Sta    Elev     Sta    Elev     Sta    Elev     Sta    Elev
     -10       8       0       3       5       2       9       1      12      -1
      14      -2      15      -3      33      -4      33      -5      35      -6
      36      -7      36      -8      40      -9      47     -10      53     -11
      62     -12      76     -13      93     -14      95     -14      96     -14
     114     -15     128     -15     129     -15     144     -14     159     -13
     173     -12     173     -11     174     -10     175      -9     179      -8
     182      -7     186      -6     189      -5     193      -4     211      -3
     394      -3     486      -3     488      -2     491      -1     497       1
     500       2     503       3     513       8

Manning's n Values        num=       3
     Sta   n Val     Sta   n Val     Sta   n Val
     -10     .03       0    .025     503     .03

Bank Sta: Left   Right    Lengths: Left Channel   Right     Coeff Contr.   Expan.
             0     503              175     180     185             .1       .3

CROSS SECTION


RIVER: RIVER-1
REACH: Reach-1            RS: 520

INPUT
Description: 5
Station Elevation Data    num=      46
```

```
     Sta    Elev     Sta    Elev     Sta    Elev     Sta    Elev     Sta    Elev
     -10       8       0       3       3       2       5       1      16      -1
      19      -2      23      -3      27      -4      30      -5      32      -6
      35      -7      37      -8      40      -9      43     -10      46     -11
      49     -12      55     -13      60     -14      75     -15      76     -15
      88     -16     141     -16     148     -15     149     -15     158     -14
     159     -14     168     -13     169     -13     174     -12     176     -11
     179     -10     181      -9     182      -8     182      -7     183      -6
     184      -5     185      -4     204      -3     392      -3     497      -3
     499      -2     501      -1     504       1     505       2     507       3
     517       8

Manning's n Values        num=       3
     Sta   n Val     Sta   n Val     Sta   n Val
     -10     .03       0    .025     507     .03

Bank Sta: Left   Right    Lengths: Left Channel   Right     Coeff Contr.   Expan.
             0     507              190     230     250             .1       .3

CROSS SECTION


RIVER: RIVER-1
REACH: Reach-1            RS: 290

INPUT
Description: 2
Station Elevation Data    num=      43
     Sta    Elev     Sta    Elev     Sta    Elev     Sta    Elev     Sta    Elev
     -10       8       0       3       9       2      15       1      18      -1
      20      -2      21      -3      23      -4      25      -5      27      -6
      29      -7      33      -8      37      -9      40     -10      41     -10
      47     -11      51     -12      54     -13      57     -14      61     -15
      65     -15      67     -15     102     -15     113     -14     120     -13
     125     -12     129     -11     134     -10     140      -9     145      -8
     146      -7     148      -6     150      -5     153      -4     189      -3
     278      -3     389      -3     390      -2     392      -1     395       1
     397       2     399       3     409       8

Manning's n Values        num=       3
     Sta   n Val     Sta   n Val     Sta   n Val
     -10     .03       0    .025     399     .03

Bank Sta: Left   Right    Lengths: Left Channel   Right     Coeff Contr.   Expan.
             0     399              150     190     230             .1       .3

CROSS SECTION


RIVER: RIVER-1
REACH: Reach-1            RS: 100

INPUT
Description: 1
Station Elevation Data    num=      22
     Sta    Elev     Sta    Elev     Sta    Elev     Sta    Elev     Sta    Elev
     -10       8       0       3      11       2      23       1      28      -1
      31      -2      35      -3      49      -4      51      -5      53      -6
      55      -7      80      -7      88      -6     164      -5     176      -4
     211      -3     213      -2     214      -1     218       1     221       2
     224       3     234       8

Manning's n Values        num=       3
     Sta   n Val     Sta   n Val     Sta   n Val
```

-10	.03	0	.025	224	.03

Bank Sta: Left	Right	Lengths: Left	Channel	Right	Coeff Contr.	Expan.
0	224	80	100	120	.1	.3

CROSS SECTION

RIVER: RIVER-1
REACH: Reach-1 RS: 0.1

INPUT
Description: 0

Station Elevation Data num= 16

Sta	Elev	Sta	Elev	Sta	Elev	Sta	Elev	Sta	Elev
0	3	5	2	10	1	20	-1	24	-2
30	-3	33	-4	40	-5	133	-5	142	-4
145	-3	147	-2	151	-1	159	1	163	2
167	3								

Manning's n Values num= 3

Sta	n Val	Sta	n Val	Sta	n Val
0	.03	0	.025	167	.03

Bank Sta: Left	Right	Lengths: Left	Channel	Right	Coeff Contr.	Expan.
0	167	0	0	0	.1	.3

SUMMARY OF MANNING'S N VALUES

River:RIVER-1

Reach	River Sta.	n1	n2	n3
Reach-1	9715	.03	.025	.03
Reach-1	9515	.03	.025	.03
Reach-1	9305	.03	.025	.03
Reach-1	9070	.03	.025	.03
Reach-1	8780	.03	.025	.03
Reach-1	8365	.03	.025	.03
Reach-1	8015	.03	.025	.03
Reach-1	7680	.03	.025	.03
Reach-1	7205	.03	.025	.03
Reach-1	6705	.03	.025	.03
Reach-1	6185	.03	.025	.03
Reach-1	5660	.03	.025	.03
Reach-1	5160	.03	.025	.03
Reach-1	4735	.03	.025	.03
Reach-1	4295	.03	.025	.03
Reach-1	3945	.03	.025	.03
Reach-1	3755	.03	.025	.03
Reach-1	3505	.03	.025	.03
Reach-1	3503	.03	.025	.03
Reach-1	3395	Bridge		
Reach-1	3287	.03	.025	.03
Reach-1	3285	.03	.025	.03
Reach-1	3160	.03	.025	.03
Reach-1	3020	.03	.025	.03
Reach-1	2870	.03	.025	.03
Reach-1	2780	.03	.025	.03
Reach-1	2640	.03	.025	.03
Reach-1	2465	.03	.025	.03

Reach-1	2330	.03	.025	.03
Reach-1	2180	.03	.025	.03
Reach-1	2085	.03	.025	.03
Reach-1	1945	.03	.025	.03
Reach-1	1810	.03	.025	.03
Reach-1	1680	.03	.025	.03
Reach-1	1500	.03	.025	.03
Reach-1	1365	.03	.025	.03
Reach-1	1150	.03	.025	.03
Reach-1	915	.03	.025	.03
Reach-1	700	.03	.025	.03
Reach-1	520	.03	.025	.03
Reach-1	290	.03	.025	.03
Reach-1	100	.03	.025	.03
Reach-1	0.1	.03	.025	.03

SUMMARY OF REACH LENGTHS

River: RIVER-1

Reach	River Sta.	Left	Channel	Right
Reach-1	9715	220	200	180
Reach-1	9515	225	210	180
Reach-1	9305	225	235	245
Reach-1	9070	290	290	290
Reach-1	8780	415	415	415
Reach-1	8365	370	350	330
Reach-1	8015	390	335	300
Reach-1	7680	475	475	475
Reach-1	7205	480	500	520
Reach-1	6705	520	520	520
Reach-1	6185	525	525	525
Reach-1	5660	540	500	460
Reach-1	5160	520	425	350
Reach-1	4735	600	440	300
Reach-1	4295	250	350	450
Reach-1	3945	160	190	350
Reach-1	3755	250	250	250
Reach-1	3505	2	2	2
Reach-1	3503	216	216	216
Reach-1	3395	Bridge		
Reach-1	3287	2	2	2
Reach-1	3285	125	125	125
Reach-1	3160	140	140	140
Reach-1	3020	140	150	160
Reach-1	2870	80	90	110
Reach-1	2780	140	140	140
Reach-1	2640	160	175	200
Reach-1	2465	135	135	135
Reach-1	2330	150	150	150
Reach-1	2180	95	95	95
Reach-1	2085	150	140	110
Reach-1	1945	160	135	100
Reach-1	1810	155	130	100
Reach-1	1680	220	180	130
Reach-1	1500	180	135	120
Reach-1	1365	210	215	230
Reach-1	1150	245	235	225
Reach-1	915	220	215	210
Reach-1	700	175	180	185

Reach-1	520	190	230	250
Reach-1	290	150	190	230
Reach-1	100	80	100	120
Reach-1	0.1	0	0	0

SUMMARY OF CONTRACTION AND EXPANSION COEFFICIENTS
River: RIVER-1

Reach	River Sta.	Contr.	Expan.
Reach-1	9715	.1	.3
Reach-1	9515	.1	.3
Reach-1	9305	.1	.3
Reach-1	9070	.1	.3
Reach-1	8780	.1	.3
Reach-1	8365	.1	.3
Reach-1	8015	.1	.3
Reach-1	7680	.1	.3
Reach-1	7205	.1	.3
Reach-1	6705	.1	.3
Reach-1	6185	.1	.3
Reach-1	5660	.1	.3
Reach-1	5160	.1	.3
Reach-1	4735	.1	.3
Reach-1	4295	.1	.3
Reach-1	3945	.1	.3
Reach-1	3755	.1	.3
Reach-1	3505	.1	.3
Reach-1	3503	.1	.3
Reach-1	3395	Bridge	
Reach-1	3287	.1	.3
Reach-1	3285	.1	.3
Reach-1	3160	.1	.3
Reach-1	3020	.1	.3
Reach-1	2870	.1	.3
Reach-1	2780	.1	.3
Reach-1	2640	.1	.3
Reach-1	2465	.1	.3
Reach-1	2330	.1	.3
Reach-1	2180	.1	.3
Reach-1	2085	.1	.3
Reach-1	1945	.1	.3
Reach-1	1810	.1	.3
Reach-1	1680	.1	.3
Reach-1	1500	.1	.3
Reach-1	1365	.1	.3
Reach-1	1150	.1	.3
Reach-1	915	.1	.3
Reach-1	700	.1	.3
Reach-1	520	.1	.3
Reach-1	290	.1	.3
Reach-1	100	.1	.3
Reach-1	0.1	.1	.3

PART II. BATIQUITOS LAGOON

HEC-RAS Version 4.1.0 Jan 2010

U.S. Army Corps of Engineers
Hydrologic Engineering Center
609 Second Street
Davis, California

```
X     X  XXXXXX    XXXX        XXXX       XX      XXXX
X     X  X        X    X       X   X     X  X    X
X     X  X        X            X   X    X    X   X
XXXXXXX  XXXX     X       XXX  XXXX     XXXXXX    XXXX
X     X  X        X            X  X     X    X        X
X     X  X        X    X       X   X    X    X        X
X     X  XXXXXX    XXXX        X    X   X    X   XXXXX
```

PROJECT DATA
Project Title: Batiquitos Lagoon
Project File : Batiquitos.prj
Run Date and Time: 5/27/2010 7:34:45 AM

Project in English units

Project Description:
BATIQUITOS LAGOON, BATHYMETRY FROM MERKEL AND ASSOCIATES
    ORIGINAL
DATUM (MLLW)=3.58'; NGVD=6.38'; ALL ELEVS. LOWERED BY 2.8'
    HOWARD H.
CHANG, OCTBOER 2009, Q100=15,000 cfs
    BATIQUITOS LAGOON, BATHYMETRY FROM
MERKEL AND ASSOCIATES
    ORIGINAL DATUM (MLLW)=3.58'; NGVD=6.38'; ALL ELEVS.
LOWERED BY 2.8'
    HOWARD H. CHANG, OCTBOER 2009, Q100=15,000 cfs

PLAN DATA

Plan Title: Bridge Alternative
Plan File : C:\HEC Data\RAS\Batiquitos.p03

Geometry Title: Bridge Alternative
Geometry File : C:\HEC Data\RAS\Batiquitos.g03

Flow Title   : Imported Flow 02
Flow File   : C:\HEC Data\RAS\Batiquitos.f02

Plan Summary Information:
Number of: Cross Sections =   26   Multiple Openings =   0
            Culverts   =   0   Inline Structures =   0
            Bridges   =   1   Lateral Structures =   0

Computational Information
    Water surface calculation tolerance = 0.01
    Critical depth calculation tolerance = 0.01
    Maximum number of iterations   = 20
    Maximum difference tolerance   = 0.3
    Flow tolerance factor   = 0.001

Computation Options

```
    Critical depth computed only where necessary
    Conveyance Calculation Method: At breaks in n values only
    Friction Slope Method:         Average Conveyance
    Computational Flow Regime:     Subcritical Flow




FLOW DATA

Flow Title: Imported Flow 02
Flow File : C:\HEC Data\RAS\Batiquitos.f02

Flow Data (cfs)

  River           Reach           RS                 100-yr
  RIVER-1         Reach-1         120.85              15000


Boundary Conditions

  River           Reach           Profile                       Upstream
Downstream

  RIVER-1         Reach-1         100-yr
Known WS = 0




GEOMETRY DATA

Geometry Title: Bridge Alternative
Geometry File : C:\HEC Data\RAS\Batiquitos.g03

CROSS SECTION


RIVER: RIVER-1
REACH: Reach-1            RS: 120.85

INPUT
Description:
Station Elevation Data    num=      26
     Sta    Elev     Sta    Elev     Sta    Elev     Sta    Elev     Sta    Elev
     -20     8.7      32     1.7      53      .7     121      .2     190     -.3
     243     -.3     299       0     355      .4     411      .7     455     1.7
     478     2.7     539     2.7     572     1.7     607      .7     636     -.3
     709     -.8     783    -1.3     816    -1.3     866     -.8     916     -.3
     970      .2    1024      .7    1046     1.7    1059     1.7    1095     1.7
    1192     7.7

Manning's n Values        num=       3
     Sta   n Val     Sta   n Val     Sta   n Val
     -20     .03      32    .025    1192     .03

Bank Sta: Left   Right    Lengths: Left Channel   Right     Coeff Contr.   Expan.
            32    1192              650     680     710             .2       .3

CROSS SECTION


RIVER: RIVER-1
REACH: Reach-1            RS: 114.05
```

```
INPUT
Description:
Station Elevation Data    num=      18
     Sta    Elev     Sta    Elev     Sta    Elev     Sta    Elev     Sta    Elev
     -20     8.7      60     2.5     120     2.2     180       2     241     1.7
     304     1.2     368      .7     391      .7     409      .7     475      .2
     541     -.3     603    -1.3     666    -1.3     730    -1.3     758     -.3
     785      .7     815     1.7     853     7.7

Manning's n Values        num=       3
     Sta   n Val     Sta   n Val     Sta   n Val
     -20     .03      60    .025     853     .03

Bank Sta: Left   Right    Lengths: Left Channel   Right     Coeff Contr.   Expan.
            60     853              730     750     765             .2       .3

CROSS SECTION


RIVER: RIVER-1
REACH: Reach-1            RS: 106.55

INPUT
Description:
Station Elevation Data    num=      27
     Sta    Elev     Sta    Elev     Sta    Elev     Sta    Elev     Sta    Elev
     -20     8.7      23     1.7      35      .7      49      .7     102      .7
     155      .7     209      .7     262      .2     315     -.3     372     -.6
     430      -1     488    -1.3     554    -1.3     621    -1.3     688    -1.3
     755    -1.3     822    -1.3     887     -.8     953     -.3    1024      .2
    1095      .7    1146     1.2    1198     1.7    1265       2    1332     2.2
    1399     2.5    1486     7.7

Manning's n Values        num=       3
     Sta   n Val     Sta   n Val     Sta   n Val
     -20     .03      23    .025    1486     .03

Bank Sta: Left   Right    Lengths: Left Channel   Right     Coeff Contr.   Expan.
            23    1486              940     880     800             .2       .3

CROSS SECTION


RIVER: RIVER-1
REACH: Reach-1            RS: 97.75

INPUT
Description:
Station Elevation Data    num=      18
     Sta    Elev     Sta    Elev     Sta    Elev     Sta    Elev     Sta    Elev
     -20     8.7      65     2.2     131     1.7     153      .7     201     -.3
     239    -1.3     310    -1.3     381    -1.3     452    -1.3     523    -1.3
     594    -1.3     657      -1     721     -.8     784     -.5     848     -.3
     915      .7     952     1.7    1050     8.7

Manning's n Values        num=       3
     Sta   n Val     Sta   n Val     Sta   n Val
     -20     .03      65    .025    1050     .03

Bank Sta: Left   Right    Lengths: Left Channel   Right     Coeff Contr.   Expan.
            65    1050              740     770     800             .2       .3

CROSS SECTION
```

```
RIVER: RIVER-1
REACH: Reach-1            RS: 90.05

INPUT
Description:
Station Elevation Data    num=      22
     Sta    Elev     Sta    Elev     Sta    Elev     Sta    Elev     Sta    Elev
     -19     8.7      76     2.2     153     1.7     212     1.2     271      .7
     312      .2     353     -.3     399     -.8     446    -1.3     512    -2.3
     579    -3.3     657    -3.3     717    -2.8     777    -2.3     837    -1.8
     898    -1.3     975      -1    1052     -.6    1129     -.3    1165      .7
    1196     1.7    1289     8.7

Manning's n Values        num=       3
     Sta   n Val     Sta   n Val     Sta   n Val
     -19     .03      76    .025    1289     .03

Bank Sta: Left   Right    Lengths: Left Channel   Right     Coeff Contr.   Expan.
            76    1289               730     760     800              .2       .3

CROSS SECTION


RIVER: RIVER-1
REACH: Reach-1            RS: 82.45

INPUT
Description:
Station Elevation Data    num=      18
     Sta    Elev     Sta    Elev     Sta    Elev     Sta    Elev     Sta    Elev
     -19     8.7      50     2.2     100     1.7     125      .7     168     -.3
     187    -1.3     250      -2     314    -2.6     378    -3.3     449    -3.3
     520    -3.3     592    -3.3     643    -2.3     694    -1.3     712     -.3
     732      .7     790     1.7     866     8.7

Manning's n Values        num=       3
     Sta   n Val     Sta   n Val     Sta   n Val
     -19     .03      50    .025     866     .03

Bank Sta: Left   Right    Lengths: Left Channel   Right     Coeff Contr.   Expan.
            50     866               600     600     600              .2       .3

CROSS SECTION


RIVER: RIVER-1
REACH: Reach-1            RS: 76.45

INPUT
Description:
Station Elevation Data    num=      18
     Sta    Elev     Sta    Elev     Sta    Elev     Sta    Elev     Sta    Elev
     -19     8.7      50     2.2     100     1.7     125      .7     168     -.3
     187    -1.3     250      -2     314    -2.6     378    -3.3     449    -3.3
     520    -3.3     592    -3.3     643    -2.3     694    -1.3     712     -.3
     732      .7     790     1.7     866     8.7

Manning's n Values        num=       3
     Sta   n Val     Sta   n Val     Sta   n Val
     -19     .03      50    .025     866     .03

Bank Sta: Left   Right    Lengths: Left Channel   Right     Coeff Contr.   Expan.
```

```
            50     866              670     625     580             .2       .3

CROSS SECTION


RIVER: RIVER-1
REACH: Reach-1            RS: 70.2

INPUT
Description:
Station Elevation Data    num=      22
     Sta    Elev     Sta    Elev     Sta    Elev     Sta    Elev     Sta    Elev
     -20     9.7      77     1.7     130      .7     184     -.3     227    -1.3
     302      -2     378    -2.6     454    -3.3     527    -3.3     600    -3.3
     673    -3.3     746    -3.3     811    -2.6     876      -2     941    -1.3
     996     -.8    1052     -.3    1098      .7    1154     1.7    1215       2
    1276     2.4    1364     9.7

Manning's n Values        num=       3
     Sta   n Val     Sta   n Val     Sta   n Val
     -20     .03      77    .025    1364     .03

Bank Sta: Left   Right    Lengths: Left Channel   Right     Coeff Contr.   Expan.
            77    1364              670     625     530             .2       .3

CROSS SECTION


RIVER: RIVER-1
REACH: Reach-1            RS: 63.95

INPUT
Description:
Station Elevation Data    num=      25
     Sta    Elev     Sta    Elev     Sta    Elev     Sta    Elev     Sta    Elev
     -20     9.7      65     2.2     131     1.7     207      .7     259      .2
     312     -.3     362    -1.3     427      -2     492    -2.6     558    -3.3
     628    -3.3     699    -3.3     770    -3.3     840    -3.3     911    -3.3
     982    -3.3    1046    -2.6    1111      -2    1176    -1.3    1230     -.8
    1284     -.3    1314      .7    1362     1.7    1415     2.2    1494     9.7

Manning's n Values        num=       3
     Sta   n Val     Sta   n Val     Sta   n Val
     -20     .03      65    .025    1494     .03

Bank Sta: Left   Right    Lengths: Left Channel   Right     Coeff Contr.   Expan.
            65    1494              680     620     550             .2       .3

CROSS SECTION


RIVER: RIVER-1
REACH: Reach-1            RS: 57.75

INPUT
Description:
Station Elevation Data    num=      21
     Sta    Elev     Sta    Elev     Sta    Elev     Sta    Elev     Sta    Elev
     -20     9.7       7     1.7      18      .7      29     -.3      45    -1.3
      91    -3.3     168    -3.6     246      -4     324    -4.3     383    -4.8
     443    -5.3     497    -5.3     552    -5.3     603    -4.3     645    -3.3
     698    -2.3     751    -1.3     801     -.3     849      .7     871     1.7
     953     9.7
```

```
Manning's n Values        num=       3
     Sta   n Val     Sta   n Val     Sta   n Val
     -20     .03       7    .025     953     .03

Bank Sta: Left   Right    Lengths: Left Channel   Right     Coeff Contr.   Expan.
             7     953              435     435     435             .2       .3

CROSS SECTION


RIVER: RIVER-1
REACH: Reach-1            RS: 53.4

INPUT
Description:
Station Elevation Data    num=      20
     Sta    Elev     Sta    Elev     Sta    Elev     Sta    Elev     Sta    Elev
     -20     9.7       7     1.7      17      .7      34     -.3      52    -1.3
     128    -2.3     205    -3.3     264    -3.3     324    -3.3     384    -3.3
     420    -3.3     470    -3.3     534    -2.8     599    -2.3     664    -1.8
     729    -1.3     736     -.3     748      .7     765     1.7     832     9.7

Manning's n Values        num=       3
     Sta   n Val     Sta   n Val     Sta   n Val
     -20     .03       7    .025     832     .03

Bank Sta: Left   Right    Lengths: Left Channel   Right     Coeff Contr.   Expan.
             7     832              385     385     385             .2       .3

CROSS SECTION


RIVER: RIVER-1
REACH: Reach-1            RS: 49.55

INPUT
Description:
Station Elevation Data    num=      19
     Sta    Elev     Sta    Elev     Sta    Elev     Sta    Elev     Sta    Elev
     -20     9.7      19     1.7      35      .7      52     -.3      65    -1.3
     136    -2.3     208    -3.3     284    -3.3     361    -3.3     437    -3.3
     514    -3.3     577    -2.8     640    -2.3     703    -1.8     766    -1.3
     784     -.3     850      .7     869     1.7     969     9.7

Manning's n Values        num=       3
     Sta   n Val     Sta   n Val     Sta   n Val
     -20     .03      19    .025     969     .03

Bank Sta: Left   Right    Lengths: Left Channel   Right     Coeff Contr.   Expan.
            19     969              465     465     465             .2       .3

CROSS SECTION


RIVER: RIVER-1
REACH: Reach-1            RS: 44.9

INPUT
Description:
Station Elevation Data    num=      25
     Sta    Elev     Sta    Elev     Sta    Elev     Sta    Elev     Sta    Elev
     -20     9.7      68     2.2     137     1.7     193     1.2     250      .7
     313      .4     376       0     439     -.3     449    -1.3     503      -2
     558    -2.6     613    -3.3     684    -3.3     756    -3.3     812    -3.3
```

```
     869    -3.3     917    -4.3     987    -4.3    1001    -3.3    1018    -1.3
    1022     -.3    1029      .7    1046     1.7    1110     2.7    1137     9.5

Manning's n Values        num=       3
     Sta   n Val     Sta   n Val     Sta   n Val
     -20     .03      68    .025    1137     .03

Bank Sta: Left   Right    Lengths: Left Channel   Right     Coeff Contr.   Expan.
            68    1137              320     280     230             .2       .3

CROSS SECTION


RIVER: RIVER-1
REACH: Reach-1            RS: 42.1

INPUT
Description:
Station Elevation Data    num=      22
     Sta    Elev     Sta    Elev     Sta    Elev     Sta    Elev     Sta    Elev
     -20     9.7      53     2.2     106     1.7     169     1.2     232      .7
     273      .2     315     -.3     329    -1.3     404    -1.6     479    -1.9
     554    -2.2     629    -2.4     704    -2.7     779      -3     854    -3.3
     906    -3.3     921    -1.3     928     -.3     938      .7     950     1.7
     983     2.7    1013     9.5

Manning's n Values        num=       3
     Sta   n Val     Sta   n Val     Sta   n Val
     -20     .03      53    .025    1013     .03

Bank Sta: Left   Right    Lengths: Left Channel   Right     Coeff Contr.   Expan.
            53    1013              270     270     270             .2       .3

CROSS SECTION


RIVER: RIVER-1
REACH: Reach-1            RS: 39.4

INPUT
Description:
Station Elevation Data    num=      20
     Sta    Elev     Sta    Elev     Sta    Elev     Sta    Elev     Sta    Elev
     -19     9.7      76     1.7     108      .7     127     -.3     145    -1.3
     213      -2     282    -2.6     351    -3.3     419    -3.3     477    -3.3
     536    -3.3     595    -3.3     636    -3.3     677    -3.3     717    -1.3
     782     -.3     847      .7     872     1.7     916     2.7     938     9.5

Manning's n Values        num=       3
     Sta   n Val     Sta   n Val     Sta   n Val
     -19     .03     351    .025     595     .03

Bank Sta: Left   Right    Lengths: Left Channel   Right     Coeff Contr.   Expan.
           351     595              260     460     570             .2       .3

CROSS SECTION


RIVER: RIVER-1
REACH: Reach-1            RS: 34.8

INPUT
Description:
Station Elevation Data    num=       9
```

```
     Sta    Elev     Sta    Elev     Sta    Elev     Sta    Elev     Sta    Elev
      79      16      79       8      95       8     110      -7     200      -7
     290      -7     305       8     321       8     321      21

Manning's n Values        num=       3
     Sta   n Val     Sta   n Val     Sta   n Val
      79     .03      95    .025     305     .03

Bank Sta: Left   Right    Lengths: Left Channel   Right     Coeff Contr.   Expan.
            95     305              250     230     250             .2       .3

BRIDGE


RIVER: RIVER-1
REACH: Reach-1            RS: 33.65

INPUT
Description:
Distance from Upstream XS =      .3
Deck/Roadway Width        =   229.3
Weir Coefficient          =     2.6
Upstream  Deck/Roadway Coordinates
    num=       2
     Sta Hi Cord Lo Cord     Sta Hi Cord Lo Cord
      77    21.3      15     323    26.3      20

Upstream Bridge Cross Section Data
Station Elevation Data    num=       9
     Sta    Elev     Sta    Elev     Sta    Elev     Sta    Elev     Sta    Elev
      79      16      79       8      95       8     110      -7     200      -7
     290      -7     305       8     321       8     321      21

Manning's n Values        num=       3
     Sta   n Val     Sta   n Val     Sta   n Val
      79     .03      95    .025     305     .03

Bank Sta: Left   Right    Coeff Contr.   Expan.
            95     305             .2       .3

Downstream  Deck/Roadway Coordinates
    num=       2
     Sta Hi Cord Lo Cord     Sta Hi Cord Lo Cord
      77    21.3      15     323    26.3      20

Downstream Bridge Cross Section Data
Station Elevation Data    num=       9
     Sta    Elev     Sta    Elev     Sta    Elev     Sta    Elev     Sta    Elev
      79      16      79       8      95       8     110      -7     200      -7
     290      -7     305       8     321       8     321      21

Manning's n Values        num=       3
     Sta   n Val     Sta   n Val     Sta   n Val
      79     .03      95    .025     305     .03

Bank Sta: Left   Right    Coeff Contr.   Expan.
            95     305             .2       .3

Upstream Embankment side slope              =       0 horiz. to 1.0 vertical
Downstream Embankment side slope            =       0 horiz. to 1.0 vertical
Maximum allowable submergence for weir flow =     .98
Elevation at which weir flow begins         =
Energy head used in spillway design         =
Spillway height used in design              =
```

```
Weir crest shape                           = Broad Crested

Number of Piers =  2

Pier Data
Pier Station     Upstream=   150.8    Downstream=   150.8
Upstream     num=       2
    Width   Elev    Width   Elev
     4.4     -10     4.4      25
Downstream     num=       2
    Width   Elev    Width   Elev
     4.4     -10     4.4      25

Pier Data
Pier Station     Upstream=   249.2    Downstream=   249.2
Upstream     num=       2
    Width   Elev    Width   Elev
     4.4     -10     4.4      25
Downstream     num=       2
    Width   Elev    Width   Elev
     4.4     -10     4.4      25

Number of Bridge Coefficient Sets =  1

Low Flow Methods and Data
       Energy
Selected Low Flow Methods = Highest Energy Answer

High Flow Method
       Energy Only

Additional Bridge Parameters
       Add Friction component to Momentum
       Do not add Weight component to Momentum
       Class B flow critical depth computations use critical depth
           inside the bridge at the upstream end
       Criteria to check for pressure flow = Upstream energy grade line

CROSS SECTION


RIVER: RIVER-1
REACH: Reach-1            RS: 32.5

INPUT
Description:
Station Elevation Data    num=       9
     Sta    Elev     Sta    Elev     Sta    Elev     Sta    Elev     Sta    Elev
      79      16      79       8      95       8     110      -7     200      -7
     290      -7     305       8     321       8     321      21

Manning's n Values        num=       3
     Sta   n Val     Sta   n Val     Sta   n Val
      79     .03      95    .025     305     .03

Bank Sta: Left   Right    Lengths: Left Channel   Right     Coeff Contr.   Expan.
            95     305              400     410     400             .2       .3

CROSS SECTION


RIVER: RIVER-1
REACH: Reach-1            RS: 28.4
```

```
INPUT
Description:
Station Elevation Data    num=      36
     Sta    Elev     Sta    Elev     Sta    Elev     Sta    Elev     Sta    Elev
     -14     5.7      72     1.7     108      .7     133     -.3     151    -1.3
     208    -3.3     255    -3.8     303    -4.3     376    -5.3     455    -5.5
     535    -5.6     615    -5.8     694      -6     774    -6.1     854    -6.3
     919    -6.3     985    -6.3    1051    -6.3    1117    -6.3    1173    -6.3
    1230    -6.3    1274    -6.8    1318    -7.3    1370    -8.3    1428    -8.3
    1455    -7.3    1470    -6.3    1485    -5.3    1499    -4.3    1512    -3.3
    1526    -1.3    1534     -.3    1587      .7    1648     1.7    1717     2.7
    1738     8.5

Manning's n Values        num=       3
     Sta   n Val     Sta   n Val     Sta   n Val
     -14     .03      72    .025    1738     .03

Bank Sta: Left   Right    Lengths: Left Channel   Right     Coeff Contr.   Expan.
            72    1738              435     435     435             .2       .3

CROSS SECTION


RIVER: RIVER-1
REACH: Reach-1            RS: 24.05

INPUT
Description:
Station Elevation Data    num=      35
     Sta    Elev     Sta    Elev     Sta    Elev     Sta    Elev     Sta    Elev
     -14     5.7      16     1.7      33      .7      46     -.3      55    -1.3
      73    -3.3     100    -4.3     130    -5.3     159    -6.3     189    -7.3
     244    -7.3     299    -7.3     367    -6.8     436    -6.3     502    -5.8
     568    -5.3     639    -5.3     711    -5.3     782    -5.3     854    -5.3
     925    -5.3     997    -5.3    1042    -5.8    1088    -6.3    1156    -6.3
    1224    -6.3    1262    -5.3    1312    -4.3    1345    -3.3    1362    -1.3
    1368     -.3    1380      .7    1416     1.7    1456     2.7    1472     5.5

Manning's n Values        num=       3
     Sta   n Val     Sta   n Val     Sta   n Val
     -14     .03      16    .025    1472     .03

Bank Sta: Left   Right    Lengths: Left Channel   Right     Coeff Contr.   Expan.
            16    1472              370     370     370             .2       .3

CROSS SECTION


RIVER: RIVER-1
REACH: Reach-1            RS: 20.35

INPUT
Description:
Station Elevation Data    num=      32
     Sta    Elev     Sta    Elev     Sta    Elev     Sta    Elev     Sta    Elev
     -15     5.7      21     1.7      44      .7      60     -.3      68    -1.3
      84    -3.3     103    -4.3     126    -5.3     192    -6.3     263    -6.3
     334    -6.3     406    -6.3     477    -6.3     549    -6.3     590    -5.8
     632    -5.3     697    -4.8     762    -4.3     840    -4.3     918    -4.3
     996    -4.3    1056    -4.8    1117    -5.3    1144    -5.3    1178    -4.3
    1212    -3.3    1241    -1.3    1249     -.3    1260      .7    1275     1.7
    1288     2.7    1306     5.5

Manning's n Values        num=       3
```

Sta	n Val	Sta	n Val	Sta	n Val
-15	.03	21	.025	1306	.03

Bank Sta: Left	Right	Lengths: Left	Channel	Right	Coeff Contr.	Expan.
21	1306	370	340	300	.2	.3

CROSS SECTION

RIVER: RIVER-1
REACH: Reach-1 RS: 16.95

INPUT
Description:
Station Elevation Data num= 42

Sta	Elev	Sta	Elev	Sta	Elev	Sta	Elev	Sta	Elev
-14	5.7	7	1.7	16	.7	24	-.3	34	-1.3
58	-3.3	103	-4.3	150	-5.3	197	-6.3	245	-7.3
293	-7.3	349	-6.8	406	-6.3	467	-5.8	529	-5.3
582	-4.8	635	-4.3	697	-4	759	-3.6	821	-3.3
885	-3.3	949	-3.3	1013	-3.3	1077	-3.3	1105	-4.3
1114	-4.3	1155	-4.3	1197	-4.3	1211	-4.3	1278	-4
1345	-3.6	1413	-3.3	1486	-2.6	1560	-2	1634	-1.3
1643	-.3	1686	.7	1759	1.7	1817	1.7	1863	1.7
1887	2.7	1900	5.5						

Manning's n Values num= 3

Sta	n Val	Sta	n Val	Sta	n Val
-14	.03	7	.025	1900	.03

Bank Sta: Left	Right	Lengths: Left	Channel	Right	Coeff Contr.	Expan.
7	1900	445	435	410	.2	.3

CROSS SECTION

RIVER: RIVER-1
REACH: Reach-1 RS: 12.6

INPUT
Description:
Station Elevation Data num= 47

Sta	Elev	Sta	Elev	Sta	Elev	Sta	Elev	Sta	Elev
-15	5.7	62	2.2	124	1.7	138	.7	145	-.3
153	-1.3	173	-3.3	218	-4.3	281	-4.3	344	-4.3
407	-4.3	471	-4.3	512	-3.8	554	-3.3	622	-3.3
691	-3.3	762	-3.3	838	-2.6	915	-2	992	-1.3
1013	-.3	1083	-.3	1154	-.3	1202	-1.3	1271	-3.3
1323	-3.8	1375	-4.3	1402	-4.3	1432	-3.3	1497	-1.3
1554	-1	1611	-.6	1668	-.3	1733	-.3	1798	-.3
1823	-1.3	1883	-1.3	1943	-1.3	1956	-.3	1973	.7
1991	1.7	2009	2.7	2070	2.7	2101	1.7	2168	1.7
2176	2.7	2198	5.5						

Manning's n Values num= 3

Sta	n Val	Sta	n Val	Sta	n Val
-15	.03	62	.025	2198	.03

Bank Sta: Left	Right	Lengths: Left	Channel	Right	Coeff Contr.	Expan.
62	2198	450	445	440	.2	.3

CROSS SECTION

```
RIVER: RIVER-1
REACH: Reach-1            RS: 8.15

INPUT
Description:
Station Elevation Data    num=      19
     Sta    Elev     Sta    Elev     Sta    Elev     Sta    Elev     Sta    Elev
     -10     5.7       2     1.7       5      .7       8     -.3      12    -1.3
      35    -3.3      49    -4.3      62    -5.3      75    -6.3      97    -6.3
     120    -5.3     146    -4.3     180    -3.3     230    -1.3     246     -.3
     270      .7     280     1.7     289     2.7     300     5.5

Manning's n Values        num=       3
     Sta   n Val     Sta   n Val     Sta   n Val
     -10     .03       2    .025     300     .03

Bank Sta: Left   Right    Lengths: Left Channel   Right     Coeff Contr.   Expan.
             2     300              385     385     385             .2       .3

CROSS SECTION


RIVER: RIVER-1
REACH: Reach-1            RS: 4.3

INPUT
Description:
Station Elevation Data    num=      27
     Sta    Elev     Sta    Elev     Sta    Elev     Sta    Elev     Sta    Elev
     -14     5.7       5     1.7      12      .7      54      .7      66     1.7
      80     2.7     123     2.7     129     1.7     135      .7     138     -.3
     143    -1.3     159    -3.3     221    -3.3     284    -3.3     351    -3.3
     418    -3.3     458    -3.3     491    -3.3     552    -4.3     595    -4.3
     633    -3.3     652    -1.3     657     -.3     662      .7     668     1.7
     676     2.7     700     5.5

Manning's n Values        num=       3
     Sta   n Val     Sta   n Val     Sta   n Val
     -14     .03       5    .025     700     .03

Bank Sta: Left   Right    Lengths: Left Channel   Right     Coeff Contr.   Expan.
             5     700              230     230     230             .2       .3

CROSS SECTION


RIVER: RIVER-1
REACH: Reach-1            RS: 2

INPUT
Description:
Station Elevation Data    num=      23
     Sta    Elev     Sta    Elev     Sta    Elev     Sta    Elev     Sta    Elev
     -15     8.7       1     1.7       4      .7       5     -.3       8    -1.3
      14    -3.3      18    -4.3      22    -5.3      27    -6.3      33    -7.3
      40    -8.3     118    -8.3     126    -7.3     132    -6.3     137    -5.3
     143    -4.3     149    -3.3     154    -1.3     156     -.3     159      .7
     161     1.7     162     2.7     175     5.5

Manning's n Values        num=       3
     Sta   n Val     Sta   n Val     Sta   n Val
     -15     .03       1    .025     175     .03

Bank Sta: Left   Right    Lengths: Left Channel   Right     Coeff Contr.   Expan.
```

1	175	200	200	200	.2	.3

CROSS SECTION

RIVER: RIVER-1
REACH: Reach-1 RS: 0.01

INPUT
Description:
Station Elevation Data num= 33

Sta	Elev	Sta	Elev	Sta	Elev	Sta	Elev	Sta	Elev
4690	13.5	4692	12.5	4693	11.5	4695	10.5	4697	9.5
4698	8.5	4700	7.5	4701	6.5	4702	5.5	4704	4.5
4705	3.5	4706	2.5	4714	1.6	4735	1.5	4751	.5
4788	.5	4867	-1.5	4940	-1.5	5000	-3.5	5020	-3.5
5087	3.5	5116	4.5	5134	5.5	5147	6.5	5275	7.5
5279	8.5	5282	9.5	5294	10.5	5295	11.5	5297	12.5
5298	13.5	5300	14.5	5303	15.5				

Manning's n Values num= 3

Sta	n Val	Sta	n Val	Sta	n Val
4690	.03	4735	.025	5275	.03

Bank Sta: Left	Right	Lengths: Left	Channel	Right	Coeff Contr.	Expan.
4735	5275	0	0	0	.2	.3

SUMMARY OF MANNING'S N VALUES

River:RIVER-1

Reach	River Sta.	n1	n2	n3
Reach-1	120.85	.03	.025	.03
Reach-1	114.05	.03	.025	.03
Reach-1	106.55	.03	.025	.03
Reach-1	97.75	.03	.025	.03
Reach-1	90.05	.03	.025	.03
Reach-1	82.45	.03	.025	.03
Reach-1	76.45	.03	.025	.03
Reach-1	70.2	.03	.025	.03
Reach-1	63.95	.03	.025	.03
Reach-1	57.75	.03	.025	.03
Reach-1	53.4	.03	.025	.03
Reach-1	49.55	.03	.025	.03
Reach-1	44.9	.03	.025	.03
Reach-1	42.1	.03	.025	.03
Reach-1	39.4	.03	.025	.03
Reach-1	34.8	.03	.025	.03
Reach-1	33.65	Bridge		
Reach-1	32.5	.03	.025	.03
Reach-1	28.4	.03	.025	.03
Reach-1	24.05	.03	.025	.03
Reach-1	20.35	.03	.025	.03
Reach-1	16.95	.03	.025	.03
Reach-1	12.6	.03	.025	.03
Reach-1	8.15	.03	.025	.03
Reach-1	4.3	.03	.025	.03
Reach-1	2	.03	.025	.03
Reach-1	0.01	.03	.025	.03

SUMMARY OF REACH LENGTHS

River: RIVER-1

Reach	River Sta.	Left	Channel	Right
Reach-1	120.85	650	680	710
Reach-1	114.05	730	750	765
Reach-1	106.55	940	880	800
Reach-1	97.75	740	770	800
Reach-1	90.05	730	760	800
Reach-1	82.45	600	600	600
Reach-1	76.45	670	625	580
Reach-1	70.2	670	625	530
Reach-1	63.95	680	620	550
Reach-1	57.75	435	435	435
Reach-1	53.4	385	385	385
Reach-1	49.55	465	465	465
Reach-1	44.9	320	280	230
Reach-1	42.1	270	270	270
Reach-1	39.4	260	460	570
Reach-1	34.8	250	230	250
Reach-1	33.65	Bridge		
Reach-1	32.5	400	410	400
Reach-1	28.4	435	435	435
Reach-1	24.05	370	370	370
Reach-1	20.35	370	340	300
Reach-1	16.95	445	435	410
Reach-1	12.6	450	445	440
Reach-1	8.15	385	385	385
Reach-1	4.3	230	230	230
Reach-1	2	200	200	200
Reach-1	0.01	0	0	0

SUMMARY OF CONTRACTION AND EXPANSION COEFFICIENTS
River: RIVER-1

Reach	River Sta.	Contr.	Expan.
Reach-1	120.85	.2	.3
Reach-1	114.05	.2	.3
Reach-1	106.55	.2	.3
Reach-1	97.75	.2	.3
Reach-1	90.05	.2	.3
Reach-1	82.45	.2	.3
Reach-1	76.45	.2	.3
Reach-1	70.2	.2	.3
Reach-1	63.95	.2	.3
Reach-1	57.75	.2	.3
Reach-1	53.4	.2	.3
Reach-1	49.55	.2	.3
Reach-1	44.9	.2	.3
Reach-1	42.1	.2	.3
Reach-1	39.4	.2	.3
Reach-1	34.8	.2	.3
Reach-1	33.65	Bridge	
Reach-1	32.5	.2	.3
Reach-1	28.4	.2	.3

```
 Reach-1              24.05           .2        .3
 Reach-1              20.35           .2        .3
 Reach-1              16.95           .2        .3
 Reach-1              12.6            .2        .3
 Reach-1              8.15            .2        .3
 Reach-1              4.3             .2        .3
 Reach-1              2               .2        .3
 Reach-1              0.01            .2        .3
```

PART III. SAN DIEGUITO RIVER

```
                        HEC-RAS Version 4.1.0 Jan 2010
                         U.S. Army Corps of Engineers
                        Hydrologic Engineering Center
                              609 Second Street
                              Davis, California


            X     X  XXXXXX    XXXX        XXXX       XX      XXXX
            X     X  X        X    X       X   X     X  X    X
            X     X  X        X            X   X    X    X   X
            XXXXXXX  XXXX     X       XXX  XXXX     XXXXXX    XXXX
            X     X  X        X            X  X     X    X        X
            X     X  X        X    X       X   X    X    X        X
            X     X  XXXXXX    XXXX        X    X   X    X   XXXXX



PROJECT DATA
Project Title: SDGO at I-5
Project File : SDGOI5.prj
Run Date and Time: 5/6/2010 2:41:04 PM

Project in English units

Project Description:
SAN DIEGUITO RIVER I-5 BRIDGE WIDENING
    FOR CALTRANS THRU WRA

APRIL 2010




PLAN DATA

Plan Title: Alternative
Plan File : C:\HEC Data\RAS\SDGOI5.p02

           Geometry Title: Existing with Alternative bridge
           Geometry File : C:\HEC Data\RAS\SDGOI5.g02

           Flow Title    : Base flood
           Flow File     : C:\HEC Data\RAS\SDGOI5.f01

Plan Summary Information:
Number of:  Cross Sections =   31    Multiple Openings  =    0
            Culverts       =    0    Inline Structures  =    0
            Bridges        =    1    Lateral Structures =    0
```

```
Computational Information
    Water surface calculation tolerance  =  0.01
    Critical depth calculation tolerance =  0.01
    Maximum number of iterations         =  20
    Maximum difference tolerance         =  0.3
    Flow tolerance factor                =  0.001

Computation Options
    Critical depth computed only where necessary
    Conveyance Calculation Method: At breaks in n values only
    Friction Slope Method:         Average Conveyance
    Computational Flow Regime:     Subcritical Flow




FLOW DATA

Flow Title: Base flood
Flow File : C:\HEC Data\RAS\SDGOI5.f01

Flow Data (cfs)

  River           Reach           RS             Base flood     50-yr flood     35-yr
flood
  RIVER-1         Reach-1         2.24                36500           32100
22000
  RIVER-1         Reach-1         1.522               36500           32100
22000
  RIVER-1         Reach-1         1.457               42400           32100
22000


Boundary Conditions

  River           Reach           Profile                        Upstream
Downstream

  RIVER-1         Reach-1         Base flood
Known WS = 16.36
  RIVER-1         Reach-1         50-yr flood
Known WS = 15
  RIVER-1         Reach-1         35-yr flood
Known WS = 13




GEOMETRY DATA

Geometry Title: Existing with Alternative bridge
Geometry File : C:\HEC Data\RAS\SDGOI5.g02

CROSS SECTION


RIVER: RIVER-1
REACH: Reach-1            RS: 2.24

INPUT
Description:
Station Elevation Data    num=      53
     Sta    Elev     Sta    Elev     Sta    Elev     Sta    Elev     Sta    Elev
```

3530	21	3533	20	3536	19	3539	18	3543	17
3546	16	3549	15	3553	14	3651	13	3719	12
3758	11	4293	11	4665	11	4672	11	4685	11
4743	10	4760	9	4774	8	4786	7	4806	7
4836	7	4840	6	4842	5	4851	5	4856	6
4865	7	4880	7	4890	6	4912	5	4957	4
4959	3	4961	2	4968	1	4977	0	4985	-1
4986	-1.1	4988	-1	5004	-.1	5007	0	5034	1
5053	1.4	5056	2	5059	3	5060	4	5061	5
5062	6	5063	7	5064	8	5065	9	5066	10
5075	10	5108	21	5148	21				

Manning's n Values num= 3

Sta	n Val	Sta	n Val	Sta	n Val
3530	.035	4957	.035	5066	.035

Bank Sta: Left	Right	Lengths: Left	Channel	Right	Coeff Contr.	Expan.
4957	5066	456	301	162	.1	.3

CROSS SECTION

RIVER: RIVER-1
REACH: Reach-1 RS: 2.183

INPUT
Description:
Station Elevation Data num= 83

Sta	Elev	Sta	Elev	Sta	Elev	Sta	Elev	Sta	Elev
3760	32	3773	33	3784	33	3786	32	3788	31
3790	30	3792	29	3795	28	3797	27	3799	26
3802	25	3804	24	3806	23	3809	22	3811	21
3814	20	3816	19	3818	18	3821	17	3823	16
3826	15	3828	14	3836	13	3990	12	4114	11
4355	10	4405	10	4420	11	4454	11	4459	10
4466	9	4482	9	4488	9	4495	9	4498	10
4499	10	4614	11	4729	11	4894	11.2	4896	11
4897	10	4898	9	4899	8	4901	7	4902	6
4904	5	4907	4	4910	3	4912	2	4915	1.2
4918	1	4927	0	4935	-.8	4941	0	4947	1
4949	1.1	4952	2	4954	3	4956	4	4987	5
4997	5	4999	4	5001	3	5002	2	5005	.8
5012	1	5024	0	5035	-1	5041	-1.5	5050	-1
5064	0	5069	.7	5081	1	5095	2	5098	3
5101	4	5103	5	5105	6	5107	7	5116	8
5125	8.5	5162.5	21	5200	21				

Manning's n Values num= 3

Sta	n Val	Sta	n Val	Sta	n Val
3760	.035	4894	.035	5116	.035

Bank Sta: Left	Right	Lengths: Left	Channel	Right	Coeff Contr.	Expan.
4894	5116	412	325	180	.1	.3

CROSS SECTION

RIVER: RIVER-1
REACH: Reach-1 RS: 2.122

INPUT
Description:
Station Elevation Data num= 59

Sta	Elev	Sta	Elev	Sta	Elev	Sta	Elev	Sta	Elev

3590	26	3592	25	3594	24	3596	23	3598	22
3600	21	3602	20	3605	19	3607	18	3609	17
3612	16	3614	15	3619	14	3624	13	3644	12
3919	12	3985	12	4118	11	4310	10	4484	10
4576	11	4740	12	4885	12	4920	11	4922	10
4924	9	4925	8	4927	7	4930	6	4934	5
4937	4	4941	3	4945	2	4951	1	4958	0
4965	-1	4973	-1	4980	0	4986	1	4993	2
4995	3	5000	4	5012	4	5014	3	5016	2
5022	1	5030	0	5039	-1	5054	-1	5062	0
5069	1	5075	2	5077	3	5078	4	5079	5
5081	6	5090	6.5	5133.5	21	5170	21		

Manning's n Values num= 3

Sta	n Val	Sta	n Val	Sta	n Val
3590	.035	4920	.035	5081	.035

Bank Sta: Left	Right	Lengths: Left	Channel	Right	Coeff Contr.	Expan.
4920	5081	347	315	270	.1	.3

CROSS SECTION

RIVER: RIVER-1
REACH: Reach-1 RS: 2.062

INPUT
Description:
Station Elevation Data num= 39

Sta	Elev	Sta	Elev	Sta	Elev	Sta	Elev	Sta	Elev
3490	12	3543	12	3573	12	3788	11	3822	11
4119	11	4302	11	4345	11	4628	11	4751	11
4867	10	4886	9	4916	8	4922	7	4934	6
4938	5	4950	5	4958	5	4961	4	4962	3
4963	2	4969	1.2	4971	1	4981	0	4992	-1
5003	-2	5006	-2.4	5012	-2	5024	-1	5033	0
5041	1	5045	1.4	5046	2	5047	3	5049	4
5050	5	5060	6	5105	21	5140	21		

Manning's n Values num= 3

Sta	n Val	Sta	n Val	Sta	n Val
3490	.035	4958	.035	5050	.035

Bank Sta: Left	Right	Lengths: Left	Channel	Right	Coeff Contr.	Expan.
4958	5050	405	439	446	.1	.3

CROSS SECTION

RIVER: RIVER-1
REACH: Reach-1 RS: 1.979

INPUT
Description:
Station Elevation Data num= 66

Sta	Elev	Sta	Elev	Sta	Elev	Sta	Elev	Sta	Elev
3200	12	3251	12	3284	12	3484	11	3545	11
3855	11	3956	11	4264	11	4315	10	4416	10
4528	11	4543	11	4570	2	4619	2	4680	2
4688	4.5	4726	4.5	4767	4.5	4768	4.5	4769	4.5
4770	4	4771	3	4775	2	4776	1.6	4782	1
4788	0	4794	-1	4798	-2.3	4808	-1	4818	0
4824	1	4828	1.3	4832	2	4850	2	4852	1.3
4857	1	4861	0	4865	-1	4869	-2	4874	-3

4879	-4	4883	-5	4887	-6	4889	-6.3	4890	-6
4894	-5	4898	-4	4903	-3	4907	-2	4911	-1
4915	0	4919	1	4920	.2	4924	2	4930	3
4937	4	4954	5	4958	6	4961	7	4968	8
4977	9	5009	10	5040	11	5085	11.5	5115	21.5
5145	21.5								

Manning's n Values num= 3

Sta	n Val	Sta	n Val	Sta	n Val
3200	.035	4767	.035	4977	.035

Bank Sta: Left	Right	Lengths: Left	Channel	Right	Coeff Contr.	Expan.
4767	4977	286	441	472	.1	.3

CROSS SECTION

RIVER: RIVER-1
REACH: Reach-1 RS: 1.895

INPUT
Description:
Station Elevation Data num= 48

Sta	Elev	Sta	Elev	Sta	Elev	Sta	Elev	Sta	Elev
3050	12	3104	12	3149	12	3332	11	3395	11
4133	11	4176	10	4200	2	4275	2	4278	2
4286	2	4304	2	4350	2	4358	4.5	4549	4.5
4566	4.5	4575	4.5	4584	4.5	4618	4.5	4719	4.5
4848	4.5	4877	4.5	4917	4	4952	3	4954	2
4954	1.4	4958	1	4961	0	4964	-1	4968	-2
4969	-2.2	4978	-2	5001	-1.4	5007	-1	5016	0
5025	1	5030	1.3	5032	2	5036	3	5040	4
5042	5	5044	6	5045	7	5047	8	5049	9
5050	10	5080	20	5120	20				

Manning's n Values num= 3

Sta	n Val	Sta	n Val	Sta	n Val
3050	.035	4848	.035	5050	.035

Bank Sta: Left	Right	Lengths: Left	Channel	Right	Coeff Contr.	Expan.
4848	5050	154	255	305	.1	.3

CROSS SECTION

RIVER: RIVER-1
REACH: Reach-1 RS: 1.847

INPUT
Description:
Station Elevation Data num= 51

Sta	Elev	Sta	Elev	Sta	Elev	Sta	Elev	Sta	Elev
3060	17	3063	16	3066	15	3070	14	3073	13
3088	12	3144	12	3168	12	3357	11	3454	11
3951	12	4119	12	4123	11	4200	2	4277	2
4420	2	4428	4.5	4544	4.5	4553	4.5	4561	4.5
4569	4.5	4579	4.5	4595	4.5	4632	4.5	4770	4.5
4819	4.5	4833	4.5	4862	4.5	4959	4.5	4966	4
4968	3	4970	2	4980	1	4992	0	4998	-.2
5005	-1	5053	-1	5070	0	5088	1	5099	.7
5102	2	5104	3	5106	4	5108	5	5110	6
5111	7	5113	8	5115	9	5116	10	5146	20
5200	20								

Manning's n Values num= 3

Sta	n Val	Sta	n Val	Sta	n Val
3060	.035	4959	.035	5116	.035

Bank Sta: Left	Right	Lengths: Left	Channel	Right	Coeff Contr.	Expan.
4959	5116	185	222	261	.1	.3

CROSS SECTION

RIVER: RIVER-1
REACH: Reach-1 RS: 1.805

INPUT
Description:
Station Elevation Data num= 54

Sta	Elev	Sta	Elev	Sta	Elev	Sta	Elev	Sta	Elev
3090	25	3097	24	3105	23	3113	22	3121	21
3127	20	3130	19	3134	18	3138	17	3142	16
3146	15	3150	14	3156	13	3201	12	3409	11
3534	11	3850	11	3870	13	4250	13	4273	11
4300	2	4530	2	4534	2	4537	2	4556	2
4580	2	4588	4.5	4747	4.5	4837	4.5	4848	4.5
4949	4	4950	3	4951	2	4954	.9	4961	1
4974	0	4988	-1	4989	-1	5022	-1.8	5037	-1
5049	0	5061	1	5068	1.1	5071	2	5074	3
5076	4	5078	5	5079	6	5080	7	5082	8
5083	9	5086	10	5116	20	5150	20		

Manning's n Values num= 3

Sta	n Val	Sta	n Val	Sta	n Val
3090	.035	4949	.035	5086	.035

Bank Sta: Left	Right	Lengths: Left	Channel	Right	Coeff Contr.	Expan.
4949	5086	165	359	420	.1	.3

CROSS SECTION

RIVER: RIVER-1
REACH: Reach-1 RS: 1.737

INPUT
Description:
Station Elevation Data num= 54

Sta	Elev	Sta	Elev	Sta	Elev	Sta	Elev	Sta	Elev
3468	27	3500	11	3883	11	4010	11	4030	13
4620	13	4650	10	4653	9	4656	8	4659	7
4662	6	4665	5	4685	5	4700	2	4735	2
4848	2	4876	2	4886	2	4921	2	4927	4
4939	4	4942	3	4946	2	4947	1.6	4949	1.1
4952	.9	4957	1	4971	0	4985	-1	4989	-1
4999	-1.9	5000	-2	5025	-3	5046	-4.6	5047	-4
5049	-4	5052	-3	5055	-2	5058	-1	5061	0
5064	1	5065	1.2	5067	2	5070	3	5072	4
5074	4.6	5075	5	5076	6	5077	7	5079	8
5080	9	5180	10	5210	20	5240	20		

Manning's n Values num= 3

Sta	n Val	Sta	n Val	Sta	n Val
3468	.035	4939	.035	5080	.035

Bank Sta: Left	Right	Lengths: Left	Channel	Right	Coeff Contr.	Expan.
4939	5080	546	330	169	.1	.3

CROSS SECTION

RIVER: RIVER-1
REACH: Reach-1 RS: 1.674

INPUT
Description:
Station Elevation Data num= 76

Sta	Elev	Sta	Elev	Sta	Elev	Sta	Elev	Sta	Elev
3968	27	4000	11	4240	11	4290	11	4337	11
4437	11	4492	11	4602	10	4610	10	4662	10
4672	9	4675	8	4678	7	4685	6	4689	6
4692	8	4695	10	4880	10	4886	8	4893	7
4896	8	4899	9	4919	10	4920	9	4922	8
4923	7	4925	6	4928	4	4929	3	4931	2
4934	1	4941	-1	4945	-2	4949	-3	4953	-4
4960	-6	4963	-7	4966	-8	4969	-9	4975	-11
4978	-12	4981	-13	4984	-14	4987	-15	4988	-15.2
4989	-15	4996	-14	5003	-13	5011	-12	5019	-11
5022	-10.2	5029	-9	5031	-8	5037	-6	5040	-5
5043	-4	5045	-3	5051	-1	5054	0	5057	1
5059	3	5066	4	5086	4	5090	2	5104	2
5109	3	5112	4	5115	5	5134	6	5140	8
5142	9	5167	10	5210	10	5260	10	5290	20
5320	20								

Manning's n Values num= 3

Sta	n Val	Sta	n Val	Sta	n Val
3968	.035	4919	.035	5142	.035

Bank Sta: Left	Right	Lengths: Left	Channel	Right	Coeff Contr.	Expan.
4919	5142	476	413	304	.1	.3

CROSS SECTION

RIVER: RIVER-1
REACH: Reach-1 RS: 1.596

INPUT
Description:
Station Elevation Data num= 64

Sta	Elev	Sta	Elev	Sta	Elev	Sta	Elev	Sta	Elev
4326	18	4456	18	4492	17	4517	16	4564	14
4590	13	4614	12	4674	10	4842	10	4900	10
4904	8	4906	7	4907	6	4909	5	4911	4
4912	3	4913	2.1	4914	2	4918	1	4924	0
4930	-1	4937	-2	4943	-3	4947	-3.6	4949	-4
4951	-4	4959	-3	4968	-2	4976	-1	4984	0
4991	1	4993	1.4	4995	2	4996	3	4998	4
5024	4	5025	3	5026	2	5029	1.2	5031	1
5039	0	5048	-1	5057	-2	5061	-2.3	5066	-2
5075	-1	5083	0	5091	1	5093	1.1	5097	2
5101	3	5104	4	5140	5	5182	6	5191	7
5205	8	5212	9	5218	10	5224	11	5231	11
5307	11	5330	12	5351	19	5400	19		

Manning's n Values num= 3

Sta	n Val	Sta	n Val	Sta	n Val
4326	.035	4900	.035	5104	.035

Bank Sta: Left	Right	Lengths: Left	Channel	Right	Coeff Contr.	Expan.

```
          4900    5104              438     388     290             .1       .3

CROSS SECTION


RIVER: RIVER-1
REACH: Reach-1            RS: 1.522

INPUT
Description:
Station Elevation Data    num=      42
     Sta    Elev     Sta    Elev     Sta    Elev     Sta    Elev     Sta    Elev
    4500      19    4523      19    4550      10    4656      10    4916      11
    4924      10    4925       9    4927       8    4928       7    4929       6
    4930       5    4932       4    4933       3    4934       2    4935     1.3
    4938       1    4944       0    4951      -1    4957      -2    4963      -3
    4993    -3.6    5012      -3    5020      -2    5027      -1    5036       0
    5044       1    5046     1.3    5049       2    5053       3    5059       4
    5142       4    5157       3    5160       3    5180       4    5186       5
    5201       6    5204       7    5207       8    5211       9    5330      10
    5357      19    5380      19

Manning's n Values        num=       3
     Sta   n Val     Sta   n Val     Sta   n Val
    4500    .035    4916    .035    5211    .035

Bank Sta: Left   Right    Lengths: Left Channel   Right     Coeff Contr.   Expan.
          4916    5211              368     345     318             .1       .3

CROSS SECTION


RIVER: RIVER-1
REACH: Reach-1            RS: 1.457

INPUT
Description:
Station Elevation Data    num=      41
     Sta    Elev     Sta    Elev     Sta    Elev     Sta    Elev     Sta    Elev
    4440    18.8    4476    18.8    4500    10.8    4510      11    4520      11
    4543      11    4683      10    4904       9    4905       8    4907       7
    4908       6    4909       5    4910       4    4911       3    4914       2
    4917     1.1    4919       1    4925       0    4931      -1    4938      -2
    4944      -3    4948    -3.7    4991      -3    5012      -2    5032      -1
    5051       0    5070       1    5077     1.2    5080       2    5083       3
    5093       4    5107       5    5110       6    5114       7    5117       8
    5168       9    5185       9    5217       9    5260     9.5    5288    18.8
    5320    18.8

Manning's n Values        num=       3
     Sta   n Val     Sta   n Val     Sta   n Val
    4440    .035    4904    .035    5117    .035

Bank Sta: Left   Right    Lengths: Left Channel   Right     Coeff Contr.   Expan.
          4904    5117              320     348     380             .1       .3

CROSS SECTION


RIVER: RIVER-1
REACH: Reach-1            RS: 1.402

INPUT
Description:
```

Station Elevation Data num= 79

Sta	Elev	Sta	Elev	Sta	Elev	Sta	Elev	Sta	Elev
4020	8	4086	8	4273	8	4355	8	4391	7
4410	6	4435	6	4449	7	4459	7	4539	6
4649	6	4680	7	4683	7	4696	7	4718	8
4749	8	4777	7	4784	7	4794	8	4814	9
4834	9	4871	8	4875	7	4881	6	4893	5
4911	4	4913	3	4916	2	4922	1	4922	.8
4928	0	4934	-1	4941	-2	4947	-3	4960	-4
4984	-4.1	5005	-4	5027	-3.2	5030	-3	5038	-2
5046	-1	5054	0	5061	1	5064	1	5072	2
5089	3	5096	4	5160	5	5168	5	5171	4
5174	4	5178	5	5278	5	5298	5	5309	5
5311	5	5342	6	5373	7	5426	7	5453	7
5534	7	5541	7	5758	7	5826	7	5869	7
5927	7	6009	7	6033	7	6044	7	6073	6
6121	6	6177	7	6255	8	6273	8	6282	7
6286	7	6310	8	6409	9	6455	10		

Manning's n Values num= 3

Sta	n Val	Sta	n Val	Sta	n Val
4020	.04	4871	.03	5096	.04

Bank Sta: Left	Right	Lengths: Left	Channel	Right	Coeff Contr.	Expan.
4871	5096	24	24	24	.3	.5

Ineffective Flow num= 2

Sta L	Sta R	Elev	Permanent
4020	4450	27	F
5150	6455	25	F

CROSS SECTION

RIVER: RIVER-1
REACH: Reach-1 RS: 1.397

INPUT
Description:
Station Elevation Data num= 67

Sta	Elev	Sta	Elev	Sta	Elev	Sta	Elev	Sta	Elev
4030	31	4080	30	4131	29	4199	28	4297	27.3
4363	27.3	4372	26	4391.2	26	4391.3	26	4393	24
4396	23	4399	22	4402	21	4405	20	4409	19
4413	18	4417	17	4420	16	4424	15	4427	14
4431	13	4434	12	4438	11	4443	10	4677	9
4757	8	4839	7	4851	6	4852	5	4854	4
4855	3	4856	2	4860	1	4867	0	4875	-1
4882	-2	4892	-3	4912	-4	4967	-4	4972	-3
4978	-2	4983	-1	4988	0	4993	1	5001	2
5008	3	5010	4	5012	5	5014	6	5017	7
5019	8	5021	9	5024	10	5026	11	5029	12
5032	13	5034	14	5037	15	5040	16	5041.2	25.7
5041.3	25.7	5104	24	5237	24	5623	23	6021	22
6288	22	6434	23						

Manning's n Values num= 3

Sta	n Val	Sta	n Val	Sta	n Val
4030	.04	4851	.03	4988	.04

Bank Sta: Left	Right	Lengths: Left	Channel	Right	Coeff Contr.	Expan.
4851	4988	254	254	254	.3	.5

BRIDGE

```
RIVER: RIVER-1
REACH: Reach-1            RS: 1.3815

INPUT
Description: Bridge #4

Distance from Upstream XS =     .25
Deck/Roadway Width        =     253
Weir Coefficient          =     2.8
Upstream  Deck/Roadway Coordinates
    num=       3
     Sta Hi Cord Lo Cord     Sta Hi Cord Lo Cord     Sta Hi Cord Lo Cord
    4363    27.3    23.3    4700    26.5    22.5  5041.3    25.7    21.7

Upstream Bridge Cross Section Data
Station Elevation Data    num=      67
     Sta    Elev     Sta    Elev     Sta    Elev     Sta    Elev     Sta    Elev
    4030      31    4080      30    4131      29    4199      28    4297    27.3
    4363    27.3    4372      26  4391.2      26  4391.3      26    4393      24
    4396      23    4399      22    4402      21    4405      20    4409      19
    4413      18    4417      17    4420      16    4424      15    4427      14
    4431      13    4434      12    4438      11    4443      10    4677       9
    4757       8    4839       7    4851       6    4852       5    4854       4
    4855       3    4856       2    4860       1    4867       0    4875      -1
    4882      -2    4892      -3    4912      -4    4967      -4    4972      -3
    4978      -2    4983      -1    4988       0    4993       1    5001       2
    5008       3    5010       4    5012       5    5014       6    5017       7
    5019       8    5021       9    5024      10    5026      11    5029      12
    5032      13    5034      14    5037      15    5040      16  5041.2    25.7
  5041.3    25.7    5104      24    5237      24    5623      23    6021      22
    6288      22    6434      23

Manning's n Values        num=       3
     Sta   n Val     Sta   n Val     Sta   n Val
    4030     .04    4851     .03    4988     .04

Bank Sta: Left   Right    Coeff Contr.   Expan.
          4851    4988             .3       .5

Downstream  Deck/Roadway Coordinates
    num=       3
     Sta Hi Cord Lo Cord     Sta Hi Cord Lo Cord     Sta Hi Cord Lo Cord
    4363    27.3    23.3    4700    26.5    22.5    5162    25.7    21.7

Downstream Bridge Cross Section Data
Station Elevation Data    num=      43
     Sta    Elev     Sta    Elev     Sta    Elev     Sta    Elev     Sta    Elev
    4030      31    4074      30    4118      29    4181      28    4266    27.3
    4363    27.3    4442      25    4443      24    4445      23    4448      22
    4451      21    4454      20    4456      19    4458      18    4461      17
    4463      16    4465      15    4467      14    4469      13    4471      12
    4474      11    4476      10    4479       9    4839       8    4879       7
    4899       6    4901       5    4903       4    4905       3    4907       2
    4911       1    4917       0    5040    -1.3    5063    -3.5    5084    -5.9
    5139      -2    5162    25.7    5480      23    5734      22    6122      21
    6172      21    6213      21    6562      24

Manning's n Values        num=       3
     Sta   n Val     Sta   n Val     Sta   n Val
    4030     .04    4879     .03    5139     .04

Bank Sta: Left   Right    Coeff Contr.   Expan.
          4879    5139             .3       .5
```

```
Upstream Embankment side slope              =       0 horiz. to 1.0 vertical
Downstream Embankment side slope            =       0 horiz. to 1.0 vertical
Maximum allowable submergence for weir flow =     .95
Elevation at which weir flow begins         =      25
Energy head used in spillway design         =
Spillway height used in design              =
Weir crest shape                            = Broad Crested

Number of Piers =  11

Pier Data
Pier Station     Upstream=    4454    Downstream=    4504
Upstream     num=       2
    Width   Elev    Width   Elev
     1.3       5     1.3      24
Downstream     num=       2
    Width   Elev    Width   Elev
     1.3       5     1.3      24

Pier Data
Pier Station     Upstream=    4500    Downstream=    4550
Upstream     num=       2
    Width   Elev    Width   Elev
     1.3       0     1.3      24
Downstream     num=       2
    Width   Elev    Width   Elev
     1.3       0     1.3      24

Pier Data
Pier Station     Upstream=    4546    Downstream=    4596
Upstream     num=       2
    Width   Elev    Width   Elev
     1.3       5     1.3      25
Downstream     num=       2
    Width   Elev    Width   Elev
     1.3       5     1.3      25

Pier Data
Pier Station     Upstream=  4612.5    Downstream=  4662.5
Upstream     num=       2
    Width   Elev    Width   Elev
     1.3       5     1.3      24
Downstream     num=       2
    Width   Elev    Width   Elev
     1.3       5     1.3      24

Pier Data
Pier Station     Upstream=    4679    Downstream=    4729
Upstream     num=       2
    Width   Elev    Width   Elev
     1.3       5     1.3      24
Downstream     num=       2
    Width   Elev    Width   Elev
     1.3       5     1.3      24

Pier Data
Pier Station     Upstream=  4745.5    Downstream=  4795.5
Upstream     num=       2
    Width   Elev    Width   Elev
     1.3       4     1.3      24
Downstream     num=       2
    Width   Elev    Width   Elev
     1.3       4     1.3      24
```

```
Pier Data
Pier Station     Upstream=    4812    Downstream=    4862
Upstream     num=       2
    Width   Elev    Width   Elev
     1.3       4     1.3      24
Downstream     num=       2
    Width   Elev    Width   Elev
     1.3       4     1.3      24

Pier Data
Pier Station     Upstream=  4878.5    Downstream=  4928.5
Upstream     num=       2
    Width   Elev    Width   Elev
     1.3       4     1.3      24
Downstream     num=       2
    Width   Elev    Width   Elev
     1.3       4     1.3      24

Pier Data
Pier Station     Upstream=    4945    Downstream=    4995
Upstream     num=       2
    Width   Elev    Width   Elev
     1.3      -4     1.3      24
Downstream     num=       2
    Width   Elev    Width   Elev
     1.3      -5     1.3      24

Pier Data
Pier Station     Upstream=    4991    Downstream=  5061.5
Upstream     num=       2
    Width   Elev    Width   Elev
     1.3      -5     1.3      24
Downstream     num=       2
    Width   Elev    Width   Elev
     1.3      -5     1.3      24

Pier Data
Pier Station     Upstream=    5037    Downstream=  5107.5
Upstream     num=       2
    Width   Elev    Width   Elev
     1.3      -5     1.3      24
Downstream     num=       2
    Width   Elev    Width   Elev
     1.4      -5     1.3      24

Number of Bridge Coefficient Sets =  1

Low Flow Methods and Data
       Yarnell                KVal =     1.2
Selected Low Flow Methods = Yarnell

High Flow Method
       Pressure and Weir flow
           Submerged Inlet Cd          =
           Submerged Inlet + Outlet Cd = .766965
           Max Low Cord                =

Additional Bridge Parameters
       Add Friction component to Momentum
       Do not add Weight component to Momentum
       Class B flow critical depth computations use critical depth
           inside the bridge at the upstream end
       Criteria to check for pressure flow = Upstream energy grade line
```

CROSS SECTION

RIVER: RIVER-1
REACH: Reach-1 RS: 1.348

INPUT
Description:
Station Elevation Data num= 43

Sta	Elev	Sta	Elev	Sta	Elev	Sta	Elev	Sta	Elev
4030	31	4074	30	4118	29	4181	28	4266	27.3
4363	27.3	4442	25	4443	24	4445	23	4448	22
4451	21	4454	20	4456	19	4458	18	4461	17
4463	16	4465	15	4467	14	4469	13	4471	12
4474	11	4476	10	4479	9	4839	8	4879	7
4899	6	4901	5	4903	4	4905	3	4907	2
4911	1	4917	0	5040	-1.3	5063	-3.5	5084	-5.9
5139	-2	5162	25.7	5480	23	5734	22	6122	21
6172	21	6213	21	6562	24				

Manning's n Values num= 3

Sta	n Val	Sta	n Val	Sta	n Val
4030	.04	4879	.03	5139	.04

Bank Sta: Left	Right	Lengths: Left	Channel	Right	Coeff Contr.	Expan.
4879	5139	30	30	30	.3	.5

CROSS SECTION

RIVER: RIVER-1
REACH: Reach-1 RS: 1.343

INPUT
Description:
Station Elevation Data num= 41

Sta	Elev	Sta	Elev	Sta	Elev	Sta	Elev	Sta	Elev
4480	19	4500	9	4551	9	4604	9	4721	9
4793	10	4863	10	4871	9	4879	8	4893	7
4898	6	4902	5	4904	4	4905	3.4	4907	3
4910	2	4915	1	4922	0	4928	-1	4935	-2
4942	-3	4948	-4	4956	-5	4980	-5	4992	-4
5006	-3	5016	-2.3	5020	-2	5033	-1	5047	0
5061	1	5070	2	5073	2.1	5074	3	5077	4
5079	5	5083	6	5086	7	5091	8	5120	8
5140	18								

Manning's n Values num= 3

Sta	n Val	Sta	n Val	Sta	n Val
4480	.035	4863	.035	5091	.035

Bank Sta: Left	Right	Lengths: Left	Channel	Right	Coeff Contr.	Expan.
4863	5091	344	284	329	.1	.3

CROSS SECTION

RIVER: RIVER-1
REACH: Reach-1 RS: 1.29

INPUT
Description:
Station Elevation Data num= 45

Sta	Elev	Sta	Elev	Sta	Elev	Sta	Elev	Sta	Elev
4400	18	4501	18	4540	5	4562	4.6	4598	4.4
4634	4.2	4670	4	4693	3.9	4717	3.8	4740	3.7
4764	3.6	4787	3.5	4810	3.4	4834	3.3	4857	3.2
4881	3.1	4904	3	4904	2.4	4907	2	4913	1
4919	0	4924	-1	4929	-2	4934	-3	4939	-4
4944	-4.9	4984	-4	5003	-3	5012	-2	5021	-1
5031	0	5040	1	5046	2	5049	3	5053	4
5057	5	5060	6	5063	7	5065	8	5081	9
5089	9	5096	8	5130	8	5200	8	5225	23

Manning's n Values num= 3

Sta	n Val	Sta	n Val	Sta	n Val
4400	.035	4904	.035	5081	.035

Bank Sta: Left	Right	Lengths: Left	Channel	Right	Coeff Contr.	Expan.
4904	5081	316	307	305	.1	.3

CROSS SECTION

RIVER: RIVER-1
REACH: Reach-1 RS: 1.241

INPUT
Description:
Station Elevation Data num= 43

Sta	Elev	Sta	Elev	Sta	Elev	Sta	Elev	Sta	Elev
4400	18	4481	18	4520	5	4576	4.6	4624	4.4
4672	4.2	4720	4	4753	3.8	4788	3.6	4803	3.5
4821	3.4	4838	3.3	4855	3.2	4872	3.1	4889	3
4902	1	4914	0	4925	-1	4936	-2	4948	-3
4952	-3.4	4971	-3	4999	-2.4	5015	-2	5040	-1.3
5045	-1	5061	0	5077	1	5087	2	5089	3
5092	4	5094	5	5096	6	5099	7	5101	8
5104	9	5107	10	5121	10	5161	9	5202	8
5242	7	5400	6	5434	23				

Manning's n Values num= 3

Sta	n Val	Sta	n Val	Sta	n Val
4400	.035	4889	.035	5107	.035

Bank Sta: Left	Right	Lengths: Left	Channel	Right	Coeff Contr.	Expan.
4889	5107	250	258	268	.1	.3

CROSS SECTION

RIVER: RIVER-1
REACH: Reach-1 RS: 1.192

INPUT
Description:
Station Elevation Data num= 47

Sta	Elev	Sta	Elev	Sta	Elev	Sta	Elev	Sta	Elev
4380	18	4451	18	4490	5	4568	4.6	4622	4.4
4676	4.2	4730	4	4768	3.8	4806	3.6	4843	3.4
4861	3.3	4881	3.2	4900	3.1	4919	3	4919	2.3
4920	2	4927	1	4940	0	4953	-1	4966	-2
4977	-2.2	5024	-2.1	5032	-2	5053	-1.6	5061	-1
5074	0	5086	1	5093	2	5095	3	5096	3.2
5097	4	5099	5	5110	6	5112	6	5125	5
5148	5	5151	6	5153	7	5156	8	5158	9
5161	10	5168	10	5173	9	5217	8	5270	7

```
    5400       7    5420      18

Manning's n Values        num=       3
     Sta   n Val     Sta   n Val     Sta   n Val
    4380    .035    4881    .035    5161    .035

Bank Sta: Left   Right    Lengths: Left Channel   Right     Coeff Contr.   Expan.
          4881    5161              271     288     309              .1       .3

CROSS SECTION


RIVER: RIVER-1
REACH: Reach-1            RS: 1.137

INPUT
Description:
Station Elevation Data    num=      47
     Sta    Elev     Sta    Elev     Sta    Elev     Sta    Elev     Sta    Elev
    4400      18    4461      18    4500       5    4560     4.6    4600     4.4
    4640     4.2    4680       4    4703     3.9    4726     3.8    4749     3.7
    4772     3.6    4785     3.5    4818     3.4    4841     3.3    4864     3.2
    4887     3.1    4911       3    4914     2.3    4918       2    4930       1
    4947       0    4964      -1    4980    -1.5    4984      -2    5012      -3
    5038    -4.1    5057      -3    5064      -2    5072      -1    5079       0
    5087       1    5091       2    5092       3    5110       4    5113       5
    5116       6    5119       7    5122       8    5165       9    5176      10
    5189      11    5200      11    5207      10    5278       9    5420       8
    5530       8    5550      22

Manning's n Values        num=       3
     Sta   n Val     Sta   n Val     Sta   n Val
    4400    .035    4887    .035    5122    .035

Bank Sta: Left   Right    Lengths: Left Channel   Right     Coeff Contr.   Expan.
          4887    5122              241     238     239              .1       .3

CROSS SECTION


RIVER: RIVER-1
REACH: Reach-1            RS: 1.092

INPUT
Description:
Station Elevation Data    num=      54
     Sta    Elev     Sta    Elev     Sta    Elev     Sta    Elev     Sta    Elev
    4400      18    4451      18    4490       5    4564     4.6    4601     4.4
    4638     4.2    4675       4    4700     3.9    4725     3.8    4750     3.7
    4775     3.6    4800     3.5    4825     3.4    4850     3.2    4875     3.1
    4899       3    4900       2    4902       2    4912       1    4934       0
    4956      -1    4961    -1.2    4977      -2    4997      -3    5011    -3.7
    5035      -3    5045      -2    5055      -1    5065       0    5075       1
    5080       2    5080     2.2    5082       3    5084       4    5085       5
    5089       6    5094       7    5146       8    5153       9    5154       9
    5164       8    5179       8    5196       9    5202      10    5211      10
    5217       9    5223       9    5225      10    5231      12    5257      12
    5265      10    5396      10    5570      10    5590      21

Manning's n Values        num=       3
     Sta   n Val     Sta   n Val     Sta   n Val
    4400    .035    4899    .035    5094    .035

Bank Sta: Left   Right    Lengths: Left Channel   Right     Coeff Contr.   Expan.
```

```
          4899    5094              260     246     229             .1       .3

CROSS SECTION


RIVER: RIVER-1
REACH: Reach-1            RS: 1.045

INPUT
Description:
Station Elevation Data    num=      60
     Sta    Elev     Sta    Elev     Sta    Elev     Sta    Elev     Sta    Elev
    4400      17    4454      17    4490       5    4566     4.8    4600     4.6
    4633     4.4    4667     4.2    4700       4    4733     3.8    4767     3.6
    4800     3.4    4833     3.2    4867    3.15    4875     3.1    4878       3
    4890       3    4893       3    4895     2.4    4896       2    4902       1
    4915       0    4928      -1    4941      -2    4949    -2.6    4968      -3
    4992    -3.6    5019      -3    5022    -2.8    5027      -2    5036      -1
    5045       0    5054       1    5058       2    5059       3    5061       4
    5067       5    5103       5    5122       5    5139       5    5145       5
    5184       6    5210       7    5216       8    5223       9    5236      10
    5242      11    5258      12    5265      12    5270      11    5275      10
    5476      10    5484      11    5488      12    5491      13    5494      14
    5498      15    5501      16    5504      17    5507      18    5511      19

Manning's n Values        num=       3
     Sta   n Val     Sta   n Val     Sta   n Val
    4400    .035    4867    .035    5067    .035

Bank Sta: Left   Right    Lengths: Left Channel   Right     Coeff Contr.   Expan.
          4867    5067              363     413     484             .1       .3

CROSS SECTION


RIVER: RIVER-1
REACH: Reach-1            RS: 0.967

INPUT
Description:
Station Elevation Data    num=      60
     Sta    Elev     Sta    Elev     Sta    Elev     Sta    Elev     Sta    Elev
    4400      17    4434      17    4470       5    4518     4.8    4560     4.6
    4602     4.4    4644     4.2    4660     4.1    4680       4    4721     3.8
    4807     3.5    4822     3.4    4838     3.3    4850     3.2    4882     3.1
    4897       3    4901       3    4902       2    4906       1    4914       0
    4922      -1    4929      -2    4937      -3    4944      -4    4947    -4.2
    4999      -4    5038      -3    5040    -2.9    5050      -2    5059      -1
    5068       0    5078       1    5085       2    5088     1.8    5090       3
    5094       4    5097       5    5101       6    5104       7    5107       8
    5135       8    5146       8    5151       9    5154       9    5158       8
    5161       7    5217       7    5238       8    5240       9    5245      11
    5247      12    5309      12    5311      11    5314      10    5320      10
    5325      12    5327      13    5330      14    5332      15    5340      15

Manning's n Values        num=       3
     Sta   n Val     Sta   n Val     Sta   n Val
    4400    .035    4897    .035    5107    .035

Bank Sta: Left   Right    Lengths: Left Channel   Right     Coeff Contr.   Expan.
          4897    5107              458     533     569             .1       .3

CROSS SECTION
```

RIVER: RIVER-1
REACH: Reach-1 RS: 0.866

INPUT
Description:
Station Elevation Data num= 51

Sta	Elev	Sta	Elev	Sta	Elev	Sta	Elev	Sta	Elev
4480	16	4547	16	4580	5	4650	4.5	4751	4
4794	4	4813	5	4819	6	4825	7	4837	7
4839	6	4842	5	4855	4	4878	4	4899	4
4925	3	4925	2.3	4928	2	4933	1	4944	0
4954	-1	4964	-2	4975	-3	4977	-3.2	4997	-4
5019	-4.9	5032	-4	5039	-3	5045	-2	5051	-1
5058	0	5064	1	5068	2	5069	3	5070	4
5072	5	5079	6	5081	6.1	5083	7	5086	8
5088	9	5092	9	5096	8	5101	7	5105	6
5601	6	5604	7	5607	8	5610	9	5657	10
5667	10								

Manning's n Values num= 3

Sta	n Val	Sta	n Val	Sta	n Val
4480	.035	4899	.035	5088	.035

Bank Sta: Left	Right	Lengths: Left	Channel	Right	Coeff Contr.	Expan.
4899	5088	288	274	228	.1	.3

CROSS SECTION

RIVER: RIVER-1
REACH: Reach-1 RS: 0.814

INPUT
Description:
Station Elevation Data num= 50

Sta	Elev	Sta	Elev	Sta	Elev	Sta	Elev	Sta	Elev
4500	20	4530	4	4551	4	4577	3	4584	2
4650	2	4668	3	4676	3	4692	2	4714	2
4720	3	4733	3	4740	2	4778	2	4781	3
4871	4	4880	5	4881	5	4885	4	4889	3
4893	2	4902	1	4915	0	4928	-1	4941	-2
4979	-3	4992	-3.2	5027	-3.2	5030	-3	5040	-2
5051	-1	5062	0	5072	1	5078	2	5079	2.4
5080	3	5082	4	5087	5	5094	6	5109	6
5436	5	5594	5	5657	5	5678	5	5695	6
5698	7	5701	8	5704	9	5741	10	5763	10

Manning's n Values num= 3

Sta	n Val	Sta	n Val	Sta	n Val
4500	.035	4881	.035	5094	.035

Bank Sta: Left	Right	Lengths: Left	Channel	Right	Coeff Contr.	Expan.
4881	5094	210	215	168	.1	.3

CROSS SECTION

RIVER: RIVER-1
REACH: Reach-1 RS: 0.773

INPUT
Description:
Station Elevation Data num= 37

Sta	Elev	Sta	Elev	Sta	Elev	Sta	Elev	Sta	Elev
4550	19	4565	2.5	4590	3	4741	4	4766	4
4919	3	4923	2.4	4924	2.2	4929	1	4937	0
4945	-1	4953	-2	4961	-3	4963	-3.2	4999	-3.2
5010	-3	5035	-2.6	5072	-2	5074	-2	5084	-1
5096	0	5108	1	5113	1.6	5115	2	5119	3
5154	4	5167	5	5185	5	5349	5	5508	5
5782	5	5802	6	5805	7	5808	8	5810	9
5842	10	5877	10						

Manning's n Values num= 3

Sta	n Val	Sta	n Val	Sta	n Val
4550	.035	4919	.035	5119	.035

Bank Sta: Left	Right	Lengths: Left	Channel	Right	Coeff Contr.	Expan.
4919	5119	611	353	78	.1	.3

CROSS SECTION

RIVER: RIVER-1
REACH: Reach-1 RS: 0.706

INPUT
Description:
Station Elevation Data num= 65

Sta	Elev	Sta	Elev	Sta	Elev	Sta	Elev	Sta	Elev
4700	15	4722	12.5	4727	12	4755	12	4780	9
4800	8	4820	8	4840	8	4860	8	4880	8
4890	8	4900	8	4902	7.5	4916	7.5	4928	7
4929	6	4930	5	4932	3	4934	2	4939	1
4943	0	4947	-1	4951	-2	4954	-3	4958	-4
4966	-6	4970	-7	4972	-7.5	4974	-8	4977	-9
4981	-10	4984	-11	4993	-12	5002	-12.3	5005	-12
5009	-11	5014	-10	5019	-9	5024	-8	5028	-7
5032	-6	5039	-5	5046	-4	5052	-3	5058	-2
5064	-1	5071	0	5113	1	5124	2	5125	2.6
5127	3	5195	4	5269	5	5276	5	5409	5
5421	5	5441	5	5466	5	5814	5	5829	6
5835	7	5838	8	5841	9	5844	10	5864	17

Manning's n Values num= 3

Sta	n Val	Sta	n Val	Sta	n Val
4700	.035	4928	.035	5071	.035

Bank Sta: Left	Right	Lengths: Left	Channel	Right	Coeff Contr.	Expan.
4928	5071	133	103	88	.1	.3

CROSS SECTION

RIVER: RIVER-1
REACH: Reach-1 RS: 0.685

INPUT
Description:
Station Elevation Data num= 41

Sta	Elev	Sta	Elev	Sta	Elev	Sta	Elev	Sta	Elev
4720	25	4740	14	4745	12	4758	12	4770	12
4775	10.4	4780	9.4	4790	9.3	4800	9.2	4824	9
4844	8.9	4866	8.9	4882	8.8	4900	8.5	4910	7.3
4926	7.3	4950	7	4980	-11	4986	-12	5000	-13.5
5020	-12	5030	-11	5062	-5	5090	0	5110	1
5130	3	5144	3.4	5166	4	5200	4.3	5246	4.4

```
    5270     4.5    5304     4.5    5350     4.7    5400     4.8    5462     4.7
    5530     4.8    5624     4.8    5760       5    5780       6    5794       7
    5810      11

Manning's n Values        num=       3
     Sta   n Val     Sta   n Val     Sta   n Val
    4720    .035    4866    .035    5400    .035

Bank Sta: Left   Right    Lengths: Left Channel   Right     Coeff Contr.   Expan.
          4866    5400              110     110      60              .1       .3

CROSS SECTION


RIVER: RIVER-1
REACH: Reach-1            RS: 0.666

INPUT
Description:
Station Elevation Data    num=      65
     Sta    Elev     Sta    Elev     Sta    Elev     Sta    Elev     Sta    Elev
    4890      25    4891       9    4916       9    4939       9    4941       7
    4942       6    4943       5    4944       4    4945       3    4946       2
    4948       1    4950       0    4953      -1    4955      -2    4957      -3
    4960      -4    4962      -5    4964      -6    4967      -7    4969      -8
    4971      -9    4973     -10    4975     -11    4977     -12    4978   -12.5
    4979     -13    4981     -14    4983     -15    5004   -15.6    5012     -15
    5015     -14    5018     -13    5021     -12    5025     -11    5028     -10
    5032      -9    5035      -8    5039      -7    5041    -6.3    5043      -6
    5048      -5    5055      -4    5061      -3    5068      -2    5075      -1
    5081       0    5088       1    5096       2    5098       3    5099       4
    5101       5    5178       5    5208       5    5209       5    5522       4
    5592       4    5621       5    5648       6    5658       7    5661       8
    5665       9    5669      10    5695      11    5758      11    5761      10

Manning's n Values        num=       3
     Sta   n Val     Sta   n Val     Sta   n Val
    4890    .035    4941    .035    5101    .035

Bank Sta: Left   Right    Lengths: Left Channel   Right     Coeff Contr.   Expan.
          4941    5101              220     249     175              .1       .3

CROSS SECTION


RIVER: RIVER-1
REACH: Reach-1            RS: 0.619

INPUT
Description:
Station Elevation Data    num=      52
     Sta    Elev     Sta    Elev     Sta    Elev     Sta    Elev     Sta    Elev
    4830      22    4838      10    4840      10    4873      10    4880      11
    4885      11    4886      10    4887       9    4888       8    4889       7
    4890       6    4891       5    4892       4    4893       3    4894     2.1
    4895       2    4900       1    4913       0    4927      -1    4941      -2
    4949    -2.2    4977      -3    5012      -4    5029    -4.7    5082    -4.3
    5085      -4    5092      -3    5099      -2    5106      -1    5114       0
    5121       1    5125       2    5128       3    5129     3.3    5131       4
    5134       5    5136       6    5139       7    5157       7    5161       6
    5165       5    5267       4    5308       4    5387       5    5424       6
    5429       7    5433       8    5437       9    5441      10    5445      11
    5509      11    5552      10
```

Manning's n Values num= 3

Sta	n Val	Sta	n Val	Sta	n Val
4830	.035	4885	.035	5139	.035

Bank Sta: Left	Right	Lengths: Left	Channel	Right	Coeff Contr.	Expan.
4885	5139	204	196	238	.1	.3

SUMMARY OF MANNING'S N VALUES

River:RIVER-1

Reach	River Sta.	n1	n2	n3
Reach-1	2.24	.035	.035	.035
Reach-1	2.183	.035	.035	.035
Reach-1	2.122	.035	.035	.035
Reach-1	2.062	.035	.035	.035
Reach-1	1.979	.035	.035	.035
Reach-1	1.895	.035	.035	.035
Reach-1	1.847	.035	.035	.035
Reach-1	1.805	.035	.035	.035
Reach-1	1.737	.035	.035	.035
Reach-1	1.674	.035	.035	.035
Reach-1	1.596	.035	.035	.035
Reach-1	1.522	.035	.035	.035
Reach-1	1.457	.035	.035	.035
Reach-1	1.402	.04	.03	.04
Reach-1	1.397	.04	.03	.04
Reach-1	1.3815	Bridge		
Reach-1	1.348	.04	.03	.04
Reach-1	1.343	.035	.035	.035
Reach-1	1.29	.035	.035	.035
Reach-1	1.241	.035	.035	.035
Reach-1	1.192	.035	.035	.035
Reach-1	1.137	.035	.035	.035
Reach-1	1.092	.035	.035	.035
Reach-1	1.045	.035	.035	.035
Reach-1	0.967	.035	.035	.035
Reach-1	0.866	.035	.035	.035
Reach-1	0.814	.035	.035	.035
Reach-1	0.773	.035	.035	.035
Reach-1	0.706	.035	.035	.035
Reach-1	0.685	.035	.035	.035
Reach-1	0.666	.035	.035	.035
Reach-1	0.619	.035	.035	.035

SUMMARY OF REACH LENGTHS

River: RIVER-1

Reach	River Sta.	Left	Channel	Right
Reach-1	2.24	456	301	162
Reach-1	2.183	412	325	180
Reach-1	2.122	347	315	270
Reach-1	2.062	405	439	446
Reach-1	1.979	286	441	472
Reach-1	1.895	154	255	305
Reach-1	1.847	185	222	261

Reach-1	1.805	165	359	420
Reach-1	1.737	546	330	169
Reach-1	1.674	476	413	304
Reach-1	1.596	438	388	290
Reach-1	1.522	368	345	318
Reach-1	1.457	320	348	380
Reach-1	1.402	24	24	24
Reach-1	1.397	254	254	254
Reach-1	1.3815	Bridge		
Reach-1	1.348	30	30	30
Reach-1	1.343	344	284	329
Reach-1	1.29	316	307	305
Reach-1	1.241	250	258	268
Reach-1	1.192	271	288	309
Reach-1	1.137	241	238	239
Reach-1	1.092	260	246	229
Reach-1	1.045	363	413	484
Reach-1	0.967	458	533	569
Reach-1	0.866	288	274	228
Reach-1	0.814	210	215	168
Reach-1	0.773	611	353	78
Reach-1	0.706	133	103	88
Reach-1	0.685	110	110	60
Reach-1	0.666	220	249	175
Reach-1	0.619	204	196	238

SUMMARY OF CONTRACTION AND EXPANSION COEFFICIENTS
River: RIVER-1

Reach	River Sta.	Contr.	Expan.
Reach-1	2.24	.1	.3
Reach-1	2.183	.1	.3
Reach-1	2.122	.1	.3
Reach-1	2.062	.1	.3
Reach-1	1.979	.1	.3
Reach-1	1.895	.1	.3
Reach-1	1.847	.1	.3
Reach-1	1.805	.1	.3
Reach-1	1.737	.1	.3
Reach-1	1.674	.1	.3
Reach-1	1.596	.1	.3
Reach-1	1.522	.1	.3
Reach-1	1.457	.1	.3
Reach-1	1.402	.3	.5
Reach-1	1.397	.3	.5
Reach-1	1.3815	Bridge	
Reach-1	1.348	.3	.5
Reach-1	1.343	.1	.3
Reach-1	1.29	.1	.3
Reach-1	1.241	.1	.3
Reach-1	1.192	.1	.3
Reach-1	1.137	.1	.3
Reach-1	1.092	.1	.3
Reach-1	1.045	.1	.3
Reach-1	0.967	.1	.3
Reach-1	0.866	.1	.3
Reach-1	0.814	.1	.3
Reach-1	0.773	.1	.3
Reach-1	0.706	.1	.3

Reach-1	0.685	.1	.3
Reach-1	0.666	.1	.3
Reach-1	0.619	.1	.3

APPENDIX B. INPUT/OUTPUT DESCRIPTIONS FOR FLUVIAL-12

I. INPUT DESCRIPTION

The basic data requirements for a modeling study include (1) topographic maps of the river reach from the downstream end to the upstream end of study, (2) digitized data for cross sections in the HEC-2 format with cross-sectional locations shown on the accompanying topographic maps, (3) flow records or flood hydrographs and their variations along the study stream reach, if any, and (4) size distributions of sediment samples along the study reach. Additional data are required for special features of a study river reach.

The HEC-2 format for input data is used in all versions of the FLUVIAL model. Data records for HEC-2 pertaining to cross-sectional geometry (X1 and GR), job title (T1, T2, and T3), and end of job (EJ), are used in the FLUVIAL model. If a HEC-2 data file is available, it is not necessary to delete the unused records except that the information they contain are not used in the computation. For the purpose of water- and sediment-routing, additional data pertaining to sediment characteristics, flood hydrograph, etc., are required and supplied by other data records. Sequential arrangement of data records are given in the following.

Records	Description of Record Type
T1,T2,T3	Title Records
G1	General Use Record
G2	General Use Records for Hydrographs
G3	General Use Record
G4	General Use Record for Selected Cross-Sectional Output
G5	General Use Record
G6	General Use Record for Selecting Times for Summary Output
G7	General Use Record for Specifying Erosion Resistant Bed Layer
GS	General Use Records for Initial Sediment Compositions
GB	General Use Records for Time Variation of Base-Level
GQ	General Use Records for Stage-Discharge Relation of Downstream Section
GI	General Use Records for Time Variation of Sediment Inflow
X1	Cross-Sectional Record
XF	Record for Specifying Special Features of a Cross Section
GR	Record for Ground Profile of a Cross Section
SB	Record for Special Bridge Routine
BT	Record for Bridge Deck Definition
EJ	End of Job Record

Variable locations for each input record are shown by the field number. Each record has an input format of (A2, F6.0, 9F8.0). Field 0 occupying columns 1 and 2 is reserved for the required record identification characters. Field 1 occupies columns 3 to 8; Fields 2 to 10 occupy 8 columns each. The data records are tabulated and described in the following.

T1, T2, T3 Records - These three records are title records that are required for each job.

Field	Variable	Value	Description
0	IA	T1	Record identification characters
1-10	None		Numbers and alphameric characters for title

G1 Record - This record is required for each job, used to enter the general parameters listed below. This record is placed right after the T1, T2, and T3 records.

Field	Variable	Value	Description
0	IA	G1	Record identification characters
1	TYME	+	Starting time of computation on the hydrograph, in hours
2	ETIME	+	Ending time of computation on the hydrograph, in hours
3	DTMAX	+	Maximum time increment Δt allowed, in seconds
4	ISED	1	Select Graf's sediment transport equation.
		2	Select Yang's unit stream power equation. The sediment size is between 0.063 and 10 mm.
		3	Select Engelund-Hansen sediment equation.
		4	Select Parker gravel equation.
		5	Select Ackers-White sediment equation.
		6	Select Meyer-Peter Muller equation for bed load.
5	BEF	+	Bank erodibility factor for the study reach. This value is used value between 0 and 1 may be used.
6	IUC	0	English units are used in input and output.
		1	Metric units are used in input and output.
7	CNN	+	Manning's *n* value for the study reach. This value is used for a section unless otherwise specified in Field 4 of the XF record. If bed roughness is computed based upon alluvial bedforms as specified in Field 5 of the G3 record, only an approximate *n* value needs to be entered here.
8	PTM1	+	First time point in hours on the hydrograph at which summary output and complete cross-sectional output are requested. It is usually

			the peak time, but it may be left blank if no output is requested.
9	PTM2	+	Second time point on the hydrograph in hours at which summary usually the time just before the end of the simulation. This field may be left blank if no output is needed.
10	KPF	+	Frequency of printing summary output, in number of time steps.

G2 Records - These records are required for each job, used to define the flow hydrograph(s) in the channel reach. The first one (or two) G2 records are used to define the spatial variation in water discharge along the reach; the succeeding ones are employed to define the time variation(s) of the discharge. Up to 10 hydrographs, with a maximum of 120 points for each, are currently dimensioned. See section II for tributaries. These records are placed after the G1 record.

Field	Variable	Value	Description
First G2			
0	IA	G2	Record identification characters
1	IHP1	+	Number of last cross section using the first (downstream most) hydrograph. The number of section is counted from downstream to upstream with the downstream section number being one. See also section II.
2	NP1	+	Number of points connected by straight segments used to define
3	IHP2	+	Number of last section using the second hydrograph if any. Otherwise leave it blank.
4	NP2	+	Number of points used to define the second hydrograph if any. Otherwise leave it blank.
5	IHP3	+	Number of last section using the third hydrograph if any. Otherwise leave it blank.
6	NP3	+	Number of points used to define the third hydrograph if any. Otherwise leave it blank.
7	IHP4	+	Number of last section using the fourth hydrograph if any. Otherwise leave it blank.
8	NP4	+	Number of points used to define the fourth hydrograph if any. Otherwise leave it blank.
9	IHP5	+	Number of last section using the fifth hydrograph if any. Otherwise leave it blank.

10	NP5	+	Number of points used to define the fifth hydrograph if any. Otherwise leave it blank.

Second G2: Note that this record is used only if more than 5 hydrographs are used for the job. It is necessary to place a negative sign in front of NP5 located in the 10th field of the first G2 record as a means to specify that more than 5 hydrographs are used.

0	IA	G2	Record identification characters
1	IHP6	+	Number of last cross section using the sixth hydrograph if any. Otherwise leave it blank.
2	NP6	+	Number of points connected by straight segments used to define
3	IHP7	+	Number of last section using the seventh hydrograph if any. Otherwise leave it blank.
4	NP7	+	Number of points used to define the seventh hydrograph
5	IHP8	+	Number of last section using the eighth hydrograph if any. Otherwise leave it blank.
6	NP8	+	Number of points used to define the eighth hydrograph
7	IHP9	+	Number of last section using the ninth hydrograph if any. Otherwise leave it blank.
8	NP9	+	Number of points used to define the ninth hydrograph
9	IHP10	+	Number of last section using the tenth hydrograph if any. Otherwise leave it blank.
10	NP10	+	Number of points used to define the tenth hydrograph

Succeeding G2 Record(s)

1	Q11, Q21 Q31	+	Discharge coordinate of point 1 for each hydrograph, in ft^3/sec or m^3/sec
2	TM11,TM21 TM31	+	Time coordinate of point 1 for each hydrograph, in hours
3	Q12, Q22 Q32	+	Discharge coordinate of point 2 for each hydrograph, in cfs or cms
4	TM12,TM22 TM32	+	Time coordinate of point 2 for each hydrograph, in hours

Continue with additional discharge and time coordinates. Note that time coordinates must be in increasing order.

G3 Record - This record is used to define required and optional river channel features for a job as listed below. This record is placed after the G2 records.

Field	Variable	Value	Description
0	IA	G3	Record identification characters
1	S11	+	Slope of the downstream section, required for a job
2	BSP	0	One-on-one slope for rigid bank or bank protection
		+	Slope of bank protection in BSP horizontal units on 1 vertical unit. for all cross sections unless otherwise specified in Field 8 of the XF record for a section.
3	DSOP	0	Downstream slope is allowed to vary during simulation.
		1	Downstream slope is fixed at S11 given in Field 1.
4	TEMP	0	Water temperature is 15°C.
		+	Water temperature in degrees Celsius
5	ICNN	0	Manning's n defined in Field 7 of the G1 record or those in Field 4 of the XF records are used.
		1	Brownlie's formula for alluvial bed roughness is used to calculate Manning's n in the simulation.
6	TDZAMA	0	Thickness of erodible bed layer is 100 ft (30.5 m).
		+	Thickness of erodible bed layer in ft or m. This value is applied to
7	SPGV	0	Specific gravity of sediment is 2.65.
		+	Specific gravity of sediment
8	KGS	0	The number of size fractions for bed material is 5.
		+	The number of size fractions for bed material. It maximum value is 8.
9	PHI	0	The angle of repose for bed material is 36°.
		+	Angle of repose for bed material

G4 Record - This is an optional record used to select cross sections (up to 4) to be included at each summary output. Each cross section is identified by its number which is counted from the downstream section. This record also contains other options; it is placed after the G3 record.

Field	Variable	Value	Description

0	IA	G4	Record identification characters
1	IPLT1	+	Number of cross section
2	IPLT2	+	Number of cross section
3	IPLT3	+	Number of cross section
4	IPLT4	+	Number of cross section
5	IEXCAV	+	A positive integer indicates number of cross section where sand/gravel excavation occurs.
6	GIFAC	+	A non-zero constant is used to modify sediment inflow at the upstream section.
7	PZMIN	0	Minimum bed profile during simulation run is not requested.
		1	Output file entitled TZMIN for minimum bed profile is requested.
10	REXCAV	+	A non-zero value specifies rate of sand/gravel excavation at Section IEXCAV.

G5 Record - This is an optional record used to specify miscellaneous options, including unsteady-flow routing for the job based upon the dynamic wave, bend flow characteristics. If the unsteady flow option is not used, the water-surface profile for each time step is computed using the standard-step method. When the unsteady flow option is used, the downstream water-surface elevation must be specified using the GB records.

Field	Variable	Value	Description
0	IA	G5	Record identification characters
1	DT	0	The first time step is 100 seconds.
		+	Size of the first time step in seconds.
2	IROUT	0	Unsteady water routing is not used; water-surface profiles are computed using standard-step method.
		1	Unsteady water-routing based upon the dynamic wave is used to compute stages and water discharges at all cross sections for each
3	PQSS	0	No output of gradation of sediment load
		3	Gradation of sediment load is included in output in 1,000 ppm by weight.
5	TSED	0	Rate of tributary sediment inflow is 1 times the discharge ratio.
		+	Rate of tributary sediment inflow is TSED times the discharge ratio.

6	PTV	0	No output of transverse distribution of depth-averaged velocity
		1	Transverse distribution of depth-averaged velocity is printed. The velocity distribution is for bends with fully developed transverse flow.
10	DYMAX	0	No GR points are inserted for cross sections.
		+	Maximum value of spacing between adjacent points at a cross

G6 Record - This is an optional record used to select time points for summary output. Up to 30 time points may be specified. The printing frequency (KPF) in Field 10 of the G1 Record may be suppressed by using a large number such as 9999.

Field	Variable	Value	Description
First G6 Record			
0	IA	G6	Record identification characters
1	NKPS	+	Number of time points
Succeeding G6 Record(s)			
0	IA	G6	Record identification characters
1	SPTM(1)	+	First time point, in hours
2	SPTM(2)	+	Second time point, in hours

Continue with additional time points.

G7 Record - This is an optional record used to specify erosion resistant bed layer, such as a caliche layer, that has a lower rate of erosion.

Field	Variable	Value	Description
First G7 Record			
0	IA	G7	Record identification characters
1	KG7	+	Number of time points used to define the known erosion rate in relation to flow velocity
2	THICK	+	Thickness of erosion resistant layer, in feet
Succeeding G7 Record(s)			
0	IA	G7	Record identification characters
1	ERATE(1)	+	Erosion rate, in feet per hour

2	G7V(2)	+	Velocity, in feet per second

Continue with additional time points.

GS Record - At least two GS records are required for each job, used to specify initial bed-material compositions in the channel at the downstream and upstream cross sections. The first GS record is for the downstream section; it should be placed before the first X1 record and after the G4 record, if any. The second GS record is for the upstream section; it should be placed after all cross-sectional data and just before the EJ record. Additional GS records may be inserted between two cross sections within the stream reach, with the total number of GS records not to exceed 15. Each GS record specifies the sediment composition at the cross section located before the record. From upstream to downstream, exponential decay in sediment size is assumed for the initial distribution. Sediment composition at each section is represented by five size fractions.

Field	Variable	Value	Description
0	IA	GS	Record identification characters
1	DFF	+	Geometric mean diameter of the smallest size fraction in mm
2	PC	+	Fraction of bed material in this size range

Continue with other DFF's and PC's.

GB Records - These optional records are used to define time variation of stage (water-surface elevation) at a cross section. The first set of GB records is placed before all cross section records (X1); it specifies the downstream stage. When the GB option is used, it supersedes other methods for determining the downstream stage. Other sets of GB records may be placed in other parts of the data set; each specifies the time variation of stage for the cross section immediately following the GB records.

Field	Variable	Value	Description
First GB Record			
0	IA	GB	Record identification characters
1	KBL	+	Number of points used to define base-level changes
Succeeding GB Record(s)			
0	IA	GB	Record identification characters
1	BSLL(1)	+	Base level of point 1, in ft or m
2	TMBL(1)	+	Time coordinate of point 1, in hours

3	BSLL(2)	+	Base level of point 2, in ft or m
4	TMBL(2)	+	Time coordinate of point 2, in hours

Continue with additional elevations and time coordinates, in the increasing order of time.

GQ Records - These optional records are used to define stage-discharge relation at the downstream section. The GQ input data may not used together with the GB records.

Field	Variable	Value	Description
First GQ Record			
0	IA	GQ	Record identification characters
1	KQL	+	Number of points used to define base-level changes
Succeeding GQ Record(s)			
0	IA	GQ	Record identification characters
1	BSLL(1)	+	Base level of point 1, in ft or m
2	TMQ(1)	+	Discharge of point 1, in cfs or cms
3	BSLL(2)	+	Base level of point 2, in ft or m
4	TMQ(2)	+	Discharge of point 2, in cfs or cms

Continue with additional elevations and discharges, in the increasing order of discharge.

GI Records - These optional records are used to define time variation of sediment discharge entering the study reach through the upstream cross section. The GI input data, if included, will supersede other methods for determining sediment inflow. The sediment inflow is classified into the two following cases: (1) specified inflow at the upstream section, such as by a rating curve; and (2) sediment feeding, such as from a dambreach or a sediment feeder. These two cases are distinguished by DXU in Field 2 of this record. For the first case, sediment discharge at the upstream section is computed using size fractions of bed-material at the section, but for the second case, the size fractions of feeding material need to be specified using the PCU values in this record. The upstream section does not change in geometry for the first case but it may undergo scour or fill for the second case.

Field	Variable	Value	Description
First GI Record			
0	IA	GI	Record identification characters
1	KGI	+	Number of points used to define time variation of sediment inflow.

2	DXU	+ or 0	Channel distance measured from the upstream section to the and KGI signify case 2, for which PCU values are required.
3-10	PCU	+	Size fractions of inflow material. The number of size fractions is given in Field 8 of the G3 record and the sizes for the fractions are given in the second GS record.

Succeeding GI Record(s)

0	IA	GI	Record identification characters
1	QSU(1)	+	Sediment discharge of point 1, in cubic ft or m (net volume) per second
2	TMGI(1)	+	Time coordinate of point 1, in hours
3	QSO(2)	+	Sediment discharge of point 2
4	TMGI(2)	+	Time coordinate of point 2.

Continue with additional sediment discharges and time coordinates, in the increasing order of time coordinates.

X1 Record - This record is required for each cross section (175 cross sections can be used for the study reach); it is used to specify the cross-sectional geometry and program options applicable to that cross-section. Cross sections are arranged in sequential order starting from downstream.

Field	Variable	Value	Description
0	IA	X1	Record identification characters
1	SECNO	+	Original section number from the map
2	NP	+	Total number of stations or points on the next GR records for
7	DX	+	Length of reach between current cross section and the next downstream section along the thalweg, in feet or meters
8	YFAC	0	Cross-section stations are not modified by the factor YFAC.
		+	Factor by which all cross-section stations are multiplied to increase or decrease area. It also multiplies YC1, YC2 and CPC in the XF record, and applies to the CI record.
9	PXSECE	0	Vertical or Z coordinate of GR points are not modified.
		±	Constant by which all cross-section elevations are raised or lowered

10	NODA	0	Cross section is subject to change.
		1	Cross section is not subject to change.

XF Record - This is an optional record used to specify special features of a cross section.

Field	Variable	Value	Description
0	IA	XF	Record identification characters
1	YC1	0	Regular erodible left bank
		+	Station of rigid left bank in ft or m, to the left of which channel dinates in GR records but not the first Y coordinate.
2	YC2	0	Regular erodible right bank
	+		Station of rigid right bank, to the right of which channel is non-erodible. Note: This station is located at toe of rigid bank; its value must be equal to one of the Y coordinates in GR records but not the last Y coordinate.
3	RAD	0	Straight channel with zero curvature
		+	Radius of curvature at channel centerline in ft or m. Center of radius is on same side of channel where the station (Y-coordinate) starts.
		-	Radius of curvature at channel centerline in ft or m. Center of radius is on opposite side of zero station. Note: RAD is used only if concave bank is rigid and so specified using the XF record. RAD produces a transverse bed scour due to curvature.
4	CN	0	Roughness of this section is the same as that given in Field 7 of the G1 record.
		+	Manning's *n* value for this section
5	CPC	0	Center of thalweg coincides with channel invert at this section.
		+	Station (Y-coordinate) of the thalweg in ft or m
6	IRC	0	Regular erodible cross section
		1	Rigid or nonerodible cross section such as drop structure or road crossing. There is no limit on the total number of such cross sections.
8	BSP	0	Slope of bank protection is the same as that given in Field 2 of the G3 record.
		+	Slope of bank protection at this section in BSP horizontal units
		5	Slope of rigid bank is defined by the GR coordinates.
9	BEFX	0	Bank erodibility factor is defined in Field 5 of the G1 record.
		+	A value between 0.1 and 1.0 for BEFX specifies the bank

			erodibility factor at this section.
	RWD	+	RWD is the width of bank protection of a small channel in the specified by a value greater than 1 (ft or m) in this field. When RWD is used, BEFX is not specified.
10	TDZAM	0	Erodible bed layer at this section is defined by TDZAMA in Field
		+	Thickness of erodible bed layer in ft or m. Only one decimal place is allowed for this number.
	ENEB	±	Elevation of non-erodible bed, used to define the crest elevation of a grade-control structure which may be above or below the existing channel bed. In order to distinguish it from TDZAM, ENEB must have the value of 1 at the second decimal place. For example, the ENEB value of 365 should be inputted as 365.01 and the ENEB value of -5.2 should be inputted as -5.21. When ENEB is specified, it supersedes TDZAM and TDZAMA

CI Record - This is an optional record used to specify channel improvement options due to excavation or fill. The excavation option modifies the cross-sectional geometry by trapezoidal excavation. Those points lower than the excavation level are not filled. The fill option modifies the cross-sectional geometry by raising the bed elevations to a prescribed level. Those points higher than the fill level are not lowered. Excavation and fill can not be used at the same time. This record should be placed after the X1 and XF records but before the GR records. The variable ADDVOL in Field 10 of this record is used to keep track of the total volume of excavation or fill along a channel reach. ADDVOL specifies the initial volume of fill or excavation. A value greater or less than 0.1 needs to be entered in this field to keep track of the total volume of fill or excavation until another ADDVOL is defined.

Field	Variable	Value	Description
0	IA	G5	Record identification characters
1	CLSTA	+	Station of the centerline of the trapezoidal excavation, expressed according to the stations in the GR records, in feet or meter.
2	CELCH	+	Elevation of channel invert for trapezoidal channel, in feet or meters.
4	XLSS	+	Side slope of trapezoidal excavation, in XLSS horizontal units for 1 vertical unit.
5	ELFIL	+	Fill elevation on channel bed, in feet or meters.
6	BW	+	Bed width of trapezoidal channel, in feet or meters. This width is measured along the cross section line; therefore, a larger value should be used if a section is skewed.
10	ADDVOL	0	Volume of excavation or fill, if any, is added to the total volume already defined.

+	Initial volume of fill on channel bed, in cubic feet or cubic meters.
-	Initial volume of excavation from channel bed, in cubic feet or meters.

GR Record - This record specifies the elevation and station of each point for a digitized cross section; it is required for each X1 record.

Field	Variable	Value	Description
0	IA	GR	Record identification characters
1	Z1	"	Elevation of point 1, in ft or m. It may be positive or negative.
2	Y1	"	Station of point 1, in ft or m
3	Z2	"	Elevation of point 2, in ft or m
4	Y2	"	Station of point 2, in ft or m

Continue with additional GR records using up to 79 points to describe the cross section. Stations should be in increasing order.

SB Record - This special bridge record is used to specify data in the special bridge routine. This record is used together with the BT and GR records for bridge hydraulics. This record is placed between cross sections that are upstream and downstream of the bridge.

Field	Variable	Value	Description
0	IA	SB	Record identification characters
1	XK	+	Pier shape coefficient for pier loss
2	XKOR	+	Total loss coefficient for orifice flow through bridge opening
3	COFQ	+	Discharge coefficient for weir flow overtopping bridge roadway
4	IB	+	Bridge index, starting with 1 from downstream toward upstream
5	BWC	+	Bottom width of bridge opening including any obstruction
6	BWP	0	No obstruction (pier) in the bridge
		i	Total width of obstruction (piers)
7	BAREA	+	Net area of bridge opening below the low chord in square feet
9	ELLC	+	Elevation of horizontal low chord for the bridge

10	ELTRD	+	Elevation of horizontal top-of-roadway for the bridge

BT Record - This record is used to compute conveyance in the bridge section. The BT data defines the top-of -roadway and the low chord profiles of bridge. The program uses the BT, SB and GR data to distinguish and to compute low flow, orifice flow and weir flow.

Field	Variable	Value	Description
0	IA	BT	Record identification characters
1	NRD	+	Number of points defining the bridge roadway and bridge low chord to be read on the BT records
2	RDST(1)	+	Roadway station corresponding to RDEL(1) and XLCEL(1)
3	RDEL(1)	+	Top of roadway elevation at station RDST(1)
4	XLCEL(1)	+	Low chord elevation at station RDST(1)
5	RDST(2)	+	Roadway station corresponding to RDEL(2) and XLCEL(2)
6	RDEL(2)	+	Top of roadway elevation at station RDST(2)
7	XLCEL(2)	+	Low chord elevation at station RDST(2)

Continue with additional sets of RDST, RDEL, and XLCEL.

EJ Record - This record is required following the last cross section for each job. Each group of records beginning with the T1 record is considered as a job.

Field	Variable	Value	Description
0	IA	EJ	Record identification characters
1-10			Not used

II. OUTPUT DESCRIPTION

Output of the model include initial bed-material compositions, time and spatial variations of the water-surface profile, channel width, flow depth, water discharge, velocity, energy gradient, median sediment size, and bed-material discharge. In addition, cross-sectional profiles are printed at different time intervals.

Symbols used in the output are generally descriptive, some of them are defined below:

SECTION	Cross section
TIME	Time on the hydrograph
DT	Size of the time step or Δt in sec
W.S.ELEV	Water-surface elevation in ft or m
WIDTH	Surface width of channel flow in ft or m
DEPTH	Depth of flow measured from channel invert to water surface in ft or m
Q	Discharge of flow in cfs or cms
V	Mean velocity of a cross-section in fps or mps
SLOPE	Energy gradient
D50	Median size or d_{50} of sediment load in mm
QS	Bed-material discharge for all size fractions in cfs or cms
FR	Froude number at a cross section
N	Manning's roughness coefficient
SED.YIELD	Bulk volume or weight of sediment having passed a cross section since beginning of simulation, in cubic yards or tons.
WSEL	Water-surface elevation, in ft or m
Z	Vertical coordinate (elevation) of a point on channel boundary at a cross-section, in ft or m
Y	Horizontal coordinate (station) of a point on channel boundary at a cross-section, in ft or m
DZ	Change in elevation during the current time step, in ft or m
TDZ	Total or accumulated change in elevation, in ft or m

Appendix C

WRA, Inc. 2010. Topographic and Vegetation Analysis of Batiquitos Lagoon and Agua Hedionda Lagoon. Prepared by WRA, Inc. 2169 E Francisco Blvd Suite G San Rafael, CA 94901 8 pp + Figures.

Topographic and Vegetation Analysis of Batiquitos Lagoon and Agua Hedionda Lagoon

I-5 North Coast Corridor Project
San Diego County, California

Prepared For:

Caltrans, District 11 and San Diego Association of Governments

Contact:

Michael Josselyn, PhD, PWS
josselyn@wra-ca.com
WRA, Inc.
2169 E Francisco Blvd Suite G
San Rafael, CA 94901

Date:

August 2010

ENVIRONMENTAL CONSULTANTS

TABLE OF CONTENTS

1.0 INTRODUCTION 1
2.0 METHODS 1
3.0 RESULTS 3
3.1 Topography and Hydrology 3
3.2 Land Cover and Vegetation 3
3.3 Batiquitos Lagoon 4
3.4 Agua Hedionda 6

TABLE OF FIGURES

Figure 1: Location 2
Figure 2: Habitat Distribution and Elevation on Batiquitos Lagoon Perimeter 5
Figure 3: Habitat Distribution and Elevation on Agua Hedionda Lagoon Perimeter 7

APPENDICES

Appendix A: Topographic and Transect Data
Appendix B: 3D Topographic and Bathemetry Model of Lagoons
Appendix C: Photo Appendix

1.0 INTRODUCTION

The California Department of Transportation (Caltrans), District 11, is developing plans and supporting environmental studies for the proposed Interstate 5 (I-5) North Coast Corridor Project. The project would improve an approximately 27-mile-long portion of I-5 within the County of San Diego, extending from the City of San Diego north to the City of Oceanside. Improvements may include widening of existing bridge structures along this portion of I-5, specifically at coastal lagoons, and would therefore have impacts to tidal and nontidal wetlands that will require mitigation. The I-5 North Coast Corridor Project will permanently impact 24.4 to 32 acres of wetland habitat depending on the alternative chosen. The majority of those impacts will be at the lagoons. Approximately 23 to 29 acres of the habitat impacted is Army Corps of Engineers (Corps) jurisdictional waters of the U.S, including up to 8 acres of coastal salt marsh habitat (San Diego Association of Governments [SANDAG] 2005). Such impacts would require permits from federal and state agencies that would mandate mitigation for any permitted fill placement in wetlands.

Caltrans is investigating opportunities to expand, restore, or enhance existing tidal wetlands as part of a potential mitigation program. The Phase I Study conducted by WRA, Inc. and AECOM in 2009 evaluated the potential restoration opportunities within six coastal lagoons traversed by I-5—Buena Vista, Aqua Hedionda, Batiquitos, San Elijo, San Dieguito, and Los Peñasquitos (listed north to south). The analysis sought to specifically identify: (a) conventional earthmoving restoration opportunities, and (b) those that could occur as a result of changes in bridge structures that might remove tidal muting east of I-5 (hydrodynamic approach).

Upon completion of the Phase I Study, Batiquitos and Agua Hedionda Lagoon were identified as having the greatest potential for salt marsh creation and enhancement using the hydrodynamic approach. The following report is a component of the Phase II Study designed to assess the potential benefits of the hydrodynamic approach for salt marsh habitat within these two lagoons (Figure 1). For this portion of the Study, WRA conducted an analysis of elevation and vegetation changes above the existing Mean High Water (MHW) within the portion of the lagoon east of I-5. By combining topographic and bathymetric data, along with collected elevation and vegetation data, WRA was able to model the area of wetland habitat located within six inche bands from MHW to two feet above MHW. This analysis was conducted to facilitate the assessment of the net increase of salt marsh habitat that could be expected from incremental increases in tidal levels within the lagoon.

2.0 METHODS

The methodology used to complete the analysis topographic model of Batiquitos and Agua Hedionda Lagoons involved data collection of elevations measured at each lagoon, and the integration and modeling of these elevations with existing bathymetry and topography data. The field work and data collection was conducted by WRA between February 22 -25, 2010. Using an Auto Level and a hand held Trimble GPS unit with sub-foot accuracy, elevation transects were shot and vegetation composition transects were collected throughout each lagoon.

For the elevation transects, representative areas of topography were selected throughout each lagoon using existing topographic data mapped upon lagoon aerials. For each representative area, a metered transect tape was run from MHW moving upslope and perpendicular to the edge of water. During data collection, MHW was determined through the use of physical and biological field indicators such as wrack lines, vegetation changes, algae growth on the ground and on low vegetation, etc… Using an Auto Level, a MHW elevation was recorded and a geo-referenced point was taken using the Trimble GPS. The collected data and transect locations are presented in Appendix A

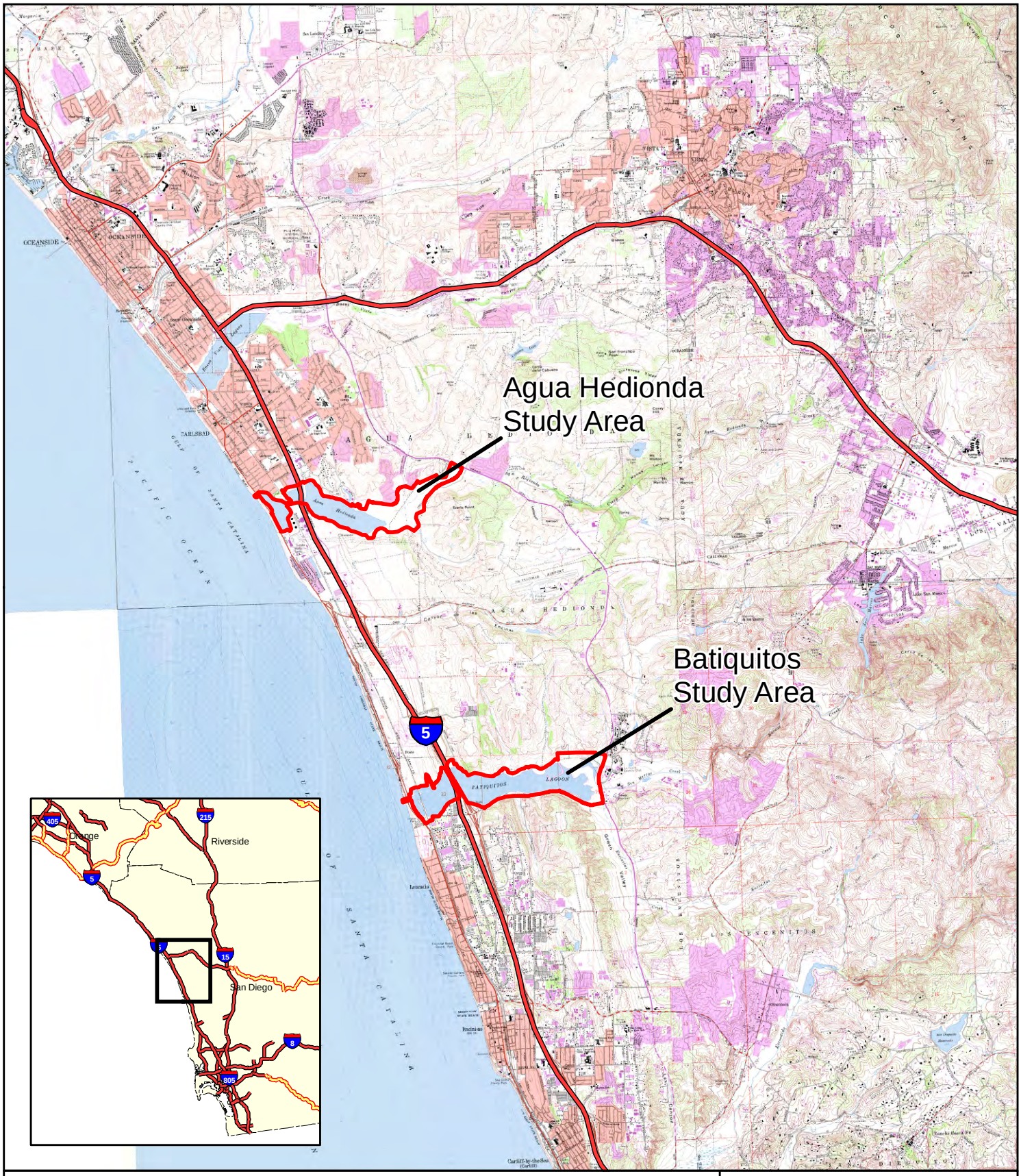

Figure 1. Location Map

SANDAG
San Diego County, CA

N
W E
S

0 0.5 1 2 Miles

wra
ENVIRONMENTAL CONSULTANTS

Date: April 2010
Map By: Sundaran Gillespie
Filepath:I:\Acad2000\16000\16165\gis\Arcmap\Phase 2\Location Map.mxd

Moving up the transect tape, elevation points were taken in six inch vertical increments, representing MHW + 6", MHW +1', MHW +1'6" and MHW +2'. GPS points were taken at each elevation point, and the horizontal distance along the transect tape was recorded. For each location, additional transects were shot east and west of the transect tape using the elevation levels recorded with the Auto Level for each of the MHW through MHW +2' increments. All recorded elevations and all Auto Level set-ups were geo-referenced with the Trimble GPS unit.

The analytical modeling consisted of creating a 3-dimensional terrain model of Batiquitos and Agua Hedionda Lagoons using existing 2 foot contours (Appendix B). Data collected in the field was then overlaid on to the terrain model to determine the elevation of each data point. Variation in the elevations of data points across multiple transects existed due to the limitations in accuracy of both the GPS unit and the terrain model. To compensate for the variations in the data and to determine the appropriate MHW elevation for each lagoon, the mean elevation of all of the MHW points was used. This averaging procedure was repeated to create the 6", 1', 1.5' and 2' above MHW contour lines.

Shifts in vegetation were identified along each transect and GPS points were taken at each shift location. Vegetation shifts were identified as areas where there was a change in dominant plant species or a change in overall vegetative cover. These data were used as reference points to identify different vegetation signatures visible on aerial photographs of the Lagoons and to group these signatures into one of three land cover types (Wetland, Upland or Sand/Rock). The extent of each land cover type was then digitized using aerial photographs and the area of each land cover type within each topographic band (MHW-6", 6"-1', 1'-1.5', 1.5'-2') was calculated using GIS. Representative photographs of the lagoon habitats are presented in Appendix C.

3.0 RESULTS

Presented below are the results for the analytical modeling of Batiquitos and Agua Hedionda Lagoons created with the use of collected field elevation data and vegetation data, and existing topography and bathymetry data. These results are modeled to represent potential vegetation changes under incremental tidal increase above MHW up to 2 feet.

3.1 Topography and Hydrology

The area of MHW was delineated for the east basins of Batiquitos and Agua Hedionda Lagoons, along with concentric rings representing elevation increases of 6 inches ranging from MHW up to MHW + 2'. The potential hydrodynamic inundation is currently under analysis by the hydrologists of Chang Consultants. Upon completion of the hydrodynamic model, the potential tidal inundation increases can be modeled in respect to the developed concentric elevation levels created for this report to allow for analytical modeling of potential vegetation changes.

3.2 Land Cover and Vegetation

<u>Wetlands</u>

The extent of wetlands and waters that form the east basins of Batiquitos and Agua Hedionda Lagoons consist mostly of open water and tidal mudflats that are permanently or semi-permanently inundated. The vegetated portions immediately surrounding the subtidal areas of the lagoons consist primarily of saltwater marsh habitat that can be categorized as low marsh habitat which is regularly inundated during most tides and is dominated by cordgrass (*Spartina spp.*), middle marsh habitat which is regularly to semi-regularly inundated at high tides and is

dominated by pickleweed (*Salicornia virginica*) and fleshy jaumea (*Jaumea carnosa*), or high marsh habitat which is occasionally inundated by very high tides and is dominated by pickleweed, salt grass (*Distichlis spicata*) and alkali heath *(Frankenia salina*). At elevations slightly above the high marsh habitats, a wetland-transition zone is common which is dominated by salt grass, spiny rush (*Juncus acutus*) and golden bush (*Isocoma menziesii*).

At locations in and adjacent to the lagoons where there are high levels of freshwater input, brackish and freshwater marsh occur and are characterized by cattail (*Typha* spp.) and California bulrush (*Shoeneoplectus californicus*). These brackish and freshwater marsh habitats can exist at varying elevations around the lagoons and are limited more by freshwater inputs than by a specific elevation range. Associated with these brackish and freshwater marsh habitats is often a drier riparian habitat dominated by arroyo willow (*Salix lasiolepis*).

Uplands

Above the wetland-transition zones are a variety of upland habitats. These upland habitats include, annual grasslands dominated by non-native annual grasses, wild radish (*Raphanus sativus*) and black mustard (*Brassica nigra*), non-native woodlands dominated by eucalyptus trees (*Eucalyptus spp.*), and a variety of scrub habitats which can be dominated by coyote brush (*Baccharis pilularis*), California sage (*Artemisia californica*), lemonade berry (*Rhus integrifolia*) or arroyo willow.

Unvegetated Areas

In several locations of around both lagoons there are unvegetated areas, some of these are naturally occurring sand/mud flats while others are areas disturbed by existing and historic land uses. The disturbed unvegetated areas around the lagoons consist of rock (riprap) infrastructure designed to prevent erosion, concrete walls and boat ramps, sandy areas associated with historic disturbances, manicured sandy beaches and least tern nesting islands.

3.3 Batiquitos Lagoon

The area of land that extends from MHW of Batiquitos Lagoon up to an elevation two feet above MHW totals 65.8 acres. The elevational distribution of that area is as follows: MHW to six inches above MHW covers 19.67 acres, six inches above MHW to one foot above MHW covers 12.52 acres, one foot above MHW to one foot six inches above MHW covers 8.02 acres and the area from one foot six inches above MHW to two feet above MHW covers 25.59 acres. The total distribution of land cover types within the MHW to two feet above MHW elevation range is split into 61.7 acres of wetlands, 4.06 acres of uplands and .04 acres of sand/rock, see Figure 2.

In the 19.67 acre area that extends from MHW to six inches above MHW the land cover is 98.9% wetland vegetation (19.47 acres). The remaining 0.2 acre consists of upland vegetation that is located in disturbed areas along the margins of the two maintained least tern nesting islands.

The 12.52 acre area that lies between six inches above MHW to one foot above MHW is 95% wetland (11.91 acres) with the remaining acreage consisting of 0.6 acre of upland habitat and 0.01 acre of rock. The upland habitats within this elevation range are concentrated around the margins of disturbed areas, specifically the tern islands and a historic roadbed located in the southeast portion of the lagoon. The rock area is a riprapped road bed along Interstate 5.

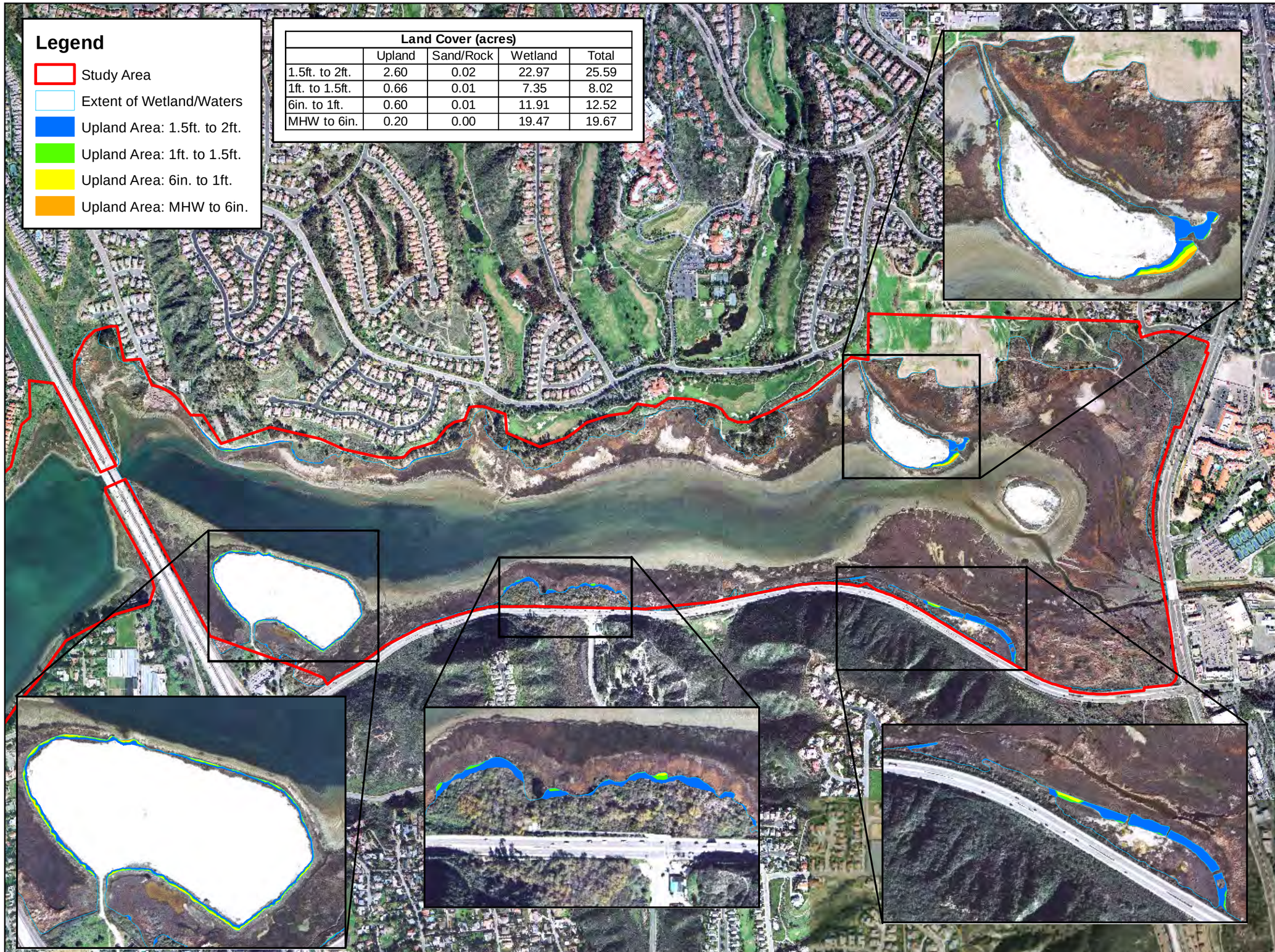

Land Cover (acres)				
	Upland	Sand/Rock	Wetland	Total
1.5ft. to 2ft.	2.60	0.02	22.97	25.59
1ft. to 1.5ft.	0.66	0.01	7.35	8.02
6in. to 1ft.	0.60	0.01	11.91	12.52
MHW to 6in.	0.20	0.00	19.47	19.67

wra
ENVIRONMENTAL CONSULTANTS
2169-G East Francisco Blvd.
San Rafael, CA 94901
(415) 454-8868 Phone
(415) 454-0129 Fax

SANDAG

Batiquitos Lagoon
San Diego County,
California

Figure 2.
Habitat Distribution and Elevation on Batiquitos Lagoon Perimeter

N
W E
S

0 400 800 1,600
Feet

Map Date: April 10
Map By: Sundaran Gillespie
Image Date: Jan 08
Base Source: Terraserver
Filepath: I:\ACAD2000\16000\16165\GIS\ArcMap\Phase 2\Bat Mit Potential.mxd

The area between one foot above MHW and one foot six inches above MHW is an 8.02 acre area that is 91.6% covered with wetland vegetation (7.35 acres). This elevation range supports 0.66 acres of upland habitat that is dispersed across several locations around the lagoon including the tern islands, the historic roadbed and a naturally occurring scrubby rise along the south shore of the lagoon. This elevation range also contains 0.01 acre of rock along the I-5 corridor.

From one foot six inches above MHW to two feet above MHW is an area totaling 25.59 acres that is 89.7%covered by wetland vegetation (22.97 acres). This elevation range supports 2.6 acres of upland habitats that are spread around the perimeter of the lagoon and have larger areas concentrated at the historic roadbed and the natural rise along the south shore of the lagoon. There is an additional 0.02 acre of rock located along the I-5 corridor in this elevation range.

3.4 Agua Hedionda

The area of land that extends from MHW of Agua Hedionda Lagoon up to an elevation two feet above MHW totals 32.52 acres. The elevational distribution of that area is as follows: MHW to six inches above MHW covers 17.73 acres, six inches above MHW to one foot above MHW covers 4.79 acres, one foot above MHW to one foot six inches above MHW covers 5.45 acres and the area from one foot six inches above MHW to two feet above MHW covers 4.55 acres. The total distribution of land cover types within the MHW to two feet above MHW elevation range is split into 30.24 acres of wetlands, 0.89 acre of uplands and 1.39 acres of sand/rock, see Figure 3.

In the 17.73 acre area that extends from MHW to six inches above MHW the land cover is 97.5% wetland vegetation (17.29 acres). This elevation range supports upland vegetation (0.19 acre) that is located in two disturbed areas along the north shore. One of these areas is on top of a small embankment reinforced with riprap near single family homes, and the other is located in a site of historic disturbance known as the Hallmark Parcel. The remaining 0.25 acre consists of disturbed sandy areas in the Hallmark Parcel.

The 4.79 acre area that lies between six inches above MHW to one foot above MHW is 92% wetland (4.41 acres) with the remaining acreage consisting of 0.1 acre of upland habitat and 0.28 acre of sand. The upland habitats within this elevation range are concentrated near the riprapped embankment on the north shore of the lagoon. The sand areas are located along the private beaches just east of the riprapped embankment and also within the disturbed portions of the Hallmark Parcel.

The area between one foot above MHW and one foot six inches above MHW is a 5.45 acre area that is 87.3% covered with wetland vegetation (4.76 acres). This elevation range supports 0.25 acres of upland habitat that is dispersed across several locations around the lagoon. This elevation range also contains 0.44 acre of sand within the private north shore beaches and within the disturbed portions of the Hallmark Parcel.

From one foot six inches above MHW to two feet above MHW is an area totaling 4.55 acres that is 83% covered by wetland vegetation (3.78 acres). This elevation range supports 0.35 acre of upland habitats that are spread around the perimeter of the lagoon. There is an additional 0.42 acre of sand located on the private north shore beaches and within the disturbed areas of the Hallmark Parcel.

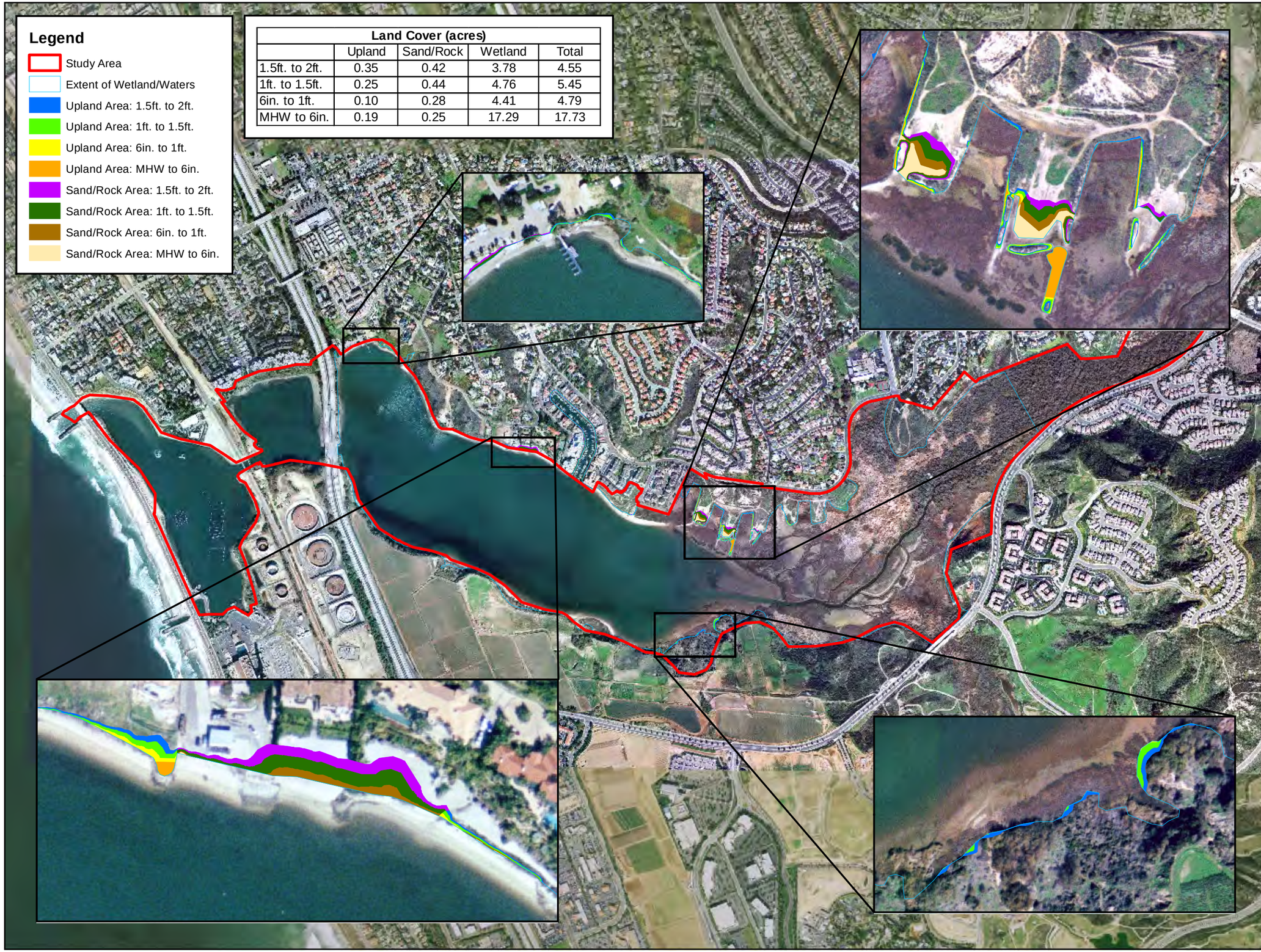

Land Cover (acres)				
	Upland	Sand/Rock	Wetland	Total
1.5ft. to 2ft.	0.35	0.42	3.78	4.55
1ft. to 1.5ft.	0.25	0.44	4.76	5.45
6in. to 1ft.	0.10	0.28	4.41	4.79
MHW to 6in.	0.19	0.25	17.29	17.73

wra
ENVIRONMENTAL CONSULTANTS
2169-G East Francisco Blvd.
San Rafael, CA 94901
(415) 454-8868 Phone
(415) 454-0129 Fax

SANDAG

Agua Hedionda Lagoon
San Diego County,
California

Figure 3.
Habitat Distribution and Elevation on Agua Hedionda Lagoon Perimeter

N
W E
S

0 495 990 1,980
Feet

Map Date: April 10
Map By: Sundaran Gillespie
Image Date: Jan 08
Base Source: Terraserver
Filepath: I:\ACAD2000\16000\16165\GIS\ArcMap\Phase 2\AH Mit Potential.mxd

APPENDIX A: TOPOGRAPHIC AND TRANSECT DATA

wra
ENVIRONMENTAL CONSULTANTS
2169-G East Francisco Blvd.
San Rafael, CA 94901
(415) 454-8868 Phone
(415) 454-0129 Fax

SANDAG

Agua Hedionda Lagoon
San Diego County,
California

Transect Locations in Agua Hedionda Lagoon

N
W E
S

0 250 500 1,000
Feet

Map Date: August 10
Map By: Sundaran Gillespie
Image Date: Jan 08
Base Source: Terraserver
Filepath: I:\ACAD2000\16000\16165\GIS\ArcMap\Phase 2\AH Transects.mxd

wra
ENVIRONMENTAL CONSULTANTS
2169-G East Francisco Blvd.
San Rafael, CA 94901
(415) 454-8868 Phone
(415) 454-0129 Fax

SANDAG

Batiquitos Lagoon
San Diego County,
California

Transect Locations in Batiquitos Lagoon

N
W E
S

0 400 800 1,600
Feet

Map Date: August 10
Map By: Sundaran Gillespie
Image Date: Jan 08
Base Source: Terraserver
Filepath: I:\ACAD2000\16000\16165\GIS\ArcMap\Phase 2\Bat Transects.mxd

Survey Crew: DC, NB

Batiquitos Lagoon - Phase II Survey Data

Survey Date: Feb 22 and 23, 2010

Transect	Feature	Station (Feet)	Stadia Rod Height (Feet)	GPS Location/Name	Set up
1	Mudflat Edge	0	8' 11"00	P1	1
1	MHW	30' 8"	6' 11" 1/4	MHW 01	
1	MHW + 1/2'	38' 3"	6' 5" 2/4	6"_01	
1	MHW + 1'	47' 1"	5' 11" 1/4	1'_01	
1	MHW + 1 1/2'	56' 7"	5' 5" 1/4	1.5'_01	
1	MHW + 2'	65' 10"	4' 11" 2/4	2'_01	
Note: Set of elevations shot about 25' SE and about 25' west of Transect 01					
2	MHW	0	9' 4" 00	MHW_02	2
2	MHW + 1/2'	6' 5"	8' 10" 00	6"_02	
2	MHW + 1'	11' 2"	8' 4" 00	1'_02	
2	MHW + 1 1/2'	14' 2"	7' 10" 00	1.5'_02	
2	MHW + 2'	17' 2"	7' 4" 00	2'_02	
Note: Elevations for Transect 02A located about 40' east of Transect 02 tape; Transect 02B about 50' northwest of tape.					
3	MHW	0	6' 4" 1/2	MHW_03	3
3	MHW + 1/2'	6' 6"	5' 10" 1/2	6"_03	
3	MHW + 1'	11' 3"	5' 4" 1/2	1'_03	
3	MHW + 1 1/2'	13' 2"	4' 10" 1/2	1.5'_03	
3	MHW + 2'	22' 6"	4' 4" 1/2	2'_03	
Note: Elevations for Transect 03A about 30' east of Transect 03 tape; Transect 03B about 40' west tape.					
4	MHW	0	6' 3" 00	MHW_04	4
4	MHW + 1/2'	29' 4"	5' 9" 00	6"_04	
4	MHW + 1'	65' 4"	5' 3" 00	1'_04	
4	MHW + 1 1/2'	72' 0"	4' 9" 00	1.5'_04	
4	MHW + 2'	98' 1"	4' 3" 00	2'_04	
Note: Elevations for Transect 04A about 50-60' east of Transect 04 tape; Transect 04B other side of small channel from tape; Transect 04C located between Transect 04B and Transect 04 tape.					
5	MHW	21' 8"	6' 5" 1/4	MHW_05	5
5	MHW + 1/2'	40' 0"	5' 11" 1/4	6"_05	
5	MHW + 1'	49' 3"	5' 5" 1/4	1'_05	
5	MHW + 1 1/2'	64' 1"	4' 11" 1/4	1.5'_05	
5	MHW + 2'	80' 0"	4' 5" 1/4	2'_05	
Note: Elevations for Transect 05A about 40' east of Transect 05 tape; Transect 05B about 40' west tape.					
6	MHW	0	5' 1" 1/4	MHW_06	6
6	MHW + 1/2'	16' 0"	4' 7" 1/4	6"_06	
6	MHW + 1'	22' 5"	4' 1" 1/4	1'_06	
6	MHW + 1 1/2'	27' 0"	3' 7" 1/4	1.5'_06	
6	MHW + 2'	29' 7"	3' 1" 1/4	2'_06	
Note: Elevations for Transect 06A about 30' east of Transect 06 tape; Transect 06B about 25' northwest tape.					
7	Edge of Slough	0	5' 11" 3/4	sloughedge	7
7	MHW	53' 4"	5' 3" 00	MHW_07	
7	MHW + 1/2'	88' 5"	4' 9" 00	6"_07	
7	MHW + 1'	125' 7"	4' 3" 00	1'_07	
7	MHW + 1 1/2'	187' 4"	3' 9" 00	1.5'_07	

7	MHW + 2'	214' 5"	3' 3" 00	2'_07	
Note: Elevations for Transect 07A about 35' east of Transect 07 tape; Transect 07B about 45' west tape.					
8	MHW	0	5' 2" 1/2	MHW_08	8
8	MHW + 1/2'	29' 3"	4' 8" 1/2	6"_08	
8	MHW + 1'	47' 3"	4' 2" 1/2	1'_08	
8	MHW + 1 1/2'	63' 0"	3' 8" 1/2	1.5'_08	
8	MHW + 2'	79' 3"	3' 2" 1/2	2'_08	
Note: No additional A or B transects taken with Transect 08.					
9	MHW	0	6' 7" 00	MHW_09	9
9	MHW + 1/2'	1' 5"	6' 1" 00	6"_09	
9	MHW + 1'	3' 3"	5' 7" 00	1'_09	
9	MHW + 1 1/2'	5' 0"	5' 1" 00	1.5'_09	
9	MHW + 2'	6' 2"	4' 7" 00	2'_09	
9	Top of Berm	11' 11"	3' 10" 1/2	Top of berm_09	
9	Depression	22' 9"	4' 11" 3/4	Depression_09	
Note: Elevations for Transect 09A about 40' east of Transect 09 tape; Transect 09B about 80' west tape.					
10	MHW	0	5' 5" 3/4	MHW_10	10
10	MHW + 1/2'	31' 7"	4' 11" 3/4	6"_10	
10	MHW + 1'	---	4' 5" 3/4	1'_10	
10	Edge of Freshwater Marsh, MHW + 2 1/2'	114' 6"	5' 3" 1/4	Edge of marsh_10	
Note: No additional A or B transects taken with Transect 10.					
11	MHW	---	5' 5" 3/4	MHW_11	10
11	MHW + 1/2'	---	4' 11" 3/4	6"_11	
11	MHW + 1'	---	4' 5" 3/4	1'_11	
Note: Elevations for Transect 11A - MHW, several MHW and MHW + 6" shot near Transect 11. Same Set up used for Transect 10 and 11.					

Survey Crew: DC, NB

Agua Hedionda Lagoon - Phase II Survey Data

Survey Date: Feb 24 and 25, 2010

Transect	Feature	Station (Feet)	Stadia Rod Height (Feet)	GPS Location/Name	Set up
AH1	MHW	0	6' 0" 1/2	MHW_AH1	AH1
AH1	MHW + 1/2'	0' 11"	5' 6" 1/2	6"_AH1	
AH1	MHW + 1'	114' 2"	5' 0" 1/2	1'_AH1	
AH1	MHW + 1 1/2'	126' 5"	4' 6" 1/2	1.5'_AH1	
AH1	MHW + 2'	128' 6"	4' 0" 1/2	2'_AH1	
Note: Elevations for Transect AH1A about 75' east of Transect AH1 tape; Transect AH1B about 60' west of the tape; Transect AH1C located about 120' west of the tape.					
AH2	MHW	0	4' 9" 1/2	MHW_AH2	AH2
AH2	MHW + 1/2'	47' 6"	4' 3" 1/2	6"_AH2	
AH2	MHW + 1'	71' 10"	3' 9" 1/2	1'_AH2	
AH2	MHW + 1 1/2'	81' 7"	3' 3" 1/2	1.5'_AH2	
AH2	MHW + 2'	96' 2"	2' 9" 1/2	2'_AH2	
Note: Elevations for Transect AH2A about 50' east of Transect AH2 tape; Transect AH2B about 40' west tape.					

AH3	MHW	0	5' 5" 00	MHW_AH3	AH3
AH3	MHW + 1/2'	197' 6"	4' 11" 00	6"_AH3	
AH3	MHW + 1'	+300'	4' 5" 00	1'_AH3	
AH3	MHW + 1 1/2'	---	3' 11" 00	1.5'_AH3	
Note: Elevations for Transect AH3A about 150' east of Transect AH2 tape.					
AH4	MHW	0	5' 4" 1/4	MHW_AH4	AH4
AH4	MHW + 1/2'	126' 1"	4' 10" 1/4	6"_AH4	
AH4	MHW + 1'	133' 4"	4' 4" 1/4	1'_AH4	
AH4	MHW + 1 1/2'	135' 3"	3' 10" 1/4	1.5'_AH4	
AH4	MHW + 2'	136' 10"	3' 4" 1/4	2'_AH4	
Note: Elevations for Transect AH4A about 90' east of Transect AH4 tape; Transect AH4B about 70' west tape.					
AH5	MHW	0	9' 6" 3/4	MHW_AH5	AH5
AH5	MHW + 1/2'	12' 1"	9' 0" 3/4	6"_AH5	
AH5	MHW + 1'	61' 10"	8' 6" 3/4	1'_AH5	
AH5	MHW + 1 1/2'	82' 3"	8' 0" 3/4	1.5'_AH5	
AH5	MHW + 2'	95' 5"	7' 6" 3/4	2'_AH5	
Note: Elevations for Transect AH5A about 60' east of Transect AH5 tape; two additional transects shot off of Transect AH5.					
AH6	MHW	0	8' 3" 1/2	MHW_AH6	AH6
AH6	MHW + 1/2'	5' 9"	7' 9" 1/2	6"_AH6	
AH6	MHW + 1'	21' 11"	7' 3" 1/2	1'_AH6	
AH6	MHW + 1' 3" 3/4	23' 9"	---	1' 3 3/4"_AH6	
AH6	base of berm north of beach	---	8' 10" 3/4	Base of berm_AH6	
AH6	MHW + 1' base of residential hill	---	---	1'_AH6	
Note: Elevations for Transect AH6B about 40' east of Transect AH6 tape; Transect AH6A about 90' west tape.					
AH7	MHW	0	8' 8" 1/4	MHW_AH7	AH7
AH7	MHW + 1/2'	3' 3"	8' 2" 1/4	6"_AH7	
AH7	MHW + 1'	6' 8"	7' 8" 1/4	1'_AH7	
AH7	MHW + 1 1/2'	12' 7"	7' 2" 1/4	1.5'_AH7	
AH7	MHW + 2'	20' 6"	6' 8" 1/4	2'_AH7	
Note: Elevations for Transect AH7B about 50' east of Transect AH7 tape; Transect AH7C about 200' east tape.					

Survey Notes

- MHW stands for Mean High Water
- Survey locations selected based off of general topography trends for each lagoon.
- Feature corresponds to the physical feature surveyed and GPS'd. Example is the MHW line.
- Station corresponds to the horizontal distance along the transect tape for the main transect.
- Set up locations were georeferenced using a Trimble GPS unit with sub-foot accuracy.
- Meter tape run for one main transect at each location. The distance and elevation recorded for MHW with 6" intervals for main transect. Additional A and B transects used elevations take from main transect and no horizontal distance was measure. GPS points taken at every location surveyed.

APPENDIX B: 3D TOPOGRAPHIC AND BATHEMETRY MODEL OF LAGOONS

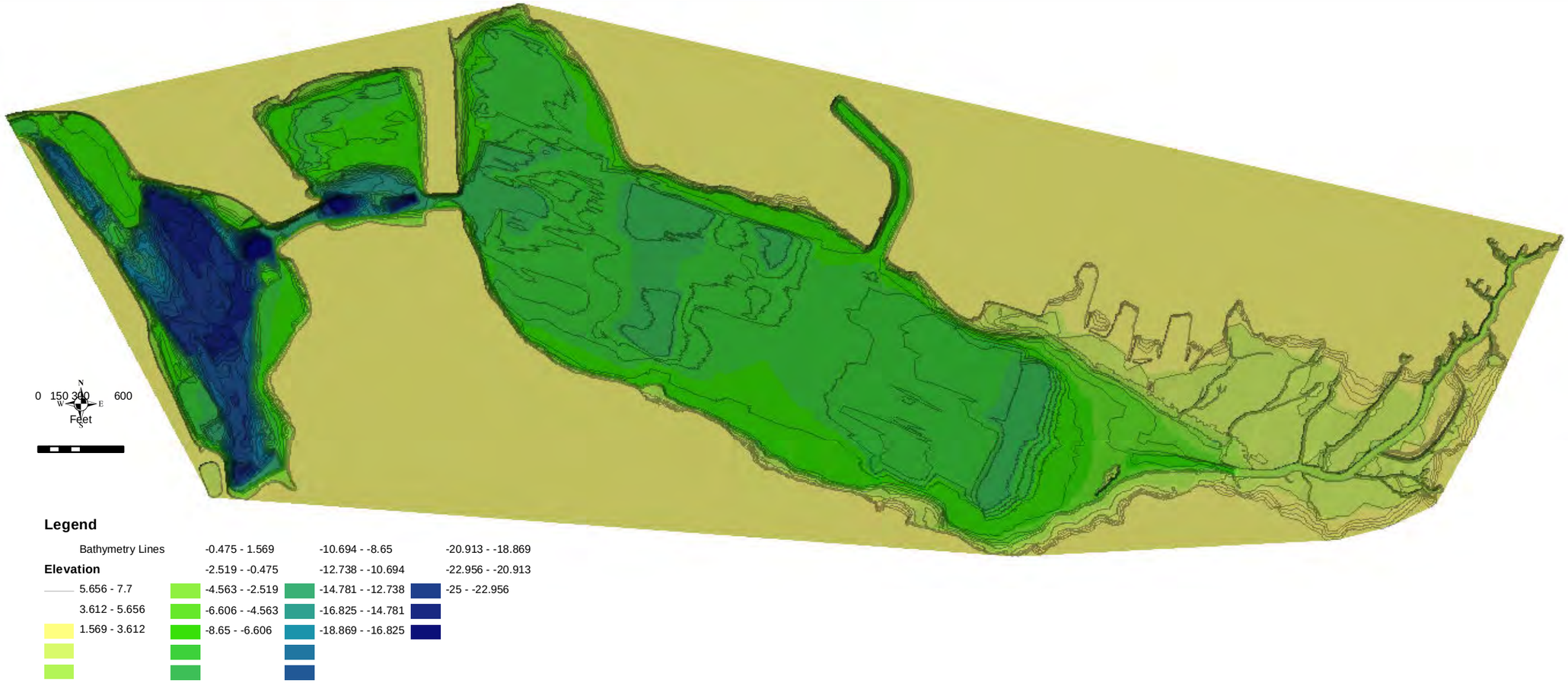

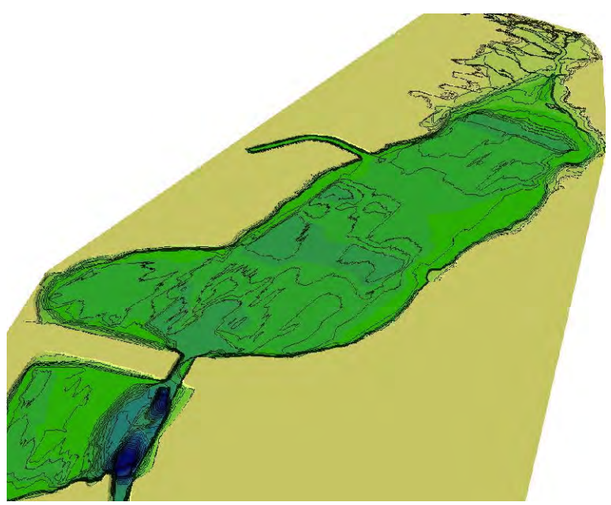

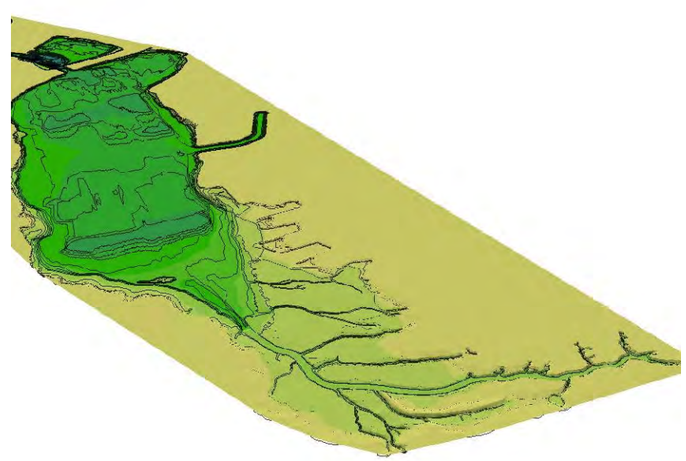

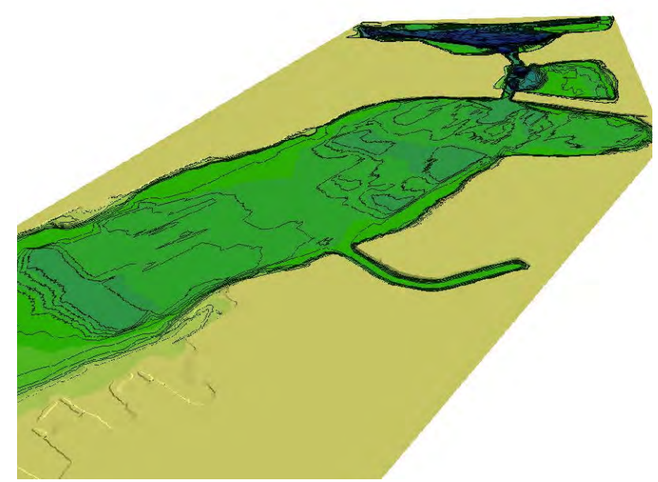

wra
ENVIRONMENTAL CONSULTANTS
2169-G East Francisco Blvd.
San Rafael, CA 94901
(415) 454-8868 Phone
(415) 454-0129 Fax

SANDAG

Agua Hedionda Lagoon
San Diego County,
California

Bathymetry of Agua Hedionda Lagoon

Map Date: August 10
Map By: Sundaran Gillespie
Filepath: I:\ACAD2000\16000\16165\GIS\ArcMap\Phase 2\AH Bathymetry.mxd

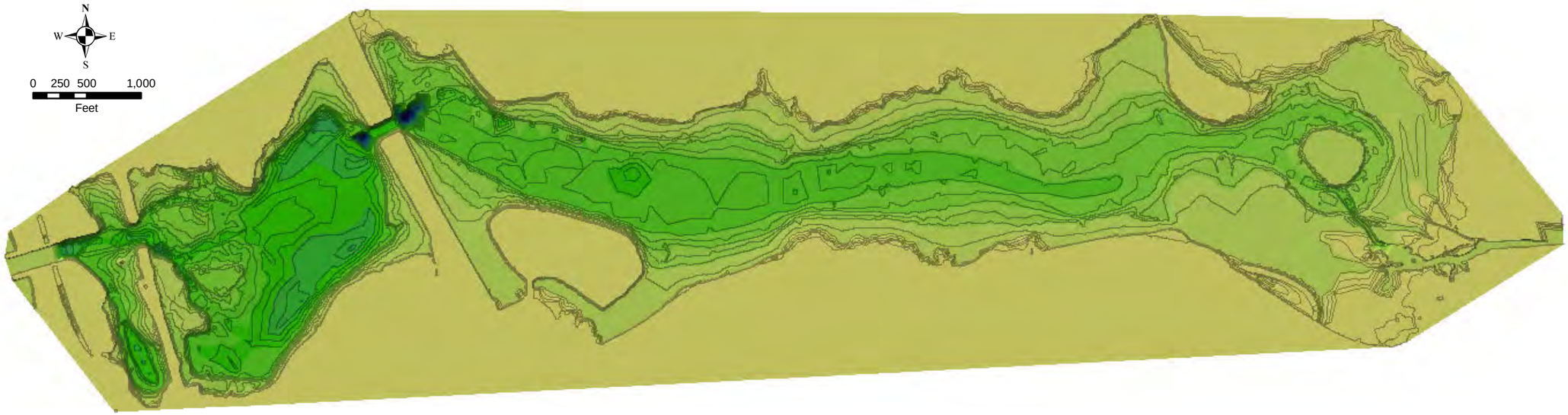

Legend

Bathymetry Lines

Elevation

- 6.187 - 8.2
- 4.175 - 6.187
- 2.162 - 4.175
- 0.15 - 2.162
- -1.863 - 0.15
- -3.875 - -1.863
- -5.888 - -3.875
- -7.9 - -5.888
- -9.913 - -7.9
- -11.925 - -9.913
- -13.938 - -11.925
- -15.95 - -13.938
- -17.963 - -15.95
- -19.975 - -17.963
- -21.988 - -19.975
- -24 - -21.988

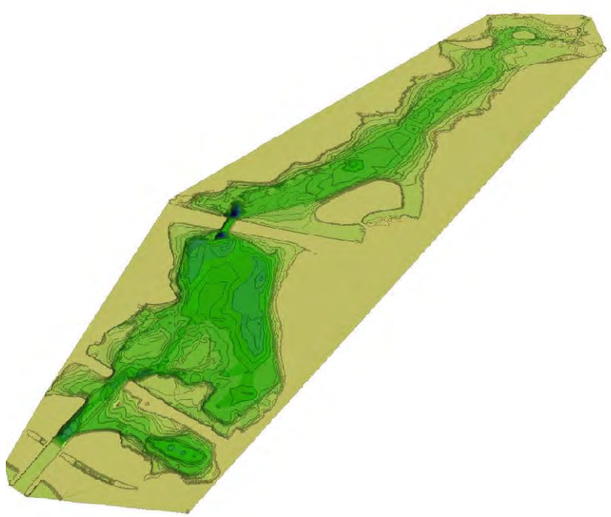

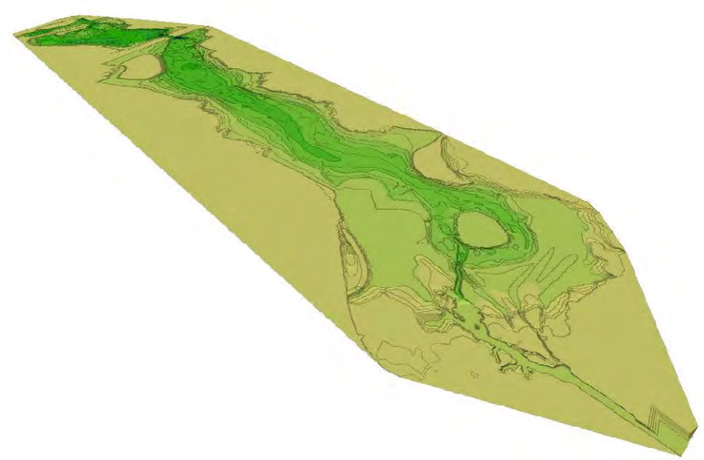

wra
ENVIRONMENTAL CONSULTANTS
2169-G East Francisco Blvd.
San Rafael, CA 94901
(415) 454-8868 Phone
(415) 454-0129 Fax

SANDAG

Batiquitos Lagoon
San Diego County,
California

Bathymetry of Batiquitos Lagoon

Map Date: August 10
Map By: Sundaran Gillespie
Filepath: I:\ACAD2000\16000\16165\GIS\ArcMap\Phase 2\Bat Bathymetry.mxd

APPENDIX C: PHOTO APPENDIX

Top: Batiquitos Lagoon Public Access through Marsh

Bottom: Batiquitos Lagoon rack line and sudden marsh shift.

wra
ENVIRONMENTAL CONSULTANTS

Top: Batiquitos Lagoon topography and vegetation shift.

Bottom: Batiquitos lagoon rack line.

wra
ENVIRONMENTAL CONSULTANTS

Top: Agua Hedionda Lagoon showing extensive eastern marsh habitats

Bottom: Agua Hedionda Lagoon slough in eastern reach of the east basin.

wra
ENVIRONMENTAL CONSULTANTS

Top: Cut Bank of Slough in Hedionda Lagoon showing dark OHW line.

Bottom: Tidal Channel adjacent to disturbed unvegetated berm at Agua Hedionda Lagoon.

wra
ENVIRONMENTAL CONSULTANTS